ACTA PHYSICA

ACADEMIAE SCIENTIARUM HUNGARICAE

TOMUS XLIII FASCICULUS 1

AKADÉMIAI KIADÓ, BUDAPEST

1977

ACTA PHYS. HUNG. APAHAQ 43 (1) 1—106 (1977)

ACTA PHYSICA

ACADEMIE SCIENTIRAUM HUNGARICAE

SZERKESZTI

KOVÁCS ISTVÁN

Az *Acta Physica* angol, német, francia vagy orosz nyelven közöl értekezéseket. Évente két kötetben, kötetenként 4—4 füzetben jelenik meg. Kéziratok a szerkesztőség címére (1521 Budapest XI., Budafoki út 8.) küldendők.

Megrendelhető a belföld számára az Akadémiai Kiadónál (1363 Budapest Pf. 24. Bankszámla 215-11488), a külföld számára pedig a „Kultura" Külkereskedelmi Vállalatnál (1389 Budapest 62, P.O.B. 149. Bankszámla 217-10990), vagy annak külföldi képviseleteinél.

The *Acta Physica* publish papers on physics in English, German, French or Russian, in issues making up two volumes per year. Subscription: $ 36.00 per volume. Distributor: "Kultura" Foreign Trading Company (1389 Budapest 62, P.O. Box 149) or its representatives abroad.

Die *Acta Physica* veröffentlichen Abhandlungen aus dem Bereich der Physik in deutscher, englischer, französischer oder russischer Sprache, in Heften, die jährlich zwei Bände bilden.

Abonnementspreis pro Band: $ 36.00. Bestellbar bei »Kultura« Außenhandelsunternehmen (1389 Budapest 62, Postfach 149) oder seinen Auslandsvertretungen.

Les *Acta Physica* publient des travaux du domaine de la physique en français, anglais, allemand ou russe, en fascicules qui forment deux volumes par an.

Prix de l'abonnement: $ 36.00 par volume. On peut s'abonner à l'Entreprise du Commerce Extérieur «Kultura» (1389 Budapest 62, P.O.B. 149) ou chez représentants à l'étranger.

«*Acta Physica*» публикуют трактаты из области физических наук на русском, немецком, английском и французском языках.

«*Acta Physica*» выходят отдельными выпусками, составляющими два тома в год.

Подписная цена — $ 36.00 за том. Заказы принимает предприятие по внешней торговле «Kultura» (1389 Budapest 62, P.O.B. 149) или его заграничные представительства.

ACTA PHYSICA

ACADEMIAE SCIENTIARUM HUNGARICAE

TOMUS XLIII

AKADÉMIAI KIADÓ, BUDAPEST

1977

ACTA PHYS. HUNG.

INDEX

Tomus 43

ACTA PHYSICA

ACADEMIAE SCIENTIARUM HUNGARICAE

TOMUS XLIII FASCICULUS 1

AKADÉMIAI KIADÓ, BUDAPEST

1977

ACTA PHYS. HUNG.

INDEX

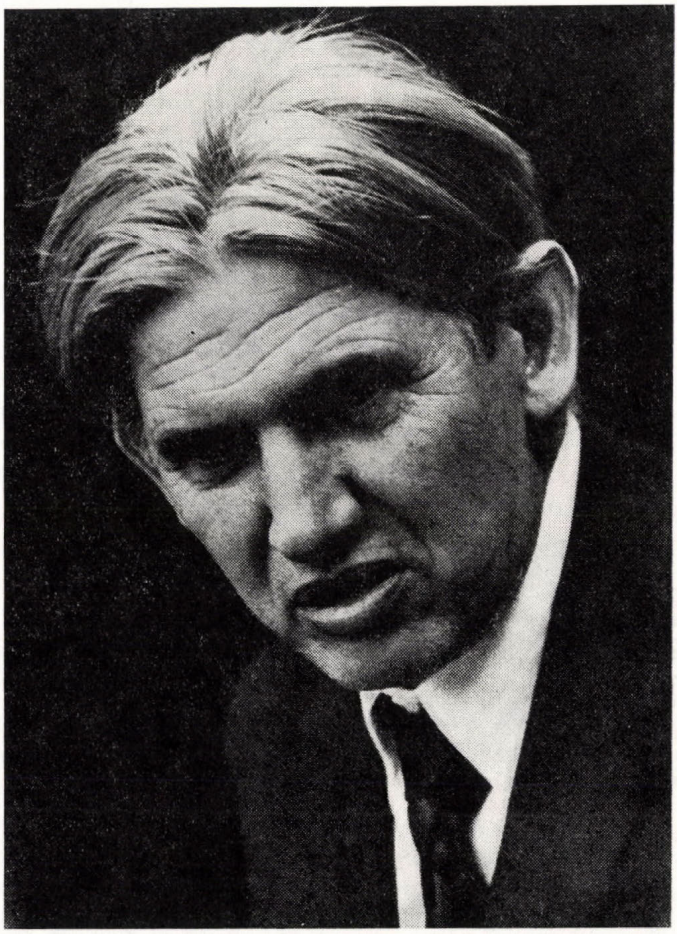

L. JÁNOSSY
1912–1978

On the 2nd of March, 1978, a prominent personality of Hungarian physics, Professor LAJOS JÁNOSSY, whose name and work are known the world over, passed away at age 66. His death is a great loss to both Hungarian and international scientific life, for he was an outstanding physicist and also a keen-sighted critic of physical science.

The present author, who has been a friend and fellow-worker of Professor JÁNOSSY for more than a quarter of a century, may perhaps take the liberty of recalling a conversation of long ago, still alive in his memory. When in the summer of 1950 Professor JÁNOSSY returned from Dublin to Budapest

for good, we discussed if it was worth reproducing measurements which had already been carried out by others. It was then that I learned from him that if a reproduction was cleverly performed it was not a simple imitation but possibly a source of some important new revelation. The correctness of this statement was later often experienced in my own investigations. We, who wanted to do something absolutely new at that time, found out later that the way to some new results led from past experience and that the difficulty lay in the choice of the proper way.

We were often surprised at the unusual turns of his questions. It was particularly fascinating to watch how theorems thought to be trivial could be ingeniously thought over anew and critically revised. I was deeply impressed by all our discussions since — mainly because of his critical perspicacity — the reasoning never remained within the scope of conventional concepts.

The earliest papers by Professor JÁNOSSY were written in 1934 reporting on his work in the Laboratory of WERNER KOLHÖRSTER in Potsdam. In his paper on the invariants of counter tubes it is shown that the intensities of cosmic radiation measured in the vertical and horizontal positions of the tubes are obtained as a linear combination of four quantities uniquely characteristic of the radiation. In another paper the angular distribution of cosmic radiation on sea level is determined. The results published in 1936 in the thesis for his doctorate are the basic concepts of a new theory of counter tubes and of coincidence. After some further reports written at the Berlin Laboratory of Cosmic Radiation Research from 1938 onward he continued his highly successful work at the Manchester Laboratory of P.M.S. BLACKETT. At this time his attention was focussed on the laws governing cosmic showers. The frequencies of these showers were measured on sea level and also underground at a depth equivalent to 60 m of water. He recognized the importance of penetrating showers and for several years he carried out thorough measurements to identify the penetrating component. In the meantime, together with B. ROSSI, he started investigations on the photon component of cosmic radiation, which made him interested in the theory of cascades. In 1941 he disproved the existence of an apparent second maximum in ROSSI's curve by showing that this false second maximum is due to SCHMEISER and BOTHE's measuring arrangement. The high energy particles of cosmic radiation passing through an absorber (e.g. lead) produce secondary particles in a cascade process. This makes the transmitted radiation intensity increase with increasing absorber thickness up to a given value past which the intensity gradually decreases. The dependence of the transmitted intensity on absorber thickness was thought by some investigators to show a second maximum for the explanation of which far-fetched hypotheses were proposed. Later, in 1956, JÁNOSSY reinvestigated the problem of the second maximum in ROSSI's curve and showed again that its existence should be unquestionably excluded.

One of his remarkable papers on the production of mesons was published in The Physical Review in 1943. It is shown in this paper by means of cloud chamber photographs that several mesons are produced at the same point and that this can only be understood on assuming that high energy particles undergo several collisions within an atomic nucleus. Investigations into the properties of penetrating showers resulted in his determination of the transition and of the barometric effects. The study of the production of mesons led him to the formulation of the "diffusion equations" describing the energy losses of high energy particles. This work was followed by the development of the cascade theory of cosmic showers and, in 1952, already in Budapest he published the general theory of cascades referred to since then in a large number of monographs and papers. In this theory he utilizes the so-called first collision method which is of great importance also in the general theory of branching stochastic processes.

His intensive engagement in problems of both mathematical statistics and probability calculus was prompted partly by the evaluation of cosmic radiation data, partly by the actual description of the processes of cosmic radiation. In a completely original way he reinvestigated the fundamentals of probability theory by a thorough analysis of reality and elaborated highly useful practical procedures for dealing with problems of data evaluation in a great variety of measurements. The majority of Hungarian physicists adopted Professor JÁNOSSY's exacting methods he always applied in connection with conclusions to be drawn from experimental data.

JÁNOSSY was much intrigued by the two grandiose theories of the twentieth century: the theory of relativity and the quantum theory. This manifested itself first of all in his courageous and ingenious attempt to revise theorems thought to be irrefutable. He transformed the whole reasoning of the theory of relativity to reconstruct it in terms of expressions closely related to real physical processes and to bring it in agreement with his concept of relativity which remains, of course, in harmony with the generally accepted theory — both formally and in respect of its actual results.

Upon the advent of the quantum theory, the controversy under debate was again one of those problems Professor JÁNOSSY thought worth reinvestigating. Assisted by his fellow-workers, he even decided to carry out the so-called "Gedanken"-experiments, frequently referred to in bygone days. The photon experiments — coincidence and interference measurements — did not only serve the above objectives, but also provided a sound basis for advanced optics (laser physics) research in the Central Research Institute for Physics. He developed the theory of the fluctuation of light, which explains the origin of excess coincidences observed in experiments with very short (10^{-7}—10^{-8} sec) coincidence times. His aim was to check the potentiality of quantum theory within its scope by calculations possibly without the use of neglections. That

is why he chose the hydrodynamical form of SCHROEDINGER's equation with all the mathematical intricacies it presents. The possible consequences of the theory are thoroughly analysed in his papers, which introduce a truly new aspect into the considerations of quantum physical phenomena.

Professor JÁNOSSY had always shown great interest in the philosophical aspect of physics expounding in many articles and lectures his standpoint based on deep Marxist conviction to contradict metaphysical views. In recent times he paid increased attention to problems connected with the teaching of mathematics and physics in secondary schools and he suggested several original initiatives.

The name of Professor JÁNOSSY is closely linked with the establishment of up-to-date physical research in Hungary, with the foundation of the Central Research Institute for Physics and that of the Atomic Physics Department of the Eötvös Lóránd University in Budapest.

He is the author of a number of important monographs, the best known of which are: Cosmic Rays, Oxford, Clarendon Press 1950; Theory and Practice of the Evaluation of Measurements, Oxford, Clarendon Press, 1965; Theory of Relativity Based on Physical Reality, Akadémiai Kiadó, Budapest, 1971.

Professor JÁNOSSY played an active part in the Editorial Board of Acta Physica Hungarica and greatly contributed to increasing the scientific standard of the publications. His own reports considerably promoted the international reputation of the journal.

We are deeply grieved by the death of Professor JÁNOSSY, who will be remembered by all of us for ever. His scientific achievements will outlive him and become sources of inspiration for new creative ideas and development.

Budapest, 6th April 1978.

L. PÁL

Member of the Hungarian Academy of Sciences

Acta Physica Academiae Scientiarum Hungaricae, Tomus 43 (1), pp. 3—16 (1977)

INELASTIC INTERACTIONS OF 69 GeV/c PROTONS WITH EMULSION NUCLEONS

By

O. E. BADAWY, A. A. EL-NAGHY, A. HUSSEIN, N. METTWALI

and

M. M. SHERIF

HIGH ENERGY PHYSICS EXPERIMENTAL LABORATORY
DEPARTMENT OF PHYSICS, FACULTY OF SCIENCE
UNIVERSITY OF CAIRO, CAIRO, EGYPT

(Received 14. IV. 1977)

Tracks of 69.0 GeV/c protons are followed in nuclear emulsion. In 768 m of proton tracks, 1887 inelastic stars are found, yielding a mean free path of proton inelastic interactions with emulsion nucleons and nuclei of 38.74 ± 1.01 cm. The average charged multiplicities $\langle n_{ch} \rangle$ of p-p and p-n interactions are found to be 6.93 ± 0.26 and 5.62 ± 0.20, respectively. The multiplicity distribution of the emitted charged secondaries for p-nucleon interactions prefers the WANG first model, reflecting the cell structure of the nucleon. KNO scaling of partial cross-section is found to be obeyed in case of p-p interactions more than in the other interactions between other hadrons.

The pseudorapidity distribution of the emitted charged secondaries is found to confirm the limiting fragmentation hypothesis.

A test of a composite proton model through the p-p multiplicity distribution and its moments prefers the construction of a proton out of three quarks.

1. Introduction

In this work the results of the study of the inelastic proton-nucleon scattering in nuclear emulsion at 69 GeV/c are presented. The multiplicity distribution of the emitted charged secondaries are compared with the various theoretical and empirical predictions. The tendency of the ratio $\langle n_{ch} \rangle / D$, where D is the dispersion of the multiplicity distributions, to approach a constant value at high energy is discussed in terms of a two component model of high energy interactions.

The study of the different moments of the multiplicity distribution of p—p interaction to test the KNO scaling behaviour of cross-section is discussed. A comparison of these moments with the predictions of a semi-classical composite model for p—p collisions at high energies are found to prefer the construction of a proton out of three quarks.

A study of the rapidity distribution of the emitted secondaries considered all to be pions indicates the coincidence of the distribution of the parameter η (where $\eta = -(\ln \tan \Theta/2)$ at the momentum 69 GeV/c with that at 200 and 3000 GeV/c, in the region of target fragmentation.

2. Experimental procedures

The exposure of an emulsion stack type, Br-2, of 20 cm × 10 cm × 0.065 cm size to the 69 GeV/c protons was tangentially performed at the Serpukhov accelerator (USSR). The admixture of pions and kaons in the beam was less than 1%. This beam was extracted by diffraction scattering and was highly collimated in a concentrated strip at the centre of the stack. The projected angular distribution of the beam tracks after about 1.5 cm from the entrance is shown in Fig. 1. The angular spread is shown to be 10^{-3} rad.

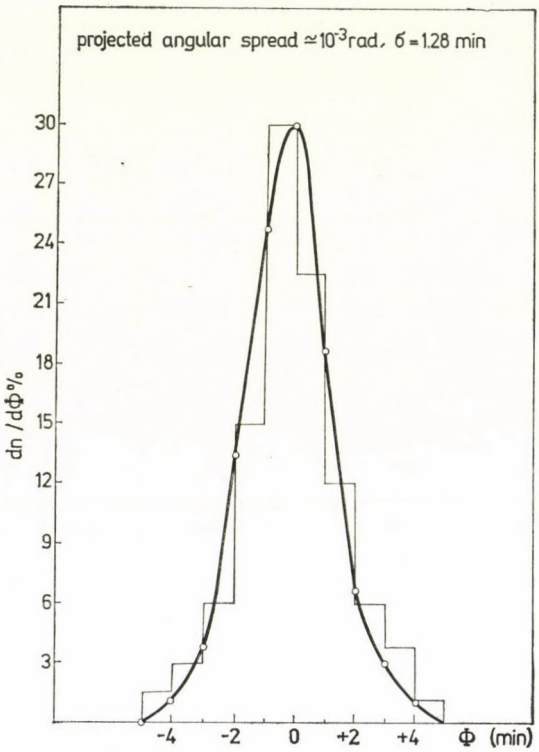

Fig. 1. Distribution of projected angles of particles from the beam irradiating the emulsion stack. The measurements were made a few centimeters (~1.5 cm) after the entrance of the particles in the stack

Starting 0.5 cm from the beam entrance, and along the track, scanning was performed.

The space angles at which the emitted secondaries are emitted relative to the primary beam direction are determined through accurate measurements of both the projected and dip angles of each secondary. Then using the usual trigonometric relations both the space and the azimuthal angles of each secondary can be calculated.

3. Results

3.1 *Inelastic interactions of protons with emulsion nucleons and nuclei*

Using the previously mentioned scanning procedures, a total of 768 meters track length was followed. For the calculation of the inelastic-interaction length "λ_{int}" the following types of events were excluded.

i) Stars with single relativistic tracks deflected by less than 7 mrad (mostly due to elastic scattering);
ii) Electron-positron pairs on the beam track;
iii) Knock-out electrons.

Altogether 1887 inelastic nuclear interactions were found, which corresponds to an interaction mean free path $\lambda_{\text{int}} = 38.74 \pm 1.01$ cm (a 5% correction was added to the total number of events found due to scanning losses. The missed events are mostly with $n_h = 0$ and $n_s \leq 4$, where n_h is the number of heavy ionizing tracks and n_s is the number of prongs due to relativistic particles.) This value of λ_{int} is not very far from that calculated for our emulsion composition and assuming an $A^{2/3}$ dependence of cross-section on the atomic weight A which amounts to a value of 35.9 cm.

3.2 *Inelastic interactions of protons with free and quasifree nucleons*

Interactions with free and quasifree nucleons were selected as those with at most one grey track (for protons this corresponds to kinetic energy between 25 MeV and 400 MeV), in the forward hemisphere in the laboratory system, and without a visible recoil nucleus. It should be pointed out that the resolution of our nuclear emulsion allows the observation of slow recoils ($\sim$ 0.2 MeV for a proton and $\sim$ 1.0 MeV for a carbon nucleus [1]). For even prong number (p – p) events there was the additional criterion of the absence of an accompanying electron. This may be due to excitation of the target nucleus, i.e. such stars may show no evidence of β-decay at the interaction point [2].

Altogether 300 proton–nucleon interactions were found (173 events with odd prong number i.e. the p – n interactions and 127 due to even prong number i.e. due to p – p interactions) which represent about 16% of all inelastic nuclear interactions in the emulsion. This ratio becomes about 20% after applying the 5% correction due to scanning losses (considering that all the 5% losses are due to events with $N_h = 0$ and $n_s \leq 4$) as mentioned before.

All the odd prong number (p – n) events correspond to collisions with quasi-free neutrons of the emulsion nuclei. As can be seen in Section 3.3 there is an admixture of coherent interactions in the odd-prong number (p – n) events.

3.3 *Prong-number distribution of proton—nucleon events*

The prong number distribution of the proton-nucleon events is shown in Fig. 2.

An overabundance of $n_{ch} = 3$ and $n_{ch} = 1$ is due to coherent interactions. The number of the coherent three prong events present in our sample was estimated to be 25, [3], giving rise to a production cross-section of 6.5 mb of coherent three prong events in p-nucleus interactions at 69 GeV/c. The

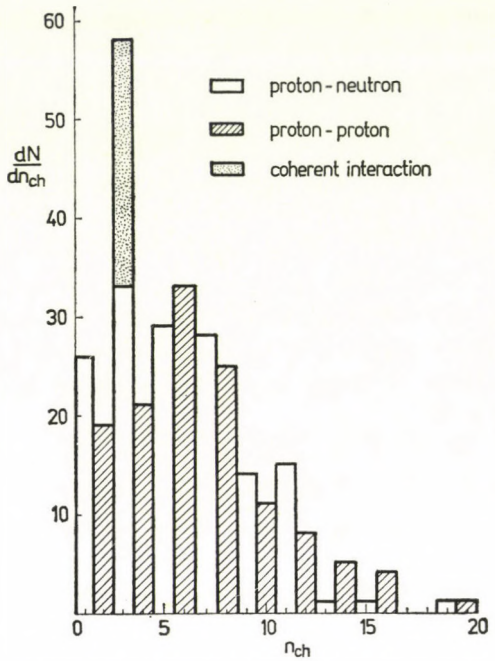

Fig. 2. Multiplicity distribution of proton-nucleon interactions by 69 GeV/c protons

average charged multiplicities for p—p and p—n interactions are 6.93 ± 0.2, and 5.62 ± 0.2, respectively. The latter multiplicity becomes 5.13 ± 0.17 without correction for the coherent events.

Our value for the average charged multiplicity $\langle n_{ch} \rangle$ for p—p interactions is greater than the value obtained in a hydrogen bubble chamber (H.B.Ch.) experiment at the same energy and which is equal to 5.89 ± 0.07 [4]. This may be due to cascading effects taking place in emulsion nuclei.

3.4 *Multiplicity distribution and current models for pion production*

The resemblance of the multiplicity distribution of charged secondaries to a Poisson distribution has been observed at low energies, [5], and some theoretical models have predicted the Poisson distribution.

WANG [6] has proposed two models which give predictions of multiplicity distributions.

Fig. 3 and Fig 4 compare these two models with the multiplicity distribution of charged secondaries produced in p—p and p—n interactions, respectively. Table I gives the results of the χ^2-test for our experimental data to the different

Table I

χ^2-values comparing the experimental multiplicity distribution of p—p and p—n inelastic interactions with the predictions of the different models (this experiment)

Model	χ^2-value p-p (8 points)	χ^2-value p-n (7 points)
Poisson	0.621	0.631
W_I	0.135	0.116
W_{II}	2.677	1.463

predictions for 8 points in case of p—p and 7 points in case of p—n. Our results are shown to be inconsistent with a Poisson distribution. The WANG second model W_{II} predictions are inconsistent with the data, while WANG first model (W_I) gives a better overall fit.

The W_I model was also found to give a better fit for the data of the k^-—p [4] at momentum 33.8 GeV/c, π^-—p [4], at 50 GeV/c, and π^-—p, π^-—n at 40 GeV/c [7].

Table II

χ^2-values obtained from fitting the experimental points of the multiplicity distribution of p—p inelastic interactions to different distributions (7 points in each case)

Model \ $P_{GeV/c}$	25 Emulsion	67 Emulsion	69 Emulsion	19 H.B.Ch.	50 H.B.Ch.	69 H.B.Ch.	102 H.B.Ch.	205 H.B.Ch.	303 H.B.Ch.
POISSON	11.82	24.90	31.54	1.09	6.50	10.25	16.08	32.75	35.25
WANG I	5.11	6.36	8.60	3.70	0.59	0.67	2.23	5.41	3.80
WANG II	62.77	119.01	150.05	7.50	56.27	66.35	89.30	168.80	171.65
Inverse square fall-off	163.28	179.00	179.50	93.27	129.20	149.74	167.10	218.86	266.30

Table II presents the results of the χ^2-fit of the experimental data of the multiplicity distribution of p—p inelastic interactions in the proton energy range from 19 up to 303 GeV [4, 8, 9], to the predictions of the inverse square fall off, the Poisson and the WANG first and second models (W_I & W_{II}). The experimental data are compiled from both H.B.Ch. and emulsion experi-

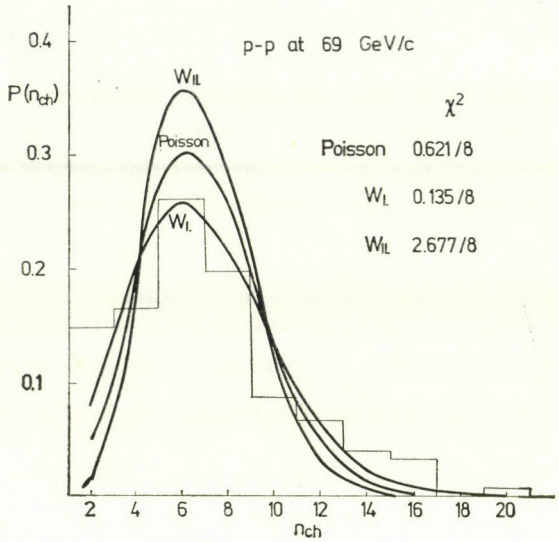

Fig. 3. Comparison of charged particle multiplicities in p-p reactions at 69 GeV/c with a Poisson distribution and with the WANG I and WANG II models

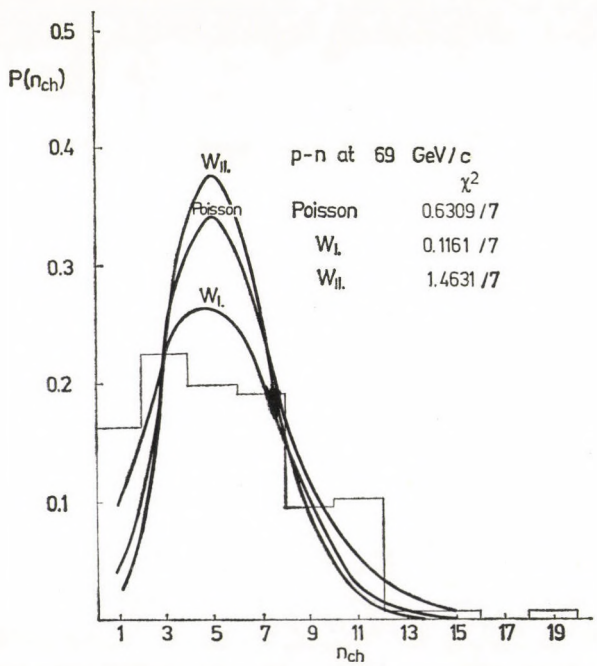

Fig. 4. Comparison of charged particle multiplicities in p-n reactions at 69 GeV/c with a Poisson distribution and with the WANG I and WANG II models

ments beside our results. The values of the χ^2 are calculated for seven points (six degrees of freedom) in each case.

The experimental results for energies below 25 GeV are fitted by a Poisson distribution to a better degree than the fitting obtained from the WANG's first and WANG's second models. As the incident energy increases, the deviation of the experimental points from the Poisson distribution increases. The χ^2-values shown in Table II indicate that WANG's first model agrees with the experimental data at energies higher than or equal to 25 GeV.

Table III

χ^2-values comparing the $\langle n_{ch} \rangle P n_{ch}$ graph for different reactions with respect to Slattery's fit

Reaction	χ^2/N for $\langle n_{ch} \rangle P n_{ch}$ with respect to the Slattery's fit	Reference
32 GeV/c K^+—p	18.5	21
32 GeV/c K^-—p	2.3	21
32 GeV/c p^-—0	0.7	21
50 GeV/C $^+$—p	10.0	21
50 GeV/c $^+$—p	8.0	21
69 GeV/c p~p	0.05	Present work

Relative to the inverse square fall off predictions, the χ^2-values show that the experimental results are inconsistent with this prediction in the whole energy range.

All the above results may reflect the cell structure of the nucleon in this energy range of interactions.

3.5 *Scaling property of multiplicity distribution*

A "scaling" behaviour of multiplicity distributions was predicted by Z. KOBA, H. B. NIELSON and P. OLESON (KNO) [10, 11].

A detailed comparison of p—p emulsion data [9, 12, 13, 14], at momenta from 19.8 up to our results at 69 GeV/c with this scaling behaviour is carried out here.

In Fig. 5, the experimental points of the multiplicity distribution for the emitted charged secondaries in this mentioned range of energy are presented on a

$$\langle n_{ch} \rangle \frac{\sigma n_{ch}}{\sigma_{inel}} \quad \text{vs} \quad \frac{n_{ch}}{\langle n_{ch} \rangle} \quad \text{graph.}$$

It is clear that they can indeed lie on one curve as expected by the KNO scaling predictions. The emulsion data for p—p interactions analyzed here give

some deviation from that universal curve fitting the H.B.Ch. data [15], which is drawn as a continuous curve in Fig. 5. This may be due to the higher values of $\langle n_{ch} \rangle$ in case of emulsion experiments as mentioned before.

It is interesting to compare the degree of consistency between the experimental results for different reactions and the calculated curve fitting the p — p data from 50 — 303 GeV/c, [15]. In Table III the values of χ^2 are given for this fit.

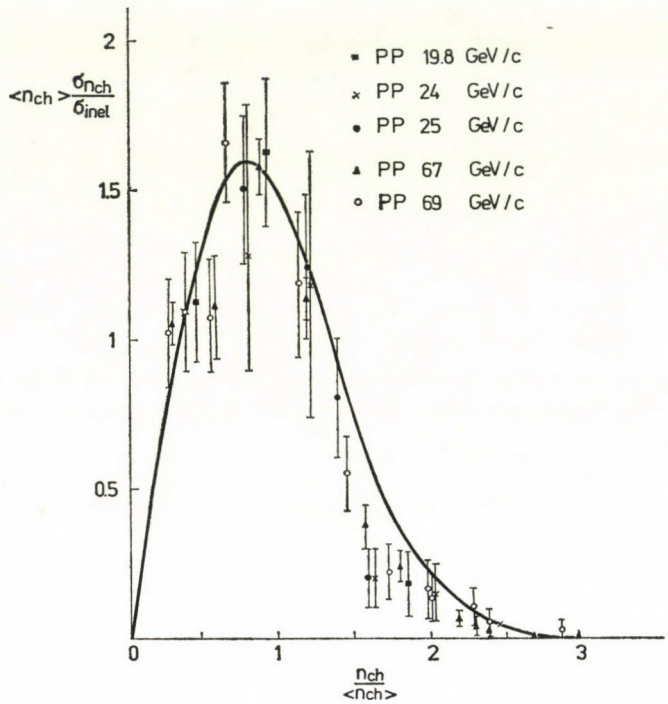

Fig. 5. Variation of $\langle n_{ch} \rangle \cdot \sigma_{nch}/\sigma_{inel.}$ vs $n_{ch}/\langle n_{ch} \rangle$. The curve represents the results of the fit of [15]

Table IV

Experimental values for the parameter C_q for the reaction pp → n charged particles at incident momenta from 19.8 up to 69.0 GeV/c and for q running from 2 through 5

q P_{lab} (GeV/c)	$C_q = \langle n_{ch}{}^q \rangle / \langle n_{ch} \rangle^q$				
	19.8	24	25	67	69
2	1.24±0.14	1.27±028.	1.25±0.12	1.25±0.07	1.29±0.11
3	1.83±0.27	1.88±0.59	1.82±0.23	1.83±0.14	2.02±0.23
4	3.13±0.59	3.14±1.29	2.99±0.48	3.05±0.30	3.55±0.54
5	5.99±1.39	5.75±2.94	5.36±1.08	5.64±1.02	7.04±1.30

In spite of the acceptable χ^2-values for $K^- - p$ and $p - p$ data, it is clear that the degree of consistency in our case of $p - p$ at 69 GeV/c is better. This may be attributed to the fitting curve being due to $p - p$ interactions, beside the low energy range of the data of the other stated reactions.

Table IV presents the experimental values of the parameter $C_q = \frac{\langle n_{ch}^q \rangle}{\langle n_{ch} \rangle^q}$ for $q = 2, 3, 4, 5$ (predicted to be energy-independent), for each value of beam momentum. Despite some indication of a slow increase with energy, the 19.8 – 69 GeV/c ratios are consistent with being constants, consequently in Table V, we present the weighted averages using just these used data, and, also

Table V

Average $C_q = \langle n_{ch}^q \rangle / \langle n_{ch} \rangle^q$ values for q running from 2 through 5. The χ^2-values compare these averages with the data of C_q shown in Table IV

q	C_q	χ^2
2	1.26	0.001
3	1.876	0.015
4	3.172	0.061
5	5.956	0.281

the χ^2-values between these data and the calculated constants. The deviation from constant may become higher for higher values of q.

Fig. 6 shows the value of $\frac{\langle n_{ch} \rangle}{D}$ as a function of the incident momentum for the data of $p - p$ interactions. It is clear that the experimental values of the

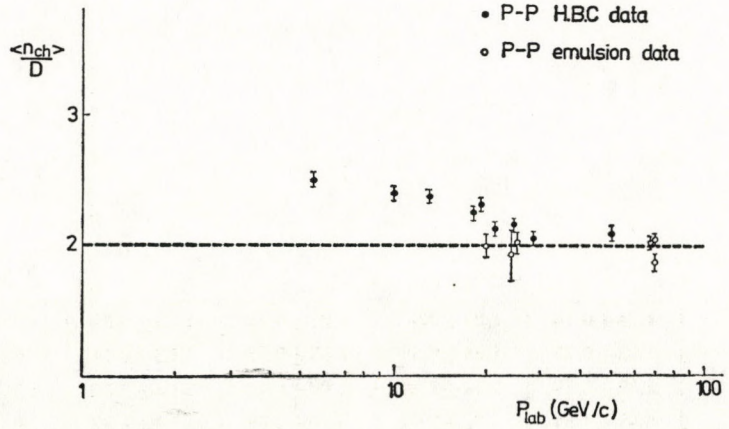

Fig. 6. $\langle n_{ch} \rangle / D$ ratio as a function of the incident momentum in p-p reactions

parameter $\frac{\langle n_{ch} \rangle}{D}$ approach its asymptotic value $\simeq 2$ as the momentum increases. This approach is from above as predicted by VAN HOVE [4, 16], using a two component model. The same behaviour was established in case of $\pi^+ - p$ and $K^+ - p$ interactions [4]. These results shed some light upon the fact that the general trend of the meson—proton reactions is similar to that of the proton—proton reactions.

3.6 *Multiplicity distribution and Czyzewski—Rybicki empirical relations*

CZYZEWSKI and RYBICKI [17] have proposed an empirical fit to multiplicity distributions which works well over the range from 4.0 to 60 GeV/c for $\pi^- - p$, from 4.0 to 18.0 GeV/c for $\pi^+ - p$ and from 4.0 to 28.5 GeV/c for $p - p$ reactions.

They proposed plotting $x = \frac{(n_{ch} - \langle n_{ch} \rangle)}{D}$ against $y = DP_n$ where P_n is the probability of n_{ch} charged particles being emitted (and $\Sigma P_n = 1$).

V. V. AMMOSOW et al [4] obtained a good fit for the experimental data of the multiplicity distribution of $K^- - p$ and $\pi^- - p$ reactions at 33.8 GeV/c and 50 GeV/c, respectively, to the CZYZEWSKI—RYBICKI empirical fit.

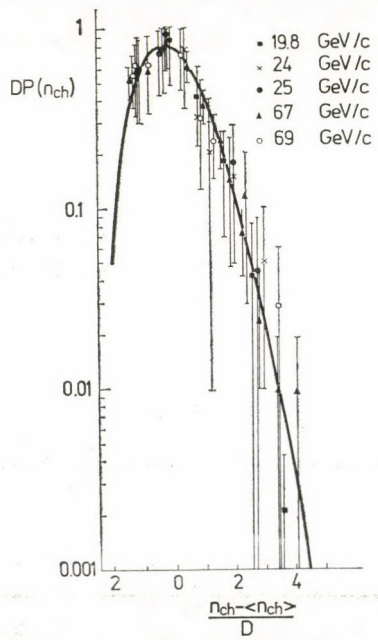

Fig. 7. Comparison of p-p data (19.8—69.0 GeV/c) with CZYZEWSKI and RYBIECKI formula [17]

The present emulsion data for p – p interactions at 19.8, 24, 67 and 69 GeV/c are plotted in Fig. 7, using the parameter of the x-y curve obtained by CZYZEWSKI and RYBICKI from fitting the earlier data. It may be seen that a good agreement is obtained.

3.7 *Pseudorapidity and angular distribution of the emitted charged secondaries*

Fig. 8 shows the distribution of the parameter η where

$$\eta = - \ln \tan (\Theta_L/2)$$

with Θ_L = the space angle with which the charged secondaries are emitted with respect to the direction of the incident beam in the laboratory

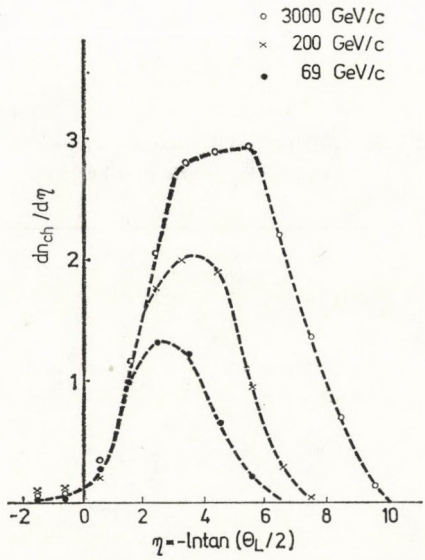

Fig. 8. Pseudo-rapidity $\eta(\eta = - \ln \tan \Theta_L/2)$ distribution of charged secondaries emitted in p-nucleon interactions at 69.0, 200 and 3000 GeV/c

system, for p—N collisions at 69 GeV/c, 200 GeV/c and at 3000 GeV/c. This parameter η is approximately proportional to the rapidity value in the laboratory system considering all the emitted secondaries as pions. From Fig. 8 it is clear that a scaling behaviour in the rapidity distribution for the secondaries emitted in p—N collisions occurs, especially for the slow pions in the target fragmentation region. This is in accordance with the limiting fragmentation hypothesis [18].

3.8 *Moments of the multiplicity distribution in a semiclassical composite mode for p—p collisions at high energies*

According to GOVORKOV [19], the scaling in the behaviour of the multiplicity moments is accounted for by the VAN HOVE overlap function being a Gaussian in impact parameter within a semiclassical composite model for p—p collisions at high energies. Within the framework of this model, the multiplicity distribution and its different moments of the emitted secondaries in p—p collisions were calculated on the basis of the following suppositions:

(1) The early onset of the VAN HOVE regime of the overlap function;
(2) The composite structure of protons and the independence of quark-proton collisions, and
(3) Narrow single particle distribution for each of these collisions compared with the overall multiplicity distribution.

Table VI

Calculated values $C_m^{\text{theor.}} = \langle N^m \rangle / \langle N \rangle^m$ (N = number of quark—proton collisions) for the quark number $\nu = 2, 3, 4$ and ∞, and experimental values $C_m^{\text{exp.}} = \langle n_{ch}^m \rangle / \langle n_{ch} \rangle^m$ (N cannot exceed a quark number ν)

m	$C_m^{\text{theor.}}$				$C_m^{\text{exp.}}$ $\langle n_{ch} \rangle = 5.02$—$6.93$
	$\nu = 2$	$\nu = 3$	$\nu = 4$	$\nu = \infty$	
2	1.117	1.191	1.240	1.50	1.26
3	1.40	1.71	1.92	3.45	1.89
4	1.94	2.82	3.57	11.24	2.99
5	2.89	5.17	7.47	47.40	5.60
6	4.48	10.12	16.98	244.0	10.78

In Table VI, the theoretical values of the different moments of the multiplicity distribution, C_m^{theor}, are compared with the experimental values $C_m^{\text{exp.}}$, for the data compiled here from 25 up to 69 GeV/c. It is clear that the best agreement is observed for the quark number "ν" equal to three. In this case single, double, and triple quark—proton collisions can occur, with the probabilities $p_1 = 0.723$, $p_2 = 0.218$ and $p_3 = 0.059$, respectively.

Adding to the above mentioned hypothesis the following two assumptions, about the particle production in each quark—proton collision.

1. The distribution of the secondaries produced in this collision is supposed to be independent of the impact parameter.

2. This distribution is a Poisson type one with the average particle number $\langle n_{ch} \rangle$ and making use of the charge-independence hypothesis to perform the

transition from the overall multiplicity distribution to the charged multiplicity distribution both the multiplicity distribution and its moments for the case of the quark number $\nu = 3$ and in both cases of $\langle n_{ch} \rangle = 6.41$ and 9.05 were calculated. The results are shown in Fig. 9, and Table VII, respectively. From Table VII, it is clear that the values of the relative moments for the charged particles multiplicity distribution obtained experimentally at 67 GeV/c and at 69 GeV/c (our work), are indeed close to the calculated values. However,

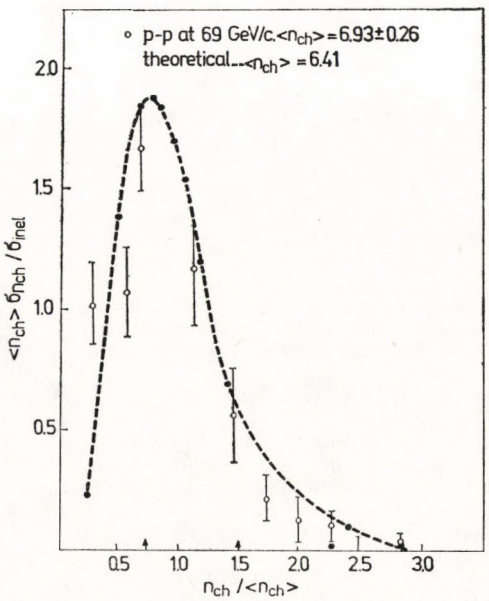

Fig. 9. KNO-plot: $\langle n_{ch} \rangle \sigma_{nch}/\sigma_{inel.}$ vs $n_{ch}/\langle n_{ch} \rangle$ for the p-p data. The continuous curves are calculated according to the composite proton model [19]. The arrows on the z-axis indicate the places where the maximum of individual distributions corresponding to a single, double, and triple quark—proton collision would be located.

Table VII

Values of $C_m^{\text{theor.}} = \langle n_{ch}^m \rangle / \langle n_{ch} \rangle^m$ calculated for the composite proton model with three quarks. In the last column the $C_m^{\text{exp.}}$ averaged over the results at 67 GeV/c and our results 69 GeV/c is given.

m	$\langle n_{ch} \rangle = 6.41$	$\langle n_{ch} \rangle = 8.05$	$\langle n_{ch} \rangle = 6.78$ 67 and 69 GeV/c
2	1.250	1.240	1.27
3	1.880	1.850	1.93
4	3.250	3.19	3.30
5	6.270	6.15	6.34
6	13.11	12.86	11.07

the KNO-plot presented in Fig. 9 shows a disagreement between the theoretical and experimental values in the range of the maximum. This may be due to the assumption that the secondary particle distribution in each quark—proton collision is a Poisson distribution as stated before. This could be broken down by the production of resonances or clusters [20].

Acknowledgement

We wish to express our deep thanks to Professor M. EL-NADI who has made this work possible by his own great efforts in establishing the experimental high energy physics laboratory at Cairo University. His continued support, scientific discussions and encouragement are greatly appreciated.

Thanks are also due to Professor K. D. TOLSTOV of the Joint Institute of Nuclear Research in Dubna (USSR) for his cooperation in supplying us with nuclear emulsion plates.

REFERENCES

1. K. D. TOLSTOV et al., Phys. Letters, **31B,** 237, 1970.
2. T. F. HOANG et al., Phys. Rev., **107,** 1968, 1957.
3. O. E. BADWAY et al., to be published in Nuclear Physics B.
4. France—Soviet Union and CERN—Soviet Union Collaborations, Nucl. Phys. **B58,** 77, 1974.
5. S. BRANDT, Phys. Letters, **32B,** 338, 1970.
6. C. P. WANG, Phys. Rev., **180,** 1463, 1969.
7. A. V. ABDURAKHIMOV et al., Dubna preprint P_1-6491, 1972.
8. P. G. BIZZETI et al., Nuovo Cimento, **27,** 6, 1963.
9. K. D. TOLSTOV et al., Phys. Letters, **39B,** 282, 1972.
10. Z. KOBA, Dubna preprint E2 No. 6918, 1973.
11. Z. KOBA, H. B. NIELSON and P. OLESEN, Nucl Phys., **B40,** 317, 1973.
12. M. MEYER et al., Nuovo Cimento, **28,** 1399, 1963.
13. A. MARZARI-CHIESA et al., Nuovo Cimento, **27,** 155, 1963.
14. E. G. BOSS et al., Soviet Physics J.E.T.P., **20,** 1371, 1965.
15. P. SLATTERY, Phys. Rev. **D7,** 2073, 1973.
16. L. VAN HOVE, CERN Preprint TH 1581, 1971.
17. O. CZYZEWSKI and K. RYBICKI, Nucl. Phys., **B47,** 633, 1972.
18. J. BENECHE et al., Phys. Rev., **188,** 2159, 1969.
19. A. B. GOVORKOV, Dubna preprint E2 — 7916, 1974.
20. D. HORN and A. S. SCHWIMMER, Nucl. Phys., **B52,** 627, 1973.
21. France—Soviet Union and CERN—Soviet Union Collaborations, Nucl. Phys., **B75,** 401, 1974.

Acta Physica Academiae Scientiarum Hungaricae, Tomus 43 (1), pp. 17—22 (1977)

MÖSSBAUER EFFECT STUDY OF CO-FERRITE FORMATION

By

NABIL A. EISSA,* ALAA EL-DIN A. BAHGAT and SALAH H. SALAH

MÖSSBAUER LABORATORY, FACULTY OF SCIENCE, AL-AZHAR UNIVERSITY, CAIRO, EGYPT

(Received in revised form 21. IV. 1977)

The activation energy (Q) for the formation of $CoFe_2O_4$ was calculated from a series of Mössbauer effect spectra measured during the formation process. This was calculated by applying the Jander's reaction kinetics equation to determine the reaction rate constant, on applying the Arrhenius equation. The obtained value of Q was found to be 56 K · cal/mol.

Introduction

Recently EISSA et al [1] studied the applicability of Mössbauer effect (ME) to follow the reaction kinetics. It was proved that ME is a powerful tool in the field of solid state reaction kinetics. Co-Ferrite ($CoFe_2O_4$) has the inverse spinel structure [1], where the tetrahedral A-sites are occupied by Fe^{3+} ions only, and the octahedral B-sites by Fe^{3+} and Co^{2+} ions with a distribution ratio of 1:1 [2]. In the present work the same method of analysis of EISSA et al [1] was applied to the $CoFe_2O_4$.

Experimental procedure

Iron oxide Fe_2O_3, having a particle size of about 370 Å as measured from the X-ray line broadening, was mixed with CoO in the stoichiometric ratio for the formation of the Co-Ferrite. The mixture was milled and many pellets were pressed at 3 tons/cm^2.

These pellets were then inserted in a preheated electric furnace at 900 up to 1200 °C. They were then heated for periods varying from 1 minute up to 120 minutes. The samples were then withdrawn and air-cooled to room temperature. X-ray diffraction measurements confirmed the formation of the ferrite after 60 minutes at 1200 °C.

Also, solid solutions having the composition (by weight)

$$(1-y)\,CoO + (1+y)\,Fe_2O_3 \rightarrow (1-y)\,CoFe_2O_4 + (2y)\,Fe_2O_3 \qquad (1)$$
$$0 \leqslant y \leqslant 1.0$$

* Present address: Physics Department, Faculty of Education, Doha, State of Qatar.

were prepared by the usual ceramic method. Previous work [5] suggests that the reaction proceeds by the following steps:

(i) Vapour phase transport of CoO to the surface of the Fe_2O_3;

(ii) Diffusion of cobalt and iron cations throughout the continuous oxygen lattice obtained by rearrangement of the oxygen ions. X-ray diffraction revealed two solid phases, as given in the right hand side of the above chemical formula. The following relation was obtained by substituting the atomic weights in formula (1):

$$X = (1 - y)/(1 + 0.36y)\,, \tag{2}$$

where x is the percent of ferrite in the final reacted mixture. Several ME absorbers which have different compositions and firing periods, were prepared to contain the same amount of iron. The ME spectra were measured at room temperature using a constant acceleration spectrometer connected to a 256 multichannel analyser. The source was 7 m Ci $^{57}Co(Cr)$.

Results and discussion

The measured spectra were analyzed by the same method applied by EISSA et al [1]. The room temperature ME spectra shown in Fig. 1 show a gradual increase in the absorption intensity corresponding to $CoFe_2O_4$. These peaks were compared after normalization with the spectra measured for the solid solutions (Fig. 2). The normalized areas of corresponding peaks give the percentage of the ferrite formed to the fully formed ferrite (x) (Fig. 3), which was confirmed by X-ray diffraction measurements. The resulting percentages were analyzed according to reduced-time plots [4], which leads to that applying Jander's equation is the suitable one to follow this kind of reaction that is [4, 5]

$$(1 - \sqrt[3]{1 - x})^2 = Kt\,, \tag{3}$$

where t is the firing period and K is the reaction rate constant, which depends on the material under study.

The above relation was applied and shows a good agreement at lower firing time intervals. Deviation at longer time intervals may be due to the change in the diffusion rate of the moving species, which is a slow homogenizing process in the almost completely reacted material.

The constant K is the slope of the $(1 - \sqrt[3]{1-x})^2$ vs t curves (Fig. 4). Values of K over a temperature range are used to find the activation energy Q from

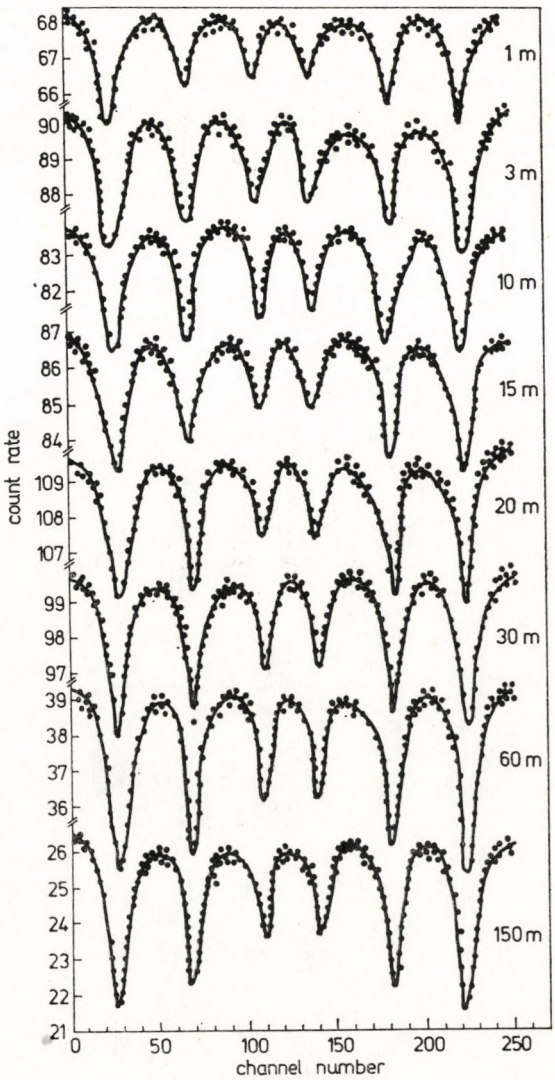

Fig. 1. Mössbauer effect spectra, measured at room temperature for the mixture $CoO-Fe_2O$ fired at 1200 ° C, for different periods. The letter (*m*) represent the period in minutes

the Arrhenius equation:

$$K = Z \exp(-Q/RT), \tag{4}$$

where Z is a constant, R is the gas constant, T is the firing temperature, and Q is the reaction activation energy (cal/mol). Fig. 5 represents a plot of the values of $\ln K$ vs $1/T$.

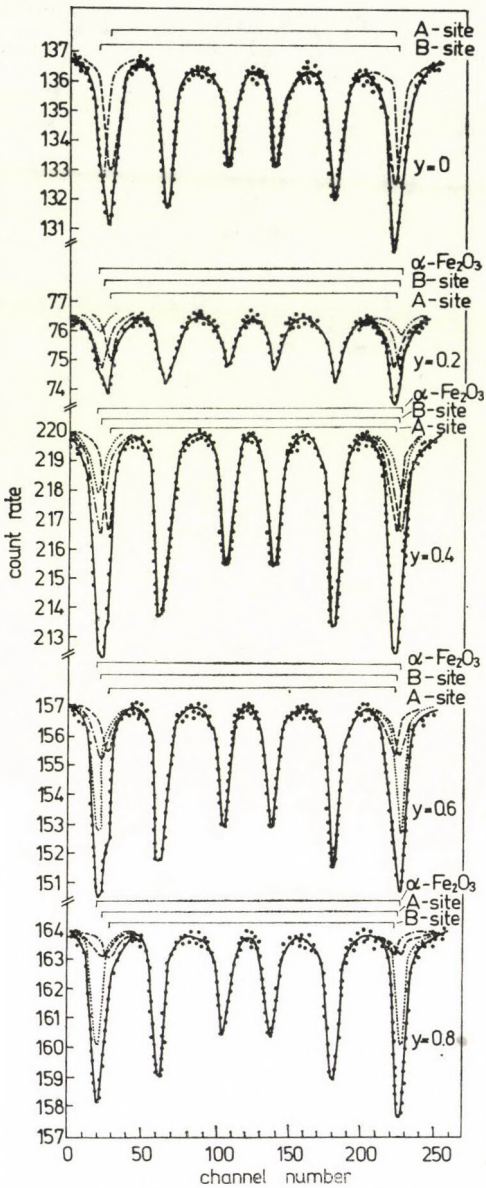

Fig. 2. Mössbauer effect spectra measured at room temperature for the solid solution (1-y) $CoFe_2O_4$: (2y)Fe_2O_3. The letters A and B represent the tetrahedral and octahedral sites, respectively

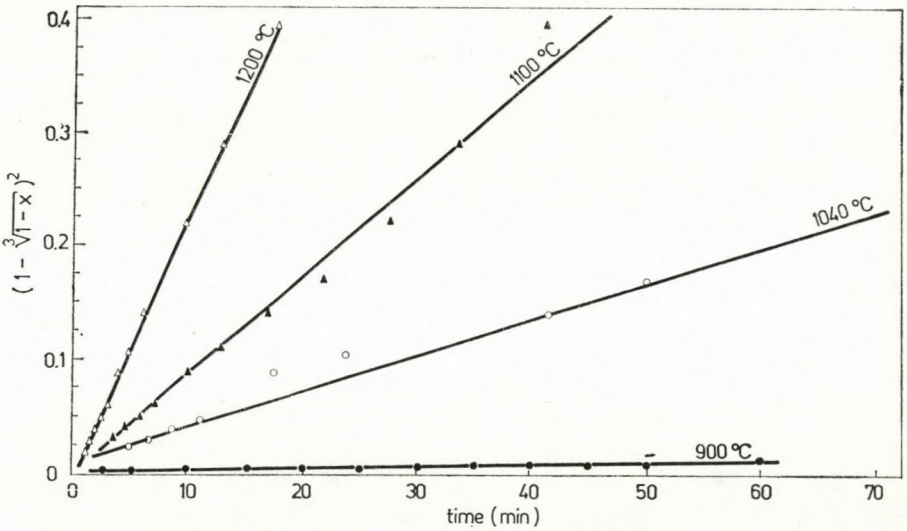

Fig. 3. Fraction of the reacted mixture (x) vs time (t) at various temperatures

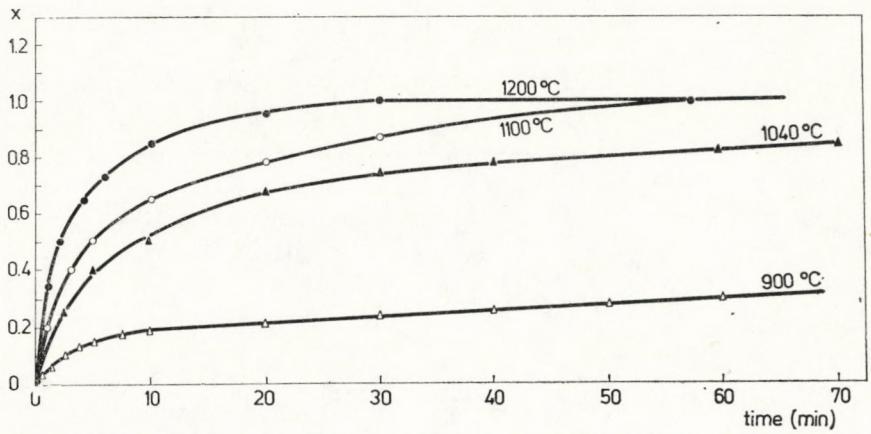

Fig. 4. Experimental results plotted according to Jander's equation

The slope of this curve determines the activation energy listed in Table I, with previous results of other ferrites for comparison.

The value of 56 Kcal/mol for Co-ferrite fits into the range of activation energy to produce other ferrites. The scattering of data can have various causes as chemical purity, physical form, method of preparation, particle size, and method of heating.

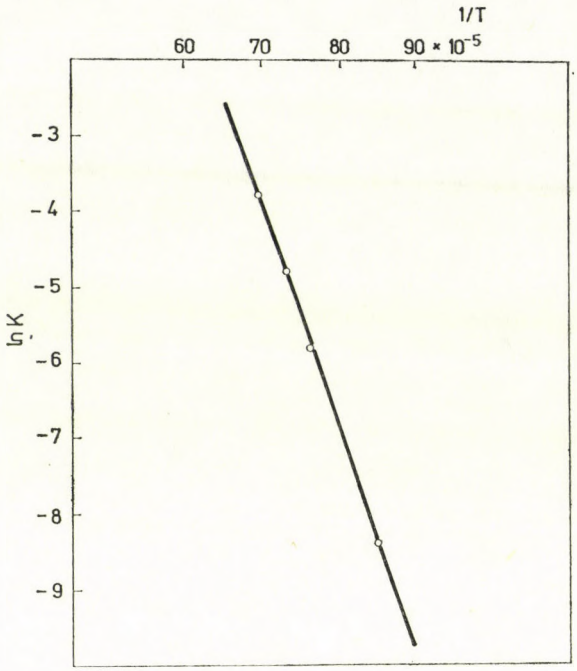

Fig. 5. Relation between ln K vs $1/T$

Table I

Activation energies of ferrites

Ferrite	Q KCal/mol	References
Co Fe_2O_4	56 ± 10*	present work
Ni Fe_2O_4	78+	[1]
	$54-70\pm3$	[5]
Zn Fe_2O_4	70 (3.02 eV)	[1]
Cd Fe_2O_4	67 (2.9 eV)**	[1]

* For pellet samples, depending on particle size of Fe(III).
** For powder samples.

REFERENCES

1. N. A. Eissa, A. A. Bahgat, A. H. Mohamed and S. A. Saleh, J. Amer. Cer. Soc., **59,** (7/8), 327, 1976.
2. P. J. Murray and J. W. Linnett, J. Phys. Chem. Solids, **37,** 619, 1976.
3. W. D. Kingery, H. K. Bowen and D. R. Uhlmann, "Introduction to Ceramics", 2nd ed., John Wiley and Sons, New York, 1976.
4. D. Dollimore, Chemistry Department, University of Salford, Lancashire, England; Private communication.
5. G. Economos and T. R. Clevenger, Jr., J. Amer. Cer. Soc., **43,** (1), 48, 1960.
6. J. F. Duncan and D. J. Stewart, Trans. Faraday Soc., **63,** (4), 1031, 1967.

Acta Physica Academiae Scientiarum Hungaricae, Tomus 43 (1), pp. 23—29 (1977)

EFFECTIVE TARGET MASS DISTRIBUTION IN RELATIVISTIC PROTON–NUCLEON INELASTIC INTERACTIONS

By

O. E. BADAWY and M. T. HUSSEIN

HIGH ENERGY PHYSICS EXPERIMENTAL LABORATORY
DEPARTMENT OF PHYSICS, FACULTY OF SCIENCE
UNIVERSITY OF CAIRO CAIRO, EGYPT

(Received 17. V. 1977)

The aim of the present work is the study of the effective target mass distribution in inelastic proton-nucleon collisions at 6 GeV/c and 69 GeV/c proton momentum. The angle, momentum and grain density are measured for each emitted secondary particle. It is proved that the average effective target mass in p-nucleon events decreases with the energy of the primary particle.

1. Introduction

Several investigations have confirmed that the nucleon consists of a dense core surrounded by a virtual meson cloud. A study of effective target M_T (the part of the target nucleon which actually participated in the interaction in which mesons are produced) reveals the existence of two types of interactions, the incident particle may interact with the central core of the nucleon or with the pion of the virtual meson cloud surrounding the core.

It is the purpose of this experiment to provide further information about the question of whether the effective mass will depend upon the energy of the primary particles.

The interactions of 6 GeV/c and 69 GeV/c incident proton beams are studied using nuclear emulsion technique.

2. Selection of central and peripheral interactions [1]

One can estimate the mass of the target particle purely from the conservation laws of energy and momentum. The target mass M_t is defined as

$$M_t = \sum_i (E_i - P_i \cos \theta_i) - (E_0 - P_0) , \qquad (1)$$

where E_i, P_i and Θ_i denote the total energy, momentum and angle of emission in the laboratory system with respect to the direction of the incident particle,

respectively, of the ith particle given out in the interaction, and E_0, P_0 represent the energy and momentum of the incident particles. For high incident energy $E_0 - P_0 \ll 1$,

$$M_t = \sum_i E_i - P_i \cos \theta_i \,. \tag{2}$$

In case of nucleon–nucleon collision, we have

$$M_n = \sum_i ((E_i - P_i) \cos \theta_i) + (E_p - P_p \cos \theta_p) \,. \tag{3}$$

M_n denotes the mass of the nucleon, subscript p denotes the recoil target nucleon and Σ denotes the summation over all secondary particles except the recoil nucleon. The effective target mass is defined as:

$$M_T = \sum_j (E_j - P_j \cos \theta_j) \,. \tag{4}$$

Thus M_T denotes the mass of the nucleon which actually participated in the production of secondaries, mainly pions.

The experimental difficulties in the direct determination of M_T are twofold. Firstly, the angles of emission and the momenta carried by neutral particles are unknown and secondly, not all the emitted charged shower particles are amenable to scattering and ionization measurements. In view of these difficulties we have followed an empirical method to determine M_T.

According to this method a quantity δ_j defined as:

$$\delta_j = \frac{1}{m_j} ((E_j - P_j) \cos \theta_j) \tag{5}$$

is computed for all the secondary shower tracks emitted from an interaction on the basis of emission angle θ_j in laboratory system. The summation of δ_j is connected with M_T by a constant conversion factor

$$K = M_T / \sum \delta_j \,. \tag{6}$$

In those cases where the scattering measurements of steepness of secondary tracks, but only the angles could be measured, the effective target mass M_t can be found by the following approximation method.

If the secondary particles have high energies, then

$$M_T \simeq \sum_i P_i (1 - \cos \theta_i) = P_t \sum_i \frac{1 - \cos \theta_i}{\sin \theta_i} \,, \tag{7}$$

where the sum is taken over all shower particles produced in nuclear interactions, and P_t is the average transverse momentum.

3. Experimental technique

Two stacks of nuclear emulsion type Бр-2 and each of size 20 cm × 10 cm × × 600 μ were used in the present work. The first one was irradiated by 6 GeV/c protons at the Dubna Synchrophasotron. The second one was exposed to the 69 GeV/c proton beam from the high energy accelerator at Serpukhov, USSR.

The scanning was carried out along the track by the following method in the central plates, starting 0.5 cm from the edge facing the incident beam. The momentum and grain density of the secondary particle were measured in the case of the 6.0 GeV/c irradiation.

The momentum is measured for each particle having small dip angle by means of Coulomb scattering using the coordinate method [2]. Each track is measured twice using cell lengths of 500 μ and 1000 μ. Noise and spurious scattering are eliminated by standard methods [3]. The average statistical errors in the values of PB were 15%, the maximum allowed error being 25%.

The grain density is measured in terms of g^* the ratio of the grain density of the track to be measured to that of the incident proton beam. A correction is made for the average depth of the track, since ionization loss differs from the depth of the emulsion. About 1000 blobs were counted for which the average blob density is determined for each track.

Identification of the particles is made using the coupled momentum-ionization measurement technique. The results of measurements of multiple scattering and blob density of the shower particles are plotted and compared with the theoretical curves [4] calculated for different particles (pion, keon and protons).

4. Results and discussion

About 151 and 300 proton—nucleon events are found in the 6 GeV/c and in the 69 GeV/c incident proton interactions, respectively.

For the 6 GeV/c proton interaction we were able to measure both the momentum and grain density of all the products of about 50 events and so for these events the effective target mass is calculated exactly by using Eq. (4). The average conversion factor K is 0.62. For the remaining events (100 events) where not all the products could be identified but only the angles are measured, the values of δ_j are determined using Fig. 1 which gives the relation between δ_j and $\sin \theta_j$. The effective target mass for these events is calculated by Eq. (6).

Fig. 2 shows the effective target mass distribution for the events produced at 6 GeV/c incident proton momentum. The distribution shows two peaks corresponding to M_π and M_n. The nucleon mass peak is twice larger. The average effective target mass is 0.85 M_n.

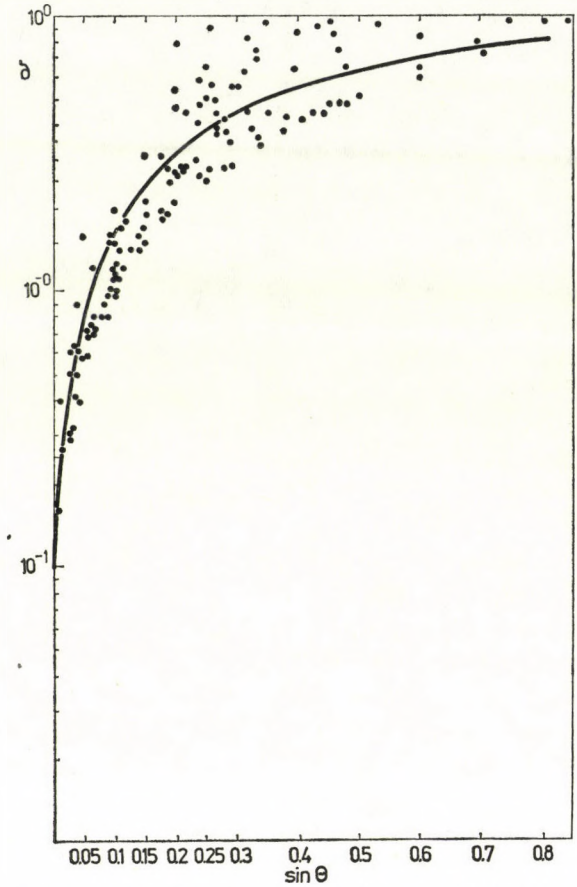

Fig. 1. $\delta_j = (E_j - P_j \cos \Theta_j)/M_j$. Plotted against laboratory emission angle Θ_j, solid curve (empirical relation) is the average fit for all types of particles. The dotted points are the experimental results for protons and pions.

Fig. 3 shows the effective target mass distribution for the 69 GeV/c incident proton interaction. The M_T values in this case are calculated according to Eq. (7) using the approximate angular method. This approximation is valid at this high energy where the average transverse momentum is constant $\langle P_t \rangle = 0.4$ GeV/c.

It is evident from the Figure that strong peak at M_π and a smaller one at M_n exist. As to the ambiguous peak between 2 and $3M_\pi$, it may be interpreted as being due to multiperipheral interactions. A mean value of $M_T \simeq \simeq 0.4\, M_n$ is obtained at this energy. Table I shows the variation of $\langle M_T \rangle$ with the energy of the incident particle.

The events are classified according to their effective target mass into p-cloud events (those having $M_T \leq M_n$) and the proton-core events (having $M_\pi < M_T \leq M_n$).

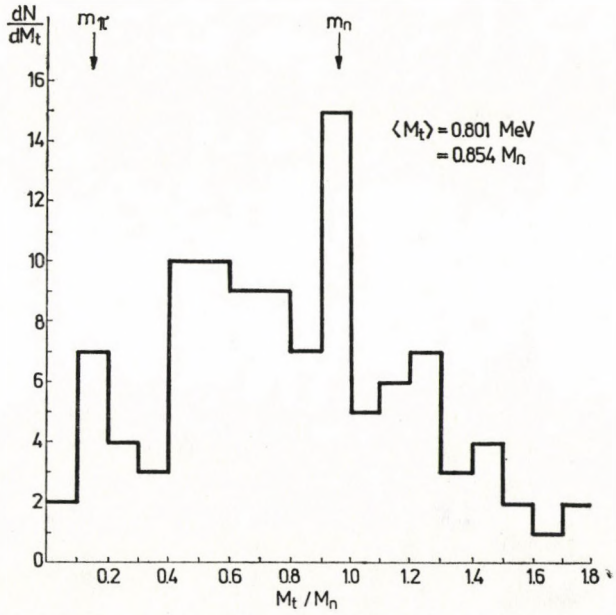

Fig. 2. The effective target mass distribution in $P-_n$ interactions at 6.0 GeV/c incident proton momentum

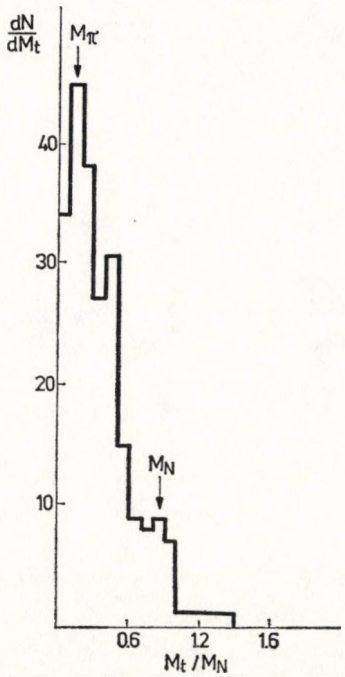

Fig. 3. The effective target mass distribution in $P-_n$ interactions at 69 GeV/c incident proton momentum

Table I

Energy	Type of incident particle	$\langle M_T \rangle$	Ref.
6 GeV	Proton	0.85 M_n	Present work
16 GeV	Pion	0.73 M_n	[5]
26.7 GeV	Proton	0.7 M_n	[6]
28 GeV	Proton	0.72 M_n	[5]
69 GeV	Proton	0.4 M_n	Present work
1000 GeV	Cosmic rays	0.3 M_n	[7], [8]

The average charged particle multiplicity and the average emission angle for the outgoing particles in each class of events are calculated.

For 6 GeV/c incident proton momentum we have

$$\langle n_{ch} \rangle_{\text{p-cloud}} = 1.941$$
$$\langle n_{ch} \rangle_{\text{p-core}} = 2.95$$
$$\langle \theta \rangle_{\text{p-cloud}} = 10.33^\circ$$
$$\langle \theta \rangle_{\text{p-core}} = 25.15^\circ$$

For 69 GeV/c incident proton interactions we have

$$\langle n_{ch} \rangle_{\text{p-cloud}} = 5.42$$
$$\langle n_{ch} \rangle_{\text{p-core}} = 8.47$$
$$\langle \theta \rangle_{\text{p-cloud}} = 5.3^\circ$$
$$\langle \theta \rangle_{\text{p-core}} = 10.4^\circ$$

The decrease in the average charged particle multiplicity in the p-cloud events is due to the lower values of the average energy available in the C.M. system for these events.

At both energies, the secondary particles emitted in proton—cloud events are confined in a much smaller cone than those from proton—core interactions. Also it is clear that the outgoing showers are collimated in a smaller cone as the momentum increases (from 6 GeV/c up to 69 GeV/c in both the peripheral and central collisions).

Acknowledgements

We wish to express our deep thanks to Professor M. EL-NADI, who has made this work possible by his own great efforts in establishing the experimental high energy physics laboratory at Cairo University.

Our thanks are due to Professor K. D. TOLSTOV, Joint Institute of Nuclear Research, Dubna, for supplying us with nuclear emulsion plates.

Our thanks are also due to our Colleagues, especially to M. M. SHERIF, in the emulsion group of Cairo University for their help.

REFERENCES

1. J. M. KOHLI, Nucl. Phys., **B4**, 620, 1968.
2. CERN European Organization for Nuclear Research, Cern 63—3.
3. WALTER H. BARKAS, Nuclear Research Emulsion, p. 263, Academic Press, New York and London, 1963.
4. B. BHOWMIK and R. K. SHIVPURI, Phys. Rev., **160**, 1227, 1967.
   O. E. BADAWY and M. T. HUSSEIN, Accepted for publication in Annalen der Physik.
5. P. Y. WANG and P. L. JAIN, Il Nuovo Cimento, A**61**, 567, 1969.
6. Y. K. LIM, Nuovo Cimento, **26**, 1221, 1962.
7. P. L. JAIN, Nuovo Cimento, **31**, 764, 1964.
8. N. A. DOBROTIN and S. A. SLAVATINSKY, Procedings of the 1960 Annual International Conference on High Energy Physics of Rochester, p. 819.
   N. A. DOBROTIN, V. V. GUSEVA, K. A. KOTEINIKOV, A. M. LEBEDEV, S. V. RYABIKOV, A. A. SLAVATINSKY and N. G. ZELEVINSKAYA, Nucl. Phys., **35**, 152, 1962.

Acta Physica Academiae Scientiarum Hungaricae, Tomus 43 (1), pp. 31—44 (1977)

PENETRATION THROUGH AND REFLECTION ON TWO THIN POTENTIAL BARRIERS

By

L. JÁNOSSY, P. KIRÁLY and A. WERNER

CENTRAL RESEARCH INSTITUTE FOR PHYSICS, BUDAPEST

(Received 19. V. 1977)

The quantum mechanical problem of a wave packet falling on two thin potential barriers of equal strength and arbitrary separation is discussed. The solution is given in the individual regions as weighted integrals over a free-particle solution, the weight functions depending on a single essential parameter (separation times strength) only. A discussion is given of the physical interpretation of the results.

Introduction

§ 1. The escape of a particle from a small region of space surrounded by a potential barrier is often discussed in quantum mechanics, in particular in the theory of α decay. The wave function can be assumed to be known and confined to this "cavity" at $t = 0$ and the Schrödinger equation can then be solved for the future development. In such an approach one is usually dissuaded from asking about the past development of the state. If one is not so easily discouraged and follows the development back in time according to the Schrödinger equation, usually very unlikely and peculiar states are obtained in the distant past. Thus this description of the whole process including both the formation of the decaying state and the subsequent decay is not even qualitatively correct, although some quantitative features of the decay obtained from such calculations might agree well with experiments.

In the present paper a very strongly simplified model will be discussed, which does not give the quantitative details of any actual experiment, but gives a good *qualitative* description of the formation of a trapped part of the wave function and its subsequent decay. The model is in one dimension. The region of space in which the wave function can be trapped is thus represented by an interval. The two potential barriers "surrounding" that interval are assumed to be infinitely thin, i.e. the potential in each of the two end-points is proportional to a Dirac delta function (the constant of proportionality is the same for both ends of the interval). A wave packet arriving for example from the left (see Fig. 1) is then partly reflected from the first barrier and moves back with essentially the original velocity towards the left. The other part of the packet penetrates into the region in between the barriers, then it is

partly reflected from the second barrier, the reflected part is again partly reflected from the first barrier, etc. If the barriers always reflect the major part of the wave function falling on them, then a trapped state evolves in between the barriers and it later decays away slowly and can thus be considered as a model for a decaying system.

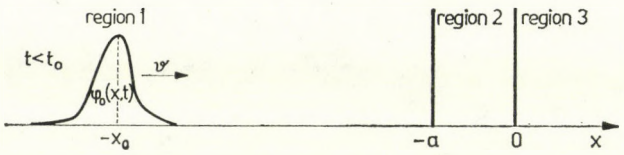

Fig. 1. The incoming packet and the two potential barriers

The phenomena connected with the passage of particles through potential barriers are relatively simple both mathematically and physically. The numerical solution for a wave-packet initial condition is fairly straightforward (for some examples see [1]). The analytical treatment in terms of energy-eigenfunctions is also easy in principle, but the solutions are given in terms of integrals which have to be evaluated numerically.

It is important that the method of solution should emphasize the *qualitative features* of the process. Such an approach was applied by one of the present authors (L. J.) to the case of the passage through one thin potential barrier [2]. Although the present problem is more difficult and the physical character of the solutions is more complex, the method used successfully in [2] is also useful in our case.

The Schrödinger equation is to be solved for a wave packet arriving from the left into the region of the potential barriers. The solution is given by free-particle solutions inside the three regions separated by the two barriers. At the barriers themselves the potential is infinitely high, but this singularity can be shown to be equivalent to a simple boundary condition connecting the free-particle solutions in adjacent regions. The three free-particle solutions connected by the two boundary conditions can then be generated from a single auxiliary function, which in turn can be shown to satisfy the free-particle Schrödinger equation for all x and t. The solution for the auxiliary function would be easily obtained if the initial condition for that function was known.

This initial condition — and also the auxiliary function for arbitrary times — can be expressed in terms of the free development of the arriving wave packet, that is in terms of the free-particle solution of the Schrödinger equation with an initial condition corresponding to the incoming packet.

The solution will turn out to be analogous to the multiple reflections of light on a set of two parallel semi-transparent mirrors, with the individual

terms in a sum corresponding to reflections of given order. The analogy is even closer if the optical model is refined to include dispersive effects and a frequency dependent reflectivity.

The exponential nature of the decay can be shown in some special cases, but in general the situation is more complex. It appears plausible that the decay is complicated by the strict phase-relations among successive reflections, and one must not expect a smooth behaviour for a precisely defined incoming packet. If, however, the subsequent incoming packets show some statistical fluctuations, then a statistical averaging should be done and the averaged decay is expected to show a smooth behaviour.

Wave equation and boundary conditions

§ 2. The one dimensional Schrödinger wave equation

$$i\dot{\Psi}(x,t) = -\frac{1}{2}\Psi''(x,t) + V(x)\Psi(x,t) \tag{1}$$

is to be solved for the potential

$$V(x) = \gamma\big(\delta(x+a) + \delta(x)\big), \quad \text{where} \quad \gamma \geq 0\,, \tag{2}$$

and for initial conditions corresponding to a wave packet arriving from the left (Fig. 1). Throughout the paper atomic units ($\hbar = m = 1$) and the denotations

$$\dot{\psi} = \frac{\partial\psi}{\partial t} \quad \text{and} \quad \psi' = \frac{\partial\psi}{\partial x}$$

will be used.

The problem can be re-formulated in terms of free-particle solutions obeying certain boundary conditions. The solution of (1) should satisfy the free-particle equation

$$i\dot{\psi} = -\frac{1}{2}\psi'' \tag{3}$$

except in the points $x = -a$ and $x = 0$ where the barriers are. These free-particle solutions are different in the three regions and they are connected by simple boundary conditions obtained by integrating (1) in small vicinities of the barriers:

$$\Psi(x+0,t) = \Psi(x-0,t) \qquad \text{for} \quad x = 0, -a, \tag{4}$$

$$\Psi'(x+0,t) - \Psi'(x-0,t) = 2\gamma\Psi(x,t) \quad \text{for} \quad x = 0, -a\,. \tag{5}$$

Thus the wave function is continuous but has a break at each barrier.

Now it will be shown that the three properly connected free-particle solutions and thus also the solution of (1) can be expressed in terms of a single free-particle solution. To do so Ψ is first written in a form which will turn out to be convenient for initial conditions as shown in Fig. 1:

$$\Psi(x,t) = \begin{cases} \psi_1(x,t) - \psi_2(x,t) - \psi_3(x,t) & \text{for} \quad x < -a, \\ \psi_1(x,t) - \psi_2(x,t) & \text{for} \quad -a < x < 0, \\ \psi_1(x,t) & \text{for} \quad x > 0, \end{cases} \tag{6}$$

where ψ_i $(i = 1,2,3)$ are free-particle solutions. The boundary conditions (4), (5) are satisfied if

$$\psi_2(0,t) = \psi_3(-a,t) = 0, \tag{7a}$$

$$\psi_2'(0,t) = 2\gamma\psi_1(0,t)\,, \tag{7b}$$

$$\psi_3'(-a,t) = 2\gamma[\psi_1(-a,t) - \psi_2(-a,t)]\,. \tag{7c}$$

These conditions are of course not enough for determining the three functions $\psi_i (i = 1,2,3)$, therefore further conditions should be imposed. First, (7a) is automatically fulfilled if ψ_2 and ψ_3 are taken to be antisymmetric with respect to the points 0 and $-a$, respectively:

$$\psi_2(x,t) = \gamma[u(x,t) - u(-x,t)], \tag{8a}$$

$$\psi_3(x,t) = \gamma[v(x+a,t) - v(-(x+a),t)], \tag{8b}$$

where u and v are also solutions of (3). Second, (8a) and the choice of ψ_1 as

$$\psi_1(x,t) = u'(x,t) \tag{9}$$

satisfy (7b) identically. Third, as can be seen from (8a), (8b) and (9), the condition (7c) is also satisfied if

$$v'\big((x+a),t\big) = u'(x,t) - \gamma[u(x,t) - u(-x,t)]\,. \tag{10}$$

Now we introduce a single free-particle solution $U(x,t)$ in terms of which u and v are expressed as

$$u(x,t) = U'(x,t)\,, \tag{11}$$

$$v\big((x+a),t\big) = U'(x,t) - \gamma[U(x,t) + U(-x,t)]\,, \tag{12}$$

in accordance with (10). By using equations (6) and (8)—(12) the solutions of

1) can then be given as

$$\begin{aligned}\Psi(x,t) = U''(x,t) + \Delta(x)\,\gamma\{U'(x,t) - U'(-x,t)\} + \\ + \Delta(x+a)\,\gamma\{U'(x,t) - U'(-(x+2a),t) - \\ - \gamma[U(x,t) + U(-x,t) - U(-(x+2a),t) - U((x+2a),t)]\}\,,\end{aligned} \tag{13}$$

where

$$\Delta(x) = \begin{cases} -1 & \text{for} \quad x < 0, \\ 0 & \text{for} \quad x > 0. \end{cases}$$

Thus for any given free-particle solution U it is easy to calculate a particular solution of (1). The solutions $\Psi(x, t)$ obtained from simple solutions for $U(x, t)$ (e.g. from simple wave packets) are, however, very artificial and thus of little physical interest. In order to have meaningful solutions, one should be able to calculate $U(x, 0)$ for given initial conditions $\Psi(x, 0)$, and then according to (13) obtain $\Psi(x, t)$ in terms of the free-particle solution. This problem will be discussed in the next Section.

Initial conditions

§ 3. The initial condition for Ψ cannot be chosen arbitrarily, since the boundary conditions (4), (5) have to be satisfied at any time. Supposing that the initial condition

$$\Psi(x, 0) = \psi_0(x) \tag{14}$$

satisfies these restrictions, (13) can be considered as a complicated differential-difference equation for $U(x, 0)$. Instead of solving this general equation, we restrict the treatment to initial conditions corresponding to wave packets approaching from the left. We suppose that at $t = t_0$ the wave packet is so for to the left that its values at and beyond the barriers are negligibly small (see Fig. 1). One further advantage of such an assumption is that it can be taken to hold for *any* time before the packet reaches the vicinity of the barriers, thus there is no need to single out a particular "initial" time. Instead of an initial state we can speak then about a time-dependent "incoming packet" and instead of (14) we can write

$$\Psi(x, t) = \psi_0(x, t) \quad \text{for} \quad t < t_0\,. \tag{15}$$

As can be seen from (13), $\Psi(x, t)$ will vanish at $x > -a$ for $t < t_0$ if it is assumed that

$$U(x, t) = 0 \quad \text{for} \quad x > -a, t < t_0\,. \tag{16}$$

For $t < t_0$ the incoming packet is then obtained from (13) as

$$\psi_0(x, t) = U''(x, t) - 2\gamma U'(x, t) + \gamma^2 U(x, t) - \gamma^2 U(x + 2a, t) \ . \qquad (17)$$

Both sides of (17) represent free-particle solutions for $t < t_0$. Since the right hand side continues to satisfy (3) for $t > t_0$, (17) holds for all times if $\psi_0(x, t)$ is the free development of the incoming packet.

Equation (17) leads to an interesting decomposition of $\psi_0(x, t)$ into three parts. Writing (17) as

$$\psi_0(x, t) = U''(x, t) - \gamma \{U'(x, t)\} - \gamma \{U'(x, t) - \gamma [U(x, t) - U(x + 2a, t)]\} \qquad (18)$$

it can be directly compared with $\Psi(x, t)$ as given in (13). Before the incoming packet reaches the barriers, both expressions (13) and (18) vanish for positive values of x and are identical for negative values. After the barriers have been reached, (13) and (18) behave differently. The three parts of (13) can, however, be obtained with the help of the parts of (18) in the following manner. The wave corresponding to the first part of (13) continues to propagate freely just as the first part of the free solution (18) does. The wave described by the second part crosses the first barrier unattenuated but is totally reflected from the second barrier, while the third part is totally reflected from the first barrier and thus it is not affected by the second barrier. Thus the solution in the presence of the barriers is easily obtained once the decomposition (18) is known.

It should be stressed that the three parts of (13) do not satisfy the bounds ary conditions at the barriers, only their sum does so. Thus the three part- of (18) do not represent some kind of "basic solutions" of (1) and (2) and are not determined by the potentials alone as is the case for eigenfunctions, but depend in an essential way on the incoming packet $\psi_0(x, t)$.

In what follows it will be assumed that the free-particle solution $\psi_0(x, t)$ is known for all values of x and t; one might take it e.g. to be a Gaussian packet or a superposition of such packets. If one knew the decomposition given in (18), $\Psi(x, t)$ could be easily obtained by the above simple procedure. In order to have the decomposition, however, $U(x, t)$ should be expressed in terms of $\psi_0(x, t)$, that is equation (17) should be solved for $U(x, t)$.

The solution for U(x, t)

§ 4. It will be convenient to write the differential-difference equation (17) in the form

$$U''(x, t) - 2\gamma\ U'(x, t) + \gamma^2\ U(x, t) = \psi_0(x, t) + \gamma^2\ U(x + 2a, t). \qquad (19)$$

The derivation of the solution will not be given in detail, only the important steps will be indicated. First, one should note that if the inconvenient term $U(x + 2a, t)$ is not there, then (19) is a well-known inhomogeneous linear differential equation of mathematical physics, the solutions of which are given in many handbooks (see e.g. [3]). Second, for $t < t_0$ $U(x, t)$ was assumed to vanish in a good approximation for $x > -a$. Similarly one might suppose that for an arbitrary time t there is a coordinate value $X(t)$ beyond which $U(x, t)$ practically vanishes. Then in the interval $X(t) - 2a < x < X(t)$ one has $U(x + 2a, t) = 0$ and (19) can be solved. In the next interval to the left, $X(t) - 4a < x < X(t) - 2a$, $U(x + 2a, t)$ is known from the previous solution and thus (19) is again a similar differential equation, but with a modified right-hand side. Continuing this step-by-step procedure, always making sure that the solutions in neighbouring regions match smoothly, one obtains

$$U(x, t) = \sum_{n=0}^{\infty} \int_x^{\infty} \frac{\gamma^{2n}}{(2n + 1)!} (x' - x)^{2n+1} e^{-\gamma(x'-x)} \psi_0(x' + 2an, t) \, dx' . \quad (20)$$

As can be directly verified, this expression satisfies Eq. (19), (16) and (3).

The above solution can also be written as

$$U(x, t) = \frac{1}{\gamma^2} \sum_{n=0}^{\infty} \int_x^{\infty} \Gamma_{2n+1}(x' - x; \gamma) \psi_0(x' + 2an, t) \, dx' , \quad (21)$$

where

$$\Gamma_{2n+1}(x' - x; \gamma) = \frac{\gamma^{2(n+1)}}{(2n + 1)!} (x' - x)^{2n+1} e^{-\gamma(x'-x)}, \quad n = 0, 1, 2, \ldots$$

are the normalized density functions of the gamma-distribution familiar from probability theory (see e.g. [4]). The gamma-densities are concentrated in fairly small vicinities of their maxima (with the parameters used here, $(x' - x)_{\max}$ and the standard deviations are given by $\frac{2n + 1}{\gamma}$ and $\frac{\sqrt{2n + 1}}{\gamma}$, respectively).

It should be noted that in practical cases the summation in (21) can be taken to extend to a finite number of n values only. Since both ψ_0 and Γ_{2n+1} are small outside a certain neighbourhood of their maxima, the overlap integrals of $\psi_0(x' + 2an, t)$ and $\Gamma_{2n+1}(x' - x; \gamma)$ are vanishingly small in most cases. It is particularly instructive to consider the case when the major contribution to $U(x, t)$ is given by a single integral. This occurs for moderate x and t values if a, the separation between the two barriers is much larger than both the width of the incoming packet and γ^{-1}. Let us fix the value of x (to be specific, we take it to be somewhat beyond the barriers). The development in time of $U(x, t)$ is then described as follows.

Before the free packet ψ_0 would reach x, all the integrals in (21) vanish and thus $U(x, t) = 0$. Then $\psi_0(x, t)$ starts to overlap with $\Gamma_1(x' - x; \gamma)$ but all the rest of the integrals vanish because the free packet would reach $x + 2an$ $(n = 1,2, \ldots)$ only much later. Before the second integral appears, ψ_0 gets beyond $\Gamma_1(x' - x; \gamma)$ and thus the first integral practically vanishes. Then the overlap and with it $| U(x, t) |$ starts to increase again and then decreases to very small values before the third integral appears, and this strongly fluctuating character continues until either the width of $\psi_0(x, t)$ or that of $\Gamma_{2n+1}(x' - x; \gamma)$ becomes comparable with $2a$. From that time on an increasing number of integrals contribute and $| U(x, t) |$ is getting smoother.

One is tempted to interpret U in terms of distortions and multiple reflections of the incoming packet. The distortions are represented by gamma-densities while the multiple reflections themselves are given by the shift by $2an$ in the argument of ψ_0. The same interpretation also applies to the case when the separation of the barriers is small, but then several reflected and distorted versions of the initial packet are superimposed at any place and time and thus it is more difficult to disentangle the picture.

The above interpretation of $U(x\ t)$ is physically meaningful for $x > 0$ only, where $\Psi = U''$, that is where there is a simple relationship between Ψ and U. For $x < 0$ U cannot be interpreted in terms of reflections from the barriers, instead it should be thought of as a mere auxiliary function generating the useful decompositions of ψ_0 and Ψ as given in (18) and (13), respectively.

Before going over to the solution for $\Psi(x, t)$, another useful expression will be derived for $U(x, t)$. By substituting $s = \gamma(x' - x) + 2a\gamma n$, (20) can be written as

$$U(x, t) = \int_0^\infty g_\sigma(s; a\gamma) \frac{1}{\gamma^2} \psi_0\left(x + \frac{s}{\gamma}, t\right) \mathrm{d}s\,, \tag{22}$$

where

$$g_\sigma(s; a\gamma) = \begin{cases} \sum_{n=0}^{\left[\frac{s}{2a\gamma}\right]} \dfrac{(s - 2na\gamma)^{2n+1}}{(2n+1)!} \mathrm{e}^{-(s-2na\gamma)} & \text{for } s > 0 \\ 0 & \text{for } s < 0\,. \end{cases} \tag{23}$$

The upper limit of summation is the integral part of $s/2a\gamma$ as indicated by the square brackets. The subscript σ indicates that the terms to be summed are the gamma-densities with odd indices $\Gamma_{2n+1}(s - 2na\gamma; 1)$.

The main advantage of the representation (22) is that it gives U as a simple weighted integral over ψ_0. The weight function depends only on the parameters of the barriers, that is on the boundary conditions, and is independent of the initial conditions. A further interesting property of $g_\sigma(s; a\gamma)$ is that

it depends on the separation a and strength γ of the barriers through the combination $a\gamma$ only, thus it is easy to tabulate. It should also be stressed that the summation in (23) extends to a finite number of terms only, although the number of terms changes with s.

The solution $\Psi(x, t)$

§ 5. The solution for the Schrödinger equation (1) with potential (2) and initial condition (15) is now obtained by substituting (22) into (13). The derivatives of ψ_0 can then be eliminated by partial integration; the resulting expression then contains the weight function $g_\sigma(s; a\gamma)$ and its first and second derivatives into s. The result can be further simplified by introducing another weight function $g_e(s; a\gamma)$ defined in a similar way to $g_\sigma(s; a\gamma)$, but containing gamma-densities with even indices instead of odd ones:

$$g_e(s; a\gamma) = \begin{cases} \sum_{n=0}^{\left[\frac{s}{2a\gamma}\right]} \frac{(s - 2an\gamma)^{2n}}{(2n)!} e^{-(s-2na\gamma)} & \text{for } s > 0 \\ 0 & \text{for } s < 0 . \end{cases} \tag{24}$$

The solution is then obtained in the following form:

$$\Psi(x, t) =$$

$$= \begin{cases} \psi_0(x,t) - \int_0^\infty g_e''(s; a\gamma)\, \psi_0\left(-x - 2a + \frac{s}{\gamma}, t\right) ds & \text{for } x < -a , \quad (25a) \\ \psi_0(x,t) + \int_0^\infty g_e'(s; a\gamma)\, \psi_0\left(x + \frac{s}{\gamma}, t\right) ds - & \\ \quad - \int_0^\infty g_\sigma'(s; a\gamma)\, \psi_0\left(-x + \frac{s}{\gamma}, t\right) ds & \text{for } -a < x < 0 , \quad (25b) \\ \psi_0(x,t) + \int_0^\infty g_\sigma''(s; a\gamma)\, \psi_0\left(x + \frac{s}{\gamma}, t\right) ds & \text{for } x > 0 , \quad (25c) \end{cases}$$

where the primes denote differentiation into s. At $s = 0$ the derivatives are defined by continuity from the right.

Thus the modifying effect of the barriers is represented by weighted integrals of the free-particle solution, the weight functions being different before, in between and after the barriers. The quantitative description of the solution requires numerical integration. Some qualitative features, however, can be revealed by an analysis of the general behaviour of the weight functions and of the free-particle solutions.

Discussion

§ 6. Let us consider the behaviour of the weight functions first. As can be seen from (24) and (23), g_e and g_σ vanish for $s < 0$ and are also very simple for $0 < s < 2a\gamma$, where

$$g_e(s; a\gamma) = e^{-s} \quad \text{and} \quad g_0(s; a\gamma) = se^{-s} . \tag{26}$$

As s increases, more and more gamma-densities appear and the resulting functions are generally rather complicated. There are, however, two particular cases when the behaviour of g_e and g_σ (and also of their derivatives) is fairly simple. First, for $a\gamma \to 0$ the summation in (23) and (24) can be easily carried out and one obtains

$$g_e(s; 0) = \frac{1 + e^{-2s}}{2} \quad \text{and} \quad g_\sigma(s; 0) = \frac{1 - e^{-2s}}{2} . \tag{27}$$

This limit corresponds to a single potential barrier of finite strength. Second, for $a\gamma \gg 1$ the subsequent gamma-densities are shifted relative to each other so much that they do not overlap for moderate values of s, that is g_e and g_σ start as trains of widely separated "bumps". For large enough values of s, however, the gamma-densities begin to overlap and smooth out the functions. It can be shown that in the asymptotic region both g_e and g_σ are well represented by the sum of a constant and of a sinusoidal term, the amplitude of the latter decreasing exponentially. Since the weight functions in (25a—c) are derivatives of g_e and g_σ they contain the damped oscillation type term only.

The behaviour of the weight functions is shown in Fig. 2 for $a\gamma = 0.5$, 1 and 3. The three curves coincide for very small values of s in accordance with (26). The new terms in (23) and (24), and thus also in the four weight functions, appear at $s = 2a\gamma n$, and the transition becomes smoother and smoother as n increases. If $a\gamma$ is of the order of unity or less, then the curves show a very strongly damped oscillation about zero. In the special case of $a\gamma = 0$ there are no oscillations at all, as can be seen from (27).

Now we return to the interpretation of (25a—c) which gives the solution for any time t and place x. The lower limit of integration in the integrals expressing the modifying effect of the barriers is $s = 0$, corresponding to different values x' of the argument of ψ_0 in different regions. For $x < -a$ we have $x' = -x-2a$, that is the integration starts from the mirror image of x relative to the first barrier. For $-a < x < 0$ there are two integrals, one starting from $x' = x$ and the other from $x' = -x$, that is from the mirror image of x relative to the second barrier. Finally, for $x > 0$ the integration starts from $x' = x$. The integration extends in each case to such parts of ψ_0 that have al-

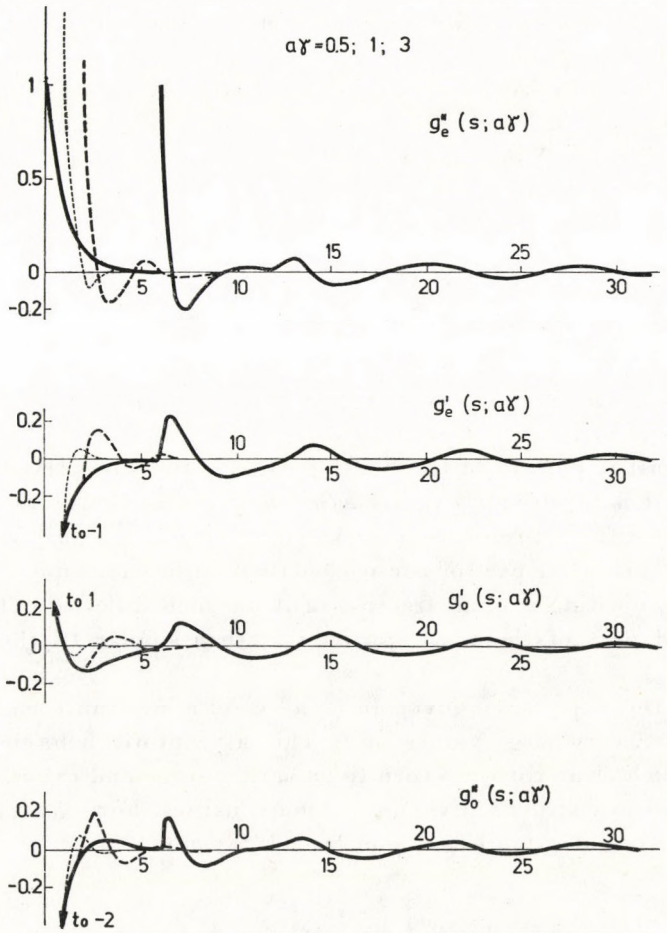

Fig. 2. The weight functions (for discussion see text)

ready passed through x as the wave packet moved to the right, that is the values of the free-particles solution $\psi_0(\xi, t)$ with $\xi < x$ have no influence on $\Psi(x, t)$.

The argument of ψ_0 in the integrals can be given in the above notation as $\xi = x' + s/\gamma$. Thus ψ_0 as a function of the integration variable s is obtained by shifting $\psi_0(\xi)$ by $-x'$ and then stretching it by a factor γ. The values of the integrals depend then separately on a and γ, whereas the weight functions depend on the product $a\gamma$ alone. It is sometimes convenient to eliminate the derivatives of g_e and g_σ by integrating by parts and also to return to the representation of g_e and g_σ in terms of gamma-densities as given in (23) and (24).

The behaviour of $\Psi(x, t)$ will now be described for some interesting limiting cases. First consider the behaviour of the solution when the separation a of the barriers is arbitrary but their strength γ tends to zero. By introducing the new variable of integration $\xi = x' + s/\gamma$ a factor γ appears before the in-

tegrals and since the integrals are finite, for $\gamma \to 0$ one has $\Psi(x, t) \to \psi_0(x, t)$ for any time as expected.

As a second limiting case we assume that γ is arbitrarily fixed but a, the separation of the barriers tends to zero. The weight functions are then obtained from (27). Using the variable of integration $\xi = x' + s/\gamma$ again we obtain

$$\Psi(x, t) = \begin{cases} \psi_0(x\, t) - 2\gamma\, e^{-2\gamma x} \int_{-x}^{\infty} e^{-2\gamma\xi} \psi_0(\xi, t)\, \mathrm{d}\xi & \text{if} \quad x < 0, \\ \psi_0(x, t) - 2\gamma\, e^{2\gamma x} \int_{x}^{\infty} e^{-2\gamma\xi} \psi_0(\xi, t)\, \mathrm{d}\xi & \text{if} \quad x > 0. \end{cases}$$

The expressions given above describe the passage of a wave packet through a single potential barrier of strength 2γ.

The most important of the limiting cases is when a is fixed and γ tends to infinity. It is intuitively expected that for very large values of γ most of the packet is reflected from the first barrier and only a small fraction passes through it. This latter part of the packet then suffers multiple reflections on the barriers, ejecting a small fraction of it on each reflection. The decay of this trapped part of the wave packet is rather similar to the radioactive decay.

From the expressions given in (25a—c) it is not quite easy to see the behaviour for very large values of γ. This asymptotic behaviour becomes, however, much clearer if we return to an earlier stage and express the weight functions as sums of derivatives of gamma-densities. For example, for $x > 0$ one obtains the following expression from (25c) and (23):

$$\Psi(x, t) = \psi_0(x, t) + \int_0^{\infty} \sum_{n=0}^{\left[\frac{s}{2a\gamma}\right]} \Gamma''_{2n+1}(s - 2na\gamma;\, 1)\ \psi_0\left(x + \frac{s}{\gamma}, t\right) \mathrm{d}s\,. \quad (28)$$

By interchanging the order of summation and integration and then integrating twice by parts one obtains

$$\Psi(x, t) = \frac{1}{\gamma^2} \sum_{n=0}^{\left[\frac{s}{2a\gamma}\right]} \int_0^{\infty} \Gamma_{2n+1}(s - 2n\, a\gamma;\, 1)\, \psi_0''\left(x + \frac{s}{\gamma}, t\right) \mathrm{d}s\,, \quad (29)$$

that is $\Psi(x, t)$ is of the order of γ^{-2} beyond the barriers. The term $\psi_0(x, t)$ describing the free propagation has been cancelled by $-\psi_0(x, t)$ obtained from the first term of the sum in (28). Similarly, it is easy to see that Ψ is of the order of γ^{-1} in between the barriers, that is much larger than for $x > 0$, and $\psi_0(x, t)$ is again cancelled. The situation is different for the region $x < -a$

from where the packet arrives. In that region both $\psi_0(x, t)$ and the directly reflected packet $\psi_0(-x - 2a, t)$ contribute along with the multiply reflected waves of order γ^{-2}. However, the incoming and directly reflected packets give appreciable contributions near the first barrier for a short time interval only, after which the slow leakage from between the barriers dominates for a very long time. This is not strictly true for all conceivable packets, but it is a good qualitative description for packets propagating fast and diffusing slowly.

The decay of that part of ψ_0 which is trapped in between the barriers has in general a rather complicated nature. The complication arises because of the strict phase relations among the many superimposed multiply reflected images of ψ_0. It is therefore worthwhile to give some attention to a special case which is free of this difficulty.

Suppose that the width of the incoming wave packet is much smaller than a, the separation between the barriers, but much larger than γ^{-1}, the reciprocal of the barrier strength. We shall describe the behaviour of $\Psi(x, t)$ in the vicinity of the barriers. Suppose that the time elapsed since the arrival of the wave packet to the barriers is not too large, so that the free wave packet is in the region where the separation of the gamma-densities in (29) is much larger than their width, thus the solution $\Psi(x, t)$ is nearly zero in a given point x for most of the time and is appreciable only when $\psi_0(x, t)$ overlaps with one of the gamma-densities, say with Γ_{2n+1}. Supposing that $x > 0$, the following integral should be evaluated:

$$\Psi_n(x, t) = \frac{1}{\gamma^2} \int_0^\infty \Gamma_{2n+1}(s - 2n\, a\gamma;\, 1)\, \psi_0'' \left(x + \frac{s}{\gamma}, t \right) \mathrm{d}s \,.$$

If the gamma-density is much narrower than $\psi_0''(x + s/\gamma, t)$, then ψ_0 can be written as a quickly oscillating term multiplied by a smooth function that changes little in the region where Γ_{2n+1} is appreciable. Treating this latter term as a constant and approximating Γ_{2n+1} by a Gaussian, the integration can be carried out. Then one can go over to the density $\varrho_n = \Psi_n^* \Psi_n$ and the following result is obtained:

$$\varrho_n(x, t) = \varrho_{0n}\big(2n(a + \gamma^{-1}) - v(t - t_x)\big)\; e^{-\frac{v}{a}\left(\frac{v}{\gamma}\right)^2 (t - t_x)}, \tag{30}$$

where t_x denotes the time at which the free packet would reach x, v is the translational velocity of ψ_0 and ϱ_{0n} is the term obtained from the smooth part of ψ_0. The function ϱ_{0n} has a sharp maximum when its argument is about zero.

The behaviour of $\varrho(x, t) = \Psi^*(x, t)\, \Psi(x, t)$ in a point to the right of the barriers can then be described in the following way. Before the freely propagating packet would reach x, the density is practically zero. Then a train of

bumps passes through x, the successive bumps containing exponentially decreasing amounts of the density. The bumps also spread out and finally lose their individuality and then more complicated interference phenomena set in. The characteristic time of the decay is the product of a/v, that is the time needed for the wave packet to cross the distance between the barriers, and of $(\gamma/v)^2$, the squared ratio of the strength of barriers to v, the velocity of the packet.

The behaviour of ϱ for $x < -a$ and for $-a < x < 0$ can be similarly calculated. For $x < -a$ the behaviour is the same as for $x > 0$, apart from the presence there of a directly reflected packet which, however, goes away fast. In between the barriers a huge bump is found going to and fro and decaying exponentially. The smaller bumps in the regions outside the barriers can be thought of as those parts of that bump that have leaked through the barriers at successive reflections.

The interference phenomena start to be important when the width of the central bump becomes comparable with the distance of the barriers. In practical experiments, however, the initial conditions are never exactly reproducible and therefore a statistical approach taking account of the distribution of the initial conditions is more appropriate. It appears likely that in such an approach the interference phenomena average out and a smooth decay is obtained.

REFERENCES

1. L. I. SCHIFF, Quantum Mechanics (third edition) p. 100. McGraw-Hill Book Co.
2. L. JÁNOSSY, Acta Phys. Hung., **2**, 171, 1952.
3. E. KAMKE, Differentialgleichungen, Lösungsmethoden und Lösungen 4. Aufl. S. 412, Leipzig, 1951.
4. L. JÁNOSSY, Theory and Practice of the Evaluation of Measurements, p. 172, Oxford, Clarendon Press, 1965.

Acta Physica Academiae Scientiarum Hungaricae, Tomus 43 (1), pp. 45—57 (1977)

ARTIFICIAL MECHANISM OF HEAT CONDUCTION FOR THE DISCUSSION OF MAGNETOGASDYNAMIC SHOCKS

By

B. G. VERMA and R. C. SRIVASTAVA

DEPARTMENT OF MATHEMATICS, UNIVERSITY OF GORAKHPUR
GORAKHPUR 273001, INDIA

(Received 26. V. 1977)

The artificial mechanism of heat conduction introduced by SACHDEV and PRASAD into ordinary gasdynamics has been extended to the case of magnetogasdynamics. This requires an additional field equation, alters the momentum and energy equations and at the same time needs satisfaction of the conditions adopted by SACHDEV and PRASAD. Although the stability conditions of the difference and differential equations are slightly disturbed, they remain almost the same. We observe that in place of ordinary medium if we take magnetised medium into consideration, the same order of artificial heat conduction can smear out the shock discontinuity easily but on account of the magnetic field, the shock region is divided into two subregions.

1. Introduction

VON NEUMANN and RICHTMYER [1] developed a method of artificial viscosity in the shock layer to smear out the shock. Following his method, LAX [2], BRODE [3], COLGATE and JOHNSON [4] and CHRISTY [5] solved various shock problems. In particular, BRODE carried out extensive computations for the blast wave problem. On account of the complexities arising in the problems taking artificial viscosity, SACHDEV and PRASAD [6] introduced a new technique of artificial heat conduction to spread out the shock in ordinary gasdynamics. The choice of this artificial heat conduction was made to satisfy the following conditions:

(i) The altered equations with the heat conduction term must possess a continuous solution.
(ii) The thickness of shock layers must be everywhere of the same order as the interval length Δx in the numerical computation and must be independent of the shock strength.
(iii) The effect of terms containing artificial heat conduction must be small outside the shock region.
(iv) The Rankine—Hugoniot conditions must hold.

In the present work, it has been shown that when gasdynamic equations are coupled with magnetic terms, all the four conditions enumerated above as well as the stability conditions for difference and differential equations are

almost satisfied also for this case. The artificial heat conduction is assumed to be effective only in the shock region and we have attempted to investigate whether the same phenomenon of spreading out of the shock occurs. We conclude that the shock region divides itself into two sub-regions on the transition layer of which the perturbation in specific volume is constant. It has also been shown that by using the artificial heat conduction method the shock discontinuity is more easily smoothened in the magnetogasdynamic case than in ordinary gasdynamics.

2. The governing equations

The one-dimensional Lagrangian equations governing the motion of an ideal, compressible fluid with artificial heat conduction, subjected to a transverse magnetic field are given by

$$V = \frac{1}{\varrho_0}\frac{\partial X}{\partial x}\,, \tag{2.1}$$

$$U(x,t) = \frac{\partial X}{\partial t}\,, \tag{2.2}$$

$$\varrho_0 \frac{\partial U}{\partial t} = -\frac{\partial p}{\partial x} - H\frac{\partial H}{\partial x}\,, \tag{2.3}$$

$$\frac{\partial H}{\partial t} + \frac{H^2}{K\varrho_0}\frac{\partial U}{\partial x} = 0\,, \tag{2.4}$$

$$\frac{\partial E}{\partial t} + \left(p + \frac{H^2}{2}\right)\frac{\partial V}{\partial t} + \frac{\partial R}{\partial t} = 0\,. \tag{2.5}$$

In these equations, x is the Lagrangian coordinate, X is the Eulerian coordinate, t is the time, V is specific volume, U is particle velocity, ϱ_0 is density at $t = 0$, p is the pressure, H is the magnetic field, E is the internal energy per unit mass given by $E = pV/\gamma - 1$, $HV = K, \gamma$ being the ratio of specific heats and K is a constant. The term $-\partial R/\partial t$ in the Eq. (2.5) represents the rate at which heat is being added to the unit mass of fluid where R is given by

$$R = \frac{1}{2}(\varrho_0 C\Delta x)^2 \frac{\partial V}{\partial t}\left\{\left|\frac{\partial V}{\partial t}\right| - \frac{\partial V}{\partial t}\right\}, \tag{2.6}$$

C being a dimensionless constant. As a consequence of (2.1) and (2.2), the above expression for R can be written as

$$R = \frac{1}{2}(C\Delta x)^2 \frac{\partial U}{\partial x}\left\{\left|\frac{\partial U}{\partial x}\right| - \frac{\partial U}{\partial x}\right\}. \tag{2.7}$$

We now prove that (2.6) satisfies the conditions enumerated in Section 1. First of all, R is large in the shock region where the derivative $\partial V/\partial t$ is large but small outside where $\partial V/\partial t$ is much smaller. Also, R is zero for expansion waves when $\partial V/\partial t > 0$. For real shocks $\partial V/\partial t < 0$ and then,

$$R = -(\varrho_0 C\Delta x)^2 \left(\frac{\partial V}{\partial t}\right)^2 . \tag{2.8}$$

In the following Section, we show that the above form of R also satisfies the conditions (i), (ii) and (iii) of Section 1 for steady-state magnetogasdynamic shocks.

3. Steady state plane shocks

Let a magnetogasdynamic shock of constant strength move with a constant Lagrangian velocity S. Then all the flow parameters will be functions of Lagrangian distance w (from the shock) given by $w = x - St$.

We now introduce a quantity $M(= \varrho_0 S)$ which is the rate of flow of mass per unit area across the shock, in the Eq. (2.1)—(2.5) to obtain

$$\frac{MK}{H} + U = C_1 , \tag{3.1}$$

$$MV + U = C_2 , \tag{3.2}$$

$$p + \frac{H^2}{2} + M^2 V = C_3 , \tag{3.3}$$

$$E + \left(p + \frac{H^2}{2}\right) V + \frac{M^2 V^2}{2} + R = C_4 , \tag{3.4}$$

where C_1, C_2, C_3, C_4 are constants. Also, in terms of M the expression (2.8) becomes

$$R = -(M C\Delta x)^2 \left(\frac{\mathrm{d}V}{\mathrm{d}w}\right)^2 . \tag{3.5}$$

Applying the boundary conditions

$$w \to \infty,\ V \to V_i,\ p \to p_i,\ H \to H_i,\ E \to E_i,\ R \to 0 ,$$
$$w \to -\infty,\ V \to V_f,\ p \to p_f,\ H \to H_f,\ E \to E_f,\ R \to 0 ,$$

where the suffixes i and f refer to the initial and final values of the quantities involved, to obtain the constants, substituting for R from (3.5) and putting

$pV/\gamma - 1$ for E, in Eq. (3.4), we get,

$$\left(\frac{\mathrm{d}V}{\mathrm{d}w}\right)^2 = \frac{\gamma+1}{2(\gamma-1)(C\Delta x)^2}(V_i - V)(V - V_f) + \frac{(\gamma+1)K^2}{2(\gamma-1)(C\,\Delta x\,M)^2} \cdot \left\{\left(\frac{1}{V_i} + \frac{1}{V_f}\right) - \frac{V}{K}\left(\frac{V_f}{V_i} + \frac{K}{\gamma+1}\right)\right\}. \tag{3.6}$$

In what follows, we discuss separately the significance of the two terms on the right hand side of Eq. (3.6).

Case I. The non-magnetic case

When the second term on the R.H.S. of Eq. (3.6) is zero, we proceed to obtain [6]

$$V = \frac{V_i + V_f}{2} + \frac{V_i - V_f}{2}\sin\left(\frac{w}{w_0}\right), \tag{3.7}$$

where

$$w_0 = \left[\frac{2(\gamma-1)}{\gamma+1}\right]^{\frac{1}{2}}(C\,\Delta x)\,.$$

Also, the width of the shock is

$$\pi\, w_0 = \pi\left[\frac{2(\gamma-1)}{\gamma+1}\right]^{\frac{1}{2}}(C\,\Delta x)\,, \tag{3.8}$$

which shows that it is independent of the shock strength and the initial state of the medium into which the shock propagates and is of the order of the interval Δx of computation. This satisfies the condition (ii) of Section 1.

The pressure p in the shock region is given by

$$\frac{p}{p_i} = \frac{2\gamma}{\gamma+1}\left[\frac{V_f}{V_i} - \frac{\gamma-1}{\gamma+1}\right]^{-1}\left[\frac{1}{2\gamma}\left(1 + \frac{V_f}{V_i}\right) - \frac{1}{2}\left(1 - \frac{V_f}{V_i}\right)\sin\left(\frac{w}{w_0}\right)\right]. \tag{3.9}$$

Case II. The magnetic case

When the first term on the R.H.S. of Eq. (3.6) is neglected to study explicitly the effect of the magnetic field, we have

$$\left(\frac{\mathrm{d}V}{\mathrm{d}w}\right)^2 = \frac{(\gamma+1)K^2}{2(\gamma-1)(MC\,\Delta x)^2}\left[\left(\frac{1}{V_i} + \frac{1}{V_f}\right) - \frac{V}{K}\left(\frac{V_f}{V_i} + \frac{K}{\gamma+1}\right)\right]. \tag{3.10}$$

We assume,

$$\Psi = \frac{V}{K}\left(\frac{V_f}{V_i} + \frac{K}{\gamma+1}\right)\left[\frac{1}{V_i} + \frac{1}{V_f}\right]^{-1}$$

so that Eq. (3.10) takes the form

$$\left(\frac{\mathrm{d}\Psi}{\mathrm{d}w}\right) = \left[\frac{\dfrac{V_f}{V_i} + \dfrac{K}{\gamma+1}}{\dfrac{1}{V_i} + \dfrac{1}{V_f}} \cdot \frac{\gamma+1}{2(\gamma-1)\,(C\Delta x\, M)^2}\right]^{\frac{1}{2}} (1-\Psi)^{1/2} \qquad (3.11)$$

which on integration and thereafter being written in terms of V becomes

$$V = \frac{K\left(\dfrac{1}{V_i} + \dfrac{1}{V_f}\right)}{\left(\dfrac{V_f}{V_i} + \dfrac{K}{\gamma+1}\right)} - \frac{K}{8} L\, w^2\,, \qquad (3.12)$$

where

$$L = \frac{(\gamma+1)}{(\gamma-1)\,(C\Delta x\, M)^2}\left(\frac{V_f}{V_i} + \frac{K}{\gamma+1}\right).$$

The pressure p in this case in the shock region is given by

$$p = \left\{\frac{\gamma+1}{\gamma} - \frac{2K}{V_i V_f\left(\dfrac{V_f}{V_i} + \dfrac{K}{\gamma+1}\right)}\right\}\left(\frac{V_i + V_f}{2}\right) M^2 - \frac{K^2}{2V2} \times \qquad (3.13)$$

$$\times \left(1 + \frac{V^2}{V_i V_f} \cdot \frac{\gamma+1}{\gamma}\right) + \frac{K}{8}\left(\frac{\gamma+1}{\gamma-1}\right)\left(\frac{w}{C\Delta x}\right)^2\left(\frac{V_f}{V_i} + \frac{K}{\gamma+1}\right)$$

or

$$\frac{p}{p^1} = \left\{\left(\frac{\gamma+1}{\gamma} - \frac{2K}{V_i V_f\left(\dfrac{V_f}{V_i} + \dfrac{K}{\gamma+1}\right)}\right)\left(\frac{V_i + V_f}{2}\right) M^2 - \frac{K^2}{2V^2} \times \right. \qquad (3.14)$$

$$\left. \times \left(1 + \frac{V^2}{V_i V_f} \cdot \frac{\gamma+1}{\gamma}\right) + \frac{K}{8}\left(\frac{\gamma+1}{\gamma-1}\right)\left(\frac{w}{C\Delta x}\right)^2\left(\frac{V_f}{V_i} + \frac{K}{\gamma+1}\right)\right\} \times$$

$$\times \left(\frac{2\gamma}{\gamma+1}\right)\left\{M^2 V_i\left(\frac{V_f}{V_i} - \frac{\gamma-1}{\gamma+1}\right) - \frac{K^2}{V^2}\left(1 + \frac{V^2}{V_i V_f} \cdot \frac{\gamma+1}{\gamma}\right)\right\}^{-1}.$$

4. Stability of differential equations

Substituting $E = pV/\gamma - 1$, the energy equation (2.5) can be written as

$$V\frac{\partial p}{\partial t} + \gamma p\frac{\partial V}{\partial t} + (\gamma - 1)\frac{H^2}{2}\frac{\partial V}{\partial t} + (\gamma - 1)\frac{\partial R}{\partial t} = 0 \,. \tag{4.1}$$

Now, we perturb the differential equations in order to study their stability. If δU, δp, δV and δH be the perturbations in U, p, V and H, the equations for the perturbations from (2.1)—(2.4) and (4.1) are

$$\varrho_0\frac{\partial}{\partial t}(\delta U) = -\frac{\partial}{\partial x}(\delta p) - \frac{\partial}{\partial x}(H\delta H)\,, \tag{4.2}$$

$$\frac{\partial}{\partial t}(\delta H) + \frac{H^2}{K\varrho_0}\frac{\partial}{\partial x}(\delta U) + \frac{2H}{K\varrho_0}(\delta H)\frac{\partial U}{\partial x} = 0 \,, \tag{4.3}$$

$$\varrho_0\frac{\partial}{\partial t}(\delta V) = \frac{\partial}{\partial x}(\delta U)\,, \tag{4.4}$$

$$\begin{aligned}\frac{\partial p}{\partial t}(\delta V) + V\frac{\partial}{\partial t}(\delta p) + \gamma p\frac{\partial}{\partial t}(\delta V) + \gamma\frac{\partial V}{\partial t}(\delta p) + \\ + (\gamma - 1)\frac{H^2}{2}\frac{\partial}{\partial t}(\delta V) + (\gamma - 1)H\delta H\frac{\partial V}{\partial t} + (\gamma - 1)\frac{\partial}{\partial t}(\delta R) = 0 \,.\end{aligned} \tag{4.5}$$

Let us assume these perturbations to be of the form

$$\begin{aligned}\delta U &= \delta U_0\, e^{i\beta x + \alpha t}, \qquad \delta V = \delta V_0\, e^{i\beta x + \alpha t}\,, \\ \delta p &= \delta p_0\, e^{i\beta x + \alpha t}, \qquad \delta H = \delta H_0\, e^{i\beta x + \alpha t}\,,\end{aligned} \tag{4.6}$$

where δU_0, δp_0, δV_0 and δH_0 are constants, β is a real constant and α is another constant, real or complex. The perturbation equations from the equations of flow then become

$$\varrho_0\,\alpha(\delta U)_0 + i\beta(\delta p_0 + H\delta H_0) + (\delta H_0)\frac{\partial H}{\partial x} = 0 \,, \tag{4.7}$$

$$\left(\alpha + \frac{2H}{K\varrho_0}\frac{\partial U}{\partial x}\right)(\delta H_0) + \frac{H^2}{K\varrho_0}i\beta(\delta H)_0 = 0 \,, \tag{4.8}$$

$$i\beta(\delta U_0) - \varrho_0\alpha(\delta V_0) = 0 \,. \tag{4.9}$$

Also,

$$\delta R = (C\Delta x)^2\left\{\left|\frac{\partial U}{\partial x}\right| - \frac{\partial U}{\partial x}\right\}\frac{\partial}{\partial x}(\delta U)\,, \tag{4.10}$$

it being assumed that the perturbation in R is not so large as to alter the sign of $\partial U/\partial x$. Since the width of the shock is very small, we consider the perturbations of very small wave length, that is, large β. From each of the Eqs. (4.7), (4.8) or (4.9) it follows that $|\alpha|$ should also be very large. Thus we consider perturbations that rapidly change in x and t and under such conditions, the coefficients of δV, δU_0, δp and δH can be regarded as constants for small time and space intervals.

Eliminating δp_0, δV_0 and δH_0 between (4.7), (4.8) and (4.9) we have,

$$\begin{aligned}
&\varrho_0^3 VK\alpha^4 + \varrho_0^2\alpha^3\left\{\gamma p_0 K\frac{\partial V}{\partial t} + 2HV\frac{\partial U}{\partial x} + (\gamma-1)\beta^2(C\Delta x)^2 K\left(\left|\frac{\partial U}{\partial x}\right| - \frac{\partial U}{\partial x}\right)\right\} \\
&+ \varrho_0\alpha^2\left\{\gamma p\beta^2 K + 2H\gamma\varrho_0\frac{\partial V}{\partial t}\cdot\frac{\partial U}{\partial x} + VH^2\beta^2 + i\beta H^2 V\frac{\partial H}{\partial x} + \right. \\
&\left. + \frac{\gamma-1}{2}H^2\beta^2 K + (\gamma-1)\beta^2(C\Delta x)^2 2H\frac{\partial U}{\partial x}\left(\left|\frac{\partial U}{\partial x}\right| - \frac{\partial U}{\partial x}\right)\right\} + \\
&+ \varrho_0\alpha\left\{\frac{2\gamma p}{\varrho_0}\beta^2 H\frac{\partial U}{\partial x} + \beta^2 H^3\frac{\partial V}{\partial t} - \gamma H^2 i\beta\frac{\partial V}{\partial t}\cdot\frac{\partial H}{\partial x} + \right. \\
&\left. + \beta^2 K\frac{\partial p}{\partial t} + \frac{\gamma-1}{2}\frac{H^2\beta^2}{\varrho_0}\frac{\partial U}{\partial x} + 2\beta^2 H\frac{\partial U}{\partial x}\cdot\frac{\partial p}{\partial t}\right\} = 0\,.
\end{aligned} \tag{4.11}$$

Since $|\alpha|$ and β are large, we can write the dominant terms in Eq. (4.7) for the shock region and shock free region separately.

In the shock region

$$\alpha = -\frac{(\gamma-1)}{\varrho_0}\frac{\beta^2(C\Delta x)^2}{V}\left(\left|\frac{\partial U}{\partial x}\right| - \frac{\partial U}{\partial x}\right) \tag{4.12}$$

which is negative for a real shock and hence the differential equations are stable in the shock region as small disturbances decay with time.

This expression is similar to the non-magnetic case discussed by VON NEUMANN and RICHTMYER [1]. The next value of α in the shock region is given by

$$\begin{aligned}
\alpha^2 = &-\frac{\beta^2}{\varrho_0^2 VK}\left\{\gamma pK + VH^2 + \frac{\gamma-1}{2}H^2 K + \right. \\
&\left. + (\gamma-1)(C\Delta x)^2 2H\frac{\partial U}{\partial x}\left(\left|\frac{\partial U}{\partial x}\right| - \frac{\partial U}{\partial x}\right)\right\}.
\end{aligned} \tag{4.13}$$

Eq. (4.13) gives the value of α in the shock region where artificial heat conduction and magnetic field both play an important role.

In the normal region,

$$\alpha^3 = -\frac{\beta^2}{\varrho_0^2 VK}\left\{\frac{2\gamma pH}{\varrho_0}\frac{\partial U}{\partial x} + K\frac{\partial p}{\partial t} + (\gamma-1)\frac{H^3}{2\varrho_0}\frac{\partial U}{\partial x}\right\}, \tag{4.14}$$

which shows that the stability of differential equations is unaffected in magneto-gasdynamic case.

In the shock region the dominant terms give

$$\frac{V\partial(\delta p)}{\partial t} = -(\gamma-1)\frac{\partial(\delta R)}{\partial t} \tag{4.15}$$

and

$$\frac{V\partial(\delta p)}{\partial t} + \gamma p\frac{\partial(\delta V)}{\partial t} + (\gamma-1)\frac{H^2}{2}\frac{\partial(\delta V)}{\partial t} + (\gamma-1)\frac{\partial(\delta R)}{\partial t} = 0. \tag{4.16}$$

From the Eqs (4.15) and (4.16) we conclude that the shock region has been divided into two subregions. In the first, only artificial heat conduction is prominent, and in the second, artificial heat conduction and magnetic field both play an important role. On the transition layer of these two regions, the perturbation in specific volume neither grows nor decays but remains constant.

As a consequence of Eqs (4.7), (4.8) and (4.10), Eq. (4.15) yields for a real shock

$$\frac{\partial}{\partial t}(\delta p) = \sigma\frac{\partial^2}{\partial x^2}(\delta p), \tag{4.17}$$

which has the form of a diffusion equation where σ is given by

$$\sigma = \frac{(\gamma-1)(C\Delta x)^2}{\varrho_0 V}\left(\left|\frac{\partial U}{\partial x}\right| - \frac{\partial U}{\partial x}\right)(1-N) \tag{4.18}$$

and N is given by

$$N = H^3\beta^2\left\{\varrho_0\alpha + \frac{H^3\beta^2}{\lambda}\right\}\left\{(\varrho_0\lambda^2 + H^3\beta^2\lambda)^2 + \beta^2 H^4\left(\frac{\partial U}{\partial x}\right)^2\right\}^{-1} \tag{4.19}$$

where we have put

$$K\varrho_0\alpha + 2H\frac{\partial U}{\partial x} = \lambda.$$

In the normal regions the dominant terms in Eq. (4.5) give

$$V\frac{\partial}{\partial t}(\delta p) + \gamma p\frac{\partial}{\partial t}(\gamma V) + (\gamma-1)\frac{H^2}{2}\frac{\partial}{\partial t}(\delta V) = 0, \tag{4.20}$$

which is simplified to an alternate form

$$\frac{\partial^2}{\partial t^2}(\delta U) = S_0^2 \frac{\partial^2(\delta U)}{\partial x^2}, \tag{4.21}$$

where

$$S_0^2 = \frac{\gamma p}{\varrho_0^2 V} + \frac{\gamma - 1}{2} \cdot \frac{H^2}{\varrho_0^2 V},$$

The Eq. (4.21) is the wave equation type so that the perturbations propagate like sound waves. From Eqs (4.16) and (4.21), we conclude that on the transition layer of shock region and normal region, the perturbation in artificial heat conduction is constant, an assumption made by SACHDEV and PRASAD [6] but proved mathematically by us.

5. Finite difference equations and their stability

Following the method of finite differences exactly on the same pattern as used by VON NEUMANN and RICHTMYER, we ensure the stability of difference equations in the normal region and shock region separately.

A) Normal region

Considering only the terms which are dominant in this region, and writing difference equations for the perturbations corresponding to differential equations (4.2), (4.4) and (4.20) we get,

$$\varrho_0(\delta U_0)\, \xi^{-1/2}(\xi - 1) = -(\delta p_0)\zeta^{-1/2}(\zeta - 1)\frac{\Delta t}{\Delta x} - H(\delta H_0)\zeta^{1/2}(\xi - 1)\frac{\Delta t}{\Delta x}, \tag{5.1}$$

$$\varrho_0(\delta V_0)\zeta^{1/2}(\xi - 1) = \frac{\Delta t}{\Delta x}(\delta U_0)\xi^{1/2}(\zeta - 1), \tag{5.2}$$

$$\left(\gamma p + \frac{\gamma - 1}{2} \cdot H^2\right)(\delta V_0) + V(\delta p_0) = 0, \tag{5.3}$$

where perturbations have been taken in the form as given below

$$\delta U_1^{n+1} = \delta U_0\, \zeta^1 \xi^{n+1/2} \quad \text{etc.} \tag{5.4}$$

where

$$\zeta = e^{i\beta \Delta x}, \quad \xi = e^{\alpha \Delta t}.$$

Eliminating δp_0, δU_0, δV_0 and δH_0 between (5.1)—(5.3) and making use of (4.8) we obtain

$$\left\{1 - \frac{HZ\zeta^{1/2}\,\xi^{1/2}}{\varrho_0}\left(\frac{\Delta t}{\Delta x}\right)\right\}\left(\xi + \frac{1}{\xi} - 2\right) = 2\left(\frac{\Delta t}{\Delta x}\,S_0\right)^2(\cos\beta\,\Delta x - 1), \quad (5.5)$$

where

$$Z = -\frac{H^2\,i\beta}{K\,\varrho_0\,\alpha + 2H\dfrac{\partial U}{\partial x}}\,.$$

Considering only the real part of Eq. (5.5) and then solving it for ξ, we have

$$\xi_{1,2} = b \pm \sqrt{b^2 - 1}\,, \quad (5.6)$$

where

$$b = 1 - \mu^2\,(1 - \cos\beta\,\Delta x)\,, \quad (5.7a)$$

$$\mu = S_0\frac{\Delta t}{\Delta x}\,. \quad (5.7b)$$

The relation (5.7a) shows that b is always less then one. Two cases may then arise:

$$-1 < b < 1,\ |\,\xi_1\,| = |\,\xi_2\,| = 1, \quad \text{(i)}$$

which gives the stability in the sense that the perturbation will not grow and

$$b < -1,\ |\,\xi_1\,| < 1 < |\,\xi_2\,| \quad \text{(ii)}$$

showing that the system of difference equations are unstable. Thus, equations will always be stable if $\mu < 1$.

B) Shock region

Writing the difference equations corresponding to (4.2), (4.10), (4.15) and (4.16) and making use of (4.6) and (5.4) we obtain the following expressions:

$$\varrho_0\,\delta U_0\,\xi^{-1/2}(\xi - 1) = -\frac{\Delta t}{\Delta x}\{\delta p_0\,\varrho^{-1/2}\,(\zeta - 1) - HZ\,\zeta^{-1/2}(\xi - 1)\,\delta U_0\}, \quad (5.9)$$

$$V\delta p_0\zeta^{1/2} = -\frac{(\gamma - 1)}{\Delta x}\cdot\delta U_0(C\Delta x)^2\left\{\left|\frac{\partial U}{\partial x}\right| - \frac{\delta U}{\partial x}\right\}\xi^{1/2}(\zeta - 1)\,. \quad (5.10)$$

Eliminating δp_0 and δU_0 between (5.9) and (5.10) and taking only real part we get

$$\xi - 1 = 2\eta(\cos\beta\,\Delta x - 1)\frac{\Delta t}{\Delta x}, \tag{5.11}$$

where

$$\eta = \frac{(\gamma-1)}{\varrho_0 V}\cdot(C\Delta x)^2\left\{\left|\frac{\partial U}{\partial x}\right| - \frac{\partial U}{\partial x}\right\}.$$

For stability $|\xi| \leq 1$ for which

$$\Delta t \leqslant \frac{(\Delta x)^2}{2\eta}. \tag{5.12}$$

We define the shock strength as

$$\theta = \frac{V_i}{V_f}. \tag{5.13}$$

In terms of this shock strength, η is expressed as

$$\Delta t \leqslant \frac{\varrho_0 K}{2(\gamma-1)(CM)^2}\left\{\frac{\theta+1}{V_f\left(1+\frac{\theta K}{\gamma+1}\right)} - \frac{w^2(\gamma+1)}{(\gamma-1)\,8\,(CM\Delta x)^2}\left(1+\frac{\theta K}{\gamma+1}\right)\right\}.$$

This equation gives the condition for stability of differential equations in the shock region. From the Rankine–Hugoniot conditions, S can be written as

$$S = \left\{\frac{2}{(\gamma+1)\theta-(\gamma-1)}\right\}^{1/2}\left\{\frac{\gamma p_f}{\varrho_0^2 V_f} + \frac{(\gamma+1)}{2\varrho_0^2 V_i}H_f^2 + \frac{V_f}{2\varrho_0^2 V_i}H_f^2\right\}^{1/2}. \tag{5.14}$$

In non-magnetic case this reduces to the form

$$S = \left\{\frac{2}{(\gamma+1)\theta-(\gamma+1)}\right\}^{1/2} S_{0f},$$

where

$$S_{0f} = \left\{\frac{\gamma p_f}{\varrho_0^2 V_f}\right\}^{1/2},$$

which gives the sound speed relative to the Lagrangian coordinate. Thus we see that the stability of difference equations is slightly disturbed in magneto-gasdynamic case but is not affected anywhere else. Since the differential equation (3.6) has been discussed by taking both parts on the right hand side separately, we cannot deduce non-magnetic conditions only by dropping the magnetic field term but have to proceed afresh in a similar way. This case has been thoroughly studied by SACHDEV and PRASAD [6].

6. Discussion and results

To have the qualitative picture, we use one set of data used by LAX [2], $\gamma = 2$, $V_i = 3$, $U_i = 0, p_i = -2/3, p_f = 6$, $V_f = 1$, $U_f = 4$. For our convenience we have taken $C = 2$, $\Delta x = 0.025$, $K = 2$. Fig. 1 represents pressure distribution in the shock region with Lagrangian distance. The four conditions of Section 1 are satisfied in the present case and the stability of difference and

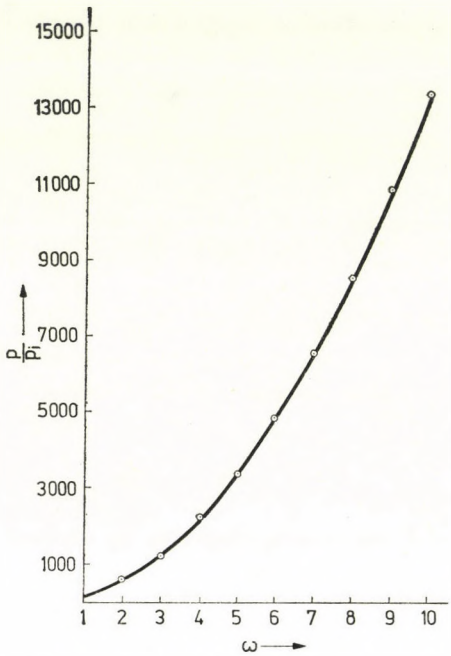

Fig. 1. Pressure distribution in shock region

differential equations are almost satisfied. As a result of the following discussions we observe that the shock region is divided into two sub-regions on the transition layer of which the perturbation in specific volume is constant. One layer behaves like the non-magnetic case while in the other sub-region the magnetic field and artificial heat conduction both play an important role. Thus, the shock region has been spread out and artificial heat conduction introduced to smoothen out the shock is more effective in the magnetised medium rather than in the ordinary gasdynamic case.

REFERENCES

1. J. Von Neumann and R. D. Richtmyer, J. Appl. Phys., **21**, 232, 1950.
2. P. D. Lax, Comm. on Pure and App. Math., **7**, 159, 1954.
3. H. L. Brode, Report of the Rand Corporation, P-571-AEC, 1954.
4. S. A. Colgate and M. H. Johnson, Phy. Rev. Letters., **5**, 235, 1960.
5. R. F. Christy, Rev. Mod. Phys., **36**, 555, 1964.
6. P. L. Sachdev and P. Prasad, J. Phys. Soc. Japan, **21**, 12, 1966.
7. R. Becker, Z. Phys., **8**, 321, 1922.
8. R. D. Richtmyer, Difference method for initial value problem, 1957.

Acta Physica Academiae Scientiarum Hungaricae, Tomus 43 (1), pp. 59—63 (1977)

NON-EQUILIBRIUM THEORY OF UNSTEADY HEAT CONDUCTION

By

P. SINGH

DEPARTMENT OF MATHEMATICS
INDIAN INSTITUTE OF TECHNOLOGY, KHARAGPUR
INDIA

(Received 26. V. 1977)

The governing principle of dissipative processes is formulated for unsteady heat conduction phenomenon. The dual field method is applied to find the temperature distribution in a finite insulated rod whose ends are maintained at a constant temperature. The variational solution obtained by this new method is in excellent agreement with the exact solution given by CARSLAW and JAEGER. The result is also obtained in the force representation of the governing principle which is exactly similar to that obtained by local potential method.

Introduction

On the basis of non-equilibrium theory of irreversible processes GYARMATI [1, 2] formulated a variational principle which describes the evolution of dissipative processes in time and space. The formulation which is called the governing principle of dissipative processes is written in most general form as

$$\delta \int_V [\sigma - \Psi - \Phi]\, dv = 0. \tag{1}$$

Here σ denotes the entropy production inside the system and it is a bilinear function of thermodynamic forces $\Delta\Gamma_i$ and current $\mathbf{J}_i$ i. e.

$$\sigma = \sum_{i=1}^{f} \mathbf{J}_i \cdot \nabla\Gamma_i \geq 0\,. \tag{2}$$

Γ_i are the state parameters, the gradients of which are the thermodynamic forces. In the linear Onsager theory, the currents are linear functions of the forces, i. e.

$$\mathbf{J}_i = \sum_{k=1}^{f} L_{ik} \nabla\Gamma_k\,, \quad \nabla\Gamma_i = \sum_{k=1}^{f} R_{ik} J_k\,, \qquad (i = 1, 2, \ldots f) \tag{3}$$

where the constant coefficients L_{ik} and R_{ik} are the conductivities and resistances, respectively, and these satisfy the famous reciprocal relations

$$L_{ik} = L_{ki}, \quad R_{ik} = R_{ki}\ (\mathrm{i}, k = 1,2, \ldots f). \tag{4}$$

Ψ and Φ are the local dissipation potentials which are defined as [1, 2]

$$\Psi(\nabla\Gamma, \nabla\Gamma) \equiv \frac{1}{2} \sum_{i,k=1}^{f} L_{ik} \nabla\Gamma_i \cdot \nabla\Gamma_k \geq 0\,, \tag{5}$$

$$\Phi(\mathbf{J}, \mathbf{J}) \equiv \frac{1}{2} \sum_{i,k=1}^{f} R_{ik} \mathbf{J}_i \cdot \mathbf{J}_k \geq 0\,. \tag{6}$$

These functions, in Onsager's linear theory, are equal to half of the entropy production for real processes, i.e. Ψ and Φ are the local measures of irreversibility. Using (2), (5) and (6), the variational principle (1) can be given in the following detailed form

$$\delta \int_V \left[\sum_{i=1}^{f} \mathbf{J}_i \cdot \nabla\Gamma_i - \frac{1}{2} \sum_{i,k=1}^{f} L_{ik} \nabla\Gamma_i \cdot \nabla\Gamma_k - \frac{1}{2} \sum_{i,k=1}^{f} R_{ik} \mathbf{J}_i \cdot \mathbf{J}_k \right] dv = 0\,. \tag{7}$$

It should be noted that the principle (7) is operative if and only if the balance equations

$$\varrho_i + \nabla \cdot \mathbf{J}_i = \sigma_i \qquad (i = 1,2, \ldots f), \tag{8}$$

are regarded as auxiliary conditions for whose variations the restrictions

$$\delta(\dot{\varrho}_i - \sigma_i) = -\delta\Delta \cdot \mathbf{J}_i = -\nabla \cdot \mathbf{J}\delta_i \; (i = 1,2, \ldots f) \tag{9}$$

are valid. Here $\dot{\varrho}_i$ is the partial time derivative of the density ϱ_i and σ_i is the rate of production of the transport quantities.

The principle is already used extensively for the derivation of equations of heat conduction, diffusion etc. Recently SINGH [3, 4, 5] applied this principle to get the variational solution of the Bénard convection. The critical wave and Rayleigh numbers for the linearised Bénard convection were obtained when the principle of exchange of stability is valid. In the following, the principle is applied to get the solution of the time dependent process of heat conduction in a finite insulated rod, the ends of which are maintained at constant temperature say zero. Assuming that the initial temperature is given by $T_0(1-x^2)$ where T_0 is constant and x is the distance measured along the rod, the temperature distribution which depends on both time and position is obtained. The result obtained using the universal form of principle is quite close to the exact result given by CARSLAW and JAEGER [6]. The result was also obtained in force representation which is same as obtained by SCHECHTER [7].

Formulation of the problem

Let us assume that the physical properties of the rod are independent of temperature, then the process of cooling is determined by the energy balance

$$\varrho c_v \frac{\partial T}{\partial t} + \nabla \cdot \mathbf{J}_q = 0\,, \tag{10}$$

where ϱ is the density and c_v is the heat capacity at constant volume. $\mathbf{J}_q$ is the heat current density and T is the temperature of the rod. The constitutive equation of the system is

$$\mathbf{J}_q = -\lambda \nabla T, \tag{11}$$

where λ is the conductivity of the rod and it is constant. The entropy production of the system in Fourier picture is [2]

$$\sigma = -J_q \cdot \nabla T \tag{12}$$

and Ψ and Φ are

$$\psi = \frac{1}{2}\lambda \nabla T \cdot \nabla T, \qquad \Phi = \frac{1}{2\lambda}\mathbf{J}_q \cdot \mathbf{J}_q\,. \tag{13}$$

Principle (1) becomes

$$\delta \int_0^\infty \int_V \left[-\mathbf{J}_q \cdot \nabla T - \frac{1}{2}\lambda \nabla T \cdot \nabla T - \frac{1}{2\lambda}\mathbf{J}_q \cdot \mathbf{J}_q \right] dv dt = 0\,. \tag{14}$$

The problem is one-dimensional, therefore relation (11) becomes

$$J_{q_1} = -\lambda \frac{\partial T}{\partial x}\,, \tag{15}$$

where x is the distance measured along the rod. In the dual method we introduce by definition, an approximate temperature field T^* which is connected with current density, J_{q_1}, by the relation

$$J_{q_1} = -\lambda \nabla T^* = -\lambda \frac{\partial T^*}{\partial x}\,. \tag{16}$$

With the help of this approximate value of J_{q_1}, energy balance (10) and the principle (14) become

$$\varrho c_v \frac{\partial T}{\partial t} - \frac{\partial}{\partial x}\left(\lambda \frac{\partial T^*}{\partial x}\right) = 0\,, \tag{17}$$

$$\delta \int_0^\infty \int_{-1}^1 \left[\frac{\partial T}{\partial x}\,\frac{\partial T^*}{\partial x} - \frac{1}{2}\left(\frac{\partial T}{\partial x}\right)^2 - \frac{1}{2}\left(\frac{\partial T^*}{\partial x}\right)^2 \right] dt dx = 0. \tag{18}$$

The initial and boundary conditions are

$$\begin{aligned} t = 0; \quad & T = T_0(1 - x^2), \\ t \geq 0; \quad & T = 0 \text{ at } x = \pm 1. \end{aligned} \tag{19}$$

It is assumed that T^* satisfies the conditions (19). Let us assume T in the following form

$$T = T_0(1 - x^2)\alpha(t), \tag{20}$$

where $\alpha(t) = 1$ when $t = 0$. Here $\alpha(t)$ is the variational parameter to be determined. Use of (20) in (17) gives

$$T^* = \frac{T_0}{\lambda}\left(x - \frac{x^3}{3} - \frac{5}{12}\right)\dot{\alpha}(t). \tag{21}$$

Using the expressions for T and T^* in (18) and integrating w.r.t. x we get the final form of the principle as

$$\delta\int_0^\infty [84\lambda\alpha\dot{\alpha} + 105\lambda^2\alpha^2 + 17\dot{\alpha}^2]dt = 0. \tag{22}$$

As the Euler–Lagrange equation of this variational formulation, we get the following equation for $\alpha(t)$

$$\ddot{\alpha} - \frac{105}{17}\lambda^2\alpha = 0. \tag{23}$$

Integrating (23) we get α as

$$\alpha = e^{-\left(\frac{105}{17}\right)^{1/2}\lambda t} \tag{24}$$

since $\alpha(0) = 1$. The temperature field is

$$T/T_0 = (1 - x^2)\, e^{-\sqrt{\frac{105}{17}}\,\lambda t}. \tag{25}$$

This variational solution is compared with the exact solution

$$T = \frac{32}{\pi^2}T_0\sum_{n=0}^{\infty}\frac{(-1)^n}{(2n+1)^3}\exp\left[-\frac{(2n+1)^2\pi^2\lambda t}{4}\right]\cos\frac{2n+1}{2}x \tag{26}$$

in Table I.

A brief study of this Table will reveal that the approximate solution, though a first approximation, is in excellent agreement with the exact result.

Table I

x	$\lambda t = 1$			$\lambda t = 0.1$			$\lambda t = 0.01$
	Exact T/T_0	Universal T/T_0	Force T/T_0	Exact T/T_0	Universal T/T_0	Force T/T_0	Universal T/T_0
0.0	0.0850	0.0833	0.0820	0.792	0.7799	0.779	0.9755
0.2	0.0823	0.0799	0.0787	0.755	0.7487	0.747	0.9364
0.4	0.0696	0.0699	0.068	0.640	0.6551	0.654	0.7194
0.6	0.0509	0.0533	0.0525	0.472	0.4992	0.498	0.6243
0.8	0.0267	0.0299	0.295	0.249	0.2808	0.280	0.3512
1.0	0.000	0.0000	0.00	0.000	0.0000	0.000	0.0000

A better approximation can be developed by using a more complex expression for temperature field.

It is well known that the governing principle of dissipative processes results in two partial forms of the principle. Though these two partial forms are no more actual variational principles, but to establish the fact that the force representation of GYARMATI's principle is equivalent to the local potential method of GLANSDORFF and PRIGOGINE, we have calculated the parameter α in the force representation and its value is found to be

$$\alpha = e^{-5/2\,\lambda t} \tag{27}$$

and therefore the temperature distribution is

$$T/T_0 = (1 - x^2)\, e^{-5/2\,\lambda t}, \tag{28}$$

which is exactly the same as obtained by SCHECHTER [7] with the help of the local potential method of GLANSDORFF and PRIGOGINE. This result proves the theoretically established fact [1, 3], that the local potential method is equivalent to the force representation of GPDP as far as the approximation procedure is concerned.

REFERENCES

1. I. GYARMATI, Ann. Phys., **23,** 353, 1969.
2. I. GYARMARI, Non-Equilibrium Thermodynamics, Field Theory and Variational Principles, Springer, Berlin, 1970.
3. P. SINGH, The Applications of the Governing Principle of Dissipative Processes to Thermo-hydrodynamical Stability, D. Sc. Dissertation, Hungarian Academy of Sciences, Budapest, 1973.
4. P. SINGH, Int. J. Heat Mass Transfer, **19,** 581, 1976.
5. P. SINGH, J. Non-Equilibrium Thermodyn., **1,** 1976.
6. H. S. CARSLAW and J. C. JAEGER, Conduction of Heat in Solids, Oxford University Press, London, 1959.
7. R. S. SCHECHTER, The Variational Method in Engineering, McGraw-Hill, New York, 1967.

Acta Physica Academiae Scientiarum Hungaricae, Tomus 43 (1), pp. 65—71 (1977)

THE SCHLIEREN DISTRIBUTION OF THE CATHODIC DIFFUSION LAYER

By

M. F. KOTKATA

PHYSICS DEPARTMENT, FACULTY OF SCIENCE, AIN SHAMS UNIVERSITY, CAIRO, EGYPT

(Received 10. VI. 1977)

The optical density distribution in cell containing electrolyte solutions of Schmidt number greater than 2500, Sc > 2500, [1], has been investigated. The "Shadow Schlieren" method is used to record the free convective flow caused by the difference in gravity between the electrode film and bulk fluid. The two roots of the imaging law of the diffusion boundary layer have been achieved in the vicinity of the cathode.

Introduction

The problem of mass transfer has been studied for acidified copper-sulphate solutions under the condition of free-convection [1]. In such a case, the deposition of metal ions on vertical cathodes is accompanied by the formation of a concentration gradient in the y-direction (Fig. 1). On this condition, the optical density is considered to be a function of the concentration distribution of the fluid.

The "Shadow Schlieren" method is based on the fact that parallel light rays passing through a medium with a continuously changing refractive index are deviated towards the optically denser parts of the medium. In this case, the image is formed by the projection of a shadow without the use of lenses and so a "Shadow Schlieren" can be photographed. The method is quite valuable for the investigation at the cathode while it is less valuable at the anode film. This is because the light passing through the boundary layer will be deviated towards and deflected by the anode. This will result in a broadening of the electrode shadow. There is, however, also an opposite effect, which results in a narrowing of the shadow, due to the light passing close to the rear edge of the anode.

When the rays are incident on the cell in the z-direction as in Fig. 2, the differential equation of the ray path in one dimensional refracting field is given from geometrical optics [2] by

$$\frac{y''}{1+y'^2} = \frac{d\ln(n)}{dy}, \tag{1}$$

where $y' = dy/dz$ is the slope of the ray, and n is the refractive index.

For a small concentration (0.1 M/L $CuSo_4$), y'^2 is practically negligible compared with unity [3]. Accordingly, the slope of any ray incident parallel to the cathode at a distance y_0 from it is given by

$$y' = \int_0^z \frac{1}{n} \frac{dn}{dy} dz . \tag{2}$$

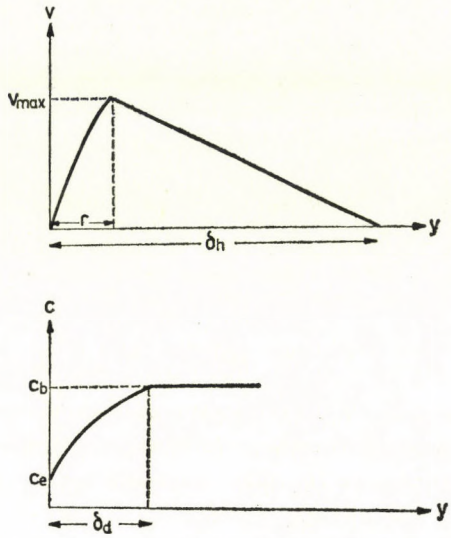

Fig. 1. Schematic representation for the fluid velocity and concentration distribution near the cathode

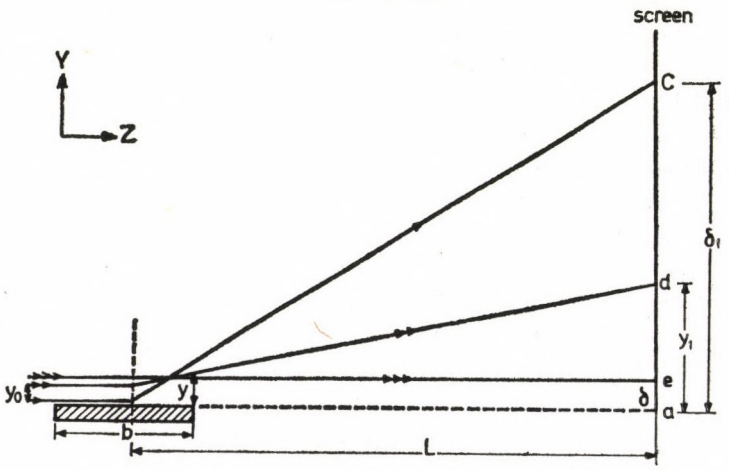

Fig. 2. Approximation of the path of parallel light through the diffusion boundary layer. a: denotes the position of the cathode edge on a screen at a distance L from the mid point of the cathode, in the absence of any concentration gradient; c: at a distance δ_l from a, denotes the maximum deviation of a beam incident just on the front edge of the cathode; d: at a distance y_1 from a, denotes the deviation of a beam incident at a distance y_0 from the front edge of the cathode. Its deviation at the rear end of the cathode is y; e: at a distance δ from a, denotes the deviation of a beam incident just outside the diffusion boundary layer

Assuming the total deviation of this ray to remain small, the concentration and its gradient do not change during the light path and, so, at the outlet of the electrode, i.e. at $z = b$,

$$y'_b = \frac{n'}{n} b \tag{3}$$

and so the total deviation of the ray at the end of the electrode is

$$y - y_0 = \frac{n'}{2n} b^2 , \quad n' = dn/dy . \tag{4}$$

Thus, the path of the light beam across the diffusion boundary layer, δ_d, describes a parabola. From Eqs. (3) and (4), one can write for the slope of the ray

$$y'_b = \frac{y - y_0}{b/2} . \tag{5}$$

The curved form of the light beam could, however, be replaced to the first approximation by two straight lines in Fig. 2. If the deviation of the light beam on a screen, at distance L away from the central point of the cathode, is denoted by y_1, then the slope of the ray is

$$y'_b = \frac{y_1 - y_0}{L} , \tag{6}$$

or, with the help of equation (3);

$$\frac{y_1 - y_0}{L} = \frac{n'}{n} b . \tag{7}$$

Fig. 3 gives a schematic diagram for the optical arrangement for the study of the density distribution in the electrolysing cell made of planparallel plates of flow-free glass [1].

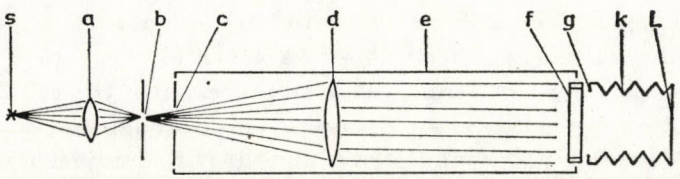

Fig. 3. Optical Schlieren arrangement for the study of the hydrodynamical motion of the fluid in the electrolysis cell. S: Sodium lamp; b: circular slit; d: collimating lens group; f: electrolysis cell; k: camera box; a: condenser lens; c: camera shutter; e: rectangular box; g: camera slit; L: screen

The diffusion boundary layer

Introducing the relative deviation $\eta_1 = y_1/\delta_1$ and the relative wall distance $\eta = y_0/\delta$, the imaging law of the diffusion boundary layer could be obtained, after Eq. (7), in the form

$$\eta_1 = \frac{n' n_e}{n n_e'} + \frac{\delta}{\delta_1} \eta, \tag{8}$$

where n_e is the refractive index on the cathode, and n_e' is the refractive index gradient perpendicular to the ray.

From the International Critical Tables giving the relation between the refractive index and the concentration, one can find for the concentration region of cupric sulphate solutions between $C = 0.0 \rightarrow 0.1$ M/L, that $\partial n/\partial C$ is positive and constant. That is, one can give for the refractive index field the same equations for the concentration field. Consequently, in Fig. 2, the illumination strength has its maximum value when $dy_1/dy = 0$. This leads for the imaging law of the diffusion boundary layer to the relation

$$\frac{d\eta_1}{d\eta} = \frac{\delta}{\delta_1} \cdot \frac{dy_1}{dy} = \frac{\delta}{\delta_1} - 6\eta + 6\eta^2 = 0. \tag{9}$$

This means that two bright lines are observed on the screen originated from the places of the diffusion boundary layer, since

$$\eta_{a,b} = 1/2 \left(1 \pm \sqrt{1 - \frac{2}{3} \frac{\delta}{\delta_1}}\right), \tag{10}$$

with η_a and η_b being the two roots of the quadratic equation (9).

This has been achieved from the Schlieren photos recorded through the present work. The image obtained on a screen at a distance $L = 28$ cm from the centre of the cell shows two bright lines to arise along the cathode. For the concentration (0.01 M/L $CuSo_4$ + 1.5 M/L H_2SO_4) during the passage of 0.306 mA/cm^2 for 90 min, Plate 1 shows the two bright lines that appeared along the cathode. They are very near to each other because of the small concentration gradient. Such photo has been taken for the cathode film using a punched rectangular slit 3 mm wide clamped close to the cell face so that light incident on the cell is allowed to pass only through the layer adjacent to the cathode surface. Also, the edge of the slit is well adjusted in the plane of the cathode edge to record the deviation due to the cathode film.

In the cathode diffusion layer, the concentration and refractive index are lower than those in the bulk solution. The light beam is, therefore, deviated

from the electrode as given in Fig. 2. Such deviation is proportional to the refractive index gradient. Since the gradient is greatest close to the cathode surface, so the light rays that enter the solution near the cathode surface will undergo the greatest deviation. Plate 2 is a Schlieren photo showing the deviation of light from the diffusion boundary layer. The course of the second bright line, denoted by C in Fig. 2, gives the variation of the concentration gradient $(\partial C_i/\partial y)_e$ at the surface of the cathode, which may be obtained from Eq. (7) and so

$$y_1 - y_0 = \frac{n'}{n} Lb \,. \tag{11}$$

As

$$y_0 \to 0, \; y_1 - y_0 \to \delta_1$$

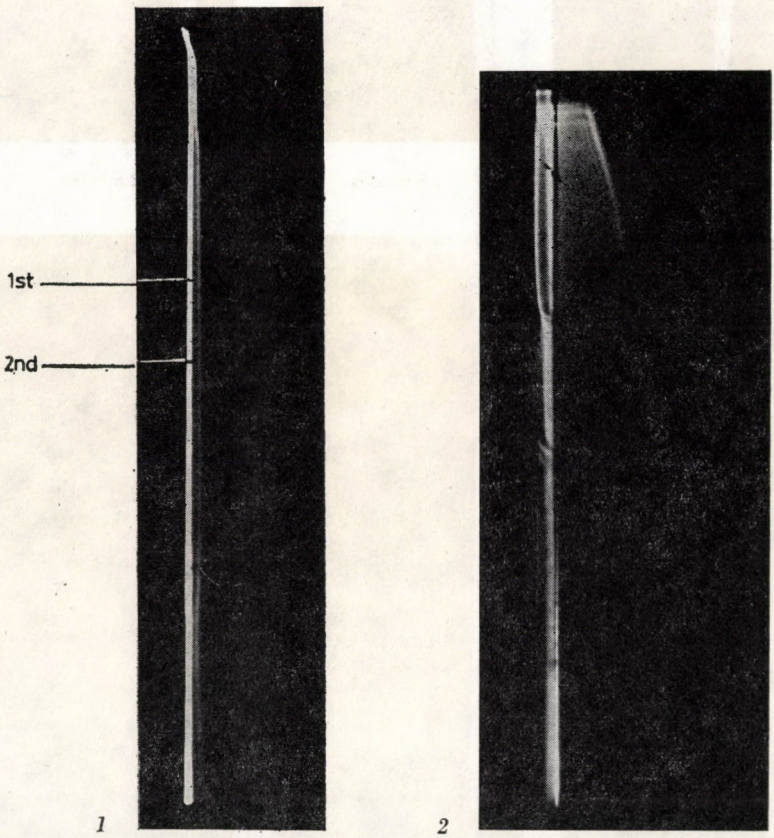

Plate 1. Schlieren photo, 90 min after closing the circuit for the composition: 0.01 M/L $CuCO_4$ + + 1.5 M/L H_2SO_4 at 0.306 mA/cm²

Plate 2. Schlieren photo shows the deviation of light from the diffusion boundary layer and illustrates the variation of the concentration gradient at the cathode surface

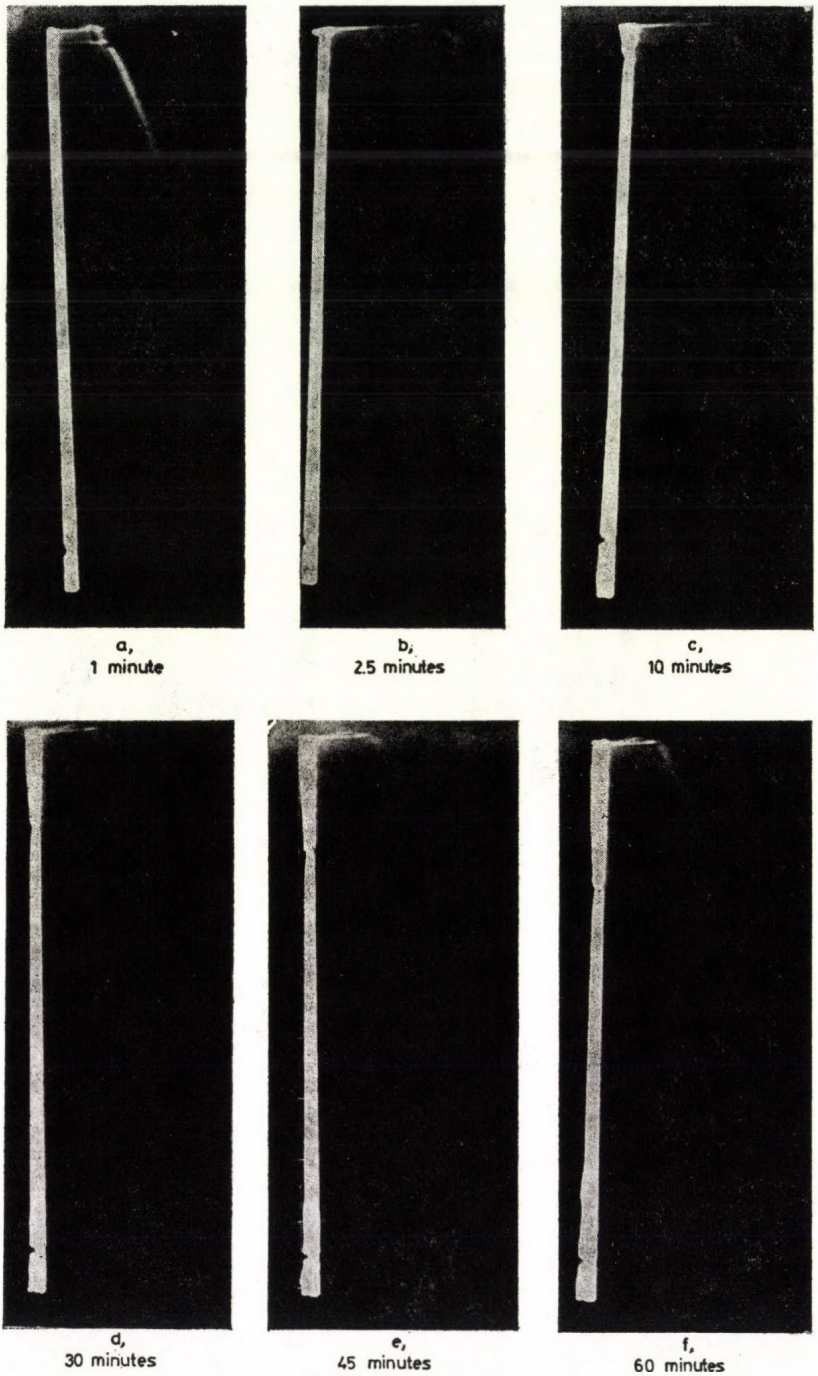

Plate 3. Schlieren photos for the cathode film showing the distribution changes of the local current along the cathode surface at different times from passing 1.787 mA/cm² current density

i.e.

$$\delta_1 = \frac{Lb}{n_e}\left(\frac{\partial n}{\partial C}\right)_e\left(\frac{\partial C}{\partial y}\right)_e \tag{12}$$

and

$$\left(\frac{\partial C}{\partial y}\right)_e = \frac{\delta_1}{Lb} \cdot \frac{n_e}{(\partial n/\partial C)_e}.$$

From this one can see the distribution of the current density along the cathode surface. The distance of the course line from the cathode surface at any point is, therefore, a measure of the concentration gradient at such point on the cathode surface.

The cathodic local current

Plates 3 are Schlieren photos for the cathode film showing the distribution changes of the local current along the surface of the cathode during one hour in the cell filled with solution (0.05 M/L $CuSO_4$ + 1.5 M/L H_2SO_4) at passage of 1.787 mA/cm^2 current density. Photos (a) to (c) illustrate the variation of the diffusion boundary layer with time before reaching the limiting current. Photos (d) to (f) show that such region remains unchanged with the time going up. This indicates that after a considerable time, (30 min for such composition,) the limiting current is reached and more or less it is constant along the surface of the cathode. Evidently, it is the case detected from the electrical measurements [1] of the local current density along the surface of the cathode. However, such constancy for the limiting current density is attributed to the presence of the back-flow which has been found to grasp the original flow [1].

Acknowledgement

The author wishes to express his gratitude to Prof. F. A. El-Bedewi, Head of the Physics Department, Ain-Shams University, for his deep interest and stimulating suggestions.

REFERENCES

1. M. F. Kotkata and Y. K. Badawy, Acta Phys. Hung., **41**, 231, 1976.
2. F. J. Weinberg, "Optics of Flames", Butterworths, London, 1963.
3. A. B. Wahba, Diss. T. H. München (in German), 1964.

Acta Physica Academiae Scientiarum Hungaricae, Tomus 43 (1), pp. 73—79 (1977)

PROPAGATION AND GROWTH OF MAGNETOGASDYNAMIC SHOCK WAVES IN INHOMOGENEOUS FLUIDS

By

B. G. VERMA and R. C. SRIVASTAVA

DEPARTMENT OF MATHEMATICS, UNIVERSITY OF GORAKHPUR
GORAKHPUR 273001, INDIA

(Received in revised form 10. VI. 1977)

This paper presents a numerical study of the propagation of magnetogasdynamic shocks in inhomogeneous medium. The natural state of the medium is defined by the assumption that the pressure, internal energy and temperature are determined at each spatial point and time by the density and entropy.

1. Introduction

Propagation of a shock wave through a non-uniform medium, in the absence of thermodynamic influences, has been considered by CHISNELL [1], who obtained the strength of the shock wave throughout the region of varying density. STRACHAN et al [2] also considered the shock propagation in a similar medium but included the initial variation in the pressure, particle velocity as well as density. Recently, NUNZIATO and WALSH [3] discussed the propagation, growth and decay behaviour of shock waves and found that a globally steady wave, in general, was not possible in a non-uniform fluid.

In the present work we study the effects of a magnetic field on the propagation and growth of shock waves in inhomogeneous fluids, and find that the equation determining the strength of the shock wave is of the same form as obtained by NUNZIATO and WALSH with the addition of magnetic field terms. Qualitative picture shows that the time derivative of the strength of the shock wave decreases with space coordinates in both cases while magnetic field creates retardation in the decrement of the derivative of the strength of the shock wave. After travelling a certain distance, the time derivative of the strength of the shock wave becomes constant.

2. Fundamental equations for the problem

We consider a Lagrangian coordinate system so that the basic equations governing the motion of a magnetogasdynamic shock wave in a non-viscous

and non-heat conducting medium are

$$\varrho_R = J\varrho\,, \tag{2.1}$$

$$\varrho_R \frac{\partial V}{\partial t} + \frac{\partial p}{\partial a} + H\frac{\partial H}{\partial a} = 0\,, \tag{2.2}$$

$$\frac{\varrho_R}{\varrho}\,\frac{\partial H}{\partial t} + H\frac{\partial V}{\partial a} = 0\,, \tag{2.3}$$

$$\frac{\partial}{\partial t}\left(e + \frac{H^2}{2\varrho}\right) + \frac{(p + H^2/2)}{\varrho_R}\,\frac{\partial V}{\partial a} = 0\,, \tag{2.4}$$

where p is the pressure, ϱ is the density, $V(=\dot{x})$ is the particle velocity, e is the internal energy and $J = \partial x/\partial a$. The position of the particle which had the position 'a' in the initial configuration is given, at time t, by $x = x(a, t)$. Initially, the mass density of the medium is given by $\varrho_R = \varrho_R(a)$ which is assumed to be once continuously differentiable.

The variables characterising the medium in its initial reference configuration are defined as

$$p_* = \hat{p}_*(\varrho, \eta), \tag{2.5}$$

$$e_* = \hat{e}_*(\varrho, \eta), \tag{2.6}$$

$$\theta = \hat{\theta}(\varrho, \eta)\,, \tag{2.7}$$

where $p_* = p + H^2/2$, $e_* = e + H^2/2\varrho$, $\theta > 0$ is the absolute temperature and η is the entropy. From the second law of thermodynamics, we have[4],

$$\hat{p}_* = \varrho^2 \partial_\varrho \hat{e}_*,\ \hat{\theta} = \partial_\eta^{\hat{e}} \tag{2.8}$$

3. Shock waves of arbitrary strength

Consider the shock wave as a singular surface propagating with the intrinsic velocity $U = d\,Y(t)/dt > 0$ where $Y(t)$ is the material point where the wave is to be found at time t. Let the jump in any function $f(a, t)$ across the wave at time t be defined as

$$[f] = \bar{f} - f^+,\quad f^\pm = \lim_{a \to Y\pm} f(a, t) \tag{3.1}$$

so that, at the wave, the following well known compatibility conditions

$$\frac{d[f]}{dt} = [\dot{f}] + U[\partial_a f] \tag{3.2}$$

and

$$[fg] = f^+[g] + g^+[f] + [f][g] \tag{3.3}$$

hold. Let the region ahead of the wave be at rest. Then, by (3.1) we have,

$$(\partial_a x)^+ = 1, \tag{3.4}$$

$$V^+ = 0. \tag{3.5}$$

Now, defining, as in [5], the strength of the shock waves

$$\delta = \frac{[\varrho]}{\bar{\varrho}} = -[\partial_a x] \tag{3.6}$$

and considering only compressive shocks so that $0 < \delta < 1$, we see from (3.4)—(3.6) that the shock strength can also be expressed as

$$\delta = \bar{V}/U. \tag{3.7}$$

Using the general conservation law the jump relations across the singular surface may be written as

$$\varrho_R U[V] = [p] + \left[\frac{H^2}{2}\right], \tag{3.8}$$

$$K \varrho_R U\left[\frac{1}{H}\right] + [V] = 0, \tag{3.9}$$

$$U \varrho_R \left\{[e] + \frac{1}{2}[V^2] + \left[\frac{H^2}{2}\right]\right\} = [pV] + \left[\frac{H^2}{2} V\right], \tag{3.10}$$

Taking into consideration that the region ahead of the wave is in equilibrium the Hugoniot relation for magnetogasdynamic case is obtained from equation (3.10) as

$$\left[e + \frac{H^2}{2\varrho}\right] + \frac{(\bar{p}_* + p_*^+)}{2}\left(\frac{1}{\bar{\varrho}} - \frac{1}{\varrho_R}\right) = 0,$$

or

$$\hat{e}(\bar{\varrho}, \bar{\eta}) - e_R + \left(\frac{H^2}{2\varrho}\right)^- - \left(\frac{H^2}{2\varrho}\right)^+ + \left(\frac{p_*^- + p_*^+}{2}\right)\left(\frac{1}{\bar{\varrho}} - \frac{1}{\varrho_R}\right) = 0, \tag{3.11}$$

where $e_R = \hat{e}(\varrho_R, \eta_R)$ and $p_R = \hat{p}(\varrho_R, \eta_R)$. Thus (3.11) implies that $\bar{\varrho}$, $\bar{\eta}$ must be related to each other. Let there exist a function η_h so that the relations

$$\bar{\eta} = \eta_h(\bar{\varrho}), \quad \eta_R = \eta_h(\varrho_R)$$

hold which are called the 'Hugoniot, entropy-density function'. From this the Hugoniot pressure density function and temperature density function

are defined by

$$\bar{p} = \hat{p}\,(\bar{\varrho}, \bar{\eta}) = \hat{p}\,[\bar{\varrho}, \eta_h(\bar{\varrho})] = p_h(\bar{\varrho})\ , \tag{3.12}$$

and

$$\bar{\theta} = \hat{\theta}\,(\bar{\varrho}, \bar{\eta}) = \hat{\theta}\,[\bar{\varrho}, \eta_h(\bar{\varrho})] = \theta_h(\bar{\varrho}) > 0\,. \tag{3.13}$$

Then, the intrinsic shock velocity U is given by

$$U^2 = \frac{(\bar{p} - p_R) + 1/2\,(\bar{H}^2 - H_R^2)}{\varrho_R\,\delta}\ . \tag{3.14}$$

It is now a matter of simple verification that WEYL's theorem [6] about shock waves of arbitrary strength holds good in the magnetogasdynamic case as well.

4. Strength of compressive shock waves

Now we shall derive an expression for the strength of the shock wave. Using the Eq. (3.2) with $f = \partial_a x$ and V, the definition of shock strength δ and conservation of momentum we obtain the formula

$$2U\frac{d\delta}{dt} + \delta\frac{dU}{dt} = -\varrho_R^{-1}\left[\partial_a\left(p + \frac{H^2}{2}\right)\right] - U^2[\partial_a^2 x]\,, \tag{4.1}$$

where we have yet to evaluate $[\partial_a^2 x]$, $[\partial_a p]$, and dU/dt. To this end we proceed as follows. From the continuity equation (2.1) we have

$$\partial_a^2 x = \varrho^{-1}\{\partial_a \varrho_R - (\partial_a x)\,(\partial_a \varrho)\} \tag{4.2}$$

while from (3.4) we get

$$(\partial_a x)^- = \frac{\varrho_R}{\bar{\varrho}} = 1 - \delta > 0. \tag{4.3}$$

Then, (4.2) evaluated at the wave yields

$$[\partial_a^2 x] = \left\{\frac{(1-\delta)}{\varrho_R}\right\}\{\partial_a \varrho_R - (1-\delta)(\partial_a \varrho)^-\}\,. \tag{4.4}$$

From the smoothness of $\hat{p}_*(\varrho, \eta)$, we have

$$[\partial_a p_*] = \bar{E}\,(\partial_a \varrho)^- - E_R\,(\partial_a \varrho_R) + \bar{L}\,(\partial_a \eta)^- - L_R\,(\partial_a \eta_R)\,, \tag{4.5}$$

where

$$\bar{E} = \frac{\partial \hat{p}_*}{\partial \bar{\varrho}}\,, \qquad L = \frac{\partial \hat{p}_*}{\partial \eta}\ .$$

In (4.5), $(\partial_a \varrho_R)$ and $(\partial_a \eta_R)$ will be determined by the initial configuration of the medium. We shall determine $(\partial_a \bar{\eta})$ in terms of $(\partial_a \varrho_R)$ and the shock strength δ. Differentiating (4.3) and making use of (3.2) and the Hugoniot entropy density function we get,

$$(\partial_a \eta)^- = \frac{\eta_h'(\bar{\varrho})}{(1-\delta)} \left(\partial_a \varrho_R + \frac{\varrho_R}{U(1-\delta)} \frac{d\delta}{dt} \right), \tag{4.6}$$

Lastly, differentiating Hugoniot function (3.11) with respect to density and using (2.8), (3.12), (3.13), (3.14) and (4.3) we obtain,

$$\eta_h'(\bar{\varrho}) = \frac{\alpha v}{\bar{L}}, \tag{4.7}$$

where

$$\alpha = \frac{1}{2\varrho_R} \left\{ \frac{\partial p_h(\bar{\varrho})}{\partial \bar{\varrho}} + \bar{H} \frac{\partial \bar{H}}{\partial \bar{\varrho}} - (1-\delta)^2 U^2 \right\}.$$

$$v = \frac{\bar{L}\delta}{\bar{\theta}}.$$

Substituting (4.7) along with (4.6) in (4.5) we get

$$[\partial_a p_* = \frac{\varrho_R \alpha v}{U(1-\delta)^2} \frac{d\delta}{dt} + \bar{E}(\partial_a \varrho)^- + \left\{ \frac{\alpha v}{1-\delta} - E_R \right\} (\partial_a \varrho_R) - L_R(\partial_a \eta_R). \tag{4.8}$$

To obtain dU/dt, we use (3.14) and also the definition of E, L and the total derivative of (4.3) evaluated at the wave to obtain

$$\frac{dU}{dt} = \frac{\varrho_R \alpha}{U\delta(1-\delta)^2} \frac{d\delta}{dt} + \frac{1}{4} [(\xi + \varepsilon)(\partial_a \varrho_R) - \varphi \partial_a \eta_R], \tag{4.9}$$

where

$$\xi = \frac{2}{\varrho_R \delta(1-\delta)} \left[\frac{\partial p_h(\bar{\varrho})}{\partial \bar{\varrho}} + \bar{H} \frac{\partial \bar{H}}{\partial \bar{\varrho}} - (1-\delta) U^2 \right],$$

$$\varepsilon = \frac{2}{\varrho_R \delta} [(1-\delta) U^2 - E_R],$$

$$\varphi = 2L_R/\varrho_R \delta.$$

Substitution of (4.8) and (4.9) in (4.1) gives the following differential equation for the strength of the shock wave

$$\frac{d\delta}{dt} = M(\delta) \{\zeta - (\partial_a \bar{\varrho})\}, \tag{4.10}$$

where

$$\zeta = -(\beta)^{-1}\left\{\left[(\xi + 3\varepsilon) + \frac{4\alpha\nu}{(1-\delta)\,\varrho_R}\right]\frac{\partial_a \varrho_R}{4} - \frac{3}{4}\varphi\,\partial_a \eta_R\right\},$$

$$\beta = \frac{1}{\varrho_R \delta}\{\bar{E} - (1-\delta)^2 U^2\},$$

$$M(\delta) = \frac{(\beta\delta)}{2U\left\{1 + \frac{\alpha(\varrho_R + \nu)}{2U^2(1-\delta)^2}\right\}} > 0.$$

Using the consequences of WEYL's theorem we can easily prove for a compressive shock that $\alpha > 0$, $\beta > 0$, $0 < \nu < 2$, $\varepsilon > 0$ and $\varphi > 0$.

Considering the motion of a magnetogasdynamic shock in a non-uniform medium at rest we have,

$$\begin{aligned}
(\partial_a \varrho)^- < \zeta &\iff \frac{d\delta}{dt} > 0, \\
(\partial_a \varrho)^- = \zeta &\iff \frac{d\delta}{dt} = 0, \qquad (4.11) \\
(\partial_a \varrho)^- > \zeta &\iff \frac{d\delta}{dt} < 0.
\end{aligned}$$

Then following the arguments as in [3], we see that, since ϱ depends on the density, magnetic field, and entropy gradients ahead of the wave as well as on the shock strength, the strength of shock wave may become stationary at one instant and be increasing (or decreasing) at the next instant, i.e. a globally steady wave, in general, cannot exist in a non-uniform fluid. But for a particular set of numerical values of physical quantities, the time derivative of strength of shock wave becomes stationary at one place and decreases with space coordinate.

5. Numerical solution and result

To have the qualitative picture, we take one set of numerical values, that is, $\gamma = 1.1$, $p_R = 1000$, $\theta = 2\times 10^4$ °K. From these numerical data we determine that the time derivative of the shock wave decreases with space coordinate in both cases. It is clear from the Figure that the magnetic field retards the decrement of the derivative of the shock strength. After travelling a certain distance, the strength of shock wave becomes constant in the ordinary as well as in the magnetogasdynamic case.

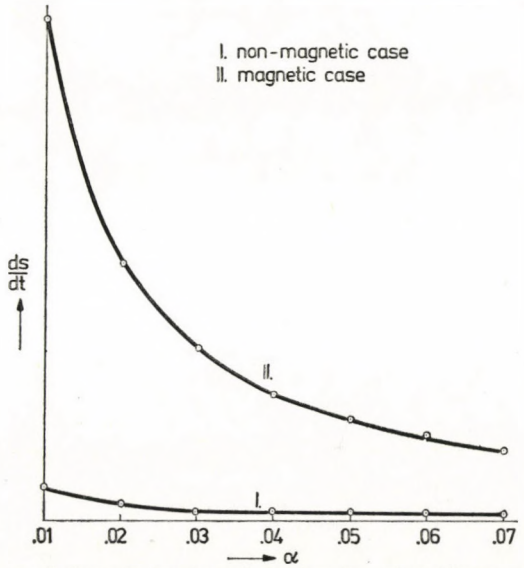

Fig. 1. Variation of time derivative of shock strength with space coordinate

REFERENCES

1. R. F. CHISNELL, Proc. Roy. Soc. London, A**232**, 350, 1955.
2. J. D. STRACHAN, J. P. HUNI aud B. AHLBORN, J. Fluid Mech., **83**, 487, 1970.
3. J. W. NUNZIATO and E. K. WALSH, The Phys. of Fluids, **15**, 8, 1972.
4. R. COURANT and K. O. FRIEDRICHS, Supersonic Flow and Shock Waves, Interscience, New York, 1948. p. 4.
5. C. TRUESDELL and R. A. TOUPIN, Handbuch der Physik, edited by S. Flügge, Springer-Verlag, Berlin 1960. Vol. III, Pt. 1, p. 522.
6. H. WEYL, Commun. Pure. Appl. Math., **2**, 103, 1949.

Acta Physica Academiae Scientiarum Hungaricae, Tomus 43 (1), pp. 81—91 (1977)

MIXED BOUNDARY VALUE PROBLEMS IN MAGNETO-ELASTO DYNAMICS

By

ANIMESH BASU

THE UNIVERSITY OF NEW SOUTH WALES
DUNTROON, ACT, AUSTRALIA

(Received 11. VI. 1977)

The interaction of magnetic fields and displacements in an elastic solid is considered as a mixed initial and boundary value problem in magneto-elasto dynamics. The solution is reduced to a system of Fredholm equations of the second kind, which in certain particular cases become Fredholm equations of the first kind. A general solution for free and forced motion problems of circular plate is obtained in the applied magnetic field and also frequency equations are obtained for free-vibrations of circular plates.

1. Introduction

Primarily due to the success of the merger of electromagnetic theory and fluid mechanics in magnetohydrodynamics, considerable attention has been given recently to the area of magneto-elastic solid interactions. Applications of magneto-elastic action are evidenced in seismology, high speed engines in a strong magnetic field, rapid rail magneto-trains, as well as in the study of the phenomena of aero-magneto flutter.

Although there has been some progress in the study of magneto-elasticity the development of effective methods of solution of the general mixed initial boundary value problem in magneto-elastodynamics remains a challenge. In this investigation complete and systematic mathematical formulation for mixed initial and boundary value problems in MED with mixed boundary conditions is developed.

The method is based on NOWACKI's general method of solving problems of elastostatics and later extended [1] to problems in elastodynamics with mixed boundary conditions. In deducing our results in magneto-elastic medium it is assumed that the magnetic field is much more conducive to inter-action effects associated with the body force coupling than is the electric field. Consequently, we investigate the problems of MED in a large magnetic field and ignore the similar electrical effect. Moreover, in a perfect conducting body, conduction current dominates, and as a result we may neglect the displacement current term.

2. Equations of motion and their solution

Assuming that the elastic displacements are infinitesimal and that the displacement currents are negligible compared with the conductivity currents, we can write the linearised exact three dimensional magneto-elastic equations for a perfectly conducting homogeneous isotropic body in vector form:

$$\frac{\partial^2 \mathbf{u}}{\partial t^2} = c_2^2 \nabla^2 \mathbf{u} + (c_1^2 - c_2^2) \operatorname{grad} \operatorname{div} \mathbf{u} + \\ + R_H [\operatorname{curl} \operatorname{curl} (\mathbf{u} \times \mathbf{H}) \times \mathbf{H} + \mathbf{X}, \tag{2.1}$$

where $\mathbf{H}$ is the vector of the original steady magnetic field, $\mathbf{u}$ is the displacement vector, c_1 and c_2 are the longitudinal and shear wave velocities, $R_H = \mu_e/\varrho$, μ_e is the magnetic permeability, ϱ is the density of the medium, and X is the body force.

Consider a conducting, isotropic, and homogeneous circular plate of radius 'a' and assuming that the magnetic field acts along the Z-direction of the circular plate we write the equations of motion (2.1) in polar co-ordinates:

$$\frac{\partial^2 u_r}{\partial t^2} = \left[c_2^2 \nabla^2 u_r - c_2^2 \frac{u_r}{r^2} + (c_1^2 - c_2^2 + R_Z^2) \frac{\partial}{\partial r} \left\{ \frac{1}{r} \frac{\partial}{\partial r} (r u_r) \right\} \right] + \\ + \left[c_1^2 - c_2^2 + R_Z^2) \frac{\partial}{\partial r} \left(\frac{\partial u_\theta}{r \partial \theta} \right) - \frac{2 c_2^2}{r^2} \frac{\partial u_\theta}{\partial \theta} \right| + X_r,$$

$$\frac{\partial^2 u_\theta}{\partial t^2} = \left[(c_1^2 - c_2^2 + R_Z^2) \frac{\partial}{r \partial \theta} \left\{ \frac{1}{r} \frac{\partial}{\partial r} (r u_r) \right\} + \frac{2 c_2^2}{r^2} \frac{\partial u_r}{\partial \theta} \right] + \tag{2.2}$$

$$+ \left[c_2^2 \nabla_{u_\theta}^2 - c_2^2 \frac{u_\theta}{r^2} + (c_1^2 - c_2^2 + R_Z^2) \frac{\partial}{r \partial \theta} \left\{ \frac{\partial u_\theta}{r \partial \theta} \right\} \right] + X_\theta,$$

where

$$\nabla^2 \equiv \frac{1}{r} \frac{\partial}{\partial r} \left(r \frac{\partial}{\partial r} \right) + \frac{\partial^2}{r^2 \partial \theta^2},$$

$$R_Z^2 = \frac{\mu_e H_{Z^2}}{\varrho}. \tag{2.3}$$

The external conditions are such that within the medium a state of plane deformation occurs. The conditions which must be satisfied at the plate-vacuum interfaces are: (1) the continuity of the magnetic field vector; (2) the continuity of the total normal and shear stresses across the surface $S_2(a)$, where the loads are prescribed, and (3) the given boundary displacements on the surface $S_1(a)$.

We find Green tensor-field of displacements $g_{ij}(r, \theta; r_0, \theta_0; t)$ of the Eq. (2.2) as follows:

We apply at the point (r_0, θ_0) inside the plate an instantaneous concentrated force, first parallel to radial direction, and then cross-radial direction subject to boundary conditions:

$$\text{(i)}\ g_{rr} = g_{r\theta} = 0 \ \text{on}\ r = a\,; \tag{2.4}$$

$$\text{(ii)}\ g_{\theta r} = g_{\theta\theta} = 0 \ \text{on}\ r = a. \tag{2.5}$$

As a preliminary to the analysis of the forced vibration we first consider the free vibration.

Let us assume that the boundary conditions are homogeneous (i.e. $u_r = u_\theta = 0$ on $r = a$) and consider the solutions in the form

$$\begin{aligned} u_r(r, \theta, t) &= f_n(r) \cos n\theta\, e^{i\omega_0 t}, \\ u_r(r, \theta, t) &= g_n(r) \sin n\theta\, e^{i\omega_0 t}. \end{aligned} \tag{2.6}$$

It can be shown that an infinite set of values for w_0 are obtained from a frequency equation which will be derived later.

The modal functions $f_n(r)$ and $g_n(r)$ satisfy the differential equations:

$$\begin{aligned} &c_2^2\left\{\frac{d^2 f_n}{dr^2} + \frac{1}{r}\frac{df_n}{dr} - \frac{n^2}{r^2} f_n\right\} - c_2^2 \frac{f_n}{r^2} + \\ &\quad + (c_1^2 - c_2^2 + R_Z^2)\left\{\frac{d^2 f_n}{dr^2} + \frac{1}{r}\frac{df_n}{dr} - \frac{f_n}{r^2}\right\} + \\ &\quad + (c_1^2 - c_2^2 + R_Z^2)\left\{\frac{n}{r}\frac{dg_n}{dr} - \frac{n}{r^2} g_n\right\} - \frac{2c_2^2 n}{r^2} g_n = -w_{0n}^2 f_n(r)\,, \\ &(c_1^2 - c_2^2 + R_Z^2)\left(-n\frac{f_n}{r^2} - \frac{n}{r}\frac{df_n}{dr}\right) - \frac{2c_2^2 n}{r^2} f_n + \\ &\quad + c_2^2\left(\frac{d^2 g_n}{dr^2} + \frac{1}{r}\frac{dg_n}{dr} - \frac{n^2 g_n}{r^2} - \frac{g_n}{r^2}\right) - \\ &\quad - n^2(c_1^2 - c_2^2 + R_Z^2)\frac{g_n}{r^2} = -w_{0n}^2 g_n(r)\,. \end{aligned} \tag{2.7}$$

For free vibrations subject to the boundary conditions $u_r = u_\theta = 0$ on $r = a$ we assume

$$u_r(r, \theta, t) = \left[A_n \frac{\partial J_n(\alpha r)}{\partial r} - nB_n \frac{J_n(\beta r)}{r}\right] \cos n\theta e^{i\omega_{0n} t}\,, \tag{2.8}$$

$$u_\theta(r, \theta, t) = \left[-nA_n \frac{J_n(\alpha r)}{r} + B_n \frac{\partial}{\partial r} J_n(\beta r)\right] \sin n\theta e^{i\omega_{0n} t}. \tag{2.9}$$

If we compare (2.6) and (2.9) we can easily see

$$f_n(r) = A_n \frac{\partial J_n(\alpha r)}{\partial r} - nB_n \frac{J_n(\beta r)}{r},$$
$$g_n(r) = -nA_n \frac{J_n(\alpha r)}{r} + B_n \frac{\partial}{\partial r} J_n(\beta r). \tag{2.10}$$

Substituting (2.9) into (2.8) we get

$$A_n \frac{\partial J_n(\alpha a)}{\partial a} - nB_n \frac{J_n(\beta a)}{a} = 0,$$
$$-nA_n \frac{J_n(\alpha a)}{a} + B_n \frac{\partial J_n(\beta a)}{\partial a} = 0. \tag{2.11}$$

In order that A_n and B_n can be determined 'a' and 'β' must satisfy:

$$\begin{vmatrix} \dfrac{\partial J_n(\alpha a)}{\partial a} & -n\dfrac{J_n(\beta a)}{a} \\ -n\dfrac{J_n(\alpha a)}{a} & \dfrac{\partial J_n(\beta a)}{\partial a} \end{vmatrix} = 0$$

or,

$$\alpha\beta J_n'(\alpha a) J_n'(\beta a) - \frac{n^2}{a^2} J_n(\alpha a) J_n(\beta a) = 0. \tag{2.12}$$

Substituting (2.10) into (2.7) and simplifying we get:

$$A_n\{w_{0n}^2 - \alpha^2(c_1^2 + R_Z^2)\} \frac{\partial J_n(\alpha r)}{\partial r} - nB_n(w_{0n}^2 - c_2^2\beta^2) \frac{J_n(\beta r)}{r} = 0, \tag{2.13}$$

$$-nA_n\{w_{0n}^2 - \alpha^2(c_1^2 + R_Z^2)\} \frac{J_n(\alpha r)}{r} + B_n(w_{0n}^2 - c_2^2\beta^2) \frac{\partial J_n(\beta r)}{\partial r} = 0. \tag{2.14}$$

The relations (2.13) and (2.14) hold provided

$$\alpha^2(c_1^2 + R_Z^2) = w_{0n}^2,$$
$$c_2^2 \beta^2 = w_{0n}^2. \tag{2.15}$$

Using the relations (2.15) in the Eqs. (2.12) we get the frequency equations as

$$\alpha^2 \sqrt{\frac{c_1^2 + R_Z^2}{c_2^2}} J_n'(\alpha a) J_n'\left(\alpha \sqrt{\frac{c_1^2 + R_Z^2}{c_2^2}}\, a\right) - \frac{n^2}{a^2} J_n'(\alpha a) J_n\left(\sqrt{\frac{c_1^2 + R_Z^2}{c_2^2}}\, \alpha a\right) = 0 \tag{2.16}$$

from which we determine α_n.

From (2.15) we then determine β_n and natural frequencies w_{0n}. Results for various values of magnetic permeability are shown in Table I.

Table I

$n=0$	D	w	$n=1$	D	w
	0	3.825		0	3.365
	0	6.635		0	5.380
	0	7.010		0	8.485
	0	10.170 etc.		0	9.275 etc.
	0.1	3.830		0.1	3.405
	0.1	6.750		0.1	5.382
	0.1	7.015		0.1	8.490
	0.1	10.175 etc.		0.1	9.420 etc.

Assuming a plate of radius unity, i.e. $a = 1$, we get the roots w of the frequency equation (2.16) for different values of

$$D = \frac{R_Z^2}{c_2^2}$$

for two modes $n = 0$ and $n = 1$.

We determine the ratio A_n/B_n from the equations (2.11).

Hence natural modes are known:

$$\begin{aligned}(u_r)_n &= f_n(r)\cos n\theta,\\ (u_\theta)_n &= g_n(r)\sin n\theta.\end{aligned} \tag{2.17}$$

Consider now the forced vibration due to a unit harmonic concentrated load in r-direction at (r_0, θ_0) with forcing frequency w. The Green functions g_{rr}, $g_{r\theta}$ satisfy the equations of motion.

$$\begin{aligned}&\left[c_2^2\nabla^2 g_{rr} - c_2^2\frac{g_{rr}}{r^2} + (c_1^2 - c_2^2 + R_Z^2)\frac{\partial}{\partial r}\left\{\frac{1}{r}\frac{\partial}{\partial r}\right\} - w^2 g_{rr}\right] +\\ &\quad + \left[(c_1^2 - c_2^2 + R_Z^2)\frac{\partial}{\partial r}\left(\frac{1}{r}\frac{\partial g_{r\theta}}{\partial\theta}\right) - \frac{2c_2^2}{r^2}\frac{\partial g_{r\theta}}{\partial\theta}\right] + \frac{\delta(r-r_0)\,\delta(\theta-\theta_0)}{r} = 0,\\ &\left[(c_1^2 - c_2^2 + R_Z^2)\frac{\partial}{r d_\theta}\left\{\frac{1}{r}\frac{\partial}{\partial r}(r g_{rr})\right\} + \frac{2c_2^2}{r^2}\frac{\partial g_{rr}}{\partial\theta}\right] +\\ &\quad + \left[c_2^2\nabla^2 g_{r\theta} - c_2^2\frac{g_{r\theta}}{r^2} + (c_1^2 - c_2^2 + R_Z^2)\frac{1}{r}\frac{\partial}{\partial\theta}\left\{\frac{1}{r}\frac{\partial g_{r\theta}}{\partial\theta}\right\} - w^2 g_{r\theta}\right] = 0.\end{aligned} \tag{2.18}$$

The solutions to (2.18) are assumed in the form of modal functions

$$g_{rr} = \sum_n f_n(r) \cos n\theta \, T_n \, e^{iwt},$$
$$g_{r\theta} = \sum_n g_n(r) \sin n\theta \, T_n \, e^{iwt}. \tag{2.19}$$

We also expand the given loading functions in terms of the modal functions

$$Q_r = \sum_n q_n f_n(r),$$
$$Q_\theta = \sum_n q_n g_n(r), \tag{2.20}$$

where the loading functions Q_r and Q_θ are the components in the r-direction and θ-direction, respectively.

From (2.18) we can easily see that

$$Q_r = \frac{\delta(r - r_0)}{\pi r} \cos n\theta_0,$$
$$Q_\theta = 0. \tag{2.21}$$

Substituting (2.19) into (2.18) and multiplying by $\cos m\theta$ and integrating with respect to θ we get

$$T_n c_2^2 \left\{ \frac{d^2 f_n}{dr^2} + \frac{1}{r} \frac{df_n}{dr} - \frac{n^2}{r^2} f_n \right\} -$$
$$- c_2^2 \, T_n \frac{f_n}{r^2} + T_n(c_1^2 - c_2^2 + R_Z^2) \left\{ \frac{d^2 f_n}{dr^2} + \frac{1}{r} \frac{df_n}{dr} - \frac{f_n}{r^2} \right\} +$$
$$+ T_n(c_1^2 - c_2^2 + R_Z^2) \left\{ \frac{n}{r} \frac{dg_n}{dr} - \frac{n}{r^2} g_n \right\} -$$
$$- \frac{2c_2^2 n}{r^2} T_n g_n + \frac{\delta(r - r_0) \cos n\theta_0}{\pi r} = - T_n w^2 f_n(r),$$

$$T_n(c_1^2 - c_2^2 + R_Z^2) \left(- \frac{n f_n}{r^2} - \frac{n}{r} \frac{df_n}{dr} \right) -$$
$$- \frac{2c_2^2 n}{r^2} T_n f_n + T_n c_2^2 \left(\frac{d^2 g_n}{dr^2} + \frac{1}{r} \frac{dg_n}{dr} - \frac{n^2}{r^2} g_n - \frac{g_n}{r^2} \right) -$$
$$- T_n \cdot n \frac{(c_1^2 - c_2^2 + R_Z^2)}{r^2} g_n = - T_n w^2 g_n(r), \text{ for each '}n\text{'}. \tag{2.22}$$

We define the operators as

$$L_1 = c_2^2\left\{\frac{d^2}{dr^2} + \frac{1}{r}\frac{d}{dr} - \frac{n^2}{r^2}\right\} - \frac{c_2^2}{r^2} + \\ + (c_1^2 - c_2^2 + R_Z^2)\left\{\frac{d^2}{dr^2} + \frac{1}{r}\frac{d}{dr} - \frac{1}{r^2}\right\},$$

$$L_2 = (c_1^2 - c_2^2 + R_Z^2)\left\{\frac{n}{r}\frac{d}{dr} - \frac{n}{r^2}\right\} - \frac{2c_2^2 n}{r^2},$$

$$L_3 = (c_1^2 - c_2^2 + R_Z^2)\left(-\frac{n}{r^2} - \frac{n}{r}\frac{d}{dr}\right) - \frac{2c_2^2 n}{r^2},$$

$$L_4 = c_2^2\left(\frac{d^2}{dr^2} + \frac{1}{r}\frac{d}{dr} - \frac{n^2}{r^2} - \frac{1}{r^2}\right) - \frac{n(c_1^2 - c_2^2 + R_Z^2)}{r^2}. \quad (2.23)$$

Using the relations (2.23) we can re-write the equations (2.22) as

$$T_n(L_1 f_n + L_2 g_n) + q_n f_n = -w^2 T_n f_n,$$
$$T_n(L_3 f_n + L_4 g_n) + q_n g_n = -w^2 T_n g_n. \quad (2.24)$$

We can also re-write the homogeneous equations (2.7) in the operator forms

$$L_1 f_n + L_2 g_n = -w_{0n}^2 f_n,$$
$$L_3 f_n + L_4 g_n = -w_{0n}^2 g_n. \quad (2.25)$$

Using the relations (2.25) into the relations (2.24) we get

$$\{T_n(w^2 - w_{0n}^2) + q_n\} f_n(r) = 0,$$
$$\{T_n(w - w_{0n}^2) + q_n\} g_n(r) = 0. \quad (2.26)$$

These two relations of (2.26) will be satisfied if

$$T_n(w^2 - w_{0n}^2) + q_n = 0. \quad (2.27)$$

Orthogonality relations:

If X_i, p_i denote body and surface forces respectively, which produce in a body the displacements, u_i, while X_i', p_i' belong to the other system of forces producing the displacements u_i'.

We have by BETTI's reciprocal theorem [1]

$$\int_{(B)} X_i u_i' \, dv + \int_{(S)} p_i u_i' \, ds = \int_{(B)} X_i' u_i \, dv + \int_{(S)} p_i' u_i \, ds, \quad (2.28)$$

where B is the whole body bounded by the surface S.

In our case the surface integrals are zero as the displacements are zero on the boundary.

Hence (2.28) reduces to

$$\int_B X_i u_i' \, dv = \int_B X_i' \, u_i \, dv \ . \tag{2.29}$$

The only body forces are the inertia forces $\varrho \, \partial^2 u_i / \partial t^2$.

If the displacements in such a system be assumed in the form $u_i = U_i \, e^{iwt}$, with U_i dependent of time, and if u_i is the displacement in the m^{th} mode and u_i the displacement in the n^{th} mode, then the time reduced form of (2.29) is

$$\left| w_m^2 - w_n^2 \right| \int_{(B)} \varrho \overset{(m)}{U_i} \overset{(n)}{U_i} \, dv = 0 \, .$$

Thus

$$\int_{(B)} \overset{(m)}{U_i} \overset{(n)}{U_i} \, dv = 0, \text{ if } m \neq n \, ,$$
$$\neq 0, \text{ if } m = n \, . \tag{2.30}$$

(Summation convention is used on i).

This is the general orthogonality condition for undamped elastic systems.

Now we multiply the first equation of (2.20) by $f_m(r)$ and the second equation of (2.20) by $g_m(r)$ and then add, we get

$$Q_r f_m + Q_\theta g_m = \sum_n q_n (f_n f_m + g_n g_m) \, . \tag{2.31}$$

Integrating (2.31) over the whole plate

$$\int_0^a \left[Q_r f_m + Q_\theta g_m \right] r \, dr = \Sigma q_n \left[\int_0^a \{ f_n f_m + g_n g_m \} \right] r \, dr \, . \tag{2.32}$$

Using the expression for Q_r and Q_θ from (2.21) in the relation (2.32) we get, with the help of (2.30)

$$q_m = \frac{\int_0^a r \cdot \dfrac{\delta(r - r_0)}{\pi r} \cos n\theta_0 \cdot f_m \, dr}{\int_0^a r \, [f_m^2 + g_m^2] \, dr} = \frac{f_m(r_0) \cos m\theta_0}{\pi l^2} \, ,$$

where l^2 is the scale factor,

$$\int_0^a r \, [f_m^2 + g_m^2] \, dr \, . \tag{2.33}$$

Using (2.33) into (2.27) we get

$$T_n = -\frac{q_n}{w^2 - w_{0n}^2} = \frac{f_n(r_0)\cos n\theta_0}{\pi l^2 (w_{0n}^2 - w^2)} . \tag{2.34}$$

Hence we know the Green's functions g_{rr}, $g_{r\theta}$ in the case of harmonic unit concentrated load as

$$g_{rr} = \sum_n \frac{f_n(r_0)\, f_n(r) \cos n\theta \cos n\theta_0}{\pi l^2 (w_{0n}^2 - w^2)} e^{iwt} ,$$

$$g_{r\theta} = \sum_n \frac{f_n(r_0)\, g_n(r) \sin n\theta \cos n\theta_0}{\pi l^2 (w_{0n}^2 - w^2)} e^{iwt} . \tag{2.35}$$

We now apply to the fundamental system (the system in which the elastic body is entirely fixed along the circumference) an instantaneous harmonic unit concentrated force, parallel to cross-radial direction subject to the boundary conditions

$$g_{\theta r} = g_{\theta\theta} = 0 \text{ on } r = a. \tag{2.36}$$

The Green's functions $g_{\theta r}$, $g_{\theta\theta}$ satisfy the equation of motion

$$\left[c_2^2 \nabla^2 g_{\theta r} - c_2^2 \frac{g_{\theta r}}{r^2} + (c_1^2 - c_2^2 + R_Z^2) \frac{\partial}{\partial r}\left\{\frac{1}{r}\frac{\partial}{\partial r}(r g_{\theta r})\right\} - w^2 g_{\theta r}\right] +$$

$$+\left[(c_1^2 - c_2^2 + R_Z^2) \frac{\partial}{\partial r}\left(\frac{1}{r}\frac{\partial g_{\theta\theta}}{\partial \theta}\right) - \frac{2c_2^2}{r^2}\frac{\partial g_{\theta\theta}}{\partial \theta}\right] = 0$$

$$\left[(c_1^2 - c_2^2 + R_Z^2) \frac{\partial}{r\partial\theta}\left\{\frac{1}{r}\frac{\partial}{\partial r}(r g_{\theta r})\right\} + \frac{2c_2^2}{r^2}\frac{\partial g_{\theta r}}{\partial \theta}\right] +$$

$$+\left[c_2^2 \nabla^2 g_{\theta\theta} - c_2^2 \frac{g_{\theta\theta}}{r^2} + (c_1^2 - c_2^2 + R_Z^2) \frac{1}{r}\frac{\partial}{\partial \theta}\left\{\frac{1}{r}\frac{\partial}{\partial \theta}\right\} - w^2 g_{\theta\theta}\right] +$$

$$+ \frac{\delta(r - r_0)\, \delta(\theta - \theta_0)}{r} = 0 . \tag{2.37}$$

If we follow the same method as before we find

$$g_{\theta r} = \sum_n \frac{g_n(r_0)\, f_n(r) \cos n\theta \sin n\theta_0}{\pi l^2 (w_{0n}^2 - w^2)} e^{iwt},$$

$$g_{\theta\theta} = \sum_n \frac{g_n(r_0)\, g_n(r) \sin n\theta \sin n\theta_0}{\pi l^2 (w_{0n}^2 - w^2)} e^{iwt} . \tag{2.38}$$

Now we know all the components of the Green's functions $g_{ij}(r, \theta; r_0, \theta_0; w)$ and we can use them to find the displacement functions $u_i(r, \theta, w)$.

Applying BETTI's reciprocal theorem [1] we can find the relations for circular case:

$$u_k(r_0, \theta_0, w) = u_k^0(r_0, \theta_0, w) - \int_{S_2(a)} U_i(a, w)\, L[g_{ik}]\, ds(a)\,, \tag{2.39}$$

where

$$u_k^0(r_0, \theta_0, w) = \iint_{(R)} g_{ik}\, X_i\, dv - \int_{S_1(a)} f_i L[g_{ik}]\, ds(a) \tag{2.40}$$

and

$$L = \mu\left(\nabla^2 - \frac{1}{c_1^2}\frac{\partial^2}{\partial t^2}\right)\delta_{ij} + (\lambda + \mu)\,\partial_i\,\partial_j,\ \ (i, j, k = 1,2).$$

Here $S_1(a)$ is the surface where the displacements are given and $S_2(a)$ is the surface where the loads are specified, and R represents the whole region of the body.

Since all the quantities X_i, g_{ik}, and f_i in (2.40) are known, the displacements u_k^0 in the fundamental system are known.

Re-writing the Eq. (2.39) in component forms we get

$$u_r(r_0, \theta_0, w) = u_r^0(r_0, \theta_0, w) - \int_{\theta_1}^{\theta_2}\left[2\mu\frac{\partial g_{rr}}{\partial r}\,U_r + \right.$$

$$\left. + \mu\left\{\frac{1}{r}\frac{\partial g_{rr}}{\partial \theta} + \frac{\partial g_{r\theta}}{\partial r} - \frac{g_{r\theta}}{r}\right\}U_\theta + \lambda U_r\left\{\frac{1}{r}\frac{\partial}{\partial r}(r g_{rr}) + \frac{1}{r}\frac{\partial g_{r\theta}}{\partial \theta}\right\}\right] a\,d\theta\,,$$

$$u_\theta(r_0, \theta_0, w) = u_\theta^0(r_0, \theta_0, w) - \int_{\theta_1}^{\theta_2}\left[2\mu\frac{\partial g_{\theta r}}{\partial r}\,U_r + \mu\left\{\frac{\partial g_{\theta\theta}}{\partial \theta} + \frac{\partial g_{\theta\theta}}{\partial r} - \frac{g_{\theta\theta}}{r}\right\}U_\theta + \right.$$

$$\left. + \lambda U_r\left\{\frac{1}{r}\frac{\partial}{\partial r}(r g_{\theta r}) + \frac{1}{r}\frac{\partial g_{\theta\theta}}{\partial \theta}\right\}\right] a\,d\theta\,, \tag{2.41}$$

Here U_r, U_θ are the unknown reactions on the boundary $S_2(a)$ and they are to be found out from the boundary conditions $S_2(a)$.

In order to determine the unknown functions U_r, U_θ we perform on the expression (2.41) the operation $L'(\ldots)$. The prime on the operator L denotes that the operation refers to the point (r_0, θ_0). Then we pass from the interior point (r_0, θ_0) εR to the point (a, θ) on the boundary and get

$$Q_r(a, \theta, w) = -\int_{\theta_1}^{\theta_2}\left[2\mu L'\left(\frac{\partial g_{rr}}{\partial r}\right)U_r + \mu\left\{L'\left(\frac{1}{r}\frac{\partial g_{rr}}{\partial \theta}\right) + L'\left(\frac{\partial g_{r\theta}}{\partial r}\right) - L'\left(\frac{g_{r\theta}}{r}\right)\right\} + \right.$$

$$\left. + \lambda U_r\left\{L'\left(\frac{1}{r}\frac{\partial}{\partial r}(r g_{rr})\right) + L'\left(\frac{1}{r}\frac{\partial g_{r\theta}}{\partial \theta}\right)\right\}\right] a\,d\theta\,,$$

$$Q_\theta(a, \theta, w) = -\int_{\theta_1}^{\theta_2}\left[2\mu L'\left(\frac{\partial g_{\theta r}}{\partial r}\right)U_r + \mu\left\{L'\left(\frac{1}{r}\frac{\partial g_{\theta r}}{\partial \theta}\right) + L'\left(\frac{\partial g_{\theta\theta}}{\partial r}\right) - L'\left(\frac{g_{\theta\theta}}{r}\right)\right\}U_\theta + \right.$$

$$\left. + \lambda U_r\left\{L'\left(\frac{1}{r}\frac{\partial}{\partial r}\right)(r g_{\theta r}) + L'\left(\frac{1}{r}\frac{\partial g_{\theta\theta}}{\partial \theta}\right)\right\}\right] a\,d\theta\,, \tag{2.42}$$

where r, $r_0 = a$ and $\theta_0 = \theta'$. As Q_r, Q_θ are known and (2.42) represents two Fredholm integral equations, we can easily determine U_r and U_θ from the system of equations.

By choosing different sets of loadings on $S_2(a)$, where the loadings are prescribed, we can find different values of U_r and U_θ for different mixed boundary value problems. Thus it is easy to find displacement functions u_r and u_θ. After having determined the displacements u_i we obtain the deformations e_{ij} and stresses σ_{ij}.

It is clear that we can extend our considerations to the case in which on the surfaces S_2, S_4 and S_6, . . . are the prescribed loadings, while on the surfaces S_1, S_3 and S_5, . . . are the given displacements.

We can also see from the above results that if we know the modal functions of the free vibrations we can find the solutions of the forced vibration problems in eigen-functions expansion. This method is very useful for any forced vibration of circular plate. From the Table of free vibrations we see that the numerical values are shifted considerably in the magneto-elastic from that of elastic case in all orders of frequency equations.

Next we will consider a number of applications of this method in subsequent papers.

Acknowledgement

I am thankful to DR. W. W. RECKER, Associate Professor, the State University of New York at Buffalo, for his continuous help and interest in the preparation of this paper.

REFERENCES

1. W. NOWACKI, Mixed Boundary Value Problems of Elastodynamics, Proc. Vibr. Probl., 3(5), 1964, pp. 161—177.
2. YU CHEN, Vibrations: Theoretical Methods, Addison-Wesley Publ. Co. Inc., Reading, Massachusetts, 1966.
3. I. STAKGOLD, Boundary Value Problems of Mathematical Physics, Vol. II, MacMillan Co., New York, 1968.
4. R. KUMAR, Magneto-elastic Vibrations of a Perfectly Conducting Isotropic Solid Cyclinder, Proc. Vibr. Probl., 3(8), 1967, pp. 273—278.

Acta Physica Academiae Scientiarum Hungaricae, Tomus 43 (1), pp. 93—97 (1977)

EVENT HORIZONS AROUND A PARTICLE SURROUNDED BY A STATIC CONFINEMENT POTENTIAL

By

K. L. NAGY*

JOINT INSTITUTE FOR NUCLEAR RESEARCH
LABORATORY OF THEORETICAL PHYSICS
DUBNA, USSR

(Received 21. VI. 1977)

After solving one of the Einstein's equations in the case of a spherically symmetric confinement potential, the locations of event horizons are discussed in gravitational theory and in the "strong black hole" picture of RECAMI and CASTORINA.

1. In elementary particle physics, in order to explain the confinement of quarks in mesons and hadrons it is widely accepted to take a two body "confinement potential" in the form

$$V(r) = \frac{e^{-mr}}{r}(\alpha_0 + K_0 r^2)\,. \tag{1}$$

For instance, [1] gives in the case of the charmonium for the $c-\bar{c}$ interaction

$$\alpha_0 = -0{,}2,\ K_0 = -\frac{\alpha_0}{a^2},\ a = 0{,}2\,fm,\ m = 0\,.$$

In the $c\,c$ $(\bar{c}\,\bar{c})$ interaction the potential is supposed to be repulsive; $V_{cc} = V_{\bar{c}\bar{c}} = -V_{c\bar{c}}$, i.e. $\alpha_0 = +0.2$ in Eq. (1).

Our aim here is to investigate the space-time structure around an object (c or $\bar{c}$) which for the following arguments, tentatively, is supposed to exist alone, surrounded by a field representing (1).

The relativistic considerations necessary to carry out our program are quite straightforward, we quote [2] only, where similar calculations for the Yukawa field have been performed.

2. The total potential energy of an object described by a distribution ϱ,

$$\int \varrho(x)\,dx = 1$$

self-interacting through (1) is

$$W = \frac{1}{2}\int \varrho(x)\,\varrho(x')\,\frac{e^{-m|x-x'|}}{|x-x'|}\,|(\alpha + K\,|\,x-x'\,|^2)\,d^3x\,d^3x'\,. \tag{2}$$

* On leave of absence from the Institute of Theoretical Physics, Roland Eötvös University, Budapest, Hungary.

Introducing

$$\Phi(x) = \int \varrho(x') \frac{e^{-m|x-x'|}}{|x-x'|} (\alpha + K \mid x-x' \mid^2)\, d^3x'$$

W takes the form

$$W = -\frac{1}{2} \int \varrho(x)\, \Phi(x)\, d^3x \,.$$

A direct calculation gives

$$\Delta\Phi - m^2\Phi = -4\pi\alpha\varrho + K\varphi,$$

$$\varphi = \int \varrho(x')\, e^{-m|x-x'|} \left(\frac{2}{|x-x'|} - 4m \right) d^3x.$$

Substituting ϱ into (2), after performing the integration over x', W is

$$W = \frac{1}{8\pi\alpha} \int (|\nabla\Phi|^2 + m^2\Phi^2 + K\Phi\varphi)\, d^3x\,, \tag{3}$$

therefore the energy density in our case is the following:

$$u(x) = \frac{1}{8\pi\alpha} (|\nabla\Phi|^2 + m^2\Phi^2 + K\Phi\varphi). \tag{4}$$

One might notice the non-definiteness of (4), which, from a field theoretical point of view, seems to be related to an indefinite metric quantization [3, 4].

For a point source

$$\Phi = \frac{e^{-mr}}{r} (\alpha + Kr^2)\,, \quad \varphi = \frac{e^{-mr}}{r} (2 - 4mr)\,,$$

and

$$u = \frac{1}{8\pi\alpha}\, e^{-2mr} \left[\frac{\alpha^2}{r^4} + \frac{2\alpha^2 m}{r^3} + \frac{2\alpha^2 m^2}{r^2} - \frac{4\alpha\, Km}{r} + \right.$$
$$\left. + 3K^2 + 4\alpha K m^2 - 6K^2 mr + 2K^2 mr^2 \right]. \tag{5}$$

Writing

$$ds^2 = e^{\nu(r)} c^2\, dt^2 - e^{\lambda(r)}\, dr^2 - r^2(d\theta^2 + \sin^2\theta\, d\varphi^2)\,,$$

one of the Einstein's equations gives [2]:

$$-\frac{8\pi G}{c^4} u = e^{-\lambda} \left(\frac{1}{r^2} - \frac{\lambda'}{r} \right) - \frac{1}{r^2}\,, \tag{6}$$

where G is the gravitational constant. With the notation

$$g(r) = e^{-\lambda(r)},$$

Eq. (6) reads

$$rg' + g = 1 - \frac{8\pi G}{c^4} r^2 u\,, \tag{7}$$

for which the solution is

$$g = 1 - \frac{2\,m_0}{r} - \frac{8\pi G}{c^4 r} \int r^2 u(r)\, dr\,,$$

where $m_0 = GMc^{-2}$ is an integration constant.

Substituting (5) into Eq. (7) one gets

$$g(r) = 1 - \frac{2m_0}{r} + \frac{G}{c^4} e^{-2mr} \left(\frac{\alpha}{r^2} + \frac{\alpha m}{r} + 2Kmr - \frac{K^2}{\alpha} r^2 + \frac{K^2 m^2}{\alpha} r^3 \right). \tag{8}$$

$g(r) = 0$ gives the locations of the event horizons if there $\exp \nu(r)$ is finite. Note that the metric tends to the Minkowski's one only if $m \neq 0$.

Let us suppose, however, that $mr \ll 1$ in the whole relevant interval. Then

$$g(r) \approx 1 - \frac{2m_0}{r} + \frac{G}{c^4} \left(\frac{\alpha}{r^2} - \frac{K^2}{\alpha} r^2 \right) \equiv f(r)\,, \tag{9}$$

and $f = 0$ leads to a fourth order equation. For $r \gg a$ one immediately observes the possibility of an event horizon (from (8) actually two) around ($\alpha > 0$!)

$$r^2 \sim \frac{\alpha c^4}{GK^2}\,,$$

with the above data for α and $K(\alpha = \alpha_0 \hbar c)$

$$r \sim 5{,}5 \cdot 10^5 \text{ cm},$$

an enormously large value. The assumption $mr \ll 1$ leads to the ratio

$$\frac{m}{m_\pi} \ll 2{,}5 \cdot 10^{-19},$$

where m_π is the pion mass.

It is quite obvious that the starting formula (1) for the potential cannot be extrapolated for such distances. Indeed, as c and $\bar{c}$ separate, the energy

grows until a pair of light quarks is created, which together with c and $\bar{c}$ form a pair of mesons, therefore the whole former simple picture breaks down.

Lonely lived quarks, therefore, in reality do not seem to produce some type of "exotic" gravitational black holes.

3. Next we wish to discuss the ideas of RECAMI and CASTORINA [5, 6] concerning the concept of "strong black holes" in our case.

According to the classical mechanics, two particles with the same mass due to their gravitational interaction move around each other in a flat space-time as if they were led by the force

$$F = -G\frac{M^2}{r^2}\,. \tag{10}$$

General relativity tells us that the motion is actually a geodetic one in a curved space-time, the structure of which is described by Einstein's equations. In an attractive strong interaction e.g. with

$$F = -\frac{\alpha}{r^2}e^{-mr}, \quad \alpha > 0, \tag{11}$$

for those distances where $mr \ll 1$, at the classical level one may say that the interaction is of a "gravitational" nature, but G is replaced by

$$G \to \frac{\alpha}{M^2}\,. \tag{12}$$

In analogy with the gravitational theory, let us suppose now that the expression (11) is just as crude a description of the reality as (10) is in the gravitational case. Instead, the motion of a strongly interacting particle (for attraction) is a geodetic one in a (strongly) curved space-time, where the (strong) space-time structure (measured by pion or gluon signals?) is determined by Einstein's equations, but according to (12) G is replaced by αM^{-2}.

Adopting this idea, introducing

$$K = -\frac{\alpha}{a^2}\,,\ x = \frac{r}{a}\,,\ A = \frac{Mc^2 a}{\alpha}\,,\ G \to \frac{\alpha}{M^2}\,,$$

the equation $f(r) = 0$, where f is given by (9) takes the form

$$x^4 - A^2x^2 + 2Ax - 1 = 0. \tag{13}$$

The value of A with the data of [1] ($M = M_c = 1{,}6$ GeV) is $A = 8{,}5$. With this value of A from Eq. (13) one immediately observes that there are three

positive real roots, two of them lie close to A^{-1}, the third one is in the immediate neighbourhood of A. Keeping in mind the former picture, this means that a lonely lived quark produces a "strong black hole" for its antiparticle (attraction) of the radius: $R \approx aA = 1{,}7\,fm$, then the antiparticle falls down to

$$R_c \approx aA^{-1} = 0{,}02\,fm\,.$$

The condition $mr \ll 1$ gives for the gluon mass

$$\frac{m}{m_\pi} \ll 1\,.$$

4. Apart from the above considerations, one might notice that one of the Einstein's equations (for the coefficient of dr^2) can exactly be solved for those situations where a particle is surrounded by a given field representing a spherically symmetric static potential V in the form

$V =$ Yukawa times an arbitrary polynomial in r.

REFERENCES

1. E. Eichten et al., Phys. Rev. Lett., **34**, 369, 1975.
2. D. K. Ross, Nuovo Cimento, **8A**, 603, 1972.
3. J. E. Kiskis, Phys. Rev., D**10**, 4268, 1974.
4. K. L. Nagy, Acta Phys. Hung., **39**, 171, 1975.
5. E. Recami and P. Castorina, Lett. Nuovo Cimento, **15**, 347, 1976.
6. R. Mignani, Lett. Nuovo Cimento, **16**, 6, 1976.

Acta Physica Academiae Scientiarum Hungaricae, Tomus 43 (1), pp. 99—103 (1977)

UNIFIED THEORY OF FERROELECTRIC PHASE TRANSITIONS: QUANTUM LIMIT

By

S. STAMENKOVIĆ

"BORIS KIDRIC" INSTITUTE FOR NUCLEAR SCIENCES, VINČA, YUGOSLAVIA

N. M. PLAKIDA, V. L. AKSIENOV

JOINT INSTITUTE FOR NUCLEAR RESEARCH, DUBNA, USSR

and

T. SIKLÓS

CENTRAL RESEARCH INSTITUTE FOR PHYSICS, BUDAPEST, HUNGARY

(Received 13. VII. 1977)

In the framework of the unified theory of ferroelectrics displacive type phase transitions are investigated in the $T = 0K$ quantum limit, when the phase transition is due to the zero-point fluctuations. The critical value of the zero-point energy is evaluated in the case of the completely ordered and disordered lattices, not taking into account tunnelling.

In [1] a unified model for ferroelectric phase transitions has been presented, which took into account both the statistical disordering of the ions in the cells and the dynamic instability of the fluctuations of the lattice leading to displacive phase transitions. The solution of the self-consistent system of equations for the two order parameters, $\sigma_\alpha = < \sigma_i^\alpha >$, the average number of ions in the state $\alpha = \pm 1$, and $\vec{b}_\alpha = < \vec{S}_i^\alpha >$, the average displacement of ions in the cell in the state α has been obtained in [1] and subsequently in [2], in the classical limit of high temperatures, $kT \gg \hbar\omega_D$.

It is also interesting to investigate the quantum limit of zero temperature when the phase transition is determined by the quantum fluctuations and the energy of the zero point fluctuations and not by thermal excitations. Displacive phase transitions in the model of ferroelectrics in the quantum case has been investigated also in [3].

1. Self-consistent system of equations

The model of ferroelectrics [1] is described by a system of harmonically coupled ions, each of which can occupy one of the two minima ($\alpha = \pm 1$) of a one-particle potential well:

$$H = \sum_{i,\alpha} \sigma_i^\alpha \left\{ \frac{1}{2m} (\vec{p}_i^\alpha)^2 - \frac{A}{2} (\vec{S}_i^\alpha)^2 + \frac{B}{4} (\vec{S}_i^\alpha)^4 \right\} + \\ + \frac{1}{2} \sum_{i,j}' \sum_{\alpha,\beta} \sigma_i^\alpha \sigma_j^\beta \varphi_{ij} (\vec{S}_i^\alpha - \vec{S}_j^\beta)^2 , \tag{1}$$

where the projection operators $\sigma_i^+ = 1$ or 0 (accordingly $\sigma_i^- = 1-\sigma_i^+ = 0$ or 1) if at the i-th lattice point the ion is in the state $\alpha = +1$ or $\alpha = -1$ respectively. $\vec{p}_i^{\alpha}$ and $\vec{S}_i^{\alpha}$ are the momenta and the coordinate of the ion, A and B are parameters of the one-particle potential well, φ_{ij} is the coupling constant between the ions in the three dimensional lattice.

From the condition of equilibrium $d < \vec{p}_i^{\alpha}(t) > /dt = 0$ in [1] the following equation has been obtained

$$\eta_\alpha^3 - (1 - 3y_\alpha)\,\eta_\alpha + (\eta_+ + \eta_-)\,f_0\,\sigma_{-\alpha} = 0\,, \tag{2}$$

which relates the equilibrium position of ions $\eta_\alpha = (B/A)^{1/2} < S_i^{\alpha} >$ to the average number of ions $\sigma_\alpha = < \sigma_i^{\alpha} >$ in the state α. Here $f_0 = \sum_j \varphi_{ij}/A = \varphi_0/A$ is the dimensionless coupling constant.

The quantity y_α is the average squared displacement of ions from the equilibrium position in the state α. It has been determined by the help of the phonon Green's function in the form

$$\begin{aligned} y_\alpha &= \frac{B}{A} < (S_i^{\alpha} - b_i^{\alpha})^2 > = \frac{B}{A} < (u_i^{\alpha})^2 > = \\ &= \frac{B}{NA^2} \sum_q \int_0^\infty d\omega \, \coth \frac{\omega}{2\theta} \left[-\frac{1}{\pi} Im\, D_q^{\alpha}(\omega + i\varepsilon) \right], \end{aligned} \tag{3}$$

$$D_q^{\alpha}(\nu) = \frac{\nu^2 - (\Delta_{-\alpha}^2 + f_0)}{(\nu^2 - \nu_{q+}^2)\,(\nu^2 - \nu_{q-}^2) - \sigma_+\sigma_- f} = \frac{\nu^2 - (\Delta_{-\alpha}^2 + f_0)}{(\nu^2 - \nu_{q1}^2)\,(\nu^2 - \nu_{q2}^2)}\,, \tag{4}$$

where

$$\nu^2 = \omega^2/(A/m);\ \nu_{q\alpha}^2 = \Delta_\alpha^2 + (f_0 - \sigma_\alpha f_q);$$

$$\nu_{q(1,2)}^2 = \frac{1}{2}(\nu_{q+}^2 + \nu_{q-}^2) \pm \frac{1}{2}\{(\nu_{q+}^2 - \nu_{q-}^2)^2 + 4\sigma_+\sigma_- f_q^2\}^{1/2};$$

$$\Delta_\alpha^2 = -1 + 3\,(\eta_\alpha^2 + y_\alpha);\ f_q = (1/A)\sum_j \varphi_{ij} e^{i\vec{q}(\vec{l}_i - \vec{l}_j)}).$$

Performing the integration in (3) in the case of zero temperature, when $\coth(\omega/2\theta) = 1$, taking into account (4) one obtains:

$$y_\alpha = \frac{\lambda}{N} \sum_q \frac{1}{2(\nu_{q_1} + \nu_{q_2})} \left(1 + \frac{\Delta_{-\alpha}^2 + f_0}{\nu_{q_1}\,\nu_{q_2}} \right), \tag{5}$$

where $\lambda = (A/m)^{1/2}/(A^2/B)$ is a quantum parameter, proportional to the ratio of the energy of zero point fluctuations, $\hbar\omega_0 = (A/m)^{1/2}$ and the height of the barrier in the one-particle potential well, $\mathbf{u}_0 = (A^2/4B)$.

For the determination of the average population σ_α or the pseudospin variable $\sigma = \langle \sigma_i^z \rangle = (2\sigma_+ - 1)(1-2\sigma_-)$, an effective pseudospin Hamiltonian has been introduced:

$$\tilde{H}_s = \sum_i h_i \sigma_i^z - \frac{1}{2} \sum_{i,j} \tilde{J}_{ij} \sigma_i^z \sigma_j^z , \tag{6}$$

where $\sigma_i^z = \pm 1$, h_i and $\tilde{J}_{ij}$ are the average effective field and the "exchange integral" which depend on the state of phonon subsystem [1].

In the Hamiltonian (1) and (6) the tunnelling between states $\alpha = \pm 1$ is not taken into account and therefore in the limit $\theta \to 0$ a unique solution $\sigma = 1$ appears (if $\tilde{J}_{ij} > 0$, $h_i > 0$). The effect of tunnelling, suggested in [4], makes it possible to generalize the Hamiltonian (1) and to introduce in (6) the transverse field, $\Omega \sum_i \sigma_i^x$, which in turn may lead to the solution $\sigma \to 0$ in the case $\theta \to 0$. In the present work we will not discuss the solution of the self-consistent system of equations for the phonon system and the pseudospin system in the range $0 < \sigma < 1$; instead we will investigate only two cases, namely the case of the completely ordered, $\sigma = 1$ lattice and the case of the completely disordered, $\sigma = 0$ lattice. Doing so, we will assume that the right choice of the value of the transverse field Ω, can ensure the transition from $\sigma = 1$ to $\sigma = 0$ in the case of zero temperature, $\theta = 0$.

2. Displacive type phase transition in ordered lattices

In the completely ordered lattice all the ions are in the same state, for example $\alpha = +1$ and $\sigma = 1$. In this case the equation of selfconsistency (5) takes the following form:

$$y_+ = \frac{\lambda}{2N} \sum_q \frac{1}{\sqrt{\Delta_+^2 + f_0 - f_q}} = \frac{\lambda}{2} \int_0^{\omega_D} \frac{g(\omega^2)\, d\omega^2}{\sqrt{\Delta_+^2 + \omega^2}}, \tag{7}$$

where the density of the phonon frequencies

$$g(\omega^2) = \frac{1}{N} \sum_q \delta\,(f_0 - f_q - \omega^2),\ \omega < \omega_D \tag{8}$$

has been introduced.

Taking into account the condition of equilibrium (2), in the case of $\sigma = 1$ ($\sigma_- = 0$) we obtain one equation for the self-consistent determination of the equilibrium displacement η or the gap in the spectrum of the frequencies $\Delta_+^2 = 2\eta^2$, in the ferroelectric phase:

$$\eta^2 = 1 - \frac{3}{2} \lambda \int_0^{\omega_D} \frac{g(\omega^2)\, d\omega^2}{\sqrt{2\eta^2 + \omega^2}} . \tag{9}$$

As can be seen the solution of this equation for the ferroelectric phase with $\eta \neq 0$ exists only if $\lambda < \lambda_{c(1)}$, where the critical value $\lambda_{c(1)}$ is determined by

$$\lambda_{c(1)} = \frac{2}{3}\left\{\int_0^{\omega_D} \frac{g(\omega^2)\, d\omega^2}{\omega}\right\}^{-1} = \frac{2}{3}\frac{\sqrt{f_0}}{\mu_{-1}}\,. \tag{10}$$

Here $\mu_{-1} = \overline{\omega^{-1}}$ is the average of the inverse of the frequency; for the Debye spectrum $g(\omega^2) = 3\omega/2\omega_D^3$; $\mu_{-1} = 3/2\sqrt{2} \approx 1$ if $\omega_D^2 = 2f_0$. Consequently, displacive type transition in ordered lattice can take place only if the lattice consists of sufficiently heavy ions, that is if

$$m > \left(\frac{2}{3}\frac{\sqrt{\varphi_0}}{\mu_{-1}}\frac{A}{B}\right)^{-2} \tag{11}$$

for a given coupling constant φ_0 between the ions and a given width $S_0 = \sqrt{A/B}$ of the one-particle potential well in accordance with [3].

3. Displacive type phase transition in disordered lattices

Let us discuss the effect of disordering on the displacive type phase transition. Putting in (2) and (3) $\sigma = 0$, corresponding to equal number of ions in the states $\alpha = +1$ and $\alpha = -1$ and consequently meaning that $\Delta_+^2 = \Delta_-^2 = \Delta_0^2$; $\eta_+ = \eta_- = \eta$ we get the following system of equations:

$$\eta^2 = 1 - f_0 - 3y\,, \tag{12}$$

$$y = \frac{\lambda}{2}\int_0^{\omega_D} \frac{g(\omega^2)\, d\omega^2}{\sqrt{\Delta_0^2 + \omega^2}}\,, \tag{13}$$

Therefore the self-consistent equation for the determination of the gap, $\Delta_0^2 > 0$ in the phonon spectrum in the case of $\sigma = 0$ and $\eta > 0$ takes the following form

$$\Delta_0^2 = 2\eta^2 - f_0 = 2 - 3f_0 - 3\lambda\int_0^{\omega_D} \frac{g(\omega^2)\, d\omega^2}{\sqrt{\Delta_0^2 + \omega^2}}\,. \tag{14}$$

Displacive type phase transition, $\eta > 0$, can take place if $\lambda < \lambda_{c(0)}$, where the critical value of λ is determined by the condition $\Delta_0^2(\lambda_{c(0)}) = 0$, that is

$$\lambda_{c(0)} = \frac{2}{3}\frac{\sqrt{f_0}}{\mu_{-1}}\left(1 - \frac{3}{2}f_0\right) = \lambda_{c(1)}\left(1 - \frac{3}{2}f_0\right)\,. \tag{15}$$

Consequently, the occurrence of the disordering decreases both the limiting value of the allowed energy of the zero-point fluctuations and the limiting value of the temperature of the phase transition in the classical limit of high temperatures: $\tau_c^{(0)} = \tau_c^{(1)} \{1-(3/2)f_0\}$ [1]. However, it has to be mentioned that the transition into the state $\sigma = 0$ can take place only if $f_0 \ll 1$, and therefore formula (15) is valid only if $f_0 \ll 1$. In the case $f_0 \gg 1$, in accordance with [1], only the state with $\sigma = 1$ is possible and formula (1) is valid.

The explicit effect of tunnelling and the evaluation of the limiting value of the quantum parameter λ in this case will be dealt with in a separate paper.

REFERENCES

1. S. Stamenković, N. M. Plakida, V. L. Aksienov and T. Siklós, Phys. Rev., **B14**, 5080, 1976.
2. V. L. Aksienov, H. Breter, J. M. Kovalski, N. M. Plakida and V. B. Priezzhev, Fiz. tv. tela, **18**, 2920, 1976.
3. T. R. Koehler and N. S. Gillis, Phys. Rev., **B7**, 4980, 1973.
4. S. Stamenković, N. M. Plakida, V. L. Aksienov and T. Siklós, Report KFKI-77—4 Budapest, 1977; Acta Phys. Hung. **42**, 265, 1977.

RECENSIONES

T. MITSUI, J. TATSUZAKI and E. NAKAMURA:

An Introduction to the Physics of Ferroelectrics

Gordon and Breach Science Publishers, London—New York—Paris, 1976

The book issued as the first volume of the "Ferroelectricity and Related Phenomena" series was in its original Japanese edition a textbook for advanced students. Though in this rapidly developing field it is impossible to write down a truly systematic theory of ferroelectricity, the book in its present revised and completed form is not simply an introduction to the contents of the literature but a presentation of the present status of the field of ferroelectrics in a systematic form. So it is suitable not only for students interested in this topic but also for young scientists, particularly experimental researchers, concerned with ferroelectricity.

While in the first part of the volume the theory of ferroelectricity is built up on the basis of experimental results based on the investigation of concrete types of crystals, in chapters V—VII the reader can also get acquainted with the theoretical treatment of both order-disorder and displacive types of ferroelectrics. In these chapters the emphasis is laid on the theory of phase transformations in ferroelectric materials.

The appendices contain the domain structures and the chemical and physical data of ferroelectrics and antiferroelectrics known so far.

Finally, the book contains a copious collection of references.

G. GROMA

Molecular Fluids — Les Houches 1973

Edited by R. Balian and G. Weill. Gordon and Breach Science Publishers, London—New York—Paris 1976, p. 459

The volume contains the material of the Molecular Fluids Summer School organized in Les Houches. As is well known, the term "molecular fluids" should always be used with caution, because it has been created by necessity and is used only owing to the lack of a better and more concise way of specifying the field in question. The subject is the physics of the condensed assemblies of large molecules, forming amorphous polymers or liquid crystals, or simply: fluids of high viscosity, etc. The School, offering a fruitful discussion for the specialists, and now the volume, publishing the lecture notes, both aim at bridgeing the gap between theoretical, and experimental investigations in the field, where, tending to describe and understand the nature of real matter, theoreticians and experimentalists have to master each other's language not only the words but also the notions and ideas. The volume contains the following contributions: Linear Response Theory (R. ZWANZIG), Correlation Functions (C. BROT), Dynamics of Chain Molecules (W. H. STOCKMAYER), Configurations and Dynamics of the Polymer Chain (S. F. EDWARDS), Viscoelasticity of Polymers (J. D. FERRY), Structural Problems in Liquid Crystal Physics (R. B. MEYER), Nematodynamics (P. G. DE GENNES), Electrodynamics of Liquid Crystals (G. DURAND), and some special seminars.

I. ABONYI

M. MLADJENOVIC: Development of Magnetic Beta-Ray Spectroscopy

Springer-Verlag, Berlin—Heidelberg—New York, 1976, p. 282

The book which appeared in the series "Lecture Notes in Physics" surveys the past and present state of magnetic beta-spectroscopy.

First of all in a short historical review the most important stages of development are given from the second decade of the century up to our days.

Separate chapters are devoted to different types of spectrometers: semicircular focused ones, prismatic spectrometers (magnetic prisms), toroidal and trochoidal types; one chapter about each type of magnetic lenses (short, long and intermediate). Similarly, individual chapters are dealing with different types of special spectrometers, i.e. those with bidirectional and higher order focusing characteristics.

Preceding the chapters dealing with the different instrument types there are separate chapters on general issues, like the most important parameters and component parts of spectrometers, the basic characteristics and equations of electron movement and those of magnetic optics. Further, among the chapters dealing with the different types of spectrometers, the necessary and possible ways of magnetic field correction are given.

The final chapter of the book gives an account of magnetic spectrometers developed on optical analogy i.e. which consist of two magnetic lenses with a magnetic prism between them.

The book of Prof. MLADJENOVIC, the first monograph in the literature on beta-spectrometers, is really very easy to follow, and as far as magnetic spectroscopes are concerned, it gives a complete summary of the different types of beta-spectroscopes. The author himself has been working actively in this field, and the contents of the book originate from the university lectures and seminar talks delivered by him at different Universities (Belgrade, Rome, Cairo, Nashville).

It should be noted here that it is spectrometers that are nearly exclusively dealt with here, other instrumental relations (like preparation of sources, or problems of detection) are just touched or even not mentioned at all. No attempt is made to survey the results of investigations carried out with beta-spectroscopes, though one might expect to find chapters about them considering the title of the book. This field of research is extremely rich that is why the material, in spite of its limitation mentioned above, makes a book of 300 pages. Anyway, it might be disputable, whether certain types of beta-spectroscopes of historical interest only (e.g. magnetic lens types) are worth the detailed discussion, as given in the book.

D. BERÉNYI

WOLFGANG MEILING; Kernphysikalische Elektronik

Akademie-Verlag, Berlin, 1975

The book published in the "Wissenschaftliche Taschenbücher" series is a very good summary of the principles of nuclear electronics. Prof. W. MEILING defines the subject matter as the instrumentation problems of data acquisition processing and handling but he omits all problems of the regulation and control of reactors as well as the special electronic instruments of high energy physics. Starting from the interaction of radiation with matter, the first Chapter makes the reader acquainted with the most important features of detectors (G. M. counter, semi-conductors, scintillation counters). In Chapter 2 a very good survey of pulse amplifiers is given and also some circuit diagrams are presented. In the third Chapter the problems of nonlinear pulse shaping are reviewed. The subject of the fourth Chapter is the pulse counter together with a universal scaler and the ratemeters. Chapter 5 is devoted to measurement problems of time differences and time correlations. A good survey of pulse height analysis is presented in Chapter 6. The last Chapter gives information on the on-line use of small computers and on CAMAC interfaces. This paperback book of small format is recommended to electronicians and senior students, and also to physicists, engineers, medical researchers and all specialists concerned with radioactive isotopes and other nuclear radiation sources.

L. MEDVECZKY

Printed in Hungary

A kiadásért felel az Akadémiai Kiadó igazgatója. Műszaki szerkesztő: Botyánszky Pál

A kézirat nyomdába érkezett: 1977. VIII. 18. — Terjedelem: 9,25 (A/5) ív, 27 ábra

78.4834 Akadémiai Nyomda, Budapest — Felelős vezető: Bernát György

NOTES TO CONTRIBUTORS

I. PAPERS will be considered for publication in Acta Physica Hungarica, only if they have not previously been published or submitted for publication elsewhere. They may be written in English, French, German or Russian.

Papers should be submitted to

Prof. I. Kovács, Editor
Department of Atomic Physics, Technical University
1521 Budapest, Budafoki út 8, Hungary

Papers may be either articles with abstracts or short communications. Both should be as concise as possible, articles in general not exceeding 25 typed pages, short communications 8 typed pages.

II. MANUSCRIPTS

1. Papers should be submitted in five copies.

2. The text of papers must be of high stylistic standard, requiring minor corrections only.

3. Manuscripts should be typed in double spacing on good quality paper, with generous margins.

4. The name of the author(s) and of the institutes where the work was carried out should appear on the first page of the manuscript.

5. Particular care should be taken with mathematical expressions. The following should be clearly distinguished, e.g. by underlining in different colours: special founts (italics, script, bold type, Greek, Gothic, etc.); capital and small letters; subscripts and superscripts, e.g. x_2, x^3; small l and 1; zero and capital O; in expressions written by hand: e and l, n and u, v and v, etc.

6. References should be numbered serially and listed at the end of the paper in the following form: J. Ise and W. D. Fretter, Phys. Rev., *76*, 933, 1949.

For books, please give the initials and family name of the author(s), title, name of publisher, place and year of publication, e.g.: J. C. Slater, Quantum Theory of Atomic Structures, I. McGraw-Hill Book Company, Inc., New York, 1960.

References should be given in the text in the following forms: Heisenberg [5] or [5].

7. Captions to illustrations should be listed on a separate sheet, not inserted in the text.

III. ILLUSTRATIONS AND TABLES

1. Each paper should be accompanied by five sets of illustrations, one of which muts be ready for the blockmaker. The other sets attached to the copies of the manuscript may be rough drawings in pencil or photocopies.

2. Illustrations must not be inserted in the text.

3. All illustrations should be identified in blue pencil by the author's name, abbreviated title of the paper and figure number.

4. Tables should be typed on separate pages and have captions describing their content. Clear wording of column heads is advisable. Tables should be numbered in Roman numerals (I, II, III, etc.).

IV. MANUSCRIPTS not in conformity with the above Notes will immediately be returned to authors for revision. The date of receipt to be shown on the paper will in such cases be that of the receipt of the revised manuscript.

Reviews of the Hungarian Academy of Sciences are obtainable at the following addresses:

AUSTRALIA
C.B.D. LIBRARY AND SUBSCRIPTION SERVICE, Box 4886, G.P.O., *Sydney N.S.W.2001*
COSMOS BOOKSHOP, 145 Ackland Street, *St. Kilda (Melbourne), Victoria 3182*

AUSTRIA
GLOBUS, Höchstädtplatz 3, *1200 Wien XX*

BELGIUM
OFFICE INTERNATIONAL DE LIBRAIRIE, 30 Avenue Marnix, *1050 Bruxelles*
LIBRAIRIE DU MONDE ENTIER, 162 Rue du Midi, *1000 Bruxelles*

BULGARIA
HEMUS, Bulvar Ruszki 6, *Sofia*

CANADA
PANNONIA BOOKS, P.O. Box 1017, Postal Station "B", *Toronto, Ontario M5T 2T8*

CHINA
CNPICOR, Periodical Department, P.O. Box 50, *Peking*

CZECHOSLOVAKIA
MAD'ARSKÁ KULTURA, Národní třida 22, *115 66 Praha*
PNS DOVOZ TISKU, Vinohradská 46, *Praha 2*
PNS DOVOZ TLAČE, *Bratislava 2*

DENMARK
EJNAR MUNKSGAARD, Norregade 6, *1165 Copenhagen*

FINLAND
AKATEEMINEN KIRJAKAUPPA, P.O. Box 128, *SF-00101 Helsinki 10*

FRANCE
EUROPERIODIQUES S. A., 31 Avenue de Versailles, *78170 La Celle St.-Cloud*
LIBRAIRIE LAVOISIER, 11 rue Lavoisier, *75008 Paris*
OFFICE INTERNATIONAL DE DOCUMENTATION ET LIBRAIRIE, 48 rue Gay-Lussac, *75240 Paris Cedex 05*

GERMAN DEMOCRATIC REPUBLIC
HAUS DER UNGARISCHEN KULTUR, Karl-Liebknecht-Strasse 9, *DDR-102 Berlin*
DEUTSCHE POST ZEITUNGSVERTRIEBSAMT, Strasse der Pariser Kommüne 3—4, *DDR-104 Berlin*

GERMAN FEDERAL REPUBLIC
KUNST UND WISSEN ERICH BIEBER, Postfach 46, *7000 Stuttgart 1*

GREAT BRITAIN
BLACKWELL'S PERIODICALS DIVISION, Hythe Bridge Street, *Oxford OX1 2ET*
BUMPUS, HALDANE AND MAXWELL LTD., Cowper Works, *Olney, Bucks MK46 4BN*
COLLET'S HOLDINGS LTD., Denington Estate, *Wellingborough, Northants NN8 2QT*
W.M. DAWSON AND SONS LTD., Cannon House, *Folkestone, Kent CT19 5EE*
H. K. LEWIS AND CO., 136 Gower Street, *London WC1E 6BS*

GREECE
KOSTARAKIS BROTHERS, International Booksellers, 2 Hippokratous Street, *Athens-143*

HOLLAND
MEULENHOFF-BRUNA B.V., Beulingstraat 2, *Amsterdam*
MARTINUS NIJHOFF B.V., Lange Voorhout 9—11, *Den Haag*
SWETS SUBSCRIPTION SERVICE, 347b Heereweg, *Lisse*

INDIA
ALLIED PUBLISHING PRIVATE LTD., 13/14 Asaf Ali Road, *New Delhi 110001*
150 B-6 Mount Road, *Madras 600002*
INTERNATIONAL BOOK HOUSE PVT. LTD., Madame Cama Road, *Bombay 400039*
THE STATE TRADING CORPORATION OF INDIA LTD., Books Import Division, Chandralok, 36 Janpath, *New Delhi 110001*

ITALY
EUGENIO CARLUCCI, P.O. Box 252, *70100 Bari*
INTERSCIENTIA, Via Mazzé 28, *10149 Torino*
LIBRERIA COMMISSIONARIA SANSONI, Via Lamarmora 45, *50121 Firenze*
SANTO VANASIA, Via M. Macchi 58, *20124 Milano*
D. E. A., Via Lima 28, *00198 Roma*

JAPAN
KINOKUNIYA BOOK-STORE CO. LTD., 17-7 Shinjuku-ku 3 chome, Shinjuku-ku, *Tokyo 160-91*
MARUZEN COMPANY LTD., Book Department, P.O. Box 5050 Tokyo International, *Tokyo 100-31*
NAUKA LTD. IMPORT DEPARTMENT, 2-30-19 Minami Ikebukuro, Toshima-ku, *Tokyo 171*

KOREA
CHULPANMUL, *Phenjan*

NORWAY
TANUM-CAMMERMEYER, Karl Johansgatan 41—43, *1000 Oslo*

POLAND
WĘGIERSKI INSTYTUT KULTURY, Marszalkowska 80, *Warszawa*
CKP I W ul. Towarowa 28 *00-958 Warsaw*

ROMANIA
D. E. P., *Bucureşti*
ROMLIBRI, Str. Biserica Amzei 7, *Bucureşti*

SOVIET UNION
SOJUZPETCHATI — IMPORT, *Moscow* and the post offices in each town
MEZHDUNARODNAYA KNIGA, *Moscow G-200*

SPAIN
DIAZ DE SANTOS, Lagasca 95, *Madrid 6*

SWEDEN
ALMQVIST AND WIKSELL, Gamla Brogatan 26, *101 20 Stockholm*
GUMPERTS UNIVERSITETSBOKHANDEL AB, Box 346, *401 25 Göteborg 1*

SWITZERLAND
KARGER LIBRI AG, Petersgraben 31, *4011 Basel*

USA
EBSCO SUBSCRIPTION SERVICES, P.O. Box 1943, *Birmingham*, Alabama 35201
F. W. FAXON COMPANY, INC., 15 Southwest Park, *Westwood*, Mass. 02090
THE MOORE-COTTRELL SUBSCRIPTION AGENCIES, *North Cohocton, N. Y. 14868*
READ-MORE PUBLICATIONS, INC., 140 Cedar Street, *New York, N. Y. 10006*
STECHERT-MACMILLAN, INC., 7250 Westfield Avenue, *Pennsauken* N. J. 08110

VIETNAM
XUNHASABA, 32, Hai Ba Trung, *Hanoi*

YUGOSLAVIA
JUGOSLAVENSKA KNJIGA, Terazije 27, *Beograd*
FORUM, Vojvode Mišiča 1, *21000 Novi Sad*

Index: 26.025
Acta Phys. Hung. Tom. 43. No. 1. Budapest, 14. IV. 1978 HU-ISSN 0001-6705

ACTA PHYSICA

ACADEMIAE SCIENTIARUM HUNGARICAE

TOMUS XLIII FASCICULUS 2

AKADÉMIAI KIADÓ, BUDAPEST

1977

ACTA PHYS. HUNG. APAHAQ 43 (2) 107—200 (1977)

ACTA PHYSICA

ACADEMIAE SCIENTIARUM HUNGARICAE

SZERKESZTI

KOVÁCS ISTVÁN

Az *Acta Physica* angol, német, francia vagy orosz nyelven közöl értekezéseket. Évente két kötetben, kötetenként 4—4 füzetben jelenik meg. Kéziratok a szerkesztőség címére (1521 Budapest XI., Budafoki út 8.) küldendők.

Megrendelhető a belföld számára az Akadémiai Kiadónál (1363 Budapest Pf. 24. Bankszámla 215-11488), a külföld számára pedig a „Kultura" Külkereskedelmi Vállalatnál (1389 Budapest 62, P.O.B. 149. Bankszámla 217-10990), vagy annak külföldi képviseleteinél.

The *Acta Physica* publish papers on physics in English, German, French or Russian, in issues making up two volumes per year. Subscription: $ 36.00 per volume. Distributor: "Kultura" Foreign Trading Company (1389 Budapest 62, P.O. Box 149) or its representatives abroad.

Die *Acta Physica* veröffentlichen Abhandlungen aus dem Bereich der Physik in deutscher, englischer, französischer oder russischer Sprache, in Heften, die jährlich zwei Bände bilden.

Abonnementspreis pro Band: $ 36.00. Bestellbar bei »Kultura« Außenhandelsunternehmen (1389 Budapest 62, Postfach 149) oder seinen Auslandsvertretungen.

Les *Acta Physica* publient des travaux du domaine de la physique en français, anglais, allemand ou russe, en fascicules qui forment deux volumes par an.

Prix de l'abonnement: $ 36.00 par volume. On peut s'abonner à l'Entreprise du Commerce Extérieur «Kultura» (1389 Budapest 62, P.O.B. 149) ou chez représentants à l'étranger.

«*Acta Physica*» публикуют трактаты из области физических наук на русском, немецком, английском и французском языках.

«*Acta Physica*» выходят отдельными выпусками, составляющими два тома в год.

Подписная цена — $ 36.00 за том. Заказы принимает предприятие по внешней торговле «Kultura» (1389 Budapest 62, P.O.B. 149) или его заграничные представительства.

ACTA PHYSICA

ACADEMIAE SCIENTIARUM HUNGARICAE

TOMUS XLIII FASCICULUS 2

AKADÉMIAI KIADÓ, BUDAPEST

1977

ACTA PHYS. HUNG.

INDEX

COMMUNICATIONES BREVES

Acta Physica Academiae Scientiarum Hungaricae, Tomus 43 (2), pp. 109—115 (1977)

THE DETERMINATION OF TRUE DECAY TIME OF FLUORESCENCE OF DYE SOLUTIONS AT A VERY LOW CONCENTRATION

By

I. KETSKEMÉTY, L. GÁTI, A. GYŐRI and L. KOZMA

INSTITUTE OF EXPERIMENTAL PHYSICS, JÓZSEF ATTILA UNIVERSITY, SZEGED

(Received 23. V. 1977)

By determining the luminescence characteristics of dye solutions at a very low concentration ($10^{-8}-10^{-7}$ mole/l) the effect of secondary luminescence cannot be neglected, even in the case of the integrating spherical cuvette, since the luminescence light leaves the cuvette after several meters of "rambling". In our present paper the calculation method is described, considering the effect of secondary luminescence, taking into account the determination of true decay time.

1. The method of determining the luminescence characteristics of dye solutions at a very low concentration with integrating spherical cuvette has been described in [1—4]. In these articles by determining the luminescence characteristics — fluorescence spectrum, yield, decay time — the effect of secondary luminescence was assumed to be negligible owing to very low concentration ($10^{-9}-10^{-6}$ mole/l).

In the course of our later experiments on decay time, it has been observed that the decay times determined on the basis of the method published in the above mentioned articles showed a concentration dependence even in the range of very low concentrations, namely τ was increasing with the increase of concentration. From the further fact that τ', τ'' obtained by measurements, the mean rambling time of the exciting and luminescence photons respectively is of an order of several ns in the spherical cuvette (further abbreviation G), in this way the luminescence light covers a path of several meters in G, it has been assumed that the above mentioned variation in τ can be attributed to the effect of the secondary luminescence.

2. Instead of Eq. (14) of [1] $\left(V\frac{dn'}{dt} = N_f - N_{fr}\right)$ concerning the time-dependent part of density n' of primary luminescence photon gas, we start from the differential equation

$$V\frac{dn'}{dt} = V\left(\frac{dn_1}{dt} + \frac{dn_2}{dt}\right) = N_{f1} + N_{f2} - N_{f1r} - N_{f2r} \tag{1}$$

in the determination of the true decay time, where N_{f1} is the number of primary luminescence photons emitted by exciting photons in G during unit

time, N_{f2} means the number of secondary luminescence photons emitted by primary luminescence photons in G during unit time, N_{f1r} and N_{f2r} mean the loss of primary and secondary luminescence photons, respectively, owing to non-complete diffuse reflexion on the interior surface of G. (The loss of escaped photons through uncoated areas of the surface of G can be neglected.) Furthermore $n' = n_1 + n_2$ (n_1, n_2 mean the density of primary and secondary fluorescence photon gas, respectively).

Based on the consideration mentioned in [1], the following relations are valid for N_{f1r} and N_{f1}

$$N_{f1r} = n_1 \frac{c}{n} (1 - R') \, r^2 \pi \, , \tag{2}$$

$$N_{f1} = \frac{1}{\tau} \eta^* V \frac{c}{n} k(\nu) \int_0^\infty e^{-t'/\tau} n_\nu (t - t') \, dt' . \tag{3}$$

Here $k(\nu)$ is the absorption coefficient of the examined solution at the exciting frequency ν, R the reflexion coefficient at mean frequency of luminescence light of the interior surface of G, r radius, V volume, n_ν density of exciting photon gas, n refractive index of the solution, c velocity of light.

The values of N_{f2r} and N_{f2} concerning secondary luminescence can be given in the same way

$$N_{f2r} = n_2 \frac{c}{n} (1 - R') \, r^2 \pi \, , \tag{4}$$

$$N_{f2} = \frac{1}{\tau} V \frac{c}{n} \int_0^\infty e^{-t'/\tau} n_1 (t - t') \left[\int_0^\infty f(\nu'') \, \eta^*(\nu'') \, k(\nu'') \, d\nu'' \right] dt' , \tag{5}$$

where $f(\nu'')$, $\eta^*(\nu'')$ and $k(\nu'')$ mean the normalised luminescence quantum spectrum, the function of absolute quantum yield, and absorption spectrum, respectively, in the overlapping range of the spectra.

Substituting the formula n_ν, the density of photon gas, obtained by solving the differential equation (11) [1], into the formula N_{f1} (3) — taking into consideration the sinusoidal excitement of intensity $N(t) = N \sin \omega t$ applied at phase fluorometer —

$$n_\nu = \frac{N}{V \sqrt{\omega^2 + \left[\frac{c}{n} k(\nu) + \frac{3c}{4rn} (1 - R) \right]^2}} \sin \omega (t - \tau') \, , \tag{6}$$

here ω is the angular frequency of the sinusoidal exciting fluxus, R is the reflexion coefficient of the interior surface of G at the exciting light frequency ν. Having done the indicated integration, and substituting the formula obtained for N_{f1} in the first part of differential equation (1), after integration we have

the following formula for the time-dependence of primary fluorescence photon gas density

$$n_1(t) = A_1 \sin \omega(t - \tau' - \tau'' - \tau) \,. \tag{7}$$

Here the value of constant A_1 is

$$A_1 = \frac{N/V \cdot \eta^* \cdot c/n \cdot k(\nu)}{\sqrt{\left\{\omega^2 + \left[\frac{3c}{4rn}(1 - R')\right]^2\right\}\left\{\omega^2 + \left[ck(\nu) + \frac{3c}{4rn}(1 - R)\right]^2 \cdot (1 + \omega^2\tau^2)\right\}}} \,. \tag{8}$$

According to Eq. (7) the density of primary fluorescence photon gas follows the variation of the intensity of the exciting light with a phase delay corresponding to time $\tau + \tau' + \tau'' = \tau^*$. Thus if no secondary luminescence occurs, the decay time of the fluorescence can be obtained from delay time τ^* measured by the fluorometer, based on the relation $\tau = \tau^* - \tau' - \tau''$. Here τ' and τ'' are the mean rambling time already mentioned above of exciting and luminescence photon gas in the solution in G, respectively, which can be determined by calculation from the formula given by solving the corresponding differential equation

$$\tau' = \frac{1}{\omega} \operatorname{arc\,tg} \frac{\omega n}{ck(\nu) + \frac{3c}{4r}(1 - R)} \tag{9}$$

and

$$\tau'' = \frac{1}{\omega} \operatorname{arc\,tg} \frac{\omega n}{\frac{3c}{4r}(1 - R')} \,. \tag{10}$$

Since the reflexion coefficients R, R' of G are difficult to determine directly, rambling time τ_0' of the exciting photons in the solvent in G has been introduced, which is immediately measurable in the integrating cuvette containing the pure solvent. For in this case $k(\nu) = 0$ based on Eq. (9)

$$\tau_0' = \frac{1}{\omega} \operatorname{arc\,tg} \frac{\omega n}{\frac{3c}{4r}(1 - R)} \,, \tag{11}$$

comparing this equation with Eq. (9) the formula

$$\tau' = \frac{1}{\omega} \operatorname{arc\,tg} \frac{\omega n}{ck(\nu) + \frac{\omega n}{\operatorname{tg} \tau_0 \omega}} \tag{12}$$

is given. In case of the small arguments on the right side of Eq. (12) (with $\operatorname{tg}\varphi \approx \varphi$ approximation)

$$\tau' \approx \frac{n}{ck(\nu) + \dfrac{n}{\tau_0'}} .$$

If τ_0' is measured either at ν exciting, or at ν' mean frequency of luminescence and R, R' can be calculated from (10) and (11)

$$\tau'' \approx \tau_0' \frac{1 - R}{1 - R'} \tag{13}$$

we obtain a very simple approximative formula.

3. If the intensity of the secondary luminescence can be neglected, its effect of τ is to be calculated as follows.

We substitute the formula for n_1 in Eq. (7) into the formula written for secondary luminescence photons N_{f2} (5), and integrate according to time t'. We substitute N_{f2} gained in the second part of differential equation (1)

$$V \frac{dn_2}{dt} = N_{f2} - N_{f2r} . \tag{1/b}$$

Having solved Eq. (1/b) in similar steps as above, we obtain for the time-dependence of density of secondary luminescence photon gas in G:

$$n_2(t) = A_2 \sin \omega(t - \tau' - 2\tau'' - 2\tau) , \tag{14}$$

where

$$A_2 = \frac{N/V \cdot \eta^* (c/n)^2 \, k(\nu)}{(1 + \omega^2\tau^2) \cdot \left\{\omega^2 + \left[\dfrac{3c}{4rn}(1 - R')\right]^2 \cdot \sqrt{\omega^2 + \left[ck(\nu) + \dfrac{3c}{4rn}(1 - R)\right]^2}\right\}} \times$$

$$\times \int_0^\infty \eta^*(\nu'') f(\nu'') \, k(\nu'') \, d\nu'' . \tag{15}$$

From formula (14) it is easy to see that the density of the secondary fluorescence photon gas produced in G follows the variation of the intensity of the exciting light with a phase delay corresponding to $\tau' + 2\tau'' + 2\tau$.

The quotient of the intensity of secondary and primary fluorescence light being proportional to the quantity obtained according to $\varkappa$ — which has been introduced previously in the course of secondary fluorescence cor-

rection [5] — from Eq. (7), (14) and Eq. (8), (15) in the following formula

$$\frac{n_2(t)_{\max}}{n_1(t)_{\max}} = \frac{A_2}{A_1} = \frac{c/n}{\sqrt{(1+\omega^2\tau^2)\left\{\omega^2 + \left[\frac{3c}{4rn}(1-R')\right]^2\right\}}} \times$$

$$\times \int_0^\infty \eta^*(\nu'')\, f(\nu'')\, k(\nu'')\, d\nu'' \approx \frac{c}{n} \frac{\tau''}{\sqrt{(1+\omega^2\tau^2)\,(1+\omega^2\tau''^2)}} \times \tag{16}$$

$$\int_0^\infty \eta^*(\nu'')\, f(\nu'')\, k(\nu'')\, d\nu''.$$

Here we substituted $\frac{3c}{4rn}(1-R')$ from the approximate formula $\tau'' \approx \omega n/(3c/4rn)(1-R')$ from Eq. (10) in case of small arguments.

4. The timewise variations of the primary and secondary luminescence photons can be considered harmonical vibrations in phase delay as compared to each other, and by superposing them we apply the relation concerning superposition of harmonical parallel vibrations of equal frequency. Thus the phase constant of the resulting vibration is

$$\operatorname{tg}\alpha = \frac{A_1 \sin\alpha_1 + A_2 \sin\alpha_2}{A_1 \cos\alpha_1 + A_2 \cos\alpha_2}, \tag{17}$$

applying it to our case $\alpha = \operatorname{arc\,tg}\,\omega\tau^*$, $\alpha_1 = \operatorname{arc\,tg}\,\omega(\tau' + \tau'' + \tau)$, $\alpha_2 = \operatorname{arc\,tg}\,\omega(\tau' + 2\tau'' + 2\tau)$.

We denoted the delay time of primary fluorescence occurring together with the secondary luminescence with τ^*, measured directly by fluorometer. We come to the formula containing the true decay time τ by adequate trigonometrical transformation of Eq. (17), by substituting the formula for α, α_1 and α_2, and by denoting the value of A_2/A_1 calculated in the way given in Eq. (16) with K.

$$\tau^* = \frac{\sqrt{1+\omega^2(\tau_2+2\tau)^2}\,(\tau_1+\tau) + K\sqrt{1+\omega^2(\tau_1+\tau)^2}\,(\tau_2+2\tau)}{\sqrt{1+\omega^2(\tau_2+2\tau)^2} + K\sqrt{1+\omega^2(\tau_1+\tau)^2}} \tag{18}$$

where $\tau_1 = \tau' + \tau''$ and $\tau_2 = \tau' + 2\tau''$.

Eq. (18) contains true decay time τ implicitly and as it is easy to see from Eq. (16) K is also dependent on τ, therefore instead of the explicit, seemingly very complicated formula of decay time, τ is calculated from the equation above with the successive approximation method with a pocket calculator. Starting from the first approximate value $\tau^0 = \tau^* - \tau' - \tau''$ in the case of

neglecting secondary luminescence ($K = 0$) the calculation can be completed quite quickly with arbitrary accuracy.

The details of the method to determine τ' and τ'' in Eq. (18) are given in Part 3. The "overlapping" integral in the second part of formula $K = A_2/A_1$ (16) has been determined with a graphical integrating method by using the results of the measurements $\eta^*(\nu'')$, $f(\nu'')$ and $k(\nu'')$ taken from [2].

5. From our several experimental results on dye solutions, we publish our data obtained on Rhodamine 6G aqueous solution as an example. The dye concentration was varied from $2.5 \cdot 10^{-8}$ mole/l to $2.5 \cdot 10^{-7}$ mole/l on a logarithmic scale. 6 per cent acetic acide was applied as an additive material.

We placed the integrating cuvette of 4 cm diameter, having coated the exterior surface with diffuse reflecting MgO in a way described in [6] into the phase fluorometer applied in [7, 8].

The luminescence was excited by the light of 546 nm wavelength of a light source type OSRAM HBO 450 and the exciting light scattered in the solution was eliminated with a crossing filter type OG3.

The experimental results are shown in Table I and Fig. 1, where τ^* is the delay time measured directly with the fluorometer, and $\tau^0 (= \tau^* - \tau' - \tau'')$ decay time uncorrected for the effect of secondary luminescence, τ the true decay time corrected for the effect of secondary luminescence. Rambling time τ'' in Table I in our case equivalent to rambling time τ_0', is calculated on the basis of Eq. (10), and rambling time τ' based on Eq. (9) by using absorption coefficient $k(\nu)$ is indicated in the Table as well. The Table also contains the value K calculated from Eq. (16).

As can be seen on the curve giving the dependence of τ^0 on dye concentration, the uncorrected decay time similarly to the ones published in numerous previous references [6—10] increases with the concentration due to the effect of secondary luminescence. The corrected true decay time τ holds continually under τ^0. Disregarding the value τ belonging to the last, highest concentration (where according to [1, 2] the condition $k(\nu) \cdot r < 10^{-2}$ to produce a homogeneous and isotropic photon gas is by no means given) a mean value 4.4 ns is given for decay time (with a mean error less than 10 per cent). This value agrees to a good approximation with the results concerning this dye, measured by several authors, by means of laser pulse fluorometer (e.g. [10—12]) it is, however, considerably greater than our values determined in a concentration range 10^{-5}—10^{-3} mole/l [13]. This deviation seems to be right, based on the data of our experiments up to the present, and is due to physical processes depending on dye concentrations. The fact is also worth mentioning that the deviation of τ from τ^0 is important even at the lowest concentration applied ($\approx$20 per cent) which exceeds the error of measurement considerably. Consequently, the correction to the effect of secondary luminescence cannot be neglected even in the case of

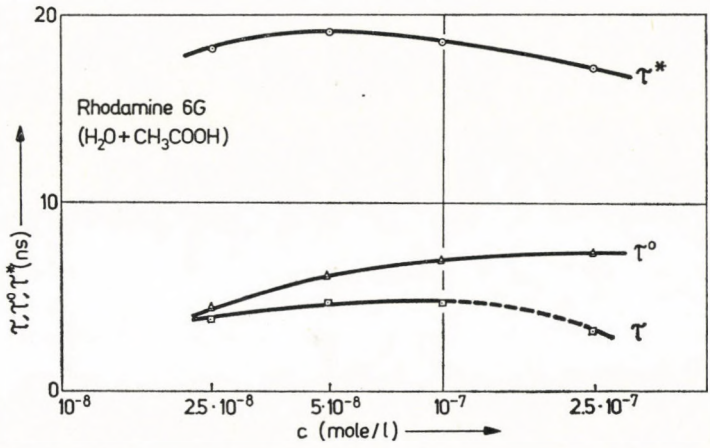

Fig. 1

Table I

Decay time of Rhodamine 6 G aqueous solution at several dye concentrations

Dye concentr. c (mole/l)	τ^* (ns)	$\tau'' = \tau_0'$ (ns)	τ' (ns)	$k(\nu)$ (cm^{-1})	K	τ^0 (ns)	τ (ns)
$2.5 \cdot 10^{-8}$	18.17	7.48	6.22	$1.288 \cdot 10^{-3}$	0.0928	4.47	3.78
$5 \cdot 10^{-8}$	18.95	7.48	5.31	$2.577 \cdot 10^{-3}$	0.1829	6.16	4.79
$1 \cdot 10^{-7}$	18.51	7.48	4.09	$5.153 \cdot 10^{-3}$	0.3667	6.94	4.52
$2.5 \cdot 10^{-7}$	17.22	7.48	2.40	$1.288 \cdot 10^{-2}$	0.9376	7.34	3.11

solutions of the lowest concentration showing an intensity of luminescence still suitable for measuring, especially in case of Rhodamine 6G and similar dyes showing a strong overlapping of absorption and emission spectra.

REFERENCES

1. I. Ketskeméty and L. Kozma, Acta Phys. Hung., **29,** 331, 1970.
2. I. Ketskeméty, L. Kozma, É. Farkas and B. Rácz, Magyar Fiz. F. i., **19,** 315, 1971.
3. I. Ketskeméty, L. Kozma, É. Farkas, Acta Phys. et Chem., Szeged, **16,** 7, 1970.
4. И. Кечкемети, Л. Козма, Э. Фаркаш, ЖПС, **17,** 59, 1972.
5. A. Budó and I. Ketskeméty, Acta Phys. Hung., **7,** 207, 1957.
6. A. Győri, University Doctoral Dissertation (in preparation).
7. L. Gáti and I. Szalma, Acta Phys. et Chem. Szeged, **14,** 3, 1968.
8. L. Gáti, Candidate Dissertation, Szeged, 1968.
9. A. Schmillen, Z. Phys., **135,** 294, 1953.
10. H. J. Cirkel, L. Ringwelski and F. P. Schäfer, Z. Phys. Chem., **81,** 158, 1972.
11. R. R. Alfano, S. L. Shapiro and W.-Yu, Optics Commun., **7,** 191, 1973.
12. M. E. Mack, J. Appl. Phys., **39,** 2483, 1969.
13. L. Gáti, Acta Phys. et Chem. Szeged (to be published).

Acta Physica Academiae Scientiarum Hungaricae, Tomus 43 (2), pp. 117—123 (1977)

KINETICS OF DISORDER-ORDER TRANSITION IN S—Se ALLOYS

By

M. K. EL-MOUSLY and M. F. KOTKATA

PHYSICS DEPARTMENT, FACULTY OF SCIENCE, AIN SHAMS UNIVERSITY, CAIRO, EGYPT

(Received 1. VI. 1977)

Three different parameters; d (density), χ (thermal conductivity), and σ (electrical conductivity) have been used to investigate the crystal growth in two Se—S glassy alloys. The kinetic analysis indicates that the crystallization process takes place through switching of the chemical bonds with energy 26—28 kcal/mole.

Introduction

The quantitative study of the dependence of the crystallization rate of Se—S alloys on the percent concentration of S-atoms showed a minimum rate at about 5 at. % S [1, 2]. This has been explained by the microheterogeneity of the states of S in both chains and rings of Se. The minimum microheterogeneity in amorphous Se—S alloys is expected to lie between SSe_{50} and SSe_{20} [2]. At the same time, the number of crystalline centres increases, also, in this region ($SSe_{50} \rightarrow SSe_{20}$), while the rate of linear growth of crystallites drastically decreases in the presence of S.

Experimental

$SSe_{32.5}$ and $SSe_{22.5}$ glassy alloys have been prepared by quenching from the melts [3]. Each sample has been subjected to isothermal aging at three different temperatures between T_g and T_m, namely 70, 80 and 90 °C. The process of aging led to great change in all the measured physical quantities; the density (d), thermal conductivity (χ) and electrical conductivity (σ). The measuring techniques were described in previous publications [4].

Results and analysis

Fig. 1 shows the annealing time dependence of d, $\chi_{20°}$, $\log \sigma_{20°}$ and E_σ for $SSe_{32\cdot5}$ and $SSe_{22\cdot5}$ samples isothermally aged at 80 °C. The dependence of χ, σ or E_σ shows firstly a miscellaneous variation referring to the presence

of an induction period [5, 6], after which the growth of the crystalline phase proceeds monotonically with time. The induction period, which may be due to a relaxation in the mechanical stresses possibly present in the amorphous matrix or due to destruction of some chemical bonds, is not detected during the density measurements.

At the other two aging temperatures, 70 and 90 °C, a similar behaviour has been found but with different durations. Table I gives the average initial-amorphous and final-crystalline values of the measured quantities as calculated for the different temperatures.

Table I

Values of the initial-amorphous and final-crystalline physical quantities in the temperature range 70—90 °C for both $SSe_{32.5}$ and $SSe_{22.5}$

Physical property	Initial value		Final value	
	$SSe_{32.5}$	$SSe_{22.5}$	$SSe_{32.5}$	$SSe_{22.5}$
d (g/c.c.)	4.26	4.19	4.52	4.44
$-\log \sigma_{20°}$ (Ω^{-1} cm^{-1})	9.46 $\pm$ 0.07	9.42 $\pm$ 0.05	5.87 $\pm$ 0.15	5.62 $\pm$ 0.12
E_σ (eV)	0.96	1.0	0.51	0.60
$\chi_{20°}$ (cal/cm S °C)	0.017 $\pm$ 0.003	0.04	0.006 $\pm$ 0.001	0.006 $\pm$ 0.001

For each composition, it can be found that the period of induction decreases from about 2.5 hr at 70 °C to 1.5 hr at 80 °C and nearly disappears at 90 °C. Also, the time required for attaining a complete crystalline modification is decreased from about 15 to 5.4 hr with the aging temperature (70 → 90 °C) indicating an increase in the rate of crystallization.

The increase of S-content in sample $SSe_{22.5}$ as in $SSe_{32.5}$ slows down the process of crystallization. It also causes a little decrease in $\sigma_{20°}$, E_σ and χ depending on the states of S in Se which, in turn, depend on temperature [7]. However, the big change of $\sigma_{20°}$ and E_σ at any aging temperature is mainly due to the disorder-order transformation of the samples. The X-ray study of the resulting solids showed that they have hexagonal structure. Heat treatment, however, causes the formation of microcrystalline areas in the disorder mode and an increase in the number of dispersed centres by which phonons are scattered. This leads to increase the density (d) during the transition and decrease the distance between the chains. That is, decreasing the phonon free path and hence the value of χ during the transition.

These experimental data are presented in terms of the formal theory of phase transformation developed by AVRAMI [8]. It gives the untransformed fraction Θ at any time moment t by the equation

$$\Theta = \exp. [-Kt^n] , \qquad (1)$$

where d, $\log \sigma$, E_σ and χ have been considered to be characteristic quantities for the two-phase system [3] (the part B—C of curves of Fig. 1). In terms of these quantities, Θ has been calculated using the suggested empirical equation [9];

$$\Theta = (H_c - H_t)/(H_c - H_a) \ , \tag{2}$$

where H stands for a measured characteristic property which can be considered linearly dependent on the crystal content.

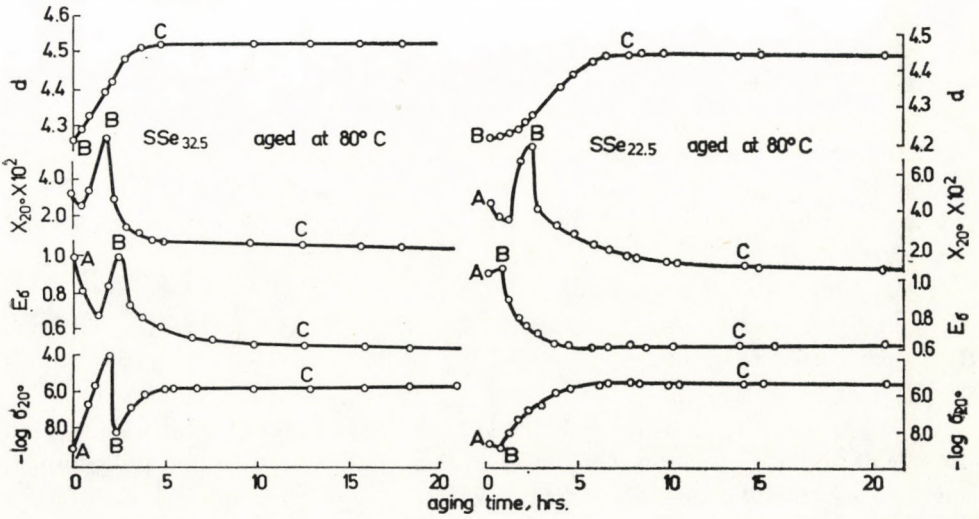

Fig. 1. The annealing time dependence of log $\sigma_{20°}$, E_σ, $\chi_{20°}$ and d for $SSe_{22\cdot5}$ and $SSe_{32\cdot5}$ samples aged at 80 °C

The parameter n of AVRAMI's equation, defining the mechanism of nucleation and crystal geometry [10], has been calculated in terms of the experimental values of Θ from the equation

$$\ln(-\ln \Theta_t) = \ln(K) + n \ln(t),$$

where the plot of $\ln(-\ln \Theta_t)$ vs $\ln(t)$ gave linear dependence for $SSe_{32\cdot5}$ and $SSe_{22\cdot5}$ at 70, 80 and 90 °C. However, for each composition, the values of n obtained on the basis of $\log \sigma$, E_σ and χ agree fairly with each other, whereas increasing the aging temperature causes a decrease in n to a limiting value about unity (Table II). This means that the growth is in one dimension and gradually changes from sporadic to predetermined one [10]. At the same time, n shows little increase with the increase of S-content, from 2.99 to 4.29 at.%. This may mean that the presence of S-atoms, in such concentration range, leads to increase the possibility of nucleation of the crystalline phase.

Table II

Values of the parameter n of AVRAMI's equation as obtained from slopes of the lines $\ln(-\ln\Theta)$ vs $\ln(t)$ at the temperatures 70, 80 and 90 °C for both $SSe_{32.5}$ and $SSe_{22.5}$

Composition	n		
	70 °C	80 °C	90 °C
$SSe_{32.5}$	1.1	0.93	0.87
$SSe_{22.5}$	1.2	1.10	1.00

The rate constant (K) of the disorder-order transition process has been calculated from Eq. (3), for all the intermediate states during the transition at the different temperatures. It has been found that the rate K has a constant value and does not depend on Θ. This may be attributed to the high degree of dispersion of the order (crystalline) phase in the disorder (amorphous) matrix as a result of the large number of the formed nuclei in the disordered volume.

The mean constant rate of crystallization ($\overline{K}$) showed an increase with the aging temperature, from 4×10^{-5} at 70 °C to 8.7×10^{-4} at 90 °C for $SSe_{22.5}$. Decreasing the S-content in the $SSe_{32.5}$ sample gives the respective values 2×10^{-4} and 10^{-3} for $\overline{K}$.

It is possible, however, to prove that the empirical relation (2) used to calculate the different values of Θ indicates that the conductivity σ of a mixture of two-phases highly dispersed in each other; amorphous (of conductivity σ_a) and crystalline (of conductivity σ_c) can be represented by a formula

$$\sigma_{\text{mix}} = \sigma_a^{\Theta}\ \sigma_c^{(1-\Theta)}\,. \tag{4}$$

Such latter formula is similar to that obtained for a mixture of two metallic phases randomly distributed in case of alloys [11].

The plotting of $\ln\overline{K}$ vs $1/T$ gave a straight line relationship for both $SSe_{32.5}$ and $SSe_{22.5}$. The slopes of these lines represent a measure for the activation energy of the crystallization process E [9]. On these conditions, the average value of E calculated on the basis of the electrical conduction (σ) and the thermal conduction (χ) has been found to be 26.16 for $SSe_{32.5}$ and 28.15 kcal/mole for $SSe_{22.5}$. This means that increasing the S-atoms in the sample, from $SSe_{32.5}$ to $SSe_{22.5}$, makes the process of crystal growth easier. However, any of these values obtained for E is less than the energy of destruction of the Se—Se or S—S bonds which, respectively, are 57 and 49 kcal/mole [12]. It is also less than the energy of self-diffusion of Se-atoms which equals 53 kcal/mole [13]. This means that the presence of S-atoms within such concentration range (2.99—4.26 at.%) does not affect the switching of

the covalent bonds known for pure Se during the viscous flow or the crystallization process [12].

To provide more information about the physical processes taking place during the amorphous-crystal ($a \rightarrow c$) transition, a piece of $SSe_{22.5}$ sample was sealed in an evacuated (10^{-4} mmHg) pyrex tube provided with two-tungsten electrodes [9]. The sample has been subjected to different isothermal aging, ranging from 98 to 132 °C. At each temperature, the electrical conductivity (σ) has been recorded continuously during the crystallization process.

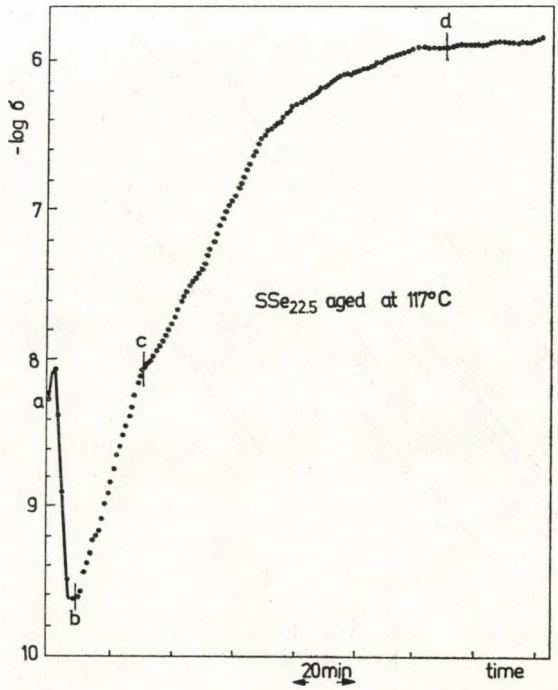

Fig. 2. The continuous variation of log σ with time for $SSe_{22.5}$ as isothermally aged at 117 °C

A typical spectrum for the isothermal time variation of log σ is given in Fig. 2 for $SSe_{22.5}$ sample aged at 117 °C. The initial value of log σ corresponding to the prepared amorphous state is -9.63 (point a) and reaches a value -5.84 corresponding to the final crystalline modification (point d) after a period of 165 min. During this period, three different stages can be distinguished:

ab: a miscellaneous change in σ due to a relaxation accompanied by an increase of temperature of the sample;

bc: a less pronounced increase in σ due to nucleation and growth of electrically isolated fine crystallites on the expense of the amorphous phase, and

cd: a big increase in σ by more than two orders related to the growth of cross-linked non-isolated crystallites forming a more ordered crystalline network.

Increasing the annealing temperature leads, generally, to decrease in the total time of the crystallization process, from 355 min at 98 °C to 87 min at 132 °C, as well as that of the individual stages during the transition.

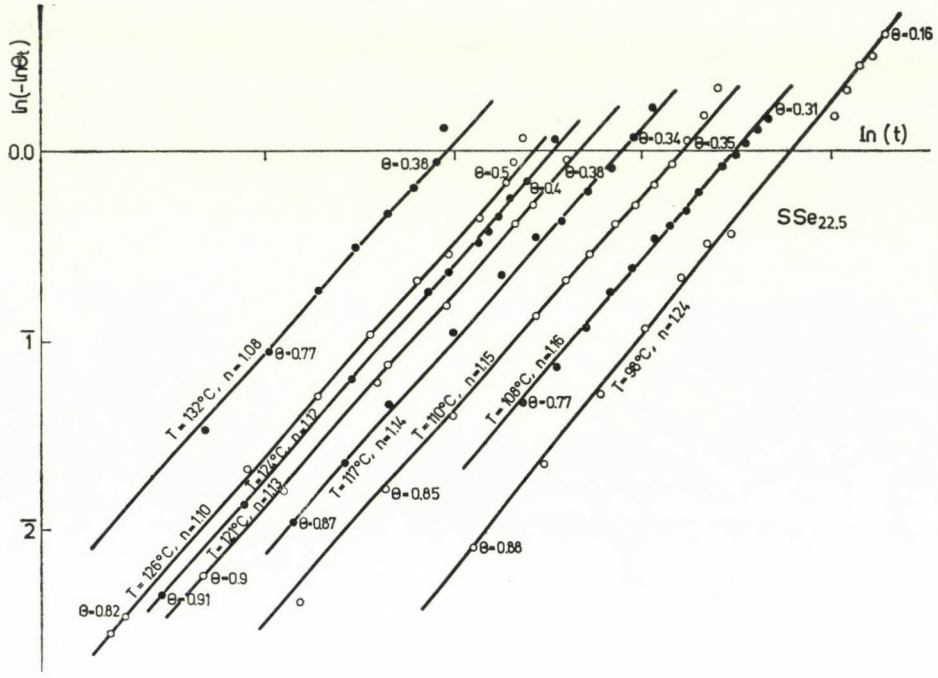

Fig. 3. The plotting of the function $\ln(-\ln\Theta)$ vs $\ln(t)$ as calculated from Eq. (2) on the basis of $\log\sigma$ for $SSe_{22\cdot5}$

Kinetics of the $a \rightarrow c$ transition has been studied for $SSe_{22\cdot5}$ sample in the range 98—132 °C by applying AVRAMI's principles. The quantity $\log\sigma$ has been used as a characteristic quantity and so the untransformed fraction Θ was calculated using Eq. (2).

Fig. 3 shows that plotting of $\ln(-\ln\Theta)$ vs $\ln(t)$ yields straight line relationships at the different temperatures. The parameter n of AVRAMI's equation as calculated from slopes of lines of Fig. 3 decreases from 1.24 to 1.08 with temperature (98 → 132 °C). The relation between $\log\overline{K}$ and $1/T$ given in Fig. 4 indicates an activation energy for the crystallization growth $E = 29.28$ kcal/mole. Such value is in agreement with that obtained from studying the electrical and thermal conduction during the transition step by step.

Evidently, the results confirm the suggested explanation for the mechanism of crystallization of the samples. That is, the $a \rightarrow c$ transition generally proceeds through nearly one-dimensional growth with binding the terminals of the formed crystallites as they come close to each other forming the final crystalline modification.

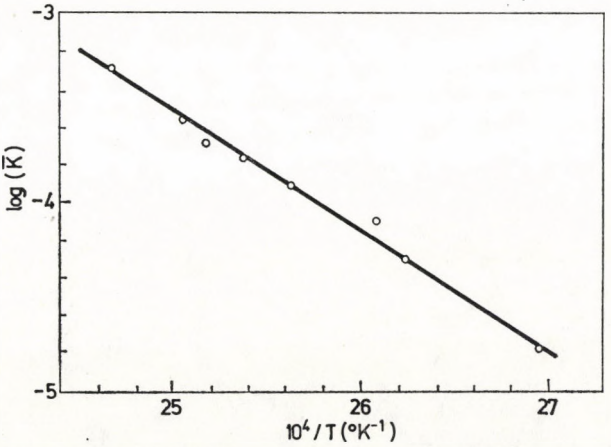

Fig. 4. The relation between the logarithm of mean crystallization rate (K) and the reciprocal of absolute temperature (T) for $SSe_{22.5}$

REFERENCES

1. B. V. Sokolov and I. A. Paribok-Alexandrovich, Bulletin Uch. Zap. of Volozodski Inst. (USSR), **30,** 64, 1966.
2. M. K. El-Mously, J. Neorg. Mat. (USSR), **13,** 801, 1977.
3. M. K. El-Mously, M. F. Kotkata and M. Fadel, Proc. Conf. Solid State Phys. and Relaxation Phenomena, 113—121, Cairo, 1977.
4. M. F. Kotkata, M. K. El-Mously and S. R. Atalla, Proc. 14th Int. Conf. on Thermal Conductivity, 39—44, USA, 1975.
5. M. Sugi, S. Iizima, M. Kikuchi and K. Tanaka, J. Non-Cryst. Solids, **5,** 358, 1971.
6. M. K. El-Mously and M. M. El-Zaidia, J. Non-Cryst. Solids, **11,** 519, 1973.
7. G. B. Abdullaev, G. M. Aliev, S. I. Mekhtieva and D. Sh. Abdinov, Phys. Stat. Sol., **13,** K109, 1966.
8. M. Avrami, J. Chem. Phys., **8,** 212, 1940.
9. M. K. El-Mously and F. A. Gani, Advanced Research in Science and Tech. of Mat., 189—196, Plenum Pub. Corp. 1974.
10. J. N. Hay, Br. Polym. J., **3,** 74, 1971.
11. R. Landauer, J. App. Phys., **23,** 779, 1952.
12. R. L. Myuller, "Glassy State", Izd. Akademy of Science (USSR) 1960, p. 61.
13. B. I. Boltax and B. T. Placheev, J. Tech. Phys. (USSR), **27,** 2229, 1957.

Acta Physica Academiae Scientiarum Hungaricae, Tomus 43 (2), pp. 125—132 (1977)

EINSTEIN—MAXWELL FIELDS WITH NULL KILLING VECTOR

By

D. KRAMER

PHYSICS DEPARTMENT, FRIEDRICH SCHILLER UNIVERSITY, JENA, GDR

(Received 14. VI. 1977)

The field equations for Einstein—Maxwell fields admitting a normal null Killing vector are reduced to a 2-covariant system of equations, which can be derived from a variational principle. Using the invariance of the associated Lagrangian one can generate a class of Einstein—Maxwell fields from the corresponding vacuum solutions.

1. Introduction

For stationary Einstein—Maxwell fields it is possible to construct from the field tensor F_{ab} and the time-like Killing vector ζ^a *scalar potentials*, and the field equations follow from a 3-dimensional variational principle [1, 2]. The Lagrangian contains these potentials and their first partial derivatives. The SU (2, 1) symmetry [3] of the Lagrangian leads to the possibility to generate new solutions [1]. Similar results hold for a space-like Killing vector. The trajectories of a *non-null* Killing vector determine a 3-dimensional space V_3 [4], and the Einstein—Maxwell equations can be written as 3-covariant equations over V_3. This relevant property breaks down in the case of a null Killing vector. Therefore, this case has been excluded from considerations on generating new solutions. However, a twistfree null Killing vector k^a

$$k_{(a;b)} = 0, \qquad k_a k^a = 0, \qquad k_a = W u_{,a} \tag{1}$$

admits finite 2-dimensional surfaces V_2 orthogonal to k^a [5]. The reduction of the field equations on equations over V_2 is possible. Moreover, we can introduce scalar potentials and find a simple Lagrangian for Einstein—Maxwell fields under the conditions (1) (with $W = 1$).

DEBNEY [6] investigated expansionfree Einstein—Maxwell fields which are of Kerr—Schild type and for which the preferred null direction is simultaneously an eigendirection of the electromagnetic field tensor F_{ab}. In place of these restrictions we impose the conditions (1) on the null vector field.

2. Coordinate system

In particular, the conditions (1) imply that k^a is a geodesic, shearfree, expansionfree, and twistfree congruence. We introduce coordinates $x^i = (x, y, v, u)$ adapted to this null congruence [5],

$$k^i = \delta^i_3 , \qquad k_i = W\delta^4_i = g_{3i} . \tag{2}$$

The space-like coordinates $x^A = (x, y)$ are chosen orthogonal to k^a. It is always possible to take a conformally flat metric in the 2-spaces V_2 ($u, v =$ = const).

$$g_{ij} = \begin{pmatrix} p^2 & 0 & 0 & m_1 \\ 0 & p^2 & 0 & m_2 \\ 0 & 0 & 0 & W \\ m_1 & m_2 & W & -2H \end{pmatrix} g_{ij,3} = 0, \ \sqrt{\det(-g_{ij})} = Wp^2 . \tag{3}$$

In general, a coordinate transformation making $W = 1$ would destroy the v-independence of g_{ij}. The following transformations preserve the form of the metric (3):

$$\begin{array}{ll} \text{(a)} & z' = F(z, u), \quad z = x + \mathrm{i}y, \\ \text{(b)} & u' = h(u), \\ \text{(c)} & v' = v + g(x, y, u) \end{array} \tag{4}$$

By means of the last transformation we can achieve $m_2 = 0$.

3. Electromagnetic null field. Scalar potential

For a geodesic null congruence k^a one obtains from the identity

$$2k_{a;[b;c]} = k_d R^d_{abc} \tag{5}$$

an equation for the derivative of the complex expansion Z with respect to the affine parameter v [8],

$$\frac{dZ}{dv} + Z^2 + \sigma\bar{\sigma} = -\frac{1}{2} R_{ab}k^a k^b . \tag{6}$$

Thus, the conditions (1) have the immediate consequence

$$R_{ab}\, k^a k^b = 0 . \tag{7}$$

From the conditions (1) we get the relation

$$k_{a;b} = W_{,[b}u_{,a]}, \qquad W_{,a}\, u'^{a} = 0 \ . \tag{8}$$

Calculating the contraction of the Ricci identity (5) we obtain

$$k^{b;a}{}_{n} = R^{ab}k_{b} = \lambda k^{a} \ . \tag{9}$$

i.e., k^a is an eigenvector of the energy-momentum tensor T_{ab}. In Section 5 we shall show that the electromagnetic field is necessarily a null field,

$$F_{ab} = 2p_{[a}k_{b]}, \qquad p_a k^a = 0 \ , \tag{10}$$
$$T_{ab} = nk_a k_b, \qquad n = p_a p^a \ .$$

The eigenvalue λ in (9) must vanish,

$$\lambda = 0 = W_{,A,A} \qquad A = 1, 2, \tag{11}$$

so that the function W satisfies a potential equation in V_2. In the case of a time-like Killing vector ζ^a the complex electromagnetic potential Φ has been defined by

$$\zeta^a F^{*}_{ab} = \Phi_{,b}, \qquad F^{*}_{ab} \equiv F_{ab} + \frac{i}{2}\,\varepsilon_{abcd}F^{cd} \tag{12}$$

[1]. It does not make sense to substitute ζ^a by k^a in this equation. The investigation of the relation

$$2A_{[b,a]} = F_{ab} = 2p_{[a}k_{b]} \tag{13}$$

in the metric (3) with (2) shows that with the aid of a gauge transformation

$$\tilde{A}_a = A_a + \chi_{,a} \tag{14}$$

the vector potential A_a can always be transformed to the form

$$A_a = \psi\, u_{,a}, \qquad \psi = \psi(x^A, u). \tag{15}$$

The gauge function χ is linear in v. Eq. (15) defines a real scalar potential ψ. The vector potential (15) satisfies the Lorentz gauge condition

$$A^{a}{}_{;a} = 0 \leftrightarrow \psi_{,a}k^{a} = 0 \ . \tag{16}$$

Thus, the Lie derivative of the field tensor

$$F_{ab} = 2\psi_{,[a}u_{,b]} \tag{17}$$

with respect to k^a vanishes. F_{ab} determines the vector p^a in (13) up to a term proportional to k^a. This freedom can be used such that a gradient $\psi_{,a}$ appears in the representation (17). The Maxwell equations

$$F_{ab}{}^{;b} = -\psi_{,b}{}^{;b}u_{,a} = 0 = \psi_{,A,A} \tag{18}$$

demand that the potential ψ is the real part of a function $f(z, u)$ analytic in z. For the complex self-dual field tensor F^*_{ab} we get

$$F^*_{ab} = 2f_{,[a}u_{,b]}, \qquad f = f(z, u) \equiv \psi + i\varphi. \tag{19}$$

The real and imaginary parts of f are related by the Cauchy—Riemann equations

$$\varphi_{,A} = -\varepsilon_{AB}\psi_{,A}\ , \tag{20}$$

so that the full system of the Maxwell equations

$$F^{*;b}_{ab} = 0 \tag{21}$$

is fulfilled because of (18).

4. Einstein equations

We have to solve the Einstein equations for the null field (17),

$$R_{ab} = \varkappa\psi_{,c}\psi^{,c}u_{,a}u_{,b}\ . \tag{22}$$

The solutions are contained in the general class investigated by KUNDT [5, 9]. We use the coordinate system (3) and apply the transformations (4) to simplify the metric.

Starting with the potential equation (11) we have to distinguish two cases:

$$\begin{aligned} &\text{I.} \quad W = 1, \\ &\text{II.} \quad W = x. \end{aligned} \tag{23}$$

The first case is characterized by the existence of a covariantly constant null vector,

$$W = 1 : k_{a;b} = 0\,. \tag{24}$$

In the second case the coordinate transformation (4a) has been used. Without the special choice $W = x$ in case II we get from the equations $R_{AB} = 0$:

$$p^2 = W^{-1/2}W_{,A}W_{,A}\,. \tag{25}$$

The Eqs. (22) lead to the statements listed in Table I where the transformations (4a—c) used are indicated.

Table I

I.			II.	
$R_{3A} = 0$:	$W = 1$		$W = x$	(4a)
$R_{AB} = 0$:	$p^2 = 1$	(4a)	$p^2 = x^{-1/2}$	(4b)
$R_{4A} = 0$:	$m_1 = 0$	(4a, c)	$m_1 = N(u) y x^{-3/2}$	(4c)

$N(u)$ is an arbitrary function of u. The last field equation of (22) is a differential equation for the remaining function H. In the case II we introduce a new function M,

$$M \equiv x^{-1} H + \frac{2}{3} x^{-3/2} \left(\frac{dN}{du} y - \frac{1}{3} N^2 \right) . \tag{26}$$

The second term in (26) takes into account the nonvanishing function m_1. In the case I the functions H and M coincide. Then, the total system of the Einstein—Maxwell equations reduces to very simple equations over the 2-spaces V_2 (u, v = const) or, equivalently, over the Euclidean plane:

$$\psi_{,A,A} = 0 , \tag{27}$$
$$(W M_{,A})_{,A} = \varkappa \psi_{,A} \psi_{,A} , \quad W = 1; \; W = x .$$

Derivatives with respect to u do not occur.

We consider the two cases separately.

Case I. ($W = 1$):

In terms of the complex coordinate z we have the equations

$$\psi = \frac{1}{2}(f + \bar{f}), \quad \frac{\partial^2 H}{\partial z \partial \bar{z}} = \varkappa \frac{\partial f}{\partial z} \frac{\partial \bar{f}}{\partial \bar{z}}$$

leading to the final form of the metric

$$ds^2 = dz\, d\bar{z} + 2du\, dv - 2H\, du^2, \tag{28}$$
$$H = \varkappa f \bar{f} + g + \bar{g}, \quad f = f(z, u), \quad g = g(z, u),$$

where f and g are arbitrary analytic functions of z depending arbitrarily on the retarded time coordinate u.

If the gravitational field is entirely caused by the electromagnetic null field, the solution of the homogeneous equation for H can be put equal to zero, and H is just the squared modulus of an analytic function. The solutions (28) are in general of Petrov type N. For the special function $f = \alpha(u)\, z$ they are even conformally flat [6]. In the case under consideration we can derive the field equations (27) from a *variational principle* with the Lagrangian

$$\boxed{\begin{aligned} L &= \Gamma_{,A}\Gamma_{,A} \\ \Gamma &\equiv H - \frac{\varkappa}{2}\psi^2 + i\psi^2. \end{aligned}} \tag{29}$$

The complex scalar potential Γ contains the gravitational potential H as well as the electromagnetic potential ψ. The invariance transformation

$$\Gamma' = e^{ia}\,\Gamma \tag{30}$$

generates solutions of the Einstein—Maxwell equations from vacuum *pp*-waves ($\psi = 0$). The parameter a in (30) can depend on u.

Case II. ($W = x$):

In this case the field equations (22) lead to one single inhomogeneous differential equation for the real function M,

$$2(z+\bar{z})\frac{\partial^2 M}{\partial z \partial \bar{z}} + \frac{\partial M}{\partial z} + \frac{\partial M}{\partial \bar{z}} = \varkappa \frac{\partial f}{\partial z}\frac{\partial \bar{f}}{\partial \bar{z}}\,. \tag{31}$$

The solutions are of Petrov type II or D (5). The metric

$$ds^2 = \frac{1}{\sqrt{x}}\,(dx^2 + dy^2) + 2x\,du\,dv - 2\varkappa C^2 x^2\,du^2, \tag{32}$$

$$\psi = Cx, \qquad C = \text{const}$$

provides the simplest example of an Einstein—Maxwell field of this kind. It can be interpreted as a stationary cylindrically symmetric field with rotating charges and curvature singularities on the axis of symmetry. If the electromagnetic field is switched off, the solution is not flat: For $C = 0$, the solution (32) is the static Levi—Civita metric which is of Petrov type D and admits two null Killing vectors.

5. Electromagnetic non-null field

Finally, we have to investigate the case of an electromagnetic non-null field with the eigendirection k^a,

$$F_{ab} = 2F(n_{[a}k_{b]} + \bar{r}_{[a}r_{b]}), \qquad T_{ab} = F\bar{F}(n_{(a}k_{b)} + \bar{r}_{(a}r_{b)}) . \tag{33}$$

The complex null tetrad $(r_a, \bar{r}_a, n_a, k_a)$ is adapted to the eigendirections of the electromagnetic field tensor. The eigenvalue λ in Eq. (9) must not vanish in this case

$$-\lambda = (2p^2W)^{-1} W_{,A,A} = \frac{\varkappa}{2} F\bar{F} \neq 0 . \tag{34}$$

We consider the Einstein equations

$$R_{AB} = \varkappa T_{AB} = -\lambda p^2 \delta_{AB} \begin{cases} \text{(a)} & R_{11} - R_{22} = 0 = R_{12} , \\ \text{(b)} & R_{11} + R_{22} = -2\lambda p^2. \end{cases} \tag{35}$$

From Eq. (35, a) we obtain

$$\sqrt{W}\lambda = \frac{-\partial A(W, u)}{\partial W}, \qquad q^{-2} = A(W, u), \qquad q^2 \equiv \sqrt{W}p^2(W_{,A}W_{,A})^{-1}, \tag{36}$$

where $A(W, u)$ is an arbitrary function of its arguments. From the relations (34), (36) it follows that there exists a function $Y = Y(W)$ satisfying the potential equation $Y_{,A,A} = 0$, so that we can put $Y = x$. The remaining Eq. (36,b) requires $\lambda = 0$, which is contradictory to the premise (34). Therefore, under the conditions (1) solutions of the Einstein—Maxwell equations with electromagnetic non-null field do not exist.

6. Summary

If the existence of a twistfree null Killing vector k^a is presumed, the Einstein—Maxwell equations can be reduced to the system (27). These equations are derivable from a variational principle with the Lagrangian (29), provided that $k_a = u_{,a}$ (covariantly constant null vector). Only electromagnetic *null* fields are compatible with the conditions (1).

In this paper we have shown that there exists an internal invariance group which can be exploited to generate *pp*-wave solutions in the Einstein—Maxwell theory from the corresponding vacuum solutions. Of course, the resulting metrics are well-known. The main result is the new generation theorem for solutions admitting a *null* Killing vector.

To find Einstein—Maxwell fields with *twisting* null Killing vectors, it might be useful to apply similar methods: introduction of scalar potentials, reduction to equations containing only derivatives with respect to two spatial coordinates.

REFERENCES

1. G. NEUGEBAUER und D. KRAMER, Ann. Physik, **24**, 62, 1969.
2. D. KRAMER, G. NEUGEBAUER und H. STEPHANI, Fortschr. Physik, **20**, 1, 1972.
3. W. KINNERSLEY, J. Math. Phys., **14**, 651, 1973.
4. R. GEROCH, J. Math. Phys., **12**, 918, 1971.
5. W. KUNDT, Z. Phys., **163**, 77, 1961.
6. G. DEBNEY, J. Math. Phys., **15**, 992, 1974.
7. G. DEBNEY, Lett. Nuovo Cim., **5**, 954, 1972.
8. P. JORDAN, J. EHLERS und R. SACHS, Beiträge zur Theorie der reinen Gravitationsstrahlung, Abh. Mainz. Akad., math.-naturw. Kl., Nr 1, 17, 1961.
9. W. KUNDT und M. TRÜMPER, Beiträge zur Theorie der Gravitationsstrahlungsfelder, Abh. Mainz. Akad., math.-naturw. Kl., Nr. 12, 980, 1962.

Acta Physica Academiae Scientiarum Hungaricae, Tomus 43 (2), pp. 133—140 (1977)

LAGRANGIAN THERMODYNAMICS AS A PARTICULAR CASE OF GOVERNING PRINCIPLE OF DISSIPATIVE PROCESSES

By

P. SINGH

DEPARTMENT OF MATHEMATICS, INDIAN INSTITUTE OF TECHNOLOGY, KHARAGPUR, INDIA

(Received 7. VII. 1977)

This note deals with the relation between the Governing Principle of Dissipative Processes and the Lagrangian thermodynamics of BIOT. The governing principle is introduced in its universal form and then the flux representation is deduced as a partial form of it for the heat conduction phenomenon. Finally, the Lagrangian thermodynamics of BIOT is introduced in its original form and it is compared with the flux representation for heat conduction in solids. It is shown that for heat conduction phenomena for which the Lagrangian thermodynamics was proposed and applied by BIOT, it is equivalent to the flux representation of GPDP.

Introduction

It is well-known that the non-equilibrium theory of irreversible processes was initiated by ONSAGER in 1931 [1, 2]. He proposed that the irreversible phenomena can be expressed by phenomenological relations of the general type:

$$\mathbf{J}_i = \sum_{k=1}^{f} L_{ik}\mathbf{X}_k \quad (i = 1, 2 \ldots f) \tag{1}$$

stating that any current $\mathbf{J}_i$, is caused by contributions of all thermodynamic forces $\mathbf{X}_i$. The coefficients L_{ik} $(i, k = 1, \ldots, f)$ are called the phenomenological coefficients. ONSAGER's fundamental theorem states that the matrix of phenomenological coefficients L_{ik} is symmetric, i.e.,

$$L_{ik} = L_{ki} \quad (i, k = 1, 2 \ldots f)\,. \tag{2}$$

These symmetries are called the ONSAGER reciprocal relations and they express a connection between two reciprocal phenomena which arise from mutual interference of simultaneously occurring irreversible processes.

Using these phenomenological relations and the reciprocal relations GYARMATI [3, 4, 5], in 1965, formulated a variational principle which is valid for the linear, quasi-linear and non-linear systems of dissipative pro-

cesses and, therefore, it is called the Governing Principle of Dissipative Processes (briefly: GPDP). In its most general form, it is expressed as

$$\delta \int_v [\sigma - \Psi - \Phi] \, dv = 0 \,, \tag{3}$$

where σ denotes the entropy production per unit time and volume and it can be expressed as

$$\sigma = \sum_{i=1}^{f} \mathbf{J}_i \cdot \mathbf{X}_i \geq 0 \,. \tag{4}$$

It is a positive definite quantity according to the second law of thermodynamics. It should be noted that in (4), f represents the number of independent current densities, $\mathbf{J}_i$, and thermodynamic forces, $\mathbf{X}_i$. Using (1), σ can be given as the homogeneous quadratic expression of the independent thermodynamic forces, i.e.

$$\sigma \equiv \sum_{i,k=1}^{f} L_{ik} \mathbf{X}_i \cdot \mathbf{X}_k \geq 0 \,. \tag{5}$$

The alternative forms of (1), (2) and (5) are also obtained when the phenomenological coefficients L_{ik} are expressed in terms of the resistances R_{ik}. The constitutive equations (1) take the form

$$\mathbf{X}_i = \sum_{k=1}^{f} R_{ik} \mathbf{J}_k \qquad (i = 1, 2, \ldots f) \,, \tag{6}$$

where R_{ik} and L_{ik} satisfy the relations

$$\sum_{m=1}^{f} L_{im} R_{mk} = \sum_{m=1}^{f} R_{im} L_{mk} = \delta_{ik} \qquad (i, k = 1, 2, \ldots, f) \,. \tag{7}$$

Here δ_{ik} is the Kronecker symbol, i.e. $\delta_{ik} = 1$; $i = k$; $\delta_{ik} = 0$; $i \neq k$. Thus the alternative reciprocal relations are

$$R_{ik} = R_{ki} \qquad (i, k = 1, 2, \ldots, f) \,. \tag{8}$$

Using (6), σ can be expressed in terms of currents as

$$\sigma \equiv \sum_{i,k=1}^{f} R_{ik} \mathbf{J}_i \cdot \mathbf{J}_k \geq 0 \,. \tag{9}$$

The forms of σ in (5) and (9) are called the force and flux representations of the entropy production. These terms are very appropriate but it is important to note that expressions (5) and (9) of σ are based on the validity of

linear constitutive equations (1) and (6), respectively. The most important fact is that the expressions (5) and (9) for σ may be considered now as local potential functions with respect to currents and forces, respectively, due to the validity of the symmetry relations (2) and (8). More exactly we can accept the expressions (5) and (9) of σ as non-equilibrium local potentials for linear theory, if and only if the ONSAGER's reciprocal relations are valid.

However, if we accept the validity of ONSAGER's relations, we can directly define the non-equilibrium local dissipation potentials, Ψ and Φ, in the following homogeneous quadratic forms [4].

$$\Psi(\mathbf{X}, \mathbf{X}) \equiv \frac{1}{2} \sum_{i,k=1}^{f} L_{ik}\mathbf{X}_i \cdot \mathbf{X}_k \geq 0 \,, \tag{10}$$

$$\Phi(\mathbf{J}, \mathbf{J}) \equiv \frac{1}{2} \sum_{i,k=1}^{f} R_{ik}\mathbf{J}_i \cdot \mathbf{J}_k \geq 0 \,, \tag{11}$$

which correspond to entropy forms (5) and (9), respectively. These potential functions are equal to half of the entropy production in case of the validity of linear laws and reciprocal relations. Hence Ψ and Φ are the local measures of irreversibility and they differ from one another only in the way of description of the non-equilibrium state. The potential character of Ψ and Φ can be seen from the relations

$$\mathbf{J}_i = \frac{\partial \Psi}{\partial \mathbf{X}_i} = \sum_{k=1}^{f} L_{ik}\mathbf{X}_k \qquad (i = 1, 2, \ldots, f) \,, \tag{12}$$

$$\mathbf{X}_i = \frac{\partial \Phi}{\partial \mathbf{J}_i} = \sum_{k=1}^{f} R_{ik}\mathbf{J}_k \qquad (i = 1, 2, \ldots, f) \,, \tag{13}$$

which represent the linear constitutive relations (1) and (6), respectively.

Substituting the expressions for σ, Ψ and Φ from (4), (10) and (13), respectively, in the principle (3), it becomes

$$\delta \int_v \left[\sum_{i=1}^{f} \mathbf{J}_i \cdot \nabla \Gamma_i - \frac{1}{2} \sum_{i,k=1}^{f} L_{ik} \nabla \Gamma_i \cdot \nabla \Gamma_k - \frac{1}{2} \sum_{i,k=1}^{f} R_{ik}\mathbf{J}_i \cdot \mathbf{J}_k \right] dv = 0 \,, \tag{14}$$

where $\mathbf{X}_i = \nabla \Gamma_i$ has been used for the dissipative forces $\mathbf{X}_i$. It should be noted that in the case of irreversible transport processes the forces can always be generated as the gradients of certain 'Γ' variables which are state variables and simultaneously internal parameters with respect to the forces [3] [4]. It should also be noted that the variational principle (14) is operative if and only if, the balance equations

$$\dot{\varrho}_i + \nabla \cdot \mathbf{J}_i = \sigma_i \qquad (i = 1, 2, \ldots, f) \tag{15}$$

are regarded as auxiliary conditions for whose variation the following restrictions [3]:

$$\delta(\dot{\varrho}_i - \sigma_i) = -\delta(\nabla \cdot \mathbf{J}_i) = \nabla \cdot \delta\mathbf{J}_i\,, \quad (i = 1, 2, \ldots, f) \tag{16}$$

are valid. Here $\dot{\varrho}_i$ is the partial time derivative of the density ϱ_i; $\mathbf{J}_i$ is the corresponding current density and σ_i is the rate of production per unit time and volume.

Flux representation of GPDP

The flux representation of the principle can be obtained from the Governing Principle of Dissipative Processes simply by varying it with respect to currents only. It is obvious that in (3), ψ is the functional of thermo-dynamic forces only and therefore its variation with currents is simply zero. Thus (3) in this case, reduces to

$$\delta \int_v [\sigma - \Phi]\, dv = 0\,,$$

which with the help of expressions for σ and Φ becomes

$$\delta \int_v \left[\sum_{i=1}^{f} \mathbf{J}_i \cdot \nabla \Gamma_i - \frac{1}{2} \sum_{i,k=1}^{f} R_{ik} \mathbf{J}_i \cdot \mathbf{J}_k \right] dv = 0. \tag{17}$$

It may be mentioned that the original formulation of ONSAGER's principle of least dissipation of energy was in flux representation and the variation was taken, naturally, with respect to currents only.

Since our aim, in this paper, is to discuss the relation between this partial form of GYARMATI's principle and the Lagrangian thermodynamics which was formulated originally for heat conduction problems, we shall formulate the partial principle (17) for the purely heat conduction phenomena. Let us denote the heat current density by $\mathbf{J}_q$ and the dissipative force by ∇T which represents the temperature gradient. Entropy production, σ, in Fourier picture [4] becomes:

$$\sigma = -\mathbf{J}_q \cdot \nabla T \geq 0. \tag{18}$$

The constitutive equation for heat conduction phenomena is well defined by Fourier's law

$$\mathbf{J}_q = -\lambda \nabla T, \tag{19}$$

here λ denotes the coefficient of heat conduction. The alternative form of this constitutive relation may be expressed as

$$\nabla T = -\frac{1}{\lambda} \mathbf{J}_q\,. \tag{20}$$

For the case under consideration, the potential function, Φ, is

$$\Phi \equiv \frac{1}{2\lambda} \mathbf{J}_q \cdot \mathbf{J}_q \geq 0 \,. \tag{21}$$

Using (18) and (21), the principle (17) for the heat conduction phenomena becomes

$$\delta \int \left[-\mathbf{J}_q \cdot \nabla T - \frac{1}{2\lambda} \mathbf{J}_q \cdot \mathbf{J}_q \right] dv = 0 \,. \tag{22}$$

We have already mentioned that in the flux representation, the principle is varied with respect to fluxes only, while the forces are kept constant. Performing the variation, (22) becomes

$$\int_v \left[\nabla T + \frac{1}{\lambda} \mathbf{J}_q \right] \cdot \delta \mathbf{J}_q \, dv = 0 \,. \tag{23}$$

In the next Section, we shall show that the Lagrangian thermodynamics of BIOT reduces to the form (23) when the phenomenon of heat conduction is considered.

In (23) the element of volume, dV, is arbitrary, therefore, it gives

$$\nabla T = -\frac{1}{\lambda} \mathbf{J}_q \,,$$

which is nothing but the constitutive relation (20). Thus it is to be noted that flux representation of GPDP leads to the constitutive equations only. It means it is useless for the practical purposes. This was the reason for the original formulation of ONSAGER principle of least dissipation of energy not having received any attention.

Lagrangian thermodynamics and its equivalency with flux representation

Since BIOT [6, 7, 8, 9] treats mainly heat conduction in solids, we shall focus our attention on this phenomenon. In this case the internal energy balance without source term is

$$\frac{\partial u}{\partial t} + \nabla \cdot \mathbf{J}_q = 0 \,, \tag{24}$$

where u denotes the specific internal energy and $\mathbf{J}_q$ is the heat current density. BIOT [6, 7, 8, 9] introduces the field quantity, $\mathbf{H}$, defined as

$$\mathbf{J}_q \equiv \frac{\partial H}{\partial t} \tag{25}$$

that is, heat current density $\mathbf{J}_q$ is a priori defined as the partial time derivative of something labelled by BIOT as $\mathbf{H}$ and called 'heat flow' or 'heat displacement vector'. It should be noted that there is, however, no macroscopic physical quantity, the time derivative of which would be identical to the heat current density. In general, there are no physical quantities from which the conductive current densities of dissipative processes may be generated by time derivation. Consequently, BIOT's method (Lagrangian thermodynamics) is based on a physically empty assumption (25). Using (25), the internal energy balance (24) was written by BIOT [9]:

$$u + \nabla \cdot \mathbf{H} = 0 \ , \tag{26}$$

which was considered analogous to a holonomic constrain in classical mechanics. The temperature field $T(\mathbf{r}, t)$ was assumed in the form

$$T = T(\mathbf{r}, t;\ q_1, q_2, \ldots, q_n) \ . \tag{27}$$

Taking the boundary conditions into considerations for $\mathbf{H}$, BIOT determines the corresponding field $\mathbf{H}$ from (26) as

$$\mathbf{H} = \mathbf{H}(\mathbf{r}, t;\ q_1, q_2, \ldots, q_n) \ . \tag{28}$$

In other words, the field $\mathbf{H}$ was assumed to be a given function of the space co-ordinates $\mathbf{r}$, of time t and of a certain number of parameters $q_1, q_2, \ldots, q_n$. These parameters are unknown functions of time and are considered as 'generalised co-ordinates' by BIOT. Using the expressions (27) and (28) for the field T and $\mathbf{H}$ respectively, BIOT formulates his 'fundamental variational principle' as [9].

$$\int_v \left[\nabla T + \frac{\dot{\mathbf{H}}}{\lambda}\right] \cdot \delta \mathbf{H}\, dv = 0 \ , \tag{29}$$

which is essentially the reformulation of the Fourier's law

$$\dot{\mathbf{H}} \equiv \mathbf{J}_q = -\lambda \nabla T.$$

Thus as a variational principle it reproduces only the constitutive relations. The situation is same with the flux representation of GPDP as we have

already seen. As an approximate variational method for the field quantity **H**, the formulation (29) contains Ritz parameters $q_1, q_2, \ldots, q_n$ which are unknown functions of time. Regarding this point FINLAYSON and SCRIVEN's [10] remarks are worth quoting: "The functions $q_1, q_2, \ldots, q_n$, which are analogous to variational parameters in classical variational method are named generalized coordinates by BIOT, who unfortunately failed to distinguish between exact and trial solutions".

Let us accept the variation

$$d\mathbf{H} = \sum_{i=1}^{n} \frac{\partial \mathbf{H}}{\partial q_i} dq_i \ , \tag{30}$$

which was used by BIOT [9]. Variation with time becomes

$$\dot{\mathbf{H}} \equiv \frac{\partial \mathbf{H}}{\partial t} = \sum_{i=1}^{n} \frac{\partial \mathbf{H}}{\partial q_i} \dot{q}_i \ . \tag{31}$$

From (30) and (31), we get

$$\frac{\partial \mathbf{H}}{\partial q_i} = \frac{\partial \dot{\mathbf{H}}}{\partial \dot{q}_i} \ . \tag{32}$$

Consequently, principle (29) with the help of (31) becomes

$$\int_v \left[\nabla T + \frac{\dot{\mathbf{H}}}{\lambda}\right] \cdot \sum_{i=1}^{n} \frac{\partial \mathbf{H}}{\partial q_i} \delta \dot{q}_i dv = 0 \ , \tag{33}$$

which with (32) yields

$$\int_v \left[\nabla T + \frac{\dot{\mathbf{H}}}{\lambda}\right] \cdot \sum_{i=1}^{n} \frac{\partial \dot{\mathbf{H}}}{\partial \dot{q}_i} \delta \dot{q}_i \, dv = 0 \ . \tag{34}$$

Finally, with the help of (25); (34) reduces to

$$\int_v \left[\nabla T + \frac{\mathbf{J}_q}{\lambda}\right] \cdot \sum_{=1}^{n} \frac{\partial \mathbf{J}_q}{\partial \dot{q}_i} \delta \dot{q}_i \, dv = 0. \tag{35}$$

This expression does not contain the field **H** and therefore, it may be remarked that there was no necessity of the field **H**. Considering the variation of $\mathbf{J}_q(\mathbf{r}, t)$ in the usual sense associated with the variational principles; (35) or (19) yields

$$\int_v \left[\nabla T + \frac{\mathbf{J}_q}{\lambda}\right] \cdot \delta \mathbf{J}_q \, dv = 0 \ , . \tag{36}$$

which is nothing but the partial principle (23). Thus BIOT's variational principle (29) reduces to (36) which is nothing but the flux (i.e. only partial) representation of governing principle of dissipative processes [3, 4]. However, for heat conduction phenomenon, this principle was already established by ONSAGER in 1931 [1, 2]. We therefore conclude that BIOT's Lagrangian thermodynamics was not a new formulation and it is based on a physically empty and incorrect hypothesis represented by (25). The criticism of this type of assumption is given by TRUESDELL (see [11] p. 128).

*

Acknowledgement

I am thankful to Prof. I. GYARMATI for his cooperation and many useful suggestions in the preparation of this paper.

REFERENCES

1. L. ONSAGER, Reciprocal relations in irreversible processes. I. Phys. Rev., **37,** 405, 1931.
2. L. ONSAGER, Reciprocal relations in irreversible processes. II. Phys. Rev., **38,** 2265, 1931.
3. I. GYARMATI, On the Governing Principle of Dissipative Processes and its Extension to Non-linear Problems. Ann. Phys., **23,** 353, 1969.
4. I. GYARMATI, Non-equilibrium Thermodynamics, Field Theory and Variational Principles. Springer Verlag, Berlin, 1970.
5. I. GYARMATI, Generalization of the Governing Principle of Dissipative Processes to Complex Scalar Fields. Ann. Phys., **31,** 18, 1974.
6. M. A. BIOT, Variational principles in irreversible thermodynamics with application to viscoelasticity. Phys. Rev., **97,** 1463, 1955.
7. M. A. BIOT, New methods in heat flow analysis with application to flight structures. J. Aeronaut, Sci., **24,** 857, 1957.
8. M. A. BIOT, Further developments of new methods in heat flow analysis. J. Aerospace Sci., **26,** 367, 1959.
9. M. A. BIOT, Variational principles in heat transfer. Oxford University-Press, 1970.
10. B. A. FINLAYSEN and L. E. SCRIVEN, On the search for variational principles. Int. J. Heat Mass Transfer, **10,** 799, 1967.
11. C. TRUESDELL, Rational Thermodynamics. McGraw-Hill, New York, 1969.

Acta Physica Academiae Scientiarum Hungaricae, Tomus 43 (2), pp. 141—145 (1977)

SINGULARITIES IN STATIC AXIALLY SYMMETRIC COUPLED FIELDS

By

D. K. DATTA and J. R. RAO

DEPARTMENT OF MATHEMATICS, INDIAN INSTITUTE OF TECHNOLOGY, KHARAGPUR, INDIA

(Received 8. VII. 1977)

In this investigation we have obtained from 'Curzon particle' solution a coupled electromagnetic and scalar meson field solution. We have studied the nature of the singularities of this solution through the evaluation of Kretschmann curvature invariant along curved trajectories approaching the origin. It has been shown that singularity in general is located along power law trajectories approaching the origin except for certain values of the power index.

I. Introduction

The problem of singularities in general relativity is one of fundamental importance since it naturally emerges in the theory. GAUTREAU and ANDERSON [1] have shown that the 'directional singularities' occur in the case of the CURZON [2] field for positive mass. Their study is based on evaluating the Kretschmann curvature scalar $\alpha = R_{\mu\nu\varrho\sigma}R^{\mu\nu\varrho\sigma}$, where $R_{\mu\nu\varrho\sigma}$ is the Riemann tensor. They have shown that α tends to infinity for every straight line trajectory approaching the origin except along the z-axis which indicates the property of 'directionality' associated with the intrinsic singularity at the origin. STACHEL [3] has analysed the same problem further and shown that in the case of 'mass' being positive the nature of the intrinsic singularity is not 'point like'. GAUTREAU [4] has shown that in the case of certain class of Weyl gravitational fields generated by the Newtonian potential of a rod, the equipotential surfaces converging on the coordinate location of the singularity become non-zero only when the singularity has directional properties. In a later work, GAUTREAU [5] has investigated the case when the zero mass scalar field is present. The above study of GAUTREAU has been extended by us (DATTA and RAO* [6]) to the case when the superposed field is coupled zero mass scalar and electromagnetic field. Our investigation reveals the persistence of the directional behaviour of the singularities, just as

* We wish to thank the referee of our paper (DATTA and RAO [7]) for drawing our attention to the mistake of not taking the effect of the factor $e^{-4\nu+4\lambda}$ in equation (30) of our earlier paper (DATTA and RAO [6]) in evaluating the limit of Kretschmann curvature invariant α. The correct conclusion thereby should be that 'directional singularities' are present in the presence of coupled fields as well.

in the corresponding cases studied by GAUTREAU and ANDERSON [1] and GAUTREAU [5] for the particle like solutions. COOPERSTOCK et al [8], [9] have examined the problem of directional singular behaviour employing curved trajectories instead of straight line paths approaching the singularity. They have shown that the behaviour of Kretschmann curvature invariant is dependent on the trajectory.

In this paper we have developed from the vacuum solution the coupled zero-mass scalar and electromagnetic solution by a method obtained by TEIXEIRA et al [10], in which two types of long-range scalar fields are considered. This solution is more general than our previous solution (DATTA and RAO [6]) in the sense that from this solution the general vacuum solution can be recovered simply by putting a constant, associated to the coupled solution, equal to zero.

In Section II, the solution for coupled superposed zero-mass scalar and electromagnetic field has been obtained by applying the technique of TEIXEIRA et al [10]. In Section III, we have analysed this solution from the point of view of the singularity. We have evaluated the Kretschmann curvature invariant α along the curved trajectories. These investigations have led us to the same qualitative conclusions as obtained by COOPERSTOCK et al [9]. The limit of α as shown in the Table I is trajectory-dependent of which the singular behaviour of the coupled solution along a straight line trajectory is a subcase. Finally some conclusions have been drawn in the last Section.

II. Technique and solution of coupled superposed fields

TEIXEIRA et al. [10] have obtained a technique which generalizes the static vacuum solution to coupled electromagnetic solution as follows:

Let a static solution (V, h_{ij}) of the Einstein's vacuum equation

$$R_{\nu\mu} = 0 \tag{1}$$

be given by the line element

$$ds^2 = e^{2v}\, dt^2 - e^{-2v}\, h_{ij}\, dx^i\, dx^j\,, \tag{2}$$

then the static solution (ψ, h_{ij}, Φ, S) of the Einstein—Maxwell-scalar equations

$$R_{\mu\nu} - \frac{1}{2} R g_{\mu\nu} = -8\pi(E_{\mu\nu} + S_{\mu\nu}) \tag{3}$$

can be obtained from the line element

$$ds^2 = e^{2\psi}\, dt^2 - e^{-2\psi}\, h_{ij}\, dz^i\, dx^j\,, \tag{4}$$

where $E_{\mu\nu}$ and $S_{\mu\nu}$ are the energy momentum tensors corresponding to electromagnetic field and scalar field, respectively. The electrostatic potential Φ is functionally related to the gravitational potential ψ, and also the scalar potential S to ψ. This ψ is to bear a functional relationship with the vacuum gravitational potential V. The solution is thus given by

$$S = \pm c_1 V, \quad c_1 = \text{constant}, \tag{5}$$

$$e^{-\psi} = \cos h\, c_2 v - (1 + a^2/c_2^2)^{1/2} \sin h\, c_2 v\ , \tag{6}$$

$$c_2 = (1 \mp c_1^2), \tag{7}$$

$$\Phi = -(a/c_2)\, e^{\psi} \sin h\, c_2 v\ , \tag{8}$$

and

$$F_{4i} = a e^{2\psi} V_i \qquad (i = 1, 2, 3) \tag{9}$$

where $F_{\mu\nu}$ is the electromagnetic field tensor.

In the case of static axially symmetric metric given by

$$ds^2 = e^{2\lambda} dt^2 - e^{2\nu - 2\lambda}(dr^2 + dz^2) - r^2 e^{-2\lambda} d\Phi^2\ , \tag{10}$$

the vacuum field equations are

$$\lambda_{11} + \lambda_{22} + \lambda_1/r = 0 \tag{11}$$

$$\nu_1 = r(\lambda_1^2 - \lambda_2^2), \qquad \nu_2 = 2r\lambda_1\lambda_2\ , \tag{12}$$

where λ and ν are functions of r and z only.

We consider the 'Curzon' solution of (11) and (12) where

$$\lambda = -\frac{m}{\varrho},$$

$$\nu = -\frac{m^2 r^2}{2\varrho^4}, \qquad \varrho = (r^2 + z^2)^{1/2}\ . \tag{13}$$

By applying the results ((1)—(9)) we obtain a solution for the coupled field from the vacuum solution (13), as

$$\lambda = -\log\left(\cos h \frac{mc_2}{\varrho} + K \sin h \frac{mc_2}{\varrho}\right)\ ,$$

$$\nu = -\frac{m^2 r^2}{2\varrho^4}, \tag{14}$$

where $K = (1 + a^2/c_2^2)^{1/2}$, a constant. (15)

Further the physical fields are given by

$$S = \mp \frac{mc_1}{\varrho}, \tag{16}$$

$$F_{14} = \frac{4amr\varrho^{-3}}{\left(\cosh \frac{mc_2}{\varrho} + K \sin h \frac{mc_2}{\varrho}\right)}, \tag{17}$$

$$F_{24} = \frac{4amz\varrho^{-3}}{\left(\cos h \frac{mc_2}{\varrho} + K \sin h \frac{mc_2}{\varrho}\right)}, \tag{18}$$

III. Coupled field singularity

The Kretschmann curvature invariant α computed for the solution (14), can be expressed in the form

$$\alpha = 8e^{-4\nu+4\lambda}\left[(R^1_{212})^2 + (R^1_{131})^2 + (R^1_{141})^2 + 2(R^3_{132})^2\right] =$$

$$= 128e^{2m^2r^2/\varrho^4 - 4mc_1/\varrho}\left[\frac{m^2c_2^2\varrho^{-6}}{(K_1 + K_2 e^{-2mc_1/\varrho})^8} \times\right.$$

$$\times \left\{\varrho^{-2}(K_1 - K_2e^{-2mc_1/\varrho})^2 + (K_1^2 - K_2^2e^{-4mc_1/\varrho})^2 + 2\varrho^{-1}(K_1 - K_2e^{-2mc_1/\varrho}) \times\right.$$

$$\left.\left. \times (K_1^2 - K_2^2e^{-4mc_1/\varrho})\right\} + \text{similar terms corresponding to other factors}\right], \tag{19}$$

where $K_1 (= 1 + K)$ and $K_2 (= 1 - K)$ are constants.

Following COOPERSTOCK et al [9] we now investigate the behaviour of α along the curved path given by the power law

$$z = Dr^n, \quad n > 0, \tag{20}$$

where D is taken to be positive and $z \to 0_+$ to the origin. The following Table is the summary for the results.

Table I
Limits for α

Range	α	Directions as $r \to 0$
$0 < n < 2/3$	0	z-axis
$n = 2/3$, $D < (m/2c_2)^{1/3}$	∞	z-axis
$D \geq (m/2c_2)^{1/3}$	0	z-axis
$2/3 < n < 1$	∞	z-axis
$n = 1$, $r \neq 0$	∞	z-axis
$r = 0$ (the z-axis trajectory)	0	z-axis
$n > 1$	∞	r-axis

IV. Conclusions

According to GAUTREAU and ANDERSON a point is said to be singular if α becomes in some way either infinite or indeterminate. Our results are similar to those of COOPERSTOCK et al [9] with the difference that for critical trajectory $n = 2/3$ the scalar α depends on the relationship between the mass of the CURZON particle, the constant c_2 and the trajectory parameter D. It should be mentioned here that the constant c_2 is not an ordinary constant but characterizes the strengths of the fields either attractive or repulsive. If c_2 is taken to be equal to 1 which implies $c_1 = 0$, our results go over to the corresponding results of COOPERSTOCK et al [9] for the vacuum field solution. The qualitative behaviour of the singularity has not changed due to the presence of the coupled field. It may also be noted as can be seen from (16)—(18) that the scalar field S is singular at the origin whereas the electric field strengths F_{14}, F_{24} tend to zero. We may therefore conclude that the singularity is essentially due to the sources of gravitating material and the zero mass scalar field.

Acknowledgement

The authors thank Prof. G. BANDYOPADHYAY for his constant encouragement. They also thank Dr. R. N. TIWARI for helpful discussions. One of the authors (D.K.D.) wishes to record his thanks to the Council of Scientific and Industrial Research, New Delhi, for financial help.

REFERENCES

1. R. GAUTREAU and J. L. ANDERSON, Phys. Letts., **25A**, 291, 1967.
2. H. E. J. CURZON, Proc. Lond. Math. Soc., **23**, 477, 1924.
3. J. STACHEL, Phys. Letts., **27A**, 60, 1968.
4. R. GAUTREAU, Phys. Letts., **28A**, 606, 1969.
5. R. GAUTREAU, Il Nuovo Cimento, **62B**, 360, 1969.
6. D. K. DATTA and J. R. RAO, J. Phys. A., Math. Nucl. Gen., **6**, 917, 1973.
7. D. K. DATTA and J. R. RAO, J. Phys. A., Math. Nucl. Gen., **8**, 190, 1975.
8. F. I. COOPERSTOCK, G. J. G. JUNEVICUS and A. R. WILSON, Phys. Letts., **42A**, 203, 1972.
9. F. I. COOPERSTOCK and G. J. G. JUNEVICUS, Int. J. Theo. Phys., **9**, 59, 1974.
10. A. F. DA F. TEIXEIRA, IDEL WOLK and M. M. SOM, J. Phys., A., Math. Nucl. Gen., **9**, 53, 1976.

Acta Physica Academiae Scientiarum Hungaricae, Tomus 43 (2), pp. 147—153 (1977)

ИССЛЕДОВАНИЕ ВОЗМОЖНОСТИ СОЗДАНИЯ ЛАВИННО-ПРОЛЕТНОГО ДИОДА НА ГЕТЕРОПЕРЕХОДЕ ГЕРМАНИЙ-АРСЕНИД ГАЛЛИЯ

К. М. ДАТИЕВ*

ИНСТИТУТ ЭКСПЕРИМЕНТАЛЬНОЙ ФИЗИКИ, УНИВЕРСИТЕТ ИМ. АТТИЛЫ ЙОЖЕФА
СЕГЕД, ВЕНГРИЯ

(Поступило в редакцию 14. VII. 1977)

Приводятся некоторые результаты исследования возможности создания лавинно-пролетных диодов (ЛПД) на гетеропереходе германий-арсенид галлия. Сообщается о разработке ЛПД с указанной структурой, на которых впервые наблюдалась генерация СВЧ колебаний.

В работах [1—4] было показано, что использование гетеропереходов Ge — GaAs для ЛПД дает возможность создания высокоэффективных генераторов СВЧ колебаний на их основе.

В работе [3] впервые сообщалось о практическом создании ЛПД с указанной структурой, на которых наблюдалась генерация СВЧ колебаний.

В предлагаемой статье приводятся некоторые результаты экспериментального исследования возможности создания ЛПД на гетеропереходе Ge — GaAs.

1. Получение гетеропереходов германий-арсенид галлия

Гетеропереходы германий-арсенид галлия были получены путем осаждения из газовой фазы на подложках из арсенида галлия с использованием известной газотранспортной реакции диспропорционирования:

$$2GeI_2 \rightleftarrows Ge + GeI_4.$$

Процесс проводился в открытой системе с применением водорода в качестве газа-носителя.

Методика подготовки подложек арсенида галлия и германиевого источника и проведение процесса эпитаксиального наращивания германия йодидными методом в настоящее время достаточно отработаны [5—8] и мы не будем на них останавливаться. Однако, укажем, что выбранные режимы процесса эпитаксиального наращивания германия на подложках из арсенида галлия, чистота аппаратуры и, в особенности, чистота приспособлений

* Постоянное место работы: Факультет Электронной Техники, Северо-Кавказский Политехнический Институт, г. Орджоникидзе (СССР).

внутри реакционной камеры позволили нам получить гетеропереходы с резким распределением атомов примесей в широком диапазоне концентраций по обе стороны от границы раздела, избавиться от взаимной диффузии материалов и содержащихся в них примесей и травления пластин-подложек арсенида галлия йодом во время роста эпитаксиального слоя.

В качестве подложек использовался двухслойный ($n — n^+$) арсенид галлия с ориентацией (100). Высокоомные эпитаксиальные пленки арсенида галлия на низкоомный подложке были получены хлоридным методом. Параметры n-слоя GaAs лежали в пределах: концентрация электронов $10^{14} \div 10^{16}$ см$^{-3}$, подвижность электронов при комнатной температуре около 5000 см^2/в. сек. толщина — 5 ÷ 8 мкм. В качестве германиевого источника использовался высокоомный германий n-типа. Легирование эпитаксиальных пленок германия галлием в процессе роста позволило нам получить двухслойные пленки германия ($p — p^+$)-типа с однородным легированием по толщине p-слоя. Параметры высокоомной эпитаксиальной пленки германия лежали в пределах: концентрация дырок $2 \cdot 10^{15} \div 6 \cdot 10^{16}$ см$^{-3}$, подвижность дырок около 30 см^2/в.сек., толщина высокоомного p-слоя в пленке ($p — p^+$)-типа 0,5 ÷ 1,0 мкм, толщина пленки p^+-типа 8 ÷ 10 мкм с удельным сопротивлением 0,001 ом. см.

На основе полученных гетероэпитаксиальных структур ($p^+ — p$)Ge — — ($n — n^+$)GaAs изготавливались опытные образцы ЛПД.

2. Изготовление опытных образцов ЛПД

Полученные гетероструктуры Ge — GaAs разрезались на кристаллы с размерами $0{,}3 \times 0{,}3$ мм^2. В качестве омического контакта к n^+ — GaAs использовалось чистое олово, вплавляемое в атмосфере водорода при температуре 470 °С в течение 5 минут, а к германию p^+-типа — сплав In — Sn вплавляемый при температуре 450 °С в течение 3 минут.

Достаточно низкие температуры процессов вплавления исключали возможность образования «ложного» гомоперехода в результате диффузии мышьяка из подложки в германий p-типа. Травлением гетеродиодов в растворе 5% H_2O_2 с добавкой КОН при температуре 70 °С обеспечивалось образование меза-структуры с диаметром $p — n$ перехода 60—70 мкм. Полученные гетеропереходы герметизировались в стандартных корпусах полупроводниковых СВЧ приборов. В работе приведены результаты измерений опытных образцов ЛПД, относящиеся к двум партиям (А и Б) с различными параметрами n-слоя: партия А (концентрация электронов $8 \cdot 10^{15}$ см$^{-3}$, толщина 7 мкм); партия Б (концентрация электронов $6 \cdot 10^{14}$ см$^{-3}$, толщина 5 мкм).

3. Исследование электрических характеристик ЛПД

Исследования электрических характеристик разработанных образцов гетеродиодов велись в направлении изучения механизма пробоя, определения распределения атомов примесей в области запирающего слоя и возможности получения генерации СВЧ колебаний. В связи с этим сначала были исследованы температурная зависимость напряжения пробоя, вольтфарадные характеристики, а затем — высокочастотные характеристики ЛПД на гетеропереходе Ge — GaAs.

3а. *Напряжение пробоя и его температурная зависимость*

Исследования обратной ветви вольтамперной характеристики гетеродиодов были проведены в широком интервале температур. На рис. 1 представлены обратные ветви вольтамперных характеристик некоторых гетеродиодов. Величина обратного тока насыщения у всех диодов при напряжении — 10 В не превышала 0,05 мка.

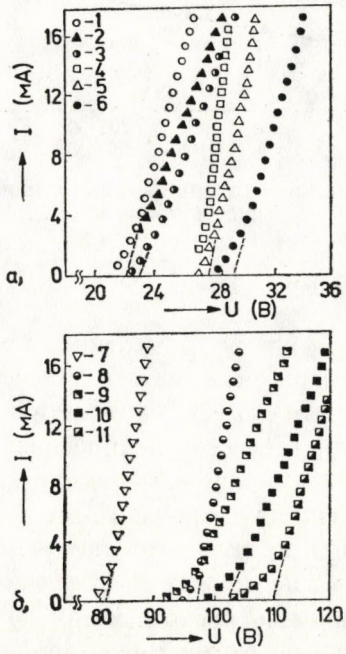

Рис. 1. Обратные ветви вольтамперных характеристик гетеродиодов:
образцы: *а)* 1—А03, 2—А14, 3—А26,
4—А43, 5—А65, 6—А78,
б) 7—Б15, 8—Б18, 9—Б27,
10—Б42, 11—Б93

Величина дифференциального сопротивления для различных диодов положительна и лежит в пределах 50—400 ом. Типичные температурные зависимости напряжений пробоя некоторых гетеродиодов в интервале температур 170 ÷ 400 °К приведены на рис. 2. Видно, что напряжение пробоя возрастает с ростом температуры, что свидетельствует о лавинном механизме пробоя в исследованных гетеродиодах.

Как известно, одним из важных моментов при создании ЛПД на основе гетероперехода является выяснение вопроса о локализации полного умножения в одной из областей запорного слоя. В работе [9] приведены некоторые результаты оценки локализации полного умножения в области объемного заряда разработанных гетеропереходов.

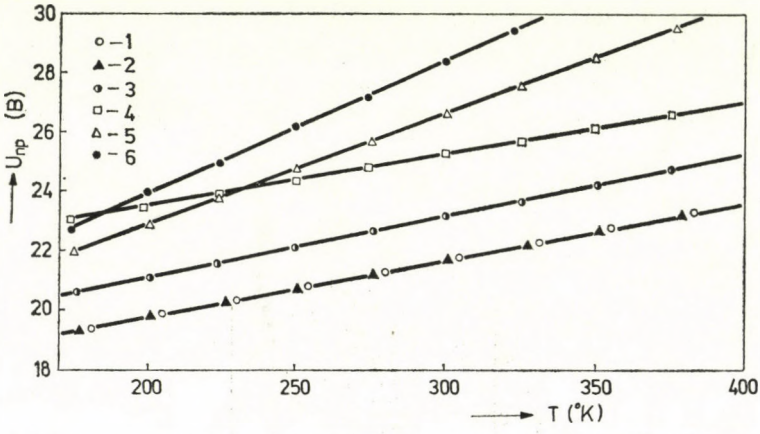

Рис. 2. Температурные зависимости напряжений лавинного пробоя гетеродиодов (обозначения образцов на рис. 1)

3б. *Вольтфарадные характеристики*

Для определения профиля распределения атомов примесей в запорном слое и закона изменения барьерной емкости полученных образцов приборов были построены их вольтфарадные характеристики.

Зависимость емкости исследуемых приборов от обратного смещения снималась методом емкостно-омического делителя на частоте 1 Мгц при величине зондирующего сигнала, равной 10 мв.

Результаты измерений представлены на рис. 3—4.

На чис. 3 приведены зависимости емкости от обратного смещения, позволяющие определить профиль распределения концентрации атомов примесей в запорном слое p-n перехода. Видно, что все исследуемые приборы имеют резкое распределение атомов примесей по обе стороны от границы раздела. Для группы приборов со структурой $(p^+ - p)$Ge — $(n - n^+)$GaAs наблюдается режим ограниченного расширения областей объемного заряда

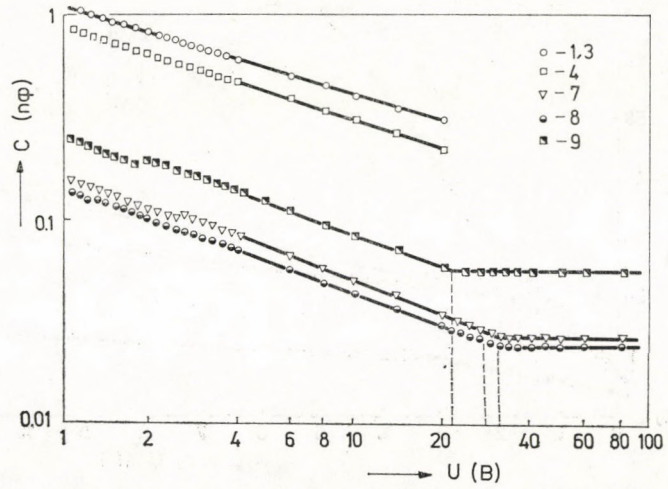

Рис. 3. Вольтфарадные характеристики гетеродиодов в логарифмическом масштабе (обозначения образцов на рис. 1)

по обе стороны от границы раздела. При малых смещениях ($|U| < 3$В) барьерная емкость гетеродиодов подчиняется уравнению

$$C = \left[\frac{q\varepsilon_0\varepsilon_1\varepsilon_2 N_1 N_2}{2(\varepsilon_1 N_1 + \varepsilon_2 N_2)} \cdot \frac{1}{\varphi_k + U}\right]^{\frac{1}{2}} \cdot S$$

и, следовательно, наклон зависимости $C^{-2}(U)$ равен

$$\operatorname{arc\,tg}\left[\frac{2\left(1 + \dfrac{\varepsilon_2 N_2}{\varepsilon_1 N_1}\right)}{q\varepsilon_0\varepsilon_2 N_2 \cdot S^2}\right].$$

(Обозначения — общепринятые: индекс 1 — германий; 2 — арсенид галлия).

При дальнейшем увеличении модуля отрицательного смещения барьерная емкость гетеродиодов определяется более толстой высокоомной областью арсенида галлия с наклоном $C^{-2}(U)$ характеристики, равным $\operatorname{arc\,tg}(2/q\varepsilon_0\varepsilon_2 N_2 S^2)$.

При напряжениях около $20 \div 40$ в область объемного заряда распространяется до низкоомного n^+-слоя арсенида галлия и при дальнейшем увеличении модуля обратного смещения барьерная емкость гетеропереходов остается постоянной. Исключение составляет ряд приборов с аналогичной структурой $(p^+ - p)$Ge — $(n - n^+)$GaAs, в которых до режима ограниченного расширения области объемного заряда в n-слое наступает лавинный пробой.

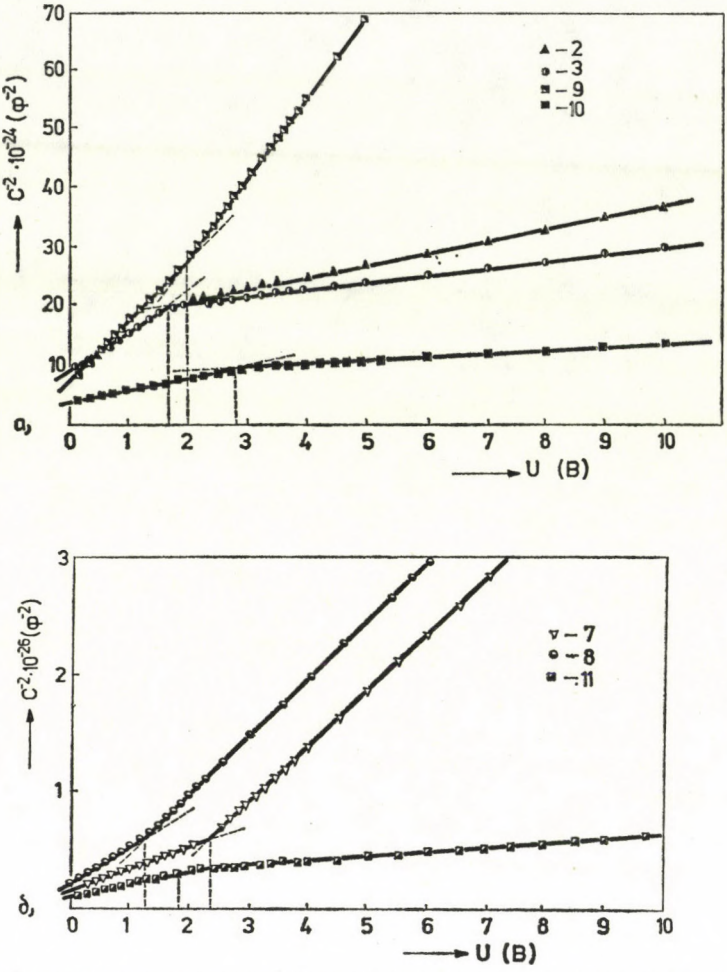

Рис. 4. Вольтфарадные характеристики гетеродиодов, построенные в координатах $C^{-2} - U$ (обозначения образцов на рис. 1)

Для определения расчетных значений напряжений пробоя по [1, 2] и сравнения их с экспериментальными данными по вольтфарадным характеристикам были рассчитаны толщины и степени легирования высокоомных областей по обе стороны от границы раздела гетеропереходов Ge — GaAs.

Анализ полученных результатов показал, что для приборов с напряжением пробоя 20 ÷ 120 в различие между расчетными и экспериментальными значениями напряжений пробоя не превышает 10—15%.

Таким образом, исследование лавинного пробоя гетеропереходов Ge — GaAs подтвердило правильность теоретических результатов полученных в работах [1, 2].

3в. *Высокочастотные характеристикиЛПД*

Разработанные образцы ЛПД исследовались в режиме генерации СВЧ колебаний в трехсантиметровом диапазоне длин волн. Нами впервые была получена эффективная генерация СВЧ колебаний на ЛПД с двухслойным запирающим слоем на основе Ge — GaAs гетеропереходов [3]. Генерация была обнаружена при импульсном режиме питания с величиной тока в импульсе 15 ÷ 250 ма, длительностью импульса 1 ÷ 10 мксек и скважностью 10^3 ÷ 10^4. Мощность генерации составляла 100 ÷ 150 мвт в импульсе. Максимальный к. п. д. —5%.

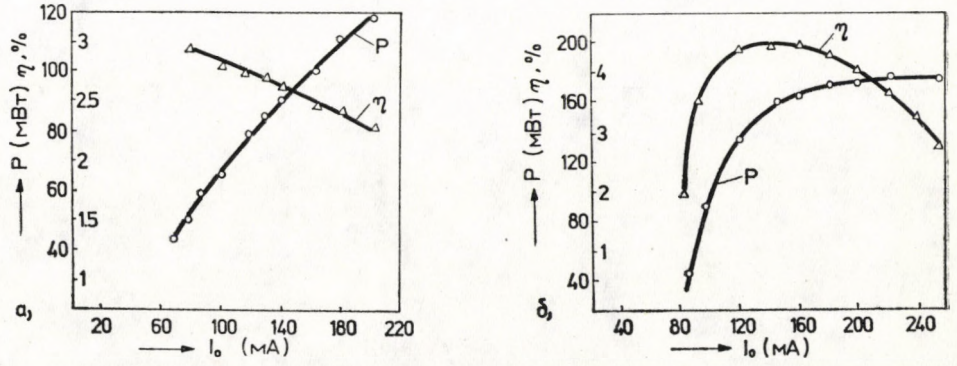

Рис. 5. Токовые зависимости мощности генерации и к. п. д. генераторов на основе гетеородиодов:
образцы: а — АО3, б — А14

На рис. 5 приведены токовые зависимости мощности и к. п. д. для двух приборов. Основные параметры первых экспериментальных образцов ЛПД на гетеропереходе Ge — GaAs, на которых была получена генерация СВЧ колебаний в X-диапазоне, приведены в таблице ($U_{пр}$ — напряжение пробоя, В; $C_{пр}$ — емкость гетероперехода при напряжении пробоя, пф; $I_{обр.}$ — обратный ток гетероперехода при обратном смещении — 10 В., мка; $R_{диф.}$ — дифференциальное сопротивление гетеродиодов в рабочем режиме, ом; I_0 — величина тока в режиме генерации, ма; P — мощность генерации, мвт; η — к. п. д., %).

Вследствие наличия достаточно толстых высокоомных слоев арсенида галлия и большой величины сопротивления омических контактов к германию и арсениду галлия, величина τ_s/τ_λ, характеризующая потери, в разработанных приборах высокая ($\tau_s/\tau_\lambda > 0{,}1$) что и обуславливает низкие значения мощности и к. п. д. [4]. Следовательно, для создания высокоэффективных ЛПД с двухслойным запирающим слоем на основе гетероперехода Ge — GaAs необходима дальнейшая отработка технологического варианта

получения гетероперехода с оптимальными параметрами структуры по обе стороны от границы раздела и улучшения свойств невыпрямляющих контактов к германию и арсениду галлия [4].

4. Выводы

1. Впервые разработаны ЛПД с двухслойным запирающим слоем на основе гетероперехода Ge — GaAs, на которых получена эффективная генерация СВЧ колебаний в сантиметровом диапазоне длин волн.

Таблица 1

Основные параметры экспериментальных образцов ЛПД на гетеропереходе Ge — GaAs

№ образца	$U_{пр.}$, В	$C_{пр.}$, пф	$I_{обр.}$ при −10В мка	$R_{диф.}$, ом	I_{0}, мА	P, мВт	η, %
A03	22,1	0,3	0,04	10	200	120	2,5
A14	22	0,2	0,04	30	135	150	4,45
A26	23	0,8	0,04	30	75	80	3,3
A43	26,2	0,2	0,03	50	55	40	2,7
A65	27	0,3	0,05	40	140	90	2,4
A78	28,9	0,3	0,03	60	40	75	5

2. Исследования электрических характеристик гетеропереходов Ge—GaAs и ЛПД на их основе показали:

а) исследуемые гетеропереходы представляют собой структуры типа $(p^+ - p)$Ge — $(n - n^+)$GaAs с однородным распределением атомов примесей по обе стороны от границы раздела;

б) обратная ветвь вольтамперной характеристики имеет резкий излом, что в сочетании с положительным ТКН пробоя свидетельствует о лавинном механизме пробоя;

в) сравнение экспериментальных и теоретических значений напряжений лавинного пробоя и оценки локализации полного умножения в одной из частей запорного слоя в исследованных гетеропереходах подтвердили правильность результатов теории лавинного пробоя гетеропереходов;

г) разработанные первые экспериментальные образцы ЛПД с двухслойным запирающим слоем обеспечивают в трехсантиметровом диапазоне мощность генерации 100 ÷ 150 мвт в импульсе с к. п. д. до 5%.

ЛИТЕРАТУРА

1. К. М. Датиев, И. М. Мартиросов, Я. А. Федотов, В сб. «Электронная техника» сер. 2, Полупроводниковые приборы, **6,** 35, 1970.
2. Я. А. Федотов, К. М. Датиев, в сб. «Электронная техника» сер. 2, Полупроводниковые приборы, **6,** 3, 1971.
3. Я. А. Федотов, И. М. Мартиросов, К. М. Датиев, Ю. А. Кузнецов ФТП, **5,** 1671, 1971.
4. Я. А. Федотов, К. М. Датиев, в сб. «Электронная техника», сер. 2., Полупроводниковые приборы, **3,** 3, 1976.
5. R. L. Anderson, IBM J., **4,** 283, 1960.
6. R. L. Anderson, Solid Stat. Electr., **5,** 341, 1962.
7. F. F. Fang, W. E. Howard, J. Appl. Phys., **35,** 612, 1964.
8. A. R. Riben, D. L. Feucht, J. Electrochem. Soc., **135, 245**, 1966.
9. K. M. Datiev, Acta Phys. Hung., **42,** 189, 1977.

Acta Physica Academiae Scientiarum Hungaricae, Tomus 43 (2), pp. 157—162 (1977)

STABILITY OF ROTATING STRATIFIED FLUID IN THE PRESENCE OF A VARIABLE HORIZONTAL MAGNETIC FIELD

By

R. C. SHARMA

DEPARTMENT OF MATHEMATICS, HIMACHAL PRADESH UNIVERSITY, SIMLA 171005, INDIA

(Received 9. VIII. 1977)

A study has been made of the stability of a rotating stratified fluid in the presence of a variable horizontal magnetic field. Both the density and the horizontal magnetic field are assumed to be exponentially varying. The dispersion relation has been obtained. Some special cases are drawn and discussed. Both rotation and magnetic field are found to have stabilizing effect on the system.

1. Introduction

The instability derived from the character of the equilibrium of an incompressible heavy fluid of variable density (i.e. of a heterogeneous fluid) is termed the Rayleigh—Taylor instability. Mention may be made of two important special cases: (a) two fluids of different densities superposed one over the other; (b) a fluid with a continuous density stratification. HIDE [1] has studied the effect of rotation on the character of the equilibrium of a stratified heterogeneous, inviscid fluid and found that rotation stabilizes the potentially unstable arrangement of certain wave number. In another study, HIDE [2] studied the case of a viscous conducting fluid with a transverse magnetic field and found that magnetic field considerably stabilizes the configuration and it is possible to have oscillatory motion in the presence of magnetic field even if the configuration is thoroughly unstable. KRUSKAL and SCHWARZSCHILD [3] have considered the stability of an inviscid plasma of infinite conductivity supported against gravity by a horizontal magnetic field. CHANDRASEKHAR [4] has given a detailed account of the Rayleigh—Taylor instability, under varying assumptions of hydrodynamics and hydromagnetics. The magnetic field, in the above studies, has been considered to be constant and uni-directional. GUPTA [5] has investigated the stability of a horizontal layer of a perfectly conducting fluid, with continuous density and viscosity stratification in the presence of a horizontal magnetic field (constant as well as variable). SHARMA [6] has studied the effect of rotation and surface tension on the stability of two superposed fluids in the presence of a variable horizontal magnetic field.

The problem of the hydromagnetic stability of conducting fluid of variable density plays an important role in astrophysics (stability of stellar atmosphere in magnetic field, heating of solar corona, theories and sunspot magnetic fields). Since the Coriolis forces play an important role in astrophysical problems, it is necessary to study the combined effect of rotation and magnetic field.

In the present paper we study the Rayleigh—Taylor instability of a fluid with a continuous density stratification in the presence of rotation and a variable horizontal magnetic field. The fluid is considered to be heterogeneous, inviscid and of zero resistivity. The fluid is assumed to be infinitely extending so that the free surface is almost horizontal. The fluid is under the action of gravity $\mathbf{g}$ $(0, 0, -g)$ and acted on by a uniform rotation $\mathbf{\Omega}$ $(0, 0, \Omega)$ and a variable horizontal magnetic field $\mathbf{H}$ $(H_0(z), 0, 0)$.

2. Basic equations

Let p, ϱ and $\mathbf{v}$ (u, v, w) denote respectively the pressure, the density and the velocity of the fluid; μ_e is the magnetic permeability. The hydromagnetic equations to be solved in the fluid are

$$\varrho\left[\frac{\partial \mathbf{v}}{\partial t} + (\mathbf{v}\cdot\nabla)\,\mathbf{v}\right] = -\nabla p + \mu_e(\nabla\times\mathbf{H})\times\mathbf{H} + \varrho\mathbf{g} + 2\varrho(\mathbf{v}\times\mathbf{\Omega})\,, \tag{1}$$

$$\nabla\cdot\mathbf{v} = 0\,, \tag{2}$$

$$\frac{\partial \mathbf{H}}{\partial t} = \nabla\times(\mathbf{v}\times\mathbf{H})\,, \tag{3}$$

$$\nabla\cdot\mathbf{H} = 0\,. \tag{4}$$

Since the density of particle moving with the fluid remains unchanged. Hence

$$\frac{\partial \varrho}{\partial t} + (\mathbf{v}\cdot\nabla)\,\varrho = 0\,. \tag{5}$$

Let $\delta\varrho$, δp, $\mathbf{v}$ (u, v, w) and $\mathbf{h}$ (h_x, h_y, h_z) denote the perturbations in density, pressure, velocity and magnetic field, respectively. Then the linearized hydromagnetic perturbation equations are

$$\varrho\frac{\partial \mathbf{v}}{\partial t} = -\nabla\delta p + \mu_e(\nabla\times\mathbf{h})\times\mathbf{H} + \mathbf{g}\delta\varrho + 2\varrho(\mathbf{v}\times\mathbf{\Omega})\,, \tag{6}$$

$$\nabla\cdot\mathbf{v} = 0\,, \tag{7}$$

$$\frac{\partial \mathbf{h}}{\partial t} = \nabla \times (\mathbf{v} \times \mathbf{H}) \ , \tag{8}$$

$$\nabla \cdot \mathbf{h} = 0 \ , \tag{9}$$

$$\frac{\partial}{\partial t} \delta\varrho = -w \frac{d\varrho}{dz} \ . \tag{10}$$

Analyzing the disturbance into normal modes, we seek solutions whose dependence on x, y and t is given by

$$\exp (ik_x x + ik_y y + nt), \tag{11}$$

where k_x and k_y are the horizontal components of the wave number, $k^2 = k_x^2 + k_y^2$ and n is the rate at which the system departs from equilibrium.

Using the expression (11), Eqs. (6)—(10) become

$$\varrho n u = -ik_x \delta p + \frac{\mu_e}{4\pi} h_z D H_0 + 2\varrho\Omega v \ , \tag{12}$$

$$\varrho n v = -ik_y \delta p + \frac{\mu_e H_0}{4\pi} (ik_x h_y - ik_y h_x) - 2\varrho\Omega u \ , \tag{13}$$

$$\varrho n w = -D\delta p + \frac{g}{n} (D\varrho)\, w + \frac{\mu_e H_0}{4\pi} \left(ik_x h_y - D h_x - h_x \frac{DH_0}{H_0} \right) \ , \tag{14}$$

$$ik_x u + ik_y v + Dw = 0 \ , \tag{15}$$

$$ik_x h_x + ik_y h_y + D h_z = 0 \ , \tag{16}$$

$$\mathbf{h} = \frac{ik_x H_0}{n} \mathbf{v} - w(DH_0)\, \mathbf{I}_x \ , \tag{17}$$

where $\mathbf{I}_x$ (1, 0, 0) is the unit vector in the direction of x-axis and $D = d/dz$.

Multiplying Eqs. (12) and (13) by $-ik_x$, $-ik_y$ respectively, adding and substituting for h_x, h_y; we get

$$\varrho n D w = -k^2 \delta p - 2\varrho\Omega\zeta + \frac{k_x k_y}{n} \frac{\mu_e H_0^2}{4\pi} \zeta + \frac{\mu_e H_0 k^2}{4\pi n} w D H_0 \ , \tag{18}$$

where ζ, the z-component of vorticity, is given by

$$\zeta = \frac{\partial v}{\partial x} - \frac{\partial u}{\partial y} = ik_x v - ik_y u \ . \tag{19}$$

Multiplying Eqs. (12) and (13) by $-ik_y$ and $+ik_x$, respectively, and adding,

we get

$$\zeta = \frac{2\Omega n\, Dw}{n^2 + k_x^2 V^2}, \tag{20}$$

where $V^2 = \mu_e H_0^2/4\pi\varrho$ is the square of the Alfvén velocity.

Eliminating δp between Eqs. (14) and (18), using (20) and the relation

$$ik^2 u = -(k_x Dw + k_y \zeta) = -\left(k_x Dw + \frac{2k_y \Omega n Dw}{n^2 + k_x^2 V^2}\right), \tag{21}$$

we get after simplification

$$\left[1 + \frac{4\Omega^2}{n^2 + k_x^2 V^2}\right] D(\varrho\, Dw) - k^2 \varrho w + \frac{\mu_e k_x^2}{4\pi n^2} [D(H_0^2 Dw) - k^2 H_0^2 w] = \\ = -\frac{gk^2}{n^2} (D\varrho)\, w\,. \tag{22}$$

Eq. (22) is the general equation formulating the effect of rotation and a variable horizontal magnetic field on the Rayleigh—Taylor instability. In the limit of vanishing magnetic field ($H_0 \to 0$), we get the particular case of the effect of rotation on the Rayleigh—Taylor instability (CHANDRASEKHAR [4], Chapter X). The particular case of the effect of constant horizontal magnetic field (CHANDRASEKHAR [4], Chapter X) can be derived in the limit of vanishing Ω.

3. The case of exponentially varying density and magnetic field

Assume the stratifications in density and magnetic field of the form

$$\varrho = \varrho_1 e^{\beta z}, \qquad H_0^2 = H_1^2 e^{\beta z}, \tag{23}$$

where ϱ_1, H_1 and β are constants and so the square of the Alfvén velocity

$$V^2 = \mu_e H_0^2/4\pi\varrho = \mu_e H_1^2/4\pi\varrho_1\,. \tag{24}$$

Using the stratification of the form (23), Eq. (22) transforms to

$$D^2 w + \beta Dw - \left\{\frac{(n^2 + k_x^2 V^2 - g\beta)(n^2 + k_x^2 V^2)}{(n^2 + k_x^2 V^2)^2 + 4\Omega^2 n^2}\right\} k^2 w = 0\,. \tag{25}$$

The general solution of Eq. (25) is

$$w = A_1 e^{q_1 z} + A_2 e^{q_2 z}, \tag{26}$$

where A_1, A_2 are two arbitrary constants and q_1, q_2 are the roots of the equation

$$q^2 + q\beta - \left\{\frac{(n^2 + k_x^2V^2 - g\beta)\,(n^2 + k_x^2V^2)}{(n^2 + k_x^2V^2)^2 + 4\Omega^2n^2}\right\}k^2 = 0\ . \tag{27}$$

If the fluid is supposed to be confined between two rigid planes at $z = 0$ and $z = d$, then the vanishing of w at $z = 0$ is satisfied by the choice

$$w = A(e^{q_1z} - e^{q_2z})\ , \tag{28}$$

while the vanishing of w at $z = d$ requires

$$\exp\,(q_1 - q_2)\,d = 1, \tag{29}$$

which imply that

$$(q_1 - q_2)\,d = 2im\pi\ , \tag{30}$$

where m is an integer.

Eq. (27) gives

$$q_{1,2} = -\frac{\beta}{2} \pm \frac{1}{2}\sqrt{\beta^2 + \frac{4k^2(n^2 + k_x^2V^2 - g\beta)\,(n^2 + k_x^2V^2)}{(n^2 + k_x^2V^2)^2 + 4\Omega^2n^2}}\ . \tag{31}$$

Inserting the values of q_1, q_2 in Eq. (30) and simplifying, we obtain

$$\begin{aligned}(1 + A)\,n^4 + [(2k_x^2V^2 + 4\Omega^2)\,A + 2k_x^2V^2 - g\beta]\,n^2 + \\ + k_x^2V^2[k_x^2V^2(1 + A) - g\beta] = 0\ ,\end{aligned} \tag{32}$$

where

$$A = \left(\frac{1}{4}\beta^2d^2 + m^2\pi^2\right)\Big/k^2d^2\ .$$

Eq. (32) is the dispersion relation studying the effect of rotation and the variable (exponentially) horizontal magnetic field on the Rayleigh—Taylor instability of fluid with exponentially varying density.

If $\beta < 0$ (stable stratification), Eq. (32) does not admit of any positive root of n^2 and the system is always stable for disturbances of all wave numbers.

If $\beta > 0$ (unstable stratification) and if

$$g\beta < k_x^2V^2(1 + A), \tag{33}$$

Eq. (32) does not allow any of the roots of n^2 to be positive. The system is therefore stable. If (33) is violated, the system may be unstable also. For the stability of the system, we must have

$$g\beta < k_x^2V^2(1 + A)\ .$$

In the special case of zero magnetic field, Eq. (32) reduces to

$$\frac{g\beta}{n^2} = 1 + \left(1 + \frac{4\Omega^2}{n^2}\right)\left(\frac{\frac{1}{4}\beta^2 d^2 + m^2\pi^2}{k^2 d^2}\right) . \tag{34}$$

If n_0^2 is the value of n^2 in the absence of rotation, Eq. (34) gives

$$n^2 = n_0^2\left[1 - \frac{4\Omega^2}{g\beta}\frac{\frac{1}{4}\beta^2 d^2 + m^2\pi^2}{k^2 d^2}\right] . \tag{35}$$

If β is positive, the rotation stabilizes the unstable arrangement for all wave numbers less than

$$g\beta k_{\min}^2 = \frac{4\Omega^2}{d^2}\left(\frac{1}{4}\beta^2 d^2 + \pi^2\right) , \tag{36}$$

and for a given Ω, $k_{\min}$ occurs for $\beta = 2\pi/d$. Distributions with β less than or greater than $2\pi/d$ are stabilized by rotation for greater ranges of k.

REFERENCES

1. R. HIDE, Proc. Roy. Soc., **A223,** 376, 1955.
2. R. HIDE, Quart. J. Appl. Math., **9,** 22, 1956.
3. M. KRUSKAL and M. SCHWARZSCHILD, Proc. Roy. Soc., *A233,* 348, 1954.
4. S. CHANDRASEKHAR, Hydrodynamic and Hydromagnetic Stability, Clarendon Press, Oxford, Chapter X, 1961.
5. A. S. GUPTA, J. Phys. Soc. Japan, **18,** 1073, 1963.
6. R. C. SHARMA, Progress of Mathematics, **7,** 1, 1973.

Acta Physica Academiae Scientiarum Hungaricae, Tomus 43 (2), pp. 163—171 (1977)

HEAT TRANSFER IN TWO-PHASE LAMINAR FLOW FOR TIMEWISE LINEAR VARIATION OF INLET TEMPERATURE IN A CIRCULAR PIPE

By

S. N. DUBE

DEPARTMENT OF MATHEMATICS, HIMACHAL PRADESH UNIVERSITY, SIMLA-171005, INDIA

(Received 1. IX. 1977)

Exact solutions of the forced convection energy equations of dust particles and of liquid with fully developed flow in a circular pipe are obtained in the present problem when the inlet temperatures vary linearly with time and an interpretation of the case of laminar flows is given.

Nomenclature

$\bar{T}_p$	temperature of dust particle
$\bar{T}$	temperature of liquid
c_p	specific heat of dust particle
c	specific heat of liquid
a	pipe radius
K_p	thermal conductivity of dust particle
K	thermal conductivity of liquid
$\bar{t}$	time
u_p	velocity component of dust particle in $\bar{z}$-direction
u	velocity component of liquid in $\bar{z}$-direction
$\bar{u}$	average velocity
$\bar{r}, \bar{\Phi}, \bar{z}$	cylindrical polar coordinates ($\bar{z}$-flow direction)
ϱ	liquid density
mN	mass of dust particle per unit volume ($= mN_0$, constant)
μ	coefficient of viscosity of liquid
ν	kinematic coefficient of viscosity of liquid
P	Prandtl number $(= \mu c/K)$
R	Reynolds number $(= a\bar{u}/\nu)$
h_p	heat transfer coefficient for flow over dust particle
A_p	surface area of dust particle
V_p	volume of dust particle
T_0, T_1, T_2	known temperature constants

The meaning of any other symbols is given in the text as they occur.

1. Introduction

Heat transfer by gas-dust suspensions in pipe flow has been the subject of many studies because of the anticipated large heat-transfer coefficient due to the high volumetric specific heat of dust particles or liquid droplets compared to a gas and the demand for high heat-transfer coefficient in gas-cooled reactors. Based on the experimental observations on gas-dust suspensions by

FARBAR and MORLEY [1] and SCHLUDERBERG [2], by JOHNSON [3] on gas suspensions of liquid droplets, and by SALOMONE and NEWMANN [4] on liquid-dust suspensions, TIEN [5, 6] has analysed the heat transfer by a gas-dust suspension in turbulent pipe flow based on a simplified model. In solutions of the forced convection energy equations of dust particles and of liquid in a circular pipe SOO [7] has assumed that the inlet temperatures of dust particles and of liquid are constants across the flow with a specified constant wall temperature. Recently DUBE and SHARMA [8] have obtained exact solutions of the forced convection energy equations of dust particles and of liquid in a channel bounded by two parallel flat plates when the inlet temperatures vary periodically with time.

In the present paper exact solutions of the forced convection energy equations of dust particles and of liquid with fully developed flow in a circular pipe are obtained under a prescribed boundary condition when the inlet temperatures of dust particles and of liquid vary linearly with time and an interpretation of the case of laminar flows is given.

2. Formulation of the problem

We consider the steady laminar flow of a dusty viscous liquid with uniform distribution of dust particles in a circular pipe of radius a. The dust particles and the liquid entering the pipe have temperatures which are spatially uniform across the entrance section but vary linearly with time. Therefore we can write the inlet conditions as

$$\overline{T}_p(\bar{r}, 0, \bar{t}) = T_0 + T_1\left(\frac{v\bar{t}}{a^2}\right) . \tag{2.1}$$

$$\overline{T}(\bar{r}, 0, \bar{t}) = T_0 + T_1\left(\frac{v\bar{t}}{a^2}\right) . \tag{2.2}$$

To obtain the heat-transfer performance and the temperatures of dust particles and of liquid it is necessary to set down two energy equations, one for the dust particles and one for the liquid-dust mixture. They are given as

$$\frac{\partial \overline{T}_p}{\partial \bar{t}} + u_p \frac{\partial \overline{T}_p}{\partial \bar{z}} = G(\overline{T} - \overline{T}_p) , \tag{2.3}$$

$$\frac{\partial \overline{T}}{\partial \bar{t}} + u \frac{\partial \overline{T}}{\partial \bar{z}} + \frac{mN_0 c_p}{\varrho c}\left(\frac{\partial \overline{T}_p}{\partial \bar{t}} + u_p \frac{\partial \overline{T}_p}{\partial \bar{z}}\right) = \frac{\nu}{P}\left(\frac{\partial^2 \overline{T}}{\partial \bar{r}^2} + \frac{1}{\bar{r}} \frac{\partial \overline{T}}{\partial \bar{r}}\right) + \beta_2(\overline{T}_p - \overline{T}) , \tag{2.4}$$

where

$$G = \frac{h_p A_p}{m N_0 c_p V_p}, \qquad \beta_2 = \frac{m N_0 c_p G}{\varrho c}.$$

Simplifying (2.4), we get

$$\frac{\partial \overline{T}}{\partial \bar{t}} + u \frac{\partial \overline{T}}{\partial \bar{z}} = \frac{\nu}{P}\left(\frac{\partial^2 \overline{T}}{\partial \bar{r}^2} + \frac{1}{\bar{r}} \frac{\partial \overline{T}}{\partial \bar{r}}\right) + 2\beta_2(\overline{T}_p - \overline{T}) . \tag{2.5}$$

The inlet and the boundary conditions of the problem are as follows:

$$\overline{T}_p = T_0 + T_1\left(\frac{\nu \bar{t}}{a^2}\right) \quad \text{when} \quad \bar{z} = 0 , \tag{2.6}$$

$$\overline{T} = T_0 + T_1\left(\frac{\nu \bar{t}}{a^2}\right) \quad \text{when} \quad \bar{z} = 0 , \tag{2.7}$$

$$\overline{T}_p \text{ is finite at } \bar{r} = 0 , \tag{2.8}$$

$$\overline{T} \text{ is finite at } \bar{r} = 0, \tag{2.9}$$

$$\overline{T}_p = T_2 \text{ at } \bar{r} = a , \tag{2.10}$$

$$\overline{T} = T_2 \text{ at } \bar{r} = a , \tag{2.11}$$

$$\bar{t} > 0 .$$

The system satisfying (2.3), (2.5) is subjected to the following restrictions (Soo [7]):

(i) Radiation effect is neglected.

(ii) The density of liquid remains constant; thus the velocity distribution is independent of the temperature distribution.

(iii) Liquid property variations are neglected.

(iv) Each dust particle is small and maintains uniform temperature due to its high thermal conductivity K_p.

(v) The liquid and dust particle cloud have similar velocity profiles. The presence of dust particles does not affect the liquid velocity profile.

(vi) The dust particles are uniformly distributed throughout the pipe.

(vii) The effect of collision with the wall is neglected.

(viii) The suspension is extremely dilute such that each particle is assumed to see the wall without interference of other particles.

(ix) Fully developed laminar velocity profiles in the pipe.

(x) Axial conduction is negligible with respect to bulk transport in the $\bar{z}$-direction. This is a reasonable assumption when Péclét number exceeds 100 [9].

(xi) Thermal resistance of the wall is negligible.

(xii) Eddy diffusivity of heat is negligible.

Further, to simplify the method of analysis the case of constant velocity will be considered here and for this purpose we substitute $\bar{u}$ ($u = u_p$) for the velocity profile in (2.3) and (2.5).

We now introduce the following non-dimensional quantities:

$$\Theta_p = \frac{\bar{T}_p - T_0}{T_1}, \quad \Theta = \frac{\bar{T} - T_0}{T_1}, \quad z = \frac{\bar{z}}{a}, \quad r = \frac{\bar{r}}{a},$$

$$t = \frac{v\bar{t}}{a^2}, \quad \Theta_0 = \frac{T_2 - T_0}{T_1}, \quad \beta_3 = \frac{a^2 G}{\nu}, \quad \beta_4 = \frac{2a^2\beta_2}{\nu}.$$

Equations (2.3) and (2.5) then become

$$\frac{\partial \Theta_p}{\partial t} + R\frac{\partial \Theta_p}{\partial z} = \beta_3(\Theta - \Theta_p). \tag{2.12}$$

$$\frac{\partial \Theta}{\partial t} + R\frac{\partial \Theta}{\partial \bar{z}} = \frac{1}{P}\left(\frac{\partial^2 \Theta}{\partial r^2} + \frac{1}{r}\frac{\partial \Theta}{\partial r}\right) + \beta_4(\Theta_p - \Theta). \tag{2.13}$$

The inlet and the boundary conditions reduce to

$$\Theta_p = t \quad \text{when} \quad z = 0\ , \tag{2.14}$$

$$\Theta = t \quad \text{when} \quad z = 0\ , \tag{2.15}$$

$$\Theta_p \quad \text{is finite at} \quad r = 0\ , \tag{2.16}$$

$$\Theta \quad \text{is finite at} \quad r = 0\ , \tag{2.17}$$

$$\Theta_p = \Theta_0 \quad \text{at} \quad r = 1\ , \tag{2.18}$$

$$\Theta = \Theta_0 \quad \text{at} \quad r = 1\ , \tag{2.19}$$

$$t > 0\ .$$

3. Solution

For the solution of the above problem we assume that

$$\Theta_p(r, z, t) = \Theta_{p1}(r, z) + t\,\Theta_{p2}(r, z)\ , \tag{3.1}$$

$$\Theta(r, z, t) = \Theta_1(r, z) + t\,\Theta_2(r, z)\ , \tag{3.2}$$

where $\Theta_{p1}, \Theta_{p2}, \Theta_1$ and Θ_2 satisfy the following problems:

$$R\frac{\partial \Theta_{p2}}{\partial z} = \beta_4(\Theta_2 - \Theta_{p2})\ , \tag{3.3}$$

$$R\frac{\partial \Theta_2}{\partial z} = \frac{1}{P}\left(\frac{\partial^2 \Theta_2}{\partial r^2} + \frac{1}{r}\frac{\partial \Theta_2}{\partial r}\right) + \beta_4(\Theta_p - \Theta_2), \tag{3.4}$$

$$\Theta_{p2} = 1 \quad \text{when} \quad z = 0 \ , \tag{3.5}$$

$$\Theta_2 = 1 \quad \text{when} \quad z = 0 \ , \tag{3.6}$$

$$\Theta_{p2} \quad \text{is finite at} \quad r = 0 \ , \tag{3.7}$$

$$\Theta_2 \quad \text{is finite at} \quad r = 0 \ , \tag{3.8}$$

$$\Theta_{p2} = 0 \quad \text{at} \quad r = 1 \ , \tag{3.9}$$

$$\Theta_2 = 0 \quad \text{at} \quad r = 1 \ . \tag{3.10}$$

$$\Theta_{p2} + R\frac{\partial \Theta_{p1}}{\partial z} = \beta_3(\Theta_1 - \Theta_{p1}) \ , \tag{3.11}$$

$$\Theta_2 + R\frac{\partial \Theta_1}{\partial z} = \frac{1}{P}\left(\frac{\partial^2 \Theta_1}{\partial r^2} + \frac{1}{r}\frac{\partial \Theta_1}{\partial r}\right) + \beta_4(\Theta_{p1} - \Theta_1) \ , \tag{3.12}$$

$$\Theta_{p1} = 0 \quad \text{when} \quad z = 0 \ , \tag{3.13}$$

$$\Theta_1 = 0 \quad \text{when} \quad z = 0 \ , \tag{3.14}$$

$$\Theta_{p1} \quad \text{is finite at} \quad r = 0 \ , \tag{3.15}$$

$$\Theta_1 \quad \text{is finite at} \quad r = 0 \ , \tag{3.1 6}$$

$$\Theta_{p1} = \Theta_0 \quad \text{at} \quad r = 1 \ , \tag{3.17}$$

$$\Theta_1 = \Theta_0 \quad \text{at} \quad r = 1 \ . \tag{3.18}$$

Solving Eqs. (3.3) and (3.4) under the conditions (3.5)—(3.10), we get

$$\Theta_{p2} = 2\sum_{n=1}^{\infty} \frac{J_0(r\alpha_n)}{\alpha_n J_1(\alpha_n)} \cdot A_n(z) \ , \tag{3.19}$$

$$\Theta_2 = 2\sum_{n=1}^{\infty} \frac{J_0(r\alpha_n)}{\alpha_n J_1(\alpha_n)} \cdot B_n(z) \ , \tag{3.20}$$

where the α_n are the positive roots of $J_0(\alpha) = 0$, and

$$A_n(z) = \frac{1}{(\lambda_n - \mu_n)}\left[\lambda_n \exp\left(-\mu_n z\right) - \mu_n \exp\left(-\lambda_n z\right)\right] \ ,$$

$$B_n(z) = \frac{\lambda_n}{(\lambda_n - \mu_n)}\left(1 - \frac{R\mu_n}{\beta_3}\right)\exp\left(-\mu_n z\right) -$$

$$- \frac{\mu_n}{(\lambda_n - \mu_n)}\left(1 - \frac{R\lambda_n}{\beta_3}\right)\exp\left(-\lambda_n z\right) \ ,$$

$$2\lambda_n = \frac{\beta_3 + \beta_4}{R} + \frac{\alpha_n^2}{PR} + \sqrt{\left[\frac{\beta_3 + \beta_4}{R} + \frac{\alpha_n^2}{PR}\right]^2 - \frac{4\alpha_n^2}{PR^2}\beta_3} \ ,$$

$$2\mu_n = \frac{\beta_3 + \beta_4}{R} + \frac{\alpha_n^2}{PR} - \sqrt{\left[\frac{\beta_3 + \beta_4}{R} + \frac{\alpha_n^2}{PR}\right]^2 - \frac{4\alpha_n^2}{PR^2}\beta_3} \ .$$

Then the solutions of (3.11) and (3.12) under the conditions (3.13)—(3.18) are given by

$$\Theta_{p1} = \Theta_0\left[1 - 2\sum_{n=1}^{\infty}\frac{J_0(r\alpha_n)}{\alpha_n J_1(\alpha_n)}\cdot A_n(z)\right] - \frac{2}{R}z\sum_{n=1}^{\infty}\frac{J_0(r\alpha_n)}{\alpha_n J_1(\alpha_n)}\cdot A_n(z)\,, \tag{3.21}$$

$$\Theta_1 = \Theta_0\left[1 - 2\sum_{n=1}^{\infty}\frac{J_0(r\alpha_n)}{\alpha_n J_1(\alpha_n)}\cdot B_n(z)\right] - \frac{2}{R}z\sum_{n=1}^{\infty}\frac{J_0(r\alpha_n)}{\alpha_n J_1(\alpha_n)}\cdot B_n(z)\,. \tag{3.22}$$

Thus

$$\Theta_p = \Theta_0\left[1 - 2\sum_{n=1}^{\infty}\frac{J_0(r\alpha_n)}{\alpha_n J_1(\alpha_n)}\cdot A_n(z)\right] + 2\left(t - \frac{z}{R}\right)\sum_{n=1}^{\infty}\frac{J_0(r\alpha_n)}{\alpha_n J_1(\alpha_n)}\cdot A_n(z)\,, \tag{3.23}$$

$$\Theta = \Theta_0\left[1 - 2\sum_{n=1}^{\infty}\frac{J_0(r\alpha_n)}{\alpha_n J_1(\alpha_n)}\cdot B_n(z)\right] + 2\left(t - \frac{z}{R}\right)\sum_{n=1}^{\infty}\frac{J_0(r\alpha_n)}{\alpha_n J_1(\alpha_n)}\cdot B_n(z)\,. \tag{3.24}$$

$\Theta_p(r, z, t)$ and $\Theta(r, z, t)$ give the dimensionless temperature distributions of dust particles and of liquid in a circular pipe for slug flow assumption when the inlet temperatures vary linearly with time.

4. Discussion

When the boundary condition on the wall for $\Theta_p(r, z, t)$ and $\Theta(r, z, t)$ is homogeneous, that is, when Θ_0 is zero, then

$$\Theta_p(r, z, t) = 2\left(t - \frac{z}{R}\right)\sum_{n=1}^{\infty}\frac{J_0(r\alpha_n)}{\alpha_n J_1(\alpha_n)}\cdot A_n(z)\,, \tag{4.1}$$

$$\Theta(r, z, t) = 2\left(t - \frac{z}{R}\right)\sum_{n=1}^{\infty}\frac{J_0(r\alpha_n)}{\alpha_n J_1(\alpha_n)}\cdot B_n(z)\,. \tag{4.2}$$

From (4.1) and (4.2) it is obvious that the temperatures of dust particles and of liquid decay exponentially along the pipe.

For a single-phase system the number of dust particles per unit volume is zero (and so $\beta_4 = 0$). Hence

$$\Theta_s(r, z, t) = 2\left(t - \frac{z}{R}\right)\sum_{n=1}^{\infty}\frac{J_0(r\alpha_n)}{\alpha_n J_1(\alpha_n)}\cdot C_n(z)\,, \tag{4.3}$$

where $C_n(z) = \exp(-\alpha_n^2/PR\, z)$ and the boundary condition on the wall is homogeneous.

In many applications heat transfer in regions away from the inlet is of interest; for such situations only the first terms in the series (4.1), (4.2) and (4.3) need to be considered. Therefore

$$\Theta_p(r, z, t) = 2\left(t - \frac{z}{R}\right) \cdot \frac{J_0(r\alpha_1)}{\alpha_1 J_1(\alpha_1)} \cdot A_1(z) \ , \tag{4.4}$$

$$\Theta(r, z, t) = 2\left(t - \frac{z}{R}\right) \cdot \frac{J_0(r\alpha_1)}{\alpha_1 J_1(\alpha_1)} \cdot B_1(z) \ , \tag{4.5}$$

$$\Theta_s(r, z, t) = 2\left(t - \frac{z}{R}\right) \cdot \frac{J_0(r\alpha_1)}{\alpha_1 J_1(\alpha_1)} \cdot C_1(z) \ , \tag{4.6}$$

where

$$A_1(z) = \frac{1}{(\lambda_1 - \mu_1)}\left[\lambda_1 \exp(-\mu_1 z) - \mu_1 \exp(-\lambda_1 z)\right] \ ,$$

$$B_1(z) = \frac{\lambda_1}{(\lambda_1 - \mu_1)}\left(1 - \frac{R\mu_1}{\beta_3}\right)\exp(-\mu_1 z) -$$

$$- \frac{\mu_1}{(\lambda_1 - \mu_1)}\left(1 - \frac{R\lambda_1}{\beta_3}\right)\exp(-\lambda_1 z) \ ,$$

$$C_1(z) = \exp\left(-\frac{\alpha_1^2}{PR} z\right) \ ,$$

$$2\lambda_1 = \frac{\beta_3 + \beta_4}{R} + \frac{\alpha_1^2}{PR} + \sqrt{\left[\frac{\beta_3 + \beta_4}{R} + \frac{\alpha_1^2}{PR}\right]^2 - \frac{4\alpha_1^2}{PR^2}\beta_3} \ ,$$

$$2\mu_1 = \frac{\beta_3 + \beta_4}{R} + \frac{\alpha_1^2}{PR} - \sqrt{\left[\frac{\beta_3 + \beta_4}{R} + \frac{\alpha_1^2}{PR}\right]^2 - \frac{4\alpha_1^2}{PR^2}\beta_3} \ .$$

The temperatures at any r, say $r = 0$, are given by

$$\Theta_p(0, z, t) = 2\left(t - \frac{z}{R}\right) \cdot \frac{1}{\alpha_1 J_1(\alpha_1)} \cdot A_1(z) \ , \tag{4.7}$$

$$\Theta(0, z, t) = 2\left(t - \frac{z}{R}\right) \cdot \frac{1}{\alpha_1 J_1(\alpha_1)} \cdot B_1(z) \ , \tag{4.8}$$

$$\Theta_s(0, z, t) = 2\left(t - \frac{z}{R}\right) \cdot \frac{1}{\alpha_1 J_1(\alpha_1)} \cdot C_1(z) \ . \tag{4.9}$$

Table I

Comparison of the temperature distributions for
$t = 2,\ P = 0.73,\ \beta_3 = 10^5,\ \beta_4/\beta_3 = 0.5,\ R = 13{,}000$

Temperatures \ z	5	10	15	20
$\Theta_p(0, z, t)$	3.1974	3.1904	3.1834	3.1763
$\Theta\ (0, z, t)$	3.1970	3.1900	3.1830	3.1759
$\Theta_s(0, z, t)$	3.1941	3.1839	3.1736	3.1634

Table II

Comparison of the temperature distributions for
$t = 2,\ P = 0.73,\ \beta_3 = 10^5,\ \beta_4/\beta_3 = 0.5,\ R = 20{,}000$

Temperatures \ z	5	10	15	20
$\Theta_p(0, z, t)$	3.1992	3.1940	3.1888	3.1836
$\Theta\ (0, z, t)$	3.1988	3.1936	3.1884	3.1832
$\Theta_s(0, z, t)$	3.1975	3.1907	3.1839	3.1771

Table III

Comparison of the temperature distributions for
$t = 2,\ P = 0.73,\ \beta_3 = 10^5,\ \beta_4/\beta_3 = 0.5,\ R = 25{,}000$

Temperatures \ z	5	10	15	20
$\Theta_p(0, z, t)$	3.2009	3.1974	3.1939	3.1904
$\Theta\ (0, z, t)$	3.2005	3.1970	3.1935	3.1900
$\Theta_s(0, z, t)$	3.1992	3.1941	3.1889	3.1838

Table IV

Comparison of the temperature distributions for
$t = 2,\ P = 0.73,\ \beta_3 = 10^9,\ \beta_4/\beta_3 = 0.5,\ R = 20{,}000$

Temperatures \ z	5	10	15	20
$\Theta_p(0, z, t)$	3.1991	3.1939	3.1887	3.1835
$\Theta\ (0, z, t)$	3.1987	3.1935	3.1883	3.1831
$\Theta_s(0, z, t)$	3.1975	3.1907	3.1839	3.1771

Table V

Comparison of the temperature distributions for
$t = 2$, $P = 0.73$, $\beta_3 = 10^9$, $\beta_4/\beta_3 = 0.5$, $R = 25{,}000$

Temperatures \ z	5	10	15	20
$\Theta_p(0, z, t)$	3.2008	3.1973	3.1938	3.1903
$\Theta(0, z, t)$	3.2004	3.1969	3.1934	3.1899
$\Theta_s(0, z, t)$	3.1992	3.1941	3.1889	3.1838

We observe the following important points:

(a) From Tables I, II and III it is obvious that the temperature distributions Θ_p, Θ and Θ_s at any point inside the pipe increase with the increase of R and

$$\Theta_p > \Theta > \Theta_s .$$

(b) Tables II and IV show that Θ_p and Θ at any point inside the pipe decrease with the increase of β_3 (and so β_4) and

$$\Theta_p > \Theta > \Theta_s .$$

(c) From Tables III and V we infer that the temperature distributions Θ_p and Θ at any point inside the pipe decrease with the increase of β_4/β_3 and

$$\Theta_p > \Theta > \Theta_s .$$

Thus, the effect of dust particle is to flatten the temperature profile and, consequently, to increase the heat transfer.

REFERENCES

1. L. Farbar and M. J. Morley, Ind. Eng. Chem., **49**, 1143, 1957.
2. D. C. Schluderberg, The Application of Gas-Ceramic Mixtures to Nuclear Power, Rept. No. CF 55-8-199 ORSORT, AEC, 1955.
3. H. A. Johnson, Trans. ASME, **77**, 1257, 1955.
4. J. J. Salomone and M. Newmann, Ind. Eng. Chem., **47**, 283, 1955.
5. C. L. Tien, Transport Processes in Two-Phase Turbulent Flow, Ph. D. thesis, Princeton University, USA, 1959.
6. C. L. Tien, Trans. ASME, **83B**, 183, 1961.
7. S. L. Soo, Fluid Dynamics of Multiphase Systems, Blaisdell Publishing Co., London, 1967.
8. S. N. Dube and C. L. Sharma, Acta Phys. Hung., **41**, 95, 1976.
9. P. J. Schneider, Trans. ASME, **79**, 765, 1957.

Acta Physica Academiae Scientiarum Hungaricae, Tomus 43 (2), pp. 173—183 (1977)

WAVE MECHANICS AND THE PHOTON III

FORMULATION OF THE SIMULTANEOUS EQUATIONS

By

L. JÁNOSSY and M. ZIEGLER-NÁRAY

CENTRAL RESEARCH INSTITUTE FOR PHYSICS, BUDAPEST

(Received 6. X. 1977)

The interaction of an H-atom with its own radiation field was treated in a former publication to a certain approximation. The calculations in this paper give a more precise formulation of the differential equations representing the interaction. In a subsequent paper we shall give the explicit solutions in a particular case of the equations derived here. It will be seen that the solutions thus obtained confirm our former results, but contain some interesting new features.

Introduction

In a previous publication [1] we have investigated the interaction of an H-atom with its own radiation field. The result of the calculation showed that the atom when in an excited state has a strongly instable configuration. Therefore a small suitable perturbation starts an avalanche which leads to emission of radiation of the total energy $h\nu$. The radiation is in general emitted inside a narrow cone. This process much resembles what one may take phenomenologically as the emission of a photon.

In the previous paper [2] we dealt with this process and carried out calculations making certain approximations. Presently we give a more precise treatment of the problem. The calculations we give presently leads to results similar to that of the former paper. Presently we show, however, that an avalanche may develop also in the case when the radiation emitted by the atom is captured by a system of perfect mirrors. In the approximation used in the former paper it appeared (incorrectly) that an avalanche can develop only if some of the radiation emitted escapes from the region occupied by the atom.

In the present paper we consider only the particular processes when one H-atom is enclosed into a cubic box with sides L, which cannot be penetrated by the atom and which acts as a perfect mirror. Further, we restrict ourselves to processes which take place when the state of the atom is the superposition of two stationary states only. So as to obtain an adequate description of the emission process it would be important to consider such processes also which occur when states consisting of the superposition of

several stationary states are present and it is also important to take into consideration the radiation which escapes out of the enclosure.

The treatment of the process as the superposition of two states leads to qualitative results only. Nevertheless in this qualitative way we obtain a phenomenon corresponding to the natural line width of spectral lines, which comes about as typical property of the non-linear oscillating system independently of the loss of energy of the oscillator. Further an effect somewhat resembling to the Lamb shift is found as the result of the non-linear interaction.

We deal presently with these more specialized configurations so as to develop mathematical methods which we hope to generalize later and which will be suitable to describe the process of emission which occurs under practical conditions.

The mathematical formulation of the problem

We investigate an H-atom described by a two-body function

$$\psi(\boldsymbol{r}) = \psi(\mathbf{r}^{(1)}, \mathbf{r}^{(2)})$$

$\mathbf{r}^{(k)}$ $(k = 1, 2)$ being the coordinate vectors of proton and electron. The Schrödinger equation can thus be written

$$(H + P)\psi = i\hbar\dot{\psi}, \tag{1}$$

where

$$H\psi_0 = i\hbar\dot{\psi}_0 \tag{2}$$

is the unperturbed wave-equation and P is the perturbation caused by the electromagnetic field of the system itself. We take thus P to be the perturbation caused by the field with potentials $\mathbf{A}$, Φ obeying

$$\nabla^2\mathbf{A} - \frac{1}{c^2}\ddot{\mathbf{A}} = -4\pi\mathbf{i}\ ,$$

$$\nabla^2\Phi - \frac{1}{c^2}\ddot{\Phi} = -4\pi\varrho\ . \tag{3}$$

The sources of $\mathbf{A}$ and Φ being the so-called semi-classical current and charge densities. Thus we derive from the wave function ψ six-dimensional source densities

$$\bar{\varrho}^{(k)}(\boldsymbol{r}) = e_k\psi^*\psi\ ,$$

$$\bar{i}^{(k)}(\boldsymbol{r}) = -\frac{i\hbar e_k}{2m_kc}(\psi^*\ \mathrm{grad}_k\,\psi - \psi\ \mathrm{grad}_k\,\psi^*) - \left[\frac{e_k^2}{m_kc^2}\psi^*\psi\mathbf{A}_k\right] \qquad k = 1, 2 \tag{4}$$

where $e_2 = -e_1 = e$ is the charge of the electron and m_1, m_2 is the mass of the proton and electron, respectively. For the potentials in three-dimensional space we introduce the notation

$$\mathbf{A}_k(\boldsymbol{r}) = \mathbf{A}(\mathbf{r}^{(k)}), \qquad \Phi_k(\boldsymbol{r}) = \Phi(\mathbf{r}^{(k)}) \qquad k = 1, 2. \tag{5}$$

The three-dimensional source densities are thus

$$\begin{aligned} \varrho^{(k)}(\mathbf{r}) &= \int \bar{\varrho}^{(k)}(\boldsymbol{r})\, d^3\mathbf{r}^{(k')} \;|_{\mathbf{r}^{(k)}=\mathbf{r}}, \\ \mathbf{i}^{(k)}(\mathbf{r}) &= \int \bar{\mathbf{i}}^{(k)}(\boldsymbol{r})\, d^3\mathbf{r}^{(k')} \;|_{\mathbf{r}^{(k)}=\mathbf{r}} \qquad k' \neq k \end{aligned} \tag{6}$$

and the total source densities caused by the electron and proton

$$\begin{aligned} \varrho(\mathbf{r}) &= \varrho^{(1)}(\mathbf{r}) + \varrho^{(2)}(\mathbf{r}) \quad , \\ \mathbf{i}(\mathbf{r}) &= \mathbf{i}^{(1)}(\mathbf{r}) + \mathbf{i}^{(2)}(\mathbf{r}) \; . \end{aligned} \tag{7}$$

We note that $\varrho(\mathbf{r})$ and $\mathbf{i}(\mathbf{r})$ thus defined cannot be represented as threefold integrals over some densities $\varrho(\boldsymbol{r})$ and $\mathbf{i}(\boldsymbol{r})$; the averaging must be taken separately over the six-dimensional proton respectively electron densities.

The perturbation operator P consists of two contributions

$$P = P^{(1)} + P^{(2)}, \tag{8}$$

where

$$P^{(k)} = \frac{ie_k\hbar}{2m_kc}\,(\nabla_k\mathbf{A}_k + \mathbf{A}_k\nabla_k) + e_k\Phi_k + \left[\frac{e_k^2}{2m_kc^2}\,\mathbf{A}^2\right]. \tag{9}$$

Remark on the magnitude of the perturbation

The H-atom being enclosed into a box with macroscopic linear dimensions L the charge and current densities as obtained by the definitions (4), (5), (6), (7) are proportional to $1/L^3$ the densities can be taken to be small. For this reason, as can be seen from (3) the potential $\mathbf{A}$ and Φ are also small, i.e. proportional to $1/L^3$. We see therefore that the perturbation operator P in (1) produces only a slow perturbation; the solutions of (1) can thus be represented as solutions of the unperturbed equation with some slowly changing parameters. In particular the frequencies of oscillations of the system have values differing only very little from those of the unperturbed system. The perturbations caused by the reaction of the atom with its own radiation field are small indeed provided

$$L \gg r_H\,, \qquad r_H = \text{Bohr radius.} \tag{10}$$

It is, however, also important for the considerations that we have to take $\psi = \psi(\boldsymbol{r})$ as a two-body wave function. If we were to take the usual one-body treatment of the H-atom, i.e. if we were to take the nucleus as a classical point particle, then the reaction of the field upon the atom would appear to cause large perturbations. The above model — as we have called it elsewhere [3] — is the "50% Bohr model". The treatment of this model involves considerable mathematical difficulties — nevertheless the solutions obtained from the 50% Bohr model do not seem to have physical reality. Some problems of this kind are treated in the literature and these are connected with the so-called "solitron" types of models.

We note further that one might suppose incorrectly that our results in the limit $m_1 \to \infty$ tend to those which could be obtained using one body wave function. This is not the case. Indeed, increasing the value of the mass m_1 one obtains configurations which show decreasing rates of diffusion. The perturbation calculation is based on stationary configurations, thus the larger m_1 the longer it takes to reach stationary configurations. Stationary configurations, however, when eventually established, fill about uniformly the volume of the box. The larger the mass m_1 the longer one has to wait until the configurations we are making use of are established. These times, however, remain very short indeed, even if the proton was replaced by a particle with mass $m \gg m_1$. The two-body treatment is thus based on wave functions which essentially differ from those used in the one-body treatment. This is so even in the limit $m_1 \to \infty$.

The perturbation energy

The perturbation energy can thus be written

$$U_P = \int \psi^* P \psi d^6\boldsymbol{r} \ . \tag{11}$$

Introducing P from (9) and making use of the expressions for the three-dimensional current and charge densities, we obtain a rather simple expression for the perturbational energy. Supposing (10) to hold we can neglect the terms containing higher powers of $\left(\frac{1}{L}\right)^3$ thus we can neglect the terms placed into square brackets in (4) and (9); we thus obtain

$$U_P = \int (\varrho\Phi - \mathbf{iA})\, d^3\mathbf{r} + \frac{ie\hbar}{2mc} \int \mathbf{A}\varrho d\mathbf{S}, \tag{12}$$

where

$$m = \frac{m_1 m_2}{m_1 + m_2}$$

is the reduced mass.

The second term on the right is to be taken as an integral over the boundary of the box containing the atom.

The perturbational equations

The effect of the perturbation P can be calculated if we introduce a complete set ψ_ν of orthogonal wave functions representing unperturbed states. Developing the wave function as linear combination of stationary states

$$\psi = \Sigma\, c_\nu \psi_\nu \,, \tag{13}$$

we find in the usual way from the wave equation (1) that the effect of the perturbation is to make the coefficients change in time in accord with

$$\dot{c}_\nu = \sum_\mu b_{\nu\mu} c_\mu \,, \tag{14}$$

where

$$b_{\nu\mu} = -\frac{i}{\hbar}\int \psi_\nu^* P \psi_\mu d^6\boldsymbol{r} \,. \tag{15}$$

(for P see Eq. (9)).

Making use of the definitions we find that the $b_{\nu\mu}$ can be expressed in terms of current and charge densities in the following manner: introducing (13) into the definitions (4), (5), (6) and (7) we may write

$$\begin{aligned} \mathbf{i}(\mathbf{r}) &= \Sigma c_\nu^* c_\mu \mathbf{i}_{\nu\mu}(\mathbf{r}) \,, \\ \varrho(\mathbf{r}) &= \Sigma c_\nu^* c_\mu \varrho_{\nu\mu}(\mathbf{r}) \,, \end{aligned} \tag{16}$$

where

$$\begin{aligned} \mathbf{i}_{\nu\mu}(\mathbf{r}) &= \mathbf{i}_{\nu\mu}^{(1)}(\mathbf{r}) + \mathbf{i}_{\nu\mu}^{(2)}(\mathbf{r}) \,, \\ \varrho_{\nu\mu}(\mathbf{r}) &= \varrho_{\nu\mu}^{(1)}(\mathbf{r}) + \varrho_{\nu\mu}^{(2)}(\mathbf{r}) \end{aligned} \tag{17}$$

and

$$\begin{aligned} \mathbf{i}_{\nu\mu}^{(k)}(\mathbf{r}) &= \int \bar{\mathbf{i}}_{\nu\mu}^{(k)}(\boldsymbol{r})\, d^3\mathbf{r}^{(k')}\,|_{\mathbf{r}^{(k)}=\mathbf{r}} \,, \\ \varrho_{\nu\mu}^{(k)}(\mathbf{r}) &= \int \bar{\varrho}_{\nu\mu}^{(k)}(\mathbf{r})\, d^3\mathbf{r}^{(k')}\,|_{\mathbf{r}^{(k)}=\mathbf{r}} \,, \quad k' \neq k \end{aligned} \tag{18}$$

finally

$$\begin{aligned} \bar{\mathbf{i}}_{\nu\mu}^{(k)}(\boldsymbol{r}) = &-\frac{ie_k\hbar}{2m_k c}(\psi_\nu^* \operatorname{grad}_k \psi_\mu - \psi_\mu \operatorname{grad}_k \psi_\nu^*) + \\ &+ \text{negligible terms} \\ \varrho_{\nu\mu}^{(k)}(\boldsymbol{r}) = &\, e_k \psi_\nu^* \psi_\mu \,. \end{aligned} \tag{19}$$

Using the above definitions, we obtain for the coefficients defined in (15)

$$b_{\nu\mu} = -\frac{i}{\hbar}\int (\varrho_{\nu\mu}\Phi - \mathbf{i}_{\nu\mu}\mathbf{A})\, d^3\mathbf{r} + \text{surface integral.} \tag{20}$$

Multiplying (20) with $c_\nu^* c_\mu$ and summing over ν and μ we find, also with the help of (16) and (11)

$$\Sigma c_\nu^* c_\mu b_{\nu\mu} = U_P \,. \tag{11a}$$

(11a) is a relation which could be derived directly from (11), (13) and (15).

Returning to the electromagnetic wave-equations, we find that the relations (3) can be written

$$\nabla^2 \mathbf{A} - \frac{1}{c^2}\ddot{\mathbf{A}} = -4\pi\Sigma c_\nu^* c_\mu \mathbf{i}_{\nu\mu} \,,$$

$$\nabla^2 \Phi - \frac{1}{c^2}\ddot{\Phi} = -4\pi\Sigma c_\nu^* c_\mu \varrho_{\nu\mu} \,. \tag{21}$$

The motion of the system is thus defined by the simultaneous solutions of (14), (20) and (21).

The stationary solutions

So as to obtain a definite set of differential equations describing the motion of the system we have to make a choice for the set of wave functions ψ_ν. We note that stationary states of the H-atom can be described by wave functions

$$\psi_\nu = \psi_{nl} = \frac{1}{L^{3/2}} e^{i\mathbf{K}_n\mathbf{R}} \varphi_l(\mathbf{s})\, e^{-i\omega_{nl}t} \,, \tag{22}$$

where

$$\mathbf{R} = \frac{m_1\mathbf{r}^{(1)} + m_2\mathbf{r}^{(2)}}{m_1 + m_2} \qquad \mathbf{s} = \mathbf{r}^{(2)} - \mathbf{r}^{(1)}$$

and

$$\omega_{nl} = \frac{K_n^2\hbar}{2(m_1 + m_2)} + \omega_l \,. \tag{23}$$

Here $\varphi_l(\mathbf{s})$ are amplitudes of the solutions of the one-body H wave equation with reduced mass m (see (12a)) and ω_l are the corresponding frequencies. We note that in the following we shall use the notation:

$$\psi_\mu = \psi_{n'l'} = \frac{1}{L^{3/2}} e^{i\mathbf{K}_{n'}\mathbf{R}} \varphi_{l'}(\mathbf{s})\, e^{-i\omega_{n'l'}t} \,. \tag{24}$$

The wave functions thus defined cannot be normalized over the whole of space. If we suppose, however, that the H-atom is captured in a finite box and the effect of the walls is to cut off the wave functions outside the box, i.e. if we suppose

$$\psi_\nu(\boldsymbol{r}) = 0 \quad \text{if} \quad \mathbf{r}^{(1)} \text{ or } \mathbf{r}^{(2)} \text{ point outside the box}$$

then the functions thus defined can be normalized and if we choose the wave vectors K_n with components

$$\mathbf{K}_n = K_{n_1},\ K_{n_2},\ K_{n_3},$$

$$K_{n_k} = \frac{2\pi n_k}{L} \text{ where } n_k \text{ are integers.} \tag{25}$$

The wave functions thus defined give a complete orthogonal set in terms of which wave functions inside the box can be developed. More exactly, the wave functions ψ_ν defined by (22), give only a nearly complete orthogonal set of functions and there is an important restriction. Indeed, the wave functions thus defined are periodic in **R**. Therefore all linear combinations of the ψ_ν are also periodic in this way. We can therefore express in terms of the ψ_ν only wave functions which are themselves periodic. Thus as we take the wave functions to vanish outside the box we can prescribe at a fixed time t the values of ψ only inside the box and on three of the walls; on the remaining opposite walls the values are repeated. We shall see further below that this restriction is not a trivial one, however, the states of the H-atom enclosed into an inpenetrable box with reflecting walls may be supposed to possess wave functions of this type.

Further below we shall carry out the perturbation calculations supposing that the stationary states of the H-atom captured into a box with reflecting walls can be described indeed by wave functions of the form ψ_{nl}.

The above assumption is not quite correct. The functions ψ_{nl} define states with definite momentum. The atom captured in the box has no total momentum, its state can thus be described only by suitable linear combination of states ψ_{nl}. We shall discuss briefly at the end of the article how our results are affected when using instead of the stationary states of the captured H-atom the wave functions ψ_{nl}.

The explicit form of the equations of motion

Introducing the wave functions ψ_{nl} defined by (22) into the expressions for the densities $\varrho_{\nu\mu}(\mathbf{r})$ and $\mathbf{i}_{\nu\mu}(\mathbf{r})$ we find as the result of a short calculation

$$\varrho_{\nu\mu}(\mathbf{r}) = \frac{e}{L^3} e^{i\theta_{\nu\mu}} R_{\nu\mu}, \tag{26a}$$

$$\mathbf{i}_{\nu\mu}(\mathbf{r}) = \frac{e}{L^3} e^{i\theta_{\nu\mu}} \mathbf{I}_{\nu\mu}. \tag{26b}$$

Here we use the following notation:

$$\Theta_{\nu\mu} = (\mathbf{K}_\mu - \mathbf{K}_\nu)\,\mathbf{r} - (\Omega_\mu - \Omega_\nu)\,t \tag{26c}$$

$$R_{\nu\mu} = \int \varphi_\nu^*(\mathbf{s})\,\varphi_\mu(\mathbf{s})\,[e^{i\alpha_2(\mathbf{K}_\mu-\mathbf{K}_\nu)\mathbf{s}} + e^{i\alpha_1(\mathbf{K}_\mu-\mathbf{K}_\nu)\mathbf{s}}]\,d^3\mathbf{s} \tag{26d}$$

$$\mathbf{I}_{\nu\mu} = \frac{\hbar}{2Mc}(\mathbf{K}_\mu + \mathbf{K}_\nu)\int (e^{-i\alpha_1(\mathbf{K}_\mu-\mathbf{K}_\nu)\mathbf{s}} + e^{i\alpha_2(\mathbf{K}_\mu-\mathbf{K}_\nu)\mathbf{s}})\,\varphi_\nu^*(\mathbf{s})\,\varphi_\mu(\mathbf{s})\,d^3\mathbf{s} -$$

$$- \frac{\hbar i}{2Mc}\int\left(\frac{e^{-i\alpha_1(\mathbf{K}_\mu-\mathbf{K}_\nu)\mathbf{s}}}{\alpha_2} - \frac{e^{i\alpha_2(\mathbf{K}_\mu-\mathbf{K}_\nu)\mathbf{s}}}{\alpha_1}\right)\left(\varphi_\nu^*\frac{\partial\varphi_\mu}{\partial\mathbf{s}} - \frac{\partial\varphi_\nu^*}{\partial\mathbf{s}}\varphi_\mu\right)d^3\mathbf{s} \tag{26e}$$

here

$$\Omega_\nu = \omega_{nl}, \qquad \Omega_\mu = \omega_{n'l'}, \qquad \mathbf{K}_\mu = \mathbf{K}_{n'l'} \qquad \mathbf{K}_\nu = \mathbf{K}_{nl} \tag{27}$$

and

$$\alpha_i = \frac{m_i}{M}, \qquad M = m_1 + m_2\,.$$

Equations (26a, b) are valid only if $L \gg r_H$. Indeed, carrying out the integrations, approximations are used the nature of which can be seen from the following example

$$\varrho^{(2)}(\mathbf{r}) = e_2 \int \psi^*\psi d^3\mathbf{r}^{(1)}\,|_{\mathbf{r}^{(2)}=\mathbf{r}}$$

introducing s as a new variable of integration, we have

$$\mathbf{R} = \mathbf{r} + \alpha_2\mathbf{s}, \qquad d^3r^{(k')} = d^3\mathbf{r}.$$

Thus

$$\varrho^{(2)}(\mathbf{r}) = \frac{e_2}{L^3}\int e^{i(\mathbf{K}_\mu-\mathbf{K}_\nu)(\mathbf{r}+\alpha_2\mathbf{s})}\,\varphi_\mu(\mathbf{s})\,\varphi_\nu(\mathbf{s})\,d^3\mathbf{s}e^{-i(\Omega_\mu-\Omega_\nu)t} =$$

$$= \frac{e}{L^3}e^{i\theta_{\nu\mu}}\int \varphi_\mu(\mathbf{s})\,e^{i(\mathbf{K}_\mu-\mathbf{K}_\nu)\mathbf{r}}\,\varphi_\nu^*(\mathbf{s})\,d^3\mathbf{s}\,.$$

Because the $\varphi(\mathbf{s})$ decreases rapidly with s, we extend the integrals over s to all values of the vector s; this procedure introduces a small error of the order of $(r_H/L)^3$.

Introducing (26) into (6) we may write in place of (2)

$$\nabla^2\mathbf{A} - \frac{1}{c^2}\ddot{\mathbf{A}} = -\frac{4\pi e}{L^3}\Sigma c_\nu^* c_\mu \mathbf{I}_{\nu\mu}e^{i\theta_{\nu\mu}},$$

$$\nabla^2\Phi - \frac{1}{c^2}\ddot{\Phi} = -\frac{4\pi e}{L^3}\Sigma c_\nu^* c_\mu R_{\nu\mu}e^{i\theta_{\nu\mu}}. \tag{28}$$

From (28) we see that $\mathbf{A}$ and Φ can be expressed by Fourier series

$$\mathbf{A} = \Sigma \mathbf{A}_{\nu\mu} e^{i\theta_{\nu\mu}} \quad \Phi = \Sigma \Phi_{\nu\mu} e^{i\theta_{\nu\mu}}, \tag{29}$$

where the coefficients $\mathbf{A}_{\nu\mu}$ and $\Phi_{\nu\mu}$ are functions of time only. It follows from (29) that $\mathbf{A}$ and Φ are periodic functions of the coordinates. From this it follows that the Poynting vector has the same value at opposite walls. Therefore the field given by potentials (29) possesses a constant amount of energy in the box; either $\mathbf{A} = \Phi = 0$ on the walls in the case there is no streaming of energy across the boundary. If $\mathbf{A}, \Phi \neq 0$ then there is a sourceless stream of energy across the volume.

We can safely restrict ourselves to solutions $\mathbf{A} = 0$, $\Phi = 0$ on the boundary. We see thus that the assumption of periodicity of the wave functions ψ_ν automatically makes a restriction to configurations enclosed by a box reflecting the radiation.

Introducing (29) into (28) with the help of (26c) we find for any one of the Fourier coefficients of (29)

$$\left[c^2(\mathbf{K}_\mu - \mathbf{K}_\nu)^2 - (\Omega_\mu - \Omega_\nu)^2\right] \mathbf{A}_{\nu\mu} - 2i(\Omega_\mu - \Omega_\nu)\, \dot{\mathbf{A}}_{\nu\mu} + \ddot{\mathbf{A}}_{\nu\mu} = \frac{4\pi c^2 e c_\nu^* c_\mu}{L^3} \mathbf{I}_{\nu\mu},$$

$$\left[c^2(\mathbf{K}_\mu - \mathbf{K}_\nu)^2 - (\Omega_\mu - \Omega_\nu)^2\right] \Phi_{\nu\mu} - 2i(\Omega_\mu - \Omega_\nu)\, \dot{\Phi}_{\nu\mu} + \ddot{\Phi}_{\nu\mu} = \frac{4\pi c^2 e c_\nu^* c_\mu}{L^3} R_{\nu\mu}.$$

The $\mathbf{A}_{\nu\mu}$ and $\Phi_{\nu\mu}$ can be eliminated from the above equations and equations containing the $b_{\nu\mu}$ only can be obtained. So as to see this, we introduce (27) into (20) and find thus

$$b_{\nu\mu} = -\frac{ie}{\hbar L^3} \int (R_{\nu\mu}\Phi - \mathbf{I}_{\nu\mu}\mathbf{A})\, e^{i\theta_{\nu\mu}}\, d^3\mathbf{r}\ . \tag{30}$$

Introducing $\mathbf{A}$ and Φ from (29) taking the orthogonality relations

$$\int e^{i(\theta_{\nu\mu} + \theta_{\mu'\nu'})}\, d^3\mathbf{r} = L^3\, \delta_{\nu\nu'}\, \delta_{\mu\mu'},$$

into consideration we have

$$b_{\nu\mu} = -\frac{ie}{\hbar} (R_{\nu\mu}\Phi_{\mu\nu} - \mathbf{I}_{\nu\mu}\mathbf{A}_{\mu\nu}), \tag{31}$$

since in accord with the definitions

$$R_{\nu\mu} = R_{\mu\nu}^* \quad \text{and} \quad \mathbf{I}_{\nu\mu} = \mathbf{I}_{\mu\nu}^*.$$

By multiplying (30) and (31) with $\frac{ie}{\hbar} R_{\nu\mu}$ and $-\frac{ie}{\hbar} R_{\nu\mu}^*$ respectively and

then adding them we obtain

$$i\gamma_{\nu\mu}^2 b_{\nu\mu} + 2(\Omega_\mu - \Omega_\nu)\,\dot{b}_{\nu\mu} - i\ddot{b}_{\nu\mu} = 2\sigma_{\nu\mu}^3 c_\nu c_\mu^* . \tag{32}$$

Equations (14) and (32) give a set of equations giving the motion of the system. The parameters $\sigma_{\nu\mu}$, $\gamma_{\nu\mu}$ appearing here are

$$\sigma_{\nu\mu}^3 = \frac{2\pi e^2 c^2}{\hbar L^3}\,(|\mathbf{I}_{\nu\mu}|^2 - |\,R_{\nu\mu}|^2) \tag{33}$$

and

$$\gamma_{\nu\mu}^2 = (\Omega_\mu - \Omega_\nu)^2 - c^2(\mathbf{K}_\mu - \mathbf{K}_\nu)^2 \tag{34}$$

are frequencies the numerical values of which can be determined from the definitions.

The system of equations of motion can be rather simplified considering systems consisting of two states only: an excited state ψ_1 and a lower state ψ_0. The amplitudes of other lower states $\psi_0^{(1)}$, $\psi_0^{(2)}$, . . ., $\psi_0^{(n)}$ should be zero. Such an assumption does not lead to inconsistency. Indeed, if we consider an initial condition so that asymptotically for $t \to -\infty$

$$|\,c_1\,| \to 1 \quad \text{and} \quad |\,c_0^{(0)}\,| = |\,c_0\,| \to 0$$

but

$$c_0^{(n)} = n \quad \text{if} \quad n > 0 .$$

Thus we permit at the beginning of the process a small admixture of one particular lower state, take the other lower states to have strictly zero amplitudes.

The full perturbation equation can be written

$$\dot{c}_1 = \sum_n b_{10}^{(n)}\, c_0^{(n)},$$

$$\dot{c}_0 = b_{10}^{(n)}\, c_1 ,$$

therefore if to begin with $b_{10}^{(n)} = 0$ for $n > 0$ we have at

$$\dot{c}_1 = bc_0,$$

$$\dot{c}_0 = -b^* c_1,$$

where we have introduced the notation $b_{10}^{(0)} = b$, thus the c_{0n} starting from zero remain zero and as a consequence the b_{0n} which start with zero values remain also permanently zero. The solution of the system of equations which thus appear at any time as a linear combination of two states only is a mathematical possible solution of our system.

It must be remembered, however, that the initial configuration in which one lower state has a very small amplitude and the others are strictly zero is a rather unstable one. In a more realistic configuration several lower states will grow up side by side.

The question of the parallel avalanches which thus develop is most important for the adequate description of the physical process and we hope to come back to the treatment of this process. In part IV of this paper [4] we shall give the explicit solutions for the two state system. In the next paper we shall confine ourselves to the two state system only, largely in order to obtain certain qualitative features of the process and also to develop mathematical methods which we hope to use later to treat the more complicated process.

REFERENCES

1. L. JÁNOSSY, Acta Phys. Hung., **35**, 141, 1974.
2. L. JÁNOSSY, Acta Phys. Hung., **41**, 71, 1976.
3. L. JÁNOSSY, Acta Phys. Hung., **39**, 109, 1975.
4. L. JÁNOSSY and M. ZIEGLER-NÁRAY, Acta Phys. Hung., **43**, 1977.

Acta Physica Academiae Scientiarum Hungaricae, Tomus 43 (2), pp. 185—196 (1977)

THE INTENSITY DISTRIBUTION OF THE $^5\Pi - ^5\Pi$ BANDS IN DIATOMIC MOLECULES

By

I. KOVÁCS and M. I. M. EL-AGRAB*

DEPARTMENT OF ATOMIC PHYSICS, TECHNICAL UNIVERSITY, BUDAPEST

(Received 11. X. 1977)

Explicit expressions are obtained for the intensity distribution in the branches of $^5\Pi(a)-^5\Pi(a)$, $^5\Pi(a)-^5\Pi(b)$, $^5\Pi(b)-^5\Pi(a)$, $^5\Pi(b)-^5\Pi(b)$ bands, including all branches which have been missing till now.

1. Introduction

In the CrO molecule the (0,0), (0,1) and (1,0) bands of a $^5\Pi-^5\Pi$ transition have been observed and analyzed rotationally by NINOMIYA [1]. In general the theoretical investigations of intensities in electronic bands relate to a wider field than the experimental data, providing hereby the experimental researcher with some guidance in case of an analysis of a new kind. So the formulas have been worked out for the line strengths of all possible transitions between Σ and Π terms of any multiplicity up to septet [2]. In the case oı transitions of higher than triplet multiplicity, general formulas, namely the formulas of the line strengths of transitions between terms belonging to the intermediate Hund's case, would be complicated. In such a case the treatment restricts to the limiting-case transitions. For $^5\Pi-^5\Pi$ transition the $^5\Pi(a)-$ $-^5\Pi(a)$, $^5\Pi(a)-^5\Pi(b)$ and $^5\Pi(b)-^5\Pi(b)$ cases have been elaborated by PREMASWARUP [3], but only 15 branches (so called main branches) arising from the transitions $\Delta J = \Delta N = 0, \pm 1$ were published of the possible 75. This is perfectly satisfactory for the $^5\Pi(a)-^5\Pi(a)$ transition because due to the $\Delta\Sigma = 0$ selection rule the line strengths of the unlisted branches are identically zero. In the case of $^5\Pi(b)-^5\Pi(b)$ transition over and above $\Delta J = 0, \pm 1$ the $\Delta N = 0, \pm 1$ selection rule is valid instead of $\Delta\Sigma = 0$ therefore over the main branches 22 further satellite branches come into being. As is known if the formulae for all branches had been included, the sum would be $(2S + 1)(2J + 1) = 5(2J + 1)$, $(S = 2)$. In the Table I the second column shows the values of $5(2J + 1)$, the fourth column the sum of the line strengths of the published main branches of $^5\Pi(b)-^5\Pi(b)$ transition for a few J values according to WHITING et al [4]. As can be seen the intensities of the satellite branches converge fast to zero with increasing rotational quantum number.

* On leave from Ain Shams University, Education College, Cairo, Egypt.

Table I

J	$5(2J+1)$	$^5\Pi(a)$—$^5\Pi(b)$	$^5\Pi(b)$—$^5\Pi(b)$
2	25	3.357	19.639
10	105	18.994	103.063
30	305	54.259	304.344
100	1005	176.849	1004.800

A quite other circumstance can be found in the case of $^5\Pi(a)$—$^5\Pi(b)$ transition. Here the selection rule $\Delta\Sigma = 0$ is no longer valid and the selection rule $\Delta N = 0, \pm 1$ is not valid yet, solely the $\Delta J = 0, \pm 1$. Therefore all the 75 branches appear and the intensities are dispersed over all branches as can be seen in the third column of the Table I. These facts make it necessary to give the line strengths of all the 75 branches.

2. Intensity distribution

As is known, in case of the thermal equilibrium the intensity of the lines of emission bands can be given by the following expression:

$$I'_{J''} = G \cdot S_{J'J''} e^{-hcF_{J'}/kT}, \tag{1}$$

where G can be regarded as constant to a good approximation within a band and $S_{J'J''}$ is the line strength. The relative intensities of the individual lines of a band arising from a multiplet transition are determined, apart from the Boltzmann factor, by the line strength; it is this latter that characterizes the intensity distribution among the branches. The task of the theory is to calculate the $S_{J'J''}$ factors for all branches occurring in the rotational transitions. For this the corresponding expression for the amplitudes

$$z_a(^5\Pi_\Omega; {}^5\Pi_{\Omega'}) = \int \psi^*_a(^5\Pi_\Omega)\, z\psi(^5\Pi_{\Omega'})\, d\tau \tag{2}$$

is used, the absolute values of which may be found in a paper by KRONIG [5]. The threefold square of (2) summed over the magnetic quantum numbers gives the $S_{J'J''}$ factors to the transition $^5\Pi(a)$—$^5\Pi(a)$ and these are to be found in the second column of Table II.

The $^5\Pi$ terms can in general be described well by the formulae of Hund's case a) only in the range of the lower rotational quantum numbers. With increasing rotational quantum numbers namely the transition starts towards the case b) and the difficulty in describing the conditions consists in that no expression is known concerning the $^5\Pi$ energies valid with a satisfactory accuracy for any value of the coupling constant. Thus we have to content

ourselves with the knowledge of the energies of the relative simple case b), respectively with the amplitudes produced by the use of the transformation matrix elements calculated with their aid

$$z(^5\Pi_{\Omega'};\, ^5\Pi_{N''}) = \int \psi_a^*(^5\Pi_{\Omega'})\, z\psi_b(^5\Pi_{N''})\, d\tau\,, \tag{3a}$$

$$z(^5\Pi_{N'};\, ^5\Pi_{\Omega''}) = \int \psi_b^*(^5\Pi_{N'})\, z\psi_a(^5\Pi_{\Omega''})\, d\tau \tag{3b}$$

and

$$z(^5\Pi_{N'};\, ^5\Pi_{N''}) = \int \psi_b^*(^5\Pi_{N'})\, z\psi_b(^5\Pi_{N''})\, d\tau\,, \tag{3c}$$

where

$$\psi_b(^5\Pi_N) = \sum_{\Omega=-1}^{+3} S_{\Omega,N}\, \psi_a(^5\Pi_\Omega) \tag{4}$$

and the elements of the transformation matrix of $^5\Pi$ state are the following

$$S_{-1,J-2} = +\sqrt{\frac{(J-2)(J+1)}{4(2J-1)(2J+1)}}; \qquad S_{0,J-2} = -\sqrt{\frac{(J-2)J}{(2J-1)(2J+1)}};$$

$$S_{+1,J-2} = +\sqrt{\frac{3(J-2)(J+1)}{2(2J-1)(2J+1)}}; \qquad S_{+2,J-2} = -\sqrt{\frac{(J-2)(J+1)(J+2)}{(J-1)(2J-1)(2J+1)}};$$

$$S_{+3,J-2} = +\sqrt{\frac{(J+1)(J+2)(J+3)}{4(J-1)(2J-1)(2J+1)}};$$

$$S_{-1,J-1} = +\sqrt{\frac{J}{2(2J+1)}}; \qquad S_{0,J-1} = -\sqrt{\frac{J+1}{2(2J+1)}};$$

$$S_{+1,J-1} = +\sqrt{\frac{3}{J(2J+1)}}; \qquad S_{+2,J-1} = +\sqrt{\frac{(J-3)^2(J+2)}{2(J-1)J(2J+1)}};$$

$$S_{+3,J-1} = -\sqrt{\frac{(J-2)(J+2)(J+3)}{2(J-1)J(2J+1)}};$$

$$S_{-1,J} = -\sqrt{\frac{3J(J+1)}{2(2J-1)(2J+3)}}; \qquad S_{0,J} = +\sqrt{\frac{3}{2(2J-1)(2J+3)}};$$

$$S_{+1,J} = +\sqrt{\frac{[J(J+1)-3]^2}{J(J+1)(2J-1)(2J+3)}}; \qquad S_{+2,J} = -\sqrt{\frac{27(J-1)(J+2)}{2J(J+1)(2J-1)(2J+3)}};$$

$$S_{+3,J} = -\sqrt{\frac{3(J-2)(J-1)(J+2)(J+3)}{2J(J+1)(2J-1)(2J+3)}};$$

$$S_{-1,J+1} = -\sqrt{\frac{J+1}{2(2,J+1)}}; \qquad S_{0,J+1} = -\sqrt{\frac{J}{2(2J+1)}};$$

$$S_{+1,J+1} = +\sqrt{\frac{3}{(J+1)(2J+1)}}; \qquad S_{+2,J+1} = +\sqrt{\frac{(J-1)(J+4)^2}{2(J+1)(J+2)(2J+1)}};$$

$$S_{+3,J+1} = +\sqrt{\frac{(J-2)(J-1)(J+3)}{2(J+1)(J+2)(2J+1)}};$$

$$S_{-1,J+2} = + \sqrt{\frac{J(J+3)}{4(2J+1)(2J+3)}}; \qquad S_{0,J+2} = + \sqrt{\frac{(J+1)(J+3)}{(2J+1)(2J+3)}};$$

$$S_{+1,J+2} = + \sqrt{\frac{3J(J+3)}{2(2J+1)(2J+3)}}; \qquad S_{+2,J+2} = + \sqrt{\frac{(J-1)J(J+3)}{(J+2)(2J+1)(2J+3)}};$$

$$S_{+3,J+2} = + \sqrt{\frac{(J-2)(J-1)J}{4(J+2)(2J+1)(2J+3)}}.$$

The threefold square of (3a), (3b) and (3c) summed over the magnetic quantum numbers gives the line strengths referring to the transitions $^5\Pi(a)-{}^5\Pi(b)$, $^5\Pi(b)-{}^5\Pi(a)$ and $^5\Pi(b)-{}^5\Pi(b)$ which are to be found in the third, fourth and fifth column in Table II, respectively.

As can be seen from Table II, the intensities of the Q branches for any transitions (if they differ from zero) are proportional to $\frac{1}{J}$ $\left(\text{except for } {}^RQ_{32}, {}^RQ_{43}, {}^PQ_{34} \text{ in the case of } {}^5\Pi(a)-{}^5\Pi(b) \text{ transition where the intensities are proportional to } \frac{1}{J^3}\right)$, therefore the observation of the Q branches cannot be expected. This is in good agreement with the experimental results [1]. The intensities of the P and R branches in the main branches ($\Delta J - \Delta N = 0$) are proportional to J and for $^5\Pi(b)-{}^5\Pi(b)$ transition in the 22 satellite branches ($\Delta J - \Delta N \neq 0$) they are proportional to $\frac{1}{J^3}$. That means that it is satisfactory in practice to know the line strengths of the main branches for $^5\Pi(b)-{}^5\Pi(b)$ transition, too. (See Table I).

On the other hand for $^5\Pi(a)-{}^5\Pi(b)$ and $^5\Pi(b)-{}^5\Pi(a)$ transitions the intensities of 21 P and 21 R branches are proportional to J and those of 4 P and 4 R branches are proportional to $\frac{1}{J^3}$. In the Table III the first column shows the line strengths of the main branches for $^5\Pi(a)-{}^5\Pi(a)$ transition and in the second column it can be seen how the intensities of the main branches among the individual branches are scattered for $^5\Pi(a)-{}^5\Pi(b)$ transition. (See Table I). This is the reason why it is necessary to know the line strengths of all branches for $^5\Pi(a)-{}^5\Pi(b)$ transition.

In Table II both $^5\Pi$ terms were assumed to be normal. In the case of inverted terms $\Omega = 3$ does not correspond to the state $N = J + 2$, but to $N = J - 2$ and for the transitions $^5\Pi_i(a)-{}^5\Pi_n(a)$, $^5\Pi_i(a)-{}^5\Pi(b)$ the first indices 1, 2, . . ., 5 in the denotation of the branches should be replaced by the denotation 5, 4, . . . (for $^5\Pi_n(a)-{}^5\Pi_i(a)$, $^5\Pi(b)-{}^5\Pi_i(a)$ this applies to the second indices).

Table II

Line strengths for $^5\Pi$—$^5\Pi$ transitions

Branches	Line strengths			
	$^5\Pi(a)$—$^5\Pi(a)$	$^5\Pi(a)$—$^5\Pi(b)$	$^5\Pi(b)$—$^5\Pi(a)$	$^5\Pi(b)$—$^5\Pi(b)$
$P_1(J)$	$\frac{(J-1)(J+1)}{J}$	$\frac{(J-2)(J-1)(J+1)^2}{4J(2J-1)(2J+1)}$	$R_1(J-1)$	$\frac{(J-3)(J-1)(2J+1)}{(J-2)(2J-3)}$
$Q_1(J)$	$\frac{2J+1}{J(J+1)}$	$\frac{J-2}{4J(2J-1)}$	$Q_1(J)$	$\frac{(J+1)(2J+1)}{(J-1)^2J}$
$R_1(J)$	$\frac{J(J+2)}{J+1}$	$\frac{(J-2)J(J+2)}{4(2J-1)(2J+1)}$	$P_1(J+1)$	$\frac{(J-2)J(2J+3)}{(J-1)(2J-1)}$
$^QP_{21}(J)$	0	$\frac{(J-2)J^2}{(2J-1)(2J+1)}$	$^QR_{12}(J-1)$	$\frac{2(2J+1)}{(J-2)(J-1)^2J}$
$^RQ_{21}(J)$	0	0	$^PQ_{12}(J)$	$\frac{2(J-2)(2J+1)}{(J-1)^2(2J-1)}$
$^SR_{21}(J)$	0	$\frac{(J-2)J(J+1)}{(2J-1)(2J+1)}$	$^OP_{12}(J+1)$	0
$^RP_{31}(J)$	0	$\frac{3(J-2)(J-1)(J+1)^2}{2J(2J-1)(2J+1)}$	$^PR_{13}(J-1)$	$\frac{6(J-2)}{(J-1)^2(2J-1)(2J-3)}$
$^SQ_{31}(J)$	0	$\frac{3(J-2)}{2J(2J-1)}$	$^OQ_{13}(J)$	0
$^TR_{31}(J)$	0	$\frac{3(J-2)J(J+2)}{2(2J-1)(2J+1)}$	$^NP_{13}(J+1)$	0

Table II (continued)

Branches	Line strengths			
	$^5\Pi(a)$—$^5\Pi(a)$	$^5\Pi(a)$—$^5\Pi(b)$	$^5\Pi(b)$—$^5\Pi(a)$	$^5\Pi(b)$—$^5\Pi(b)$
$^SP_{41}(J)$	0	$\frac{(J-2)^2(J+1)(J+2)^2}{(J-1)J(2J-1)(2J+1)}$	$^OR_{14}(J-1)$	0
$^TQ_{41}(J)$	0	$\frac{4(J-2)(J+2)}{(J-1)J(2J-1)}$	$^NQ_{14}(J)$	0
$^NR_{41}(J)$	0	$\frac{(J-2)(J+2)(J+3)}{(2J-1)(2J+1)}$	$^MP_{14}(J+1)$	0
$^TP_{51}(J)$	0	$\frac{(J-3)(J+1)(J+2)(J+3)^2}{4(J-1)J(2J-1)(2J+1)}$	$^NR_{15}(J-1)$	0
$^UQ_{51}(J)$	0	$\frac{9(J+2)(J+3)}{4(J-1)J(2J-1)}$	$^MQ_{15}(J)$	0
$^VR_{61}(J)$	0	$\frac{(J-2)(J+2)(J+3)(J+4)}{4(J-1)(2J-1)(2J+1)}$	$^LP_{15}(J+1)$	0
$^OP_{12}(J)$	0	$\frac{(J-1)(J+1)}{2(2J+1)}$	$^SR_{21}(J-1)$	0
$^PQ_{12}(J)$	0	$\frac{1}{2(J+1)}$	$^RQ_{21}(J)$	$\frac{2(J-2)(2J+1)}{(J-1)^2(2J-1)}$
$^QR_{12}(J)$	0	$\frac{J^2(J+2)}{2(J+1)(2J+1)}$	$^QP_{21}(J+1)$	$\frac{2(2J+3)}{(J-1)J^2(J+1)}$
$P_2(J)$	J	$\frac{J(J+1)}{2(2J+1)}$	$R_2(J-1)$	$\frac{(J-2)^2(J+1)(2J+1)}{(J-1)^2(2J-1)}$

Branches	Line strengths			
	$^5\Pi(a)$—$^5\Pi(a)$	$^5\Pi(a)$—$^5\Pi(b)$	$^5\Pi(b)$—$^5\Pi(a)$	$^5\Pi(b)$—$^5\Pi(b)$
$Q_2(J)$	0	0	$Q_2(J)$	$\frac{(J^2-3)^2(2J+1)}{(J-1)^2J^3(J+1)}$
$R_2(J)$	$J+1$	$\frac{(J+1)^2}{2(2J+1)}$	$P_2(J+1)$	$\frac{(J-1)^2(J+2)(2J+3)}{J^2(2J+1)}$
$^QP_{32}(J)$	0	$\frac{3(J-1)(J+1)}{J^2(2J+1)}$	$^QR_{23}(J-1)$	$\frac{3(J+1)(2J-3)}{(J-1)^2J^3}$
$^RQ_{32}(J)$	0	$\frac{3}{J^2(J+1)}$	$^PQ_{23}(J)$	$\frac{3(J-1)^2(2J+3)}{J^3(2J-1)}$
$^SR_{32}(J)$	0	$\frac{3(J+2)}{(J+1)(2J+1)}$	$^OP_{23}(J+1)$	0
$^RP_{42}(J)$	0	$\frac{(J-3)^2(J-2)(J+2)^2}{2(J-1)J^2(2J+1)}$	$^PR_{24}(J-1)$	$\frac{9(J-1)(J+1)}{J^3(2J-1)(2J+1)}$
$^SQ_{42}(J)$	0	$\frac{2(J-3)^2(J+2)}{(J-1)J^2(J+1)}$	$^OQ_{24}(J)$	0
$^TR_{42}(J)$	0	$\frac{(J-3)^2(J+2)(J+3)}{2J(J+1)(2J+1)}$	$^NP_{24}(J+1)$	0
$^SP_{52}(J)$	0	$\frac{(J-3)(J-2)(J+2)(J+3)^2}{2(J-1)J^2(2J+1)}$	$^OR_{25}(J-1)$	0
$^TQ_{52}(J)$	0	$\frac{9(J-2)(J+2)(J+3)}{2(J-1)J^2(J+1)}$	$^NQ_{25}(J)$	0
$^UR_{52}(J)$	0	$\frac{(J-2)^2(J+2)(J+3)(J+4)}{2(J-1)J(J+1)(2J+1)}$	$^MP_{25}(J+1)$	0

Table II (continued)

Branches	Line strengths			
	$^5\Pi(a)$—$^5\Pi(a)$	$^5\Pi(a)$—$^5\Pi(b)$	$^5\Pi(b)$—$^5\Pi(a)$	$^5\Pi(b)$—$^5\Pi(b)$
$^NP_{13}(J)$	0	$\frac{3(J-1)(J+1)^2}{2(2J-1)(2J+3)}$	$^TR_{31}(J-1)$	0
$^OQ_{13}(J)$	0	$\frac{3(2J+1)}{2(2J-1)(2J+3)}$	$^SQ_{31}(J)$	0
$^PR_{13}(J)$	0	$\frac{3J^2(J+2)}{2(2J-1)(2J+3)}$	$^RP_{31}(J+1)$	$\frac{6(J-1)}{J^2(2J-1)(2J+1)}$
$^OP_{23}(J)$	0	$\frac{3J}{2(2J-1)(2J+3)}$	$^SR_{32}(J-1)$	0
$^PQ_{23}(J)$	0	0	$^RQ_{32}(J)$	$\frac{3(J-1)^2(2J+3)}{J^3(2J-1)}$
$^QR_{23}(J)$	0	$\frac{3(J+1)}{2(2J-1)(2J+3)}$	$^QP_{32}(J+1)$	$\frac{3(J+2)(2J-1)}{J^2(J+1)^3}$
$P_3(J)$	$\frac{(J-1)(J+1)}{J}$	$\frac{(J-1)[J(J+1)-3]^2}{J^2(2J-1)(2J+3)}$	$R_3(J-1)$	$\frac{(J-1)^2(J+1)^2(2J-3)(2J+3)}{J^3(2J-1)(2J+1)}$
$Q_3(J)$	$\frac{2J+1}{J(J+1)}$	$\frac{(2J+1)[J(J+1)-3]^2}{J^2(J+1)^2(2J-1)(2J+3)}$	$Q_3(J)$	$\frac{[J(J+1)-3]^2(2J+1)}{J^3(J+1)^3}$
$R_3(J)$	$\frac{J(J+2)}{J+1}$	$\frac{(J+2)[J(J+1)-3]^2}{(J+1)^2(2J-1)(2J+3)}$	$P_3(J+1)$	$\frac{J^2(J+2)^2(2J-1)(2J+5)}{(J+1)^3(2J+1)(2J+3)}$
$^QP_{43}(J)$	0	$\frac{27(J-2)(J-1)(J+2)^2}{2J^2(J+1)(2J-1)(2J+3)}$	$^QR_{35}(J-1)$	$\frac{3(J-1)(2J+3)}{J^3(J+1)^2}$
$^RQ_{43}(J)$	0	$\frac{54(J-1)(J+2)(2J+1)}{J^2(J+1)^2(2J-1)(2J+3)}$	$^PQ_{35}(J)$	$\frac{3(J+2)^2(2J-1)}{(J+1)^3(2J+3)}$

Branches	Line strengths			
	$^5\Pi(a)$—$^5\Pi(a)$	$^5\Pi(a)$—$^5\Pi(b)$	$^5\Pi(b)$—$^5\Pi(a)$	$^5\Pi(b)$—$^5\Pi(b)$
$^SR_{43}(J)$	0	$\frac{27(J-1)^2(J+2)(J+3)}{2J(J+1)^2(2J-1)(2J+3)}$	$^OP_{34}(J+1)$	0
$^RP_{53}(J)$	0	$\frac{3(J-3)(J-2)(J-1)(J+2)(J+3)^2}{2J^2(J+1)(2J-1)(2J+3)}$	$^PR_{35}(J-1)$	$\frac{6(J+2)}{(J+1)^2(2J+1)(2J+3)}$
$^SQ_{53}(J)$	0	$\frac{27(J-2)(J-1)(J+2)(J+3)(2J+1)}{2J^2(J+1)^2(2J-1)(2J+3)}$	$^OQ_{35}(J)$	0
$^TR_{53}(J)$	0	$\frac{3(J-2)^2(J-1)(J+2)(J+3)(J+4)}{2J(J+1)^2(2J-1)(2J+3)}$	$^NP_{35}(J+1)$	0
$^MP_{14}(J)$	0	$\frac{(J-1)(J+1)^2}{2J(2J+1)}$	$^UR_{41}(J-1)$	0
$^NQ_{14}(J)$	0	$\frac{1}{2J}$	$^TQ_{41}(J)$	0
$^CR_{14}(J)$	0	$\frac{J(J+2)}{2(2J+1)}$	$^SP_{41}(J+1)$	0
$^NP_{24}(J)$	0	$\frac{J^2}{2(2J+1)}$	$^TR_{42}(J-1)$	0
$^OQ_{24}(J)$	0	0	$^SQ_{42}(J)$	0
$^PR_{24}(J)$	0	$\frac{J(J+1)}{2(2J+1)}$	$^RP_{42}(J+1)$	$\frac{9J(J+2)}{(J+1)^3(2J+1)(2J+3)}$
$^OP_{34}(J)$	0	$\frac{3(J-1)}{J(2J+1)}$	$^SR_{43}(J-1)$	0
$^PQ_{34}(J)$	0	$\frac{3}{J(J+1)^2}$	$^RQ_{43}(J)$	$\frac{3(J+2)^2(2J-1)}{(J+1)^3(2J+3)}$

Table II (continued)

Branches	Line strengths			
	$^5\Pi(a)$—$^5\Pi(a)$	$^5\Pi(a)$—$^5\Pi(b)$	$^5\Pi(b)$—$^5\Pi(a)$	$^5\Pi(b)$—$^5\Pi(b)$
$^QR_{34}(J)$	0	$\frac{3J(J+2)}{(J+1)^2(2J+1)}$	$^QP_{43}(J+1)$	$\frac{3J(2J+5)}{(J+1)^3(J+2)^2}$
$P_4(J)$	$\frac{(J-2)(J+2)}{J}$	$\frac{(J-2)(J-1)(J+4)^2}{2J(J+1)(2J+1)}$	$R_4(J-1)$	$\frac{(J-1)(J+2)^2(2J-1)}{(J+1)^2(2J+1)}$
$Q_4(J)$	$\frac{4(2J+1)}{J(J+1)}$	$\frac{2(J-1)(J+4)^2}{J(J+1)^2(J+2)}$	$Q_4(J)$	$\frac{[J(J+2)-2]^2(2J+1)}{J(J+1)^3(J+2)^2}$
$R_4(J)$	$\frac{(J-1)(J+3)}{J+1}$	$\frac{(J-1)^2(J+3)(J+4)^2}{2(J+1)^2(J+2)(2J+1)}$	$P_4(J+1)$	$\frac{J(J+3)^2(2J+1)}{(J+2)^2(2J+3)}$
$^QP_{54}(J)$	0	$\frac{(J-3)(J-2)(J-1)(J+3)^2}{2J(J+1)(J+2)(2J+1)}$	$^QR_{45}(J-1)$	$\frac{2(2J-1)}{J(J+1)^2(J+2)}$
$^RQ_{54}(J)$	0	$\frac{9(J-2)(J-1)(J+3)}{2J(J+1)^2(J+2)}$	$^PQ_{45}(J)$	$\frac{2(J+3)(2J+1)}{(J+2)^2(2J+3)}$
$^SR_{54}(J)$	0	$\frac{(J-2)^2(J-1)(J+3)(J+4)}{2(J+1)^2(J+2)(2J+1)}$	$^OP_{45}(J+1)$	0
$^LP_{15}(J)$	0	$\frac{(J-1)(J+1)(J+3)}{4(2J+1)(2J+3)}$	$^VR_{51}(J-1)$	0
$^MQ_{15}(J)$	0	$\frac{J+3}{4(J+1)(2J+3)}$	$^UQ_{51}(J)$	0
$^NR_{15}(J)$	0	$\frac{J^2(J+2)(J+3)}{4(J+1)(2J+1)(2J+3)}$	$^TP_{51}(J+1)$	0
$^MP_{25}(J)$	0	$\frac{J(J+1)(J+3)}{(2J+1)(2J+3)}$	$^UR_{52}(J-1)$	0

Branches	Line strengths			
	$^5\Pi(a)$—$^5\Pi(a)$	$^5\Pi(a)$—$^5\Pi(b)$	$^5\Pi(b)$—$^5\Pi(a)$	$^5\Pi(b)$—$^5\Pi(b)$
${}^{N}Q_{25}(J)$	0	0	${}^{T}Q_{52}(J)$	0
${}^{O}R_{25}(J)$	0	$\frac{(J+1)^2(J+3)}{(2J+1)(2J+3)}$	${}^{S}P_{52}(J+1)$	0
${}^{N}P_{35}(J)$	0	$\frac{3(J-1)(J+1)(J+3)}{2(2J+1)(2J+3)}$	${}^{T}R_{53}(J-1)$	0
${}^{O}Q_{35}(J)$	0	$\frac{3(J+3)}{2(J+1)(2J+3)}$	${}^{S}Q_{53}(J)$	0
${}^{P}R_{35}(J)$	0	$\frac{3J^2(J+2)(J+3)}{2(J+1)(2J+1)(2J+3)}$	${}^{R}P_{53}(J+1)$	$\frac{6(J+3)}{(J+2)^2(2J+3)(2J+5)}$
${}^{O}P_{45}(J)$	0	$\frac{(J-2)(J-1)(J+3)}{(2J+1)(2J+3)}$	${}^{S}R_{54}(J-1)$	0
${}^{P}Q_{45}(J)$	0	$\frac{4(J-1)(J+3)}{(J+1)(J+2)(2J+3)}$	${}^{R}Q_{54}(J)$	$\frac{2(J+3)(2J+1)}{(J+1)^2(2J+3)}$
${}^{Q}R_{45}(J)$	0	$\frac{(J-1)^2J(J+3)^2}{(J+1)(J+2)(2J+1)(2J+3)}$	${}^{Q}P_{54}(J+1)$	$\frac{2(2J+1)}{(J+1)(J+2)^2(J+3)}$
$P_5(J)$	$\frac{(J-3)(J+3)}{J}$	$\frac{(J-3)(J-2)(J-1)(J+3)}{4(J+2)(2J+1)(2J+3)}$	$R_5(J-1)$	$\frac{(J+1)(J+3)(2J-1)}{(J+2)(2J+3)}$
$Q_5(J)$	$\frac{9(2J+1)}{J(J+1)}$	$\frac{9(J-2)(J-1)}{4(J+1)(J+2)(2J+3)}$	$Q_5(J)$	$\frac{J(2J+1)}{(J+1)(J+2)^2}$
$R_5(J)$	$\frac{(J-2)(J+4)}{J+1}$	$\frac{(J-2)^2(J-1)J(J+4)}{4(J+1)(J+2)(2J+1)(2J+3)}$	$P_5(J+1)$	$\frac{(J+2)(J+4)(2J+1)}{(J+3)(2J+5)}$

Table III

$^5\Pi(a)$—$^5\Pi(a)$	$^5\Pi(a)$—$^5\Pi(b)$				
	S^A_1	S^A_{21}	S^A_{31}	S^A_{41}	S^A_{51}
S^A_1	$\frac{1}{16}$	$\frac{4}{16}$	$\frac{6}{16}$	$\frac{4}{16}$	$\frac{1}{16}$
	S^A_{12}	S^A_2	S^A_{32}	S^A_{42}	S^A_{52}
S^A_2	$\frac{1}{4}$	$\frac{1}{4}$	0	$\frac{1}{4}$	$\frac{1}{4}$
	S^A_{13}	S^A_{23}	S^A_3	S^A_{43}	S^A_{53}
S^A_3	$\frac{3}{8}$	0	$\frac{2}{8}$	0	$\frac{3}{8}$
	S^A_{14}	S^A_{24}	S^A_{34}	S^A_4	S^A_{54}
S^A_4	$\frac{1}{4}$	$\frac{1}{4}$	0	$\frac{1}{4}$	$\frac{1}{4}$
	S^A_{15}	S^A_{25}	S^A_{35}	S^A_{45}	S^A_5
S^A_5	$\frac{1}{16}$	$\frac{4}{16}$	$\frac{6}{16}$	$\frac{4}{16}$	$\frac{1}{16}$

$A = P$ or R

REFERENCES

1. M. NINOMIYA, J. Phys. Soc. Japan, **10,** 829, 1955.
2. I. KOVÁCS, Rotational Structure in the Spectra of Diatomic Molecules, Akadémiai Kiadó, Budapest and Adam Hilger Ltd. London, 1969.
3. D. PREMASWARUP, Ind. J. Phys., **27,** 415, 578, 1953.
4. E. E. WHITING, I. A. PATERSON, I. KOVÁCS and R. W. NICHOLLS, J. Mol. Spectr., **47,** 91, 1973.
5. R. L. KRONIG, Z. f. Phys., **45,** 458, 1927.

Acta Physica Academiae Scientiarum Hungaricae, Tomus 43 (2), pp. 197—198 (1977)

COMMUNICATIO BREVIS

MEASUREMENTS ON THE FOURTH POSITIVE BAND SYSTEM OF $^{14}C^{16}O$ MOLECULE IN THE NEAR ULTRAVIOLET REGION

By

J. Domin, U. Domin and M. Rytel

ATOMIC AND MOLECULAR PHYSICS LABORATORY, PEDAGOGICAL COLLEGE, RZESZÓW, POLAND

(Received 9. VIII. 1977)

The fourth positive system ($A^1\Pi - X^1\Sigma^+$ transition) of the $^{14}C^{16}O$ molecule was obtained by a discharge in a Geissler tube filled up with carbon monoxide having 91% ^{14}C. The bands were photographed in the third order of PGS-2 plane grating spectrograph (VEB C. Zeiss, Jena) with a dispersion of about 2.4 Å/mm on the UV—1 type ORWO plates. The thorium lines from the hollow-cathode type lamp were used as standards [1].

The band heads of the fourth positive system of the $^{14}C^{16}O$ molecule are listed in a Deslandres table. These wave numbers are in satisfactory agreement with those calculated from the origins of the natural molecule [2] using isotopic relations. We estimate that the errors of most of the given wave numbers are less than 1 cm^{-1}. The wave numbers of the heads of the bands (9,21), (11,20), (11,21), (12,22), (12,23) are especially inexact since they are overlapped by another system. The presence of the bands (13,23), (14,25) is possible but their region is strongly blended.

The detailed analysis of this system of $^{14}C^{16}O$ molecule will be undertaken subsequently.

REFERENCES

1. A. Giacchetti, J. Opt. Soc., **60**, 474, 1970.
2. J. Domin, U. Domin and M. Rytel, Acta Phys. Pol., **A51**, 783, 1977.

Table I

The band heads of fourth positive system of $^{14}C^{16}O$ molecule (in cm^{-1})

v' \ v''	11	12	13	14	15	16	17	18	19	20	21	22	23	24
1	46,310.5	44,525.4												
3	47,665.1	45,875.6	44,108.4											
4	48,991.3	47,200.5	45,434.1	43,691.4										
5		48,493.1	46,726.3	44,983.0	43,264.0	41,568.3								
6			47,988.4	46,245.1	44,525.4	42,829.3	41,156.8							
7				47,473.9	45,754.0	44,057.3	42,384.6	40,735.5	39,109.9					
8						45,259.1	43,582.5	41,933.4	40,307.1					
9							44,749.7	43,099.6	41,473.1	39,869.9	38,290.3			
10									42,608.1	41,004.9	39,417.4	37,868.9		
11										42,101.0	40,531.8	38,971.8	37,419.3	
12												40,035.5	38,497.9	36,998.4
13														38,039.7

RECENSIONES

Physique des Plasmas — Les Houches 1972

Edited by C. DE WITT and J. PEYRAUD
Gordon and Breach Science Publishers, New York—London—Paris, 1975

The volume presents the lectures delivered at the Les Houches Summer School of Theoretical Physics 1972, in the course on plasma physics. The collection gives only six contributions, evidently the most important ones of the course: 1. Collective Emission Processes in Unmagnetized Plasmas, by G. BEKEFI, 2. Linear Waves and Instabilities, by A. BERS, 3. Non-Linear Effects, by G. LAVAL and R. PELLAT, 4. Atomic and Molecular Processes in Ionized Gases, by J.-L. DELCROIX, 5. Topics on Plasma Response Functions, by G. KALMAN and 6. Strongly Magnetized Classical Plasma Models, by D. MONTGOMERY.

The collection of the articles offers an excellent and open-minded review of two fields of plasma physics, namely description of linear waves, instability criteria, study of non-linear effects, radiation on the one hand, and the study of dense plasmas with the correlation function method on the other.

The contribution of Professor J.-L. DELCROIX gives an excellent and rapid view of the individual processes of the plasma interior which is the bridge to every practical application.

I. ABONYI

T. KALLARD: Exploring Laser Light

Optosonic Press, New York, 1977, pp. 298.

Experiments with lasers today are no longer restricted to research laboratories. As a result of the widespread application of this light source lasers are present in every fundamental optics experiment. And when lasers are combined with properly chosen display elements, many old and difficult demonstrations in optics become easier to do and able to be viewed by a large audience.

The performance of the optics experiments is generally inseparable from difficulties involved. Fortunately, many of them are simply eliminated by the advantageous characteristics of laser light. Nevertheless, a careful preparation of the laboratory exercises and lecture demonstrations requires a knowledge of all the basic principles and techniques of optics.

From the points of view mentioned above T. KALLARD's book will be of advantage to those, who want to master the performance of various optics experiments and measurements.

The book is not divided into chapters explicitly. In connection with each experiment discussed in the book the author has mentioned those physical principles which form the basis both of laboratory exercises and simple practical applications.

All the exercises and lecture demonstrations contained in the book utilize low-power c.w. He-Ne lasers.

The book begins with a brief review of the properties of laser light and exploratory exercises. These are followed by the measurements with optical elements such as mirrors, lenses, prisms, etc.

The next part of the book contains measurements of the parameters of basic accessories. In these sections the author gives practical advices for the determination of the radius of curvature of mirrors, for refractive index measurements, for measuring small wedge angles and for other techniques, connected with the formation of the laser beam.

The section on "Simple polarisation demonstration" contains a short discussion on the polarisation of light, followed by exercises on the relevant problems.

The metrological possibilities of optics are realized by interferometers: interference is discussed in detail. The usefulness of the different interferometers for measuring purposes is demonstrated over a variety of practical applications. Unfortunately, the importance of the Fabry—Perot interferometer is illustrated in a too modest way. Diffraction experiments are treated as being of capital importance.

The experimental part of the book is completed with holography and its applications.

In the book relevant formulas are presented to refresh the memory and where appropriate, numerical values for parameters are given. Schematic drawings help the experimenter.

The "References" and the literature suggested "For Further Reading" make it easier for the reader to pursue any of the topics covered in the book in greater detail. Review articles are often included in the references. Relevant books are listed at the end of the volume.

T. KALLARD's book will give an invaluable aid to workers of teaching laboratories. The practical ideas it offers for planning the exercises can be very useful for young scientists, too.

Z. FÜZESSY

K. MENDELSSOHN: The Quest for Absolute Zero

Taylor & Francis Ltd., London, 1977

Professor MENDELSSOHN's book summarizes the fundamental problems of low temperature physics for a wide circle of readers in an understandable way. In my opinion, this is the best book which has ever been written about this subject.

The author is an outstanding scientist in low temperature physics and engineering. His name is connected with numerous significant results in the research of low temperatures. The fact that he has been able to describe very complicated things in such a simple, clear and understandable manner is obviously due to his perfect orientation and deep-settled knowledge in this vast field of research.

The book begins with the first experiment to liquefy the so-called "permanent" gases (Paris, 1877) and leads us as far as the presentation of the most up-to-date technical applications of superconductivity. In this way it shows the reader over the whole chronological history of the investigations of low temperatures and presents all phenomena, effects and technical results which rightly attract the interest of readers.

The principal content of approaching the absolute zero and the phenomena occurring inbetween are dealt with very clearly and vividly, pointing beyond the principles of physics and at the same time projecting the perspectives of applications.

The two most unexpected and astonishing groups of phenomena, namely the question of the flow of helium without viscosity (superfluidity) and that of the electric current without resistance (superconductivity) are analysed in detail. The process how the absolute zero can be approached through the liquefaction of the gas and further through the magnetic cooling of nuclei is described.

We are acquainted with the recent technology which has grown out of the physics of low temperatures but can be applied effectively in many fields of engineering practice.

The book is divided into the following eleven chapters: 1. Paris 1877, 2. Cracow 1883, 3. London 1898, 4. Leiden 1908, 5. The third law, 6. Quantisation, 7. Indeterminacy, 8. Magnetic cooling, 9. Superconductivity, 10. Technology near absolute zero, 11. Superfluidity.

Of these the first four can be taken essentially as the "novel" of gas liquefaction, while the others give an overall picture of low temperature physics covering all essential problems ranging from the problem of specific heat to the superconducting train.

The material contained in the book has been written and arranged in such a manner that natural scientists and experts, technicians, university students and even many of those who have an inclination for classical subjects can equally benefit from it since almost everybody interested in the results of modern natural sciences can find something interesting in it.

The neat printing and fine lay-out of the work is the merit of the Publishers.

I. KIRSCHNER

Printed in Hungary

A kiadásért felel az Akadémiai Kiadó igazgatója. Műszaki szerkesztő: Botyánszky Pál

A kézirat nyomdába érkezett: 1977. X. 19. — Terjedelem: 8,25 (A/5) ív, 12 ábra

78.5070 Akadémiai Nyomda, Budapest — Felelős vezető: Bernát György

NOTES TO CONTRIBUTORS

I. PAPERS will be considered for publication in Acta Physica Hungarica, only if they have not previously been published or submitted for publication elsewhere. They may be written in English, French, German or Russian.

Papers should be submitted to

Prof. I. Kovács, Editor
Department of Atomic Physics, Technical University
1521 Budapest, Budafoki út 8, Hungary

Papers may be either articles with abstracts or short communications. Both should be as concise as possible, articles in general not exceeding 25 typed pages, short communications 8 typed pages.

II. MANUSCRIPTS

1. Papers should be submitted in five copies.

2. The text of papers must be of high stylistic standard, requiring minor corrections only.

3. Manuscripts should be typed in double spacing on good quality paper, with generous margins.

4. The name of the author(s) and of the institutes where the work was carried out should appear on the first page of the manuscript.

5. Particular care should be taken with mathematical expressions. The following should be clearly distinguished, e.g. by underlining in different colours: special founts (italics, script, bold type, Greek, Gothic, etc.); capital and small letters; subscripts and superscripts, e.g. x^2, x_3; small l and 1; zero and capital O; in expressions written by hand: e and l, n and u, v and v, etc.

6. References should be numbered serially and listed at the end of the paper in the following form: J. Ise and W. D. Fretter, Phys. Rev., *76*, 933, 1949.

For books, please give the initials and family name of the author(s), title, name of publisher, place and year of publication, e.g.: J. C. Slater, Quantum Theory of Atomic Structures, I. McGraw-Hill Book Company, Inc., New York, 1960.

References should be given in the text in the following forms: Heisenberg [5] or [5].

7. Captions to illustrations should be listed on a separate sheet, not inserted in the text.

III. ILLUSTRATIONS ANv TABLES

1. Each paper should be accompanied by five sets of illustrations, one of which must be ready for the blockmaker. The other sets attached to the copies of the manuscript may be rough drawings in pencil or photocopies.

2. Illustrations must not be inserted in the text.

3. All illustrations should be identified in blue pencil by the author's name, abbreviated title of the paper and figure number.

4. Tables should be typed on separate pages and have captions describing their content. Clear wording of column heads is advisable. Tables should be numbered in Roman numerals

(I, II, III, etc.).

IV. MANUSCRIPTS not in conformity with the above Notes will immediately be returned to authors for revision. The date of receipt to be shown on the paper will in such cases be that of the receipt of the revised manuscript.

Reviews of the Hungarian Academy of Sciences are obtainable at the following addresses:

AUSTRALIA
C.B.D. LIBRARY AND SUBSCRIPTION SERVICE, Box 4886, G.P.O., *Sydney N.S.W. 2001*
COSMOS BOOKSHOP, 145 Ackland Street, *St. Kilda (Melbourne), Victoria 3182*

AUSTRIA
GLOBUS, Höchstädtplatz 3, *1200 Wien XX*

BELGIUM
OFFICE INTERNATIONAL DE LIBRAIRIE, 30 Avenue Marnix, *1050 Bruxelles*
LIBRAIRIE DU MONDE ENTIER, 162 Rue du Midi, *1000 Bruxelles*

BULGARIA
HEMUS, Bulvar Ruszki 6, *Sofia*

CANADA
PANNONIA BOOKS, P.O. Box 1017, Postal Station "B", *Toronto, Ontario M5T 2T8*

CHINA
CNPICOR, Periodical Department, P.O. Box 50, *Peking*

CZECHOSLOVAKIA
MAD'ARSKÁ KULTURA, Národní třida 22, *115 66 Praha*
PNS DOVOZ TISKU, Vinohradská 46, *Praha 2*
PNS DOVOZ TLAČE, *Bratislava 2*

DENMARK
EJNAR MUNKSGAARD, Norregade 6, *1165 Copenhagen*

FINLAND
AKATEEMINEN KIRJAKAUPPA, P.O. Box 128, *SF-00101 Helsinki 10*

FRANCE
EUROPERIODIQUES S. A., 31 Avenue de Versailles, *78170 La Celle St. Cloud*
LIBRAIRIE LAVOISIER, 11 rue Lavoisier, *75008 Paris*
OFFICE INTERNATIONAL DE DOCUMENTATION ET LIBRAIRIE, 48 rue Gay-Lussac, *75240 Paris Cedex 05*

GERMAN DEMOCRATIC REPUBLIC
HAUS DER UNGARISCHEN KULTUR, Karl-Liebknecht-Strasse 9, *DDR-102 Berlin*
DEUTSCHE POST ZEITUNGSVERTRIEBSAMT, Strasse der Pariser Kommüne 3—4, *DDR-104 Berlin*

GERMAN FEDERAL REPUBLIC
KUNST UND WISSEN ERICH BIEBER. Postfach 46, *7000 Stuttgart 1*

GREAT BRITAIN
BLACKWELL'S PERIODICALS DIVISION, Hythe Bridge Street, *Oxford OX1 2ET*
BUMPUS, HALDANE AND MAXWELL LTD., Cowper Works, *Olney, Bucks MK46 4BN*
COLLET'S HOLDINGS LTD., Denington Estate, *Wellingborough, Northants NN8 2QT*
W.M. DAWSON AND SONS LTD., Cannon House, *Folkestone, Kent CT19 5EE*
H. K. LEWIS AND CO., 136 Gower Street, *London WC1E 6BS*

GREECE
KOSTARAKIS BROTHERS, International Booksellers, 2 Hippokratous Street, *Athens-143*

HOLLAND
MEULENHOFF-BRUNA B.V., Beulingstraat 2, *Amsterdam*
MARTINUS NIJHOFF B.V., Lange Voorhout 9—11, *Den Haag*
SWETS SUBSCRIPTION SERVICE, 347b Heereweg, *Lisse*

INDIA
ALLIED PUBLISHING PRIVATE LTD., 13/14 Asaf Ali Road, *New Delhi 110001*
150 B-6 Mount Road, *Madras 600002*
INTERNATIONAL BOOK HOUSE PVT. LTD., Madame Cama Road, *Bombay 400039*
THE STATE TRADING CORPORATION OF INDIA LTD., Books Import Division, Chandralok, 36 Janpath, *New Delhi 110001*

ITALY
EUGENIO CARLUCCI, P.O. Box 252, *70100 Bari*
INTERSCIENTIA, Via Mazzé 28, *10149 Torino*
LIBRERIA COMMISSIONARIA SANSONI, Via Lamarmora 45, *50121 Firenze*
SANTO VANASIA, Via M. Macchi 58, *20124 Milano*
D. E. A., Via Lima 28, *00198 Roma*

JAPAN
KINOKUNIYA BOOK-STORE CO. LTD., 17-7 Shinjuku-ku 3 chome, Shinjuku-ku, *Tokyo 160-91*
MARUZEN COMPANY LTD., Book Department, P.O. Box 5050 Tokyo International, *Tokyo 100-31*
NAUKA LTD. IMPORT DEPARTMENT, 2-30-19 Minami Ikebukuro, Toshima-ku, *Tokyo 171*

KOREA
CHULPANMUL, *Phenjan*

NORWAY
TANUM-CAMMERMEYER, Karl Johansgatan 41—43, *1000 Oslo*

POLAND
WĘGIERSKI INSTYTUT KULTURY, Marszałkowska 80, *Warszawa*
CKP I W ul. Towarowa 28 *00-958 Warsaw*

ROMANIA
D. E. P., *Bucureşti*
ROMLIBRI, Str. Biserica Amzei 7, *Bucureşti*

SOVIET UNION
SOJUZPETCHATJ — IMPORT, *Moscow*
and the post offices in each town
MEZHDUNARODNAYA KNIGA, *Moscow G-200*

SPAIN
DIAZ DE SANTOS, Lagasca 95, *Madrid 6*

SWEDEN
ALMQVIST AND WIKSELL, Gamla Brogatan 26, *101 20 Stockholm*
GUMPERTS UNIVERSITETSBOKHANDEL AB, Box 346, *401 25 Göteborg 1*

SWITZERLAND
KARGER LIBRI AG, Petersgraben 31, *4011 Basel*

USA
EBSCO SUBSCRIPTION SERVICES, P.O. Box 1943, *Birmingham, Alabama 35201*
F. W. FAXON COMPANY, INC., 15 Southwest Park, *Westwood, Mass, 02090*
THE MOORE-COTTRELL SUBSCRIPTION AGENCIES, *North Cohocton, N. Y. 14868*
READ-MORE PUBLICATIONS, INC., 140 Cedar Street, *New York, N. Y. 10006*
STECHERT-MACMILLAN, INC., 7250 Westfield Avenue, *Pennsauken N. J. 08110*

VIETNAM
XUNHASABA, 32, Hai Ba Trung, *Hanoi*

YUGOSLAVIA
JUGOSLAVENSKA KNJIGA, Terazije 27, *Beogra*
FORUM, Vojvode Mišiča 1, *21000 Novi Sad*

ACTA PHYSICA

ACADEMIAE SCIENTIARUM HUNGARICAE

TOMUS XLIII FASCICULI 3–4

AKADÉMIAI KIADÓ, BUDAPEST

1977

ACTA PHYS. HUNG. APAHAQ 43 (3–4) 201–354 (1977)

ACTA PHYSICA

ACADEMIAE SCIENTIARUM HUNGARICAE

SZERKESZTI

KOVÁCS ISTVÁN

Az *Acta Physica* angol, német, francia vagy orosz nyelven közöl értekezéseket. Évente két kötetben, kötetenként 4—4 füzetben jelenik meg. Kéziratok a szerkesztőség címére (1521 Budapest XI., Budafoki út 8.) küldendők.

Megrendelhető a belföld számára az Akadémiai Kiadónál (1363 Budapest Pf. 24. Bankszámla 215-11488), a külföld számára pedig a „Kultura" Külkereskedelmi Vállalatnál (1389 Budapest 62, P.O.B. 149. Bankszámla 217-10990), vagy annak külföldi képviseleteinél.

The *Acta Physica* publish papers on physics in English, German, French or Russian, in issues making up two volumes per year. Subscription: $ 36.00 per volume. Distributor: "Kultura" Foreign Trading Company (1389 Budapest 62, P.O. Box 149) or its representatives abroad.

Die *Acta Physica* veröffentlichen Abhandlungen aus dem Bereich der Physik in deutscher, englischer, französischer oder russischer Sprache, in Heften, die jährlich zwei Bände bilden.

Abonnementspreis pro Band: $ 36.00. Bestellbar bei »Kultura« Außenhandelsunternehmen (1389 Budapest 62, Postfach 149) oder seinen Auslandsvertretungen.

Les *Acta Physica* publient des travaux du domaine de la physique en français, anglais, allemand ou russe, en fascicules qui forment deux volumes par an.

Prix de l'abonnement: $ 36.00 par volume. On peut s'abonner à l'Entreprise du Commerce Extérieur «Kultura» (1389 Budapest 62, P.O.B. 149) ou chez représentants à l'étranger.

«*Acta Physica*» публикуют трактаты из области физических наук на русском, немецком, английском и французском языках.

«*Acta Physica*» выходят отдельными выпусками, составляющими два тома в год.

Подписная цена — $ 36.00 за том. Заказы принимает предприятие по внешней торговле «Kultura» (1389 Budapest 62, P.O.B. 149) или его заграничные представительства.

ACTA PHYSICA

ACADEMIAE SCIENTIARUM HUNGARICAE

TOMUS XLIII FASCICULI 3–4

AKADÉMIAI KIADÓ, BUDAPEST

1977

ACTA PHYS. HUNG.

INDEX

Acta Physica Academiae Scientiarum Hungaricae, Tomus 43 (3—4), pp. 203—208 (1977)

ITERATION AND LANGER'S METHODS FOR COMPUTING WAVE FUNCTIONS

By

D. C. PATIL and V. M. KORWAR

DEPARTMENT OF PHYSICS, KARNATAK UNIVERSITY, DHARWAR-580 003, INDIA

(Received 13. IX. 1977)

Two approximation methods for solving the Schrödinger equation, one recently proposed by HERMAN et al., called the iteration method and the other due to LANGER, have been compared computing wave functions by these methods for (A – X) transition of AlO and using them to compute Franck–Condon factors. RKR (Rydberg – Klein – Rees) Franck – Condon factors have been taken as standard results for comparison. It is found that the iteration method is better than LANGER's. Compared to RKR procedure, the iteration method is also much simpler.

1. Introduction

Recently HERMAN et al. [1] have proposed a new approximation method for solving the Schrödinger wave equation for a diatomic molecule. These authors give explicit expressions for wave functions and further, they claim that the wave functions obtainable by their method are more accurate than those which are available (e. g., Morse oscillator wave functions); the wave functions, they claim, can be credited with accuracies at least as great as those associated with the Rydberg – Klein – Rees numerical methods. In the present work we have computed wave functions for the $A^2\Sigma - X^2\Sigma$ transition of AlO molecule using the expressions given by these authors.

We have taken this opportunity to evaluate wave functions by yet another method known as LANGER's [2] approximation method which has not found as much publicity as it deserves. Using one and the same potential, viz., the Rydberg potential we have computed wave functions and Franck – Condon factors and r-centroids thereof both by the method of iteration and LANGER's procedure. To see how both these approximate solutions compare with exact solutions of the Schrödinger equation, we have compared the Franck – Condon (FC) factors and r-centroids ($\bar{r}_{v'v''}$) calculated on approximation methods with those obtained using Morse potential wave functions, which are exact solutions of the Schrödinger equation. The Morse data on FCs on the aforesaid transition are available from the work of earlier workers [3] on this molecule.

2. Evaluation of the vibrational wave functions

(A) *Iteration method*

The Schrödinger wave equation for rotationless vibrational state governing the nuclear radial motion can be written in the form

$$\frac{d^2 \psi_v^{(x)}}{dx^2} + \{[E_v - V(x)]/_{B_e}\}\psi_v^{(x)} = 0 . \tag{1}$$

Here x represents the relative internuclear displacement, $(r - r_e)/r_e$, r and r_e being the instantaneous and equilibrium internuclear separation, respectively, and E_v is the vibrational eigen energy (in cm^{-1}) and B_e is the rotational constant.

Equation (1) is solved by first making the transformations

$$\psi_0(x) = \exp\left(-\frac{1}{2}\int_0^x y(x')\,dx'\right) \tag{2}$$

and

$$\psi_v(x) = g_v(x)\,\psi_0(x)\,, \tag{3}$$

$\psi_0(x)$ being the unnormalized wave function of the ground state $v = 0$. The functions $y(x)$ and $g_v(v)$ satisfy

$$y(x)^2 - \left[2\frac{dy(x)}{dx}\right] - \frac{4}{B_e}[v(x) - E_0] = 0 \tag{4}$$

and

$$\frac{d^2 g_v^{(x)}}{dx^2} - y(x)\frac{dg_v^{(x)}}{dx} + \frac{(E_v - E_0)}{B_e} g_v(x) = 0 . \tag{5}$$

Power series solutions to these equations have been found; these have been tabulated in [1].

With the use of Rydberg potential defined by

$$V(r) = -D[1 + a(r - r_e)]\,e^{-a(r-r_e)},$$

where D = dissociation energy, a = constant, r_e = equilibrium internuclear distance, we have, in the present investigation, computed wave functions for the vibrational states $v' = 0, 1, 2, 3, 4$ of A State and $v'' = 0, 1, 2, 3$ of X State of AlO. The integral

$$\bar{R}_e^2 \int \psi_{v'}^* \psi_{v''}\,d\tau \tag{6}$$

characterises the transition between two vibrational states v' and v''. $\bar{R}_e$ is the average electronic transition moment. The integral $\int \psi_{v'}^* \psi_{v''} d\tau$ is called the overlap integral and its square is called the Franck–Condon factor for the transition $v' \to v''$.

(B) *Langer's method*

The one-dimensional Schrödinger wave equation is written in the form

$$\frac{d^2\psi}{dx^2} + \lambda^2 [E - V^{(x)}]\psi = 0, \tag{7}$$

where μ = reduced mass, h = Planck's constant, $V(x)$ = potential energy function.

$$\lambda^2 = \frac{2\mu}{\hbar^2} .$$

One of the pre-requisites for the validity of LANGER's procedure for low vibrational quantum numbers is that λE has to be of moderate value. If this condition is satisfied let the variable in equation (7) be changed to Z, given by

$$Z = x - x_e - \left(\frac{\sigma}{\lambda}\right), \tag{8}$$

where σ is a constant to be determined through the formula

$$\sigma = -\frac{2V'''(x_e)\,\lambda E}{9[V''(x_e)]^2},$$

x_e = equilibrium internuclear distance. Primes indicate derivatives.

Then Eq. (7) becomes

$$\frac{d^2\psi}{dz^2} - (\lambda^2 \chi_0^2(z) + \lambda\chi_1 + \chi_2)\,\chi = 0, \tag{9}$$

where

$$\chi_0^2(z) = V(z + x_e),$$

$$\chi_1(z) = -\lambda E + \sigma V'(z + x_e),$$

$$\chi_2(z) = \lambda^2 \left\{ V\left(z + x_e + \frac{\sigma}{\lambda}\right) - V(z + x_e) - \frac{\sigma}{\lambda} V'(z + x_e) \right\}.$$

It is shown by LANGER that the solution of Eq. (9) which remains bounded as $z \to \infty$, is unique except for an arbitrary constant factor, and that for values of z that are positive and sufficiently large, its form is

$$\psi = \lambda^{-1/4}\, \varphi^{-1/2}\, \zeta^k\, e^{-1/2\zeta},$$

where

$$\Phi = 2\chi_0 + \frac{1}{\lambda}\left\{\frac{\chi_1}{\chi_0} + \frac{2k\chi_0}{\int_0^z \chi_0\,dz}\right\},$$

$$\zeta = \lambda\int_0^z \Phi\,dz, \quad k = \frac{\lambda E}{2[2V''(x_e)]^{1/2}} .$$

The form of the same solution for values of Z that are negative and numerically large is

$$\psi = \lambda^{-1/4} \Phi^{-1/2} [A_1 \zeta^{-k} e^{1/2} + A_2 \zeta^k e^{-1/2\zeta}],$$

where A_1 and A_2 are arbitrary constants and are given by

$$A_1 = \frac{1}{\pi} e^{2-(k-1/4)\pi i} \Gamma(k + 1/4) \Gamma(k + 3/4) \sin(2k - 1/2)\pi$$

and $A_2 = 1$.

Ultimately one obtains the following expressions for normalised wave functions

$$\psi_n = \left(\frac{2V''(x_e)}{\pi}\right)^{1/4} \left(\frac{n!}{2^n}\right)^{1/2} \frac{2(-1)^{(n-1)/2}}{\left(\frac{n-1}{2}\right)!} \frac{M_{n/2+1/4,1/4}(\zeta)}{\Phi''^2(z)},$$

where n is odd and

$$\psi_n = \left(\frac{2V''(x_e)}{\pi}\right)^{1/4} \left(\frac{n!}{2^n}\right)^{1/2} \frac{(-1)^{n/2}}{(n/2)!} \frac{M_{n/2+1/4,-(1/4)}(\zeta)}{\Phi(z)},$$

where n is even (M's are confluent hypergeometric functions.)

Using the Rydberg potential we have arrived at the following expressions for Φ and ζ:

$$\Phi = 2\sqrt{D}\,[0.707{,}107\,az - 235{,}702\,a^2z^2 + 0.049{,}105\,a^3z^3 - 0.015{,}386\,a^4z^4 + 0.000{,}641\,a^5z^5 - 0.000{,}201\,a^6z^6 \ldots .] + \frac{E}{\sqrt{D}}[-0.463{,}766\,az + 0.115{,}121\,a^2z^2 - 0.069{,}099\,a^3z^3 - 0.010{,}42\,a^4z^4 - 0.000{,}957\,a^5z^5 \ldots],$$

$$\zeta = \lambda \int_0^z \varphi\, dz .$$

By integrating the above expression for Φ, one can write explicitly for ζ.

Using these expressions wave functions have been obtained for vibrational quantum numbers ranging from 0 to 4. Wave functions have been evaluated at intervals of $0{\cdot}01$ A of r, the internuclear distance. A desk DCM calculator (Programmable) has been used and the calculations have been recorded up to sixth place of decimal.

As wave functions are available, another important parameter, r-centroid, defined by the following relation has been evaluated:

$$\bar{r}_{v'v''} = \frac{\int \psi_{v'}\, r\psi_{v''}\, \mathrm{d}r}{\int \psi_{v'}\, \psi_{v''}\, \mathrm{d}r} .$$

Table I

AlO($A^2\Sigma - X^2\Sigma$)

Band	FC Factors				r-Centroids		
	Nicholls (Morse)	RKR (Sharma)	Langer (Rydberg Potential)	Iteration	Tawde — Korwar (Morse)	Langer	Iteration
(0,0)	0.730	0.730	0.733	0.729	1.646	1.646	1.646
(0,1)	0,238	0.237	0.244	0.237	1.727	1.727	1.727
(0.2)	0.031	–	0.033	0.031	–	1.809	1.811
(0,3)	0.001	–	–	0.001	–	–	1.989
(1,1)	0.356	0.346	0.366	0.357	1.657	1.656	1.656
(1,0)	0.244	0.223	0.220	0.224	1.573	1.574	1.573
(1,2)	0.343	0.349	0.357	0.342	1.739	1.738	1.747
(1,3)	0.071	–	0.077	0.069	–	1.905	1.827
(2,2)	0.160	–	0.166	0.160	1.669	1.652	1.667
(2,0)	0.040	–	0.037	0.040	–	1.497	1.504
(2,1)	0.310	0.303	0.318	0.302	1.573	1.579	1.579
(2,3)	0.378	0.384	0.354	0.379	1.752	1.728	1.749
(3,3)	0.063	–	–	0.059	–	–	1.779
(3,0)	0.005	–	0.005	0.005	–	1.945	1.506
(3,1)	0.088	0.094	0.091	0.090	1.501	1.509	1.484
(3,2)	0.304	0.298	0.318	0.306	1.586	1.585	1.603
(4,0)	0.00043	–	–	0.00036	–	–	1.428
(4,2)	0.129	0.138	–	0.132	1.518	–	1.523
(4,3)	0.275	0.257	–	0.266	1.591	–	1.641

All these results are given in Table I. Also in Table I are given FCs and $r_{v'v''}$ s of Sharma [4] obtained on RKRV procedure and FCs and $\bar{r}_{v'v''}$'s of Nicholls [3] obtained with the use of Morse potential are given for comparison.

3. Discussion

As RKR potentials are realistic in that experimental data have been made use of in constructing potential energy curves which are later employed for obtaining potential at any inter-nuclear separation r, results of FCs and r-centroids evaluated with the use of RKR potentials may be taken as standard results with which we could compare other results.

Now, we see from Table I that, except for bands involving high quantum numbers such as (3, 1), (2, 3), (3, 2), (4, 2) and (4, 3) Morse FCs are almost the same as RKR FCs. This fact, incidentally supports the long-established

fact that Morse potential is generally valid at low quantum numbers. However there is another significance indicated by this fact and that is, we could take either RKR results or Morse results for testing the accuracy of the two approximation methods we are employing.

As one can easily see from Table I, the results of iteration method compare better with RKR results than do the results based on LANGER's procedure. It may be noted here that we have employed the same potential, viz., Rydberg's, in both the approximation methods. The difference between iteration results and LANGER's result are especially significant at high quantum numbers, for instance for (2, 3) transition. LANGER's procedure yields 8 % error whereas iteration gives only 1.3 % error; for (3,2) transition LANGER's FC is in error by 6.7 % while iteration FC is in error by 2.6 %. Thus, based on the results of FCs by the two approximations considered in the present investigation we can say that the iteration method yields better results than does LANGER's. Another point in favour of iteration procedure is that, although it is an approximation method, it yields results comparable with RKR results, and it is a much simpler method than RKR procedure.

r-centroid results could also be compared in a similar way; but *r*-centroids are not as sensitive as FCs to potentials. One can find the reason for this in the very definition of the *r*-centroid. This is also clear from the last 3 columns of Table I: there is not any appreciable difference in the various sets of *r*-centroids.

REFERENCES

1. R. M. HERMAN, R. H. TIPPING and S. SHORT, J. Chem. Phys., **53**, 595, 1970.
2. R. E. LANGER, Phys. Rev., **75**, 1573, 1949.
3. C. LINTON and R. W. NICHOLLS, JQSRT., **9**, 1, 1969.
4. A. SHARMA, JQSRT., **7**, 283, 289, 1967.

Acta Physica Academiae Scientiarum Hungaricae, Tomus 43 (3—4), pp. 209—215 (1977)

TWO-PHASE FLOW HEAT TRANSFER IN A CHANNEL WHEN THE INLET TEMPERATURE VARIES LINEARLY WITH TIME

By

K. S. SHIRKOT and SURJIT SINGH

DEPARTMENT OF MATHEMATICS, HIMACHAL PRADESH UNIVERSITY, SIMLA-171 005, INDIA

(Received 13. IX. 1977)

Exact solutions of the transient forced convection energy equations of dust particles and of liquid in a channel bounded by two parallel flat plates are obtained in the present paper when the inlet temperatures vary linearly with time and an interpretation of the case of laminar flows is given. It is found that the effect of the presence of dust particles is to increase the heat transfer.

Nomenclature

T_p	temperature of dust particles
T	temperature of liquid
C_p	specific heat of dust particles
C	specific heat of liquid
h	half distance between parallel plates
K_p	thermal conductivity of dust particle
K	thermal conductivity of liquid
$\bar{t}$	time
U_p	velocity of dust particle in $\bar{x}$-direction
U	velocity of liquid in $\bar{x}$-direction
$\bar{U}$	average velocity
ϱ	liquid density
$\bar{x}, \bar{y}$	Cartesian coordinates ($\bar{x}$—flow direction, and y—distance from channel centre line)
mN	mass of dust particle per unit volume ($= mNo$, constant)
μ	coefficient of viscosity of liquid
v	kinematic coefficient of viscosity
P	Prandtl number ($= \mu c/k$)
R	Reynolds number ($= h\bar{u}/v$)
h_p	heat transfer coefficient for flow over dust particle
A_p	surface area of dust particle
V_p	volume of dust particle

The meaning of any other symbols is given in the text as they occur.

1. Introduction

Heat transfer by gas-dust suspensions in pipe flow has been a subject of many studies. This was due partly to the demand for high heat-transfer coefficient in gas-cooled reactors and partly to the high volumetric specific heat of dust particles compared to a gas. Based on the experimental observations by FARBAR and MORLEY [1], SCHLUDERBERG [2] and SALOMONE and NEWMAN [3], TIEN [4,5], has analyzed the heat transfer by gas-dust suspen-

sion in turbulent pipe flow. Soo [6] in his solutions of the transient forced convection energy equations of dust particle and of liquid in a circular pipe has assumed that the inlet temperature of dust particles and of liquid are constant across the flow. DUBE and SHARMA [7] have analyzed a similar problem for the flow in a channel when the inlet temperatures very sinusoidally with time and the corresponding problem of flow in a pipe has been solved by SHIRKOT and SURJIT [8].

In the present investigation, exact solutions of the transient forced convection energy equations of dust particles and of liquid with fully developed flow in a parallel plate channel are obtained under given boundary conditions when the inlet temperature varies linearly with time and an interpretation of the case of laminar flows is given.

2. Formulation of the problem

We consider the steady laminar flow of a dusty viscous liquid with uniform distribution of dust particles in a parallel plate channel whose sides are separated by distance $2h$. The dust particles and the liquid entering the channel have temperatures which are spatially uniform across the entrance section but vary linearly with time. Therefore we can write the inlet conditions as

$$\overline{T}_p(0, \bar{y}, \bar{t}) = T_0 + T_1\left(\frac{v\bar{t}}{h^2}\right), \tag{2.1}$$

$$T(0, \bar{y}, \bar{t}) = T_0 + T_1\left(\frac{v\bar{t}}{h^2}\right), \tag{2.2}$$

where T_0 is the cycle mean temperature.

To obtain the heat-transfer performance and the temperatures of dust particles and of liquid it is necessary to set up two energy equations, one for the dust particles and one for the liquid—dust mixture. They are given as:

$$\frac{\partial \overline{T}_p}{\partial \bar{t}} + u_p \frac{\partial \overline{T}_p}{\partial \bar{x}} = G(\overline{T} - \overline{T}_p), \tag{2.3}$$

$$\frac{\partial \overline{T}}{\partial \bar{t}} + u \frac{\partial \overline{T}}{\partial \bar{x}} = \frac{v}{p} \frac{\partial^2 \overline{T}}{\partial \bar{y}^2} + 2\beta_2(\overline{T}_p - \overline{T}), \tag{2.4}$$

where

$$G = \frac{h_p A_p}{m N_0 C_p V_p}, \quad \beta_2 = \frac{m N_0 C_p G}{\varrho C}.$$

The inlet and the boundary conditions of the problem are as follows

$$\bar{T}_p = T_0 + T_1\left(\frac{v\bar{t}}{h^2}\right) \quad \text{when} \quad \bar{x} = 0\,. \tag{2.5}$$

$$\bar{T} = T_0 + T_1\left(\frac{v\bar{t}}{h^2}\right) \quad \text{when} \quad \bar{x} = 0\,, \tag{2.6}$$

$$\left.\begin{aligned} &\left(\frac{\partial \bar{T}_p}{\partial \bar{y}}\right)_{\bar{y}=0} = 0\,, \quad \left(\frac{\partial \bar{T}}{\partial \bar{y}}\right)_{\bar{y}=0} = 0\,, \\ &\bar{T}_p = T_\omega,\ \bar{T} = T_\omega \ \text{at} \ \bar{y} = h,\ (t > 0). \end{aligned}\right] \tag{2.7}$$

The system satisfying (2.3), (2.4) is subjected to the following restrictions (Soo [6]):

(i) Radiation effect is neglected.
(ii) The density of liquid remains constant; thus the velocity distribution is independent of the temperature distribution .
(iii) Liquid property variation is neglected.
(iv) Each dust particle is small and maintains uniform temperature due to its high thermal conductivity.
(v) The liquid and dust particle cloud have similar velocity profiles. The presence of dust particles does not affect the liquid velocity profile.
(vi) The dust particles are uniformly distributed throughout the channel.
(vii) The effect of collision with the wall is neglected.
(viii) The suspension is extremely dilute such that each particle is assumed to see the wall without interference of other particles.
(ix) Fully developed laminar velocity profiles between the parallel plates.
(x) Axial conduction is negligible with respect to bulk transport in the $\bar{x}$-direction. This is a reasonable assumption when Peclet number exceeds 100 [9].
(xi) Thermal resistance of the channel wall is negligible.
(xii) Eddy diffusivity of heat is negligible.

Further, to simplify the method of analysis the case of constant velocity will be considered here and for this purpose we substitute $\bar{u}(u = u_p)$ for the velocity profile in (2.3) and (2.4).

We introduce the following non-dimensional quantities:

$$\theta = \frac{\bar{T} - T_0}{T_1},\ \theta_p = \frac{T_p - T_0}{T_1},\ x = \frac{\bar{x}}{h},\ y = \frac{\bar{y}}{h},\ \bar{u} = u = u_0\,,$$

$$t = \frac{v\bar{t}}{h^2},\ \theta_0 = \frac{T_\omega - T_0}{T_1},\ \beta_3 = \frac{h^2 G}{v},\ \beta_4 = \frac{2h^2\beta_2}{v},\ R = \frac{h\bar{u}}{v}\,.$$

Equations (2.3) and (2.4) then become

$$\frac{\partial \theta_p}{\partial t} + R\frac{\partial \theta_p}{\partial x} = \beta_3(\theta - \theta_p), \tag{2.8}$$

$$\frac{\partial \theta}{\partial t} + R\frac{\partial \theta}{\partial x} = \frac{1}{p}\frac{\partial^2 \theta}{\partial y^2} + \beta_4(\theta_p - \theta). \tag{2.9}$$

The inlet and the boundary conditions reduce to

$$\theta_p = t \quad \text{when} \quad \bar{x} = 0, \tag{2.10}$$

$$\theta = t \quad \text{when} \quad \bar{n} = 0, \tag{2.11}$$

$$\left(\frac{\partial \theta_p}{\partial y}\right)_{y=0} = 0, \quad \left(\frac{\partial \theta}{\partial y}\right)_{y=0} = 0, \ \theta_p = \theta_0, \ \theta = \theta_0 \text{ at } y = 1, \ (t > 0). \tag{2.12}$$

3. Method of solution

The above problem can be separated into two as follows:

$$\theta_p(x, y, t) = \theta_{p_1}(x, y) + \theta_{p_2}(y, x, t), \tag{3.1}$$

$$\theta(x, y, t) = \theta_1(x, y) + \theta_2(x, y, t), \tag{3.2}$$

where θ_1, θ_2, θ_{p_1} and θ_{p_2} satisfy the following problems:

$$R\frac{\partial \theta p_1}{\partial x} = \beta_3(\theta_1 - \theta_{p_1}), \tag{3.3}$$

$$R\frac{\partial \theta_1}{\partial x} = \frac{1}{\varrho}\frac{\partial^2 \theta_0}{\partial y^2} + \beta_4(\theta_{p_1} - \theta_1), \tag{3.4}$$

$$\theta_{p_1} = 0 \text{ when } x = 0, \tag{3.5}$$

$$\theta_1 = 0 \text{ when } x = 0, \tag{3.6}$$

$$\left(\frac{\partial \theta_{p_1}}{\partial y}\right)_{y=0} = 0, \ \left(\frac{\partial \theta_1}{\partial y}\right)_{y=0} = 0, \theta_{p_1} = \theta_0, \theta_1 = \theta_0 \text{ at } y = 1, \ (t > 0). \tag{3.7}$$

and

$$\frac{\partial \theta_{p_2}}{\partial t} + R\frac{\partial \theta_{p_2}}{\partial x} = \beta_3(\theta_2 - \theta_{p_2}), \tag{3.8}$$

$$\frac{\partial \theta_2}{\partial t} + R\frac{\partial \theta_2}{\partial x} = \frac{1}{p}\frac{\partial^2 \theta_2}{\partial y^2} + \beta_u(\theta_{p_2} - \theta_2), \tag{3.9}$$

$$\theta_{p_2} = t \text{ when } x = 0, \tag{3.10}$$

$$\theta_2 = t \text{ when } x = 0, \tag{3.11}$$

$$\left.\begin{aligned} &\left(\frac{\partial \theta_{p_2}}{\partial y}\right)_{y=0} = 0, \ \left(\frac{\partial \theta_2}{\partial y}\right)_{y=0} = 0, \\ &\theta_{p_2} = 0, \ \theta_2 = 0 \text{ at } y = 1, \ (t > 0). \end{aligned}\right] \tag{3.12}$$

Solving Eqs. (3.3) and (3.4) under the conditions (3.5) – (3.7), we get

$$\theta_{p_1}(x, y) = \theta_0\left[1 - \frac{4}{\pi}\sum_{n=0}^{\infty}\frac{(-1)^n}{(2n+1)}\cos\left(\frac{2n+1}{2}\right)\pi y \times \right.$$

$$\left. \times \frac{(\lambda_n e^{-\mu_n x} - \mu_n e^{-\lambda_n x})}{\lambda_n - \mu_n}\right],$$

$$\theta_1(x, y) = \theta_0\left[1 - \frac{4}{\pi}\sum_{n=0}^{\infty}\frac{(-1)^n}{(2n+1)}\cos\left(\frac{2n+1}{2}\right)\pi y\, B_n(x)\right],$$

where

$$B_n(x) = \frac{\lambda_n}{\lambda_n - \mu_n}\left(1 - \frac{R\mu_n}{\beta_3}\right)e^{-\mu_n x} - \frac{\mu_n}{\lambda_n - \mu_n}\left(1 - \frac{R\lambda_n}{\beta_3}\right)e^{-\lambda_n x},$$

and

$$2\lambda_n = \frac{\beta_3 + \beta_4}{R} + \frac{(2n+1)^2\pi^2}{4PR} + \sqrt{\left[\frac{\beta_3+\beta_4}{R} + \frac{(2n+1)^2\pi^2}{4PR}\right]^2 - \frac{(2n+1)^2\pi^2\beta_3}{PR^2}},$$

$$2\mu_n = \frac{\beta_3 + \beta_4}{R} + \frac{(2n+1)^2\pi^2}{4PR} - \sqrt{\left[\frac{\beta_3+\beta_4}{R} + \frac{(2n+1)^2\pi^2}{4PR}\right]^2 - \frac{(2n+1)^2\pi^2\beta_3}{PR^2}}.$$

let

$$\theta_{p_1}(x, y, t) = t\varphi_{p_1}(x, y) + \psi_{p_1}(x, y),$$

$$\theta_2(x, y, t) = t\varphi_2(x, y) + \psi_2(x, y).$$

Substituting in (3.8) and (3.9) and on equating co-efficients of t and the constant terms we get

$$\varphi_{p_1} + R\frac{\partial\psi_{p_1}}{\partial x} = \beta_3(\psi_2 - \psi_{p_1}), \tag{3.13}$$

$$\varphi_2 + R\frac{\partial\psi_2}{\partial x} = \frac{1}{p}\frac{\partial^2\psi_2}{\partial y^2} + \beta_4(\psi_{p_1} - \psi_2), \tag{3.14}$$

$$R\frac{\partial\varphi_{p_1}}{\partial x} = \beta_3(\varphi_2 - \varphi_{p_1}), \tag{3.15}$$

$$R\frac{\partial\varphi_{p_1}}{\partial x} = \frac{1}{p}\frac{\partial^2\varphi_2}{\partial y^2} + \beta_4(\varphi_{p_1} - \varphi_2). \tag{3.16}$$

The boundary conditions are

$$\varphi_{p_1} = 1,\ \psi_{p_1} = 0 \text{ when } x = 0, \tag{3.17}$$

$$\varphi_2 = 1,\ \psi_2 = 0 \text{ when } x = 0, \tag{3.18}$$

$$\left(\frac{\partial\varphi_{p_1}}{\partial y}\right)_{y=0} = 0,\ \left(\frac{\partial\psi_{p_1}}{\partial y}\right)_{y=0} = 0,\ \varphi_{p_1} = 0,\ \psi_{p_1} = 0 \text{ at } y = 1, \tag{3.19}$$

$$\left(\frac{\partial\varphi_2}{\partial y}\right)_{y=0} = 0,\ \left(\frac{\partial\psi_2}{\partial y}\right)_{y=0} = 0,\ \varphi_2 = 0,\ \psi_2 = 0 \text{ at } y = 1. \tag{3.20}$$

Solving Eqs. (3.13 – 3.18) and using (3.17 – 3.20) we get

$$\varphi_{p_2} = \frac{4}{\pi} \sum_{n=0}^{\infty} \frac{(-1)^n}{2n+1} \cos\left(\frac{2n+1}{2}\right) \pi y \; A_n(x),$$

$$\varphi_2 = \frac{4}{\pi} \sum_{n=0}^{\infty} \frac{(-1)^n}{2n+1} \cos\left(\frac{2n+1}{2}\right) \pi y \; B_n(x),$$

$$\psi_{p_2} = \frac{4}{\pi} \sum_{n=0}^{\infty} \frac{(-1)^n}{2n+1} \cos\left(\frac{2n+1}{2}\right) \pi y \; C_n(x),$$

$$\psi_2 = \frac{4}{\pi} \sum_{n=0}^{\infty} \frac{(-1)^n}{2n+1} \cos\left(\frac{2n+1}{2}\right) \pi y \; D_n(x),$$

where

$$A_n(x) = \frac{\lambda_n e^{-\mu_n y} - \mu_n e^{-\lambda_n x}}{\lambda_n - \mu_n},$$

$$B_n(x) = \frac{\lambda_n}{\lambda_n - \mu_n}\left(1 - \frac{R\mu_n}{\beta_3}\right) e^{-\mu_n x} - \left(\frac{\mu_n}{\lambda_n - \mu_n}\left(1 - \frac{R\lambda_n}{\beta_3}\right) e^{-\lambda_n x},\right.$$

$$C_n(x) = -\frac{x}{R(\lambda_n - \mu_n)}\left(\lambda_n e^{-\mu_n x} - \mu_n e^{-\lambda_n x}\right),$$

$$D_n(x) = \frac{x\lambda_n \mu_n}{(\lambda_n - \mu_n)\beta_3}\left(e^{-\mu_n x} - e^{-\lambda_n x}\right) - \frac{x(\lambda_n e^{-\mu_n x} - \mu_n e^{-\lambda_n x})}{R(\lambda_n - \mu_n)}.$$

Thus

$$\theta_{p_2} = \left(t - \frac{x}{R}\right) \frac{4}{\pi} \sum_{n=0}^{\infty} \frac{(-1)^n \cos\left(\frac{2n+1}{2}\right) \pi y}{2n+1} \left(\frac{\lambda_n e^{-\mu_n x} - \mu_n e^{-\lambda_n x}}{\lambda_n - \mu_n}\right),$$

$$\theta_2 = \left(t - \frac{x}{R}\right) \frac{4}{\pi} \sum_{n=0}^{\infty} \frac{(-1)^n \cos\left(\frac{2n+1}{2}\right) \pi y}{2n+1} \times$$

$$\times \left[\frac{\lambda_n e^{-\mu_n x} - \mu_n e^{-\lambda_n x}}{\lambda_n - \mu_n} - \frac{R\lambda_n \mu_n}{(\lambda_n - \mu_n)\beta_3}\left(e^{-\mu_n x} - e^{-\lambda_n x}\right)\right],$$

where λ_n and μ_n have the values given before.

4. Discussion

When the boundary condition on the wall for θ_p and θ is homogeneous, that is when θ_0 is zero, then

$$\theta_p(x, y, t) = \theta_{p_2}(x, y, t), \tag{4.1}$$

$$\theta\,(x, y, t) = \theta_2(x, y, t). \tag{4.2}$$

Expressions for $\theta_{p_2}(x, y, t)$ and $\theta_2(x, y, t)$ show that the temperatures of dust particles and of liquid decay exponentially along the channel.

The temperatures at any y, say $y = 0$ and $t = 2$ are given in the following Tables:

Table I

$p = 0.73$, $\beta_3 = 10^5$, $\beta_4/\beta_3 = 0.5$

	R \ x	1	5	10	15	20
θ_2	13 000	2.0236955	1.9997131	1.9984316	1.9980305	1.9976402
	20 000	2.0318297	2.0028223	1.9989533	1.9984620	1.9981961
θ_{p_2}	13 000	2.0237062	1.9998234	1.9984333	1.9980306	1.9976421
	20 000	2.0318379	2.0028316	1.9989538	1.9984639	1.9981966

We observe the following important points:

(i) From Table I it is found that θ_2 and θ_{p_2} both increase with the increase of R and decrease with the increase of x. Also, $\theta_{p_2} > \theta_2$ always, for fixed values of P, β_3 and β_4/β_3.

(ii) θ_2 and θ_{p_2} increase with the increase of β_4/β_3 and decrease with the increase of x. Also, $\theta_{p_2} > \theta_2$ always, for fixed values of ϱ, β_3 and R as given in Table II.

Table II

$p = 0.73$, $\beta_3 = 10^5$, $R = 30000$

	β_4/β_3 \ x	1	5	10	15	20
θ_2	0.5	2.0381531	2.0084913	2.0004405	1.9989521	1.9985684
	0.9	2.0410775	2.0128147	2.0022515	1.999516	1.9987236
θ_{p2}	0.5	2.0387145	2.0086209	2.000632	1.9989836	1.9985736
	0.9	2.0418631	2.0128736	2.0025646	1.9995982	1.9987422

Thus it is observed that the effect of the presence of the dust particles is to flatten the temperature profile and as a result, to increase the heat transfer.

REFERENCES

1. L. FARBAR and M. J. MORLEY, Ind. Eng. Chem., **49**, 1143, 1957.
2. D. C. SCHLUDERBERG, The Application of Gas-Ceramic Mixtures to Nuclear Power. Rept. No. CF 55-8-199 ORSORT, AEC, 1955
3. J. J. SALOMANE and N. NEWMANN, Ind. Eng. Chem. **47**, 283, 1955.
4. C. L. TIEN, Transport Processes in Two-phase Turbulent Flow, Ph. D. Thesis, Princeton University U.S.A. 1959.
5. C. L. TIEN, Trans. ASME, **83C**, 183, 1961.
6. S. L. SOO, Fluid Dynamics of Multiphase Systems, Blaisdell Publishing Co., London, 1967.
7. S. N. DUBE and C. L. SHARMA, Acta Phys. Hung. **39**, 23, 1975.
8. K. S. SHIRKOT and SURJIT SINGH, Acta Phys. Hung., **42**, 201, 1977.
9. P. J. SCHNEIDER, Trans. ASME, **79**, 765, 1957.

Acta Physica Academiae Scientiarum Hungaricae, Tomus 43 (3—4), pp. 217—225 (1977)

EQUATION OF STATE OF THE SYSTEM OF ALFVÉN WAVES

By

M. Y. NASIR*

DEPARTMENT OF THEORETICAL PHYSICS, ROLAND EÖTVÖS UNIVERSITY, BUDAPEST

(Received 11. X. 1977)

The system of Alfvé nwaves is elucidated. Bose—Einstein statistics is applied to find the equation of state and thermodynamic quantities of the system. It is found that the pressure of the system is directly proportional to the square of the absolute temperature. Adiabatic changes of the system are also discussed.

1. Introduction

So far Alfvén waves have not been studied as a system. In this paper we are showing that Alfvén waves can be considered as a system. Assuming that the energy of the system of Alfvén waves is quantized by the boundary conditions imposed on the walls of the box containing the fluid and taking the aid of the formulae of electromagnetic waves we have obtained the density of states and free energy of the system which have led us to the equation of state of the system.

2. Definition

In analogy with the photon of electromagnetic waves and the phonon of acoustic waves, we assume that the quantum of energy of an Alfvén wave also exists and possesses the value $\hbar\omega$ ($\hbar$ being Dirac h and ω the angular frequency). We call this quantum "Alfvénon".

The definition is supported by the fact that magnetohydrodynamic waves can be considered as an extreme case of electromagnetic waves and that there is transition between magnetohydrodynamic and electromagnetic waves [1]. The transition also occurs between magnetohydrodynamic and acoustic waves as discussed by HERLOFSON [2].

3. Formulation of the problem

We consider the system of Alfvén waves in a cubic box having each side l and volume V. Let the system be in thermal equilibrium with the box which is assumed to have perfectly reflecting walls. Moreover, we suppose that the

* On leave from Government College, Bahawalnagar, Pakistan.

walls of the box are ideally conducting and that the wave function vanishes on all sides of the box. Due to the analogy between photons and Alfvénons, we say that Alfvénons are subject to quantum statistics, in general, and Bose–Einstein statistics, in particular. Thus, the Pauli exclusion principle is disobeyed by Alfvénons.

On the basis of the facts supporting the definition of an Alfvénon as described in the previous Section we are justified in determining thermodynamic quantities of the system of Alfvén waves with the aid of the formulae of electromegnetic waves.

4. Solution of the problem

We write the basic equations of magnetohydrodynamics for an ideal medium as follows [3]:

$$\frac{\partial \varrho}{\partial t} + \nabla \cdot (\varrho \mathbf{v}) = 0 \,, \tag{1}$$

$$\varrho \frac{\mathrm{d}\mathbf{v}}{\mathrm{d}t} = -\nabla p + \frac{1}{4\pi}[(\nabla \times \mathbf{B}) + \mathbf{B}], \tag{2}$$

$$\frac{\partial \mathbf{B}}{\partial t} = \nabla \times (\mathbf{v} \times \mathbf{B}), \tag{3}$$

$$\nabla \cdot \mathbf{B} = 0, \tag{4}$$

where $\varrho = \varrho(\mathbf{r}, t)$ is the mass density of the fluid, $\mathbf{v} = \mathbf{v}(\mathbf{r}, t)$ its velocity, p the pressure and $\mathbf{B}$ the magnetic field. Also we add an equation which in the first approximation is representing a reversible adiabatic process of an isotropic plasma:

$$p = \text{const}\ \varrho^{\gamma}, \tag{5}$$

where γ is the ratio of specific heats given by

$$\gamma = C_p/C_v. \tag{6}$$

We assume that the waves propagating in the fluid are plane harmonic waves havin gsmall amplitudes. The assumption of small amplitude helps us to linearize the Eqs. (1)–(5). Thus, we write

$$\mathbf{B} = \mathbf{B}_0 + \mathbf{B}_1 \,, \tag{7}$$

$$\mathbf{v} = \mathbf{v}_0 + \mathbf{v}_1 \,, \tag{8}$$

$$p = p_0 + p_1 \,, \tag{9}$$

$$\varrho = \varrho_0 + \varrho_1 \,, \tag{10}$$

where $\mathbf{B}_0$, $\mathbf{v}_0$, p_0 and ϱ_0 are constants and correspond to the uniform equilibrium state of the fluid. $\mathbf{B}_1$, $\mathbf{v}_1$, p_1 and ϱ_1 are small perturbations in the quantities $\mathbf{B}_0$, $\mathbf{v}_0$, p_0 and ϱ_0, respectively. The values of these perturbations and their derivatives always remain very much smaller than the constant quantities. Neglecting all but the linear terms in $\mathbf{B}_1$, $\mathbf{v}_1$, p_1 and ϱ_1, the equations (1) – (5) are linearized to:

$$\frac{\partial \varrho_1}{\partial t} + \varrho_0(\nabla \cdot \mathbf{v}_1) = 0\,, \tag{11}$$

$$\varrho \frac{\partial \mathbf{v}_1}{\partial t} = -\nabla p_1 + \frac{1}{4\pi}\left[(\nabla \times \mathbf{B}_1) \times \mathbf{B}_0\right], \tag{12}$$

$$\frac{\partial \mathbf{B}_1}{\partial t} = \nabla \times (\mathbf{v}_1 \times \mathbf{B}_0), \tag{13}$$

$$\nabla \cdot \mathbf{B}_1 = 0\,, \tag{14}$$

$$\frac{p_1}{p_0} = \gamma \frac{\varrho_1}{\varrho_0}\,. \tag{15}$$

Thus, we get a system of homogeneous, linear, partial differential equations that governs the behaviour of the perturbations is space and time. Since, the waves propagating in the fluid are plane harmonic, we may simplify the linearized equations (11) – (15) by introducing the plane wave solution

$$A = \mathcal{A}\, e^{-i(\omega t - \mathbf{K}\cdot\mathbf{r})}\,, \tag{16}$$

where A is any fluctuating quantity, $\mathcal{A}$ its amplitude, $i = (-1)^{1/2}$ and $\mathbf{K}$ the wave vector. The simplified forms of the equations will be

$$\omega\varrho_1 - \varrho_0(\mathbf{K} \cdot \mathbf{v}_1) = 0, \tag{17}$$

$$\varrho_0\, \omega \mathbf{v}_1 = p_1\, \mathbf{K} + \frac{1}{4\pi}\,[\mathbf{K}(\mathbf{B}_0 \cdot \mathbf{B}_1) - \mathbf{B}_1(\mathbf{B}_0 \cdot \mathbf{K})], \tag{18}$$

$$\omega \mathbf{B}_1 = -\left[\mathbf{v}_1(\mathbf{B}_0 \cdot \mathbf{K}) - \mathbf{B}_0(\mathbf{K} \cdot \mathbf{v}_1)\right], \tag{19}$$

$$\mathbf{K} \cdot \mathbf{B}_1 = 0\,, \tag{20}$$

$$\frac{p_1}{p_0} = \gamma \frac{\varrho_1}{\varrho_0}\,. \tag{21}$$

With the help of these equations we may obtain the following important relation connecting the kinetic and magnetic energy for any type of mode

$$\frac{1}{2}\,\varrho_0\, \mathbf{v}_1^2 = \frac{\varrho_1^2}{2\varrho_0} C_s^2 + \frac{B_1^2}{8\pi}\,, \tag{22}$$

where $C_s = (p_1/\varrho_1)^{1/2}$ is the speed of sound. Moreover, eliminating all the variables except $\mathbf{v}_1$ from the Eqs. (17)–(21), we get the following equality [4]:

$$\left[\frac{(\mathbf{B}_0 \cdot \mathbf{K})^2}{4\pi} - \varrho_0\omega^2\right]\mathbf{v}_1 + \left[\left(\frac{\mathbf{B}_0^2}{4\pi} + \gamma p_0\right)\mathbf{K} - \frac{\mathbf{B}_0(\mathbf{B}_0 \cdot \mathbf{K})}{4\pi}\right](\mathbf{K} \cdot \mathbf{v}_1) - \\ - \frac{(\mathbf{B}_0 \cdot \mathbf{v}_1)}{4\pi}(\mathbf{B}_0 \cdot \mathbf{K})\,\mathbf{K} = 0\,. \tag{23}$$

Now corresponding to different conditions, we obtain different relations for the various modes of oscillations.

If the fluid velocity $\mathbf{v}_1$ is perpendicular to the wave vector $\mathbf{K}$ and the unperturbed magnetic field $\mathbf{B}_0$, viz. Fig. 1 [5], we obtain transverse magneto-hydrodynamic waves known as Alfvén waves. On the other hand, if $\mathbf{v}_1$, $\mathbf{K}_1$, and $\mathbf{B}_0$ are coplanar, we get magneto-acoustic waves – the waves which are neither purely longitudinal nor purely transverse.

For the time being we restrict ourselves to the case of Alfvén waves and postpone the discussion of magneto-acoustic waves to some other place. For Alfvén waves we have

$$(\mathbf{K} \cdot \mathbf{v}_1) = 0 = (\mathbf{B}_0 \cdot \mathbf{v}_1). \tag{24}$$

Therefore, the expression (23) is simplified to

$$\omega^2 = \frac{(\mathbf{B}_0 \cdot \mathbf{K})^2}{4\pi\varrho_0} \tag{25}$$

or simply

$$\omega^2 = (\mathbf{C}_A \cdot \mathbf{K})^2, \tag{26}$$

where

$$\mathbf{C}_A = \frac{\mathbf{B}_0}{(4\pi\varrho_0)^{1/2}} \tag{27}$$

is known as Alfvén velocity. We can write Eq. (26) as:

$$C_{Ax}^2 K_x^2 + C_{Ay}^2 K_y^2 + C_{Az}^2 K_z^2 + 2C_{Ax}C_{Az}K_x K_y + 2C_{Ay}C_{Az}K_y K_z + \\ + 2C_{Az}C_{Ax}K_z K_x - \omega^2 = 0\,. \tag{28}$$

The discriminating cubic of this quadratic equation will be

$$\begin{vmatrix} C_{Ax}^2 - g & C_{Ax}C_A & C_{Az}C_{Ax} \\ C_{Ax}C_{Ay} & C_{Ay}^2 - g & C_{Ay}C_{Az} \\ C_{Az}C_{Ax} & C_{Ay}C_{Az} & C_{Az}^2 - g \end{vmatrix} = 0. \tag{29}$$

Solving this equation, we obtain

$$g = 0,\ 0,\ (C_{Ax}^2 + C_{Ay}^2 + C_{Az}^2).$$

Thus, the quadratic equation (28) can be reduced to the form

$$(C_{Ax}^2 + C_{Ay}^2 + C_{Az}^2)\, K_0^2 - \omega^2 = 0$$

or,

$$K_z = \pm \frac{\omega}{(C_{Ax}^2 + C_{Ay}^2 + C_{Az}^2)^{1/2}} . \tag{30}$$

Hence, the relation (26) represents a pair of parallel planes in **K** space. Moreover, the result (25) implies that the group velocity of the waves is

$$\frac{\partial \omega}{\partial \mathbf{K}} = \frac{\mathbf{B}}{(4\pi \varrho_0)^{1/2}} . \tag{31}$$

Therefore, the disturbance travels parallel to the magnetic field with the Alfvén velocity $\mathbf{C}_A$. Furthermore, with the help of the equalities (17), (21), (22) and (24), we obtain

$$\varrho_1 = 0 = p_1 \tag{32}$$

and

$$\frac{1}{2}\varrho_0 v_1^2 = \frac{B_1^2}{8\pi} . \tag{33}$$

Thus, we conclude that the compressibility of the fluid does not play any role in Alfvén waves, density or pressure perturbation does not accompany these waves, energy flow is always along the magnetic lines of force, geometrical spreading of the energy does not take place, the medium does not change thermodynamically (ϱ_1, p_1 being zero) and there is an equipartition between hydrodynamic and electromagnetic energy, a fact which serves as an important guide to recognize Alfvén waves [6].

Due to the boundary conditions imposed by us upon the walls of the box only two types of propagation of magnetohydrodynamic waves are possible; either along or across the magnetic field. Thus, the oblique propagation of magnetohydrodynamic waves in the box is not permitted by the set of boundary conditions. Now the relation (26) gives us

$$\omega = C_A K \cos \varphi , \tag{34}$$

where φ is the angle between the direction of the constant magnetic field and the wave propagation. For Alfvén waves to propagate along the magnetic

field φ vanishes (see Fig. 1). These waves do not propagate across the magnetic field because in this case $\varphi = \pi/2$ and the result (34) will imply

$$\text{phase velocity} = \omega/K = 0.$$

Thus, Alfvén waves will tend to become entropy waves. To avoid this situation, we take $\varphi = 0$ for Alfvén waves and write the relation (34) as:

$$\omega = C_A K. \tag{35}$$

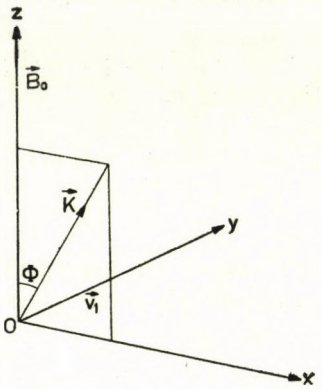

Fig. 1. Directions of the constant magnetic field $\mathbf{B}_0$, the wave vector $\mathbf{K}$ and the fluid velocity $\mathbf{v}_1$

We can find the density of states Z of the system of Alfvén waves by applying the formula given by KOMPANEYETS [7]:

$$dz = \frac{l}{\pi} \mathrm{d}K. \tag{36}$$

We are justified in utilizing this formula because we are considering the propagation of Alfvén waves along one side on the cube only. Hence, substituting the value of dk from Eq. (35) and considering all possible polarizations, we obtain the number of states included between ω and $\omega + \mathrm{d}\omega$ as:

$$dZ(\omega) = \frac{2V^{1/3}}{\pi C_A} \mathrm{d}\omega\ . \tag{37}$$

Now let us determine the thermodynamic quantities of the system of Alfvén waves. At first we shall find the expression for the free energy $\mathcal{E}$ of the system by using the formula given by GUGGENHEIM [8]:

$$\mathcal{E} = \theta \sum_k Z_k \log\left(1 - e^{-E_k/\theta}\right), \tag{38}$$

where θ is Boltzmann's constant $\times$ absolute temperature and E_k the energy of the kth Alfvénon. The expressions (37) and (38) collectively give us

$$\mathcal{E} = \frac{2V^{1/3}\theta}{\pi C_A}\int_0^\infty \log\left(1 - e^{-\hbar\omega/\theta}\right) d\omega .$$

Let $\hbar\omega/\theta = x$. Therefore,

$$\mathcal{E} = \frac{2V^{1/3}\theta^2}{\pi\hbar C_A}\int_0^\infty \log\left(1 - e^{-x}\right) dx .$$

Using power series for logarithm and integrating term by term, we obtain

$$\mathcal{E} = \frac{2V^{1/3}\theta^2}{\pi\hbar C_A}\int_0^\infty \left(-\sum_{n=1}^{\infty} n^{-1}\, e^{-nx}\right) dx .$$

Putting $nx = y$, we get

$$\mathcal{E} = -\frac{2V^{1/3}\theta^2}{\pi\hbar C_A}\int_0^\infty \left(\sum_{n=0}^{\infty}\frac{1}{n^2}\right) e^{-y}\, dy = -\frac{2V^{1/3}\theta^2}{\pi\hbar C_A}\cdot\frac{\pi^2}{6} = -\frac{\pi V^{1/3}\theta^2}{3\hbar C_A}. \quad (39)$$

Entropy S of the system will be

$$S = -\frac{\partial\mathcal{E}}{\partial\theta} = \frac{2\pi V^{1/3}\theta}{3\hbar C_A} . \quad (40)$$

Mean energy:
$$\bar{E} = \mathcal{E} + \theta S = \frac{\pi V^{1/3}\theta^2}{3\hbar C_A} . \quad (41)$$

Pressure:
$$p = -\frac{\partial\mathcal{E}}{\partial V} = \frac{\pi}{9\hbar C_A}\theta^2 V^{-1/3} , \quad (42)$$

or,

$$pV^{2/3} = \frac{\pi}{9\hbar C_A}\theta^2 . \quad (43)$$

Eq. (43) is called the equation of state of the system of Alfvén waves. Thermodynamic potential

$$\chi = \bar{E} - \theta S + pV = -\frac{2\pi V^{1/3}\theta^2}{9\hbar C_A} . \quad (44)$$

Enthalpy or heat function

$$y = \bar{E} + pV = \frac{4\pi V^{1/3}\theta^2}{9\hbar C_A} . \quad (45)$$

For reversible adiabatic changes, the entropy of the system remains constant. Therefore, Eq. (40) implies

$$V\theta^3 = \text{const.} \tag{46}$$

Eq. (43) and (46) further give us

$$pV^{4/3} = \text{const.} \tag{47}$$

The expressions (46) and (47) are also obtainable for a photon gas.

The specific heat of the system at constant volume can be determined as:

$$C_v = \left(\frac{\partial \bar{E}}{\partial \theta}\right)_V = \frac{2\pi V^{1/3}\,\theta}{3\hbar C_A} . \tag{48}$$

If C_p is the specific heat at constant pressure, then

$$C_p - C_v = -\frac{\theta\left(\frac{\partial p}{\partial \theta}\right)_v^2}{\left(\frac{\partial p}{\partial V}\right)_\theta} = \frac{2\pi\, V^{1/3}\,\theta}{3\hbar C_A}, \tag{49}$$

$$C_p = \frac{4\pi V^{1/3}\,\theta}{3\hbar C_A} . \tag{50}$$

Adiabatic index

$$\gamma = C_p/C_v = 2, \tag{51}$$

$$\varkappa = \frac{C_p - C_v}{C_p} = \frac{1}{2} . \tag{52}$$

5. Conclusion and discussion

On the basis of Eq. (42), we say that the pressure of the system of Alfvén waves is directly proportional to the square of the absolute temperature.

If we compare results obtained in the system of Alfvén waves with the corresponding results of a photon gas [4], we observe that the energy of the system of Alfvén waves is directly proportional to the square of the absolute temperature (cf. expression (41)), but for a photon gas Stefan – Boltzmann law states that energy is proportional to the fourth power of the absolute temperature. Also we note that for both systems pressure is equal to one-third of the energy density. The thermodynamic potential of the system of Alfvén waves has a definite value given by the relation (44) but for a photon gas it

vanishes. For adiabatic changes, the results (46) and (47) hold in both systems. Moreover, the adiabatic index γ for the system of Alfvén waves is 2 while for a photon gas it becomes infinity. The value of $\varkappa$ for the system of Alfvén waves is 1/2 but for a photon gas it is indeterminate.

Acknowledgement

The author expresses gratitude to Prof. IVÁN ABONYI for his kind suggestion to solve this problem, constructive criticism to strengthen the arguments and inspiration to complete the work. Financial support of the Institute of Cultural Relations, Budapest is also appreciated.

REFERENCES

1. H. ALFVÉN, Cosmical Electrodynamics, p. 84, Clarendon Press, Oxford, 1950.
2. N. HERLOFSON, Nature, **165,** 1020, 1950.
3. A. I. AKHIEZER et al., Plasma Electrodynamics I, p. 31, Pergamon Press, Oxford, 1975.
4. M. Y. NASIR, Ph. D. Thesis of Roland Eötvös University, Budapest, 1977.
5. H. ALFVÉN, Cosmical Electrodynamics, p. 96, Clarendon Press, Oxford, 1963.
6. I. ABONYI, Postepy Astronautyki, 2/3, 7, 1974.
7. A. S. KOMPANEYETS, Theoretical Physics, p. 268, Mir Publishers, Moscow, 1965.
8. E. A. GUGGENHEIM, Thermodynamics, p. 391, North Holland Publishing Company, Amsterdam, 1950.

Acta Physica Academiae Scientiarum Hungaricae, Tomus 43 (3—4), pp. 227—235 (1977)

TRAVELLING WAVES ON THE SURFACE OF A FALLING LIQUID FILM PAST A PERMEABLE BED

By

V. VIDYANIDHI and V. C. CHENCHU RAJU

DEPARTMENT OF ENGINEERING MATHEMATICS, ANDHRA UNIVERSITY, WALTAIR, INDIA

(Received 11. X. 1977)

The paper presents the existence of gravity capillary waves travelling down the surface of a falling liquid film past a permeable bed. The bed is characterized by a parameter $\beta = (\alpha + \sigma)/\alpha\sigma^2$, where α is a property of the porous material and $\sigma = h_0/\sqrt{K}$, h_0 the depth of the liquid film and K the absolute permeability of the porous medium. It is shown that the range of allowed dimensionless wave celerity widens as β increases. The celerity depends less and less on the Weber number W and also on the dimensionless wave number N, as β increases. When $\beta = 0$ we recover the gravity capillary waves on liquid films predicted by KAPITZA.

1. Introduction

An important phenomenon in physicochemical hydrodynamics [1] is the existence of travelling waves on the surface of viscous liquid films under the influence of gravity and surface tension. Such waves were first predicted by KAPITZA [2]. His procedure was refined by MASSOT, IRANI and LIGHTFOOT [3]. In this paper, following their scheme, we investigate the nature of these waves for a falling liquid film past a permeable vertical bed.

2. Nusselt solution for a liquid film past a permeable bed

At the outset, we determine the steady fully developed flow for a falling liquid film past a permeable bed. The corresponding solution for a liquid film past an impermeable bed, i.e. for the classical case was given by NUSSELT [4]. The physical model illustrating the problem is sketched in Fig. 1. It consists of a permeable vertical bed. The flow to the right of the bed (Zone 1) and through the bed (Zone 2) is caused by the gravitational acceleration g. The depth of the liquid film h_0 in the zone 1 is so maintained that the flow is laminar. In the Zone 1, we have [5]

$$0 = \frac{g}{\nu} + \frac{d^2 u}{dy^2},$$

while, in Zone 2, by the Darcy's Law

$$\frac{Q}{K} = \frac{g}{\nu},$$

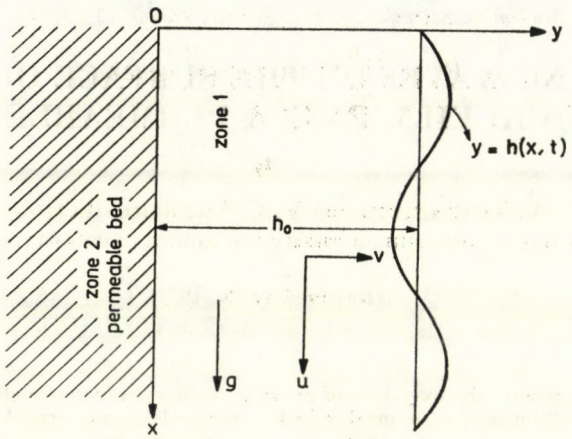

Fig. 1. Physical model

where K is the absolute permeability of the porous medium, Q the filter velocity and ν the kinematic coefficient of viscosity.

The following condition developed by BEAVERS and JOSEPH [6] is used at the permeable bed in the present analysis

$$\left.\frac{du}{dy}\right|_{y=0+} = \frac{\alpha}{\sqrt{K}}(u_B - Q),$$

where α is a dimensionless quantity depending on the material parameters which characterize the structure of permeable material within the boundary region, and u_B is the slip flow at the nominal surface at $y = 0$. At the free surface, the shear being zero, we use

$$\left.\frac{du}{dy}\right|_{y=h_0} = 0.$$

Using the dimensionless variables

$$u' = \frac{u}{u_0}, \qquad y' = \frac{y}{h_0}$$

with u_0 as a reference velocity, the solution of the foregoing equations for the liquid film is

$$u' = \frac{R}{F}\left(y' - \frac{y'^2}{2} + \beta\right), \tag{1}$$

wherein

$$R = \frac{u_0 h_0}{\nu} \quad \text{(Reynolds number)}, \tag{2}$$

$$F = \frac{u_0^2}{g h_0} \quad \text{(Froude number)}, \tag{3}$$

$$\sigma = \frac{h_0}{\sqrt{K}}, \quad \beta = \frac{\alpha + \sigma}{\alpha \sigma^2}. \tag{4}$$

Choosing u_0 as the average velocity of the liquid film, we have

$$\frac{F}{R} = \frac{1}{3} + \beta. \tag{5}$$

When $\beta \to 0$ (or $\sigma \to \infty$), we obtain the NUSSELT solution [4] for the falling liquid film past an impermeable bed.

3. Kapitza's scheme of approximation

We follow the KAPITZA's scheme of finding an approximate expression of u when the film surface assumes an arbitrary shape $y = h\,(x, t)$ which changes with time (Fig. 1). We note that u must satisfy the conditions [6],

$$y = 0: \quad \left.\frac{\partial u}{\partial y}\right|_{y=0+} = \frac{\alpha}{\sqrt{K}}\,(u_B - Q).$$

These conditions, in the absence of the permeable bed ($\sigma \to \infty$) led KAPITZA to pattern the approximate expression after the NUSSELT flow. In the same spirit, we write the following expression for u for the flow under consideration

$$u = \frac{R}{F}\,\bar{u}\,(x, t)\left(\frac{y}{h(x,t)} - \frac{y^2}{2h^2(x,t)} + \beta\right). \tag{6}$$

We substitute (6) in the equation of continuity

$$\frac{\partial u}{\partial x} + \frac{\partial v}{\partial y} = 0,$$

and integrate under the boundary condition $v\,(x, o, t) = 0$. Then

$$v = \frac{R}{F}\,\frac{\partial u}{\partial x}\left(\frac{y^3}{6h^2} - \frac{y^2}{2h} - \beta y\right) + \frac{R}{F}\,\bar{u}\,\frac{\partial h}{\partial x}\left(-\frac{y^3}{3h^3} + \frac{y^2}{2h^2}\right). \tag{7}$$

KAPITZA [2] also assumed $\partial p/\partial y = 0$, i.e. $p = p(x, h(x,t), t)$. But

$$p = p_{\text{ext}} - \varkappa \frac{\partial^2 h}{\partial x^2} \quad \text{on} \quad y = h(x,t),$$

where $\varkappa$ is the coefficient of surface tension. The radius of the curvature of the film is approximated by $\partial^2 h/\partial x^2$ since the surface slope is expected to be so small that its cube can be neglected. Therefore

$$\frac{\partial p}{\partial x} = -\varkappa \frac{\partial^3 h}{\partial x^3} . \tag{8}$$

Substituting (6–8) in the x–momentum equation

$$\frac{\partial u}{\partial t} + u\frac{\partial u}{\partial x} + v\frac{\partial u}{\partial y} = -\frac{1}{\varrho}\frac{\partial p}{\partial x} + g + \nu\left(\frac{\partial^2 u}{\partial x^2} + \frac{\partial^2 u}{dy^2}\right),$$

and integrating the result with respect to y from 0 to $h(x,t)$, we get

$$\begin{aligned} m_1\frac{\partial \bar{u}}{\partial t} + m_2\frac{\bar{u}}{h}\frac{\partial h}{\partial t} + m_3\bar{u}\frac{\partial \bar{u}}{\partial x} + m_4\frac{\bar{u}^2}{h}\frac{\partial h}{\partial x} = g\frac{F}{R} + \\ + \frac{\varkappa}{\varrho}\frac{F}{R}\frac{\partial^3 h}{\partial x^3} + \nu\left(m_1\frac{\partial^2 \bar{u}}{\partial x^2} + m_2\frac{\bar{u}}{h}\frac{\partial^2 h}{\partial x^2} - \right. \\ \left. - m_5\frac{\bar{u}}{h^2} - m_6\frac{1}{h}\frac{\partial \bar{u}}{\partial x}\frac{\partial h}{\partial x}\right), \end{aligned} \tag{9}$$

where

$$\begin{aligned} m_1 = \frac{F}{R} = \frac{1}{3} + \beta,\ m_2 = -\frac{1}{6},\ m_3 = \frac{R}{F}\left(\frac{1}{10} + \frac{\beta}{2} + \beta^2\right) \\ m_4 = \frac{R}{F}\left(-\frac{1}{30} - \frac{1}{6}\beta\right),\ m_5 = 1 \text{ and } m_6 = \frac{5}{12} . \end{aligned} \tag{10}$$

The principle here is to determine $\bar{u}$ so that (6) becomes the best representation of u in the sense that it satisfies (9) in an averaged manner.

4. Linearized travelling wave

If a solution of (9) exists such that it represents a steady travelling wave in the x-direction, it must be function of a single variable $(x - ct)$, where c is the phase velocity of the progressive undamped wave train. To search for such a solution, we can replace $\partial/\partial t$ in (9) by $-c\partial/\partial x$ and linearise Eq. (9) on the

assumption that the wavy surface is but a small perturbation on the flat surface $y = h_0$, i.e. $h(x, t) = h_0\,(1 + \psi(x, t))$ where $|\,\psi\,| < 1$.

The mass balance equation

$$\frac{\partial h}{\partial t} = \frac{\partial}{\partial x}\int_0^h u\,dy = \frac{\partial}{\partial x}(\bar{u}h)\,,$$

gives us

$$c(h - h_0) = \bar{u}h - u_0 h_0\,,$$

where u_0 is the average velocity of the liquid film referred to in Section 2 above.

In terms of ψ

$$\bar{u} = u_0 + (c - u_0)\psi\,.$$

In a similar manner

$$\frac{\partial \bar{u}}{\partial t} = -c(c - u_0)\frac{\partial \psi}{\partial x}\,,$$

$$\frac{\partial \bar{u}}{\partial x} = (c - u_0)\frac{\partial \psi}{\partial x}\,,$$

$$\frac{\bar{u}}{h} = \frac{1}{h_0}\left(u_0 + (c - 2u_0)\,\psi\right),$$

$$\frac{\bar{u}}{h^2} = \frac{1}{h_0^2}\left(u_0 + (c - 3u_0)\,\psi\right),$$

$$\frac{\partial h}{\partial t} = -ch_0\frac{\partial \psi}{\partial x}\,,$$

$$\frac{\partial h}{\partial x} = h_0\frac{\partial \psi}{\partial x}\,.$$

Substituting these quantities in (9), we arrive at a linear equation, which is expressed in a non-dimensional form using

$$\xi = \frac{2\pi x}{\lambda}\,,\quad \gamma = \frac{c}{u_0}\ \text{(wave celerity)},$$
$$P = \frac{\lambda}{2\pi}\left(\frac{\varrho g}{\varkappa}\right)^{1/2},\quad N = \frac{2\pi h_0}{\lambda}\,, \tag{11}$$

where λ is the wave length. Thus we get

$$\frac{n_1 N}{P^2}\,\frac{\partial^3 \psi}{\partial \xi^3} + \frac{n_2 F}{R}\,N^2\frac{\partial^2 \psi}{\partial \xi^2} + n_3 FN\frac{\partial \psi}{\partial \xi} -$$
$$- \frac{F}{R}\,(n_4\gamma - n_5)\psi = 0\,, \tag{12}$$

where

$$n_1 = \frac{F}{R}, \quad n_2 = m_1\gamma + (m_2 - m_1),$$

$$n_3 = m_1\gamma^2 + (-m_3 - m_1 + m_2)\gamma + (m_3 - m_4), \tag{13}$$

$$n_4 = 1, \; n_5 = 3.$$

Eq. (12), being homogeneous, will admit a sinusoidal solution only if

$$P^2 = \frac{n_1}{n_3 F}, \tag{14}$$

$$N^2 = -\frac{n_4\gamma - n_5}{n_2}. \tag{15}$$

We note that $n_1 > 0$ and that n_3 is a quadratic function of γ with a positive leading coefficient. Therefore P^2 in (13) is real if

$$\gamma > \gamma_2 \quad \text{or} \quad \gamma < \gamma_1, \tag{16}$$

where $\gamma_1 < \gamma_2$ are the roots of $n_3 = 0$. On the other hand N in (14) is real only if

$$\frac{m_2 - m_1}{m_1} < \gamma < \frac{n_5}{n_4}. \tag{17}$$

Thus an undamped, steadily travelling wave in the form of a sinusoidal function is compatible with the physical situation if positive values of τ lie within the common range of (16) and (17). No solution in the particular form under consideration exists if the two regions do not overlap.

If a value of γ does lie in the range that make both P and N real, the wave length of the corresponding wavy flow is then

$$\lambda = 2\pi h_0 \left(\frac{n_2}{n_5 - n_4\gamma}\right)^{1/2}.$$

5. Conclusions

The common range of (16 and 17) is dependent on the value of β. The result is plotted in Fig. 2. For $\beta = 0$, we have the allowed range

$$1.689 < \gamma < 3,$$

which checks with the analysis of KAPITZA [3] for the liquid film past an impermeable bed.

As β increases, the allowed range widens and reaches the maximum range

$$1 < \gamma < 3$$

corresponding to a perfect permeable bed for which $\sigma = 0$. For each β, there is always an admissible range for the wave celerity.

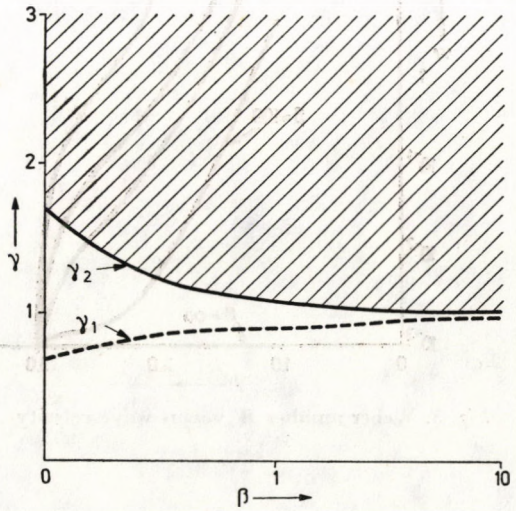

Fig. 2. Admissible range of wave celerity

The Weber number

$$W = \frac{u_0^2 h_0}{\varkappa/\varrho} = P^2 N^2 F = -\frac{n_1(n_4\gamma - n_5)}{n_2 n_3}$$

is calculated for each admissible value of γ and is plotted in Fig. 3 for various values of β. This shows that the Weber number W decreases as β increases, for the allowed range of the dimensionless celerity γ. Fig. 4 shows the dimensionless wave number N versus γ for various values of β. It is also found to decrease as β increases. Further the celerity is more sensitive to the Weber number and the dimensionless wave number as β increases. Ultimately at a perfect impermeable bed ($\sigma = 0$), both W and N vanish.

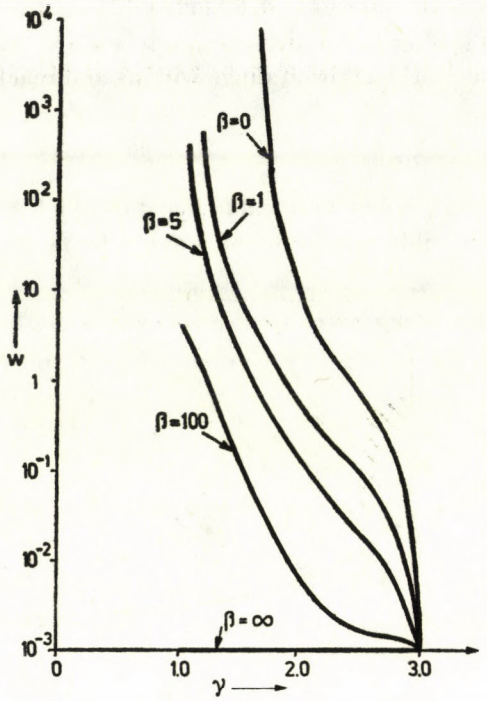

Fig. 3. Weber number W versus wave celerity

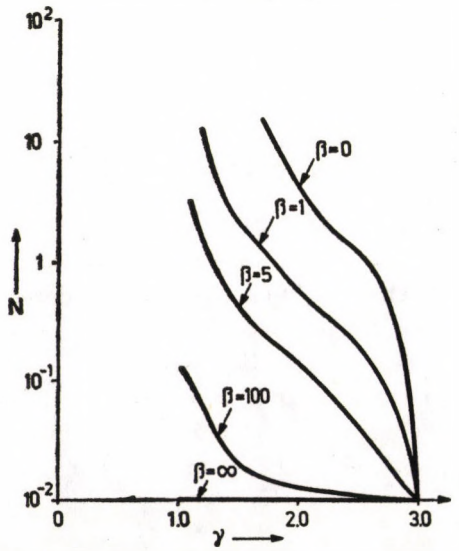

Fig. 4. Dimensionless wave length N versus wave celerity

REFERENCES

1. V. G. LEVICH, Physicochemical Hydrodynamics, Prentice Hall, Inc., New Jersey, 1962.
2. P. L. KAPITZA, Collected papers of P. L. Kapitza, II edited by D. ter Haar, Pergamon Press, Inc., New York, 1965.
3. C. MASSOT, F. IRANI and E. N. LIGHTFOOT, Am. Inst. Chem. Engr. J., **12**, 445, 1966.
4. W. NUSSELT, Z. Ver. Deut. Ingr., **60**, 541, 1916.
5. M. N. CHANNABASAPPA and G. RANGANNA, Proc. Ind. Soc. Theor. and Appl. Mech., **20**, 123, 1975.
6. G. S. BEAVERS and D. D. JOSEPH, J. Flu. Mech., **30**, 197, 1967.

Acta Physica Academiae Scientiarum Hungaricae, Tomus 43 (3—4), pp. 237—241 (1977)

ON THE INVERSE OF THE POMERANCHUK THEOREM

By

E. NAGY

CENTRAL RESEARCH INSTITUTE FOR PHYSICS, HIGH ENERGY PHYSICS DEPARTMENT, BUDAPEST

(Received 18. X. 1977)

In this note we prove the inverse of the Pomeranchuk theorem for logarithmically rising total cross sections.

Recent measurements on total cross sections and forward scattering amplitudes [1] reveal the following basic features in the 10 – 2000 GeV energy region:

1) The total cross sections rise with increasing energy and this rise is compatible with a logarithmic law;

2) the difference of the particle and anti-particle total cross sections decreases with increasing energy and this decrease is compatible with an inverse power law;

3) The forward scattering amplitudes are not dominantly real.

In 1958 POMERANCHUK proved [2] that for bounded total cross sections property 3) involves property 2). More precisely, if in the asymptotic region 3) is fulfilled and total cross sections tend to constant limits, then these limits are the same for a particle and its antiparticle hitting the same target. However, as mentioned, recent measurements do not indicate the boundedness of total cross sections at infinite energies, and for arbitrarily rising cross sections one cannot prove the zero asymptotic limit of the difference of the particle and antiparticle total cross sections. There exists a proof only on the ratio of the particle—antiparticle cross sections [3].

Therefore we consider the problem here from the inverse point of view. In this note we prove using dispersion relations that from the assumption that 1) and 2) hold asymptotically 3) follows also in the asymptotic energy region. More precisely, we repeat POMERANCHUK's line of thought in order to show that if

i) the total cross sections rise with some power β of logarithm ($\beta \geq 1$) and if

ii) the difference of the particle and antiparticle total cross sections remains finite, then

the real to imaginary ratios of both the particle and antiparticle forward scattering amplitudes are bounded.

These two amplitudes will be denoted by f and $\bar{f}$, whereas their sum and difference will be labelled by f_+ and f_-:

$$f_+ = \bar{f} + f; \quad f_- = \bar{f} - f. \tag{1}$$

The real and imaginary parts of any amplitudes will be denoted by D and A. We write the twice subtracted dispersion relations in the form [4]:

$$\left.\begin{matrix} D(E) \\ \bar{D}(E) \end{matrix}\right\} = \frac{1}{2}[\bar{D}(m) - D(m)] \mp \frac{E}{2m}[\bar{D}(m) - D(m)] +$$
$$+ \sum_i \frac{p^2}{E_i^2 - E^2}(E_i \mp E)\frac{2X_i}{E_i^2 - m^2} +$$
$$+ \frac{p^2}{\pi}\int_{E_0}^{m} \frac{\bar{A}\cdot(E' \mp E)\mathrm{d}E'}{p'^2(E'^2 - E^2)} + \tag{2}$$
$$+ \frac{p^2}{4\pi^2} P\int_m^{\infty} \frac{E'\cdot(\bar{\sigma} + \sigma) \mp E\cdot(\bar{\sigma} - \sigma)\,\mathrm{d}E'}{p'(E'^2 - E^2)}.$$

Here p, E and m are the laboratory momentum, energy and the rest mass of the incoming particle, respectively. $\bar{D}(m)$ and $D(m)$ are the two subtraction constants, the subtraction being made at zero laboratory momentum. In the integral over the physical region we have substituted A by the total cross section using the optical theorem:

$$A = \frac{p}{4\pi}\sigma_{\mathrm{t}}. \tag{3}$$

The threshold of the unphysical region, E_0, is the laboratory energy of the incoming particle corresponding to the CMS energy which is equal to the smallest mass of the physical continuum having the quantum numbers of the initial state.* The polynom represents the pole contributions, where E_i is the beam laboratory energy corresponding to the CMS energy equal to the rest mass m_i of the pole. X_i is proportional to the coupling constant square of the colliding particles to the pole [4]:

$$X_i = g_i^2 \frac{(m_i - m_t)^2 - m^2}{4m_i^2}. \tag{4}$$

* The laboratory energy corresponding to $\sqrt{s}$ energy in the CMS is:

$$E_{\sqrt{s}} = \frac{s - m_i^2 - m^2}{2m_t},$$

where m_t is the target mass.

Since we assume ii), it is enough to prove that

$$\lim_{E\to\infty}\left|\frac{D}{A_+}\right| < \infty \text{ and } \lim_{E\to\infty}\left|\frac{\bar{D}}{A_+}\right| < \infty \tag{5a}$$

or

$$\lim_{E\to\infty}\left|\frac{D_+}{A_+}\right| < \infty \text{ and } \lim_{E\to\infty}\left|\frac{D_-}{A_+}\right| < \infty . \tag{5b}$$

Hypothesis i) is equivalent to

$$|A_+| \sim cE(\ln E)^\beta \tag{6}$$

asymptotically, therefore in Eq. (2) all terms but the last one (which we denote by D^h) automatically fulfil the inequalities (5). Instead of (5) it is sufficient to prove the following inequalities:

$$\lim_{E\to\infty}\left|\frac{D_+^h}{A_+}\right| < \infty \tag{5c}$$

and

$$\lim_{E\to\infty}\left|\frac{D_-^h}{A_+}\right| < \infty . \tag{5d}$$

In Appendix 1 we calculate the integral D_+^h for $\beta = 0, 1, 2$ and show explicitly that the limit of (5c) is equal to zero. For arbitrary values of $\beta \geq 1$ we recall (see e.g. [5]) that analyticity and crossing require the following form the of amplitude in case of logarithmically rising cross sections:

$$\lim_{E\to\infty} f_+ = i \cdot c \cdot E\left(\ln E - \frac{i\pi}{2}\right)^\beta ,$$

from which we get [5] the same result as for integer values of β.

Inequality (5c) can also be proved for a very general case. FISCHER et al have given namely [6] an upper bound for

$$\varrho_+ \equiv D_+/A_+$$

if σ_+ rises unboundedly:

$$\int^\infty \left(\varrho_+(E) - \frac{\pi}{\ln E}\right)\frac{\mathrm{d}E}{E} < \infty .$$

This means that inequality (5c) is zero if ϱ_+ is positive. For this latter we recall the theorem of KHURI and KINOSHITA [7] who showed that for an unboundedly rising cross section D_+ cannot stay negative at all energies.

Turning now finally to inequality (5d) we reproduce in Appendix 2 the result of POMERANCHUK, which states that the crossing odd term, D_- approaches to

$$\lim_{E\to\infty} D_-^h = -\frac{\Delta\sigma}{2\pi^2} E \ln \frac{E}{E_1} .$$

if the difference, $\Delta\sigma$, of the antiparticle and particle cross sections remains constant beyond a certain value E_1. Combining the limits (6) and (5) we arrive to prove (5d) and hence the whole statement.

We thus conclude that extrapolating the observed properties 1)–3) up to infinite energies they are compatible with dispersion relations in the sense that 3) follows from 1) and 2), although the inverse statement may not be proved.

I am indebted to Dr. JAN FISCHER for valuable comments and suggestions.

Appendix 1

The crossing even part of the high energy integral

1. σ and $\bar{\sigma}$ are constant beyond E_1

$$D_+^h \sim E^2 \int_{E_1}^{\infty} \frac{x \cdot (\sigma + \bar{\sigma})}{x(x^2 - E^2)} \, dx \sim E \ln \left| \frac{E_1 - E}{E_1 + E} \right| \sim E_1 .$$

2. σ and $\bar{\sigma}$ are logarithmically rising: $\sigma \sim (\ln E)^\beta$; $\beta = 2$ (for $\beta = 1$ the procedure is essentially the same [8]).

$$D_+^h \sim E^2 \int_{E_1}^{\infty} \frac{\ln^2 x \, dx}{x^2 - E^2} \sim E \int_{E_1/E}^{\infty} \frac{(\ln E + \ln x)^2}{x^2 - 1} \, dx \sim$$

$$\sim E \ln^2 E \int_{E_1/E}^{\infty} \frac{dx}{x^2 - 1} + 2E \ln E \int_{E_1/E}^{\infty} \frac{\ln x \, dx}{x^2 - 1} + \int_{E_1/E}^{\infty} \frac{\ln^2 x \, dx}{x^2 - 1} .$$

If $E \to \infty$

$$D_+^h \sim c_1 \ln^2 E + c_2 E \ln E \int_{-\infty}^{\infty} \frac{u \, du}{shu} + c_3 E \int_{-\infty}^{\infty} \frac{u^2}{shu} \, du .$$

The last term is zero, the second integral is finite and non-zero, therefore:

$$D_+^h \sim c_1 \ln^2 E + c_2 E \cdot \ln E ,$$

where c_1 and c_2 are some constants.

Appendix 2

The crossing odd part of the high energy integral

$\Delta\sigma \equiv \sigma - \bar{\sigma}$ is constant beyond E_1

$$D_-^h \sim \frac{E^3 \Delta\sigma}{4\pi^2} \int_{E_1}^{\infty} \frac{\mathrm{d}x}{x(x^2 - E^2)} = \Delta\sigma \frac{E}{4\pi} \int_0^{(E/E_1)^2} \frac{du}{1-u} \sim$$

$$\sim -\frac{\Delta\sigma}{2\pi^2} E \ln \frac{E}{E_1} .$$

REFERENCES

1. See e.g. A. N. DIDDENS, Rapporteur talk at the XVIIth International Conference on High Energy Physics, London, 1974, Proceedings, p. 1—41.
2. I. JA. POMERANCHUK, ZhETF, **34,** 725, 1958.
3. G. GRUNBERG and T. N. TRUONG, Phys. Rev. Letters, **31**$_1$ 63, 1973.
4. See e.g. N. M. QUEEN, Fortschr. d. Physik, **17,** 467, 1969.
5. A. MARTIN, Proc. 8eme Renc. de Moriond, 1973, p. 91.
6. J. FISCHER, P. KOLÁR and I. VRKOČ, Phys. Rev., **D13,** 133, 1976.
7. N. KHURI and T. KINOSHITA, Phys. Rev., **B137,** 720, 1965 and Phys. Rev., **B140,** 706, 1965.
8. A more elegant method of computing this integral is given by H. ČAPRASSE and A. BURNEL, Phys. Rev., **D9,** 1980, 1974.

Acta Physica Academiae Scientiarum Hungaricae, Tomus 43 (3—4), pp. 243—249 (1977)

EFFECTS OF MASS TRANSFER ON FREE CONVECTIVE FLOW OF AN ELECTRICALLY CONDUCTING, VISCOUS FLUID PAST AN INFINITE POROUS PLATE WITH CONSTANT SUCTION AND TRANSVERSELY APPLIED MAGNETIC FIELD

By

D. D. HALDAVNEKAR

DEPARTMENT OF CHEMICAL TECHNOLOGY, UNIVERSITY OF BOMBAY
MATUNGA, BOMBAY 400019, INDIA

and

V. M. SOUNDALGEKAR

DEPARTMENT OF MATHEMATICS, INDIAN INSTITUTE OF TECHNOLOGY, POWAI,
BOMBAY 400076, INDIA

(Received in revised form 18. X. 1977)

An analysis of the mass transfer effects on the free convective flow of an incompressible, electrically conducting, viscous fluid past an infinite porous plate with constant suction and transverse magnetic field, has been carried out. Approximate solutions to coupled non-linear equations governing the flow are derived. The velocity and the temperature fields are shown graphically. The effects of G_T (Grashof number), G_c (modified Grashof number), S_c (Schmidt number), E(Eckert number), P(Prandtl number) and M(the Hartmann number) on the flow field are described during the course of discussion.

1. Introduction

There are a number of research papers published on free convective flow past infinite and semi-infinite plates and other bodies. These flows are caused by the temperature differences. In these studies, it was assumed that the fluid is free from all soluble and insoluble impurities. This is not always true. In many cases, the flow is modified by density differences caused by temperature or chemical composition differences. Such a physical situation constituting flow due to temperature and concentration differences has not received much attention. In this situation, there is transfer of mass due to temperature differences and transfer of heat due to concentration differences. In the literature, these are known as thermal diffusion and diffusion thermo effects.

Such a combined flow has been considered by a few researchers like SPARROW, MINKOWYCZ and ECKERT [2], GEBHART and PERA [3] and a few others referred to in [1, 3]. Their study was aimed at flow past semi-infinite plates without suction. In [1, 2], the thermal diffusion and diffusion thermo effects

were considered whereas in [3] only thermal diffusion effects were considered and diffusion thermo effects were assumed to be negligible. This assumption is true when the concentration level is very low. Assuming very low concentration level, the effects of free convection currents and the mass transfer on the flow past an infinite porous plate were studied by SOUNDALGEKAR [4].

All these papers deal with non-conducting fluids. But the effects of mass transfer on the free convective flow of an electrically conducting fluid under the action of the transverse magnetic field have not been studied at all. Hence it is the object of the present paper to study the effects of the mass-transfer on the free convective flow of a viscous, electrically conducting fluid past an infinite porous plate with constant suction and transverse magnetic field.

In Section 2, the problem is posed mathematically and the approximate solutions to a coupled non-linear system of equations governing the flow are derived. The velocity, the temperature, the skin-friction and the Nusselt number have been shown graphically. In Section 3, the conclusions are set out.

2. Mathematical analysis

Here the X-axis is chosen along a vertical porous plate in the upward direction and the y' axis is chosen perpendicular to the plate. u', v' are the components of velocity along x' and y' directions. The equations governing the free convective flow of non conducting fluid under proper assumptions are derived in GEBHART [5]. Following his treatment, we can show that the free convective flow on an electrically conducting, incompressible, viscous fluid on neglecting induced magnetic field, is governed by the following equations (Rossow [6])

$$v' \frac{\partial u'}{\partial y'} = \nu \frac{\partial^2 u'}{\partial y'^2} + g\beta(T' - T'_\infty) + g\beta^*(C' - C'_\infty) - \frac{\sigma B_0^2}{\varrho} u', \tag{1}$$

$$\varrho C_p v' \frac{\partial T'}{\partial y'} = K_1 \frac{\partial^2 T'}{\partial y'^2} + \sigma B_0^2 u'^2, \tag{2}$$

$$\frac{\partial v'}{\partial y'} = 0, \tag{3}$$

$$v' \frac{\partial c'}{\partial y'} = D \frac{\partial^2 C'}{\partial y'^2}. \tag{4}$$

Here all physical quantities have their usual meaning except β^* which is known as volume coefficient of expansion with concentration. D is the molecular diffusivity and C' is the species concentration. In Eq. (2), the last term re-

presents the Joule dissipative heat. The viscous dissipative heat is assumed to be negligible as compared to Joule dissipative heat.

Integrating (3) we have

$$v' = -v_0, \tag{5}$$

where v_0 is the constant suction velocity and the negative sign in (5) indicates that the suction is towards the plate.

On introducing the following non-dimensional quantities

$$u = \frac{u'}{v_0}, \; y = \frac{y' v_0}{c}, \; \theta = \frac{T' - T'_\infty}{T'_w - T'_\infty},$$

$$C = \frac{C' - C'_\infty}{C'_w - C'_\infty}, \; G_T = \frac{vg\,\beta(T'_w - T'_\infty)}{v_0^3} \text{ (the Grashof number)},$$

$$G_c = \frac{vg\beta^*(C'_w - C'_\infty)}{v_0^3} \text{ (the modified Grashof number)},$$

$$P = \frac{\mu C_p}{K_1} \text{ (the Prandtl number)}$$

$$E = \frac{v_0^2}{C_p(T'_w - T'_\infty)} \text{ (the Eckert number)} \tag{5a}$$

$$M^2 = \frac{\sigma B_4^2 v^2}{\mu v_0^2} \text{ (the Hartmann number)},$$

$$S_c = \frac{c}{D} \text{ (Schmidt number)}$$

in Eqs. (1), (2) and (4) we have

$$\frac{d^2 u}{dy^2} + \frac{du}{dy} - M^2 u = -(G_T \theta + G_c C), \tag{6}$$

$$\frac{d^2 \theta}{dy^2} + P\frac{d\theta}{dy} = -M^2 PEu^2, \tag{7}$$

$$\frac{d^2 C}{dy^2} + S_c \frac{dC}{dy} = 0. \tag{8}$$

The boundary conditions are [3],

$$\left.\begin{aligned} u = 0,\ \theta = 1,\ C = 1 \text{ at } y = 0 \\ u = 0,\ \theta = 0,\ C = 0 \text{ at } y \to \infty \end{aligned}\right\}. \tag{9}$$

Eqs. (6)–(8) are the coupled non-linear equations to be solved under the boundary conditions (9). As exact solutions are not possible, we now try to obtain approximate solutions. To solve these equations, we expand u, θ, C in

powers of E, the Eckert number, This is possible physically as E for the flow of an incompressible fluid is always less than unity. It can be interpreted physically as the flow due to the Joule dissipation heat is superimposed on the main flow. Hence we assume,

$$u = u_0 + Eu_1,\ \theta = \theta_0 + E\theta_1,\ C = C_0 + EC_1. \tag{10}$$

The terms of order E^2, E^3 . . . are neglected because as $E \ll 1$, the contribution from the coefficients of E^2, E^3 . . . will be negligibly small. Substituting (10) in (6)–(9), equating the coefficients of different powers of E, neglecting those of E^2 . . ., we get a system of coupled linear equations. The procedure being straightforward, it is not mentioned here to save space. These coupled linear equations are solved and their values are substituted in (10). The solutions are the following:

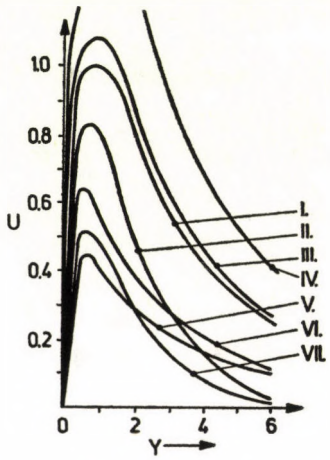

Fig. 1. Velocity profiles $P = 0.025$

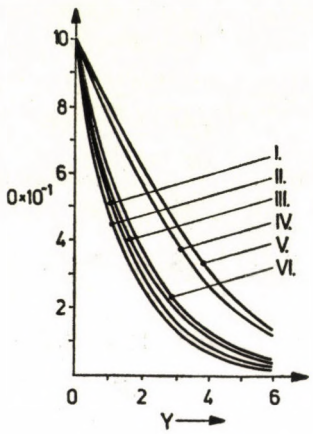

Fig. 2. Temperature profiles, $P = 0.025$

$$u = b_1 e^{-m_3 y} - b_2 e^{-Py} - b_3 e^{-S_c y} + E\left[A_8 e^{-m_3 y} - \right.$$
$$- G_T\left\{A_1 e^{-Py} - A_2 e^{-2m_3 y} - A_3 e^{-2Py} - A_4 e^{-2S_c y} + \right. \tag{11}$$
$$\left.\left. + A_5 e^{-(m_3+P)y} - A_6 e^{-(S_c+P)y} + A_7 e^{-(m_3+S_c)y}\right\}\right]$$

$$\theta = e^{-Py} + E\left[b_5 e^{-Py} - C_2 e^{-m_3 y} - C_3^{-2py} - C_4 e^{-2S_c y} + \right.$$
$$\left. + C_5 e^{-(m_3+P)y} - C_6 e^{-(S_c+S_c)y} + C_7 e^{-(m_3+S_c)y}\right]. \tag{12}$$

u and θ are shown in Fig. 1–2, respectively.

Here

$$m_2 = \frac{1 + \sqrt{1 + 4M^2}}{2},$$

$$b_1 = b_2 + b_3, \qquad b_2 = \frac{G_T}{P^2 - P - M^2}, \qquad b_3 = \frac{G_c}{S_c^2 - S_c - M^2},$$

$$C_2 = \frac{M^2 P b_1^2}{4m_2^2 - 2m_2 P}, \qquad C_3 = \frac{M^2 b_2^2}{2P},$$

$$C_4 = \frac{M^2 P b_3^2}{4Sc^2 - 2PS_c}, \qquad C_5 = \frac{2b_1 b_2 M^2 P}{m_2(m_2 + p)},$$

$$C_6 = \frac{2b_1 b_3 M^2 P}{(m_2 + S_c)(m_2 + S_c - P)}, \qquad C_7 = \frac{2b_2 b_3 M^2 P}{S_c(S_c + P)},$$

$$b_5 = C_2 + C_3 + C_4 - C_5 - C_6 + C_7,$$

$$A_1 = \frac{b_5}{P^2 - P - M^2}, \qquad A_2 = \frac{C_2}{4m_2^2 - 2m_2 - M^2},$$

$$A_3 = \frac{C_3}{4P^2 - 2P - M^2}, \qquad A_4 = \frac{C_4}{4S_c^2 - 2S_c - M_2},$$

$$A_5 = \frac{C_5}{m_2^2 + 2m_2 P + P^2 - m_2 - P - M^2},$$

$$A_6 = \frac{C_7}{S_c^2 + 2PS_c + P^2 - S_c - P - M^2},$$

$$A_7 = \frac{C_6}{m_z^2 + 2m_2 S_c + S_c^2 - m_2 - S_c - M^2,},$$

$$A = G_T [A_1 - A_2 - A_3 - A_4 + A_5 - A_6 + A_7].$$

Knowing the velocity and the temperature field, we can now calculate the skin-friction and the rate of heat transfer expressed in terms of the Nusselt number.

The skin-friction is given by

$$\tau = \mu \left.\frac{\partial u'}{\partial y'}\right|_{y'=0}, \tag{13}$$

which in view of (5a) reduces to

$$\tau = \left.\frac{du}{dy}\right|_{y'=0}. \tag{14}$$

Substituting for u from (11), in (14) we can obtain the expression for τ shown in Fig. 3. The rate of heat transfer, in terms of the Nusselt number is given by

$$Nu = -\frac{qv}{K_1(T'_w - T'_\infty)v_0} = -\left.\frac{d\theta}{dy}\right|_{y=0}. \tag{15}$$

Substituting for θ from (12) in (15) we can obtain the expression for Nu shown in Fig. 4.

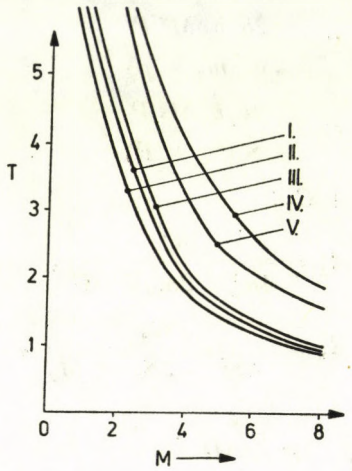

Fig. 3. Skin friction $P = 0.025$

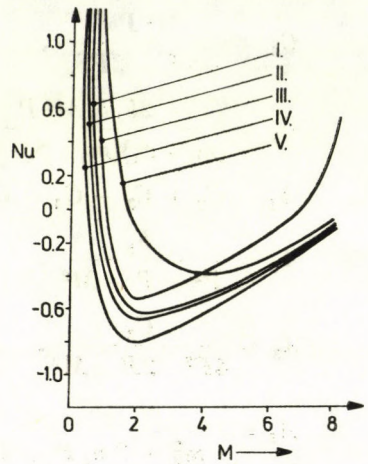

Fig. 4. Nusselt number $P = 0.025$

3. Discussion

In order to get the physical insight into the problem, numerical calculations are carried out for different values of G_T, G_c, M, E, P and S_c. In Fig. 1 the velocity profiles are shown for constant G_c and S_c. We observe that due to more addition of Joule dissipative heat, the velocity increases. The velocity increases with increasing G_T whereas an increase in the magnetic field leads to a decrease in the velocity. An increase in G_c leads to an increase in the velocity whereas an increase in S_c leads to a decrease in the velocity. Fig. 2 shows the temperature profiles. We observe from this Figure that an increase in the Schmidt number leads to a decrease in the temperature. But due to more addition of the Joule dissipative heat, the temperature increases. The temperature increases due to increasing G_T or G_c or M. Fig. 3 shows the skin-friction plotted against M. With increasing M, the skin-friction decreases. It decreases with increasing the Schmidt number. However, due to more addition of the Joule dissipative heat or due to an increase in G_T or G_c, the skin-friction increas-

es. In Fig. 4, the Nusselt number is plotted against M. For small values of M, the Nusselt number is large. It decreases due to increasing the Schmidt number or G_T and increases owing to an increase in G_c or E.

Acknowledgement

Dr. D. D. HALDAVNEKAR is grateful to the University Grants Commission, New Delhi, for the award of a research grant to carry out this research paper.

REFERENCES

1. E. M. SPARROW, Recent Studies Relating to Mass Transfer Cooling, Proceedings of 1964 Heat Transfer and Fluid Mechanics Institute, pp 1—18.
2. E. M. SPARROW, W. J. MINKOWYCZ and E. R. G. ECKERT, Trans. ASME, Journal of Heat Transfer, **86**, Sec. C. 508, 1964.
3. B. GEBHART and L. PERA, International Journal of Heat Mass Transfer, **14**, 2025, 1971.
4. V. M. SOUNDALGEKAR, Effects of Mass Transfer on Free Convective Flow of a Dissipative, Incompressible Fluid past an Infinite, Porous Plate with Suction, vol. LXXXIV A, No. 5, 194—203.
5. B. GEBHART, Heat Transfer, 2nd Ed., McGraw Hill, New York, 1971, pp 197.
6. V. J. RUSSOW, On Flow of Electrically Conducting Fluids over a Flat Plate in the Presence of a Transverse Magnetic Field, NACA TN 3971, 1957.

Acta Physica Academiae Scientiarum Hungaricae, Tomus 43 (3—4), pp. 251—258 (1977)

RAYLEIGH—TAYLOR INSTABILITY OF TWO SUPERPOSED CONDUCTING FLUIDS IN THE PRESENCE OF SUSPENDED PARTICLES

By

R. C. SHARMA and K. C. SHARMA

DEPARTMENT OF MATHEMATICS, HIMACHAL PRADESH UNIVERSITY, SIMLA-171005, INDIA

(Received 19. X. 1977)

Rayleigh—Taylor instability of two superposed conducting fluids in the presence of suspended particles is studied. The prevalent magnetic field is assumed to be uniform and horizontal. The fluids are assumed to be highly viscous and of equal kinematic viscosities, for mathematical simplicity. The system is found to be stable for stable configuration and unstable for unstable configuration in the presence of suspended particles. This is in contrast to the thermal instability problem where the suspended particles have a destabilizing effect.

1. Introduction

The instability derived from the character of the equilibrium of an incompressible heavy fluid of variable density (i.e. of a heterogeneous fluid) is termed the Rayleigh—Taylor instability. Mention may be made of two important special cases: (a) two fluids of different densities superposed one over the other; (b) a fluid with a continuous density stratification. KRUSKAL and SCHWARZSCHILD [1] have considered the stability of an inviscid plasma of infinite conductivity supported against gravity by a horizontal magnetic field. HIDE [2] studied the case of a viscous conducting fluid with a transverse magnetic field and found that magnetic field considerably stabilizes the configuration and it is possible to have oscillatory motion in the presence of magnetic field even if the configuration is thoroughly unstable. CHANDRASEKHAR [3] has given a detailed account of the Rayleigh—Taylor instability under varying assumptions of hydrodynamics and hydromagnetics.

The effect of suspended particles on the stability of superposed fluids might be of industrial and chemical engineering importance. Further motivation for this study is the fact that knowledge concerning fluid-particle mixtures is not commensurate with their industrial and scientific importance. SCANLON and SEGEL [4] considered the effect of suspended particles on the onset of Bénard convection and found that the critical Rayleigh number was reduced solely because the heat capacity of the pure gas was supplemented by that of the particles. SHARMA et al [5] studied the effect of suspended particles on the onset of Bénard convection in hydromagnetics. The effect of suspended particles was found to destabilize the layer whereas the effect of magnetic

field was stabilizing. The effect of a uniform rotation was also studied and was found to have a stabilizing effect in the presence of suspended particles on the Bénard convection.

The effect of suspended particles on the stability of two superposed fluids in hydromagnetics might be of industrial and scientific importance. This aspect forms the subject matter of the present paper.

We consider a static state in which an incompressible fluid-particle layer of variable density is arranged in horizontal strata and the pressure p and the density ϱ are functions of the vertical coordinate z only. The character of the equilibrium of this initial static state is determined by supposing that the system is slightly disturbed and then following its further evolution. The fluid is under the action of gravity $\mathbf{g}(0, 0, -g)$ and the horizontal magnetic field $\mathbf{H}(H, 0, 0)$. The particles are assumed to be nonconducting.

2. Basic equations

Let ϱ, μ, p and $\mathbf{u}(u, v, \omega)$ denote respectively the density, the viscosity, the pressure and the velocity of the pure gas; $\mathbf{V}(\bar{x}, t)$ and $N(\bar{x}, t)$ denote the velocity and number density of the particles, respectively. $\mathbf{K} = 6\pi\mu\eta$, where η is the particle radius, is a constant and $\bar{x} = (x, y, z)$. Then the equations of motion and continuity for the gas and Maxwell's equations are

$$\varrho\left[\frac{\partial \mathbf{u}}{\partial t} + (\mathbf{u}\cdot\nabla)\mathbf{u}\right] = -\nabla p + \varrho\mathbf{g} + \mu\nabla^2\mathbf{u} + \mathbf{K}N(\mathbf{V}-\mathbf{u}) + \frac{1}{4\pi}(\nabla\times\mathbf{h})\times\mathbf{H} + \left(\frac{\partial\omega}{\partial\bar{x}} + \frac{\partial\mathbf{u}}{\partial z}\right)\frac{d\mu}{dz}, \tag{1}$$

$$\nabla\cdot\mathbf{u} = 0, \tag{2}$$

$$\frac{\partial\mathbf{H}}{\partial t} = \nabla\times(\mathbf{u}\times\mathbf{H}), \tag{3}$$

$$\nabla\cdot\mathbf{H} = 0. \tag{4}$$

Since the density of a particle moving with the fluid remains unchanged, we have

$$\frac{\partial\varrho}{\partial t} + (\mathbf{u}\cdot\nabla)\varrho = 0. \tag{5}$$

The presence of particles adds an extra force term, proportional to the velocity difference between particles and fluid and appears in equations of motion (1). Since the force exerted by the fluid on the particles is equal and

opposite to that exerted by the particles on the fluid, there must be an extra force term, equal in magnitude but opposite in sign, in the equations of motion for the particles. The buoyancy force on the particles is neglected. Inter-particle reactions are not considered either for we assume that the distance between particles is quite large compared with their diameter.

The equations of motion and continuity for the particles, under the above approximations, are

$$mN\left[\frac{\partial \mathbf{V}}{\partial t} + (\mathbf{V}\cdot\nabla)\mathbf{V}\right] = mN\mathbf{g} + \mathbf{K}N(\mathbf{u}-\mathbf{V}), \tag{6}$$

$$\frac{\partial N}{\partial t} + \nabla\cdot(N\mathbf{V}) = 0, \tag{7}$$

where mN is the mass of particles per unit volume.

Let $\delta\varrho$, δp and $\mathbf{h}(hx, hy, hz)$ denote respectively the perturbations in density ϱ, pressure p and the magnetic field $\mathbf{H}$. Then the linearized perturbation equations of the fluid-particle layer are:

$$\varrho\frac{\partial \mathbf{u}}{\partial t} = -\nabla\,\delta p + \mathbf{g}\delta\varrho + \mu\nabla^2\mathbf{u} + \left(\frac{\partial\omega}{\partial\bar{x}} + \frac{\partial \mathbf{u}}{\partial z}\right)\frac{d\mu}{dz} + \\ + \frac{1}{4\pi}(\nabla\times\mathbf{h})\times\mathbf{H} + KN(\mathbf{V}-\mathbf{u}), \tag{8}$$

$$\nabla\cdot\mathbf{u} = 0, \tag{9}$$

$$\frac{\partial \mathbf{h}}{\partial t} = \nabla\times(\mathbf{u}\times\mathbf{H}), \tag{10}$$

$$\nabla\cdot\mathbf{h} = 0, \tag{11}$$

$$\left(\frac{m}{K}\frac{\partial}{\partial t} + 1\right)\mathbf{V} = \mathbf{u}. \tag{12}$$

In addition to Eqs. (8)–(12), we have the equation

$$\frac{\partial}{\partial t}\delta\varrho = -\omega\left(\frac{d\varrho}{dz}\right), \tag{13}$$

which ensures that the density of every particle remains unchanged as we follow it with its motion.

Analyzing the disturbance into normal modes, we seek solutions whose dependence on x, y and t is given by

$$\exp(ik_x x + ik_y y + nt), \tag{14}$$

where k_x, k_y are the horizontal components of the wave number, $k^2 = k_x^2 + k_2^y$ and n is the growth rate.

Using expression (14), Eqs. (8)–(13) give

$$[\varrho(\tau n + 1) + mN]\, nu = -(1 + \tau n)\, ik_x\, \delta p + \mu(1 + \tau n)(D^2 - k^2)\, u + \\ + (ik_x\omega + Du)(1 + \tau n)D\mu\,, \tag{15}$$

$$[\varrho(\tau n + 1) + mN]\, nv = -(1 + \tau n)\, ik_y\, \delta p + \mu(1 + \tau n)(D^2 - k^2)v + \\ + (ik_y\,\omega + Dv)\,(1 + \tau n)D\mu + \frac{H}{4\pi}(ik_x h_y - ik_y h_x), \tag{16}$$

$$[\varrho(\tau n + 1) + mN]\, n\omega = -(1 + \tau n)\, D\delta p + \mu\,(1 + \tau n)\,(D^2 - k^2)\,\omega + \\ + 2D\omega\,(1 + \tau n)D\mu + \frac{g}{n}(1 + \tau n)\,(D\varrho) + \frac{H}{4\pi}(ik_x h_z - Dh_x), \tag{17}$$

$$ik_x\, u + ik_y\, v + D\omega = 0\,, \tag{18}$$

$$ik_x\, h_x + ik_y\, h_y + Dh_z = 0\,, \tag{19}$$

$$n\mathbf{h} = ik_x\, H\mathbf{u}\,. \tag{20}$$

Eliminating δp between Eqs. (15)–(17) and using Eqs. (18)–(20), we obtain

$$n(\tau n + 1)\,[D(\varrho D\omega) - k^2\varrho\omega] + [D(mND\omega) - k^2(mN)\omega] - \\ - \mu(\tau n + 1)(D^2 - k^2)^2\,\omega + \frac{gk^2}{n}(D\varrho)(\tau n + 1)\,\omega + \\ - (\tau n + 1)\,[D\{(D\mu)(D^2 + k^2)\omega\} - 2k^2(D\mu)\,(D\omega)] + \\ + \frac{\mu_e H^2 k_x^2}{4\pi n}(D^2 - k^2)\omega = 0\,. \tag{21}$$

3. Two uniform fluids separated by a horizontal boundary

Consider the case of two uniform fluids of densities ϱ_1 and ϱ_2 and viscosities μ_1 and μ_2 separated by a horizontal boundary at $z = 0$. The subscripts 1 and 2 distinguish the lower and the upper fluids, respectively. In each of the two regions of constant ϱ and μ, Eq. (21) reduces to

$$(D^2 - k^2)\,(D^2 - K^2)\omega = 0\,, \tag{22}$$

where

$$K^2 = k^2 + \frac{n}{\nu} + \frac{mN}{\mu(1 + \tau n)} + \frac{\mu_e k_x^2 H^2}{4\pi k\nu\varrho n\,(1 + \tau n)}\,.$$

Since ω must vanish both when $z \to -\infty$ (in the lower fluid) and $z \to +\infty$ (in the upper fluid), the general solution of Eq. (22) can be written as

$$\omega_1 = A_1 e^{+kz} + B_1 e^{+k_1 z}, \qquad (z < 0) \tag{23}$$

$$\omega_2 = A_2 e^{-kz} + B_2 e^{-k_1 z}, \qquad (z > 0) \tag{24}$$

where A_1, B_1, A_2, B_2 are constants of integration,

$$K_1 = \sqrt{k^2 + \frac{n}{\nu_1} + \frac{mN}{\varrho_1 \nu_1 (1+\tau n)} + \frac{\mu_e k_x^2 H^2}{4\pi \nu_1 \varrho_1 n(1+\tau n)}}, \tag{25}$$

and

$$K_2 = \sqrt{k^2 + \frac{n}{\nu_2} + \frac{mN}{\varrho_2 \nu_2 (1+\tau n)} + \frac{\mu_e k_x}{4\pi \nu_2 \varrho_2 n(1+\tau n).}}. \tag{26}$$

Integrating Eq. (21) across the interface at $z = 0$, we obtain

$$\left\{\left[\varrho_2 - \frac{\mu_2}{n}(D^2 - k^2)\right] D\omega_2\right\}_{z=0} - \left\{\left[\varrho_1 - \frac{\mu_1}{n}(D^2 - k^2)\right] D\omega_1\right\}_{z=0} +$$

$$+ \frac{mN}{n(\tau n+1)}(D\omega_2 - D\omega_1)_{z=0} + \frac{\mu_e H^2 k_x^2}{4\pi n^2(\tau n+1)}(D\omega_2 - D\omega_1)_{z=0} \tag{27}$$

$$= -\frac{gk^2}{n^2}(\varrho_2 - \varrho_1)\omega_0 - \frac{2k^2}{n}(\mu_2 - \mu_1)(D\omega)_0 .$$

In addition to the condition (27), the boundary conditions to be satisfied at the interface $z = 0$ are (CHANDRASEKHAR [3], p. 432):

$$\omega, \tag{28}$$

$$D\omega \tag{29}$$

and

$$\mu(D^2 + k^2)\omega \tag{30}$$

must be continuous across an interface between two fluids.

Applying the boundary conditions (27)–(30) to the solutions given in (23) and (24), we obtain

$$A_1 + B_1 = A_2 + B_2 , \tag{31}$$

$$kA_1 + K_1 B_1 = -kA_2 - K_2 B_2 , \tag{32}$$

$$\mu_1[2k^2 A_1 + (K_1^2 + k^2)B_1] = \mu_2[2k^2 A_2 + (K_2^2 + k^2)B_2], \tag{33}$$

and

$$\left[\frac{R}{2} + C - \varrho_1 - \frac{mN}{n(\tau n+1)} - \frac{S}{n^2(\tau n+1)}\right] A_1 + \left[\frac{R}{2} + \frac{CK_1}{k}\right] B_1 +$$

$$+ \left[\frac{R}{2} - C - \varrho_2 - \frac{mN}{n(\tau n+1)} - \frac{S}{n^2(\tau n+1)}\right] A_2 + \left[\frac{R}{2} - \frac{CK_2}{k}\right] B_2 = 0, \tag{34}$$

where

$$R = \frac{gk}{n^2}(\varrho_2 - \varrho_1),\ C = \frac{k^2}{n}(\mu_2 - \mu_1) \text{ and } S = \frac{\mu_c k_x^2 H^2}{4\pi}.$$

Eqs. (31)–(34) can be written, in matrix notation, in the form of the single matrix equation

$$\begin{bmatrix} 1 & 1 & -1 & -1 \\ k & K_1 & k & K_2 \\ 2k^2\mu_1 & \mu_1(K_1^2+k^2) & -2k^2\mu_2 & -\mu_2(K_2^2+k^2) \\ \left\{\frac{R}{2}+C-\varrho_1-\right. & & \left\{\frac{R}{2}-C-\varrho_2-\right. & \\ -\frac{mN}{n(\tau n+1)}- & \left\{\frac{R}{2}+\frac{CK_1}{k}\right\} & -\frac{mN}{n(\tau n+1)}- & \left\{\frac{R}{2}-\frac{CK_2}{k}\right\} \\ \left.-\frac{S}{n^2(\tau n+1)}\right\} & & \left.-\frac{S}{n^2(\tau n+1)}\right\} & \end{bmatrix} \begin{bmatrix} A_1 \\ B_1 \\ A_2 \\ \\ B_2 \end{bmatrix} = 0. \tag{35}$$

The determinant of the linear system of equations which (35) represents must clearly vanish. The determinant can be reduced by subtracting the first column from the second, the third column from the fourth and adding the first column to the third. By this procedure, we obtain

$$\begin{bmatrix} K_1 - k & 2k & K_2 - k \\ \left(\varrho_1 n + \frac{mN}{\tau n+1} + \right. & & -\left(\varrho_2 n + \frac{mN}{\tau n+1} + \right. \\ \left. + \frac{S}{n(\tau n+1)}\right) & 2k^2(\varrho_1 v_1 - \varrho_2 v_2) & \left. + \frac{S}{n(\tau n+1)}\right) \\ \left\{\varrho_1 + \frac{mN}{n(\tau n+1)} + \right. & \left\{\frac{gk}{n^2}(\varrho_2 - \varrho_1) - \right. & \left\{\varrho_2 + \frac{mN}{n(\tau n+1)} - \right. \\ + \frac{C}{k}(K_1 - k) + & -(\varrho_1+\varrho_2) - \frac{2mN}{n(\tau n+1)} & -\frac{C}{k}(K_2 - k) + \\ \left. + \frac{S}{n^2(\tau n+1)}\right. & \left. - \frac{2S}{n^2(\tau n+1)}\right\} & \left. + \frac{S}{n^2(\tau n+1)}\right\} \end{bmatrix} = 0. \tag{36}$$

4. Discussion

Since the values of K_1 and K_2 involve square roots, the dispersion relation (36) is quite complicated. For mathematical simplicity, we make the assumptions that the kinematic viscosities of the two fluids are the same i.e.

$\nu_1 = \nu_2 = \nu$ and that the fluids are highly viscous. Under the above assumptions, we have

$$K = k\left[1 + \frac{n}{\nu k^2} + \frac{mN}{\varrho \nu k^2(\tau n+1)} + \frac{S}{k^2 \nu \varrho n(\tau n+1)}\right]^{1/2} \tag{37}$$

$$= k + \frac{n}{2\nu k} + \frac{mN}{2\varrho \nu k(\tau n+1)} + \frac{S}{2k\nu\varrho n(\tau n+1)},$$

so that

$$K_1 - k = \frac{n}{2\nu k} + \frac{mN}{2\varrho_1 \nu k(\tau n+1)} + \frac{S}{2k\nu\varrho_1 n(\tau n+1)}, \tag{38}$$

and

$$K_2 - k = \frac{n}{2\nu k} + \frac{mN}{2\varrho_2 \nu k(\tau n+1)} + \frac{S}{2k\nu\varrho_2 n(\tau n+1)}. \tag{38}$$

Substituting the values of $K_1 - k$ and $K_2 - k$ from Eqs. (38) and (39) in the determinant (36) and simplifying it, after a little algebra, we obtain

$$A_9 n^9 + A_8 n^8 + A_7 n^7 + A_6 n^6 + A_5 n^5 + A_4 n^4 + A_3 n^3 + \\ + A_2 n^2 + A_1 n + A_0 = 0, \tag{40}$$

where

$$A_9 = \varrho_1 \varrho_2 \tau^3(\varrho_1 + \varrho_2)^2,$$

$$A_8 = \varrho_1 \varrho_2 \tau^2(\varrho_1 + \varrho_2)^2 [3 + 2k^2 \nu\tau)],$$

$$A_7 = 6\nu k^2 \tau^2 \varrho_1 \varrho_2 (\varrho_1 + \varrho_2)^2 + gk\varrho_1 \varrho_2(\varrho_1 + \varrho_2)(\varrho_1 - \varrho_2)\tau^3 + \\ + 3\varrho_1 \varrho_2 \tau(\varrho_1 + \varrho_2)^2 + mN\tau^2(\varrho_1 + \varrho_2)(\varrho_1^2 + 4\varrho_1 \varrho_2 + \varrho_2^2),$$

$$A_6 = 6\nu k^2 \tau\varrho_1 \varrho_2(\varrho_1 + \varrho_2)^2 + 2\nu k^2 mN\tau^2(\varrho_1 + \varrho_2)^3 + \\ + 3gk\tau^2 \varrho_1 \varrho_2(\varrho_1 - \varrho_2)(\varrho_1 + \varrho_2) + 2mN\tau(\varrho_1 + \varrho_2) \times \\ \times (\varrho_1^2 + 4\varrho_1 \varrho_2 + \varrho_2^2) + 2\varrho_1 \varrho_2(\varrho_1 + \varrho_2)^2 - S\tau^2(\varrho_1 + \varrho_2)^3,$$

$$A_5 = 4\nu k^2 mN\tau(\varrho_1 + \varrho_2)^3 + 2\nu k^2 \varrho_1 \varrho_2(\varrho_1 + \varrho_2)^2 + \\ + 3gk\varrho_1 \varrho_2\tau(\varrho_1 + \varrho_2)(\varrho_1 - \varrho_2) + mN(\varrho_1 + \varrho_2)(\varrho_1^2 + 4\varrho_1 \varrho_2 + \varrho_2^2) + \\ + gk(\varrho_1 - \varrho_2)(\varrho_1 + \varrho_2)^2 mN\tau^2 + 3m^2N^2\tau(\varrho_1 + \varrho_2)^2 + \\ + S\tau(\varrho_1 + \varrho_2)[2(\varrho_1 + \varrho_2)^2 + 2\nu k^2 \tau(\varrho_1^2 + \varrho_2^2)], \tag{41}$$

$$A_4 = 2\nu k^2 m^2 N^2 \tau(\varrho_1 + \varrho_2)^2 + 2gkmN\tau(\varrho_1 - \varrho_2)(\varrho_1 + \varrho_2)^2 + \\ + gk\varrho_1\varrho_2(\varrho_1 - \varrho_2)(\varrho_1 + \varrho_2) + 3m^2N^2(\varrho_1 + \varrho_2)^2 + \\ + 2k^2\nu mN(\varrho_1 + \varrho_2)^3 + S(\varrho_1 + \varrho_2)^3 + S\tau(\varrho_1 + \varrho_2)[4k^2\nu(\varrho_1^2 + \varrho_2^2) + \\ + gk\tau(\varrho_1 - \varrho_2)(\varrho_1 + \varrho_2) + 4mN(\varrho_1 + \varrho_2)],$$

$$A_3 = gkmN(\varrho_1 - \varrho_2)(\varrho_1 + \varrho_2)^2 + gk(\varrho_1 - \varrho_2)(\varrho_1 + \varrho_2)m^2N^2\tau +$$
$$+ 2m^3N^3(\varrho_1 + \varrho_2) + 2\nu k^2m^2N^2(\varrho_1 + \varrho_2)^2 + S\tau(\varrho_1 + \varrho_2)\times$$
$$\times [2k^2\nu mN(\varrho_1 + \varrho_2) + S(\varrho_1 + \varrho_2) + 2gk(\varrho_1 - \varrho_2)(\varrho_1 + \varrho_2)] +$$
$$+ S(\varrho_1 + \varrho_2)[4k^2\nu\varrho_1\varrho_2 + 2k^2\nu(\varrho_1 - \varrho_2)^2],$$

$$A_2 = gkm^2N^2(\varrho_1 - \varrho_2)(\varrho_1 + \varrho_2) + gkS(\varrho_1 - \varrho_2)(\varrho_1 + \varrho_2)\times$$
$$\times [\varrho_1 + \varrho_2 + 2mN\tau] + 4m^2N^2S(\varrho_1 + \varrho_2) + S^2(\varrho_1 + \varrho_2)^2,$$

$$A_1 = gkS(\varrho_1 - \varrho_2)(\varrho_1 + \varrho_2)[2mN + S\tau] + 2S^2mN(\varrho_1 + \varrho_2),$$

$$A_0 = S^2gk(\varrho_1 - \varrho_2)(\varrho_1 + \varrho_2).$$

For the potentially stable arrangement $\varrho_1 > \varrho_2$, we find that all the coefficients in (40) are positive and so all the roots of n are either real and negative or there are complex roots (which occur in pairs) with negative real parts and the rest negative real roots. The system is therefore stable in each case. Thus the potentially stable configuration $\varrho_1 > \varrho_2$, remains stable for the case of two superposed fluids in the presence of suspended particles.

For the unstable configuration $\varrho_2 > \varrho_1$, there is at least one change of sign in (40) and so Eq. (40) has one positive root. The occurrence of positive root implies that the system is unstable. The unstable configuration, therefore, remains unstable for the case of two superposed fluids in the presence of suspended particles.

We conclude therefore that the system is stable for stable configuration and unstable for unstable configuration in the presence of suspended particles. This is in contrast to the thermal instability (Bénard convection) problem where the suspended particles have a destabilizing effect.

REFERENCES

1. M. KRUSKAL and M. SCHWARZSCHILD, Proc. Roy. Soc., A **233,** 348, 1954.
2. R. HIDE, Quart. J. Appl. Math., **9,**, 22, 1956.
3. S. CHANDRASEKHAR, Hydrodynamic and Hydromagnetic Stability, Oxford University Press, 1961, Chap. 10.
4. J. W. SCANLON and L. A. SEGEL, Phys. Fluids, **16,** 1573, 1973.
5. R. C. SHARMA, K. PRAKASH, and S. N. DUBE, Acta Phys. Hung. **40,** 3, 1976.

Acta Physica Academiae Scientiarum Hungaricae, Tomus 43 (3—4), pp. 259—268 (1977)

STATISTICAL FLUCTUATIONS OF (d, p) AND (d, α) REACTIONS ON ^{32}S TARGET NUCLEI AT 135°

By

O. E. BADAWY

PHYSICS DEPARTMENT, FACULTY OF SCIENCE, CAIRO UNIVERSITY, CAIRO, EGYPT

and

A. A. EL-SOUROGY

PHYSICS DEPARTMENT, ATOMIC ENERGY COMMISSION, ARE, CAIRO, EGY.

(Received in revised form 20. X. 1977)

The auto-correlation analysis of the fluctuations of the differential cross-sections of the (d, p) and (d, α) reactions on ^{32}S target at 135° gave a mean level width "Γ" of 20 ± 5 keV for the ^{34}Cl compound nucleus at 13.630 MeV average excitation energy. This value of "Γ" eflects the nuclear shell structure ef fects for even mass numb er nuclei beside confirming the rermigas model predictions. The abs e nce of correlation between associated as well as between Fon-associated decay groups is confirmed. The validity of the Thomas-Porter distribution for nescribing the probability distribution of cross-sections around their averages is attributed do a very small contribution of the direct process to the reaction mechanism if present. The tprobability of the α-isospin forbidden transition to the ^{30}P first excited state is discussed in the frame of the isospin mixing.

I. Introduction

The angular distributions of the different groups emitted in the $^{32}S(d, p)^{33}S$ reaction were studied [1—7] in the deuteron energy range from 1.0 up to 5.0 MeV, and a contribution from both the direct and compound nucleus processes to the reaction mechanism was recognised. The angular distribution of the (d, α) reaction in ^{32}S targets in the energy range from 2.0 up to 5.5 MeV [8, 9] showed the characteristic features of the compound nucleus mechanism.

In all these previous studies the mechanism of the (d, p) and (d, α) reaction on the ^{32}S target nuclei was investigated via the analysis of the measured angular distributions in terms of both the direct and compound nucleus processes beside the interference between both. The use of thick ^{32}S targets beside the big energy steps used in measurements prevented the obtained data from being suitable for ERICSON analysis of the present cross-section fluctuations.

Accordingly, we still have to investigate these reaction mechanisms, especially in the low energy range of incident deuterons. This is carried out here via the analysis of the accurately measured yield curves of these reactions in terms of the ERICSON methods [10], on the one hand. On the other hand the

study of the ERICSON fluctuations of these reactions is used as a tool for the determinations of the isospin mixing leading to the appearance of the α-isospin forbidden transitions in this low energy range of bombarding deuterons.

This paper presents the experimental results of the excitation functions of the above mentioned reactions in the deuteron energy range from 2.0 to 2.5 MeV, in 10 keV steps at 135° scattering angle. The observed fluctuations are attributed to a statistical origin and thus analyzed according to the method proposed by ERICSON [10].

II. Experimental techniques and analysis

^{32}S targets of thickness equivalent to ~ 10 keV energy loss at 2.20 MeV deuterons were prepared from "Ag_2S" by evaporation onto thin "Ag" backings.

The same experimental techniques given in [11] were performed here for the yield curves measurements. The methods of analysis of the results in terms of the ERICSON theory of statistical fluctuations [10] are given in detail in [11].

III. Results and discussion

1. *Energy spectra and yield curves*

Fig. 1a shows a typical energy spectrum of the elastically scattered deuterons at $E_d = 2.20$ MeV, and at 135° angle of scattering. Peaks corresponding to (d, α) reactions upon ^{32}S target nuclei as well as those due to "Ag" nuclei used as backings and present in target material (Ag_2S) are well seen. Peaks of ^{12}C impurities are also present. Considering the elastic scattering due to Rutherford, the target thickness was determined to be equivalent to $\simeq 10$ keV energy loss at 2.20 MeV deuteron energy.

Figs. 1b and 1c present the energy spectra of the protons and α-groups emitted in the (d, p) and (d, α) reactions on the ^{32}S targets, respectively, at $E_d = 2.0$ MeV and $\theta = 135°$). The first six proton groups leading to the shown ^{32}S levels are well separated from the $^{12}C(d, p_0)^{13}C$ group shown at the low energy end of the spectrum (Fig. 1b). The first emitted four α-groups, with α_1 and α_2 recorded as one group (α_{1-2}) due to lack of such very high energy resolution, are clearly seen in the spectrum of Fig. 1c. The identification of the reaction groups was performed by the reaction kinematics. In view of this, one can carry out the study of six proton groups and three α-groups with fair certainty. Accordingly, the excitation function curves of these six proton and three alpha-groups are measured in the deuteron energy range from 2.0 up to 2.4 MeV in the fairly accepted steps of 10 keV. Proton and α-spectra at

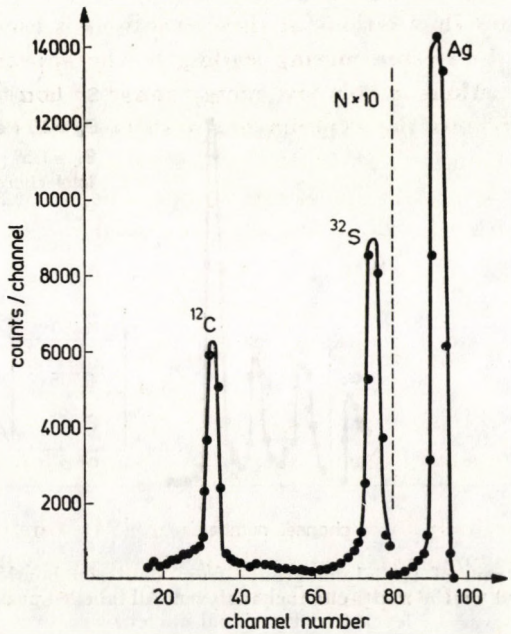

Fig. 1a. Spectrum of elastically scattered deuterons from ^{32}S target on Ag backing measured at $E_d = 2.2$ MeV and 135° angle of scattering

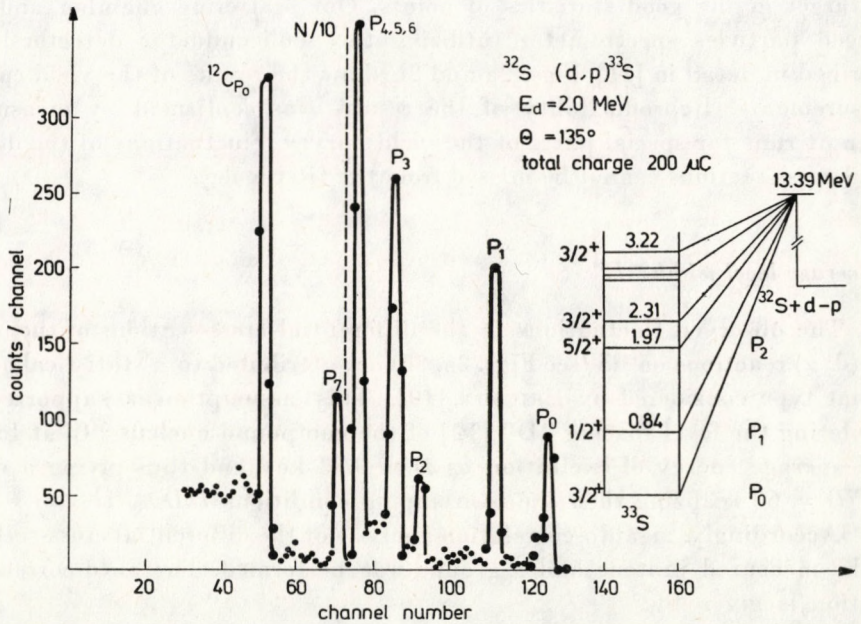

Fig. 1b. Typical spectrum of the proton groups from deuteron bombardment of a natural sulphur target, recorded on the multi-channel analyzer. All labelled peaks correspond to single levels in ^{33}S residual nucleus

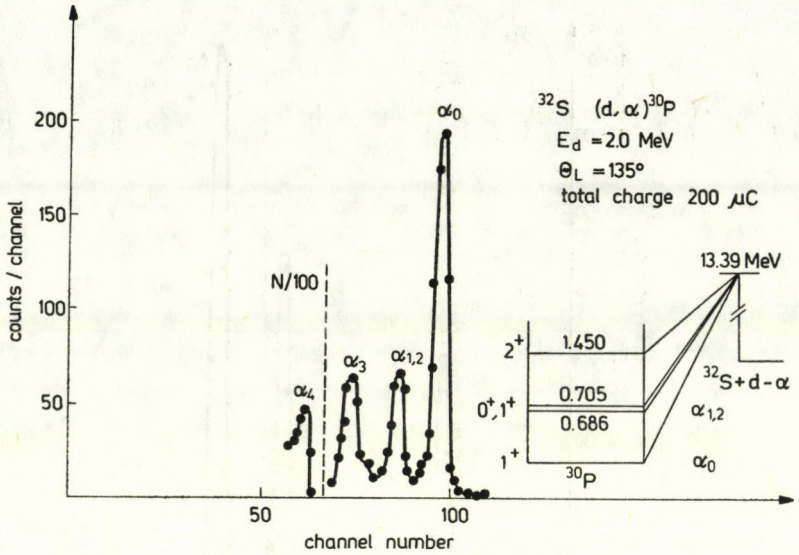

Fig. 1c. Typical spectrum of the alpha groups from deuteron bombardment of a natural sulphur target, recorded on the multi-channel analyzer. All labelled peaks correspond to single levels in ^{30}P residual nucleus

each deuteron energy were measured for a deuteron charge accumulated on the target giving good statistics of points. Our scattering chamber and the charged particles spectrometer (utilizing the semiconductor detectors) are described in detail in [11]. Figs. 2a and 2b show the results of the yield curves measurements. Reproducibility of the results was confirmed by measuring different runs for special parts of the yield curves. Fluctuations of the differential cross-sections cannot be missed from the first look.

2. *Average level width "Γ"*

The observed fluctuations in the differential cross-sections of the (d, p) and (d, α) reactions on ^{32}S (see Figs. 2a, 2b) are attributed to a statistical origin of that type considered by ERICSON [10]. This assumption is supported by calculating the level spacing "D" [12] of the compound nucleus ^{34}Cl at 13.630 MeV average energy of excitation as $D \simeq 0.33$ keV and thus giving a value of $\Gamma/D = 60$ realizing then the overlapping conditions $\Gamma/D \gg 1$.

Accordingly, an auto-correlation analysis of the differential cross-sections of the measured protons and α-groups was performed. The auto-correlation function is given by:

$$R(\epsilon) = \left\langle \left(\frac{\sigma(E_i)}{\langle \sigma(E_i) \rangle} - 1 \right) \cdot \left(\frac{\sigma(E_i + \epsilon)}{\langle \sigma(E_i + \epsilon) \rangle} - 1 \right) \right\rangle \qquad (1)$$

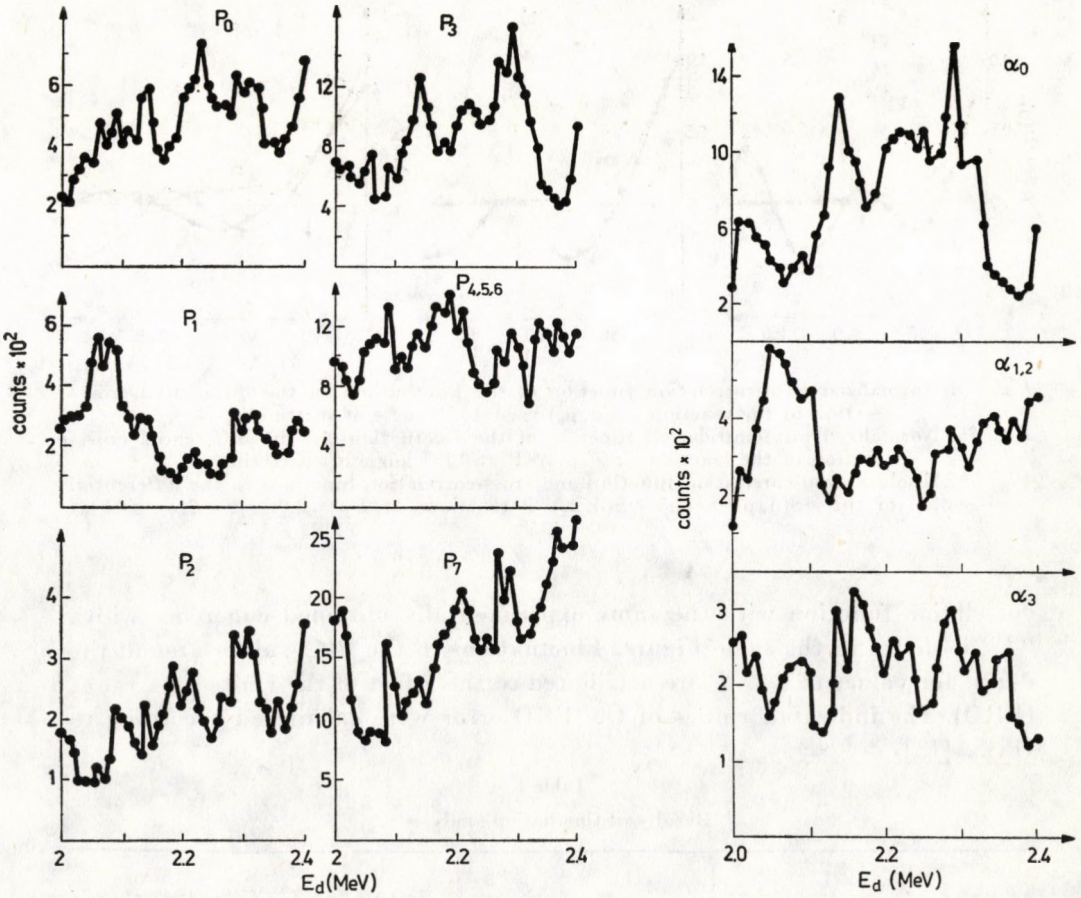

Fig. 2a. Excitation functions of the $^{32}S(d, p)^{33}S$ reaction leading to the first eight excited states of the ^{33}S nucleus for the scattering angle 135°, and deuteron energy range from 2.0 to 2.4 MeV. The statistical errors are within the dots.

Fig. 2b. Excitation function of the $^{32}S(d, \alpha)^{30}P$ reaction leading to the first four excited states of the ^{30}P nucleus, for the scattering angle 135° and in the deuteron energy range from 2.0 to 2.4 MeV. The statistical errors are within the dots.

with "ϵ" as an increment of energy not less than the energy steps of the yield curves measurements. The average value of the cross-section at an energy $E_i \langle \sigma(E_i) \rangle$ is represented by either a straight line obtained by a least square fit of the data or by a non-periodic Fourier function with higher orders neglected. An iteration procedure for the method of average was performed until getting the coherence width "Γ" of a certain excitation function being approximately constant. The details of the procedures of analysis are given in [11].

Figs. 3a and 3b present examples of the normalized auto-correlation function (that is $R(\epsilon)$ normalized to $R(\epsilon = 0)$] of some of the studied protons and α-groups. The theoretically expected Lorentzian shape [10] of the auto-

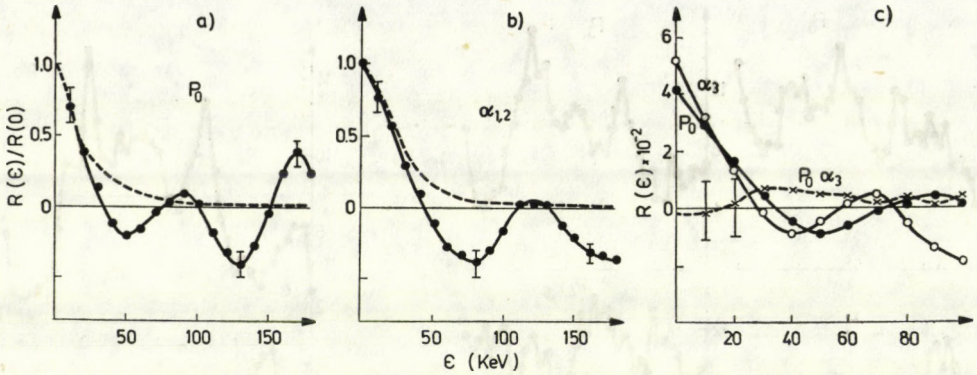

Fig. 3a. Normalized auto-correlation function of the fluctuations in the differential cross-section of the reaction $^{32}S(d, p_0)^{33}S$ at 135° angle of scattering

Fig. 3b. Normalized auto-correlation function of the fluctuations in the differential cross-section of the reaction $^{32}S(d, \alpha_{12})^{30}P$ at 135° angle of scattering

Fig. 3c. Absolute auto-correlation function and cross-correlation functions in the differential cross-section of the $^{32}S(d, p)^{33}S$ and $^{32}S(d, \alpha_3)^{30}P$ reactions at $E_d = 2.0 - 2.4$ MeV and at $\Theta = 135°$

correlation function with the same experimentally obtained coherence width "Γ" is shown in the same Figure. Fluctuations in the $R(\epsilon)$ values around the ϵ-axis for values of $\epsilon \gg \Gamma$ are attributed to the effect of the finite data range (FRD). The indicated values of the FRD error were calculated according to HALL [13].

Table I

Results of fluctuation analysis

Reaction	Group	Level spin	N	$N = 1/R(0)$	Γ_{auto} (keV)	$\overline{\Gamma}_{auto}$ (keV)	Γ_{fr} (keV)	$\overline{\Gamma}_{fr}$ (keV)	Average excitation energy (MeV)	Mean life time τ (sec)
$^{32}S(d, \alpha)\ ^{33}S$	P_0	3/2	12	23	17		17.5			
	P_1	1/2	6	9	20		21.5			
	P_2	5/2	18	19	14	18	16	19.5	13.63	3.66×10^{-20}
	P_3	3/2	12	10	26		24			
	$P_{4,5,6}$	–	–	29	15		19			
	P_7	3/2	12	22	16		18			
$^{32}S(d, \alpha)\ ^{30}P$	α_0	1	5	5	32		27.5			
	$\alpha_{1,2}$	–	–	10	23	23	20	22	13.63	2.86×10^{-20}
	α_3	2	8	19	14		18.5			

N Fluctuation damping coefficient calculated using the spin weight formula
$N = 1/R(0)$ Fluctuation damping coefficient from the experimental data
Γ_{auto} Width obtained from auto correlation analysis
Γ_{fr} Width obtained from the Fourier technique analysis
τ Average life time
The FRD error in Γ, $R(0)$ and $\tau = \pm 25$ %

Another method for the determination of the average coherence width "Γ" based on the Fourier analysis of the yield curves was used in all groups studied. The details of this method are given in our previous work [11].

Table I presents the values of the coherence width "Γ" obtained for each group by both the Lorentzian and the Fourier methods of analysis. The corresponding mean life-time "τ" of the compound nucleus ^{34}Cl at the average excitation energy of 13.630 MeV, amounts to $\sim 3.21 \times 10^{-20}$ sec in agreement with the slow reaction mechanism. Comparing this value of "Γ" for the ^{34}Cl nucleus at an average excitation energy 13.630 MeV with that at 16.30 MeV, which amounts to $\Gamma = 39 \pm 4$ keV [9], one can see that these results are in agreement with the Fermi-gas model predicition [9]. The value of "Γ" obtained here, being equal to that for the ^{33}S nucleus at an average excitation energy ~ 17.4 MeV [11], reflects the nuclear shell-structure effects for even mass nuclei [9].

3. *Associated and non-associated decay group correlation*

The correlation between the different groups emitted in a certain decay channel (i.e. protons or α-groups) can be studied through the correlation function

$$R_{a,b}(\epsilon) = \left\langle 1/2 \left[\frac{\sigma_a(E) - \langle \sigma_a(E) \rangle \left[\sigma_b(E + \epsilon) - \langle \sigma_b(E + \epsilon) \rangle \right]}{\left[\langle \sigma_a(E) \rangle \langle \sigma_b(E + \epsilon) \rangle \right]} + \right.\right. \\ \left.\left. + \frac{\left[\sigma_a(E + \epsilon) - \langle \sigma_a(E + \epsilon) \rangle \right] \left[\sigma_b(E) - \langle \sigma_a(E) \rangle \right]}{\left[\langle \sigma_a(E + \epsilon) \rangle \langle \sigma_b(E) \rangle \right]} \right] \right\rangle \tag{2}$$

with the same parameters defined in Eq. (1). In our work we studied the correlation between the emitted proton groups as well as between the emitted α-groups. The overall normalized values of the cross-correlation function (i.e. at $\epsilon = 0$) amount to (18 ± 54) % and (-8.0 ± 40) % for protons and α-groups, respectively. This confirms the absence of correlation between associated decay groups. On the other hand, the correlation between the non-associated decay groups (i.e. protons with α-groups) was also studied. Fig. 3c shows an example of this correlation parameter. Fig. 4 displays the values of the normalized cross-correlation parameter (at $\epsilon = 0$) between each emitted proton group and all the emitted α-groups. The overall average correlation amounts to (0.16 ± 1.7) which reflects the lack of correlation between non-associated decay groups, in accordance with the ERICSON predictions [10].

4. *Probability distribution of cross-section*

Fig. 5 shows the probability distribution of the measured cross-sections around their averages $\eta = \sigma / \langle \sigma \rangle$ (represented by a histogram) for some of the

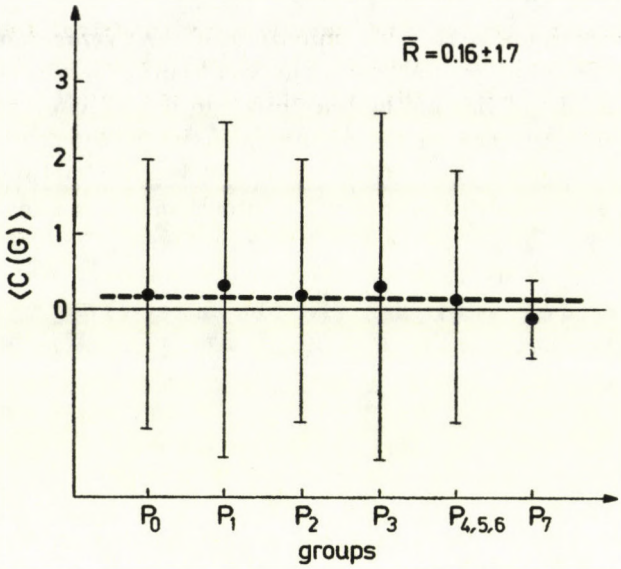

Fig. 4. The mean normalized cross-correlation function $<C(G)>$ for each proton group emitted from the $^{32}S(d, p)^{33}S$ reaction with all α-groups emitted in the $^{32}S(d, \alpha)^{30}P$ reaction. The over-all normalized cross-correlation R between all the proton and α-groups averaged over all of them is represented by the dashed line passing through the points.

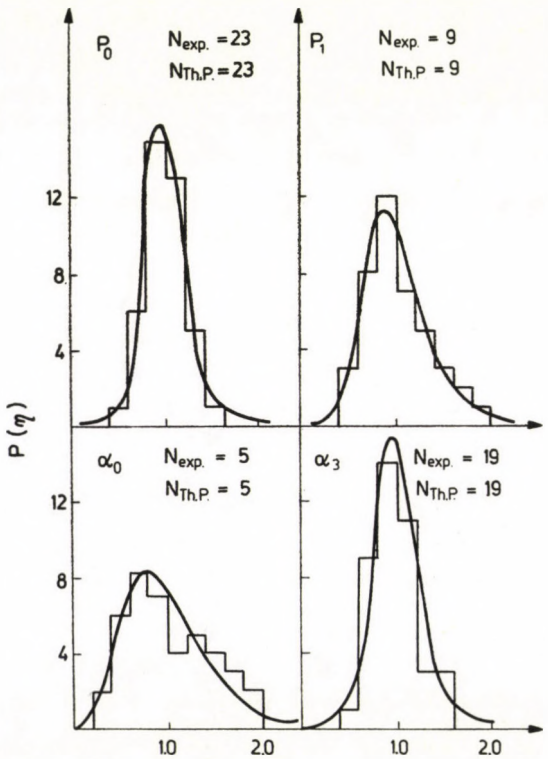

Fig. 5. The cross-section probability distribution histograms of the $^{32}S(d, p)^{33}S$ and the $^{32}(d, \alpha)^{30}P$ reaction groups. The smooth curves are calculated neglecting the direct interaction contribution

studied proton and α-groups. The smooth curves represent the distributions calculated according to the Thomas—Porter distribution, i.e. a χ^2-distribution with $2N$ degrees of freedom [10] and neglecting the direct reaction contribution, with N as the value of the fluctuation damping coefficient taken as $N = 1/R(0)$. These values of N are given in Table I where they are compared with the corresponding values calculated with the spin weight formula defining the number of incoherent statistically independent competing reaction channels [10]. The small deviations seen in Fig. 5 may be due to some small contributions of direct and/or any other than the compound nucleus mechanism if present.

5. *Isospin mixing*

In the present investigation, the isospin forbidden $T = 1$ state in ^{30}P at 0.678 MeV can be excited through the (d, α) reaction on ^{32}S. This 0^+ ($T = 1$) state of 0.678 MeV is so close to the 1^+ ($T = 0$) state at 0.709 MeV that they cannot be separated and are recorded as one group (α_{1-2}). Now, due to Coulomb forces, isospin mixing may occur before the decay of the compound nucleus state, and violations of the isospin selection rule then take place [14]. According to WILKINSON, the cross-section for an isospin forbidden transition should be inhibited by a factor $f = \langle H_c \rangle / \Gamma$ where Γ is the level width and $\langle H_c \rangle$ is the average matrix element of the Coulomb forces which are responsible for the mixing of the isospin of neighbouring states having the same spin and parities but different isospins. If we considered a probable upper limit for the value of $\langle H_c \rangle = 100$ keV [14], then a value for the inhibition factor $f = 100/20 = 5$ is obtained. This is clear from Fig. 6 where the proba-

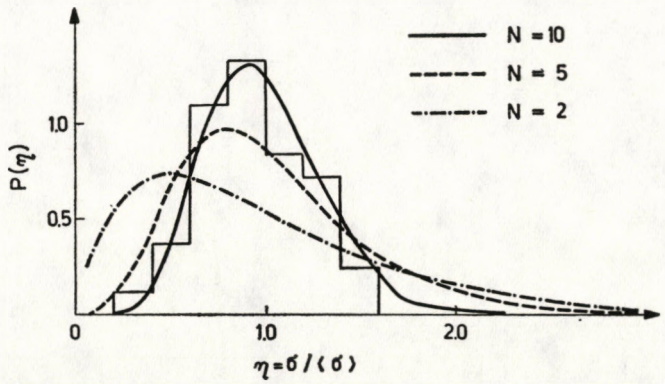

Fig. 6. The probability distribution of the cross-section of the ^{32}S(d, α_{12})^{30}P reaction group around their average. Smooth curves are calculated α_1 and α_2 alone ($N = 2$ and $N = 5$, respectively). The deviation of the $N = 2$ curve from the experimental histograms confirms the big inhibition of the isospin forbidden α_1 transition

bility distribution of cross-sections around their aevrage ($\eta = \sigma/\langle\sigma\rangle$) for the α_{1-2} group is very far from agreement with the calculated distribution with $N = 2$ (corresponding to the $T = 1$ state of spin $= 0^+$). The deviation is very clear in both the width and the peak position. This reflects the fact of the very small amount of isospin mixing in this case, a result which permits one to consider the α_{1-2} group as due to α_2 group only on the average.

Acknowledgement

We are deeply indebted to Professor Dr. M. EL-NADI who has made this work possible by this continuous encouragement and his valuable scientific discussions. Thanks are due to Professor Dr. V. Y. GONTCHAR, Professor Dr. L. M. EL-NADI and Dr. D. A. E. DARWISH for their help and advice during the experimental measurements.

REFERENCES

1. SILVESTEIN et al., CU(PNPL-234) 1964.
2. R. B. LEACHMAN, (LA-DC-8082), 1966.
3. J. B. TEPLOV and B. H. JUREV, JETP, **5**, 156, 1957.
4. J. B. TEPLOV and B. H. JUREV, JETP, **7**, 233, 1958.
5. H. R. SAAD, Z. A. SALEH, N. A. MANSOUR, E. M. SAYED and I. I. ZALOUBOVSKY, Nuclear Physics, **84**, 629, 1966.
6. KAASSANYI et al., J. de Phys. (Paris), **25**, 329, 1964.
7. F. L. WILSON, Thesis (Lawrence) 1965.
8. EL-BAHIE, M. NASSIF, M. F. AHMED and I. I. ZALOUBOVSKY, Nuovo Cimento, **38**, 521, 1965.
9. A. BOTTEGA, W. R. MCMUNOY and W. J. NAUDÉ, Nuclear Physics, Ä**136**, 265, 1969.
10. T. E. ERICSON, Adv. in Physics, **9**, 435, 1960.
    T. E. ERICSON, Annals of Physics, **23**, 390, 1963.
11. O. E. BADAWAY and A. A. EL-SOUROGY, Acta Phys. Hung., **42**, 343, 1977.
12. A. G. GILBERT and A. G. W. CAMERON, Canadian J. of Phys., **43**, 1446, 1965.
13. I. HALL, Physics Letters, **10**, 199, 1964.
14. P. H. WILKINSON, Phil. Mag., **1**, 379, 1956.

Acta Physica Academiae Scientiarum Hungaricae, Tomus 43 (3—4), pp. 269—279 (1977)

IN-ELASTIC INTERACTIONS OF 6.0 GeV/c PROTONS WITH C, N, O AND Ag, Br NUCLEI

By

O. E. BADAWY, K. M. ABDO and M. TAWFIK

EXPERIMENTAL HIGH ENERGY LABORATORY, PHYSICS DEPARTMENT, FACULTY OF SCIENCE, UNIVERSITY OF CAIRO, CAIRO, EGYPT

(Received in revised form 20. X. 1977)

Inelastic interactions of 6.0 GeV/c protons with light (C, N, O) and heavy (Ag, Br) emulsion nuclei were separated and classified by the use of two types of nuclear emulsions. The average values and the angular distributions of the emitted showers, recoil nucleons, and evaporated particles together with the intercorrelation between them are thoroughly investigated both for light (C, N, O) and heavy (Ag, Br) nuclei.

The results are compared with the predictions of the traditional cascade evaporation model and with its version taking into account many particle interaction (MPI).

I. Introduction

Inelastic interactions of 6.0 GeV/c protons with light (C, N, O) and heavy (Ag, Br) nuclei are investigated by using two types of photoemulsions I, II having different compositions (Table I). The interaction characteristics are studied and compared with their corresponding values calculated according to the cascade model with and without considering multiparticle interactions MPI [1, 2].

The intercorrelations between different emitted secondaries are studied and interesting conclusions about the mechanism of proton—nucleus interaction are obtained. The space angular distributions of secondary emitted shower, grey and black tracks producing particles are measured, and the half cone angles of the emitted particles are then obtained and compared with the values predicted by the cascade model [2, 3].

Table I

Element	Emulsion I nuclei/c.c.	Emulsion II nuclei/c.c.
H	3.15×10^{22}	5.06×10^{22}
C	1.41	1.83
N	0.39	0.16
O	0.96	1.65
Br	1.03	0.42
Ag	1.04	0.42

II. Experimental technique

NIK – FI – Br – 2 photoemulsion (denoted by I) and emulsion I enriched by ethylene glycol $[CH_2CH]_n$ (denoted by II) are used in our experiment. The nuclear composition of these photoemulsions is given Table I. Photoemulsions I and II were exposed at the Dubna Synchrophasotron, USSR, to 6 GeV/c protons.

The grain density in emulsion I was 33 per 100μ, while in emulsion II it was 21 per 100μ.

Events were searched for along the tracks. All events including one-prong at an angle $> 10°$ to the primary particle were detected and recorded.

III. Results and discussion

1. *Separation of inelastic interactions with light (C, N, O) and heavy (Ag, Br) nuclei from the total sample*

Due to the additivity of the nuclear composition of emulsion I and CH_2OH, the interactions in emulsion II are considered as a sum of interactions with emulsion I and CH_2OH nuclei.

In order to determine the number of interactions of protons with C, O nuclei we subtract the interactions with free protons (these form 4 % of events in emulsion I and about 10 % in emulsion II) according to their criteria [4].

Some events are produced showing coherent generations, which are searched for among the selected pure relativistic clean odd prong number events, i.e. among the sample of proton—neutron interactions. At our energy, events showing coherent production are of very small number.

Subtracting the p-free p events from the events in both types of emulsions (I and II) we can obtain the number of events due to proton interactions with carbon and oxygen nuclei $N_{II}(C, O)$ due to the enrichment in emulsion II by the equation:

$$N_{II}(C, O) = N_{II} - \frac{N_I}{V/V_0} \cdot \frac{L_{II}}{L_I} . \tag{1}$$

This equation makes a normalization to the scanning length equal to that of emulsion II, and decreased as much as the emulsion volume V_0 is increased to V when enriched by light nuclei $[CH_2OH]$, where the number of stars in emulsion I found along a scanning length L_I is denoted by N_I and the number of stars in emulsion II found along a length L_{II} is denoted by N_{II}.

After subtracting this number of stars $N_{II}(C, O)$ from N_{II}, the remaining number N_{IIr} will have the same n_s/n_h (n_s and n_h being the number of shower

and heavy tracks producing particles) distribution as the normal one N_I and is distributed according to the distribution ratios in N_I.

To obtain the n_s/n_h distribution of the C, O events we subtract the n_s/n_h distribution of N_{IIr} (which is similar to the n_s/n_h distribution of N_I) from that of N_{II} (this is similar to the distribution of C, N, O because the average atomic mass is the same). Since we know (by composition of emulsion I) that 22 % of the total emulsion I events N_I are due to interactions with (C, N, O) nuclei, so one can find N_I(C, N, O) in emulsion I and also its n_s/n_h distribution from its similarity to that of N_{II}(C, O).

Also to get the distribution of events due to Ag, Br nuclei in emulsion I, one subtracts the N_I(C, N, O) distribution from that of the total N_I. By a similar procedure one gets the Ag, Br events distribution in emulsion II.

From our data wa have obtained that

L_I = 298.92 metres
L_{II} = 129.91 metres
N_I (p-free p events are subtracted) = 833 events.
N_{II} (p-free p events are subtracted) = 247 events.
$V/V_0 = 2.5$

2. *Multiplicities of the shower, recoil and evaporated particles*

Table II presents the dependence of the average values characterizing particle generation for some groups of nuclei and their decay under proton bombardment. For comparison, Table II presents the mean number of charged shower particles $\bar{n}_{ch}$ and half angles $\theta_{1/2}$ (the angle through which half of the secondary particles emerge), averaged for interactions with protons and neutrons. In this Table we also present the data obtained at 69 GeV/c and 9.0 GeV/c incident proton momenta [5, 6].

The most convenient characterization of the multiplicity is the ratio R_A of the average number of shower tracks $\bar{n}_s(A)$ from a target A to $\bar{n}_{ch}$ in p—p collisions at the same energy: $R_A = \bar{n}_s(A)/\bar{n}_{ch}(pp)$. Fig. 2 shows the dependence of the ratio R on n_h for the interactions with nuclei, C, N, O and Ag, Br, where the data at 69 GeV/c [5] are introduced.

Table II shows a weak dependence of $\bar{n}_s$ on the atomic weight A. One also sees this well in Fig. 3 in which the line $A^{0.10}$ fits the data at 69 GeV/c [5], while the line $A^{0.025}$ fits our data at 6 GeV/c.

The average values of interaction characteristics $n_s^{\pm}$, $n_g^{\pm}$, $n_h^{\pm}$ of our data obtained for the interactions of 6.0 GeV/c protons with emulsion nuclei are presented in Table III, where they are compared with their corresponding values calculated for 6.2 GeV primary protons according to the cascade model with and without taking into account MPI [2, 3].

Table II

The different characteristics of the in-elastic interactions of protons with light and heavy emulsion nuclei at different momenta

Nuclei	A	Momentum GeV/c	$\bar{n}_s$	$\bar{n}_g$	$\bar{n}_b$
C		6	2.77 ± 0.12	0.96 ± 0.07	1.71 ± 0.12
N	14	9	3.0 ± 0.1	1.4 ± 0.1	3.3 ± 0.1
O		69	7.53 ± 0.27	0.90 ± 0.05	2.57 ± 0.13
Ag		6	2.92 ± 0.07	2.54 ± 0.06	5.51 ± 0.09
Br	92	9	3.5 ± 0.3	4.1 ± 0.5	6.1 ± 0.6
		69	10.53 ± 0.48	2.98 ± 0.1	6.6 ± 0.5
		$6\bar{n}_{ch}=$			
nucleon	1		2.6 ± 0.3		
		69	6.0 ± 0.2		

Nuclei	A	Momentum GeV/c	n_h	$\theta_{s,1/2}$	$\theta_{g,1/2}$
C		6	2.67 ± 0.12	23.0° ± 0.5°	60.5° ± 5°
N	14	9		22.5° ± 1°	56.5° ± 3°
O		69	3.47 ± 0.16	9.6° ± 1°	60° ± 3°
Ag		6	8.05 ± 0.11	34.6° ± 1°	67.8° ± 2.5°
Br	92	9		27.5° ± 1.5°	65.0° ± 3°
		69	9.58 ± 0.6	14.0° ± 0.5°	66.4° ± 1°
		$6\bar{n}_{ch}=$			
nucleon	1			11°	
		69		6.5°	

Table III

The 6.0 GeV/c interaction characteristics compared with theoretical values

Interaction characteristics	Present data at 6 GeV/c	Calculated values according to the cascade evaporation model ref. [5]	Calculated values according to cascade model with MPI ref. [4]
$\bar{n}_s^{\pm}$	2.89 ± 0.05	2.80 ± 0.15	2.7 ± 0.1
$\bar{n}_g^{\pm}$	2.18 ± 0.05	2.10 ± 0.15	2.3 ± 0.1
$\bar{n}_h^{\pm}$	6.81 ± 0.09	8.30 ± 0.40	7.8 ± 0.4
θ°_{s12}	25.0° ± 0.5°	28° ± 2°	29° ± 1.5
$\theta^{\circ}_{g1/2}$	65.5° ± 3°	70° ± 4°	66° ± 3°

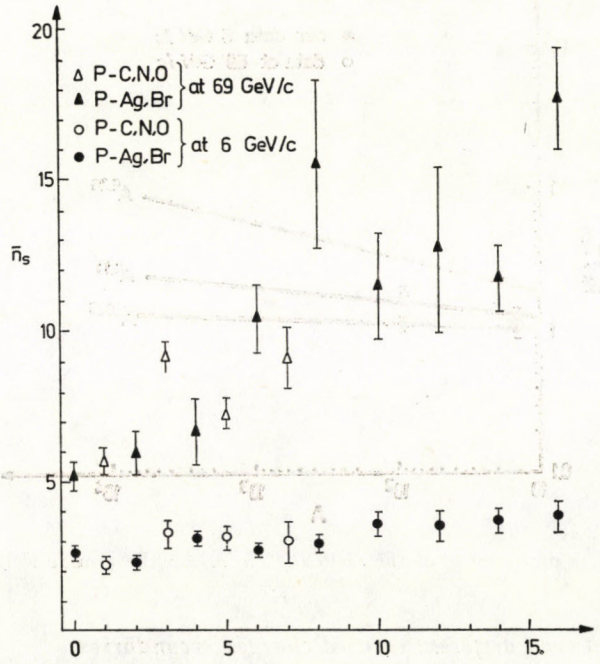

Fig. 1. The dependence of the average number of shower tracks on the number of heavy tracks producing particles

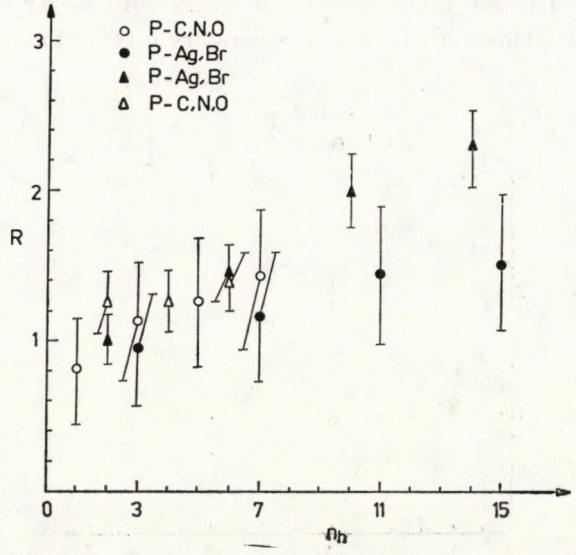

Fig. 2. The dependence of the ratio $R = n_s/n_h$ on the number of heavy tracks producing particles. Circles are our data at 6 GeV/c, and triangles are data at 69 GeV/c incident proton momentum

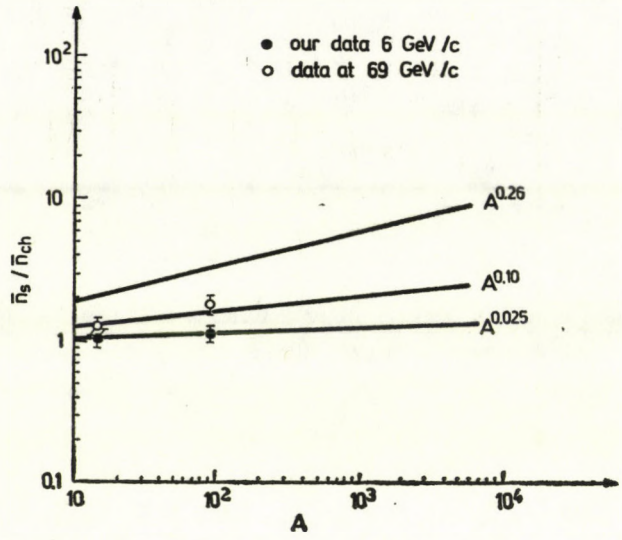

Fig. 3. The dependence of the ratio $R = \bar{n}_s/\bar{n}_{ch}$ on the atomic weight A

3. *Correlation between different emitted charged secondaries*

The intercorrelations between n_b, n_g and n_s are given in Figs 4, 5, 6 and 7.

In the representation of the frequency distribution of stars for n_s as a function of their grey and black prong number n_h (Figs. 1,6), it was found that for both light and heavy nuclei events the stars with larger n_h show, on the average, a large n_s. This must be due to secondary interactions for two reasons:

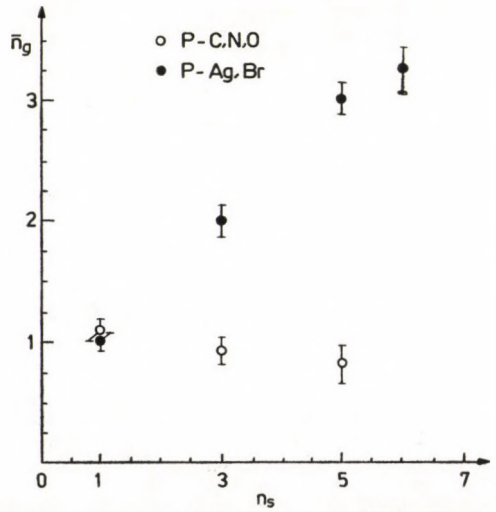

Fig. 4. The dependence of the average number of grey tracks producing particles on the number of shower tracks producing particles at 6 GeV/c

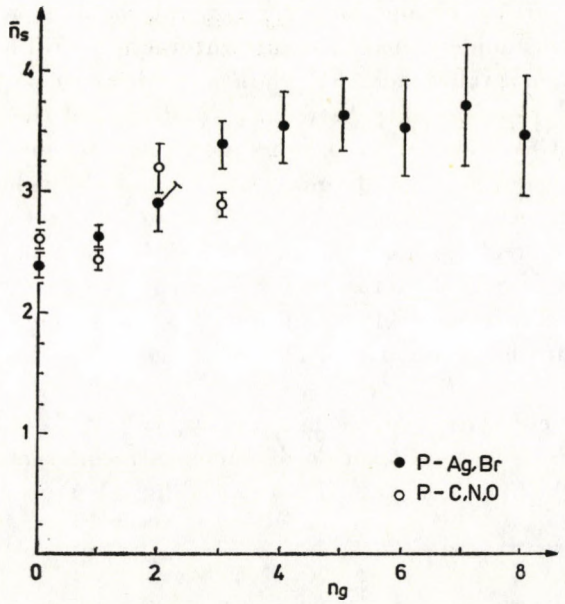

Fig. 5. The dependence of the average number of the shower tracks producing particles on the number of grey tracks producing particles at 6 GeV/c incident proton momentum

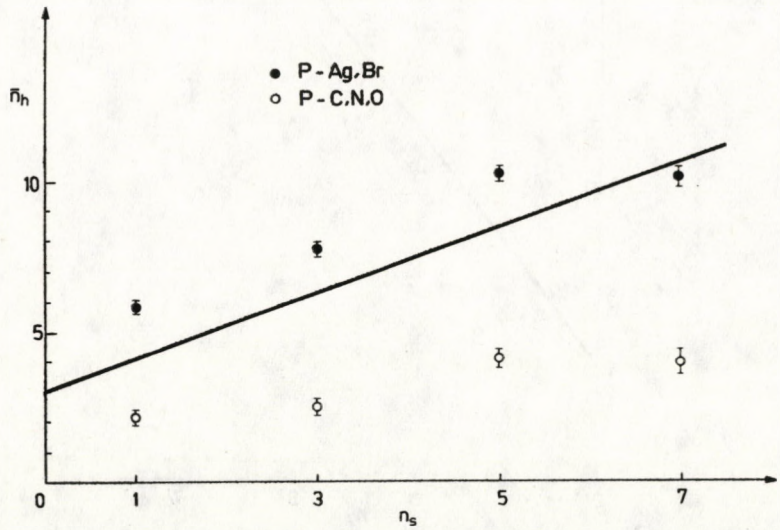

Fig. 6. The dependence of the average number of heavy tracks producing particles on the number of shower tracks producing particles

(i) If n_s is larger; the change for secondary interactions increases.
(ii) Fast particles undergoing secondary interactions still have some change to lead to additional thin tracks by producing other fast particles.

From the proportionality between n_g and n_b, and the constancy of the ratio n_g/n_b at 6 GeV/c and other protons momenta [4], one may think of the high energy collision as proceeding in spatially and chronologically separable steps: the fast particles undergo an independent process, not directly connected with the nuclear break-up mechanism. The link between the jet and the evaporation process is formed by the recoils from the high energy collision. These recoil particles excite the nucleus and serve as the strong "buffer" which is needed to explain the observations. The existence of this buffer is entirely an effect of elementary particle physics.

The linear correlation between n_g and n_b indicated that normally every recoil particle finds its own fraction of nucleons to interact with.

The straight lines in Figs. 6, 7 are drawn for all emulsion nuclei by least square fitting.

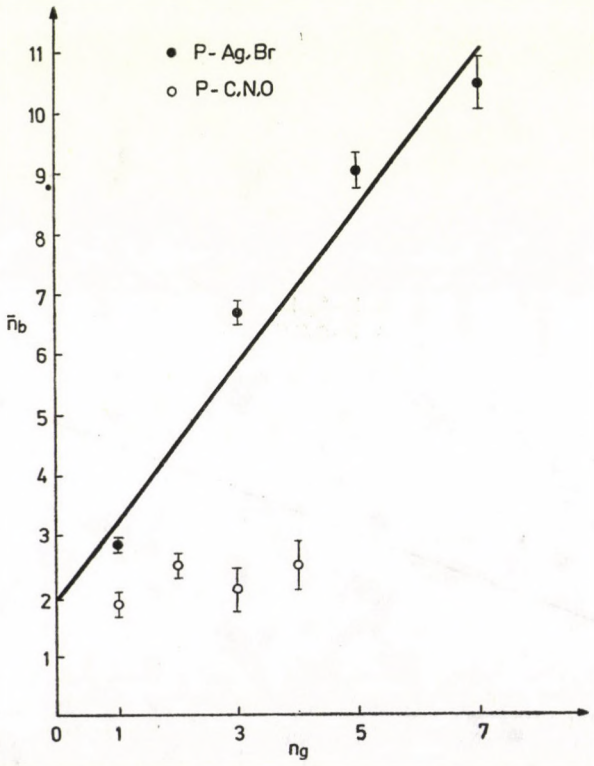

Fig. 7. Correlation between the number of grey tracks producing particles and the average number of black tracks producing particles

4. *Angular distribution of different charged secondaries*

The angular distributions of shower, grey and black tracks producing particles emitted from the interactions of protons with both light (C, N, O) and heavy (Ag, Br) nuclei are given in Figs. 8, 9, 10, respectively. From these

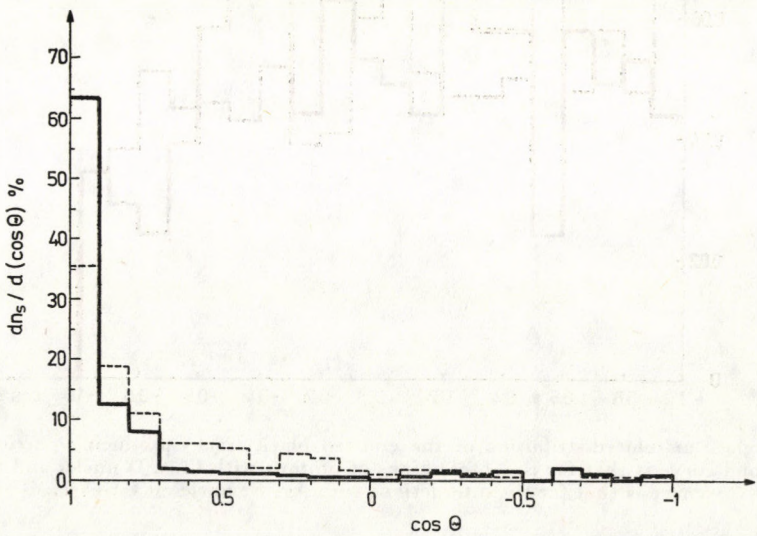

Fig. 8. Space angular distribution of the emitted shower tracks producing particles in the lab. system. The solid curve is that for the interactions of protons with nuclei C, N, O and the dashed curve is that for the interactions with Ag, Br nuclei, at our 6 GeV/c proton momentum.

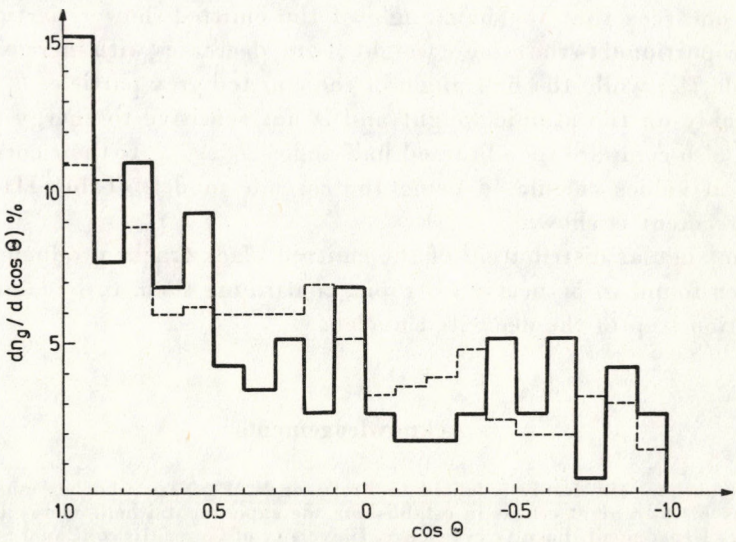

Fig. 9. Space angular distribution of the emitted grey tracks producing particles in the lab. system. Solid curve is that for the interactions of protons with nuclei C, N, O, and the dashed curve is that for the interactions with nuclei Ag, Br at 6 GeV/c incident proton momentum.

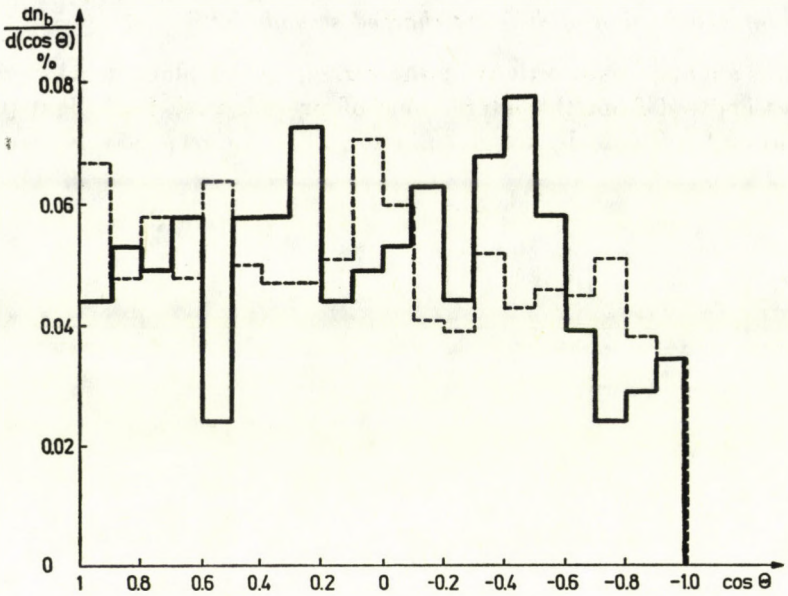

Fig. 10. Space angular distribution of the emitted black tracks producing particles in lab. system. Solid curve is that for the interactions of protons with C, N, O nuclei and the dashed curve is that for the interactions with Ag, Br nuclei at 6 GeV/c.

Figures one sees that the half angle of the emitted shower particles $\theta_{1/2s}$ is about proportional to the atomic weight A and decreases with increasing energy (see Table II); while the half angle of the emitted grey particles $\theta_{1/2g}$ depends very weakly on the atomic weight and is not sensitive to energy (Table II). One can also compare the obtained half angles $\theta_{1/2s}$, $\theta_{1/2g}$ to their corresponding theoretical values calculated using the cascade models (Table III), where a good agreement is shown.

The angular distribution of the emitted black tracks producing particles have been found to be nearly isotropic, confirming them to be emitted in the evaporation step of the deexcited nucleus.

Acknowledgements

The authors are deeply indebted to Professor M. EL-NADI who has made this work possible by his own great efforts in establishing the experimental high energy laboratory in the Physics Department, Faculty of Science, University of Cairo. His continual help, valuable scientific discussions are highly appreciated.

Thanks are due to Professor K. D. TOLSTOV, from the Joint Institute for Nuclear Research JINR in Dubna, USSR, for supplying the irradiated plates.

REFERENCES

1. A. DAR and J. VARY, Phys. Rev., **D6**, 2412, 1972.
2. J. Z. ARTYKOV and V. S. BARASHENKOV, Nucl. Phys., **136**, 11, 1968.
3. J. Z. ARTYKOV and V. S. BARASHENKOV, Journal of Nucl. Phys., Vol. **4** part I (1966).
4. H. WINZELER, Il Nuovo Cimento, **17**, 8, 1960.
5. K. D. TOLSTOV, Dubna reprint El-7548, (USSR) 1973.
6. V. S. BARASHENKOV, Nucl. Phys. **14**, 522, 1959/60.
7. P. L. JAIN, Nucl. Phys., **67**, 641, 1965.

Acta Physica Academiae Scientiarum Hungaricae, Tomus 43 (3—4), pp. 281—291 (1977)

WAVE MECHANICS AND THE PHOTON IV

By

L. JÁNOSSY and M. ZIEGLER-NÁRAY

CENTRAL RESEARCH INSTITUTE FOR PHYSICS, BUDAPEST

(Received 29. XII. 1977)

In Part III we have given in a suitable form the system of differential equations describing the interaction of an excited H-atom with its own radiation field. In the present paper we give a particular solution of the system; i.e. we give such a solution which corresponds to the superposition of two stationary solutions only. For the ultimate description of the process it seems necessary to extend the present calculation and to obtain the more general solutions corresponding to the simultaneous transition of an excited state into a number of lower states.

The solutions obtained in the particular case dealt with presently show interesting qualitative features. So one finds a feature of the solution which seems to be related with the Lamb shift.

Introduction

In the preceding part of this paper (see [1]) we have given in a peculiar form the system of differential equations which governs the motion of a H-atom interacting with its own radiation field. The atom was supposed to be enclosed into a cubic box of sides $L \gg r_H$ and the walls of the box were taken to be perfect mirrors. In the present paper we give an explicit particular solution of the system of equation derived in [1].

In [1] we developed the wave function of the H-atom in a series of stationary wave functions

$$\psi = \sum c_\nu \psi_\nu .$$

In the present paper we confine ourselves to wave functions which can be expressed as the superposition of two states only, thus we suppose

$$\psi = c_0 \psi_0 + c_1 \psi_1. \tag{1}$$

The differential equations given in [1] admit solutions of the form (1); this can be seen considering the solutions of those equations with initial condition

$$c_\nu = 0 , \qquad \nu \neq 0, 1 ,$$
$$b_{\nu\mu} = \dot{b}_{\nu\mu} = 0 , \qquad \nu\mu \neq 0, 1 . \tag{2}$$

(For the definition of $b_{\nu\mu}$ see [1] (15)) The initial conditions (2) are in fact Cauchy conditions; i.e. if (2) is satisfied at any time $t = t_0$ then it remains satisfied at any time $t \neq t_0$.

Simplifying the notation of [1] we can thus write the equations of motion for the two-state system

$$i\gamma_0^2 b + 2\Omega\dot{b} - i\ddot{b} = 2\sigma_0^3 c_0 c_1^*, \tag{3}$$

$$\begin{aligned} \dot{c}_0 &= bc_1, \\ \dot{c}_1 &= -b^* c_0 . \end{aligned} \tag{3a}$$

We obtain (3) from Equ. (32) [1] writing

$$\begin{gathered} \gamma_{01} = \gamma_0, \ \Omega_1 - \Omega_0 = \Omega, \ \sigma_{01} = \sigma_0 \\ b_{01} = -b_{10}^* = b . \end{gathered} \tag{4}$$

The definitions of $\gamma_{\nu\mu}, \sigma_{\nu\mu}, b_{\nu\mu}$ are given in [1]. Here we note that b is a quantity proportional to the transition probability $1 \to 0$, Ω is the combination frequency between the two states ψ_0 and ψ_1. We suppose

$$\Omega > 0 \tag{5}$$

thus we choose ψ_1 to be a state of higher energy than ψ_0 Further:

$$\gamma_0^2 = \Omega^2 - c^2 K^2 , \tag{6}$$

where

$$\mathbf{K} = \mathbf{K}_1 - \mathbf{K}_2$$

is the wave vector of the relative translational motions of the two states. It will be seen that (3) possesses non trivial solutions only if

$$\gamma_0 \sim 0,$$

i.e. in the case of close resonance between de Broglie wave length and the wave length of the emitted radiation. From [1] one finds

$$\sigma_0 \sim \frac{c}{137L} . \tag{7}$$

This is a frequency which plays the role of the coupling constant between atom and radiation. It must be emphasized that this coupling decreases with increasing volume L^3 of the box containing the atom.

The latter fact may appear surprising at first sight – however, it can be understood clearly in this manner: Increasing the box into which the atom

spreads out we decrease the current and charge densities by spreading them out. In this way the density of radiation emitted by the current charge density decreases with increasing spread.

Because of the volume dependence of the coupling constant, in accord with (7), the rate of the process described by (3) will be the slower the larger the volume L^3. So as to eliminate this dependence from the mathematical formalism it is convenient to introduce as the unit of time

$$\Delta t = \frac{\Omega^{1/2}}{\sigma_0^{3/2}} .$$

The above unit is thus proportional to $L^{3/2}$; in such units we have

$$\Omega = \sigma_0^3 \tag{8}$$

and the equations of motion (3) can be written

$$i\gamma_0^2 b + 2\Omega\dot{b} - i\ddot{b} = 2\Omega c_0 c_1^* . \tag{9}$$

Elimination of the coefficient c_ν

The coefficients c_0, c_1^* appearing in (3) and (9) can be eliminated with the help of (3a). Indeed, introduce two new quantities

$$B = 2c_0 c_1^* \text{ and } U = |c_1|^2 - |c_0|^2 . \tag{10}$$

Using the normalization

$$|c_0|^2 + |c_1|^2 = 1 \tag{11}$$

we have from (10)

$$U = \sqrt{1 - BB^*} . \tag{12}$$

In a transition where the atom starts in the excited state $|c_1| = 1$ finishes in the lower state $|c_0| = 1$ we find that U changes from $+1 \to -1$. $|B|$ changes from $0 \to 1 \to 0$; the sign of the square root has to be changed while B passes through unity.

Differentiating the second equation (10) into time, we find with the help of (3a)

$$\dot{U} = -(Bb^* + B^* b) \tag{13}$$

and similarly

$$\dot{B} = 2bU. \tag{14}$$

Thus differentiating (9) into time we find with the help of (10) and (14)

$$i\gamma_0^2 \dot{b} + 2\Omega\ddot{b} - i\dddot{b} = 2\Omega b \sqrt{1 - BB^*}. \tag{15a}$$

For the sake of completeness we write down Eq. (9) here again using the expression B given in (10):

$$i\gamma_0^2 b + 2\Omega\dot{b} - i\ddot{b} = \Omega B\,. \tag{15b}$$

B can be eliminated from the relations (15) and thus we are left with a strongly non linear differential equation for b.

An approximate solution

So as to see better the properties of the system (15) we give first an approximate solution. For this purpose we neglect the imaginary terms and look for real solutions of the approximate system. Thus we write in place of (15b)

$$\dot{b} = \frac{1}{2} B\,,$$

$$\ddot{b} = b\sqrt{1 - B^2} = b\sqrt{1 - 4b^2}\,.$$

Integrating in the usual way we get

$$2\dot{b} = \sin \int 2\, b\, dt\,.$$

Thus introducing

$$2\int b\, dt = \beta\,,$$

we are left with the equation of the pendulum, i.e.

$$\ddot{\beta} = \cos\beta\,.$$

The explicit solution of which, with initial conditions

$$b, \dot{b} \to 0 \quad \text{if} \quad t \to -\infty$$

is found as

$$b = \frac{1}{cht}\,. \tag{16}$$

Thus b increases monotonically from zero to its maximum value one at $t = 0$ and then it falls back monotonically to zero. Further

$$B = 2\dot{b} = -\frac{2\,sht}{ch^2 t},$$

thus B increases from zero to one and then falls back to zero.

The process thus described amounts to the atom falling down gradually from the excited state 1 into the lower state zero. However, once the lower state is reached the radiation emitted by the system is reabsorbed and eventually the initial excited state is re-established.

Complex solutions

So as to obtain more exact solutions it is necessary to take into consideration the imaginary terms also. For this purpose it is useful to introduce phases and amplitudes of b as new variables. Let us write

$$b = e^{T+iS}, \tag{17}$$

where T and S are real functions of the time. It is convenient to introduce further a notation for time derivatives, thus

$$\dot{T} = \tau, \quad \dot{S} = \sigma. \tag{18}$$

We shall always consider initial conditions

$$b, \dot{b} \to 0 \quad \text{if} \quad t \to -\infty,$$

thus we also suppose

$$T \to -\infty \quad \text{if} \quad t \to -\infty.$$

With the help of the above notation we obtain two integrals of the equations of motion as we show presently. Indeed, multiplying (15b) with b^* and adding to the equation so obtained the complex conjugate equation we have

$$\frac{d}{dt}\left(\Omega b b^* - i(\dot{b}b^* - \dot{b}^* b)\right) = \Omega(B b^* + B^* b).$$

Using (13) we can integrate both sides into t. Using the initial condition

$$b, \dot{b} \to 0, \; U \to 1 \text{ if } t \to \infty$$

we find

$$\Omega bb^* - i(\dot{b}b^* - \dot{b}^* b) = \Omega(1 - U).$$

With the help of (17) and (18)

$$\dot{b}b^* - \dot{b}^* b = 2i\sigma bb^*$$

thus

$$bb^* = \frac{1 - U}{1 + \dfrac{2\sigma}{\Omega}} . \tag{19}$$

(19) is an integral of the equations of motion, valid for the initial conditions (18a).

If $\sigma \ll \Omega$ then $bb^* \sim 1 - U$ thus bb^* represents the energy irradiated by the system.

Another integral is obtained by multiplying (15a) by b^* and subtracting from the equation thus obtained its complex conjugate value. The right hand sides are thus zero and we find

$$\frac{d}{dt}\left[-i\gamma_0^2 bb^* + 2\Omega(\dot{b}^* b - b^* \dot{b}) + i(\ddot{b}\, b^* + \ddot{b}^* b - \dot{b}^* \dot{b})\right] = 0 .$$

Integrating the above equation into time we note that the expression inside the square bracket is constant. However, as the above expression tends to zero for $t \to -\infty$ we see that the value of the bracket must be zero. With the help of (17) and (18) the expression in the square bracket can be expressed in terms of σ, τ and its derivatives; we find thus

$$\gamma_0^2 + 4\Omega\sigma - 2\dot{\tau} - \tau^2 + 3\sigma^2 = 0 \tag{20}$$

as a condition which must be fulfilled for any value of t if the process starts from the initial configuration (18a). Eq. (20) is thus a second integral of the equations of motion, valid for the initial condition (18a).

Equation of motion in terms of the phases

Introducing (17) and (18) into (15) and separating it into real and imaginary parts, we obtain two real differential equations expressing $\ddot{\sigma}$ and $\ddot{\tau}$ in terms of lower derivatives. Such a system can be solved e.g. by numerical integration. However, using (20) $\dot{\tau}$ can be expressed in terms of σ, τ therefore it is sufficient to take from the equations which can be derived from (15) only the one

which contains $\ddot{\sigma}$; the one containing $\ddot{\tau}$ can be replaced by the simpler relation (20).

We find thus considering the real part of (15) and simplifying the expression thus obtained making use of (20)

$$2\Omega(\sigma^2 + \tau^2 + \dot{\tau}) + \theta = 2\Omega(1 - e^{2T}) \tag{21}$$

with

$$\theta = 2\sigma^3 + 2\tau^2\sigma + \dot{\tau}\sigma + 3\dot{\sigma}\tau + \ddot{\sigma} + 2\sigma e^{2T} .$$

The advantage of using (20) instead of the imaginary part of (15) is that (21) which is obtained in this way does not contain the parameter γ_0 explicitly.

Thus (20) and (21) is a system equivalent to the original equations of motion provided the initial condition (18b) is used.

Solutions by successive approximations in powers of $1/\Omega$

The solutions of (20) and (21) can be obtained by successive approximation supposing $\Omega \gg 1$ and writing

$$\sigma = \sigma_1 + \frac{1}{\Omega}\sigma_2 + \dots$$

$$\tau = \tau_1 + \frac{1}{\Omega}\tau_2 + \dots$$

similarly (22)

$$T = T_1 + \frac{1}{\Omega}T_2 + \dots .$$

Indeed, inserting (20), (22) into (21) and considering the first terms only in the development we find from (20)

$$\gamma_0^2 + 4\Omega\sigma_1 = 0 ,$$

thus

$$\sigma_1 = -\frac{\gamma_0^2}{4\Omega} \tag{23}$$

and since σ_1 does not change in time, also, we have

$$\dot{\sigma}_1 = 0.$$

In (21) we can neglect in our first approximation the terms lumped together into θ, we find thus

$$\tau_1^2 + \dot{\tau}_1 = (1 - \sigma_1^2 - e^{2T_1}) . \tag{24}$$

Let us write further

$$e^{T_1} = y, \tag{25}$$

thus

$$\ddot{y} = (\tau_1^2 + \dot{\tau}_1) y .$$

Multiplying (24) by y we find therefore

$$\ddot{y} = (1 - \sigma_1^2) y - y^3 .$$

Multiplying this with y and integrating into t we find

$$\frac{1}{2} \dot{y}^2 = \frac{1}{2} (1 - \sigma_1^2)\, y^2 - \frac{1}{4} y^4 .$$

The integration constant is chosen so as to satisfy the initial condition, $y_1 \to 0$ i.e. $y \to 0$ for $t \to -\infty$. The above equation possesses non-trivial real solution only if

$$\sigma_1^2 < 1.$$

Integrating once more into t we obtain (with the initial condition given above) as non-trivial solution

$$y = \frac{\sqrt{2}\,\alpha}{ch \alpha t} , \quad \alpha = \sqrt{1 - \sigma_1^2} . \tag{26}$$

According to (19) we get (neglecting terms of $1/\Omega$)

$$U_{\min} = 1 - |\, b_{\max}|^2 .$$

Thus using (25) and (26) we find:

$$U_{\min} = \sigma_1^2 - 1 . \tag{27}$$

In the case of perfect resonance $\sigma_1 = 0$

$$U_{\min} = -1$$

and we find

$$|\, c_0 \,|^2 = 1 \quad |\, c_1 \,|^2 = 0 \quad \text{at } t = 0 ,$$

thus the atom falls from the excited state into the pure lower state; however, the radiation field appears exactly suitable to reverse the position and to bring back the system into its original configuration. If there is lack of resonance ($\sigma_1 \neq 0$) then the reversal takes place before the pure lower state has been reached. For $|\, \sigma_1 \,| > 1$ the process does not start at all.

We note, if radiation was allowed to escape from the enclosure, the reversal could not take place – presumably it does not take place if the energy is split among a number of lower states of about equal energies. Thus the symmetric process (see Fig. 1) takes place only in the idealized case considered above.

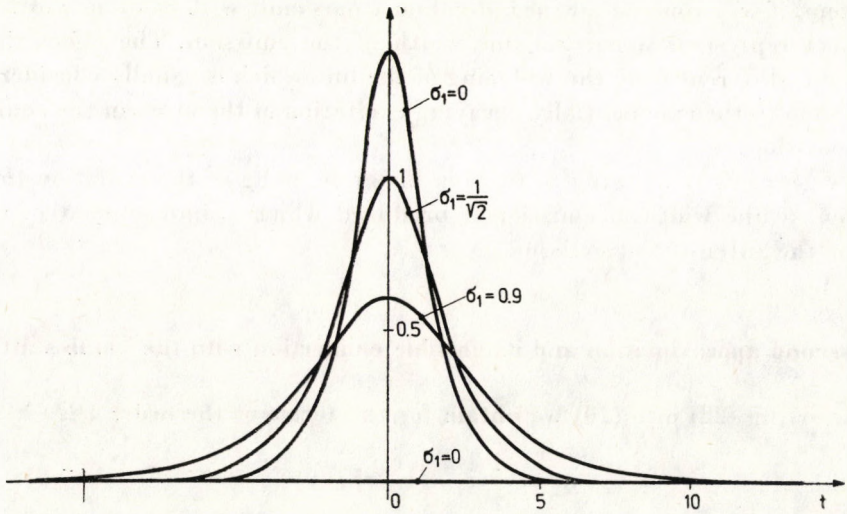

Fig. 1

A qualitative remark

An electromagnetic wave of arbitrarily small amplitude with frequency $\Omega + \sigma_1$ sweeping over the excited H-atom starts an avalanche which leads to the process described above. The avalanche starts, however, only if

$$|\sigma_1| < 1$$

this means, only if there is a very close resonance between the atomic frequency and the exciting radiation. From (6) and (23) we find

$$\Delta\Omega = |cK - \Omega| < \frac{1}{2}.$$

The above expression is another form of the relation defining the state of resonance in which an avalanche will start.

The physical significance of σ is that the radiation field emitted by the atom has a frequency $\Omega + \sigma$. Thus owing to the nonlinearity oi the process, frequencies slightly deviating from the combination frequency appear. How-

ever, these deviations are small. The physical significance of these deviations is as follows. The H-atoms enclosed into the box will emit frequencies inside a frequency range $\Omega \pm \Delta\Omega$. The actual frequency of an individual emission depends on the mode of initial excitation of the state. Considering the emission of several atoms we expect therefore a band with $2\Delta\Omega$ of the line emitted by the system, if we suppose that the individual atoms emit with random width σ. This effect represents a natural line width of the emission. The effect thus described is different from the widening of the line which is usually considered as being due to the exponentially decaying excitation of the atom in the course of the emission.

We see thus that owing to the non linear coupling of the radiation field and atom, a line width of emission is produced which is independent of the decay of the intensity of emission.

The second approximation and its possible connection with the Lamb shift

Inserting (22) into (20) we obtain for the terms of the order $1/\Omega$

$$\sigma_2 = \frac{1}{2}\dot{\tau}_1 + \frac{1}{4}\tau_1^2 .$$

Taking expressions (24) and (26) into account we find

$$\Delta\sigma = \sigma_2(0) - \sigma_2(-\infty) = \frac{1}{2}(1 - \sigma_1^2) .$$

We see thus that the frequency σ which is superposed to the combination frequency varies in the course of the emission. The shift itself $\Delta\sigma > 0$ is positive independently of the sign of σ_1.

An important qualitative feature of this shift is that it depends explicitly on σ_0 and thus it depends on the exact configuration of the states ψ_1 and ψ_0.

Considering thus two types of transitions so that for

$$\psi_2 \to \psi_0, \quad \sigma_0 = \sigma_0^{(2)},$$
$$\psi_1 \to \psi_0, \quad \sigma_0 = \sigma_0^{(1)}.$$

($\sigma_0^{(1)}$, $\sigma_0^{(2)}$ the respective parameters defined further above).

In case of degenerancy we may have

$$\Omega_{20} = \Omega_{10}.$$

However, even if the supposition concerning σ_0 given in [1] is strictly correct we may have independently

$$\sigma_0^{(2)} \neq \sigma_0^{(1)}.$$

In the latter case the corresponding shifts are also different, i.e.

$$\Delta\sigma^{(2)} \neq \Delta\sigma^{(1)} .$$

Thus owing to the interaction of the system with its own radiation field, the frequency shift depends on the distributions $\varphi_0(s)$ and $\varphi_1(s)$. Appart from small terms it is proportional to the expression

$$| \int \varphi_0^*(\mathbf{s}) \operatorname{grad} \varphi_1(\mathbf{s}) |^2,$$

i.e. to what is taken as the "transition probability" in the usual terminology.

The above effect qualitatively resembles the Lamb shift. Indeed, in case of the H-atom the transitions

$$^2P_{3/2} \rightarrow {}^1S_{1/2} ,$$
$$^2S_{1/2} \rightarrow {}^1S_{1/2}$$

possess exactly the same combination frequency. Nevertheless, the two transitions produce emission of slightly different frequencies. This difference is the Lamb shift. We see that an effect qualitatively of this kind follows from the strict solutions of the system of simultaneous equations consisting of wave equations and classical equations.

A qualitative comparison of the observed Lamb shift and the frequency change $\Delta\sigma_2$ calculated here is not possible at this stage – as the real process can only be dealt with considering the simultaneous transitions of an excited state into a number of lower states. This is a problem we hope to come back to shortly.

REFERENCES

1. L. JÁNOSSY and M. ZIEGLER-NÁRAY, Acta Phys. Hung., **42**, 173, 1977.

Acta Physica Academiae Scientiarum Hungaricae, Tomus 43 (3—4), pp. 293—318 (1977)

CONTRIBUTION TO THE INTENSITY DISTRIBUTIONS OF THE MULTIPLET BANDS IN DIATOMIC MOLECULES I

By

I. KOVÁCS and I. PÉCZELI
DEPARTMENT OF ATOMIC PHYSICS, TECHNICAL UNIVERSITY, BUDAPEST

(Received 3. I. 1978)

Explicit expressions are obtained for the intensity distribution in the branches of sextet transitions of any type with $\Delta\Lambda = 0$ and $\Delta\Lambda = \pm 1$ where the upper and lower electronic states may belong to one of the limiting Hund's cases a) or b). Moreover, general formulae are given for the transitions of any type and any multiplicity where both the upper and lower electronic states may belong to the same limiting case.

1. Introduction

In the case of spin multiplets formulae of the intensity distributions (line strengths, Hönl-London factors) for transitions between terms of any type are known in general form only for doublet and triplet transitions where both the upper and lower electronic states may belong to a coupling case intermediate between Hund's cases a) and b) [1]. For transitions between terms of higher than triplet multiplicity formulas have been worked out till now only for special cases, namely for $\Sigma - \Sigma$, $\Pi - \Pi$ and $\Pi - \Sigma$ transitions where the upper and lower electronic states may belong only to one of the limiting cases a) or b). In addition, in the case of (a)—(b) transitions formulae for the intensity factors of several branches with significant intensity have not been published yet and the list of the intensity factors for (b)—(b) transitions is not complete either [2]. Recently one of the authors (I. K.) eliminated this lack for ${}^5\Pi - {}^5\Pi$ transition [3]. Lately PUILLY, SCHAMPS, LUMELY and BARROW [4] observed and analyzed a ${}^6\Pi - {}^6\Delta$ and ${}^6\Delta - {}^6\Phi$ transition on the spectra of iron monofluoride (FeF). The formulae of the line strengths for these transitions are not known so far, which makes it necessary to give the line strengths also for these transitions. Instead of the formulae of the line strengths of the ${}^6\Pi - {}^6\Delta$ and ${}^6\Phi - {}^6\Delta$ transitions, however, general formulae will be given for all branches of the sextet transitions of any type with $\Delta\Lambda = 0$ and $\Delta\Lambda = \pm 1$ where the upper and lower terms may belong to one of the limiting cases a) or b). These formulae give after substitution of the proper Λ values the line strengths of all branches for $\Sigma - \Sigma$, $\Pi - \Pi$, $\Delta - \Delta \ldots$ and $\Pi - \Sigma$, $\Delta - \Pi$, $\Phi - \Delta \ldots$ transitions completing with the line strengths of the lacking branch-

es the $\Pi - \Pi$ and $\Pi - \Sigma$ transitions already published. Moreover, general formulae are published for the transitions of *any type* and *any multiplicity* where both the upper and lower electronic states may belong to the same limiting coupling case (e.g. (a)–(a) or (b)–(b) transition). Algebraic expressions where both states may belong to a coupling case intermediate between Hund's cases a) and b) in general form would be very complicated. For a given transition of higher than triplet multiplicity with the known value of the coupling constant Y, however, numerical values of the line strengths for each value of the rotational quantum number can be calculated by the numerical diagonalization of the Hamiltonian with the aid of electronic computer (e.g. LAMBERT, GAURE, ALBRITTON [5] for the $b^4\Sigma_g - a^4\Pi_n$ transition of O_2^+ molecule).

2. Intensity distribution

In case of the thermal equilibrium the intensity of an emission line can be written

$$I_{J''}^{J'} = GS_{J'J''} e^{-\frac{hcF_{J'}}{kT}}, \tag{1}$$

where G can be regarded as constant to a good approximation within a particular band and $S_{J'J''}$ is the line strength. Thus the intensities of the spectral lines within a band, apart from the Boltzmann factor, written explicitly, depend only on the line strength. The theoretical prediction of these line strengths is therefore of considerable importance. For this the corresponding expressions for the amplitudes

$$\begin{aligned} z_a({}^{2S+1}X_{J',\Omega,M'} {}^{2S+1}X_{J'',\Omega,M''}) &= \int \psi_a^*({}^{2S+1}X_{J',\Omega,M'}) z\psi_a({}^{2S+1}X_{J'',\Omega,M''})\, d\tau, \\ z_a({}^{2S+1}X_{J',\Omega\pm1,M'} {}^{2S+1}X_{J'',\Omega,M''}) &= \int \psi_a^* ({}^{2S+1}X_{J',\Omega\pm1,M'}) z\psi_a({}^{2S+1}X_{J'',\Omega,M''})\, d\tau \end{aligned} \tag{2}$$

are used, the absolute values of which may be found among others in a paper by KRONIG [6]. As can be shown over and above $\Delta J = 0, \pm 1$ the selection rule relating to (2) is $\Delta\Omega = 0$ and ± 1, respectively. Since in the Hund's case a) the selection rule $\Delta\Sigma = 0$ also holds, the above relations are equivalent to the selection rule $\Delta\Lambda = 0$ and ± 1. The threefold square of (2) summed over the magnetic quantum numbers M gives the $S_{J'J''}$ factors to the transition ${}^{2S+1}X_\Lambda - {}^{2S+1}X_\Lambda$ and ${}^{2S+1}X_{\Lambda\pm1} - {}^{2S+1}Y_\Lambda$ where both the upper and the lower electronic state may belong to the Hund's case a). These are to be found for the case of sextet transition in the second and third column of the Tables I and II, respectively and in general form for transition ${}^{2S+1}X_\Lambda(a) - {}^{2S+1}X_\Lambda(a)$ and ${}^{2S+1}X_{\Lambda\pm1}(a) - {}^{2S+1}Y_\Lambda(a)$ in the second and third column of the Tables III and IV, respectively.

The multiplet terms where $\Lambda > 0$ can in general be well described by the formulae of Hund's case a) only in the range of the lower rotational quantum numbers. With increasing rotational quantum numbers, namely, the transition starts toward the case b) while the multiplet Σ terms ($\Lambda = 0$) already in the range of the lower rotational quantum numbers also belong to the Hund's case b). The difficulty in describing the conditions consists in that no algebraic expressions are known concerning the multiplet energies ($\Lambda > 0$) higher than quartet valid with a satisfactory accuracy for any value of the coupling constant. Thus we have to restrict ourselves to the knowledge of the energies of the relatively simple case b), and to the amplitudes produced by the use of the proper transformation matrix elements calculated with their aid

$$\begin{aligned} z(^{2S+1}X_{J'\Omega'M'}\,{}^{2S+1}X_{J''\Omega''M''}) &= \int \psi_a^*(^{2S+1}X_{J'\Omega'M'})\, z\psi_b(^{2S+1}X_{J''N''M''})\, d\tau, \\ z(^{2S+1}X_{J'N'M'}\,{}^{2S+1}X_{J''\Omega''M''}) &= \int \psi_b^*(^{2S+1}X_{J'N'M'})\, z\psi_a(^{2S+1}X_{J''\Omega''M''})\, d\tau, \\ z(^{2S+1}X_{J'N'M'}\,{}^{2S+1}X_{J''N''M''}) &= \int \psi_b^*(^{2S+1}X_{J'N'M'})\, z\psi_a(^{2S+1}X_{J''N''M''})\, d\tau, \end{aligned} \tag{3a}$$

and

$$\begin{aligned} z(^{2S+1}X_{J'\Omega'M'}\,{}^{2S+1}Y_{J''N''M''}) &= \int \psi_a^*(^{2S+1}X_{J'\Omega'M'})\, z\psi_b(^{2S+1}Y_{J''N''M''})\, d\tau\,, \\ z(^{2S+1}X_{J'N'M'}\,{}^{2S+1}Y_{J''\Omega''M''}) &= \int \psi_b^*(^{2S+1}X_{J'N'M'})\, z\psi_a(^{2S+1}Y_{J''\Omega''M''})\, d\tau, \\ z(^{2S+1}X_{J'N'M'}\,{}^{2S+1}Y_{J''N''M''}) &= \int \psi_b^*(^{2S+1}X_{J'N'M'})\, z\psi_b(^{2S+1}Y_{J''N''M''})\, d\tau, \end{aligned} \tag{3b}$$

where

$$\begin{aligned} \psi_b(^{2S+1}X_{J'N'M'}) &= \sum_{\Omega'=\Lambda'-S}^{\Lambda'+S} S_{\Omega'N'}(J')\psi_a(^{2S+1}X_{J'\Omega'M'})\,, \\ \psi_b(^{2S+1}Y_{J''N''M''}) &= \sum_{\Omega''=\Lambda''-S}^{\Lambda''+S} S_{\Omega''N''}(J'')\psi_a(^{2S+1}Y_{J''\Omega''M''})\,. \end{aligned} \tag{4}$$

The elements of the transformation matrix of sextet terms of any type are the following

$$S_{\Lambda-5/2,J-5/2} = +\sqrt{\frac{u_3^- u_4^- u_5^- u_6^- u_7^-}{2C_{J-5/2}(J)}}\,;\quad S_{\Lambda-3/2,J-5/2} = -\sqrt{\frac{5u_3^- u_4^- u_5^- u_6^- u_3^+}{2C_{J-5/2}(J)}}$$

$$S_{\Lambda-1/2,J-5/2} = +\sqrt{\frac{5\,u_3^- u_4^- u_5^- u_3^+ u_4^+}{C_{J-5/2}(J)}}\,;\quad S_{\Lambda+1/2,J-5/2} = -\sqrt{\frac{5\,u_3^- u_4^- u_3^+ u_4^+ u_5^+}{C_{J-5/2}(J)}}\,;$$

$$S_{\Lambda+3/2,J-5/2} = +\sqrt{\frac{5\,u_3^- u_3^+ u_4^+ u_5^+ u_6^+}{2C_{J-5/2}(J)}}\,;\quad S_{\Lambda+5/2,J-5/2} = -\sqrt{\frac{u_3^+ u_4^+ u_5^+ u_6^+ u_7^+}{2\,C_{J-5/2}(J)}}\,;$$

$$S_{\Lambda-5/2.J-3/2} = + \sqrt{\frac{5u_4^- u_5^- u_6^- u_7^- u_3^+}{2C_{J-3/2}(J)}}\ ;\ S_{\Lambda-3/2,J-3/2} = - \sqrt{\frac{(3u_3^+ + 2\Lambda)^2 u_4^- u_5^- u_6^-}{2C_{J-3/2}(J)}}\ ;$$

$$S_{\Lambda-1/2,J-3/2} = + \sqrt{\frac{(u_3^+ + 4\Lambda)^2 u_4^- u_5^- u_4^+}{C_{J-3/2}(J)}}\ ;\ S_{\Lambda+1/2\,J-3/2} = + \sqrt{\frac{(u_3^+ - 4\Lambda)^2 u_4^- u_4^+ u_5^+}{C_{J-3/2}(J)}}\ ;$$

$$S_{\Lambda+3/2,J-3/2} = - \sqrt{\frac{(3u_3^- - 2\Lambda)^2 u_4^+ u_5^+ u_6^+}{2C_{J-3/2}(J)}}\ ;\ S_{\Lambda+5/2,J-3/2} = + \sqrt{\frac{5u_3^- u_4^+ u_5^+ u^+ u_7^+}{2C_{J-3/2}(J)}}\ ; \qquad (5a)$$

$$S_{\Lambda-5/2,J-1/2} = - \sqrt{\frac{5\,u_5^- u_6^- u_7^- u_3^+ u_4^+}{C_{J-1/2}(J)}}\ ;\ S_{\Lambda-3/2,J-1/2} = + \sqrt{\frac{(u_1^- + 4\Lambda)^2 u_5^- u_6^- u_4^+}{C_{J-1/2}(J)}}\ ;$$

$$S_{\Lambda-1/2,J-1/2} = + \sqrt{\frac{2[u_4^- u_6^- - 3\Lambda(2\Lambda-1)]^2 u_5^-}{C_{J-1/2}(J)}}\ ;$$

$$S_{\Lambda+1/2,J-1/2} = - \sqrt{\frac{2[u_4^+ u_6^+ - 3\Lambda(2\Lambda+1)]^2 u_5^+}{C_{J-1/2}(J)}}\ ;$$

$$S_{\Lambda+3/2,J-1/2} = - \sqrt{\frac{(u_1^- - 4\Lambda)^2 u_4^- u_5^+ u_6^+}{C_{J-1/2}(J)}}\ ;\ S_{J+5/2,J-1/2} = + \sqrt{\frac{5u_3^- u_4^- u_5^+ u_6^+ u_7^+}{C_{J-1/2}(J)}}\ ;$$

$$S_{\Lambda-5/2,J+1/2} = - \sqrt{\frac{(5\,u_6^- u_7^- u_3^+ u_4^+ u_5^+}{C_{J+1/2}(J)}}\ ;\ S_{\Lambda-3/2,J+1/2} = - \sqrt{\frac{(u_9^- - 4\Lambda)^2\, u_6^- u_4^+ u_5^+}{C_{J+1/2}(J)}}\ ;$$

$$S_{\Lambda-1/2,J+1/2} = + \sqrt{\frac{2[u_4^+ u_6^+ - 3\Lambda(2\Lambda-1)]^2 u_5^+}{C_{J+1/2}(J)}}\ ;$$

$$S_{\Lambda+1/2,J+1/2} = + \sqrt{\frac{2[u_4^- u_6^- - 3\Lambda(2\Lambda+1)]^2\, u_5^-}{C_{J+1/2}(J)}}\ ;$$

$$S_{\Lambda+3/2.J+1/2} = - \sqrt{\frac{(u_9^+ + 4\Lambda)^2 u_4^- u_5^- u_6^+}{C_{J+1/2}(J)}}\ ;\ S_{\Lambda+5/2,J+1/2} = - \sqrt{\frac{5\,u_3^- u_{1\frac{1}{2}}^- u_5^- u_6^+ u_7^+}{C_{J+1/2}(J)}}\ ;$$

$$S_{\Lambda-5/2,J+3/2} = - \sqrt{\frac{5u_7^- u_3^+ u_4^+ u_5^+ u_6^+}{2C_{J+3/2}(J)}}\ ;\ S_{\Lambda-3/2,J+3/2} = - \sqrt{\frac{(3u_7^- - 2\Lambda)^2 u_4^+ u_5^+ u_6^+}{2C_{J+3/2}(J)}}\ ;$$

$$S_{\Lambda-1/2,J+3/2} = - \sqrt{\frac{(u_7^- - 4\Lambda)^2 u_6^- u_5^+ u_6^+}{C_{J+3/2}(J)}}\ ;\ S_{\Lambda+1/2,J+3/2} = + \sqrt{\frac{(u_7^+ + 4\Lambda)^2 u_5^- u_6^- u_6^+}{C_{J+3/2}(J)}}\ ;$$

$$S_{\Lambda+3/2,J+3+2} = + \sqrt{\frac{(3u_7^+ + 2\Lambda)^2 u_4^- u_5^- u_6^-}{2C_{J+3/2}(J)}}\ ;\ S_{\Lambda+5/2,J+3/2} = + \sqrt{\frac{5\,u_3^- u_4^- u_5^- u_6^- u_7^+}{2\,C_{J+3/2}(J)}}$$

$$S_{\Lambda-5/2,J+5/2} = -\sqrt{\frac{u_3^+ u_4^+ u_5^+ u_6^+ u_7^-}{2C_{J+5/2}(J)}}\ ;\ S_{\Lambda-3/2,J+5/2} = -\sqrt{\frac{5u_7^- u_4^+ u_5^+ u_6^+ u_7^+}{2C_{J+5/2}(J)}}\ ;$$

$$S_{\Lambda-1/2,J+5/2} = -\sqrt{\frac{5u_6^- u_7^- u_5^+ u_6^+ u_7^+}{C_{J+5/2}(J)}}\ ;\ S_{\Lambda+1/2,J+5/2} = -\sqrt{\frac{5u_5^- u_6^- u_7^- u_6^+ u_7^+}{C_{J+5/2}(J)}}\ ;$$

$$S_{\Lambda+3/2,J+5/2} = -\sqrt{\frac{5u_4^- u_5^- u_6^- u_7^- u_7^+}{2C_{J+5/2}(J)}}\ ;\ S_{\Lambda+5/2,J+5/2} = -\sqrt{\frac{u_3^- u_4^- u_5^- u_6^- u_7^-}{2C_{J+5/2}(J)}}$$

where $u_{n+1}^{\pm} = u_n^{\pm} + 1$ and $u_{-1}^{\pm} = J \pm \Lambda - 11/2$

$$\begin{aligned}
C_{J-5/2}(J) &= 2(J-1)J(2J-3)(2J-\Lambda)(2J+1),\\
C_{J-3/2}(J) &= 2J(J+1)(2J-3)(2J-1)(2J+1),\\
C_{J-1/2}(J) &= 2(J-1)(J+1)(2J-1)(2J+1)(2J+3),\\
C_{J+1/2}(J) &= 2J(J+2)(2J-1)(2J+1)(2J+3),\\
C_{J+3/2}(J) &= 2J(J+1)(2J+1)(2J+3)(2J+5),\\
C_{J+5/2}(J) &= 2(J+1)(J+2)(2J+1)(2J+3)(2J+5).
\end{aligned} \tag{5b}$$

After substitution of 0, 1, 2, . . . for the value Λ these formulae give the transformation matrix elements for ${}^6\Sigma$, ${}^6\Pi$, ${}^6\Delta$, . . . terms.

The threefold square of (3a) and (3b) summed over the magnetic quantum numbers gives the line strengths referring to the transition ${}^6X_\Lambda(a) - {}^6X_\Lambda(b)$, ${}^6X_\Lambda(b) - {}^6X_\Lambda(b)$ and ${}^6X_{\Lambda+1}(a) - {}^6Y_\Lambda(b)$, ${}^6X_{\Lambda+1}(b) - {}^6Y_\Lambda(a)$, ${}^6X_{\Lambda+1}(b) - {}^6Y_\Lambda(b)$ that is to the sextet transitions of any type which are to be found in the third and fifth column in Table I, and in the fourth, fifth and sixth column in Table II, respectively and in general form referring to the transitions of any type and multiplicity ${}^{2S+1}X_\Lambda(b) - {}^{2S+1}X_\Lambda(b)$ and ${}^{2S+1}X_{\Lambda+1}(b) - {}^{2S+1}Y_\Lambda(b)$ in the third column in Table III and the fourth column in Table IV, respectively. In the case of the $(b) - (b)$ transition of any type and multiplicity we have used the amplitude factors determined by HILL and VAN VLECK [6] starting directly from Hund's case b).

For $(a) - (a)$ transition due to the $\Delta\Sigma = 0$ selection rule there are $3(2S+1)$ branches, the so called main branches, the intensities of which differ from zero. In the case of $(a) - (b)$ transition the selection rule $\Delta\Sigma = 0$ is no longer valid and the selection rule of $(b) - (b)$ transition $\Delta N = 0, \pm 1$ is not valid yet, solely the $\Delta J = 0, \pm 1$. Therefore all the $3(2S+1)^2$ branches appear and the intensities are dispersed over all branches (see for the dispersion of quintet transition [5]). This fact makes it necessary to give the line strengths of all the $3(2S+1)^2$ (for sextet transition 108) branches. For $(b) - (b)$ transi-

Table I

Line strengths for ${}^6X_\Lambda - {}^6X_\Lambda$ transitions

Branches	Line strengths			
	${}^6X(a) - {}^6X(a)$	${}^6X(a) - {}^6X(b)$	${}^6X(b) - {}^6X(a)$	${}^6X(b) - {}^6X(b)$
$P_1(J)$	$\dfrac{u_7^- u_2^+}{J}$	$\dfrac{u_3^- u_4^- u_5^- u_6^- u_7^{-2} u_2^+}{2C_1(P)}$	$R_1(J-1)$	$\dfrac{u_2^- u_2^+(2J+1)}{(J-2)(2J-5)}$
$Q_1(J)$	$\left(\Lambda - \dfrac{5}{2}\right)^2 \dfrac{2(J+1/2)}{J(J+1)}$	$\left(\Lambda - \dfrac{5}{2}\right)^2 \dfrac{u_3^- u_4^- u_5^- u_6^- u_7^-}{C_1(Q)}$	$Q_1(J)$	$\Lambda^2 \dfrac{4(J+1)(2J+1)}{J(2J-3)^2}$
$R_1(J)$	$\dfrac{u_8^- u_3^+}{J+1}$	$\dfrac{u_3^- u_4^- u_5^- u_6^- u_7^- u_8^- u_3^+}{2C_1(R)}$	$P_1(J+1)$	$\dfrac{u_3^- u_3^+(2J+3)}{(J-1)(2J-3)}$
${}^QP_{21}(J)$	0	$\dfrac{5u_3^- u_4^- u_5^- u_6^{-2} u_3^{+2}}{2C_1(P)}$	${}^QR_{12}(J-1)$	$\Lambda^2 \dfrac{20(2J+1)}{J(2J-5)(2J-3)^2}$
${}^RQ_{21}(J)$	0	$\left(\Lambda - \dfrac{3}{2}\right)^2 \dfrac{5u_3^- u_4^- u_5^- u_6^- u_3^+}{C_1(Q)}$	${}^PQ_{12}(J)$	$\dfrac{5u_3^- u_3^+(2J+1)}{(J-1)J(2J-3)^2}$
${}^SR_{21}(J)$	0	$\dfrac{5u_3^- u_4^- u_5^- u_6^- u_7^- u_3^+ u_4^+}{2C_1(R)}$	${}^OP_{12}(J+1)$	0
${}^RP_{31}(J)$	0	$\dfrac{5u_3^- u_4^- u_5^{-2} u_3^+ u_4^{+2}}{C_1(P)}$	${}^PR_{13}(J-1)$	$\dfrac{10u_3^- u_3^+}{(J-2)(J-1)J(2J-3)^2}$
${}^SQ_{31}(J)$	0	$\left(\Lambda - \dfrac{1}{2}\right)^2 \dfrac{10u_3^- u_4^- u_5^- u_3^+ u_4^+}{C_1(Q)}$	${}^OQ_{13}(J)$	0
${}^TR_{31}(J)$	0	$\dfrac{5u_3^- u_4^- u_5^- u_6^- u_3^+ u_4^+ u_5^+}{C_1(R)}$	${}^NP_{13}(J+1)$	0
${}^SP_{41}(I)$	0	$\dfrac{5u_3^- u_4^{-2} u_3^+ u_4^+ u_5^{+2}}{C_1(P)}$	${}^OR_{14}(J-1)$	0
${}^TQ_{41}(J)$	0	$\left(\Lambda + \dfrac{1}{2}\right)^2 \dfrac{10u_3^- u_4^- u_3^+ u_4^+ u_5^+}{C_1(Q)}$	${}^NQ_{14}(J)$	0
${}^UR_{41}(J)$	0	$\dfrac{5u_3^- u_4^- u_5^- u_3^+ u_4^+ u_5^+ u_6^+}{C_1(R)}$	${}^MP_{14}(J+1)$	0

${}^{T}P_{51}(J)$	0	$\frac{5u_3^{-2}u_3^{+}u_4^{+}u_5^{+}u_6^{+2}}{2C_1(R)}$	${}^{N}R_{15}(J-1)$	0
${}^{U}Q_{51}(J)$	0	$\left(\Lambda+\frac{3}{2}\right)^2\frac{5u_3^{-}u_3^{+}u_4^{+}u_5^{+}u_6^{+}}{C_1(Q)}$	${}^{M}Q_{15}(J)$	0
${}^{V}R_{51}(J)$	0	$\frac{5u_3^{-}u_4^{-}u_3^{+}u_4^{+}u_5^{+}u_6^{+}u_7^{+}}{2C_1(R)}$	${}^{L}P_{15}(J+1)$	0
${}^{U}P_{61}(J)$	0	$\frac{u_2^{-}u_3^{+}u_4^{+}u_5^{+}u_6^{+}u_7^{+2}}{2C_1(P)}$	${}^{M}R_{16}(J-1)$	0
${}^{V}Q_{61}(J)$	0	$\left(\Lambda+\frac{5}{2}\right)^2\frac{u_3^{+}u_4^{+}u_5^{+}u_6^{+}u_7^{+}}{C_1(Q)}$	${}^{L}Q_{16}(J)$	0
${}^{W}R_{61}(J)$	0	$\frac{u_3^{-}u_3^{+}u_4^{+}u_5^{+}u_6^{+}u_7^{+}u_8^{+}}{2C_1(R)}$	${}^{K}P_{16}(J+1)$	0
${}^{O}P_{12}(J)$	0	$\frac{5u_4^{-}u_5^{-}u_6^{-}u_7^{-2}u_2^{+}u_3^{+}}{2C_2(P)}$	${}^{S}R_{21}(J-1)$	0
${}^{P}Q_{12}(J)$	0	$\left(\Lambda-\frac{5}{2}\right)^2\frac{5u_4^{-}u_5^{-}u_6^{-}u_7^{-}u_3^{+}}{C_2(Q)}$	${}^{R}Q_{21}(J)$	$\frac{5u_3^{-}u_3^{+}(2J+1)}{(J-1)J(2J-3)^2}$
${}^{Q}R_{12}(J)$	0	$\frac{5u_4^{-}u_5^{-}u_6^{-}u_7^{-}u_8^{-}u_3^{+2}}{2C_2(R)}$	${}^{Q}P_{21}(J+1)$	$\Lambda^2\frac{20(2J+3)}{(J+1)(2J-3)(2J-1)^2}$
$P_2(J)$	$\frac{u_6^{-}u_3^{+}}{J}$	$\frac{(3u_3^{+}+2\Lambda)^2u_4^{-}u_5^{-}u_6^{-2}u_3^{+}}{2C_2(P)}$	$R_2(J-1)$	$\frac{(J+1)u_3^{-}u_3^{+}(2J-5)(2J+1)}{(J-1)J(2J-3)^2}$
$Q_2(J)$	$\left(\Lambda-\frac{3}{2}\right)^2\frac{2(J+1/2)}{J(J+1)}$	$\left(\Lambda-\frac{3}{2}\right)^2\frac{(3u_3^{+}+2\Lambda)^2u_4^{-}u_5^{-}u_6^{-}}{C_2(Q)}$	$Q_2(J)$	$\Lambda^2\frac{4(2J^2-J-8)^2(2J+1)}{J(J+1)(2J-3)^2(2J-1)^2}$
$R_2(J)$	$\frac{u_7^{-}u_4^{+}}{J+1}$	$\frac{(3u_3^{+}+2\Lambda)^2u_4^{-}u_5^{-}u_6^{-}u_7^{-}u_4^{+}}{2C_2(R)}$	$P_2(J+1)$	$\frac{(J+2)u_4^{-}u_4^{+}(2J-3)(2J+3)}{J(J+1)(2J-1)^2}$
${}^{Q}P_{32}(J)$	0	$\frac{(u_3^{+}+4\Lambda)^2u_4^{-}u_5^{-2}u_4^{+2}}{C_2(P)}$	${}^{Q}R_{23}(J-1)$	$\Lambda^2\frac{128(J-2)(J+1)}{J(2J-3)^2(2J-1)^2}$
${}^{R}Q_{32}(J)$	0	$\left(\Lambda-\frac{1}{2}\right)^2\frac{2(u_3^{+}+4\Lambda)^2u_4^{-}u_5^{-}u_4^{+}}{C_2(Q)}$	${}^{P}Q_{23}(J)$	$\frac{2u_4^{-}u_4^{+}(2J-3)(2J+1)(2J+3)}{(J-1)J^2(J+1)(2J-1)^2}$

Table I (continued)

Branches	Line strengths			
	${}^{6}X(a) - {}^{6}X(a)$	${}^{6}X(a) - {}^{6}X(b)$	${}^{6}X(b) - {}^{6}X(a)$	${}^{6}X(b) - {}^{6}X(b)$
${}^{S}R_{32}(J)$	0	$\frac{(u_3^+ + 4\Lambda)^2 u_4^- u_5^- u_6^- u_4^+ u_5^+}{C_2(R)}$	${}^{O}P_{32}(J+1)$	0
${}^{R}P_{42}(J)$	0	$\frac{(u_3^- - 4\Lambda)^2 u_4^{-2} u_4^+ u_5^{+2}}{C_2(P)}$	${}^{P}R_{24}(J-1)$	$\frac{18 u_4^- u_4^+}{(J-1)J^2(2J-1)^2}$
${}^{S}Q_{42}(J)$	0	$\left(\Lambda + \frac{1}{2}\right)^2 \frac{2(u_3^- - 4\Lambda)^2 u_4^- u_4^+ u_5^+}{C_2(Q)}$	${}^{O}Q_{24}(J)$	0
${}^{T}R_{42}(J)$	0	$\frac{(u_3^- - 4\Lambda)^2 u_4^- u_5^- u_4^+ u_5^+ u_6^+}{C_2(R)}$	${}^{N}P_{24}(J+1)$	0
${}^{S}P_{52}(J)$	0	$\frac{(3u_3^- - 2\Lambda)^2 u_3^- u_4^+ u_5^+ u_6^{+2}}{2C_2(P)}$	${}^{O}R_{25}(J-1)$	0
${}^{T}Q_{52}(J)$	0	$\left(\Lambda + \frac{3}{2}\right)^2 \frac{(3u_3^- - 2\Lambda)^2 u_4^+ u_5^+ u_6^+}{C_2(Q)}$	${}^{N}Q_{25}(J)$	0
${}^{U}R_{52}(J)$	0	$\frac{(3u_3^- - 2\Lambda)^2 u_4^- u_4^+ u_5^+ u_6^+ u_7^+}{2C_2(R)}$	${}^{M}P_{25}(J+1)$	0
${}^{T}P_{62}(J)$	0	$\frac{5u_2^- u_3^- u_4^+ u_5^+ u_6^+ u_7^{+2}}{2C_2(P)}$	${}^{N}R_{26}(J-1)$	0
${}^{U}Q_{62}(J)$	0	$\left(\Lambda + \frac{5}{2}\right)^2 \frac{5u_3^- u_4^+ u_5^+ u_6^+ u_7^+}{C_2(Q)}$	${}^{M}Q_{26}(J)$	0
${}^{V}R_{62}(J)$	0	$\frac{5u_4^{-2} u_4^+ u_5^+ u_6^+ u_7^+ u_8^+}{2C_2(R)}$	${}^{L}P_{26}(J+1)$	0
${}^{N}P_{13}(J)$	0	$\frac{5u_5^- u_6^- u_7^{-2} u_2^+ u_3^+ u_4^+}{C_3(P)}$	${}^{T}R_{31}(J-1)$	0
${}^{O}Q_{13}(J)$	0	$\left(\Lambda - \frac{5}{2}\right)^2 \frac{10u_5^- u_6^- u_7^- u_3^+ u_4^+}{C_3(Q)}$	${}^{S}Q_{31}(J)$	0
${}^{P}R_{13}(J)$	0	$\frac{5u_5^- u_6^- u_7^+ u_8^- u_3^{+2} u_4^+}{C_3(R)}$	${}^{R}P_{31}(J+1)$	$\frac{10 u_4^- u_4^+}{(J-1)J(J+1)(2J-1)^2}$

${}^{O}P_{23}(J)$	0	$\dfrac{(u_1^+ + 4\Lambda)^2\, u_5^- u_6^{-2} u_3^+ u_4^+}{C_3(P)}$	${}^{S}R_{32}(J-1)$	0
${}^{P}Q_{23}(J)$	0	$\left(\Lambda - \dfrac{3}{2}\right)^2 \dfrac{2(u_1^+ + 4\Lambda)^2\, u_5^- u_6^- u_4^+}{C_3(Q)}$	${}^{R}Q_{32}(J)$	$\dfrac{2u_4^- u_4^+(2J-3)(2J+1)(2J+3)}{(J-1)J^2(J+1)(2J-1)}$
${}^{Q}R_{23}(J)$	0	$\dfrac{(u_1^+ + 4\Lambda)^2\, u_5^- u_6^- u_7^- u_4^{+2}}{C_3(R)}$	${}^{Q}P_{32}(J+1)$	$\Lambda^2 \dfrac{128(J-1)(J+2)}{(J+1)(2J-1)^2(2J+1)^2}$
$P_3(J)$	$\dfrac{u_6^- u_3^+}{J}$	$\dfrac{2[u_4^- u_6^- - 3\Lambda(2\Lambda-1)]^2\, u_5^{-2} u_4^+}{C_3(P)}$	$R_3(J-1)$	$\dfrac{(J-2)(J+1)\, u_4^- u_4^+(2J-3)(2J+3)}{(J-1)J^2(2J-1)^2}$
$Q_3(J)$	$\left(\Lambda - \dfrac{3}{2}\right)^2 \dfrac{2(J+1/2)}{J(J+1)}$	$\left(\Lambda - \dfrac{1}{2}\right)^2 \dfrac{4[u_4^- u_6^- - 3\Lambda(2\Lambda-1)]^2\, u_5^-}{C_3(Q)}$	$Q_3(J)$	$\Lambda^2 \dfrac{4(2J^2+J-9)^2}{J(J+1)(2J-1)^2(2J+1)}$
$R_3(J)$	$\dfrac{u_7^- u_4^+}{J+1}$	$\dfrac{2[u_4^- u_6^- - 3\Lambda(2\Lambda-1)]^2\, u_5^- u_6^- u_5^+}{C_3(R)}$	$P_3(J+1)$	$\dfrac{(J-1)(J+2)\, u_5^- u_5^+(2J-1)(2J+5)}{J(J+1)^2(2J+1)^2}$
${}^{Q}P_{43}(J)$	0	$\dfrac{2[u_4^+ u_6^+ - 3\Lambda(2\Lambda+1)]^2\, u_4^- u_5^{+2}}{C_3(P)}$	${}^{Q}R_{34}(J-1)$	$\Lambda^2 \dfrac{36(2J-3)(2J+3)}{J(2J-1)^2(2J+1)^2}$
${}^{R}Q_{43}(J)$	0	$\left(\Lambda + \dfrac{1}{2}\right)^2 \dfrac{4[u_4^+ u_6^+ - 3\Lambda(2\Lambda+1)]^2\, u_5^+}{C_3(Q)}$	${}^{P}Q_{34}(J)$	$\dfrac{9(J-1)(J+2)\, u_5^- u_5^+}{J^2(J+1)^2(2J+1)}$
${}^{S}R_{43}(J)$	0	$\dfrac{2[u_4^+ u_6^+ - 3\Lambda(2\Lambda+1)]^2\, u_5^- u_5^+ u_6^+}{C_3(R)}$	${}^{O}P_{34}(J+1)$	0
${}^{R}P_{53}(J)$	0	$\dfrac{(u_1^- - 4\Lambda)^2\, u_3^- u_4^- u_5^+ u_6^{+2}}{C_3(P)}$	${}^{P}R_{35}(J-1)$	$\dfrac{18u_5^- u_5^+}{J^2(J+1)(2J+1)^2}$
${}^{S}Q_{53}(J)$	0	$\left(\Lambda + \dfrac{3}{2}\right)^2 \dfrac{2(u_1^- - 4\Lambda)^2\, u_4^- u_5^+ u_6^+}{C_3(Q)}$	${}^{O}Q_{35}(J)$	0
${}^{T}R_{53}(J)$	0	$\dfrac{(u_1^- - 4\Lambda)^2\, u_4^{-2} u_5^+ u_6^+ u_7^+}{C_3(R)}$	${}^{N}P_{35}(J+1)$	0
${}^{S}P_{63}(J)$	0	$\dfrac{5u_2^- u_3^- u_4^- u_5^+ u_6^+ u_7^{+2}}{C_3(P)}$	${}^{O}R_{36}(J-1)$	0
${}^{T}Q_{63}(J)$	0	$\left(\Lambda + \dfrac{5}{2}\right)^2 \dfrac{10u_3^- u_4^- u_5^+ u_6^+ u_7^+}{C_3(Q)}$	${}^{N}Q_{36}(J)$	0
${}^{U}R_{63}(J)$	0	$\dfrac{5u_3^{-2} u_4^- u_5^+ u_6^+ u_7^+ u_8^+}{C_3(R)}$	${}^{M}P_{36}(J+1)$	0

Table I (continued)

Branches	Line strengths			
	${}^{e}X(a) - {}^{e}X(a)$	${}^{e}X(a) - {}^{e}X(b)$	${}^{e}X(b) - {}^{e}X(a)$	${}^{e}X(b) - {}^{e}X(b)$
${}^{M}P_{14}(J)$	0	$\dfrac{5u_6^- u_7^{-2} u_2^+ u_3^+ u_4^+ u_5^+}{C_4(P)}$	${}^{U}R_{41}(J-1)$	0
${}^{N}Q_{14}(J)$	0	$\left(\Lambda - \dfrac{5}{2}\right)^2 \dfrac{10u_6^- u_7^- u_3^+ u_4^+ u_5^+}{C_4(Q)}$	${}^{T}Q_{41}(J)$	0
${}^{O}R_{14}(J)$	0	$\dfrac{5u_6^- u_7^- u_8^- u_3^{+2} u_4^+ u_5^+}{C_4(R)}$	${}^{S}P_{41}(J+1)$	0
${}^{N}P_{24}(J)$	0	$\dfrac{(u_9^- - 4\Lambda)^2 u_6^{-2} u_3^+ u_4^+ u_5^+}{C_4(P)}$	${}^{T}R_{42}(J-1)$	0
${}^{O}Q_{24}(J)$	0	$\left(\Lambda - \dfrac{3}{2}\right)^2 \dfrac{2(u_9^- - 4\Lambda)^2 u_6^- u_4^+ u_8^+}{C_4(Q)}$	${}^{S}Q_{42}(J)$	0
${}^{P}R_{24}(J)$	0	$\dfrac{(u_9^- - 4\Lambda)^2 u_6^- u_7^- u_4^{+2} u_5^+}{C_4(R)}$	${}^{R}P_{42}(J+1)$	$\dfrac{18u_5^- u_5^+}{J(J+1)^2(2J+1)^2}$
${}^{O}P_{34}(J)$	0	$\dfrac{2[u_4^+ u_6^+ - 3\Lambda(2\Lambda-1)]^2 u_5^- u_4^+ u_5^+}{C_4(P)}$	${}^{S}R_{43}(J-1)$	0
${}^{P}Q_{34}(J)$	0	$\left(\Lambda - \dfrac{1}{2}\right)^2 \dfrac{4[u_4^+ u_6^+ - 3\Lambda(2\Lambda-1)]^2 u_5^+}{C_4(Q)}$	${}^{R}Q_{43}(J)$	$\dfrac{9(J-1)(J+2)\,u_5^- u_5^+}{J^2(J+1)^2(2J+1)}$
${}^{Q}R_{34}(J)$	0	$\dfrac{2[u_4^+ u_6^+ - 3\Lambda(2\Lambda-1)]^2 u_6^- u_5^{+2}}{C_4(R)}$	${}^{Q}P_{43}(J+1)$	$\Lambda^2 \dfrac{36(2J-1)(2J+5)}{(J+1)(2J+1)^2(2J+3)^2}$
$P_4(J)$	$\dfrac{u_4^- u_5^+}{J}$	$\dfrac{2[u_4^- u_6^- - 3\Lambda(2\Lambda+1)]^2 u_4^- u_5^- u_5^+}{C_4(P)}$	$R_4(J-1)$	$\dfrac{(J-1)(J+2)\,u_5^- u_5^+ (2J-3)(2J+3)}{J^2(J+1)(2J+1)^2}$
$Q_4(J)$	$\left(\Lambda + \dfrac{1}{2}\right)^2 \dfrac{2(J+1/2)}{J(J+1)}$	$\left(\Lambda + \dfrac{1}{2}\right)^2 \dfrac{4[u_4^- u_6^- - 3\Lambda(2\Lambda+1)]^2 u_5^-}{C_4(Q)}$	$Q_4(J)$	$\Lambda^2 \dfrac{4(2J^2+3J-8)^2}{J(J+1)(2J+1)(2J+3)^2}$
$R_4(J)$	$\dfrac{u_5^- u_6^+}{J+1}$	$\dfrac{2[u_4^- u_6^- - 3\Lambda(2\Lambda+1)]^2 u_5^{-2} u_6^+}{C_4(R)}$	$P_4(J+1)$	$\dfrac{J(J+3)\,u_6^- u_6^+ (2J-1)(2J+5)}{(J+1)^2(J+2)(2J+3)^2}$
${}^{Q}P_{54}(J)$	0	$\dfrac{(u_9^+ + 4\Lambda)^2 u_3^- u_4^- u_5^- u_6^{+2}}{C_4(P)}$	${}^{Q}R_{45}(J-1)$	$\Lambda^2 \dfrac{128(J-1)(J+2)}{J(2J+1)^2(2J+3)^2}$

Acta Physica Academiae Scientiarum Hungaricae 43, 1977

${}^{R}Q_{54}(J)$	0
${}^{S}R_{54}(J)$	0
${}^{R}P_{64}(J)$	0
${}^{S}Q_{64}(J)$	0
${}^{T}R_{64}(J)$	0
${}^{L}P_{15}(J)$	0
${}^{M}Q_{15}(J)$	0
${}^{N}R_{15}(J)$	0
${}^{M}P_{25}(J)$	0
${}^{N}Q_{25}(J)$	0
${}^{O}R_{25}(J)$	0
${}^{N}P_{35}(J)$	0
${}^{O}Q_{35}(J)$	0
${}^{P}R_{35}(J)$	0
${}^{O}P_{35}(J)$	0
${}^{P}Q_{45}(J)$	$\dfrac{2u_6^- u_6^+(2J-1)(2J+1)(2J+5)}{J(J+1)^2(J+2)(2J+3)^2}$
${}^{O}P_{45}(J+1)$	0
${}^{P}R_{46}(J-1)$	$\dfrac{10u_6^- u_6^+}{J(J+1)(J+2)(2J+3)^2}$
${}^{O}Q_{46}(J)$	0
${}^{N}P_{46}(J+1)$	0
${}^{V}R_{51}(J-1)$	0
${}^{U}Q_{51}(J)$	0
${}^{T}P_{51}(J+1)$	0
${}^{U}R_{52}(J-1)$	0
${}^{T}Q_{52}(J)$	0
${}^{S}P_{52}(J+1)$	0
${}^{T}R_{53}(J-1)$	0
${}^{S}Q_{53}(J)$	0
${}^{R}P_{53}(J+1)$	$\dfrac{18u_6^- u_6^+}{(J+1)^2(J+2)(2J+3)^2}$
${}^{S}R_{54}(J-1)$	0

$\left(\Lambda+\frac{3}{2}\right)^2 \dfrac{2(u_3^+ + 4\Lambda)^2 u_4^- u_5^- u_6^+}{C_4(Q)}$	
$\dfrac{(u_9^+ + 4\Lambda)^2 u_4^{-2} u_5^- u_6^+ u_7^+}{C_4(R)}$	
$\dfrac{5u_3^- u_4^- u_5^- u_6^+ u_7^{+2}}{C_4(P)}$	
$\left(\Lambda+\frac{5}{2}\right)^2 \dfrac{10u_3^- u_4^- u_5^- u_6^+ u_7^+}{C_4(Q)}$	
$\dfrac{5u_3^{-2} u_4^- u_5^- u_6^+ u_7^+ u_8^+}{C_4(R)}$	
$\dfrac{5u_7^{-2} u_2^+ u_3^+ u_4^+ u_5^+ u_6^+}{2C_5(P)}$	
$\left(\Lambda-\frac{5}{2}\right)^2 \dfrac{5u_7^- u_3^+ u_4^+ u_5^+ u_6^+}{C_5(Q)}$	
$\dfrac{5u_7^- u_8^- u_3^{+2} u_4^+ u_5^+ u_6^+}{2C_5(R)}$	
$\dfrac{(3u_7^- - 2\Lambda)^2 u_6^- u_3^+ u_4^+ u_5^+ u_6^+}{2C_5(P)}$	
$\left(\Lambda-\frac{3}{2}\right)^2 \dfrac{(3u_7^- - 2\Lambda)^2 u_4^+ u_5^+ u_6^+}{C_5(Q)}$	
$\dfrac{(3u_7^- - 2\Lambda)^2 u_7^- u_4^{+2} u_5^+ u_6^+}{2C_5(R)}$	
$\dfrac{(u_7^- - 4\Lambda)^2 u_5^- u_6^- u_4^+ u_5^+ u_6^+}{C_5(P)}$	
$\left(\Lambda-\frac{1}{2}\right)^2 \dfrac{2(u_7^- - 4\Lambda)^2 u_6^- u_5^+ u_6^+}{C_5(Q)}$	
$\dfrac{(u_7^- - 4\Lambda)^2 u_6^{-2} u_5^{+2} u_6^+}{C_5(R)}$	
$\dfrac{(u_7^+ + 4\Lambda)^2 u_4^- u_5^- u_6^- u_5^+ u_6^+}{C_5(P)}$	

Table I (continued)

Branches	Line strengths			
	${}^6X(a) - {}^6X(a)$	${}^6X(a) - {}^6X(b)$	${}^6X(b) - {}^6X(a)$	${}^6X(b) - {}^6X(b)$
${}^PQ_{45}(J)$	0	$\left(\Lambda + \frac{1}{2}\right)^2 \frac{2(u_7^+ + 4\Lambda)^2 u_5^- u_6^- u_6^+}{C_5(Q)}$	${}^RQ_{54}(J)$	$\frac{2u_6^- u_6^+(2J-1)(2J+1)(2J+5)}{J(J+1)^2(J+2)(2J+3)^2}$
${}^QR_{45}(J)$	0	$\frac{(u_7^+ + 4\Lambda)^2 u_5^{-2} u_6^- u_6^{+2}}{C_5(R)}$	${}^QP_{54}(J+1)$	$\Lambda^2 \frac{128J(J+3)}{(J+1)(2J+3)^2(2J+5)^2}$
$P_5(J)$	$\frac{u_3^- u_6^+}{J}$	$\frac{(3u_7^+ + 2\Lambda)^2 u_3^- u_4^- u_5^- u_6^+}{2C_5(P)}$	$R_5(J-1)$	$\frac{(J-1)\,u_6^- u_6^+(2J-1)(2J+5)}{J(J+1)(2J+3)^2}$
$Q_5(J)$	$\left(\Lambda + \frac{3}{2}\right)^2 \frac{2(J+1/2)}{J(J+1)}$	$\left(\Lambda + \frac{3}{2}\right)^2 \frac{(3u_7^+ + 2\Lambda)^2 u_4^- u_5^- u_6^-}{C_5(Q)}$	$Q_5(J)$	$\Lambda^2 \frac{4(2J^2+5J-5)^2(2J+1)}{J(J+1)(2J+3)^2(2J+5)^2}$
$R_5(J)$	$\frac{u_4^- u_7^+}{J+1}$	$\frac{(3u_7^+ + 2\Lambda)^2 u_4^{-2} u_5^- u_6^- u_7^+}{2C_5(R)}$	$P_5(J+1)$	$\frac{Ju_7^- u_7^+(2J+1)(2J+7)}{(J+1)(J+2)(2J+5)^2}$
${}^QP_{65}(J)$	0	$\frac{5u_2^- u_3^- u_4^- u_5^- u_6^- u_7^{+2}}{2C_5(P)}$	${}^QR_{56}(J-1)$	$\Lambda^2 \frac{20(2J-1)}{(2J+3)^2(2J+5)}$
${}^RQ_{65}(J)$	0	$\left(\Lambda + \frac{5}{2}\right)^2 \frac{5u_3^- u_4^- u_5^- u_6^- u_7^+}{C_5(Q)}$	${}^PQ_{56}(J)$	$\frac{5u_7^- u_7^+(2J+1)}{(J+1)(J+2)(2J+5)^2}$
${}^SR_{65}(J)$	0	$\frac{5u_3^{-2} u_4^- u_5^- u_6^- u_7^+ u_8^+}{2C_5(R)}$	${}^OP_{56}(J+1)$	0
${}^KP_{16}(J)$	0	$\frac{u_7^- u_2^+ u_3^+ u_4^+ u_5^+ u_6^+ u_7^+}{2C_6(P)}$	${}^WR_{61}(J-1)$	0
${}^LQ_{16}(J)$	0	$\left(\Lambda - \frac{5}{2}\right)^2 \frac{u_3^+ u_4^+ u_5^+ u_6^+ u_7^+}{C_6(R)}$	${}^VQ_{61}(J)$	0
${}^MR_{16}(J)$	0	$\frac{u_8^- u_3^{+2} u_4^+ u_5^+ u_6^+ u_7^+}{2C_6(R)}$	${}^UP_{61}(J+1)$	0
${}^LP_{26}(J)$	0	$\frac{5u_6^- u_7^- u_3^+ u_4^+ u_5^+ u_6^+ u_7^+}{2C_6(P)}$	${}^VR_{62}(J-1)$	0
${}^MQ_{26}(J)$	0	$\left(\Lambda - \frac{3}{2}\right)^2 \frac{5u_7^- u_4^+ u_5^+ u_6^+ u_7^+}{C_6(Q)}$	${}^UQ_{62}(J)$	0

${}^{N}R_{26}(J)$	0	$\frac{5u_7^{-2}u_4^{+2}u_5^{+}u_6^{+}u_7^{+}}{2C_6(R)}$	${}^{T}P_{62}(J+1)$	0
${}^{M}P_{36}(J)$	0	$\frac{5u_5^{-}u_6^{-}u_7^{-}u_4^{+}u_5^{+}u_6^{+}u_7^{+}}{C_6(P)}$	${}^{U}R_{63}(J-1)$	0
${}^{N}Q_{36}(J)$	0	$\left(\Lambda-\frac{1}{2}\right)^2\frac{10u_6^{-}u_7^{-}u_5^{+}u_6^{+}u_7^{+}}{C_6(Q)}$	${}^{T}Q_{63}(J)$	0
${}^{O}R_{36}(J)$	0	$\frac{5u_6^{-2}u_7^{-}u_5^{+2}u_6^{+}u_7^{+}}{C_6(R)}$	${}^{S}P_{63}(J+1)$	0
${}^{N}P_{46}(J)$	0	$\frac{5u_4^{-}u_5^{-}u_6^{-}u_7^{-}u_5^{+}u_6^{+}u_7^{+}}{C_6(P)}$	${}^{T}R_{64}(J-1)$	0
${}^{O}Q_{46}(J)$	0	$\left(\Lambda+\frac{1}{2}\right)^2\frac{10u_5^{-}u_6^{-}u_7^{-}u_6^{+}u_7^{+}}{C_6(Q)}$	${}^{S}Q_{64}(J)$	0
${}^{P}R_{46}(J)$	0	$\frac{5u_5^{-2}u_6^{-}u_7^{-}u_6^{+2}u_7^{+}}{C_6(R)}$	${}^{R}P_{64}(J+1)$	$\frac{10u_7^{-}u_7^{+}}{(J+1)(J+2)(J+3)(2J+5)^2}$
${}^{O}P_{56}(J)$	0	$\frac{5u_3^{-}u_4^{-}u_5^{-}u_6^{-}u_7^{-}u_6^{+}u_7^{+}}{2C_6(P)}$	${}^{S}R_{65}(J-1)$	0
${}^{P}Q_{56}(J)$	0	$\left(\Lambda+\frac{3}{2}\right)^2\frac{5u_4^{-}u_5^{-}u_6^{-}u_7^{-}u_7^{+}}{C_6(Q)}$	${}^{R}Q_{65}(J)$	$\frac{5u_7^{-}u_7^{+}(2J+1)}{(J+1)(J+2)(2J+5)^2}$
${}^{Q}R_{56}(J)$	0	$\frac{5u_4^{-2}u_5^{-}u_6^{-}u_7^{-}u_7^{+2}}{2C_6(R)}$	${}^{Q}P_{65}(J+1)$	$\Lambda^2\frac{20(2J+1)}{(J+1)(2J+5)^2(2J+7)}$
$P_6(J)$	$\frac{u_2^{-}u_7^{+}}{J}$	$\frac{u_2^{-}u_3^{-}u_4^{-}u_5^{-}u_6^{-}u_7^{-}u_7^{+}}{2C_6(P)}$	$R_6(J-1)$	$\frac{u_7^{-}u_7^{+}(2J-1)}{(J+2)2(J+5)}$
$Q_6(J)$	$\left(\Lambda+\frac{5}{2}\right)^2\frac{2(J+1/2)}{J(J+1)}$	$\left(\Lambda+\frac{5}{2}\right)^2\frac{u_3^{-}u_4^{-}u_5^{-}u_6^{-}u_7^{-}}{C_6(Q)}$	$Q_6(J)$	$\Lambda^2\frac{4J(2J+1)}{(J+1)(2J+5)^2}$
$R_6(J)$	$\frac{u_3^{-}u_8^{+}}{J+1}$	$\frac{u_3^{-2}u_4^{-}u_5^{-}u_6^{-}u_7^{-}u_8^{+}}{2C_6(R)}$	$P_6(J+1)$	$\frac{u_8^{-}u_8^{+}(2J+1)}{(J+3)(2J+7)}$

Table II

Line strengths

Branches		Line	
$\Delta\Lambda = +1$	$\Delta\Lambda = -1$	${}^{s}X(a) - {}^{s}Y(a)$	${}^{s}X(a) - {}^{s}Y(b)$
$P_1(J)$	$R_1(J-1)$	$\frac{u_6^- u_7^-}{2J}$	$\frac{u_3^- u_4^- u_5^- u_6^{-2} u_7^{-2}}{4C_1(P)}$
$Q_1(J)$	$Q_1(J)$	$\frac{u_7^- u_3^+ (J+1/2)}{J(J+1)}$	$\frac{u_3^- u_4^- u_5^- u_6^- u_7^{-2} u_3^+}{2C_1(Q)}$
$R_1(J)$	$P_1(J+1)$	$\frac{u_3^+ u_4^+}{2(J+1)}$	$\frac{u_3^- u_4^- u_5^- u_6^- u_7^- u_3^+ u_4^+}{4C_1(R)}$
${}^{Q}P_{21}(J)$	${}^{Q}R_{12}(J-1)$	0	$\frac{5u_3^- u_4^- u_5^{-2} u_6^{-2} u_3^+}{4C_1(R)}$
${}^{R}Q_{21}(J)$	${}^{P}Q_{12}(J)$	0	$\frac{5u_3^- u_4^- u_5^- u_6^{-2} u_3^+ u_4^+}{2C_1(Q)}$
${}^{S}R_{21}(J)$	${}^{O}P_{12}(J+1)$	0	$\frac{5u_3^- u_4^- u_5^- u_6^- u_3^+ u_4^+ u_5^+}{4C_1(R)}$
${}^{R}P_{31}(J)$	${}^{P}R_{13}(J-1)$	0	$\frac{5u_3^- u_4^{-2} u_5^{-2} u_3^+ u_4^+}{2C_1(P)}$
${}^{S}Q_{31}(J)$	${}^{O}Q_{13}(J)$	0	$\frac{5u_3^- u_4^- u_5^{-2} u_3^+ u_4^+ u_5^+}{C_1(Q)}$
${}^{T}R_{31}(J)$	${}^{N}P_{13}(J+1)$	0	$\frac{5u_3^- u_4^- u_5^- u_3^+ u_4^+ u_5^+ u_6^+}{2C_1(R)}$
${}^{S}P_{41}(J)$	${}^{O}R_{14}(J-1)$	0	$\frac{5u_3^{-2} u_4^{-2} u_3^- u_4^+ u_5^+}{2C_1(P)}$
${}^{T}Q_{41}(J)$	${}^{N}Q_{14}(J)$	0	$\frac{5u_3^- u_4^{-2} u_3^+ u_4^+ u_5^+ u_6^+}{C_1(Q)}$
${}^{U}R_{41}(J)$	${}^{M}P_{14}(J+1)$	0	$\frac{5u_3^- u_4^- u_3^+ u_4^+ u_5^+ u_6^+ u_7^+}{2C_1(R)}$
${}^{T}P_{51}(J)$	${}^{N}R_{15}(J-1)$	0	$\frac{5u_2^- u_3^{-2} u_3^+ u_4^+ u_5^+ u_6^+}{4C_1(P)}$
${}^{U}Q_{51}(J)$	${}^{M}Q_{15}(J)$	0	$\frac{5u_3^{-2} u_3^+ u_4^+ u_5^+ u_6^+ u_7^+}{2C_1(Q)}$
${}^{V}R_{51}(J)$	${}^{L}P_{15}(J+1)$	0	$\frac{5u_3^- u_3^+ u_4^+ u_5^+ u_6^+ u_7^+ u_8^+}{4C_1(R)}$
${}^{U}P_{61}(J)$	${}^{M}R_{16}(J-1)$	0	$\frac{u_1^- u_2^- u_3^+ u_4^+ u_5^+ u_6^+ u_7^+}{4C_1(P)}$
${}^{V}Q_{61}(J)$	${}^{L}Q_{16}(J)$	0	$\frac{u_2^- u_3^+ u_4^+ u_5^+ u_6^+ u_7^+ u_8^+}{2C_1(Q)}$
${}^{W}R_{61}(J)$	${}^{K}P_{16}(J+1)$	0	$\frac{u_3^+ u_4^+ u_5^+ u_6^+ u_7^+ u_8^+ u_9^+}{4C_1(R)}$
${}^{O}P_{12}(J)$	${}^{S}R_{21}(J-1)$	0	$\frac{5u_4^- u_5^- u_6^{-2} u_7^{-2} u_3^+}{4C_2(P)}$

for ${}^6X_{A+1} - {}^6Y_A$ transitions

strengths

${}^6X(b) - {}^6Y(a)$	${}^6X(b) - {}^6Y(b)$
$\frac{u_1^- u_2^- u_3^- u_4^- u_5^- u_6^- u_7^-}{4C_1^-(P)}$	$\frac{u_1^- u_2^-(2J+1)}{2(J-2)(2J-5)}$
$\frac{u_2^- u_3^- u_4^- u_5^- u_6^- u_7^- u_3^+}{2C_1(Q)}$	$\frac{2(J+1)\,u_2^- u_3^+(2J+1)}{J(2J-3)^2}$
$\frac{u_3^- u_4^- u_5^- u_6^- u_7^- u_3^+ u_4^+}{4C_1^+(R)}$	$\frac{u_3^+ u_4^+(2J+3)}{2(J-1)(2J-3)}$
$\frac{5u_2^- u_3^- u_4^- u_5^- u_6^- u_7^- u_3^+}{4C_2^-(P)}$	$\frac{10u_2^- u_3^+(2J+1)}{J(2J-5)(2J-3)^2}$
$\frac{5u_3^- u_4^- u_5^- u_6^- u_7^- u_3^+ u_4^+}{2C_2(Q)}$	$\frac{5u_3^+ u_4^+(2J+1)}{2(J-1)J(2J-3)^2}$
$\frac{5u_4^- u_5^- u_6^- u_7^- u_3^+ u_4^+ u_5^+}{4C_2^+(R)}$	0
$\frac{5u_3^- u_4^- u_5^- u_6^- u_7^- u_3^+ u_4^+}{2C_3^-(P)}$	$\frac{5u_3^+ u_4^+}{(J-2)(J-1)J(2J-3)^2}$
$\frac{5u_4^- u_5^- u_6^- u_7^- u_3^+ u_4^+ u_5^+}{C_3(Q)}$	0
$\frac{5u_5^- u_6^- u_7^- u_3^+ u_4^+ u_5^+ u_6^+}{2C_3^+(R)}$	0
$\frac{5u_4^- u_5^- u_6^- u_7^- u_3^+ u_4^+ u_5^+}{2C_4^-(P)}$	0
$\frac{5u_5^- u_6^- u_7^- u_3^+ u_4^+ u_5^+ u_6^+}{C_4(Q)}$	0
$\frac{5u_6^- u_7^- u_3^+ u_4^+ u_5^+ u_6^+ u_7^+}{2C_4^+(R)}$	0
$\frac{5u_5^- u_6^- u_7^- u_3^+ u_4^+ u_5^+ u_6^+}{4C_5^-(P)}$	0
$\frac{5u_6^- u_7^- u_3^+ u_4^+ u_5^+ u_6^+ u_7^+}{2C_5(Q)}$	0
$\frac{5u_7^- u_3^+ u_4^+ u_5^+ u_6^+ u_7^+ u_8^+}{4C_5^+(R)}$	0
$\frac{u_6^- u_7^- u_3^+ u_4^+ u_5^+ u_6^+ u_7^+}{4C_6^-(P)}$	0
$\frac{u_7^- u_3^+ u_4^+ u_5^+ u_6^+ u_7^+ u_8^+}{2C_6(Q)}$	0
$\frac{u_3^+ u_4^+ u_5^+ u_6^+ u_7^+ u_8^+ u_9^+}{4C_6^+(R)}$	0
$\frac{5u_1^- u_2^- u_3^- u_4^- u_5^- u_6^- u_3^+}{4C_1^-(P)}$	0

Table II

Branches		Line	
$\Delta\Lambda = +1$	$\Delta\Lambda = -1$	${}^{6}X(a) - {}^{6}Y(a)$	${}^{6}X(a) - {}^{6}Y(b)$
${}^{P}Q_{12}(J)$	${}^{R}Q_{21}(J)$	0	$\frac{5u_4^- u_5^- u_6^- u_7^{-2} u_3^{+2}}{2C_2(Q)}$
${}^{Q}R_{12}(J)$	${}^{Q}P_{21}(J+1)$	0	$\frac{5u_4^- u_5^- u_6^- u_7^- u_3^{+2} u_4^+}{4C_2(R)}$
$P_2(J)$	$R_2(J-1)$	$\frac{u_5^- u_6^-}{2J}$	$\frac{[3u_3^+ + 2\Lambda]^2 u_4^- u_5^{-2} u_6^{-2}}{4C_2(P)}$
$Q_2(J)$	$Q_2(J)$	$\frac{u_6^- u_4^+(J+1/2)}{J(J+1)}$	$\frac{[3u_3^+ + 2\Lambda]^2 u_4^- u_5^- u_6^{-2} u_4^+}{2C_2(Q)}$
$R_2(J)$	$P_2(J+1)$	$\frac{u_4^+ u_5^+}{2(J+1)}$	$\frac{[3u_3^+ + 2\Lambda]^2 u_4^- u_5^- u_6^- u_4^+ u_5^+}{4C_2(R)}$
${}^{Q}P_{32}(J)$	${}^{Q}R_{23}(J-1)$	0	$\frac{[u_3^+ + 4\Lambda]^2 u_4^{-2} u_5^{-2} u_4^+}{2C_2(P)}$
${}^{R}Q_{32}(J)$	${}^{P}Q_{23}(J)$	0	$\frac{[u_3^+ + 4\Lambda]^2 u_4^- u_5^{-2} u_4^+ u_5^+}{C_2(Q)}$
${}^{S}R_{32}(J)$	${}^{O}P_{23}(J+1)$	0	$\frac{[u_3^+ + 4\Lambda]^2 u_4^- u_5^- u_4^+ u_5^+ u_6^+}{2C_2(R)}$
${}^{R}P_{42}(J)$	${}^{P}R_{24}(J-1)$	0	$\frac{[u_3^- - 4\Lambda]^2 u_3^- u_4^{-2} u_4^+ u_5^+}{2C_2(P)}$
${}^{S}Q_{42}(J)$	${}^{O}Q_{24}(J)$	0	$\frac{[u_3^- - 4\Lambda]^2 u_4^{-2} u_4^+ u_5^+ u_6^+}{C_2(Q)}$
${}^{T}R_{42}(J)$	${}^{N}P_{24}(J+1)$	0	$\frac{[u_3^- - 4\Lambda]^2 u_4^- u_4^+ u_5^+ u_6^+ u_7^+}{2C_2(R)}$
${}^{S}P_{52}(J)$	${}^{O}R_{25}(J-1)$	0	$\frac{[3u_3^- - 2\Lambda]^2 u_2^- u_3^- u_4^+ u_5^+ u_6^+}{4C_2(P)}$
${}^{T}Q_{52}(J)$	${}^{N}Q_{25}(J)$	0	$\frac{[3u_3^- - 2\Lambda]^2 u_3^- u_4^+ u_5^+ u_6^+ u_7^+}{2C_2(Q)}$
${}^{U}R_{52}(J)$	${}^{M}P_{25}(J+1)$	0	$\frac{[3u_3^- - 2\Lambda]^2 u_4^+ u_5^+ u_6^+ u_7^+ u_8^+}{4C_2(R)}$
${}^{T}P_{62}(J)$	${}^{N}R_{26}(J-1)$	0	$\frac{5u_1^- u_2^- u_3^- u_5^+ u_6^+ u_7^+}{4C_2(P)}$
${}^{U}Q_{62}(J)$	${}^{M}Q_{26}(J)$	0	$\frac{5u_2^- u_3^- u_4^+ u_5^+ u_6^+ u_7^+ u_8^+}{2C_2(Q)}$
${}^{V}R_{62}(J)$	${}^{L}P_{26}(J+1)$	0	$\frac{5u_3^- u_4^+ u_5^+ u_6^+ u_7^+ u_8^+ u_9^+}{4C_2(R)}$
${}^{N}P_{13}(J)$	${}^{T}R_{31}(J-1)$	0	$\frac{5u_5^- u_6^{-2} u_7^{-2} u_3^+ u_4^+}{2C_3(P)}$
${}^{O}Q_{13}(J)$	${}^{S}Q_{31}(J)$	0	$\frac{5u_5^- u_6^- u_7^{-2} u_3^{+2} u_4^+}{C_3(Q)}$
${}^{P}R_{13}(J)$	${}^{R}P_{31}(J+1)$	0	$\frac{5u_5^- u_6^- u_7^- u_3^{+2} u_4^{+2}}{2C_3(R)}$

(continued)

strengths

${}^6X(b) - {}^6Y(a)$	${}^6X(b) - {}^6Y(b)$
$\frac{5u_2^- u_3^- u_4^- u_5^- u_6^- u_4^{+2}}{2C_1(Q)}$	$\frac{5u_2^- u_3^-(2J+1)}{2(J-1)J(2J-3)^2}$
$\frac{5u_3^- u_4^- u_5^- u_6^- u_3^+ u_5^{+2}}{4C_1^+(R)}$	$\frac{10u_3^- u_4^+(2J+3)}{(J+1)(2J-3)(2J-1)^2}$
$\frac{[3u_3^+ + 2(\Lambda+1)]^2\, u_2^- u_3^- u_4^- u_5^- u_6^-}{4C_2^-(P)}$	$\frac{(J+1)\, u_2^- u_3^-(2J-5)(2J+1)}{2(J-1)J(2J-3)^2}$
$\frac{[3u_4^+ + 2(\Lambda+1)]^2\, u_3^- u_4^- u_5^- u_6^- u_4^+}{2C_2(Q)}$	$\frac{2(2J^2-J-8)^2\, u_3^- u_4^+(2J+1)}{J(J+1)(2J-3)^2(2J-1)^2}$
$\frac{[3u_5^+ + 2(\Lambda+1)]^2\, u_4^- u_5^- u_6^- u_4^+ u_5^+}{4C_2^+(R)}$	$\frac{(J+2)\, u_4^+ u_5^+(2J-3)(2J+3)}{2J(J+1)(2J-1)^2}$
$\frac{[u_1^+ + 4(\Lambda+1)]^2\, u_3^- u_4^- u_5^- u_6^- u_4^+}{2C_3^-(P)}$	$\frac{64(J-2)(J+1)\, u_3^- u_4^+}{J(2J-3)^2(2J-1)^2}$
$\frac{[u_2^+ + 4(\Lambda+1)]^2\, u_4^- u_5^- u_6^- u_4^+ u_5^+}{C_3(Q)}$	$\frac{u_4^+ u_5^+(2J-3)(2J+1)(2J+3)}{(J-1)J^2(J+1)(2J-1)^2}$
$\frac{[u_3^+ + 4(\Lambda+1)]^2\, u_5^- u_6^- u_4^+ u_5^+ u_6^+}{2C_3^+(R)}$	0
$\frac{[u_7^+ - 4(\Lambda+1)]^2\, u_4^- u_5^- u_6^- u_4^+ u_5^+}{2C_4^-(P)}$	$\frac{9u_4^+ u_5^+}{(J-1)J^2(2J-1)^2}$
$\frac{[u_8^- - 4(\Lambda+1)]^2\, u_5^- u_6^- u_4^+ u_5^+ u_6^+}{C_4(Q)}$	0
$\frac{[u_9^- - 4(\Lambda+1)]^2\, u_6^- u_4^+ u_5^+ u_6^+ u_7^+}{2C_4^+(R)}$	0
$\frac{[3u_5^- - 2(\Lambda+1)]^2\, u_5^- u_6^- u_4^+ u_5^+ u_6^+}{4C_5^-(P)}$	0
$\frac{[3u_6^- - 2(\Lambda+1)]^2\, u_6^- u_4^+ u_5^+ u_6^+ u_7^+}{2C_5(Q)}$	0
$\frac{[3u_7^- - 2(\Lambda+1)]^2\, u_4^+ u_5^+ u_6^+ u_7^+ u_8^+}{4C_5^+(R)}$	0
$\frac{5u_5^{-2} u_6^- u_4^+ u_5^+ u_6^+ u_7^+}{4C_6^-(P)}$	0
$\frac{5u_6^{-2} u_4^+ u_5^+ u_6^+ u_7^+ u_8^+}{2C_6(Q)}$	0
$\frac{5u_7^- u_4^+ u_5^+ u_6^+ u_7^+ u_8^+ u_9^+}{4C_6^+(R)}$	0
$\frac{5u_1^- u_2^- u_3^- u_4^- u_5^- u_3^+ u_4^+}{2C_1^-(P)}$	0
$\frac{5u_2^- u_3^- u_4^- u_5^- u_4^+ u_5^{+2}}{C_1(Q)}$	0
$\frac{5u_3^- u_4^- u_5^- u_5^{+2} u_6^{+2}}{2C_1^+(R)}$	$\frac{5u_3^- u_4^-}{(J-1)J(J+1)(2J-1)^2}$

Table II

Branches		Line	
$\Delta\Lambda = +1$	$\Delta\Lambda = -1$	${}^{6}X(a) - Y^{6}(a)$	${}^{6}X(a) - {}^{6}Y(b)$
${}^{O}P_{23}(J)$	${}^{S}R_{32}(J-1)$	0	$\frac{[u_1^+ + 4\Lambda]^2 u_5^- {}^2 u_6^- {}^2 u_4^+}{2C_3(P)}$
${}^{P}Q_{23}(J)$	${}^{R}Q_{32}(J)$	0	$\frac{[u_1^+ + 4\Lambda]^2 u_5^- u_6^- {}^2 u_4^{+2}}{C_3(Q)}$
${}^{Q}R_{23}(J)$	${}^{Q}P_{32}(J+1)$	0	$\frac{[u_1^+ + 4\Lambda]^2 u_5^- u_6^- u_4^{+2} u_5^+}{2C_3(R)}$
$P_3(J)$	$R_3(J-1)$	$\frac{u_4^- u_5^-}{2J}$	$\frac{[u_4^- u_6^- - 3\Lambda(2\Lambda-1)]^2 u_4^- u_5^- {}^2}{C_3(P)}$
$Q_3(J)$	$Q_3(J)$	$\frac{u_4^- u_5^+ (J+1/2)}{J(J+1)}$	$\frac{2[u_4^- u_6^- - 3\Lambda(2\Lambda-1)]\, u_5^- {}^2 u_5^+}{C_3(Q)}$
$R_3(J)$	$P_3(J+1)$	$\frac{u_5^+ u_6^+}{2(J+1)}$	$\frac{[u_4^- u_6^- - 3\Lambda(2\Lambda-1)]^2 u_5^- u_5^+ u_6^+}{C_3(R)}$
${}^{Q}P_{43}(J)$	${}^{Q}R_{34}(J-1)$	0	$\frac{[u_4^+ u_6^+ - 3\Lambda(2\Lambda+1)]^2 u_3^- u_4^- u_5^+}{C_3(P)}$
${}^{R}Q_{43}(J)$	${}^{P}Q_{34}(J)$	0	$\frac{2[u_4^+ u_6^+ - 3\Lambda(2\Lambda+1)]^2 u_4^- u_5^+ u_6^+}{C_3(Q)}$
${}^{S}R_{43}(J)$	${}^{O}P_{34}(J+1)$	0	$\frac{[u_4^+ u_6^+ - 3\Lambda(2\Lambda+1)]^2 u_5^+ u_6^+ u_7^+}{C_3(R)}$
${}^{R}P_{53}(J)$	${}^{P}R_{35}(J-1)$	0	$\frac{[u_1^- - 4\Lambda]^2 u_2^- u_3^- u_4^- u_5^+ u_6^+}{2C_3(P)}$
${}^{S}Q_{53}(J)$	${}^{O}Q_{35}(J)$	0	$\frac{[u_1^- - 4\Lambda]^2 u_3^- u_4^- u_5^+ u_6^+ u_7^+}{C_3(Q)}$
${}^{T}R_{53}(J)$	${}^{N}P_{35}(J+1)$	0	$\frac{[u_1^- - 4\Lambda]^2 u_4^- u_5^+ u_6^+ u_7^+ u_8^+}{2C_3(R)}$
${}^{S}P_{63}(J)$	${}^{O}R_{36}(J-1)$	0	$\frac{5u_1^- u_2^- u_3^- u_4^- u_5^+ u_6^+ u_7^+}{2C_3(P)}$
${}^{T}Q_{63}(J)$	${}^{N}Q_{36}(J)$	0	$\frac{5u_2^- u_3^- u_4^- u_5^+ u_6^+ u_7^+ u_8^+}{C_3(Q)}$
${}^{U}R_{63}(J)$	${}^{M}P_{36}(J+1)$	0	$\frac{5u_3^- u_4^- u_5^+ u_6^+ u_7^+ u_8^+ u_9^+}{2C_3(R)}$
${}^{M}P_{14}(J)$	${}^{U}R_{41}(J-1)$	0	$\frac{5u_6^- {}^2 u_7^- {}^2 u_3^+ u_4^+ u_5^+}{2C_4(P)}$
${}^{N}Q_{14}(J)$	${}^{T}Q_{41}(J)$	0	$\frac{5u_6^- u_7^- {}^2 u_3^{+2} u_4^+ u_5^+}{C_4(Q)}$
${}^{O}R_{14}(J)$	${}^{S}P_{41}(J+1)$	0	$\frac{5u_6^- u_7^- u_3^{+2} u_4^{+2} u_5^+}{2C_4(R)}$
${}^{N}P_{24}(J)$	${}^{T}R_{42}(J-1)$	0	$\frac{[u_9^- - 4\Lambda]^2 u_5^- u_6^- {}^2 u_4^+ u_5^+}{2C_4(P)}$
${}^{O}Q_{24}(J)$	${}^{S}Q_{42}(J)$	0	$\frac{[u_9^- - 4\Lambda]^2 u_6^- {}^2 u_4^{+2} u_5^+}{C_4(Q)}$

(continued)

strengths

${}^6X(b) - {}^6Y(a)$	${}^6X(b) - {}^6Y(b)$
$\frac{[u_3^+ + 4(\Lambda+1)]^2 u_2^- u_3^- u_4^- u_5^- u_4^+}{2C_2^-(P)}$	0
$\frac{[u_4^+ + 4(\Lambda+1)]^2 u_3^- u_4^- u_5^- u_5^{+2}}{C_2(Q)}$	$\frac{u_3^- u_4^-(2J-3)(2J+1)(2J+3)}{(J-1)J^2(J+1)(2J-1)^2}$
$\frac{[u_5^+ + 4(\Lambda+1)]^2 u_4^- u_5^- u_5^+ u_6^{+2}}{2C_2^+(R)}$	$\frac{64(J-1)(J+2)\,u_4^- u_5^+}{(J+1)(2J-1)^2(2J+1)^2}$
$\frac{2[u_2^- u_4^- - 3(\Lambda+1)(2\Lambda+1)]^2 u_3^- u_4^- u_5^-}{2C_3^-(P)}$	$\frac{(J-2)(J+1)\,u_3^- u_4^-(2J-3)(2J+3)}{2(J-1)J^2(2J-1)^2}$
$\frac{2[u_3^- u_5^- - 3(\Lambda+1)(2\Lambda+1)]^2 u_4^- u_5^- u_5^+}{C_3(Q)}$	$\frac{2(2J^2+J-9)^2 u_4^- u_5^+}{J(J+1)(2J-1)^2(2J+1)}$
$\frac{2[u_4^- u_6^- - 3(\Lambda+1)(2\Lambda+1)]^2 u_5^- u_5^+ u_6^+}{2C_3^+(R)}$	$\frac{(J-1)(J+2)\,u_5^+ u_6^+(2J-1)(2J+5)}{2J(J+1)^2(2J+1)^2}$
$\frac{2[u_4^+ u_6^+ - 3(\Lambda+1)(2\Lambda+1)]^2 u_4^- u_5^- u_5^+}{2C_4^-(P)}$	$\frac{18u_4^- u_5^+(2J-3)(2J+3)}{J(2J-1)^2(2J+1)^2}$
$\frac{2[u_5^+ u_7^+ - 3(\Lambda+1)(2\Lambda+1)]^2 u_5^- u_5^+ u_6^+}{C_4(Q)}$	$\frac{9(J-1)(J+2)\,u_5^+ u_6^+}{2J^2(J+1)^2(2J+1)}$
$\frac{2[u_6^+ u_8^+ - 3(\Lambda+1)(2\Lambda+1)]^2 u_5^+ u_6^+ u_7^+}{2C_4^+(R)}$	0
$\frac{[u_5^- - 4(\Lambda+1)]^2 u_4^{-2} u_5^- u_5^+ u_6^+}{2C_5^-(P)}$	$\frac{9u_5^+ u_6^+}{J^2(J+1)(2J+1)^2}$
$\frac{[u_6^- - 4(\Lambda+1)]^2 u_5^{-2} u_5^+ u_6^+ u_7^+}{C_5(Q)}$	0
$\frac{[u_7^- - 4(\Lambda+1)]^2 u_6^- u_5^+ u_6^+ u_7^+ u_8^+}{2C_5^+(R)}$	0
$\frac{5u_4^{-2} u_5^{-2} u_5^+ u_6^+ u_7^+}{2C_6^-(P)}$	0
$\frac{5u_5^{-2} u_6^- u_5^+ u_6^+ u_7^+ u_8^+}{C_6(Q)}$	0
$\frac{5u_6^- u_7^- u_5^+ u_6^+ u_7^+ u_8^+ u_9^+}{2C_6^+(R)}$	0
$\frac{5u_1^- u_2^- u_3^- u_4^- u_3^+ u_4^+ u_5^+}{2C_1^-(P)}$	0
$\frac{5u_2^- u_3^- u_4^- u_4^+ u_5^+ u_6^{+2}}{C_1(Q)}$	0
$\frac{5u_3^- u_4^- u_5^+ u_6^{+2} u_7^+}{2C_1^+(R)}$	0
$\frac{[u_1^- - 4(\Lambda+1)]^2 u_2^- u_3^- u_4^- u_4^+ u_5^+}{2C_2^-(P)}$	0
$\frac{[u_2^- - 4(\Lambda+1)]^2 u_3^- u_4^- u_5^+ u_6^{+2}}{C_2(Q)}$	0

Table II

Branches		Line	
$\Delta\Lambda = +1$	$\Delta\Lambda = -1$	${}^{6}X(a) - {}^{6}Y(a)$	${}^{6}X(a) - {}^{6}Y(b)$
${}^{P}R_{24}(J)$	${}^{R}P_{42}(J+1)$	0	$\frac{[u_9^- - 4\Lambda]^2\, u_6^- u_4^{+2} u_5^{+2}}{2C_4(R)}$
${}^{O}P_{34}(J)$	${}^{S}R_{43}(J-1)$	0	$\frac{[u_4^+ u_6^+ - 3\Lambda(2\Lambda-1)]^2\, u_4^- u_5^- u_5^+}{C_4(P)}$
${}^{P}Q_{34}(J)$	${}^{R}Q_{43}(J)$	0	$\frac{2[u_4^+ u_6^+ - 3\Lambda(2\Lambda-1)]^2\, u_5^- u_5^{+2}}{C_4(Q)}$
${}^{Q}R_{34}(J)$	${}^{Q}P_{43}(J+1)$	0	$\frac{[u_4^+ u_6^+ - 3\Lambda(2\Lambda-1)]^2\, u_5^{+2} u_6^+}{C_4(R)}$
$P_4(J)$	$R_4(J-1)$	$\frac{u_3^- u_4^-}{2J}$	$\frac{[u_4^- u_6^- - 3\Lambda(2\Lambda+1)]^2\, u_3^- u_4^- u_5^-}{C_4(P)}$
$Q_4(J)$	$Q_4(J)$	$\frac{u_4^- u_6^+(J+1/2)}{J(J+1)}$	$\frac{2[u_4^- u_6^- - 3\Lambda(2\Lambda+1)]^2\, u_4^- u_5^- u_6^+}{C_4(Q)}$
$R_4(J)$	$P_4(J+1)$	$\frac{u_6^+ u_7^+}{2(J+1)}$	$\frac{[u_4^- u_6^- - 3\Lambda(2\Lambda+1)]^2\, u_5^- u_6^+ u_7^+}{C_4(R)}$
${}^{Q}P_{54}(J)$	${}^{Q}R_{45}(J-1)$	0	$\frac{[u_9^+ + 4\Lambda]^2\, u_2^- u_3^- u_4^- u_5^- u_6^+}{2C_4(P)}$
${}^{R}Q_{54}(J)$	${}^{P}Q_{45}(J)$	0	$\frac{[u_9^+ + 4\Lambda]^2\, u_3^- u_4^- u_5^- u_6^+ u_7^+}{C_4(Q)}$
${}^{S}R_{54}(J)$	${}^{O}P_{45}(J+1)$	0	$\frac{[u_9^+ + 4\Lambda]^2\, u_4^- u_5^- u_6^+ u_7^+ u_8^+}{2C_4(R)}$
${}^{R}P_{64}(J)$	${}^{P}R_{46}(J-1)$	0	$\frac{5u_1^- u_2^- u_3^- u_4^- u_5^- u_6^+ u_7^+}{2C_4(P)}$
${}^{S}Q_{64}(J)$	${}^{O}Q_{46}(J)$	0	$\frac{5u_2^- u_3^- u_4^- u_5^- u_6^+ u_7^+ u_8^+}{C_4(Q)}$
${}^{T}R_{64}(J)$	${}^{N}P_{46}(J+1)$	0	$\frac{5u_3^- u_4^- u_5^- u_6^+ u_7^+ u_8^+ u_9^+}{2C_4(R)}$
${}^{L}P_{15}(J)$	${}^{V}R_{51}(J-1)$	0	$\frac{5u_6^- u_7^{-2} u_3^+ u_4^+ u_5^+ u_6^+}{4C_5(P)}$
${}^{M}Q_{15}(J)$	${}^{U}Q_{51}(J)$	0	$\frac{5u_7^{-2} u_3^{+2} u_4^+ u_5^+ u_6^+}{2C_5(Q)}$
${}^{N}R_{15}(J)$	${}^{T}P_{51}(J+1)$	0	$\frac{5u_7^- u_3^{+2} u_4^{+2} u_5^+ u_6^+}{4C_5(R)}$
${}^{M}P_{25}(J)$	${}^{U}R_{52}(J-1)$	0	$\frac{[3u_7^- - 2\Lambda]^2\, u_5^- u_6^- u_4^+ u_5^+ u_6^+}{4C_5(P)}$
${}^{N}Q_{25}(J)$	${}^{T}Q_{52}(J)$	0	$\frac{[3u_7^- - 2\Lambda]^2\, u_6^- u_4^{+2} u_5^+ u_6^+}{2C_5(Q)}$
${}^{O}R_{25}(J)$	${}^{S}P_{52}(J+1)$	0	$\frac{[3u_7^- - 2\Lambda]^2\, u_4^{+2} u_5^{+2} u_6^+}{4C_5(R)}$
${}^{N}P_{35}(J)$	${}^{T}R_{53}(J-1)$	0	$\frac{[u_7^- - 4\Lambda]^2\, u_4^- u_5^- u_6^- u_5^+ u_6^+}{2C_5(P)}$

(continued)

strengths

${}^6X(b) - {}^6Y(a)$	${}^4X(b) - {}^4Y(b)$
$\frac{[u_3^- - 4(\Lambda+1)]^2\, u_4^- u_6^{+2} u_7^{+2}}{2C_2^+(R)}$	$\frac{9u_4^- u_5^-}{J(J+1)^2(2J+1)^2}$
$\frac{[u_4^+ u_6^+ - 3(\Lambda+1)(2\Lambda+3)]^2\, u_3^- u_4^- u_5^+}{C_3^-(P)}$	0
$\frac{2[u_5^+ u_7^+ - 3(\Lambda+1)(2\Lambda+3)]^2\, u_4^- u_6^{+2}}{C_3(Q)}$	$\frac{9(J-1)(J+2)\, u_4^- u_5^-}{2J^2(J+1)^2(2J+1)}$
$\frac{[u_6^+ u_8^+ - 3(\Lambda+1)(2\Lambda+3)]^2\, u_6^+ u_7^{+2}}{C_3^+(R)}$	$\frac{18u_5^- u_6^+(2J-1)(2J+5)}{(J+1)(2J+1)^2(2J+3)^2}$
$\frac{[u_2^- u_4^- - 3(\Lambda+1)(2\Lambda+3)]^2\, u_3^{-2} u_4^-}{C_4^-(P)}$	$\frac{(J-1)(J+2)\, u_4^- u_5^-(2J-3)(2J+3)}{2J^2(J+1)(2J+1)^2}$
$\frac{2[u_3^- u_5^- - 3(\Lambda+1)(2\Lambda+3)]^2\, u_4^{-2} u_6^+}{C_4(Q)}$	$\frac{2(2J^2+3J-8)^2\, u_5^- u_6^+}{J(J+1)(2J+1)(2J+3)^2}$
$\frac{[u_4^- u_6^- - 3(\Lambda+1)(2\Lambda+3)]^2\, u_5^- u_6^+ u_7^+}{C_4^+(R)}$	$\frac{J(J+3)\, u_6^+ u_7^+(2J-1)(2J+5)}{2(J+1)^2(J+2)(2J+3)^2}$
$\frac{[u_7^+ + 4(\Lambda+1)]^2\, u_3^{-2} u_4^{-2} u_6^+}{2C_5^-(P)}$	$\frac{64(J-1)(J+2)\, u_5^- u_6^+}{J(2J+1)^2(2J+3)^2}$
$\frac{[u_8^+ + 4(\Lambda+1)]^2\, u_4^{-2} u_5^- u_6^+ u_7^+}{C_5(Q)}$	$\frac{u_6^+ u_7^+(2J-1)(2J+1)(2J+5)}{J(J+1)^2(J+2)(2J+3)^2}$
$\frac{[u_9^+ + 4(\Lambda+1)]^2\, u_5^- u_6^- u_6^+ u_7^+ u_8^+}{2C_5^+(R)}$	0
$\frac{5u_3^{-2} u_4^{-2} u_5^- u_6^+ u_7^+}{2C_6^-(P)}$	$\frac{5u_6^+ u_7^+}{J(J+1)(J+2)(2J+3)^2}$
$\frac{5u_4^{-2} u_5^- u_6^- u_6^+ u_7^+ u_8^+}{C_6(Q)}$	0
$\frac{5u_5^- u_6^- u_7^- u_6^+ u_7^+ u_8^+ u_9^+}{2C_6^+(R)}$	0
$\frac{5u_1^- u_2^- u_3^- u_3^+ u_4^+ u_5^+ u_6^+}{4C_1^-(P)}$	0
$\frac{5u_2^- u_3^- u_4^+ u_5^+ u_6^+ u_7^{+2}}{2C_1(Q)}$	0
$\frac{5u_3^- u_5^+ u_6^+ u_7^{+2} u_8^{+2}}{4C_1^+(R)}$	0
$\frac{[3u_1^- - 2(\Lambda+1)]^2\, u_2^- u_3^- u_4^+ u_5^+ u_6^+}{4C_2^-(P)}$	0
$\frac{[3u_2^- - 2(\Lambda+1)]^2\, u_3^- u_5^+ u_6^+ u_7^{+2}}{2C_2(Q)}$	0
$\frac{[3u_3^- - 2(\Lambda+1)]^2\, u_6^+ u_7^{+2} u_8^{+2}}{4C_2^+(R)}$	0
$\frac{[u_1^- - 4(\Lambda+1)]^2\, u_2^{-2} u_3^- u_5^+ u_6^+}{2C_3^-(P)}$	0

Table II

Branches		Line	
$\Delta\Lambda = +1$	$\Delta\Lambda = -1$	${}^{6}X(a) - {}^{6}Y(a)$	${}^{6}X(a) - {}^{6}Y(b)$
${}^{O}Q_{35}(J)$	${}^{S}Q_{53}(J)$	0	$\frac{[u_7^- - 4\Lambda]^2 u_5^- u_6^- u_5^{+2} u_6^+}{C_5(Q)}$
${}^{P}R_{35}(J)$	${}^{R}P_{53}(J+1)$	0	$\frac{[u_7^- - 4\Lambda]^2 u_6^- u_5^{+2} u_6^{+2}}{2C_5(R)}$
${}^{O}P_{45}(J)$	${}^{S}R_{54}(J-1)$	0	$\frac{[u_7^+ + 4\Lambda]^2 u_3^- u_4^- u_5^- u_6^- u_6^+}{2C_5(P)}$
${}^{P}Q_{45}(J)$	${}^{R}Q_{54}(J)$	0	$\frac{[u_7^+ + 4\Lambda]^2 u_4^- u_5^- u_6^- u_6^{+2}}{C_5(Q)}$
${}^{Q}R_{45}(J)$	${}^{Q}P_{54}(J+1)$	0	$\frac{[u_7^+ + 4\Lambda]^2 u_5^- u_6^- u_6^{+2} u_7^+}{2C_5(R)}$
$P_5(J)$	$R_5(J-1)$	$\frac{u_2^- u_3^-}{2J}$	$\frac{[3u_7^+ + 2\Lambda]^2 u_2^- u_3^- u_4^- u_5^- u_6^-}{4C_5(P)}$
$Q_5(J)$	$Q_5(J)$	$\frac{u_3^- u_7^+(J+1/2)}{J(J+1)}$	$\frac{[3u_7^+ + 2\Lambda]^2 u_3^- u_4^- u_5^- u_6^- u_7^+}{2C_5(Q)}$
$R_5(J)$	$P_5(J+1)$	$\frac{u_7^+ u_8^+}{2(J+1)}$	$\frac{[3u_7^+ + 2\Lambda]^2 u_4^- u_5^- u_6^- u_7^+ u_8^+}{4C_5(R)}$
${}^{Q}P_{65}(J)$	${}^{Q}R_{56}(J-1)$	0	$\frac{5u_1^- u_2^- u_3^- u_4^- u_5^- u_6^- u_7^+}{4C_5(P)}$
${}^{R}Q_{65}(J)$	${}^{P}Q_{56}(J)$	0	$\frac{5u_2^- u_3^- u_4^- u_5^- u_6^- u_7^+ u_8^+}{2C_5(Q)}$
${}^{S}R_{65}(J)$	${}^{O}P_{56}(J+1)$	0	$\frac{5u_3^- u_4^- u_5^- u_6^- u_7^+ u_8^+ u_9^+}{4C_5(R)}$
${}^{K}P_{16}(J)$	${}^{W}R_{61}(J-1)$	0	$\frac{u_6^- u_7^- u_3^+ u_4^+ u_5^+ u_6^+ u_7^+}{4C_6(P)}$
${}^{L}Q_{16}(J)$	${}^{V}Q_{61}(J)$	0	$\frac{u_7^- u_3^{+2} u_4^+ u_8^+ u_6^+ u_7^+}{2C_6(Q)}$
${}^{M}R_{16}(J)$	${}^{U}P_{61}(J+1)$	0	$\frac{u_3^{+2} u_4^{+2} u_5^+ u_6^+ u_7^+}{4C_6(R)}$
${}^{L}P_{26}(J)$	${}^{V}R_{62}(J-1)$	0	$\frac{5u_5^- u_6^- u_7^- u_4^+ u_5^+ u_6^+ u_7^+}{4C_6(P)}$
${}^{M}Q_{26}(J)$	${}^{U}Q_{62}(J)$	0	$\frac{5u_6^- u_7^- u_4^{+2} u_5^+ u_6^+ u_7^+}{2C_6(Q)}$
${}^{N}R_{26}(J)$	${}^{T}P_{62}(J+1)$	0	$\frac{5u_7^- u_4^{+2} u_5^{+2} u_6^+ u_7^+}{4C_6(R)}$
${}^{M}P_{36}(J)$	${}^{U}R_{63}(J-1)$	0	$\frac{5u_4^- u_5^- u_6^- u_7^- u_5^+ u_6^+ u_7^+}{2C_6(P)}$
${}^{N}Q_{36}(J)$	${}^{T}Q_{63}(J)$	0	$\frac{5u_5^- u_6^- u_7^- u_5^{+2} u_6^+ u_7^+}{C_6(Q)}$
${}^{O}R_{36}(J)$	${}^{S}P_{63}(J+1)$	0	$\frac{5u_6^- u_7^- u_5^{+2} u_6^{+2} u_7^+}{2C_6(R)}$

(continued)

strengths

${}^{s}X(b) - {}^{s}Y(a)$	${}^{s}X(b) - {}^{s}Y(b)$
$\frac{[u_0^- - 4(\Lambda+1)]^2 u_3^{-2} u_6^+ u_7^{+2}}{C_3(Q)}$	0
$\frac{[u_1^- - 4(\Lambda+1)]^2 u_4^- u_7^{+2} u_8^{+2}}{2C_3^+(R)}$	$\frac{9u_5^- u_6^-}{(J+1)(J+2)(2J+3)^2}$
$\frac{[u_9^+ + 4(\Lambda+1)]^2 u_2^{-2} u_3^{-2} u_6^+}{2C_4^-(P)}$	0
$\frac{[u_{10}^+ + 4(\Lambda+1)]^2 u_3^{-2} u_4^- u_7^{+2}}{C_4(Q)}$	$\frac{u_5^- u_6^-(2J-1)(2J+1)(2J+5)}{J(J+1)^2(J+2)(2J+3)^2}$
$\frac{[u_{11}^+ + 4(\Lambda+1)]^2 u_4^- u_5^- u_7^+ u_8^{+2}}{2C_4^+(R)}$	$\frac{64J(J+3)\, u_6^- u_7^+}{(J+1)(2J+3)^2(2J+5)^2}$
$\frac{[3u_7^+ + 2(\Lambda+1)]^2 u_2^{-2} u_3^{-2} u_4^-}{4C_5^-(P)}$	$\frac{(J-1)\, u_5^- u_6^-(2J-1)(2J+5)}{2J(J+1)(2J+3)^2}$
$\frac{[3u_8^+ + 2(\Lambda+1)]^2 u_3^{-2} u_4^- u_5^- u_7^+}{2C_5(Q)}$	$\frac{2(2J^2+5J-5)^2 u_6^- u_7^+(2J+1)}{J(J+1)(2J+3)^2(2J+5)^2}$
$\frac{[3u_9^+ + 2(\Lambda+1)]^2 u_4^- u_5^- u_6^- u_7^+ u_8^+}{4C_5^+(R)}$	$\frac{Ju_7^+ u_8^+(2J+1)(2J+7)}{2(J+1)(J+2)(2J+5)^2}$
$\frac{5u_2^{-2} u_3^{-2} u_4^- u_8^- u_7^+}{4C_6^-(P)}$	$\frac{10u_6^- u_7^+(2J-1)}{J(2J+3)^2(2J+5)}$
$\frac{5u_3^{-2} u_4^- u_5^- u_6^- u_7^+ u_8^+}{2C_6(Q)}$	$\frac{5u_7^+ u_8^+(2J+1)}{2(J+1)(J+2)(2J+5)^2}$
$\frac{5u_4^- u_5^- u_6^- u_7^- u_8^+ u_9^+}{4C_6^+(R)}$	0
$\frac{u_1^- u_2^- u_3^+ u_4^+ u_5^+ u_6^+ u_7^+}{4C_1^-(P)}$	0
$\frac{u_3^- u_4^+ u_5^+ u_6^+ u_7^+ u_8^{+2}}{2C_1(Q)}$	0
$\frac{u_5^+ u_6^+ u_7^+ u_8^{+2} u_9^{+2}}{4C_1^+(R)}$	0
$\frac{5u_1^{-2} u_2^- u_4^+ u_5^+ u_6^+ u_7^+}{4C_2^-(P)}$	0
$\frac{5u_2^{-2} u_5^+ u_6^+ u_7^+ u_8^{+2}}{2C_2(Q)}$	0
$\frac{5u_3^- u_6^+ u_7^+ u_8^{+2} u_9^{+2}}{4C_2^+(R)}$	0
$\frac{5u_1^{-2} u_2^{-2} u_5^+ u_6^+ u_7^+}{2C_3^-(P)}$	0
$\frac{5u_2^{-2} u_3^- u_6^+ u_7^+ u_8^{+2}}{C_3(Q)}$	0
$\frac{5u_3^- u_4^- u_7^+ u_8^{+2} u_9^{+2}}{2C_3^+(R)}$	0

Table II (continued)

Branches		Line strengths			
$\Delta\Lambda = +1$	$\Delta\Lambda = -1$	${}^{6}X(a) - {}^{6}Y(a)$	${}^{6}X(a) - {}^{6}Y(b)$	${}^{6}X(b) - {}^{6}Y(a)$	${}^{6}X(b) - {}^{6}Y(b)$
${}^{N}P_{46}(J)$	${}^{T}R_{64}(J-1)$	0	$\frac{5u_3^- u_4^- u_5^- u_6^- u_7^- u_6^+ u_7^+}{2C_6(P)}$	$\frac{5u_1^{-2} u_2^{-2} u_3^- u_6^+ u_7^+}{2C_4^-(P)}$	0
${}^{O}Q_{46}(J)$	${}^{S}Q_{64}(J)$	0	$\frac{5u_4^- u_5^- u_6^- u_7^- u_6^{+2} u_7^+}{C_6(Q)}$	$\frac{5u_2^{-2} u_3^- u_4^- u_7^+ u_8^{+2}}{C_4(Q)}$	0
${}^{P}R_{46}(J)$	${}^{R}P_{64}(J+1)$	0	$\frac{5u_5^- u_6^- u_7^- u_6^{+2} u_7^{+2}}{2C_6(P)}$	$\frac{5u_3^- u_4^- u_5^- u_8^{+2} u_9^{+2}}{2C_4^+(R)}$	$\frac{5u_6^- u_7^-}{(J+1)(J+2)(J+3)(2J+5)^2}$
${}^{O}P_{56}(J)$	${}^{S}R_{65}(J-1)$	0	$\frac{5u_2^- u_3^- u_4^- u_5^- u_6^- u_7^- u_7^+}{4C_6(P)}$	$\frac{5u_1^{-2} u_2^{-2} u_3^- u_4^- u_7^+}{4C_5^-(P)}$	0
${}^{P}Q_{56}(J)$	${}^{R}Q_{65}(J)$	0	$\frac{5u_3^- u_4^- u_5^- u_6^- u_7^- u_7^{+2}}{2C_6(Q)}$	$\frac{5u_2^{-2} u_3^- u_4^- u_5^- u_8^{+2}}{2C_5(Q)}$	$\frac{5u_6^- u_7^-(2J+1)}{2(J+1)(J+2)(2J+5)^2}$
${}^{Q}R_{56}(J)$	${}^{Q}P_{65}(J+1)$	0	$\frac{5u_4^- u_5^- u_6^- u_7^- u_7^{+2} u_8^+}{4C_6(R)}$	$\frac{5u_3^- u_4^- u_5^- u_6^- u_8^+ u_9^{+2}}{4C_5^+(R)}$	$\frac{10u_7^- u_8^+(2J+1)}{(J+1)(2J+5)^2(2J+7)^2}$
$P_6(J)$	$R_6(J-1)$	$\frac{u_1^- u_2^-}{2J}$	$\frac{u_1^- u_2^- u_3^- u_4^- u_5^- u_6^- u_7^-}{4C_6(P)}$	$\frac{u_1^{-2} u_2^{-2} u_3^- u_4^- u_5^-}{4C_6^-(P)}$	$\frac{u_6^- u_7^-(2J-1)}{2(J+2)(2J+5)}$
$Q_6(J)$	$Q_6(J)$	$\frac{u_2^- u_8^+(J+1/2)}{J(J+1)}$	$\frac{u_2^- u_3^- u_4^- u_5^- u_6^- u_7^- u_8^+}{2C_6(Q)}$	$\frac{u_2^{-2} u_3^- u_4^- u_5^- u_6^- u_8^+}{2C_6(Q)}$	$\frac{2Ju_7^- u_8^+(2J+1)}{(J+1)(2J+5)^2}$
$R_6(J)$	$P_6(J+1)$	$\frac{u_8^+ u_9^+}{2(J+1)}$	$\frac{u_3^- u_4^- u_5^- u_6^- u_7^- u_8^+ u_9^+}{4C_6(R)}$	$\frac{u_3^- u_4^- u_5^- u_6^- u_7^- u_8^+ u_9^+}{4C_6^+(R)}$	$\frac{u_8^+ u_9^+(2J+1)}{2(J+3)(2J+7)}$

Table III

Line strengths for ${}^{2S+1}X_{\Lambda} - {}^{2S+1}X_{\Lambda}$ transitions

Branches	Line strengths	
	${}^{2S+1}X(a) - {}^{2S+1}X(a)$	${}^{2S+1}X(b) - {}^{2S+1}X(b)$
$P_i(J)$	$\dfrac{J^2-(\Lambda+\Sigma)^2}{J}$	$\dfrac{(N-\Lambda)(N+\Lambda)[(J+N-1)(J+N)-S(S+1)]\,[(J+N)(J+N+1)-S(S+1)]}{4JN^2(2N-1)(2N+1)}$
${}^{Q}P_{i+1,i}(J)$	0	$\Lambda^2\dfrac{[(J+N)(J+N+1)-S(S+1)]\,[S(S+1)-(J-N)(J-N-1)]}{4JN^2(N+1)^2}$
${}^{R}P_{i+1,i}(J)$	0	$\dfrac{(N-\Lambda+1)(N+\Lambda+1)\,[S(S+1)-(J-N-1)(J-N)][S(S+1)-(J-N-2)(J-N-1)]}{4J(N+1)^2(2N+1)(2N+3)}$
${}^{P}Q_{i-1,i}(J)$	0	$\dfrac{(N-\Lambda)(N+\Lambda)[(J+N)(J+N+1)-S(S+1)][S(S+1)-(J-N)(J-N+1)](2J+1)}{4J(J+1)N^2(2N-1)(2N+1)}$
$Q_i(J)$	$(\Lambda+\Sigma)^2\dfrac{2J+1}{J(J+1)}$	$\Lambda^2\dfrac{[J(J+1)+N(N+1)-S(S+1)]^2(2J+1)}{4J(J+1)N^2(N+1)^2}$
${}^{R}Q_{i+1,i}(J)$	0	$\dfrac{(N-\Lambda+1)(N+\Lambda+1)\,[(J+N+1)(J+N+2)-S(S+1)]\,[S(S+1)-(J-N-1)(J-N)]\,(2J+1)}{4J(J+1)(N+1)^2(2N+1)(2N+3)}$
${}^{P}R_{i-2,i}(J)$	0	$\dfrac{(N-\Lambda)(N+\Lambda)\,[S(S+1)-(J-N+1)(J-N+2)]\,[S(S+1)-(J-N)(J-N+1)^2]}{4(J+1)N^2(2N-1)(2N+1)}$
${}^{Q}R_{i-1,i}(J)$	0	$\Lambda^2\dfrac{[(J+N+1)(J+N+2)-S(S+1)]\,[S(S+1)-(J-N+1)(J-N)]}{4(J+1)N^2(N+1)^2}$
$R_i(J)$	$\dfrac{(J+1)^2-(\Lambda+\Sigma)^2}{J+1}$	$\dfrac{(N-\Lambda+1)(N+\Lambda+1)\,[(J+N+1)(J+N+2)-S(S+1)][(J+N+2)(J+N+3)-S(S+1)]}{4(J+1)(N+1)^2(2N+1)(2N+3)}$

tion due to the $\Delta N = 0, \pm 1$ selection rule there are $9\,(2S+1) - 8$ branches, i.e. their intesities are other than zero. In the Tables I and II

$$C_i^-(P) = JC_K(J-1); \qquad C_i(R) = (J+1)\,C_K(J);$$
$$C_i(Q) = \frac{J(J+1)}{J+1/2}\,C_K(J); \tag{6}$$
$$C_i(P) = JC_K(J); \qquad C_i^+(R) = (J+1)C_K(J+1);$$

where $i = 1, 2, \ldots, 6$ and $K = J - 5/2, J - 3/2, \ldots, J + 5/2$, respectively. For all the Tables the following correlation

	Case *a)*		Case *b)*
i	Ω_n	Ω_i	N
1	$\Lambda - S$	$\Lambda + S$	$J - S$
2	$\Lambda - S + 1$	$\Lambda + S - 1$	$J - S + 1$
.	.	.	.
.	.	.	.
.	.	.	.
$2S + 1$	$\Lambda + S$	$\Lambda - S$	$J + S$

holds, where the suffix of Ω n = normal, i = inverted.

For all Tables the terms of case a) were assumed to be normal. If an inverted term occurs instead of a normal one then the suffixes corresponding to the inverted terms in the branch symbols have to be changed on the basis of the above correlation according to the pattern $1 \to 2S + 1$, $2 \to 2S, \ldots$, $2S + 1 \to 1$ wherever the inverted term occurs. In the next part of this paper the quartet and quintet transitions will be discussed.

REFERENCES

1. I. Kovács, Rotational Structure in the Spectra of Diatomic Molecules, Akadémiai Kiadó, Budapest and Adam Hilger, Ltd. London, 1969.
2. E. E. Whiting, J. A. Peterson, I. Kovács, R. W. Nicholls, J. Mol. Spectr., **47**, 84, 1973.
3. I. Kovács and M. I. M. El Agrab, Acta Phys. Hung., **43**, 185, 1977.
4. B. Pouilly, J. Schamps, D. Luncley, R. F. Barrow, Coll. High Resolution Molecular Spectra, Tours, 1977.
5. A. M. Lambert, J. P. Goure, D. L. Albritton, Can. J. Phys., **55**, 1842, 1977.
6. E. L. Hill and J. H. van Vleck, Phys. Rev., **32**, 250, 1928.

Table IV

Line strengths for ${}^{2S+1}X_{\Lambda+1} - {}^{2S+1}Y_{\Lambda}$ transitions

Branches		Line strengths	
$\Delta\Lambda = +1$	$\Delta\Lambda = -1$	${}^{2S+1}X(a) - {}^{2S+1}Y(a)$	${}^{2S+1}X(b) - {}^{2S+1}Y(b)$
$P_i(J)$	$R_i(J-1)$	$\dfrac{(J-\Lambda-\Sigma-1)(J-\Lambda-\Sigma)}{2J}$	$\dfrac{(N-\Lambda)(N-\Lambda-1)[(J+N-1)(J+N)-S(S+1)][(J+N)(J+N+1)-S(S+1)]}{8JN^2(2N-1)(2N+1)}$
${}^{Q}P_{i+1,i}(J)$	${}^{Q}R_{i,i+1}(J-1)$	0	$\dfrac{(N-\Lambda)(N+\Lambda+1)[(J+N)(J+N+1)-S(S+1)][S(S+1)-(J-N)(J-N-1)]}{8JN^2(N+1)^2}$
${}^{R}P_{i+2,i}(J)$	${}^{P}R_{i,i+2}(J-1)$	0	$\dfrac{(N+\Lambda+1)(N+\Lambda+2)[S(S+1)-(J-N-1)(J-N)][S(S+1)-(J-N-2)(J-N-1)]}{8J(N+1)^2(2N+1)(2N+3)}$
${}^{P}Q_{i-1,i}(J)$	${}^{R}Q_{i,i-1}(J)$	0	$\dfrac{(N-\Lambda)(N-\Lambda-1)[(J+N)(J+N+1)-S(S+1)][S(S+1)-(J-N)(J-N+1)](2J+1)}{8J(J+1)N^2(2N-1)(2N+1)}$
$Q_i(J)$	$Q_i(J)$	$\dfrac{(J+\Lambda+\Sigma+1)(J-\Lambda-\Sigma)(2J+1)}{2J(J+1)}$	$\dfrac{(N-\Lambda)(N+\Lambda+1)[J(J+1)+N(N+1)-S(S+1)]^2(2J+1)}{8J(J+1)N^2(N+1)^2}$
${}^{R}Q_{i+1,i}(J)$	${}^{P}Q_{i,i+1}(J)$	0	$\dfrac{(N+\Lambda+1)(N+\Lambda+2)[(J+N+1)(J+N+2)-S(S+1)][S(S+1)-(J-N-1)(J-N)](2J+1)}{8J(J+1)(N+1)^2(2N+1)(2N+3)}$
${}^{P}R_{i-2,i}(J)$	${}^{R}P_{i,i-2}(J+1)$	0	$\dfrac{(N-\Lambda)(N-\Lambda-1)[S(S+1)-(J-N+1)(J-N+2)][S(S+1)-(J-N)(J-N+1)]}{8(J+1)N^2(2N-1)(2N+1)}$
${}^{Q}R_{i-1,i}(J)$	${}^{Q}P_{i,i-1}(J+1)$	0	$\dfrac{(N-\Lambda)(N+\Lambda+1)[(J+N+1)(J+N+2)-S(S+1)][S(S+1)-(J-N+1)(J-N)]}{8(J+1)N^2(N+1)^2}$
$R_i(J)$	$P_i(J+1)$	$\dfrac{(J+\Lambda+\Sigma+1)(J+\Lambda+\Sigma+2)}{2(J+1)}$	$\dfrac{(N+\Lambda+1)(N+\Lambda+2)[(J+N+1)(J+N+2)-S(S+1)][(J+N+2)(J+N+3)-S(S+1)]}{8(J+1)(N+1)^2(2N+1)(2N+3)}$

Acta Physica Academiae Scientiarum Hungaricae, Tomus 43 (3—4), pp. 319—345 (1977)

CONTRIBUTION TO THE INTENSITY DISTRIBUTIONS OF THE MULTIPLET BANDS IN DIATOMIC MOLECULES II

By

I. KOVÁCS and A. GRANDPIERRE

DEPARTMENT OF ATOMIC PHYSICS, TECHNICAL UNIVERSITY, BUDAPEST

(Received 17. I. 1978)

Explicit expressions are obtained for the intensity distributions in the branches of quartet and quintet transitions of any type with $\Delta\Lambda = 0$ and $\Delta\Lambda = \pm 1$ where the upper and lower electronic states may belong to one of the limiting Hund's cases a) or b).

In the first part of this paper the formulae of the intensity distribution of the sextet transitions and of the transitions of any type and any multiplicity in the limiting Hund's cases have been treated [1]. In this second part general formulae of the line strengths are given for all branches of the quartet and quintet transitions of any type with $\Delta\Lambda = 0$ and $\Delta\Lambda = \pm 1$ where the upper and lower terms may belong toone of the limiting Hund's cases a) or b). These formulae give after substitution of the proper Λ values (0, 1, 2, ...) the line strengths of all branches for $\Sigma - \Sigma$, $\Pi - \Pi$, $\Delta - \Delta$ ... and $\Pi - \Sigma$, $\Delta - \Pi$, $\Phi - \Delta$, ... transitions completed with the line strengths of the lacking branches of the $\Pi - \Pi$ and $\Pi - \Sigma$ transitions already published [2]. In spite of the existence of algebraic expression for the quartet terms of intermediate case [3] due to the complicated form of the transformation matrix in intermediate case we have also in this case no other choice but to restrict ourselves to the transitions of limiting cases, otherwise the formulae of line strengths would be too complicated to use. The adopted procedure has been described in the previous part of this paper [1]. The elements of the transformation matrix of quartet and quintet terms of any type for case b) required for the application are the following.

$^4X(b)$ transformation matrix

$$S_{\Lambda-3/2,J-3/2} = \sqrt{\frac{u_4^- u_5^- u_6^-}{C_{J-3/2}(J)}}\,;\quad S_{\Lambda-1/2,J-3/2} = -\sqrt{\frac{3u_4^- u_5^- u_4^+}{C_{J-3/2}(J)}}\,;$$

$$S_{\Lambda+1/2,J-3/2} = \sqrt{\frac{3u_4^- u_4^+ u_5^+}{C_{J-3/2}(J)}}\,;\quad S_{\Lambda+3/2,J-3/2} = -\sqrt{\frac{u_4^+ u_5^+ u_6^+}{C_{J-3/2}(J)}}\,;$$

$$S_{\Lambda-3/2,J-1/2} = -\sqrt{\frac{3u_5^- u_6^- u_4^+}{C_{J-1/2}(J)}}\,;\quad S_{\Lambda-1/2,J-1/2} = \sqrt{\frac{(u_4^+ + 2\Lambda)^2 u_5^-}{C_{J-1/2}(J)}}\,;$$

$$S_{\Lambda+1/2,J-1/2} = \sqrt{\frac{(u_4^- - 2\Lambda)^2 u_5^+}{C_{J-1/2}(J)}}\,;\quad S_{\Lambda+3/2.J-1/2} = -\sqrt{\frac{3\,u_4^- u_5^+ u_6^+}{C_{J-1/2}(J)}}\,;$$

$$S_{\Lambda-3/2,J+1/2} = \sqrt{\frac{3\,u_6^- u_4^+ u_5^+}{C_{J+1/2}(J)}}\,;\quad S_{\Lambda-1/2,J+1/2} = \sqrt{\frac{(u_6^- - 2\Lambda)^2 u_5^+}{C_{J+1/2}(J)}}\,;$$

$$S_{\Lambda+1/2.J+1/2} = -\sqrt{\frac{(u_6^+ + 2\Lambda)^2 u_5^-}{C_{J+1/2}(J)}}\,;\quad S_{\Lambda+3/2,J+1/2} = -\sqrt{\frac{3\,u_4^- u_5^- u_6^+}{C_{J+1/2}(J)}}\,;$$

$$S_{\Lambda-3/2,J+3/2} = -\sqrt{\frac{u_4^+ u_5^+ u_6^+}{C_{J+3/2}(J)}}\,;\quad S_{\Lambda-1/2,J+3/2} = -\sqrt{\frac{3\,u_6^- u_5^+ u_6^+}{C_{J+3/2}(J)}}\,;$$

$$S_{\Lambda+1/2,J+3/2} = -\sqrt{\frac{3\,u_5^- u_6^- u_6^+}{C_{J+3/2}(J)}}\,;\quad S_{\Lambda+3/2,J+3/2} = -\sqrt{\frac{u_4^- u_5^- u_6^-}{C_{J+3/2}(J)}}\,; \tag{1a}$$

where $u_{n+1}^{\pm} = u_n^{\pm} + 1$ and $u_0^{\pm} = J \pm \Lambda - 9/2$

$$\begin{aligned} C_{J-3/2}(J) &= 2J(2J-1)(2J+1)\,,\\ C_{J-1/2}(J) &= 2(J+1)(2J-1)(2J+1)\,,\\ C_{J+1/2}(J) &= 2J(2J+1)(2J+3)\,,\\ C_{J+3/2}(J) &= 2(J+1)(2J+1)(2J+3)\,. \end{aligned} \tag{1b}$$

$^5X(b)$ transformation matrix

$$S_{\Lambda-2,J-2} = \sqrt{\frac{v_3^- v_4^- v_5^- v_6^-}{C_{J-2}(J)}}\,;\quad S_{\Lambda-1,J-2} = -\sqrt{\frac{4\,v_3^- v_4^- v_5^- v_1^+}{C_{J-2}(J)}}\,;$$

$$S_{\Lambda,J-2} = \sqrt{\frac{6\,v_3^- v_4^- v_3^+ v_4^+}{C_{J-2}(J)}}\,;\quad S_{\Lambda+1,J-2} = -\sqrt{\frac{4 v_3^- v_4^+ v_5^+ v_6^+}{C_{J-2}(J)}}\,;$$

$$S_{\Lambda+2.J-2} = \sqrt{\frac{v_3^+ v_4^+ v_5^+ v_6^+}{C_{J-2}(J)}}\,;$$

$$S_{\Lambda-2,J-1} = \sqrt{\frac{v_4^- v_5^- v_6^- v_3^+}{C_{J-1}(J)}}\,;\quad S_{\Lambda-1,J-1} = -\sqrt{\frac{(v_3^+ + \Lambda)^2 v_4^- v_5^-}{C_{J-1}(J)}}\,;$$

$$S_{\Lambda,J-1} = \Lambda\sqrt{\frac{6\,v_4^- v_4^+}{C_{J-1}(J)}}\,;\quad S_{\Lambda+1,J-1} = \sqrt{\frac{(v_3^- - \Lambda)^2 v_4^+ v_5^+}{C_{J-1}(J)}}\,;$$

$$S_{\Lambda+2,J-1} = -\sqrt{\frac{v_3^- v_4^+ v_5^+ v_6^+}{C_{J-1}(J)}}\,;$$

$$S_{\Lambda-2,J} = \sqrt{\frac{3\,v_5^- v_6^- v_3^+ v_4^+}{C_J(J)}}\,;\quad S_{\Lambda-1,J} = -(2\Lambda-1)\sqrt{\frac{3 v_5^- v_4^+}{C_J(J)}}\,;$$

$$S_{\Lambda,J} = \sqrt{\frac{2[v_5^- v_4^+ - \Lambda(2\Lambda+1)]^2}{C_J(J)}}\,;\quad S_{\Lambda+1,J} = (2\Lambda+1)\sqrt{\frac{3v_4^- v_5^+}{C_J(J)}}\,;$$

$$S_{\Lambda+2,J} = \sqrt{\frac{3v_3^- v_4^- v_5^+ v_6^+}{C_J(J)}}\,; \tag{2a}$$

$$S_{\Lambda-2,J+1} = \sqrt{\frac{v_6^- v_3^+ v_4^+ v_5^+}{C_{J+1}(J)}}\,;\quad S_{\Lambda-1,J+1} = \sqrt{\frac{(v_6^- - \Lambda)^2 v_4^+ v_5^+}{C_{J+1}(J)}}\,;$$

$$S_{\Lambda,J+1} = -\Lambda\sqrt{\frac{6v_5^- v_5^+}{C_{J+1}(J)}}\,;\quad S_{\Lambda+1,J+1} = -\sqrt{\frac{(v_6^+ + \Lambda)^2 v_4^- v_5^-}{C_{J+1}(J)}}\,;$$

$$S_{\Lambda+2,J+1} = -\sqrt{\frac{v_3^- v_4^- v_5^- v_6^+}{C_{J+1}(J)}}\,;$$

$$S_{\Lambda-2,J+2} = \sqrt{\frac{v_3^+ v_4^+ v_5^+ v_6^+}{C_{J+2}(J)}}\,;\quad S_{\Lambda-1,J+2} = \sqrt{\frac{4v_6^- v_4^+ v_5^+ v_6^+}{C_{J+2}(J)}}\,;$$

$$S_{\Lambda,J+2} = \sqrt{\frac{6v_5^- v_6^- v_5^+ v_6^+}{C_{J+2}(J)}}\,;\quad S_{\Lambda+1,J+2} = \sqrt{\frac{4v_4^- v_5^- v_6^- v_6^+}{C_{J+2}(J)}}\,;$$

$$S_{\Lambda+2,J+2} = \sqrt{\frac{v_3^- v_4^- v_5^- v_6^-}{C_{J+2}(J)}}\,;$$

where $v_{n+1}^{\pm} = v_n^{\pm} + 1$ and $v_1^{\pm} = J \pm \Lambda - 3$

$$\begin{aligned}
C_{J-2}(J) &= 4(J-1)J(2J-1)(2J+1)\,,\\
C_{J-1}(J) &= 2(J-1)J(J+1)(2J+1)\,,\\
C_J(J) &= 2J(J+1)(2J-1)(2J+3)\,,\\
C_{J+1}(J) &= 2J(J+1)(J+2)(2J+3)\,,\\
C_{J+2}(J) &= 4(J+1)(J+2)(2J+1)(2J+3)\,.
\end{aligned} \tag{2b}$$

The line strengths referring to the transition ${}^4X_\Lambda(a) - {}^4X_\Lambda(a)$, ${}^4X_\Lambda(a) - {}^4X_\Lambda(b)$, ${}^4X_\Lambda(b) - {}^4X_\Lambda(a)$, ${}^4X_\Lambda(b) - {}^4X_\Lambda(b)$ and ${}^5X_\Lambda(a) - {}^5X_\Lambda(a)$, ${}^5X_\Lambda(a) - {}^5X_\Lambda(b)$, ${}^5X_\Lambda(b) - {}^5X_\Lambda(a)$, ${}^5X_\Lambda(b) - {}^5X_\Lambda(b)$ that is to the quartet and quintet transitions of any type with $\Delta\Lambda = 0$ can be found in the second, third, fourth, and fifth column in Table I, and in Table III, respectively. The line strengths referring to the transition ${}^4X_{\Lambda+1}(a) - {}^4Y_\Lambda(a)$, ${}^4X_{\Lambda+1}(a) - {}^4Y_\Lambda(b)$, ${}^4X_{\Lambda+1}(b) - {}^4Y_\Lambda(a)$, ${}^4X_{\Lambda+1}(b) - {}^4Y_\Lambda(b)$ and ${}^5X_{\Lambda+1}(a) - {}^5Y_\Lambda(a)$, ${}^5X_{\Lambda+1}(a) - {}^5Y_\Lambda(b)$, ${}^5X_{\Lambda+1}(b) - {}^5Y_\Lambda(a)$, ${}^4X_{\Lambda+1}(b) - {}^5Y_\Lambda(b)$ that is to the quartet and quintet transitions of any type with $\Delta\Lambda = \pm 1$ are included in the third, fourth, fifth and sixth column in Table II and in Table IV, respectively.

Table I

Line strength for ${}^4X_\Lambda - {}^4X_\Lambda$ transitions

Branches	Line strengths			
	${}^4X(a) - {}^4X(a)$	${}^4X(a) - {}^4X(b)$	${}^4X(b) - {}^4X(a)$	${}^4X(b) - {}^4X(b)$
$P_1(J)$	$\frac{u_6^- u_3^+}{J}$	$\frac{u_4^- u_5^- u_6^{-2} u_3^+}{C_1(P)}$	$R_1(J-1)$	$\frac{u_3^- u_3^+ (2J+1)}{(J-1)(2J-3)}$
$Q_1(J)$	$\left(\Lambda - \frac{3}{2}\right)^2 \frac{2J+1}{J(J+1)}$	$\left(\Lambda - \frac{3}{2}\right)^2 \frac{u_4^- u_5^- u_6^-}{C_1(Q)}$	$Q_1(J)$	$\Lambda^2 \frac{4(J+1)(2J+1)}{J(2J-1)^2}$
$R_1(J)$	$\frac{u_7^- u_4^+}{J+1}$	$\frac{u_4^- u_5^- u_6^- u_7^- u_4^+}{C_1(R)}$	$P_1(J+1)$	$\frac{u_4^- u_4^+ (2J+3)}{J(2J-1)}$
${}^Q P_{21}(J)$	0	$\frac{3u_4^- u_5^{-2} u_4^{+2}}{C_1(P)}$	${}^Q R_{12}(J-1)$	$\Lambda^2 \frac{12(2J+1)}{J(2J-1)^2(2J-3)}$
${}^R Q_{21}(J)$	0	$\left(\Lambda - \frac{1}{2}\right)^2 \frac{3u_4^- u_5^- u_4^+}{C_1(Q)}$	${}^P Q_{12}(J)$	$\frac{3u_4^- u_4^+ (2J+1)}{J^2(2J-1)^2}$
${}^S R_{21}(J)$	0	$\frac{3u_4^- u_5^- u_6^- u_4^+ u_5^+}{C_1(R)}$	${}^O P_{12}(J+1)$	0
${}^R P_{31}(J)$	0	$\frac{3u_4^{-2} u_4^+ u_5^{+2}}{C_1(P)}$	${}^P R_{13}(J-1)$	$\frac{3u_4^- u_4^+}{(J-1)J^2(2J-1)^2}$
${}^S Q_{31}(J)$	0	$\left(\Lambda + \frac{1}{2}\right)^2 \frac{3u_4^- u_4^+ u_5^+}{C_1(Q)}$	${}^O Q_{13}(J)$	0
${}^T R_{31}(J)$	0	$\frac{3u_4^- u_5^- u_4^+ u_5^+ u_6^+}{C_1(R)}$	${}^N P_{13}(J+1)$	0
${}^S P_{41}(J)$	0	$\frac{u_3^- u_4^+ u_5^+ u_6^{+2}}{C_1(P)}$	${}^O R_{14}(J-1)$	0
${}^T Q_{41}(J)$	0	$\left(\Lambda + \frac{3}{2}\right)^2 \frac{u_4^+ u_5^+ u_6^+}{C_1(Q)}$	${}^N Q_{14}(J)$	0
${}^U R_{41}(J)$	0	$\frac{u_4^- u_4^+ u_5^+ u_6^+ u_7^+}{C_1(R)}$	${}^M P_{14}(J+1)$	0

${}^{O}P_{12}(J)$	0	$\dfrac{3u_5^- u_6^{-2} u_3^+ u_4^+}{C_2(P)}$	${}^{S}R_{21}(J-1)$	0
${}^{P}Q_{12}(J)$	0	$\left(\Lambda - \dfrac{3}{2}\right)^2 \dfrac{3u_5^- u_6^- u_4^+}{C_2(Q)}$	${}^{R}Q_{21}(J)$	$\dfrac{3u_4^- u_4^+ (2J+1)}{J^2(2J-1)^2}$
${}^{Q}R_{12}(J)$	0	$\dfrac{3u_5^- u_6^- u_7^- u_4^{+2}}{C_2(R)}$	${}^{Q}P_{21}(J+1)$	$\Lambda^2 \dfrac{12(2J+3)}{(J+1)(2J-1)(2J+1)^2}$
$P_2(J)$	$\dfrac{u_5^- u_4^+}{J}$	$\dfrac{(u_4^+ + 2\Lambda)^2 u_5^{-2} u_4^+}{C_2(P)}$	$R_2(J-1)$	$\dfrac{(J+1)u_4^- u_4^+ (2J-3)(2J+1)}{J^2(2J-1)^2}$
$Q_2(J)$	$\left(\Lambda - \dfrac{1}{2}\right)^2 \dfrac{2J+1}{J(J+1)}$	$\left(\Lambda - \dfrac{1}{2}\right)^2 \dfrac{(u_4^+ + 2\Lambda)^2 u_5^-}{C_2(Q)}$	$Q_2(J)$	$\Lambda^2 \dfrac{4(2J^2+J-4)^2}{J(J+1)(2J-1)^2(2J+1)}$
$R_2(J)$	$\dfrac{u_5^+ u_6^+}{2(J+1)}$	$\dfrac{(u_4^+ + 2\Lambda)^2 u_5^- u_5^+ u_6^+}{C_2(R)}$	$P_2(J+1)$	$\dfrac{(J+2)u_5^- u_5^+ (2J-1)(2J+3)}{(J+1)^2(2J+1)^2}$
${}^{Q}P_{32}(J)$	0	$\dfrac{(u_4^- - 2\Lambda)^2 u_4^- u_5^{+2}}{C_2(P)}$	${}^{Q}R_{23}(J-1)$	$\Lambda^2 \dfrac{64(J-1)(J+1)}{J(2J-1)^2(2J+1)^2}$
${}^{R}Q_{32}(J)$	0	$\left(\Lambda + \dfrac{1}{2}\right)^2 \dfrac{(u_4^- - 2\Lambda)^2 u_5^+}{C_2(Q)}$	${}^{P}Q_{23}(J)$	$\dfrac{u_5^- u_5^+ (2J-1)(2J+3)}{J^2(J+1)^2(2J+1)}$
${}^{S}R_{32}(J)$	0	$\dfrac{(u_4^- - 2\Lambda)^2 u_5^- u_5^+ u_6^+}{C_2(R)}$	${}^{O}P_{23}(J+1)$	0
${}^{R}P_{42}(J)$	0	$\dfrac{3u_3^- u_4^- u_5^+ u_6^{+2}}{C_2(P)}$	${}^{P}R_{24}(J-1)$	$\dfrac{3u_5^- u_5^+}{2J^2(J+1)(2J+1)}$
${}^{S}Q_{42}(J)$	0	$\left(\Lambda + \dfrac{3}{2}\right)^2 \dfrac{3u_4^- u_5^+ u_6^+}{C_2(Q)}$	${}^{O}Q_{24}(J)$	0
${}^{T}R_{42}(J)$	0	$\dfrac{3u_4^{-2} u_5^+ u_6^+ u_7^+}{C_2(R)}$	${}^{N}P_{24}(J+1)$	0
${}^{N}P_{13}(J)$	0	$\dfrac{3u_6^{-2} u_3^+ u_4^+ u_5^+}{C_3(P)}$	${}^{T}R_{31}(J-1)$	0
${}^{O}Q_{13}(J))$	0	$\left(\Lambda - \dfrac{3}{2}\right)^2 \dfrac{3u_6^- u_4^+ u_5^+}{C_3(Q)}$	${}^{S}Q_{31}(J)$	0
${}^{P}R_{13}(J)$	0	$\dfrac{3u_6^- u_7^- u_4^{+2} u_5^+}{C_3(R)}$	${}^{R}P_{31}(J+1)$	$\dfrac{3u_5^- u_5^+}{J(J+1)^2(2J+1)^2}$

Table I (continued)

Branches	Line strengths			
	$^4X(a) - {}^4X(a)$	$^4X(a) - {}^4X(b)$	$^4X(b) - {}^4X(a)$	$^4X(b) - {}^4X(b)$
$^OP_{23}(J)$	0	$\frac{(u_6^- - 2\Lambda)^2 u_5^- u_4^+ u_5^+}{C_3(P)}$	$^SR_{32}(J-1)$	0
$^PQ_{23}(J)$	0	$\left(\Lambda - \frac{1}{2}\right)^2 \frac{(u_6^- - 2\Lambda)^2 u_5^+}{C_3(Q)}$	$^RQ_{32}(J)$	$\frac{u_5^- u_5^+ (2J-1)(2J+3)}{J^2(J+1)^2(2J+1)}$
$^QR_{23}(J)$	0	$\frac{(u_6^- - 2\Lambda)^2 u_6^- u_5^{+2}}{C_3(R)}$	$^QP_{32}(J+1)$	$\Lambda^2 \frac{64J(J+2)}{(J+1)(2J+1)^2(2J+3)^2}$
$P_3(J)$	$\frac{u_4^- u_5^+}{J}$	$\frac{(u_6^+ + 2\Lambda)^2 u_4^- u_5^- u_5^+}{C_3(P)}$	$R_3(J-1)$	$\frac{(J-1)u_5^- u_5^+ (2J-1)(2J+3)}{J^2(2J+1)^2}$
$Q_3(J)$	$\left(\Lambda + \frac{1}{2}\right)^2 \frac{2J+1}{J(J+1)}$	$\left(\Lambda + \frac{1}{2}\right)^2 \frac{(u_6^+ + 2\Lambda)^2 u_5^-}{C_3(Q)}$	$Q_3(J)$	$\Lambda^2 \frac{4(2J^2+J-3)^2}{2J(J+1)(2J+1)(2J+3)^2}$
$R_3(J)$	$\frac{u_5^- u_6^+}{J+1}$	$\frac{(u_6^+ + 2\Lambda)^2 u_5^{-2} u_6^+}{C_3(R)}$	$P_3(J+1)$	$\frac{Ju_6^- u_6^+ (2J+1)(2J+5)}{(J+1)^2(2J+3)^2}$
$^QP_{43}(J)$	0	$\frac{3u_3^- u_4^- u_5^- u_6^{+2}}{C_3(P)}$	$^QR_{34}(J-1)$	$\Lambda^2 \frac{24(2J+1)}{J(2J-1)(2J+1)^2(2J+3)}$
$^RQ_{43}(J)$	0	$\left(\Lambda + \frac{3}{2}\right)^2 \frac{3u_4^- u_5^- u_6^+}{C_3(Q)}$	$^PQ_{34}(J)$	$\frac{3u_6^- u_6^+ (2J+1)}{(J+1)^2(2J+3)^2}$
$^SR_{43}(J)$	0	$\frac{3u_4^- u_5^{-2} u_6^{+2}}{C_3(R)}$	$^OP_{34}(J+1)$	0
$^MP_{14}(J)$	0	$\frac{u_6^- u_5^+ u_4^+ u_5^+ u_6^+}{C_4(P)}$	$^UR_{41}(J-1)$	0
$^NQ_{14}(J)$	0	$\left(\Lambda - \frac{3}{2}\right)^2 \frac{u_4^+ u_5^+ u_6^+}{C_4(Q)}$	$^TQ_{41}(J)$	0
$^OR_{14}(J)$	0	$\frac{u_7^- u_4^{+2} u_5^+ u_6^+}{C_4(R)}$	$^SP_{41}(J+1)$	0
$^NP_{24}(J)$	0	$\frac{3u_5^- u_6^- u_4^+ u_5^+ u_6^+}{C_4(P)}$	$^TR_{42}(J-1)$	0

${}^{O}Q_{24}(J)$	0	$\left(\Lambda-\frac{1}{2}\right)^2\frac{3u_6^-u_5^+u_6^+}{C_4(Q)}$
${}^{P}R_{24}(J)$	0	$\frac{3u_6^{-2}u_5^{+2}u_6^+}{C_4(R)}$
${}^{O}P_{34}(J)$	0	$\frac{3u_4^-u_5^-u_6^-u_5^+u_6^+}{C_4(P)}$
${}^{P}Q_{34}(J)$	0	$\left(\Lambda+\frac{1}{2}\right)^2\frac{3u_5^-u_6^-u_6^+}{C_4(Q)}$
${}^{Q}R_{34}(J)$	0	$\frac{3u_5^{-2}u_6^-u_6^{+2}}{C_4(R)}$
$P_4(J)$	$\frac{u_3^-u_6^+}{J}$	$\frac{u_3^-u_4^-u_5^-u_6^-u_6^+}{C_4(P)}$
$Q_4(J)$	$\left(\Lambda+\frac{3}{2}\right)^2\frac{2J+1}{J(J+1)}$	$\left(\Lambda+\frac{3}{2}\right)^2\frac{u_4^-u_5^-u_6^-}{C_4(Q)}$
$R_4(J)$	$\frac{u_4^-u_7^+}{J+1}$	$\frac{u_4^{-2}u_5^-u_6^-u_7^+}{C_4(R)}$

${}^{S}Q_{42}(J)$	0
${}^{R}P_{42}(J+1)$	$\frac{3u_6^-u_6^+}{2(J+1)^2(J+2)(2J+3)}$
${}^{S}R_{43}(J-1)$	0
${}^{R}Q_{43}(J)$	$\frac{3u_6^-u_6^+(2J+1)}{(J+1)^2(2J+3)^2}$
${}^{Q}P_{43}(J+1)$	$\Lambda^2\frac{24(2J+3)}{(J+1)(2J+1)(2J+3)^2(2J+5)}$
$R_4(J-1)$	$\frac{u_6^-u_6^+(2J-1)}{(J+1)(2J+3)}$
$Q_4(J)$	$\Lambda^2\frac{4J(2J+1)}{(J+1)(2J+3)^2}$
$P_4(J+1)$	$\frac{u_7^-u_7^+(2J+1)}{(J+2)(2J+5)}$

Table II

Line strengths for

Branches		Line	
$\Delta\Lambda = +1$	$\Delta\Lambda = -1$	${}^4X(a) - {}^4Y(a)$	${}^4X(a) - {}^4Y(b)$
$P_1(J)$	$R_1(J-1)$	$\frac{u_5^- u_6^-}{2J}$	$\frac{u_4^- u_5^{-2} u_6^{-2}}{2C_1(P)}$
$Q_1(J)$	$Q_1(J)$	$\frac{u_6^- u_4^+ (2J+1)}{2J(J+1)}$	$\frac{u_4^- u_5^- u_6^{-2} u_4^+}{2C_1(Q)}$
$R_1(J)$	$P_1(J+1)$	$\frac{u_4^+ u_5^+}{2(J+1)}$	$\frac{u_4^- u_5^- u_6^- u_4^+ u_5^+}{2C_1(R)}$
${}^QP_{21}(J)$	${}^QR_{12}(J-1)$	0	$\frac{3u_4^{-2} u_5^{-2} u_4^+}{2C_1(P)}$
${}^RQ_{21}(J)$	${}^PQ_{12}(J)$	0	$\frac{3u_4^- u_5^{-2} u_4^+ u_5^+}{2C_1(Q)}$
${}^SR_{21}(J)$	${}^OP_{12}(J+1)$	0	$\frac{3u_4^- u_5^- u_4^+ u_5^+ u_6^+}{2C_1(R)}$
${}^RP_{31}(J)$	${}^PR_{13}(J-1)$	0	$\frac{3u_3^- u_4^{-2} u_4^+ u_5^+}{2C_1(P)}$
${}^SQ_{31}(J)$	${}^OQ_{13}(J)$	0	$\frac{3u_4^{-2} u_4^+ u_5^+ u_6^+}{2C_1(Q)}$
${}^TR_{31}(J)$	${}^NP_{13}(J+1)$	0	$\frac{3u_4^- u_4^+ u_5^+ u_6^+ u_7^+}{2C_1(R)}$
${}^SP_{41}(J)$	${}^OR_{14}(J-1)$	0	$\frac{u_2^- u_3^- u_4^+ u_5^+ u_6^+}{2C_1(P)}$
${}^TQ_{41}(J)$	${}^NQ_{14}(J)$	0	$\frac{u_3^- u_4^+ u_5^+ u_6^+ u_7^+}{2C_1(Q)}$
${}^UR_{41}(J)$	${}^MP_{14}(J+1)$	0	$\frac{u_4^+ u_5^+ u_6^+ u_7^+ u_8^+}{2C_1(R)}$
${}^OP_{12}(J)$	${}^SR_{21}(J-1)$	0	$\frac{3u_5^{-2} u_6^{-2} u_4^+}{2C_2(P)}$
${}^PQ_{12}(J)$	${}^RQ_{21}(J)$	0	$\frac{3u_5^- u_6^{-2} u_4^+}{2C_2(Q)}$
${}^QR_{12}(J)$	${}^QP_{21}(J+1)$	0	$\frac{3u_5^- u_6^- u_4^{+2} u_5^+}{2C_2(R)}$
$P_2(J)$	$R_2(J-1)$	$\frac{u_4^- u_5^-}{2J}$	$\frac{(u_4^+ + 2\Lambda)^2 u_4^- u_5^{-2}}{2C_2(P)}$

${}^4X_{\Lambda+1} - {}^4Y_\Lambda$ transitions

strengths

${}^4X(b) - {}^4Y(a)$	${}^4X(b) - {}^4Y(b)$
$\frac{u_2^- u_3^- u_4^- u_5^- u_6^-}{2C_1^-(P)}$	$\frac{u_2^- u_3^-(2J+1)}{2(J-1)(2J-3)}$
$\frac{u_3^- u_4^- u_5^- u_6^- u_4^+}{2C_1(Q)}$	$\frac{2(J+1)\, u_3^- u_4^+(2J+1)}{J(2J-1)^2}$
$\frac{u_4^- u_5^- u_6^- u_4^+ u_5^+}{2C_1^+(R)}$	$\frac{u_4^+ u_5^+(2J+3)}{2J(2J-1)}$
$\frac{3u_3^- u_4^- u_5^- u_6^- u_4^+}{2C_2^-(P)}$	$\frac{6u_3^- u_4^+(2J+1)}{J(2J-3)(2J-1)^2}$
$\frac{3u_4^- u_5^- u_6^- u_4^+ u_5^+}{2C_2(Q)}$	$\frac{3u_4^+ u_5^+(2J+1)}{2J^2(2J-1)^2}$
$\frac{3u_5^- u_6^- u_4^+ u_5^+ u_6^+}{2C_2^+(R)}$	0
$\frac{3u_4^- u_5^- u_6^- u_4^+ u_5^+}{2C_3^-(P)}$	$\frac{3u_4^+ u_5^+}{2(J-1)J^2(2J-1)^2}$
$\frac{3u_5^- u_6^- u_4^+ u_5^+ u_6^+}{2C_3(Q)}$	0
$\frac{3u_6^- u_4^+ u_5^+ u_6^+ u_7^+}{2C_3^+(R)}$	0
$\frac{u_5^- u_6^- u_4^+ u_5^+ u_6^+}{2C_4^-(P)}$	0
$\frac{u_6^- u_4^+ u_5^+ u_6^+ u_7^+}{2C_4(Q)}$	0
$\frac{u_4^+ u_5^+ u_6^+ u_7^+ u_8^+}{2C_4^+(R)}$	0
$\frac{3u_2^- u_3^- u_4^- u_5^- u_4^+}{2C_1^-(P)}$	0
$\frac{3u_3^- u_4^- u_5^- u_5^{+2}}{2C_1(Q)}$	$\frac{3u_3^- u_4^-(2J+1)}{2J^2(2J-1)^2}$
$\frac{3u_4^- u_5^- u_5^+ u_6^{+2}}{2C_1^+(R)}$	$\frac{6u_4^- u_5^+(2J+3)}{(J+1)(2J-1)(2J+1)^2}$
$\frac{(u_6^+ + 2\Lambda)^2\, u_3^- u_4^- u_5^-}{2C_2^-(P)}$	$\frac{2(J+1)\, u_3^- u_4^+(2J-3)(2J+1)}{J^2(2J-1)^2}$

Table II

Branches		Line	
$\Delta\Lambda = +1$	$\Delta\Lambda = -1$	${}^{\epsilon}X(a) - {}^{\epsilon}Y(a)$	${}^{\epsilon}X(a) - {}^{\epsilon}Y(b)$
$Q_2(J)$	$Q_2(J)$	$\frac{u_5^- u_5^+ (2J+1)}{2J(J+1)}$	$\frac{(u_4^+ + 2\Lambda)^2 u_5^{-2} u_5^+}{2C_2(Q)}$
$R_2(J)$	$P_2(J+1)$	$\frac{u_5^+ u_6^+}{2(J+1)}$	$\frac{(u_4^+ + 2\Lambda)^2 u_5^- u_5^+ u_6^+}{2C_2(R)}$
${}^{Q}P_{32}(J)$	${}^{Q}R_{23}(J-1)$	0	$\frac{(u_4^- - 2\Lambda)^2 u_3^- u_4^- u_5^+}{2C_2(P)}$
${}^{R}Q_{32}(J)$	${}^{P}Q_{23}(J)$	0	$\frac{(u_4^- - 2\Lambda)^2 u_4^- u_5^+ u_6^+}{2C_2(Q)}$
${}^{S}R_{32}(J)$	${}^{O}P_{23}(J+1)$	0	$\frac{(u_4^- - 2\Lambda)^2 u_5^+ u_6^+ u_7^+}{2C_2(R)}$
${}^{R}P_{42}(J)$	${}^{P}R_{24}(J-1)$	0	$\frac{3u_2^- u_3^- u_4^- u_5^+ u_6^+}{2C_2(P)}$
${}^{S}Q_{42}(J)$	${}^{O}Q_{24}(J)$	0	$\frac{3u_3^- u_4^- u_5^+ u_6^+ u_7^+}{2C_2(Q)}$
${}^{T}R_{42}(J)$	${}^{N}P_{24}(J+1)$	0	$\frac{3u_4^- u_5^+ u_6^+ u_7^+ u_8^+}{2C_2(R)}$
${}^{N}P_{13}(J)$	${}^{T}R_{31}(J-1)$	0	$\frac{3u_5^- u_6^{-2} u_4^+ u_5^+}{2C_3(P)}$
${}^{O}Q_{13}(J)$	${}^{S}Q_{31}(J)$	0	$\frac{3u_6^{-2} u_4^{+2} u_5^+}{2C_3(Q)}$
${}^{P}R_{13}(J)$	${}^{R}P_{31}(J+1)$	0	$\frac{3u_6^- u_4^{+2} u_5^{+2}}{2C_3(R)}$
${}^{O}P_{23}(J)$	${}^{S}R_{32}(J-1)$	0	$\frac{(u_6^- - 2\Lambda)^2 u_4^- u_5^- u_5^+}{2C_3(P)}$
${}^{P}Q_{23}(J)$	${}^{R}Q_{32}(J)$	0	$\frac{(u_6^- - 2\Lambda)^2 u_5^- u_5^{+2}}{2C_3(Q)}$
${}^{Q}R_{23}(J)$	${}^{Q}P_{32}(J+1)$	0	$\frac{(u_6^- - 2\Lambda)^2 u_5^{+2} u_6^+}{2C_3(R)}$
$P_3(J)$	$R_3(J-1)$	$\frac{u_3^- u_4^-}{2J}$	$\frac{(u_6^+ + 2\Lambda)^2 u_3^- u_4^- u_5^-}{2C_3(P)}$
$Q_3(J)$	$Q_3(J)$	$\frac{u_4^- u_6^+ (2J+1)}{2J(J+1)}$	$\frac{(u_6^+ + 2\Lambda)^2 u_4^- u_5^- u_6^+}{2C_3(Q)}$
$R_3(J)$	$P_3(J+1)$	$\frac{u_6^+ u_7^+}{2(J+1)}$	$\frac{(u_6^+ + 2\Lambda)^2 u_5^- u_6^+ u_7^+}{2C_3(R)}$

(continued)

strengths

$^4X(b) - {}^4Y(a)$	$^4X(b) - {}^4Y(b)$
$\frac{(u_7^+ + 2\Lambda)^2 u_4^- u_5^- u_5^+}{2C_2(Q)}$	$\frac{2u_4^- u_5^+ (2J^2 + J - 4)^2}{J(J+1)(2J-1)^2(2J+1)}$
$\frac{(u_8^+ + 2\Lambda)^2 u_5^- u_5^+ u_6^+}{2C_2^+(R)}$	$\frac{(J+2)\, u_5^+ u_6^+ (2J-1)(2J+3)}{2(J+1)^2(2J+1)^2}$
$\frac{(u_2^- - 2\Lambda)^2 u_4^- u_5^- u_5^+}{2C_3^-(P)}$	$\frac{16(J-1)(J+1)\, u_4^- u_5^+}{J(2J-1)^2(2J+1)^2}$
$\frac{(u_3^- - 2\Lambda)^2 u_5^- u_6^+ u_6^+}{2C_3(Q)}$	$\frac{u_5^+ u_6^+ (2J-1)(2J+3)}{2J^2(J+1)^2(2J+1)}$
$\frac{(u_4^- - 2\Lambda)^2 u_5^+ u_6^+ u_7^+}{2C_3^+(R)}$	0
$\frac{3u_4^{-2} u_5^- u_5^+ u_6^+}{2C_4^-(P)}$	$\frac{3u_5^+ u_6^+}{2J^2(J+1)(2J+1)^2}$
$\frac{3u_5^{-2} u_4^+ u_5^{+2}}{2C_4(Q)}$	0
$\frac{3u_6^- u_5^+ u_6^+ u_7^+ u_8^+}{2C_4^+(R)}$	0
$\frac{3u_2^- u_3^- u_4^- u_4^+ u_5^+}{2C_1^-(P)}$	0
$\frac{3u_3^- u_4^- u_5^+ u_6^{+2}}{2C_1(Q)}$	0
$\frac{3u_4^- u_6^{+2} u_7^{+2}}{2C_1^+(R)}$	$\frac{3u_4^- u_5^-}{2J(J+1)^2(2J+1)^2}$
$\frac{(u_0^- - 2\Lambda)^2 u_3^- u_4^- u_5^+}{2C_2^-(P)}$	0
$\frac{(u_1^- - 2\Lambda)^2 u_4^- u_6^{+2}}{2C_2(Q)}$	$\frac{u_4^- u_5^- (2J-1)(2J+3)}{2J^2(J+1)^2(2J+1)}$
$\frac{(u_2^- - 2\Lambda)^2 u_6^+ u_7^{+2}}{2C_2^+(R)}$	$\frac{32J(J+2)\, u_5^- u_6^+}{(J+1)(2J+1)^2(2J+3)^2}$
$\frac{(u_8^+ + 2\Lambda)^2 u_3^{-2} u_4^-}{2C_3^-(P)}$	$\frac{(J-1)\, u_4^- u_5^- (2J-1)(2J+3)}{2J^2(2J+1)^2}$
$\frac{(u_9^+ + 2\Lambda)^2 u_4^{-2} u_6^+}{2C_3(Q)}$	$\frac{2u_5^- u_6^+ (2J^2+3J-3)^2}{J(J+1)(2J+1)(2J+3)^2}$
$\frac{(u_{10}^+ + 2\Lambda)^2 u_5^- u_6^+ u_7^+}{2C_3^+(R)}$	$\frac{Ju_6^+ u_7^+ (2J+1)(2J+5)}{2(J+1)^2(2J+3)^2}$

Table II.

Branches		Line	
$\Delta\Lambda = +1$	$\Delta\Lambda = -1$	${}^{4}X(a) - {}^{4}Y(a)$	${}^{4}X(a) - {}^{4}Y(b)$
${}^{Q}P_{43}(J)$	${}^{Q}R_{34}(J-1)$	0	$\frac{3u_2^- u_3^- u_4^- u_5^- u_6^+}{2C_3(P)}$
${}^{R}Q_{43}(J)$	${}^{P}Q_{34}(J)$	0	$\frac{3u_3^- u_4^- u_5^- u_6^+ u_7^+}{2C_3(Q)}$
${}^{S}R_{43}(J)$	${}^{O}P_{34}(J+1)$	0	$\frac{3u_4^- u_5^- u_6^+ u_7^+ u_8^+}{2C_3(R)}$
${}^{M}P_{14}(J)$	${}^{U}R_{41}(J-1)$	0	$\frac{u_5^- u_6^- u_4^+ u_5^+ u_6^+}{2C_4(P)}$
${}^{N}Q_{14}(J)$	${}^{T}Q_{41}(J)$	0	$\frac{u_6^- u_4^{+2} u_5^+ u_6^+}{2C_4(Q)}$
${}^{O}R_{14}(J)$	${}^{S}P_{41}(J+1)$	0	$\frac{u_4^{+2} u_5^{+2} u_6^+}{2C_4(R)}$
${}^{N}P_{24}(J)$	${}^{T}R_{42}(J-1)$	0	$\frac{3u_4^- u_5^- u_6^- u_5^+ u_6^+}{2C_4(P)}$
${}^{O}Q_{24}(J)$	${}^{S}Q_{42}(J)$	0	$\frac{3u_5^- u_6^- u_5^{+2} u_6^{+2}}{2C_4(Q)}$
${}^{P}R_{24}(J)$	${}^{R}P_{42}(J+1)$	0	$\frac{3u_6^- u_5^{+2} u_6^{+2}}{2C_4(R)}$
${}^{O}P_{34}(J)$	${}^{S}R_{43}(J-1)$	0	$\frac{3u_3^- u_4^- u_5^- u_6^- u_6^+}{2C_4(P)}$
${}^{P}Q_{34}(J)$	${}^{R}Q_{43}(J)$	0	$\frac{3u_4^- u_5^- u_6^- u_6^{+2}}{2C_4(Q)}$
${}^{Q}R_{34}(J)$	${}^{Q}P_{43}(J+1)$	0	$\frac{3u_5^- u_6^- u_6^{+2} u_7^+}{2C_4(R)}$
$P_4(J)$	$R_4(J-1)$	$\frac{u_2^- u_3^-}{2J}$	$\frac{u_2^- u_3^- u_4^- u_5^- u_6^-}{2C_4(P)}$
$Q_4(J)$	$Q_4(J)$	$\frac{u_3^- u_7^+ (2J+1)}{2J(J+1)}$	$\frac{u_3^- u_4^- u_5^- u_6^- u_7^+}{2C_4(Q)}$
$R_4(J)$	$P_4(J+1)$	$\frac{u_7^+ u_8^+}{2(J+1)}$	$\frac{u_4^- u_5^- u_6^- u_7^+ u_8^+}{2C_4(R)}$

(continued)

strengths

$^4X(b) - {}^4Y(a)$	$^4X(b) - {}^4Y(b)$
$\frac{3u_3^{-2}u_4^{-2}u_6^+}{2C_4^-(P)}$	$\frac{6u_5^-u_6^+(2J-1)}{J(2J+1)^2(2J+3)^2}$
$\frac{3u_4^{-2}u_5^-u_6^+u_7^+}{2C_4(Q)}$	$\frac{3u_6^+u_7^+(2J+1)}{2(J+1)^2(2J+3)^2}$
$\frac{3u_5^-u_6^-u_6^+u_7^+u_8^+}{2C_4^+(R)}$	0
$\frac{u_2^-u_3^-u_4^+u_5^+u_6^+}{2C_1^-(P)}$	0
$\frac{u_3^-u_5^+u_6^+u_7^{+2}}{2C_1(Q)}$	0
$\frac{u_6^+u_7^{+2}u_8^{+2}}{2C_1^+(R)}$	0
$\frac{3u_2^{-2}u_3^-u_5^+u_6^+}{2C_2^-(P)}$	0
$\frac{3u_3^{-2}u_6^+u_7^{+2}}{2C_2(Q)}$	0
$\frac{3u_4^-u_7^{+2}u_8^{+2}}{2C_2^+(R)}$	$\frac{3u_5^-u_6^-}{2(J+1)^2(J+2)(2J+3)}$
$\frac{3u_2^{-2}u_3^{-2}u_6^+}{2C_3^-(P)}$	0
$\frac{3u_3^{-2}u_4^-u_7^{+2}}{2C_3(Q)}$	$\frac{3u_5^-u_6^-(2J+1)}{2(J+1)^2(2J+3)^2}$
$\frac{3u_4^-u_5^-u_7^+u_8^{+2}}{2C_3^+(R)}$	$\frac{3u_6^-u_7^+(2J+1)}{(J+1)(2J+3)^2(2J+5)}$
$\frac{u_2^{-2}u_3^{-2}u_4^-}{2C_4^-(P)}$	$\frac{u_5^-u_6^-(2J-1)}{2(J+1)(2J+3)}$
$\frac{u_3^{-2}u_4^-u_5^-u_7^+}{2C_4(Q)}$	$\frac{Ju_6^-u_7^+(2J+1)}{2(J+1)(2J+3)^2}$
$\frac{u_4^-u_5^-u_6^-u_7^+u_8^+}{2C_4^+(R)}$	$\frac{u_7^+u_8^+(2J+1)}{2(J+2)(2J+5)}$

Table III

Line strengths for ${}^5X_A - {}^5X_A$ transitions

Branches	Line strengths			
	${}^5X(a) - {}^5X(a)$	${}^5X(a) - {}^5X(b)$	${}^5X(b) - {}^5X(a)$	${}^5X(b) - {}^5X(b)$
$P_1(J)$	$\frac{v_6^- v_2^+}{J}$	$\frac{v_3^- v_4^- v_5^- v_6^{-2} v_2^+}{C_1(P)}$	$R_1(J-1)$	$\frac{v_2^- v_2^+ (2J+1)}{(J-2)(2J-3)}$
$Q_1(J)$	$(A-2)^2 \frac{2J+1}{J(J+1)}$	$(A-2)^2 \frac{v_3^- v_4^- v_5^- v_6^-}{C_1(Q)}$	$Q_1(J)$	$A^2 \frac{(J+1)(2J+1)}{2(J-1)^2 J}$
$R_1(J)$	$\frac{v_7^- v_3^+}{J+1}$	$\frac{v_3^- v_4^- v_5^- v_6^- v_7^- v_3^+}{C_1(R)}$	$P_1(J+1)$	$\frac{v_3^- v_3^+ (2J+3)}{(J-1)(2J-1)}$
${}^Q P_{21}(J)$	0	$\frac{4 v_3^- v_4^- v_5^{-2} v_3^{+2}}{C_1(P)}$	${}^P R_{12}(J-1)$	$A^2 \frac{2(2J+1)}{(J-2)(J-1)^2 J}$
${}^R Q_{21}(J)$	0	$(A-1)^2 \frac{4 v_3^- v_4^- v_5^- v_3^+}{C_1(Q)}$	${}^Q Q_{12}(J)$	$\frac{2 v_5^- v_5^+ (2J+1)}{(J-1)^2 J(2J-1)}$
${}^S R_{21}(J)$	0	$\frac{4 v_3^- v_4^- v_5^- v_6^- v_3^+ v_4^+}{C_1(R)}$	${}^O P_{12}(J+1)$	0
${}^R P_{31}(J)$	0	$\frac{6 v_3^- v_4^{-2} v_3^+ v_4^{+2}}{C_1(P)}$	${}^P R_{13}(J-1)$	$\frac{6 v_3^- v_3^+}{(J-1)^2 J(2J-3)(2J-1)}$
${}^S Q_{31}(J)$	0	$A^2 \frac{6 v_3^- v_4^- v_3^+ v_4^+}{C_1(Q)}$	${}^O Q_{13}(J)$	0
${}^T R_{31}(J)$	0	$\frac{6 v_3^- v_4^- v_5^- v_3^+ v_4^+ v_5^+}{C_1(R)}$	${}^N P_{13}(J+1)$	0
${}^S P_{41}(J)$	0	$\frac{4 v_3^{-2} v_3^+ v_4^+ v_5^{+2}}{C_1(P)}$	${}^O R_{14}(J-1)$	0
${}^T Q_{41}(J)$	0	$(A+1)^2 \frac{4 v_3^- v_3^+ v_4^+ v_5^+}{C_1(Q)}$	${}^N Q_{14}(J)$	0
${}^U R_{41}(J)$	0	$\frac{4 v_3^- v_4^- v_3^+ v_4^+ v_5^+ v_6^+}{C_1(R)}$	${}^M P_{14}(J+1)$	0

${}^{T}P_{51}(J)$	0	$\frac{v_2^- v_3^+ v_4^+ v_5^+ v_6^{+2}}{C_1(P)}$		${}^{N}R_{15}(J-1)$	0
${}^{U}Q_{51}(J)$	0	$(\Lambda+2)^2 \frac{v_3^+ v_4^+ v_5^+ v_6^+}{C_1(Q)}$		${}^{M}Q_{15}(J)$	0
${}^{V}R_{51}(J)$	0	$\frac{v_3^- v_3^+ v_4^+ v_5^+ v_6^+ v_7^+}{C_1(R)}$		${}^{L}P_{15}(J+1)$	0
${}^{O}P_{12}(J)$	0	$\frac{v_4^- v_5^- v_6^{-2} v_2^+ v_3^+}{C_2(P)}$		${}^{S}R_{21}(J-1)_4^1$	0
${}^{P}Q_{12}(J)$	0	$(\Lambda-2)^2 \frac{v_4^- v_5^- v_6^- v_3^+}{C_2(Q)}$		${}^{R}Q_{21}(J)$	$\frac{2v_5^- v_5^+(2J+1)}{(J-1)^2 J(2J-1)}$
${}^{Q}R_{12}(J)$	0	$\frac{v_4^- v_5^- v_6^- v_7^- v_3^{+2}}{C_2(R)}$		${}^{Q}P_{21}(J+1)$	$\Lambda^2 \frac{2(2J+3)}{(J-1)J^2(J+1)}$
$P_2(J)$	$\frac{v_5^- v_3^+}{J}$	$\frac{(v_3^+ + \Lambda)^2 v_4^- v_5^{-2} v_3^+}{C_2(P)}$		$R_2(J-1)$	$\frac{(J-2)(J+1) v_3^- v_3^+(2J+1)}{(J-1)^2 J(2J-1)}$
$Q_2(J)$	$(\Lambda-1)^2 \frac{2J+1}{J(J+1)}$	$(\Lambda-1)^2 \frac{(v_3^+ + \Lambda)^2 v_4^- v_5^-}{C_2(Q)}$		$Q_2(J)$	$\Lambda^2 \frac{(J^2-3)^2(2J+1)}{(J-1)^2 J^3(J+1)}$
$R_2(J)$	$\frac{v_6^- v_4^+}{J+1}$	$\frac{(v_3^+ + \Lambda)^2 v_4^- v_5^- v_6^- v_4^+}{C_2(R)}$		$P_2(J+1)$	$\frac{(J-1)(J+2) v_4^- v_4^+(2J+3)}{J^2(J+1)(2J+1)}$
${}^{Q}P_{32}(J)$	0	$\Lambda^2 \frac{6 v_4^{-2} v_4^{+2}}{C_2(P)}$		${}^{Q}R_{23}(J-1)$	$\Lambda^2 \frac{3(J+1)(2J-3)}{(J-1)^2 J^3}$
${}^{R}Q_{32}(J)$	0	$\Lambda^4 \frac{6 v_4^- v_4^+}{C_2(Q)}$		${}^{P}Q_{23}(J)$	$\frac{3(J-1) v_4^- v_4^+(2J+3)}{J^3(J+1)(2J-1)}$
${}^{S}R_{32}(J)$	0	$\Lambda^2 \frac{6 v_4^- v_5^- v_4^+ v_5^+}{C_2(R)}$		${}^{O}P_{23}(J+1)$	0
${}^{R}P_{42}(J)$	0	$\frac{(v_3^- - \Lambda)^2 v_3^- v_4^+ v_5^{+2}}{C_2(P)}$		${}^{P}R_{24}(J-1)$	$\frac{9 v_4^- v_4^+}{J^3(2J-1)(2J+1)}$
${}^{S}Q_{42}(J)$	0	$(\Lambda+1)^2 \frac{(v_3^- - \Lambda)^2 v_4^+ v_5^+}{C_2(Q)}$		${}^{O}Q_{24}(J)$	0
${}^{T}R_{42}(J)$	0	$\frac{(v_3^- - \Lambda)^2 v_4^- v_4^+ v_5^+ v_6^+}{C_2(R)}$		${}^{N}P_{24}(J+1)$	0

Table III (continued)

Branches	Line strengths			
	$^5X(a) - {}^5X(a)$	$^5X(a) - {}^5X(b)$	$^5X(b) - {}^5X(a)$	$^5X(b) - {}^5X(b)$
$^SP_{52}(J)$	0	$\frac{v_2^- v_3^- v_4^+ v_5^+ v_6^{+2}}{C_2(P)}$	$^OR_{25}(J-1)$	0
$^TQ_{52}(J)$	0	$(\Lambda+2)^2 \frac{v_3^- v_4^+ v_5^+ v_6^+}{C_2(Q)}$	$^NQ_{25}(J)$	0
$^UR_{52}(J)$	0	$\frac{v_3^{-2} v_4^+ v_5^+ v_6^+ v_7^+}{C_2(R)}$	$^MP_{25}(J+1)$	0
$^NP_{13}(J)$	0	$\frac{3 v_5^- v_6^- v_2^+ v_3^+ v_4^+}{C_3(P)}$	$^TR_{31}(J-1)$	0
$^OQ_{13}(J)$	0	$(\Lambda-2)^2 \frac{3 v_5^- v_6^- v_3^+ v_4^+}{C_3(Q)}$	$^SQ_{31}(J)$	0
$^PR_{13}(J)$	0	$\frac{3 v_5^- v_6^- v_7^- v_3^{+2} v_4^+}{C_3(R)}$	$^RP_{31}(J+1)$	$\frac{6 v_4^- v_4^+}{J^2(J+1)(2J-1)(2J+1)}$
$^OP_{23}(J)$	0	$(2\Lambda-1)^2 \frac{3 v_5^{-2} v_3^+ v_4^+}{C_3(P)}$	$^SR_{32}(J-1)$	0
$^PQ_{23}(J)$	0	$(\Lambda-1)^2(2\Lambda-1)^2 \frac{3 v_5^- v_4^+}{C_3(Q)}$	$^RQ_{32}(J)$	$\frac{3(J-1) v_4^- v_4^+ (2J+3)}{J^3(J+1)(2J-1)}$
$^QR_{23}(J)$	0	$(2\Lambda-1)^2 \frac{3 v_5^- v_6^- v_4^{+2}}{C_3(R)}$	$^QP_{32}(J+1)$	$\Lambda^2 \frac{3(J+2)(2J-1)}{J^2(J+1)^3}$
$P_3(J)$	$\frac{v_4^- v_4^+}{J}$	$\frac{2[v_5^- v_4^+ - \Lambda(2\Lambda+1)]^2 v_4^- v_4^+}{C_3(P)}$	$R_3(J-1)$	$\frac{(J-1)(J+1) v_4^- v_4^+ (2J-3)(2J+3)}{J^3(2J-1)(2J+1)}$
$Q_3(J)$	$\Lambda^2 \frac{2J+1}{J(J+1)}$	$\Lambda^2 \frac{2[v_5^- v_4^+ - \Lambda(2\Lambda+1)]^2}{C_3(Q)}$	$Q_3(J)$	$\Lambda^2 \frac{[J^2+J-3]^2(2J+1)}{J^3(J+1)^3}$
$R_3(J)$	$\frac{v_5^- v_5^+}{J+1}$	$\frac{2[v_5^- v_4^+ - \Lambda(2\Lambda+1)]^2 v_5^- v_5^+}{C_3(R)}$	$P_3(J+1)$	$\frac{J(J+2) v_5^- v_5^+ (2J-1)(2J+5)}{(J+1)^3(2J+1)(2J+3)}$
$^QP_{43}(J)$	0	$(2\Lambda+1)^2 \frac{3 v_3^- v_4^- v_5^{+2}}{C_3(P)}$	$^QR_{34}(J-1)$	$\Lambda^2 \frac{3(J-1)(2J+3)}{J^3(J+1)^2}$

${}^{R}Q_{43}(J)$	0	$(\Lambda+1)^2(2\Lambda+1)^2\dfrac{3v_4^-v_5^+}{C_3(Q)}$	${}^{P}Q_{34}(J)$	$\dfrac{3(J+2)v_5^-v_5^+(2J-1)}{J(J+1)^3(2J+3)}$
${}^{S}R_{43}(J)$	0	$(2\Lambda+1)^2\dfrac{3v_4^{-2}v_5^+v_6^+}{C_3(R)}$	${}^{O}P_{34}(J+1)$	0
${}^{R}P_{53}(J)$	0	$\dfrac{3v_2^-v_3^-v_4^-v_5^+v_6^{+2}}{C_3(P)}$	${}^{P}R_{35}(J-1)$	$\dfrac{6v_5^-v_5^+}{J(J+1)^2(2J+1)(2J+3)}$
${}^{S}Q_{53}(J)$	0	$(\Lambda+2)^2\dfrac{3v_3^-v_4^-v_5^+v_6^+}{C_3(Q)}$	${}^{O}Q_{35}(J)$	0
${}^{T}R_{53}(J)$	0	$\dfrac{3v_3^{-2}v_4^-v_5^+v_6^+v_7^+}{C_3(R)}$	${}^{N}P_{35}(J+1)$	0
${}^{M}P_{14}(J)$	0	$\dfrac{v_6^{-2}v_2^+v_3^+v_4^+v_5^+}{C_4(P)}$	${}^{U}R_{41}(J-1)$	0
${}^{N}Q_{14}(J)$	0	$(\Lambda-2)^2\dfrac{v_6^-v_3^+v_4^+v_5^+}{C_4(Q)}$	${}^{T}Q_{41}(J)$	0
${}^{O}R_{14}(J)$	0	$\dfrac{v_6^-v_7^-v_3^{+2}v_4^+v_5^+}{C_4(R)}$	${}^{S}P_{41}(J+1)$	0
${}^{N}P_{24}(J)$	0	$\dfrac{(v_6^- - \Lambda)^2v_5^-v_3^+v_4^+v_5^+}{C_4(P)}$	${}^{T}R_{42}(J-1)$	0
${}^{O}Q_{24}(J)$	0	$(\Lambda-1)^2\dfrac{(v_6^- - \Lambda)^2v_4^+v_5^+}{C_4(Q)}$	${}^{S}Q_{42}(J)$	0
${}^{P}R_{24}(J)$	0	$\dfrac{(v_6^- - \Lambda)^2v_6^-v_4^{+2}v_5^+}{C_4(R)}$	${}^{R}P_{42}(J+1)$	$\dfrac{9v_5^-v_5^+}{(J+1)^3(2J+1)(2J+3)}$
${}^{O}P_{34}(J)$	0	$\Lambda^2\dfrac{6v_4^-v_5^-v_4^+v_5^+}{C_4(P)}$	${}^{S}R_{43}(J-1)$	0
${}^{P}Q_{34}(J)$	0	$\Lambda^4\dfrac{6v_5^-v_5^+}{C_4(Q)}$	${}^{R}Q_{43}(J)$	$\dfrac{3(J+2)v_5^-v_5^+(2J-1)}{J(J+1)^3(2J+3)}$
${}^{Q}R_{34}(J)$	0	$\Lambda^2\dfrac{6v_5^{-2}v_5^{+2}}{C_4(R)}$	${}^{Q}P_{43}(J+1)$	$\Lambda^2\dfrac{3J(2J+5)}{(J+1)^3(J+2)^2}$
$P_4(J)$	$\dfrac{v_3^-v_5^+}{J}$	$\dfrac{(v_6^+ + \Lambda)^2v_3^-v_4^-v_5^-v_5^+}{C_4(P)}$	$R_4(J-1)$	$\dfrac{(J-1)(J+2)v_5^-v_5^+(2J-1)}{J(J+1)^2(2J+1)}$

Table III (continued)

Branches	Line strengths			
	${}^{5}X(a) - {}^{5}X(a)$	${}^{5}X(a) - {}^{5}X(b)$	${}^{5}X(b) - {}^{5}X(a)$	${}^{5}X(b) - {}^{5}X(b)$
$Q_4(J)$	$(\Lambda+1)^2 \frac{2J+1}{J(J+1)}$	$(\Lambda+1)^2 \frac{(v_6^+ + \Lambda)^2 v_4^- v_5^-}{C_4(Q)}$	$Q_4(J)$	$\Lambda^2 \frac{[J^2+2J-2]^2(2J+1)}{J(J+1)^3(J+2)^2}$
$R_4(J)$	$\frac{v_4^- v_6^+}{J+1}$	$\frac{(v_6^+ + \Lambda)^2 v_4^{-2} v_5^- v_6^+}{C_4(R)}$	$P_4(J+1)$	$\frac{J(J+3) v_6^- v_6^+ (2J+1)}{(J+1)(J+2)^2(2J+3)}$
${}^{Q}P_{54}(J)$	0	$\frac{v_2^- v_3^- v_4^- v_5^- v_6^{+2}}{C_4(P)}$	${}^{Q}R_{45}(J-1)$	$\Lambda^2 \frac{2(2J-1)}{J(J+1)^2(J+2)}$
${}^{R}Q_{54}(J)$	0	$(\Lambda+2)^2 \frac{v_3^- v_4^- v_5^- v_6^+}{C_4(Q)}$	${}^{P}Q_{45}(J)$	$\frac{2 v_6^- v_6^+ (2J+1)}{(J+1)(J+2)^2(2J+3)}$
${}^{S}R_{54}(J)$	0	$\frac{v_3^{-2} v_4^- v_5^- v_6^+ v_7^+}{C_4(R)}$	${}^{O}P_{45}(J+1)$	0
${}^{L}P_{15}(J)$	0	$\frac{v_6^- v_2^+ v_3^+ v_4^+ v_5^+ v_6^+}{C_5(P)}$	${}^{V}R_{51}(J-1)$	0
${}^{M}Q_{15}(J)$	0	$(\Lambda-2)^2 \frac{v_3^+ v_4^+ v_5^+ v_6^+}{C_5(Q)}$	${}^{U}Q_{51}(J)$	0
${}^{N}R_{15}(J)$	0	$\frac{v_7^- v_3^{+2} v_4^+ v_5^+ v_6^+}{C_5(R)}$	${}^{T}P_{51}(J+1)$	0
${}^{M}P_{25}(J)$	0	$\frac{4 v_5^- v_6^- v_3^+ v_4^+ v_5^+ v_6^+}{C_5(P)}$	${}^{U}R_{52}(J-1)$	0
${}^{N}Q_{25}(J)$	0	$(\Lambda-1)^2 \frac{4 v_6^- v_4^+ v_5^+ v_6^+}{C_5(Q)}$	${}^{T}Q_{52}(J)$	0
${}^{O}R_{25}(J)$	0	$\frac{4 v_6^{-2} v_4^{+2} v_5^+ v_6^+}{C_5(R)}$	${}^{S}P_{52}(J+1)$	0
${}^{N}P_{35}(J)$	0	$\frac{6 v_4^- v_5^- v_6^- v_4^+ v_5^+ v_6^+}{C_5(P)}$	${}^{T}R_{53}(J-1)$	0
${}^{O}Q_{35}(J)$	0	$\Lambda^2 \frac{6 v_5^- v_6^- v_5^+ v_6^+}{C_5(Q)}$	${}^{S}Q_{53}(J)$	0

${}^{P}R_{35}(J)$	0	$\dfrac{6v_5^{-2}v_6^{-}v_5^{+2}v_6^{+}}{C_5(R)}$	${}^{R}P_{53}(J+1)$	$\dfrac{6v_6^{-}v_6^{+}}{(J+1)(J+2)^2(2J+3)(2J+5)}$
${}^{O}P_{45}(J)$	0	$\dfrac{4\,v_3^{-}v_4^{-}v_5^{-}v_6^{-}v_5^{+}v_6^{+}}{C_5(P)}$	${}^{S}R_{54}(J-1)$	0
${}^{P}Q_{45}(J)$	0	$(\Lambda+1)^2\,\dfrac{4v_4^{-}v_5^{-}v_6^{-}v_6^{+}}{C_5(Q)}$	${}^{R}Q_{54}(J)$	$\dfrac{2v_6^{-}v_6^{+}(2J+1)}{(J+1)(J+2)^2(2J+3)}$
${}^{Q}R_{45}(J)$	0	$\dfrac{4\,v_4^{-2}v_5^{-}v_6^{-}v_6^{+2}}{C_5(R)}$	${}^{Q}P_{54}(J+1)$	$\Lambda^2\,\dfrac{2(2J+1)}{(J+1)(J+2)^2(J+3)}$
$P_5(J)$	$\dfrac{v_2^{-}v_6^{+}}{J}$	$\dfrac{v_2^{-}v_3^{-}v_4^{-}v_5^{-}v_6^{-}v_6^{+}}{C_5(P)}$	$R_5(J-1)$	$\dfrac{v_6^{-}v_6^{+}(2J-1)}{(J+2)(2J+3)}$
$Q_5(J)$	$(\Lambda+2)^2\,\dfrac{(2J+1)}{J(J+1)}$	$(\Lambda+2)^2\,\dfrac{v_3^{-}v_4^{-}v_5^{-}v_6^{-}}{C_5(Q)}$	$Q_5(J)$	$\Lambda^2\,\dfrac{J(2J+1)}{(J+1)(J+2)^2}$
$R_5(J)$	$\dfrac{v_3^{-}v_7^{+}}{J+1}$	$\dfrac{v_3^{-2}v_4^{-}v_5^{-}v_6^{-}v_7^{+}}{C_5(R)}$	$P_5(J+1)$	$\dfrac{v_7^{-}v_7^{+}(2J+1)}{(J+3)(2J+5)}$

Table IV

Line strengths for

Branches		Line	
$\Delta\Lambda = +1$	$\Delta\Lambda = -1$	${}^{5}X(a) - {}^{5}Y(a)$	${}^{5}X(a) - {}^{5}Y(b)$
$P_1(J)$	$R_1(J-1)$	$\frac{v_5^- v_6^-}{2J}$	$\frac{v_3^- v_4^- v_5^{-2} v_6^{-2}}{2C_1(P)}$
$Q_1(J)$	$Q_1(J)$	$\frac{v_6^- v_3^+ (2J+1)}{2J(J+1)}$	$\frac{v_3^- v_4^- v_5^- v_6^{-2} v_3^+}{2C_1(Q)}$
$R_1(J)$	$P_1(J+1)$	$\frac{v_3^+ v_4^+}{2(J+1)}$	$\frac{v_3^- v_4^- v_5^- v_6^- v_3^+ v_4^+}{2C_1(R)}$
${}^{Q}P_{21}(J)$	${}^{Q}R_{12}(J-1)$	0	$\frac{2v_3^- v_4^{-2} v_5^{-2} v_3^+}{C_1(P)}$
${}^{R}Q_{21}(J)$	${}^{P}Q_{12}(J)$	0	$\frac{2v_3^- v_4^- v_5^{-2} v_3^+ v_4^+}{C_1(Q)}$
${}^{S}R_{21}(J)$	${}^{O}P_{12}(J+1)$	0	$\frac{2v_3^- v_4^- v_5^- v_3^+ v_4^+ v_5^+}{C_1(R)}$
${}^{R}P_{31}(J)$	${}^{P}R_{13}(J-1)$	0	$\frac{3v_3^{-2} v_4^{-2} v_3^+ v_4^+}{C_1(P)}$
${}^{S}Q_{31}(J)$	${}^{O}Q_{13}(J)$	0	$\frac{3v_3^- v_4^{-2} v_3^+ v_4^+ v_5^+}{C_1(Q)}$
${}^{T}R_{31}(J)$	${}^{N}P_{13}(J+1)$	0	$\frac{3v_3^- v_4^- v_3^+ v_4^+ v_5^+ v_6^+}{C_1(R)}$
${}^{S}P_{41}(J)$	${}^{O}R_{14}(J-1)$	0	$\frac{2v_2^- v_3^{-2} v_3^+ v_4^+ v_5^+}{C_1(P)}$
${}^{T}Q_{41}(J)$	${}^{N}Q_{14}(J)$	0	$\frac{2v_3^{-2} v_3^+ v_4^+ v_5^+ v_6^+}{C_1(Q)}$
${}^{U}R_{41}(J)$	${}^{M}P_{14}(J+1)$	0	$\frac{2v_3^- v_3^+ v_4^+ v_5^+ v_6^+ v_7^+}{C_1(R)}$
${}^{T}P_{51}(J)$	${}^{N}R_{15}(J-1)$	0	$\frac{v_1^- v_2^- v_3^+ v_4^+ v_5^+ v_6^+}{2C_1(P)}$
${}^{U}Q_{51}(J)$	${}^{M}Q_{15}(J)$	0	$\frac{v_2^- v_3^+ v_4^+ v_5^+ v_6^+ v_7^+}{2C_1(Q)}$
${}^{V}R_{51}(J)$	${}^{L}P_{15}(J+1)$	0	$\frac{v_3^+ v_4^+ v_5^+ v_6^+ v_7^+ v_8^+}{2C_1(R)}$
${}^{O}P_{12}(J)$	${}^{S}R_{21}(J-1)$	0	$\frac{v_4^- v_5^{-2} v_6^{-2} v_3^+}{2C_2(P)}$
${}^{P}Q_{12}(J)$	${}^{R}Q_{21}(J)$	0	$\frac{v_4^- v_5^- v_6^{-2} v_3^{+2}}{2C_2(Q)}$
${}^{Q}R_{12}(J)$	${}^{Q}P_{21}(J+1)$	0	$\frac{v_4^- v_5^- v_6^- v_3^{+2} v_4^+}{2C_2(R)}$
$P_2(J)$	$R_2(J-1)$	$\frac{v_4^- v_5^-}{2J}$	$\frac{(v_3^+ + \Lambda)^2 v_4^{-2} v_5^{-2}}{2C_2(P)}$

${}^5X_{A+1} - {}^5Y_A$ transitions

strengths

${}^5X(b) - {}^5Y(a)$	${}^5X(b) - {}^5Y(b)$
$\frac{v_1^- v_2^- v_3^- v_4^- v_5^- v_6^-}{2C_1^-(P)}$	$\frac{v_1^- v_2^-(2J+1)}{2(J-2)(2J-3)}$
$\frac{v_2^- v_3^- v_4^- v_5^- v_6^- v_3^+}{2C_1(Q)}$	$\frac{(J+1)\,v_2^- v_3^+(2J+1)}{2(J-1)^2 J}$
$\frac{v_3^- v_4^- v_5^- v_6^- v_3^+ v_4^+}{2C_1^+(R)}$	$\frac{v_3^+ v_4^+(2J+3)}{2(J-1)(2J-1)}$
$\frac{v_2^- v_3^- v_4^- v_5^- v_6^- v_3^+}{2C_2^-(P)}$	$\frac{v_2^- v_3^+(2J+1)}{(J-2)(J-1)^2 J}$
$\frac{v_3^- v_4^- v_5^- v_6^- v_3^+ v_4^+}{2C_2(Q)}$	$\frac{v_3^+ v_4^+(2J+1)}{(J-1)^2 J(2J-1)}$
$\frac{v_4^- v_5^- v_6^- v_3^+ v_4^+ v_5^+}{2C_2^+(R)}$	0
$\frac{3v_3^- v_4^- v_5^- v_6^- v_3^+ v_4^+}{2C_3^-(P)}$	$\frac{3v_3^+ v_4^+}{(J-1)^2 J(2J-3)(2J-1)}$
$\frac{3v_4^- v_5^- v_6^- v_3^+ v_4^+ v_5^+}{2C_3(Q)}$	0
$\frac{3v_5^- v_6^- v_3^+ v_4^+ v_5^+ v_6^+}{2C_3^+(R)}$	0
$\frac{v_4^- v_5^- v_6^- v_3^+ v_4^+ v_5^+}{2C_4^-(P)}$	0
$\frac{v_5^- v_6^- v_3^+ v_4^+ v_5^+ v_6^+}{2C_4(Q)}$	0
$\frac{v_6^- v_3^+ v_4^+ v_5^+ v_6^+ v_7^+}{2C_4^+(R)}$	0
$\frac{v_5^- v_6^- v_3^+ v_4^+ v_5^+ v_6^+}{2C_5^-(P)}$	0
$\frac{v_6^- v_3^+ v_4^+ v_5^+ v_6^+ v_7^+}{2C_5(Q)}$	0
$\frac{v_3^+ v_4^+ v_5^+ v_6^+ v_7^+ v_8^+}{2C_5^+(R)}$	0
$\frac{2v_1^- v_2^- v_3^- v_4^- v_5^- v_3^+}{C_1^-(P)}$	0
$\frac{2v_2^- v_3^- v_4^- v_5^- v_4^{+2}}{C_1(Q)}$	$\frac{v_2^- v_3^-(2J+1)}{(J-1)^2 J(2J-1)}$
$\frac{2v_3^- v_4^- v_5^- v_4^+ v_5^{+2}}{C_1^+(R)}$	$\frac{v_3^- v_4^+(2J+3)}{(J-1)J^2(J+1)}$
$\frac{(v_4^+ + A)^2\, v_2^- v_3^- v_4^- v_5^-}{2C_2^-(P)}$	$\frac{(J-2)(J+1)\,v_2^- v_3^-(2J+1)}{2(J-1)^2 J(2J-1)}$

Table IV

Branches		Line	
$\Delta\Lambda = +1$	$\Delta\Lambda = -1$	${}^5X(a) - {}^5Y(a)$	${}^5X(a) - {}^5Y(b)$
$Q_2(J)$	$Q_2(J)$	$\frac{v_5^- v_4^+ (2J+1)}{2J(J+1)}$	$\frac{(v_3^+ + \Lambda)^2 v_4^- v_5^{-2} v_4^+}{2C_2(Q)}$
$R_2(J)$	$P_2(J+1)$	$\frac{v_4^+ v_5^+}{2(J+1)}$	$\frac{(v_3^+ + \Lambda)^2 v_4^- v_5^- v_4^+ v_5^+}{2C_2(R)}$
${}^Q P_{32}(J)$	${}^Q R_{23}(J-1)$	0	$\Lambda^2 \frac{3 v_3^- v_4^{-2} v_4^+}{C_2(P)}$
${}^R Q_{32}(J)$	${}^P Q_{23}(J)$	0	$\Lambda^2 \frac{3 v_4^{-2} v_4^+ v_5^+}{C_2(Q)}$
${}^S R_{32}(J)$	${}^O P_{23}(J+1)$	0	$\Lambda^2 \frac{3 v_4^- v_4^+ v_5^+ v_6^+}{C_2(R)}$
${}^R P_{42}(J)$	${}^P R_{24}(J-1)$	0	$\frac{(v_3^- - \Lambda)^2 v_2^- v_3^- v_4^+ v_5^+}{2C_2(P)}$
${}^S Q_{42}(J)$	${}^O Q_{24}(J)$	0	$\frac{(v_3^- - \Lambda)^2 v_3^- v_4^+ v_5^+ v_6^+}{2C_2(Q)}$
${}^T R_{42}(J)$	${}^N P_{24}(J+1)$	0	$\frac{(v_3^- - \Lambda)^2 v_4^+ v_5^+ v_6^+ v_7^+}{2C_2(R)}$
${}^S P_{52}(J)$	${}^O R_{25}(J-1)$	0	$\frac{v_1^- v_2^- v_3^- v_4^+ v_5^+ v_6^+}{2C_2(P)}$
${}^T Q_{52}(J)$	${}^N Q_{25}(J)$	0	$\frac{v_2^- v_3^- v_4^+ v_5^+ v_6^+ v_7^+}{2C_2(Q)}$
${}^U R_{52}(J)$	${}^M P_{25}(J+1)$	0	$\frac{v_3^- v_4^+ v_5^+ v_6^+ v_7^+ v_8^+}{2C_2(R)}$
${}^N P_{13}(J)$	${}^T R_{31}(J-1)$	0	$\frac{3 v_5^{-2} v_6^{-2} v_3^+ v_4^+}{2C_3(P)}$
${}^O Q_{13}(J)$	${}^S Q_{31}(J)$	0	$\frac{3 v_5^- v_6^{-2} v_3^{+2} v_4^+}{2C_3(Q)}$
${}^P R_{13}(J)$	${}^R P_{31}(J+1)$	0	$\frac{3 v_5^- v_6^- v_3^{+2} v_4^{+2}}{2C_3(R)}$
${}^O P_{23}(J)$	${}^S R_{32}(J-1)$	0	$(2\Lambda - 1)^2 \frac{3 v_3^- v_4^- v_5^- v_4^+}{2C_3(P)}$
${}^P Q_{23}(J)$	${}^R Q_{32}(J)$	0	$(2\Lambda - 1)^2 \frac{3 v_5^{-2} v_4^{+2}}{2C_3(Q)}$
${}^Q R_{23}(J)$	${}^Q P_{32}(J+1)$	0	$(2\Lambda - 1)^2 \frac{3 v_5^- v_4^{+2} v_5^+}{2C_3(R)}$
$P_3(J)$	$R_3(J-1)$	$\frac{v_3^- v_4^-}{2J}$	$\frac{[v_5^- v_4^+ - \Lambda(2\Lambda+1)]^2 v_3^- v_4^-}{C_3(P)}$
$Q_3(J)$	$Q_3(J)$	$\frac{v_4^- v_5^+ (2J+1)}{2J(J+1)}$	$\frac{[v_5^- v_4^+ - \Lambda(2\Lambda+1)]^2 v_4^- v_5^+}{C_3(Q)}$
$R_3(J)$	$P_3(J+1)$	$\frac{v_5^+ v_6^+}{2(J+1)}$	$\frac{[v_5^- v_4^+ - \Lambda(2\Lambda+1)]^2 v_5^+ v_6^+}{C_3(R)}$

(continued)

strengths

$^5X(b) - {}^5Y(a)$	$^5X(b) - {}^5Y(b)$
$\frac{(v_5^+ + \Lambda)^2 v_3^- v_4^- v_5^- v_4^+}{2C_2(Q)}$	$\frac{(J^2-3)^2 v_3^- v_4^+ (2J+1)}{2(J-1)^2 J^3 (J+1)}$
$\frac{(v_6^+ + \Lambda)^2 v_4^- v_5^- v_4^+ v_5^+}{2C_2^+(R)}$	$\frac{(J-1)(J+2)\, v_4^+ v_5^+ (2J+3)}{2J^2(J+1)(2J+1)}$
$(2\Lambda+1)^2 \frac{3v_3^- v_4^- v_5^- v_4^+}{2C_3^-(P)}$	$\frac{3(J+1)\, v_3^- v_4^+ (2J-3)}{2(J-1)^2 J^3}$
$(2\Lambda+1)^2 \frac{3v_4^- v_5^- v_4^+ v_5^+}{2C_3(Q)}$	$\frac{3(J-1)\, v_4^+ v_5^+ (2J+3)}{2J^3(J+1)(2J-1)}$
$(2\Lambda+1)^2 \frac{3v_5^- v_5^+ v_6^{+2}}{2C_3^+(R)}$	0
$\frac{(v_3^- - \Lambda)^2 v_4^- v_5^- v_4^+ v_5^+}{2C_4^-(P)}$	$\frac{9 v_4^+ v_5^+}{2J^3(2J-1)(2J+1)}$
$\frac{(v_4^- - \Lambda)^2 v_5^- v_4^+ v_5^+ v_6^+}{2C_4(Q)}$	0
$\frac{(v_5^- - \Lambda)^2 v_6^{+2} v_7^{+2}}{2C_4^+(R)}$	0
$\frac{2v_4^{-2} v_5^- v_4^+ v_5^+ v_6^+}{C_5^-(P)}$	0
$\frac{2v_5^{-2} v_4^+ v_5^+ v_6^+ v_7^+}{C_5(Q)}$	0
$\frac{2v_6^- v_6^+ v_7^{+2} v_8^{+2}}{C_5^+(R)}$	0
$\frac{3v_1^- v_2^- v_3^- v_4^- v_3^+ v_4^+}{C_1^-(P)}$	0
$\frac{3v_2^- v_3^- v_4^- v_4^+ v_5^{+2}}{C_1(Q)}$	0
$\frac{3v_3^- v_4^- v_3^+ v_4^+ v_5^+ v_6^+}{C_1^+(R)}$	$\frac{3v_3^- v_4^-}{J^2(J+1)(2J-1)(2J+1)}$
$(\Lambda+1)^2 \frac{3v_2^- v_3^- v_4^- v_4^+}{C_2^-(P)}$	0
$(\Lambda+1)^2 \frac{3v_3^- v_4^- v_5^{+2}}{C_2(Q)}$	$\frac{3(J-1)\, v_3^- v_4^- (2J+3)}{2J^3(J+1)(2J-1)}$
$(\Lambda+1)^2 \frac{3v_4^- v_4^+ v_5^+ v_6^+}{C_2^+(R)}$	$\frac{3(J+2)\, v_4^- v_5^+ (2J-1)}{2J^2(J+1)^3}$
$\frac{[v_3^- v_4^+ - (\Lambda+1)(2\Lambda+3)]^2 v_3^- v_4^-}{C_3^-(P)}$	$\frac{(J-1)(J+1)\, v_3^- v_4^- (2J-3)(2J+3)}{2J^3(2J-1)(2J+1)}$
$\frac{[v_4^- v_5^+ - (\Lambda+1)(2\Lambda+3)]^2 v_4^- v_5^-}{C_3(Q)}$	$\frac{(J^2+J-3)^2 v_4^- v_5^+ (2J+1)}{2J^3(J+1)^3}$
$\frac{[v_4^- v_5^+ - (\Lambda+1)(2\Lambda+3)]\, v_5^+ v_6^+}{C_3^+(R)}$	$\frac{J(J+2)\, v_5^+ v_6^+ (2J-1)(2J+5)}{2(J+1)^3(2J+1)(2J+3)}$

Table IV

Branches		Line	
$\Delta\Lambda = +1$	$\Delta\Lambda = -1$	${}^5X(a) - {}^5Y(a)$	${}^5X(a) - {}^5Y(b)$
${}^QP_{43}(J)$	${}^QR_{34}(J-1)$	0	$(2\Lambda+1)^2 \frac{3v_2^- v_3^- v_4^- v_5^+}{2C_3(P)}$
${}^RQ_{43}(J)$	${}^PQ_{34}(J)$	0	$(2\Lambda+1)^2 \frac{3v_3^- v_4^- v_5^+ v_6^+}{2C_3(Q)}$
${}^SR_{43}(J)$	${}^OP_{34}(J+1)$	0	$(2\Lambda+1)^2 \frac{3v_4^- v_5^+ v_6^+ v_7^+}{2C_3(R)}$
${}^RP_{53}(J)$	${}^PR_{35}(J-1)$	0	$\frac{3v_1^- v_2^- v_3^- v_4^- v_5^+ v_6^+}{2C_3(P)}$
${}^SQ_{53}(J)$	${}^OQ_{35}(J)$	0	$\frac{3v_2^- v_3^- v_4^- v_5^+ v_6^+ v_7^+}{2C_3(Q)}$
${}^TR_{53}(J)$	${}^NP_{35}(J+1)$	0	$\frac{3v_3^- v_4^- v_5^+ v_6^+ v_7^+ v_8^+}{2C_3(R)}$
${}^MP_{14}(J)$	${}^UR_{41}(J-1)$	0	$\frac{v_5^- v_6^{-2} v_3^+ v_4^+ v_5^+}{2C_4(P)}$
${}^NQ_{14}(J)$	${}^TQ_{41}(J)$	0	$\frac{v_6^{-2} v_3^{+2} v_4^+ v_5^+}{2C_4(Q)}$
${}^OR_{14}(J)$	${}^SP_{41}(J+1)$	0	$\frac{v_6^- v_3^{+2} v_4^{+2} v_5^+}{2C_4(R)}$
${}^NP_{24}(J)$	${}^TR_{42}(J-1)$	0	$\frac{(v_6^- - \Lambda)^2 v_4^- v_5^- v_4^+ v_5^+}{2C_4(P)}$
${}^OQ_{24}(J)$	${}^SQ_{42}(J)$	0	$\frac{(v_6^- - \Lambda)^2 v_5^- v_4^{+2} v_5^+}{2C_4(Q)}$
${}^PR_{24}(J)$	${}^RP_{42}(J+1)$	0	$\frac{(v_6^- - \Lambda)^2 v_4^{+2} v_5^{+2}}{2C_4(R)}$
${}^OP_{34}(J)$	${}^SR_{43}(J-1)$	0	$\Lambda^2 \frac{3v_3^- v_4^- v_5^- v_5^+}{C_4(P)}$
${}^PQ_{34}(J)$	${}^RQ_{43}(J)$	0	$\Lambda^2 \frac{3v_4^- v_5^- v_5^+ v_6^+}{C_4(Q)}$
${}^QR_{34}(J)$	${}^QP_{43}(J+1)$	0	$\Lambda^2 \frac{3v_5^- v_5^{+2} v_6^+}{C_4(R)}$
$P_4(J)$	$R_4(J-1)$	$\frac{v_2^- v_3^-}{2J}$	$\frac{(v_6^+ + \Lambda)^2 v_2^- v_3^- v_4^- v_5^-}{2C_4(P)}$
$Q_4(J)$	$Q_4(J)$	$\frac{v_3^- v_6^+ (2J+1)}{2J(J+1)}$	$\frac{(v_6^+ + \Lambda)^2 v_3^- v_4^- v_5^- v_6^+}{2C_4(Q)}$
$R_4(J)$	$P_4(J+1)$	$\frac{v_6^+ v_7^+}{2(J+1)}$	$\frac{(v_6^+ + \Lambda)^2 v_4^- v_5^- v_6^+ v_7^+}{2C_4(R)}$
${}^QP_{54}(J)$	${}^SR_{45}(J-1)$	0	$\frac{v_1^- v_2^- v_3^- v_4^- v_5^- v_6^+}{2C_4(P)}$
${}^RQ_{54}(J)$	${}^PQ_{45}(J)$	0	$\frac{v_3^{-2} v_4^- v_5^- v_6^{+2}}{2C_4(Q)}$

(continued)

strengths

${}^5X(b) - {}^5Y(a)$	${}^5X(b) - {}^5Y(b)$
$(\Lambda+1)^2 \dfrac{3v_3^{-2}v_4^-v_5^+}{C_4^-(P)}$	$\dfrac{3(J-1)\,v_4^-v_5^+(2J+3)}{2J^3(J+1)^2}$
$(\Lambda+1)^2 \dfrac{3v_4^{-2}v_5^+v_6^+}{C_4(Q)}$	$\dfrac{3(J+2)\,v_5^+v_6^+(2J-1)}{2J(J+1)^3(2J+3)}$
$(\Lambda+1)^2 \dfrac{3v_5^-v_6^+v_7^{+2}}{C_4^+(R)}$	0
$\dfrac{3v_3^{-2}v_4^{-2}v_5^+v_6^+}{C_5^-(P)}$	$\dfrac{3v_5^+v_6^+}{J(J+1)^2(2J+1)(2J+3)}$
$\dfrac{3v_4^{-2}v_5^-v_5^+v_6^+v_7^+}{C_5(Q)}$	0
$\dfrac{3v_5^-v_6^-v_7^{+2}v_8^{+2}}{C_5^+(R)}$	0
$\dfrac{2v_1^-v_2^-v_3^-v_3^+v_4^+v_5^+}{C_1^-(P)}$	0
$\dfrac{2v_2^-v_3^-v_4^+v_5^+v_6^{+2}}{C_1(Q)}$	0
$\dfrac{2v_3^-v_3^+v_4^+v_5^+v_6^+v_7^+}{C_1^+(R)}$	0
$\dfrac{(v_0^- - \Lambda)^2\, v_2^-v_3^-v_5^+v_6^+}{2C_2^-(P)}$	0
$\dfrac{(v_1^- - \Lambda)^2\, v_3^-v_5^+v_6^{+2}}{2C_2(Q)}$	0
$\dfrac{(v_2^- - \Lambda)^2\, v_4^+v_5^+v_6^+v_7^+}{2C_2^+(R)}$	$\dfrac{9v_4^-v_5^-}{2(J+1)^3(2J+1)(2J+3)}$
$(2\Lambda+3)^2 \dfrac{3v_2^{-2}v_3^-v_5^+}{2C_3^-(P)}$	0
$(2\Lambda+3)^2 \dfrac{3v_3^{-2}v_6^{+2}}{2C_3(Q)}$	$\dfrac{3(J+2)\,v_4^-v_5^-(2J-1)}{2J(J+1)^3(2J+3)}$
$(2\Lambda+3)^2 \dfrac{3v_4^-v_5^+v_6^+v_7^+}{2C_3^+(R)}$	$\dfrac{3Jv_5^-v_6^-(2J+5)}{2(J+1)^3(J+2)^2}$
$\dfrac{(v_7^+ + \Lambda)^2\, v_2^{-2}v_3^{-2}}{2C_4^-(P)}$	$\dfrac{(J-1)(J-2)\,v_4^-v_5^-(2J-1)}{2J(J+1)^2(2J+1)}$
$\dfrac{(v_8^+ + \Lambda)^2\, v_3^{-2}v_4^-v_6^+}{2C_4(Q)}$	$\dfrac{(J^2+2J-2)^2\, v_5^-v_6^+(2J+1)}{2J(J+1)^3(J+2)^2}$
$\dfrac{(v_9^+ + \Lambda)^2\, v_4^-v_5^-v_6^+v_7^+}{2C_4^+(R)}$	$\dfrac{J(J+3)\,v_6^+v_7^+(2J+1)}{2(J+1)(J+2)^2(2J+3)}$
$\dfrac{2v_2^{-2}v_3^{-2}v_4^-v_6^+}{C_5^-(P)}$	$\dfrac{v_5^-v_6^+(2J-1)}{J(J-1)^2(J+2)}$
$\dfrac{2v_3^{-2}v_4^-v_5^-v_6^+v_7^+}{C_5(Q)}$	$\dfrac{v_6^+v_7^+(2J+1)}{(J+1)(J+2)^2(2J+3)}$

Table IV

Branches		Line	
$\Delta\Lambda = +1$	$\Delta\Lambda = -1$	${}^{5}X(a) - {}^{5}Y(a)$	${}^{5}X(a) - {}^{5}Y(b)$
${}^{S}R_{54}(J)$	${}^{O}P_{45}J+1)$	0	$\frac{v_3^- v_4^- v_5^- v_6^+ v_7^+ v_8^+}{2C_4(R)}$
${}^{L}P_{15}(J)$	${}^{V}R_{51}(J-1)$	0	$\frac{v_5^- v_6^- v_3^+ v_4^+ v_5^+ v_6^+}{2C_5(P)}$
${}^{M}Q_{15}(J)$	${}^{U}Q_{51}(J)$	0	$\frac{v_6^- v_3^{+2} v_4^+ v_5^+ v_6^+}{2C_5(Q)}$
${}^{N}R_{15}(J)$	${}^{T}P_{51}(J+1)$	0	$\frac{v_3^{+2} v_4^{+2} v_5^+ v_6^+}{2C_5^+(R)}$
${}^{M}P_{25}(J)$	${}^{U}R_{52}(J-1)$	0	$\frac{2v_4^- v_5^- v_6^- v_4^+ v_5^+ v_6^+}{C_5(P)}$
${}^{N}Q_{25}(J)$	${}^{T}Q_{52}(J)$	0	$\frac{2v_5^- v_6^- v_4^{+2} v_5^+ v_6^+}{C_5(Q)}$
${}^{O}R_{25}(J)$	${}^{S}P_{52}(J+1)$	0	$\frac{2v_6^- v_4^{+2} v_5^{+2} v_6^+}{C_5(R)}$
${}^{N}P_{35}(J)$	${}^{T}R_{53}(J-1)$	0	$\frac{3v_3^- v_4^- v_5^- v_6^- v_5^+ v_6^+}{C_5(P)}$
${}^{O}Q_{35}(J)$	${}^{S}Q_{53}(J)$	0	$\frac{3v_4^- v_5^- v_6^- v_5^{+2} v_6^+}{C_5(Q)}$
${}^{P}R_{35}(J)$	${}^{R}P_{53}(J+1)$	0	$\frac{3v_5^- v_6^- v_5^{+2} v_6^{+2}}{C_5(R)}$
${}^{O}P_{45}(J)$	${}^{S}R_{54}(J-1)$	0	$\frac{2v_2^- v_3^- v_4^- v_5^- v_6^- v_6^+}{C_5(P)}$
${}^{P}Q_{45}(J)$	${}^{R}Q_{54}(J)$	0	$\frac{2v_3^- v_4^- v_5^- v_6^- v_6^{+2}}{C_5(Q)}$
${}^{Q}R_{45}(J)$	${}^{Q}P_{54}(J+1)$	0	$\frac{2v_4^- v_5^- v_6^- v_6^{+2} v_7^+}{C_5(R)}$
$P_5(J)$	$R_5(J-1)$	$\frac{v_1^- v_2^-}{2J}$	$\frac{v_1^- v_2^- v_3^- v_4^- v_5^- v_6^-}{2C_5(P)}$
$Q_5(J)$	$Q_5(J)$	$\frac{v_2^- v_7^+(2J+1)}{2J(J+1)}$	$\frac{v_2^- v_3^- v_4^- v_5^- v_6^- v_7^+}{2C_5(P)}$
$R_5(J)$	$P_5(J+1)$	$\frac{v_7^+ v_8^+}{2(J+1)}$	$\frac{v_3^- v_4^- v_5^- v_6^- v_7^+ v_8^+}{2C_5(R)}$

continued)

strengths

${}^5X(b) - {}^5Y(a)$	${}^5X(b) - {}^5Y(b)$
$\frac{2v_4^- v_5^- v_6^- v_7^+ v_8^{+2}}{C_5^+(R)}$	0
$\frac{v_1^- v_2^- v_3^+ v_4^+ v_5^+ v_6^+}{2C_1^-(P)}$	0
$\frac{v_2^- v_4^+ v_5^+ v_6^+ v_7^{+2}}{2C_1(Q)}$	0
$\frac{v_3^+ v_4^+ v_5^+ v_6^+ v_7^+ v_8^+}{2C_1^+(R)}$	0
$\frac{v_1^{-2} v_2^- v_4^+ v_5^+ v_6^+}{2C_2^-(P)}$	0
$\frac{v_2^{-2} v_5^+ v_6^+ v_7^2}{2C_2(Q)}$	0
$\frac{v_3^- v_4^+ v_5^+ v_6^+ v_7^+ v_8^+}{2C_2^+(R)}$	0
$\frac{3v_1^{-2} v_2^{-2} v_5^+ v_6^+}{2C_3^-(P)}$	0
$\frac{3v_2^{-2} v_3^- v_6^+ v_7^{+2}}{2C_3(Q)}$	0
$\frac{3v_3^- v_4^- v_5^+ v_6^+ v_7^+ v_8^+}{2C_3^+(R)}$	$\frac{3v_5^- v_6^-}{(J+1)(J+2)^2(2J+3)(2J+5)}$
$\frac{v_1^{-2} v_2^{-2} v_3^- v_6^+}{2C_4^-(P)}$	0
$\frac{v_2^{-2} v_3^- v_4^- v_7^{+2}}{2C_4(Q)}$	$\frac{v_6^- v_5^+(2J+1)}{(J+1)(J+2)^2(2J+3)}$
$\frac{v_3^- v_4^- v_5^- v_6^+ v_7^+ v_8^+}{2C_4^+(R)}$	$\frac{v_6^- v_7^+(2J+1)}{(J+1)(J+2)^2(J+3)}$
$\frac{v_1^{-2} v_2^{-2} v_3^- v_4^-}{2C_5^-(P)}$	$\frac{v_5^- v_6^-(2J-1)}{2(J+2)(2J+3)}$
$\frac{v_2^{-2} v_3^- v_4^- v_5^- v_7^+}{2C_5(Q)}$	$\frac{Jv_6^- v_7^+(2J+1)}{(J+1)(J+2)^2}$
$\frac{v_3^- v_4^- v_5^- v_6^- v_7^+ v_8^+}{2C_5^+(R)}$	$\frac{v_7^+ v_8^+(2J+1)}{2(J+3)(2J+5)}$

In the Tables

$$C_i^-(P) = JC_k(J-1); \qquad C_i(R) = (J+1)C_k(J);$$

$$C_i(Q) = \frac{J(J+1)}{J+1/2} C_k(J); \tag{3}$$

$$C_i(P) = JC_k(J); \qquad C_i^+(R) = (J+1)C_k(J+1);$$

where for quartet transitions $i = 1, 2, 3, 4$ and $k = J-3/2, J-1/2, J+1/2, J+3/2$, respectively and for quintet transitions $i = 1, 2, 3, 4, 5$ and $k = J-2, J-1, J, J+1, J+2$, respectively. For all Tables the terms of case a) were assumed to be normal. If an inverted term occurs instead of a normal one then the suffixes corresponding to the inverted terms in the branch symbols have to be changed on the basis of the above correlation according to the pattern for quartet transition $1 \to 4$, $2 \to 3$, $3 \to 2$, $4 \to 1$ and for quintet transitions $1 \to 5$, $2 \to 4$, $3 \to 3$, $4 \to 2$, $5 \to 1$, respectively, wherever the inverted term occurs.

REFERENCES

1. I. KOVÁCS and I. PÉCZELI, Acta Phys. Hung., **43**, 299, 1977.
2. I. KOVÁCS, Rotational Structure in the Spectra of Diatomic Molecules, Akadémiai Kiadó, Budapest and Adam Hilger Ltd. London, 1969.
3. W. H. BRANDT, Phys. Rev., **50**, 778, 1936.

Acta Physica Academiae Scientiarum Hungaricae, Tomus 43 (3—4), pp. 347—350 (1977)

COMMUNICATIO BREVIS

SEGREGATION OF MAGNETOHYDRODYNAMIC WAVES IN AN IDEAL MEDIUM

By

M. Y. NASIR*

DEPARTMENT OF THEORETICAL PHYSICS, LORÁND EÖTVÖS UNIVERSITY, BUDAPEST

(Received 27. IX. 1977)

1. Introduction

A. I. AKHIEZER et al in their book "Plasma Electrodynamics" describe that the fundamental equations of magnetohydrodynamics can be written in matrix form. After linearizing and solving the equations they obtain the phase velocities of different magnetohydrodynamic waves as eigenvalues of a matrix. Corresponding to these eigenvalues they calculate different column (right) eigenvectors and row (left) eigenvectors and show that an arbitrary small perturbation of a magnetohydrodynamic quantity can be written as a superposition of seven fundamental magnetohydrodynamic waves. In this paper we reproduce these results briefly and extend them to prove that the fundamental magnetohydrodynamic waves do not mix with each other.

2. Formulation and solution of the problem

We consider one dimensional wave propagation along a $Z-$axis and take all magnetohydrodynamic quantities depending upon z and time t only. The basic equations of magnetohydrodynamics for an ideal medium can be written as [1]:

$$\frac{\partial A_l}{\partial t} + \sum_{n=1}^{7} M_{ln}(A) \frac{\partial A_n}{\partial z} = 0, \; l = 1, 2, \ldots, 7, \tag{1}$$

* On leave from Government College, Bahawalnagar, Pakistan.

where A_l and M_{ln} are respectively, given by

$$A_l = \begin{bmatrix} \varrho \\ s \\ v_x \\ v_y \\ v_z \\ B_x \\ B_y \end{bmatrix} \tag{2}$$

$$M_{ln} = \begin{bmatrix} v_z & 0 & 0 & 0 & \varrho & 0 & 0 \\ 0 & v_z & 0 & 0 & 0 & 0 & 0 \\ 0 & 0 & v_z & 0 & 0 & -B_z/4\pi\varrho & 0 \\ 0 & 0 & 0 & v_z & 0 & 0 & -B_z/4\pi\varrho \\ \frac{1}{\varrho}C_s^2 & \frac{1}{\varrho}\frac{\partial p}{\partial s} & 0 & 0 & v_z & B_x/4\pi\varrho & B_y/4\pi\varrho \\ 0 & 0 & -B_z & 0 & B_x & v_z & 0 \\ 0 & 0 & 0 & -B_z & B_y & 0 & v_z \end{bmatrix}. \tag{3}$$

Here, ϱ is the mass density, s the entropy density, **v** the fluid velocity, **B** the magnetic field, p the pressure and $C_s = (\partial p/\partial \varrho)^{1/2}$ the speed of sound. We linearize the set of Eqs. (1) by substituting $A_l = A_{l(0)} + A_{l(1)}$ and assuming that the components $A_{l(1)}$ are small corrections to the unperturbed solutions $A_{l(0)}$. Thus, the Eqs. (1) will become:

$$\frac{\partial A_{l(1)}}{\partial t} + \sum_{n=1}^{7} M_{ln}(A_{(0)}) \frac{\partial A_{n(1)}}{\partial z} = 0 . \tag{4}$$

If the frame of reference moves with the fluid velocity and the coordinate system rotates about a Z-axis, the matrix (3) can obviously be simplified to a form $\mathfrak{M}_{ln}$ (say). Using a plane wave trial function for the solutions

$$A_{l(1)} = \mathfrak{A}_l \, e^{i(kz-\omega t)}, \tag{5}$$

where $\mathfrak{A}_l$ is the amplitude of $A_{l(1)}$, $i = (-1)^{1/2}$, k the wave vector and ω the angular frequency, we obtain a system of algebraic equations in terms of ω and k (or the phase velocity $u = \omega/k$). These equations are:

$$\sum_{n=1}^{7} \mathfrak{M}_{ln} \mathfrak{A}_n = u \mathfrak{A}_l . \tag{6}$$

We observe that a vector G_l having components $\mathfrak{A}_l$ is a column eigenvector and u an eigenvalue of the matrix $\mathfrak{M}_{ln}$. We write

$$\sum_{n=1}^{7} \mathfrak{M}_{ln} G_n = u G_l . \tag{7}$$

Thus, the solution of the wave problem is reduced to a proper value problem. For a non-trivial solution of Eq. (7), we must have

$$|\mathfrak{M}_{ln} - u\delta_{ln}| = 0, \tag{8}$$

δ_{ln} being Kronecker delta. It is a polynomial equation in u of degree seven. Solving this equation we obtain seven values of the phase velocity u; each two corresponding to Alfvén waves, rapid magneto-acoustic waves and slow magneto-acoustic waves and one to entropy wave. We can determine different column (right) eigenvectors and row (left) eigenvectors corresponding to these values of u. The sets of these column eigenvectors $\{G_l\}$ and row eigenvectors $\{F_n\}$ form a biorthogonal set. Therefore, we can write

$$\left.\begin{aligned} &\sum_{m=1}^{7} F_u^{(m)} G_l^{(m)} = 0, \quad \text{if } n \neq l \\ &\sum_{m=1}^{7} F_n^{(m)} G_n^{(m)} = Y \neq 0. \end{aligned}\right\} \tag{9}$$

Now the general solution of (4) can be written in the form:

$$A_{l(1)}(z, t) = \sum_{n=1}^{7} C^{(n)} \mathfrak{R}_l^{(n)} e^{i(kz-\omega t)} \tag{10}$$

$$= \sum_{n=1}^{7} C^{(n)} G_l^{(n)} e^{i(kz-\omega t)}, \tag{11}$$

where $C^{(n)}$ are coefficients to be determined later.

Let us assume that the equalities (4) are subejct to the initial condition:

$$A_{l(1)1}(z, 0) = f_l(z). \tag{12}$$

Now keeping in view the expression (5), we can write $f_l(z)$ as a Fourier integral:

$$A_{l(1)}(z, 0) = f_l(z) = \int f_l^{(k)} e^{ikz} \, dk, \tag{13}$$

where $f_l(k)$ can further be written as:

$$f_l(k) = \sum_{n=1}^{7} C^{(n)} G_l^{(n)}. \tag{14}$$

The coefficients $C^{(n)}$, with the help of the relations (9) and (14), will turn out to be

$$C^{(n)} = \frac{\sum_{n=1}^{7} F_l^{(n)} f_l(k)}{Y}. \tag{15}$$

Thus, Eq. (5) will take the form:

$$A_{l(1)}(z, t) = \sum_{n=1}^{7} \int \frac{\sum_{m=1}^{7} F_m^{(n)} f_m(k) G_l^{(n)}}{Y} e^{i(kz-\omega t)} dk . \tag{16}$$

implying that an arbitrary small perturbation can be written as a superposition of seven fundamental magnetohydrodynamic waves.

3. Segregation

Interchanging the order of summation in (16) and taking the aid of the Eq. (9), we obtain

$$A_{l(1)}(z, t) = \sum_{m=1}^{7} \int \frac{\sum_{n=1}^{7} F_m^{(n)} G_l^{(n)}}{Y} f_m(k) \, e^{i(kz-\omega t)} dk = \tag{17}$$

$$= \sum_{m=1}^{7} \int \delta_{ml} f_m(k) \, e^{i(kz-\omega t)} dk . \tag{18}$$

Therefore, if $f_m(k)$ represents one of the fundamental waves, the solution continues to belong to that very fundamental type; or cross-excitation does not take place.

From the last expression, we note that any perturbation of a magnetohydrodynamic quantity in a given mode has contributions from the same mode only and all other modes remain apart. Thus, we can conclude that magnetohydrodynamic waves do not mix with each other in an ideal medium.

Acknowledgement

I am highly obliged to Professor Iván Abonyi for his benevolence and learned guidance to complete this work. I am also thankful to the Institute of Cultural Relations, Budapest, for awarding me a research scholarship.

REFERENCE

1. A. I. Akhiezer et al., Plasma Electrodynamics I, Pergamon Press, Oxford, 1975.

RECENSIONES

Lasers and Their Applications

Edited by Alberto Sona, Gordon and Breach Science Publishers, London, 1976
pp. 629 + XIV. Price £ 23.90

The book contains the proceedings of a Course on lasers and their applications from the International School of Applied Physics held in Eric, Sicily from 31 May to 13 June, 1970. The Course was a very significant meeting of researchers active in different areas from universities and industrial laboratories. The papers of contributors are valuable for young graduate and experienced scientists interested in having basic information on laser sources and some specific applications. However, the delayed publication of the book has led to its depreciation to a certain extent. As a matter of course the basic physics does not become out of date, while the technological applications are more ramifying now as it is suggested in the book and in many cases are realized with good results even in factory environments.

The work is divided into two sections headed, "Laser Sources" and "Applications". The first section contains seven papers on 252 pages. This part of the book deals with the physical processes in laser action, properties of open resonators. In the following the detailed physics of semi-conductor, dye, gaseous and solid state lasers is given with the discussion of technological problems pointing out the advantages and difficulties in the applications of each technique. Basic principles of laser theory are applied to the experimental results observed under operation. In most cases the conclusions are supported by numerical examples.

In the second section different applications of lasers are discussed. It is difficult to estimate the expectational effectiveness of these papers because of their inopportuneness for the experienced scientist of our days. The lectures on applications dealt with theory and applications of holography, information processing with optical methods, atmospheric propagation, transmission of information with laser beams, distance measurements by laser beams, machining with laser, medical applications, scattering experiments, nonlinear optics, plasma generation and diagnostics. Valuable analysis of basic physics and some general technological problems are explored scientifically.

To summarize, in this book we have a good collection of works on topics of laser physics and its various applications. The literature listed at the end of each paper makes it easier for the reader to pursue any of the topics covered in the book in greater detail.

The book is nicely presented and has an extensive set of figures to accompany the text

Z. FÜZESSY

R. V. DICKEY: Bifurcation Problems in Nonlinear Elasticity

Pitman Publishing Ltd. London, San Francisco, Melbourne 1976

This is the 3. volume of the series "Research Notes in Mathematics" edited by an editorial board headed by Prof. A. JEFFREY (University of Newcastle-upon-Tyne). The aim of the series is to publish current material of a specialist nature whose style of exposition is mostly that of a developing subject.

The present small volume of 119 pages (it looks like a lecture note) presents the most important elements of bifurcation theory and its application to some problems in the nonlinear elasticity. Bifurcation theory deals with problems of solving differential equations of the type $F(u, \lambda) = 0$, where F is in the most general context a nonlinear transformation defined for u and λ a real parameter, when the solutions are not single valued functions of λ. The most

important mathematical bases are given in Chapter 1 (Introduction) and Chapter 6 (Bifurcation theory for second order ordinary differential equations) while the applications treated are given in the other Chapters. These are devoted to the following problems of nonlinear elasticity: the static problem for the nonlinear string and circular membrane, the rotating string and the buckling of the circular plate.

The volume is written on a rather sophisticated level, but in an elegant, clear style and with many clarifying examples. A clever balance was held between the pure and applied side of mathematics used and for every chapter references are given for a deeper study of the subject. There is, however, no subject index and a slightly more detailed introduction as well as a short conclusion would have been useful for a physicist reader, who wanted to use advanced mathematical methods in different possible fields of physics.

J. ANTAL

H. HAKEN: Synergetics—An Introduction

Springer-Verlag, Berlin, Heidelberg, New York, 1977, pp. 325

Synergetics is a very new field of interdisciplinary research. It investigates the spontaneous formation and functioning of well organized dynamic structures caused by the cooperation of many subsystems or phenomena. Such phenomena are an experience of our daily life when we observe the growth of plants and animals. On the other hand, the whole universe exhibits pronounced dynamic structures from different samples of galaxies to living cells and their constituents. In the last decades it has become evident that there are numerous examples in physical, chemical and biological systems where well organized temporal, spatial or spatial-temporal dynamic structures arise out of certain chaotic states. In contrast to artificial, man-made machines, these dynamic structures develop spontaneously, i.e. they are self-organizing and, many of the most fascinating and interesting phenomena occur in systems far from thermostatic equilibrium. Many different disciplines cooperate in the theory of "synergetics" to find general laws governing self-organizing dynamic structures.

The author, who is a pioneer of this interdisciplinary science, in this introduction tried to present the different disciplines of synergetics as a text for students of physics, chemistry and biology in an elementary fashion whenever possible. Therefore the knowledge of an undergraduate course in mathematics is sufficient and the basic knowledge required for the physical, chemical and biological systems is not very special.

The book contains twelve chapters concerned with the fundamental laws of Probability, Information, Chance, Necessity, Thermodynamics, Self-organization and applications of the general concepts and laws of these disciplines to physical, chemical, biological and sociological systems and phenomena. The book is beautifully presented and has an extensive set of figures to accompany the text. The treatise is very useful for physicists, chemists, biologists and so on and it really is indispensable for university libraries. Nevertheless, we cannot find any new and original concepts and principles in the text which would be characteristic only for the new science of "synergetics". Consequently, the real existence of this "new science" remains problematic.

I. GYARMATI

H. BACRY: Lectures on Group Theory and Particle Theory

"Documents on Modern Physics". Edited by E. W. Montroll, G. H. Vineyard, M. Lévy and P. Matthews. Gordon and Breach Science Publishers, London, New York, Paris, 1977, 586 p.

This book provides the basic concepts and theorems in group theory as well as selected applications to the fundamental symmetries of elementary particles for physics students. Complicated proofs are avoided but the notions and theorems are well enlightened. Numerous exercises are included into the volume. The inquiring reader can find also specialized works given in the bibliography.

Chapter 1 yields a description of the elements of group theory. A whole chapter (Ch. 2) is devoted to vector spaces followed by Chapter 3 treating the notion of group representation. The finite representations of the linear groups and of their principal subgroups are contained in Chapter 4. The next chapter deals with the topics of Lie groups and Lie algebras. Considering the importance of the rotation group in physics, a whole chapter (6) treats its properties. In the subsequent parts topics essential in particle physics are selected: the Lorentz group (Ch. 7), the Poincaré group (Ch. 8), the most essential internal symmetries of elementary particles (Ch. 9) and unitary symmetries of hadrons (Ch. 10). Since the SU(6)-physics (Ch. 10) there is a great progress in particle symmetries, this can be pursued on the basis of the bibliography.

It is a real plesure to see such a volume containing also applications in a well summarized way. We hope it will be good reading for those interested in theoretical physics.

G. PÓCSIK

AMON YARIV: Introduction to Optical Electronics

Holl, Rinehart and Winston, New York, 1977.

In recent years the importance of quantum electronics has considerably grown in the study of phenomena observed on both atomic and macroscopic levels. The latter field has attracted ever more attention with the progress of applied research. The book contains the basic principles of this discipline completed with new results obtained over the five years which elapsed since its first edition. The concentration on the macroscopic features of interactions between light and matter permit the phenomena to be described without recourse to quantum mechanics which reappears only in the determintaion of certain parameters characteristic of matter.

The reader is first introduced to the field of basic problems connected with the propagation of electromagnetic radiation in isotropic and anisotropic media, then to the fundamentals of geometrical optics. Finally, in this part, the propagation of optical beams and the properties of optical resonators are discussed.

Subsequently, we learn about the behaviour of electromagnetic waves interacting with atomic systems and about the basic principles of laser operation. This is followed by the description of the laser types most frequently used.

In some crystals the polarization in strong electric fields varies with the square of the electric field intensity. This phenomenon can be utilized for a number of practical applications such as the generation of second harmonics and parametric amplification. This section of the book ends with the discussion of the basic principles of the electrooptical modulation of laser beams.

Some problems of light detection are also considered with special regard to the role of noise. The operation of some of the most important light detectors is described.

The interaction between light and sound waves plays an important role in modern applications (e.g. light deflectors). For this reason the chapter on the theory of these interaction can be very useful. This applies also to the chapter dealing with the propagation of light in dielectric waveguides and with the basic principles of the so-called "integrated optics".

The book is a useful manual for university students who are interested in quantum electronics and it can be of good use to engineers starting research and development in the field of modern optics.

N. KROÓ

Progress in Crystal Growth and Characterization

Editor: B. R. Pamplin. Pergamon Press, Oxford, 1977.

A new international review journal, planned to appear as a quarterly, edited by the well-known specialist B. R. PAMPLIN, has been launched by Pergamon Press. The aim of this new journal, as expounded by the Editor in the Introduction, is to review the important technologies and methods of the rapidly developing subject of crystal growth and crystal qualification before the results become outdated and thus to give general information on this

field of research. Fast information is well served by the camera-ready copy techniques. The issues are completed by book reviews and a list of current conferences and other events. From time to time special issues are planned to appear on some up-to-date problems in the foreground of interest, as e.g. Molecular Beam Epitaxy.

Workers in this field welcome this new journal which, beside filling the gap between monographs and original papers, provides information for the beginners on the essentials of the subject as well as for more advanced readers on recent results. The journal serves equally well the interest of the experts of research and industry.

The first issue contains articles by B. R. PAMPLIN on "The Evolution of Crystal Growth-Techniques", by B. K. TANNER on "Crystal Assessment by X-ray Topography Using Synchrotron Radiation" and by K. G. BARRACLOUGH on "Crystal Growth of Ferromagnetic Semiconductors". From the high standard set by these papers one may conclude that the new periodical will be most useful in promoting work in the field of crystal growth.

R. VOSZKA

Printed in Hungary

A kiadásért felel az Akadémiai Kiadó igazgatója — Műszaki szerkesztő: Botyánszky Pál

A kézirat nyomdába érkezett: 1978. I. 23. — Terjedelem: 13,5 (A/5) ív, 31 ábra, 1 melléklet

78.5456 Akadémiai Nyomda, Budapest — Felelős vezető: Bernát György

NOTES TO CONTRIBUTORS

I. PAPERS will be considered for publication in Acta Physica Hungarica, only if they have not previously been published or submitted for publication elsewhere. They may be written in English, French, German or Russian.

Papers should be submitted to

Prof. I. Kovács, Editor
Department of Atomic Physics, Technical University
1521 Budapest, Budafoki út 8, Hungary

Papers may be either articles with abstracts or short communications. Both should be as concise as possible, articles in general not exceeding 25 typed pages, short communications 8 typed pages.

II. MANUSCRIPTS

1. Papers should be submitted in five copies.

2. The text of papers must be of high stylistic standard, requiring minor corrections only.

3. Manuscripts should be typed in double spacing on good quality paper, with generous margins.

4. The name of the author(s) and of the institutes where the work was carried out should appear on the first page of the manuscript.

5. Particular care should be taken with mathematical expressions. The following should be clearly distinguished, e.g. by underlining in different colours: special founts (italics, script, bold type, Greek, Gothic, etc.); capital and small letters; subscripts and superscripts, e.g. x_2, x^3; small *l* and 1; zero and capital O; in expressions written by hand: *e* and *l*, *n* and *u*, *v* and *v*, etc.

6. References should be numbered serially and listed at the end of the paper in the following form: J. Ise and W. D. Fretter, Phys. Rev., *76*, 933, 1949.

For books, please give the initials and family name of the author(s), title, name of publisher, place and year of publication, e.g.: J. C. Slater, Quantum Theory of Atomic Structures, I. McGraw-Hill Book Company, Inc., New York, 1960.

References should be given in the text in the following forms: Heisenberg [5] or [5].

7. Captions to illustrations should be listed on a separate sheet, not inserted in the text.

III. ILLUSTRATIONS AND TABLES

1. Each paper should be accompanied by five sets of illustrations, one of which must be ready for the blockmaker. The other sets attached to the copies of the manuscript may be rough drawings in pencil or photocopies.

2. Illustrations must not be inserted in the text.

3. All illustrations should be identified in blue pencil by the author's name, abbreviated title of the paper and figure number.

4. Tables should be typed on separate pages and have captions describing their content. Clear wording of column heads is advisable. Tables should be numbered in Roman numerals (I, II, III, etc.).

IV. MANUSCRIPTS not in conformity with the above Notes will immediately be returned to authors for revision. The date of receipt to be shown on the paper will in such cases be that of the receipt of the revised manuscript.

Reviews of the Hungarian Academy of Sciences are obtainable at the following addresses:

AUSTRALIA
C.B.D. LIBRARY AND SUBSCRIPTION SERVICE, Box 4886, G.P.O., *Sydney N.S.W.2001*
COSMOS BOOKSHOP, 145 Ackland Street, *St. Kilda (Melbourne), Victoria 3182*

AUSTRIA
GLOBUS, Höchstädtplatz 3, *1200 Wien XX*

BELGIUM
OFFICE INTERNATIONAL DE LIBRAIRIE, 30 Avenue Marnix, *1050 Bruxelles*
LIBRAIRIE DU MONDE ENTIER, 162 Rue du Midi, *1000 Bruxelles*

BULGARIA
HEMUS, Bulvar Ruszki 6, *Sofia*

CANADA
PANNONIA BOOKS, P.O. Box 1017, Postal Station "B", *Toronto, Ontario M5T 2T8*

CHINA
CNPICOR, Periodical Department, P.O. Box 50, *Peking*

CZECHOSLOVAKIA
MAD'ARSKÁ KULTURA, Národní třida 22, *115 66 Praha*
PNS DOVOZ TISKU, Vinohradská 46, *Praha 2*
PNS DOVOZ TLAČE, *Bratislava 2*

DENMARK
EJNAR MUNKSGAARD, Norregade 6, *1165 Copenhagen*

FINLAND
AKATEEMINEN KIRJAKAUPPA, P.O. Box 128, *SF-00101 Helsinki 10*

FRANCE
EUROPERIODIQUES S. A., 31 Avenue de Versailles, *78170 La Celle St.-Cloud*
LIBRAIRIE LAVOISIER, 11 rue Lavoisier, *75008 Paris*
OFFICE INTERNATIONAL DE DOCUMENTATION ET LIBRAIRIE, 48 rue Gay-Lussac, *75240 Paris Cedex 05*

GERMAN DEMOCRATIC REPUBLIC
HAUS DER UNGARISCHEN KULTUR, Karl-Liebknecht-Strasse 9, *DDR-102 Berlin*
DEUTSCHE POST ZEITUNGSVERTRIEBSAMT, Strasse der Pariser Kommüne 3—4, *DDR-104 Berlin*

GERMAN FEDERAL REPUBLIC
KUNST UND WISSEN ERICH BIEBER, Postfach 46, *7000 Stuttgart 1*

GREAT BRITAIN
BLACKWELL'S PERIODICALS DIVISION, Hythe Bridge Street, *Oxford OX1 2ET*
BUMPUS, HALDANE AND MAXWELL LTD., Cowper Works, *Olney, Bucks MK46 4BN*
COLLET'S HOLDINGS LTD., Denington Estate, *Wellingborough, Northants NN8 2QT*
W.M. DAWSON AND SONS LTD., Cannon House, *Folkestone, Kent CT19 5EE*
H. K. LEWIS AND CO., 136 Gower Street, *London WC1E 6BS*

GREECE
KOSTARAKIS BROTHERS, International Booksellers, 2 Hippokratous Street, *Athens-143*

HOLLAND
MEULENHOFF-BRUNA B.V., Beulingstraat 2, *Amsterdam*
MARTINUS NIJHOFF B.V., Lange Voorhout 9—11, *Den Haag*
SWETS SUBSCRIPTION SERVICE, 347b Heereweg, *Lisse*

INDIA
ALLIED PUBLISHING PRIVATE LTD., 13/14 Asaf Ali Road, *New Delhi 110001*
150 B-6 Mount Road, *Madras 600002*
INTERNATIONAL BOOK HOUSE PVT. LTD., Madame Cama Road, *Bombay 400039*
THE STATE TRADING CORPORATION OF INDIA LTD., Books Import Division, Chandralok, 36 Janpath, *New Delhi 110001*

ITALY
EUGENIO CARLUCCI, P.O. Box 252, *70100 Bari*
INTERSCIENTIA, Via Mazzé 28, *10149 Torino*
LIBRERIA COMMISSIONARIA SANSONI, Via Lamarmora 45, *50121 Firenze*
SANTO VANASIA, Via M. Macchi 58, *20124 Milano*
D. E. A., Via Lima 28, *00198 Roma*

JAPAN
KINOKUNIYA BOOK-STORE CO. LTD., 17-7 Shinjuku-ku 3 chome, Shinjuku-ku, *Tokyo 160-91*
MARUZEN COMPANY LTD., Book Department, P.O. Box 5050 Tokyo International, *Tokyo 100-31*
NAUKA LTD. IMPORT DEPARTMENT, 2-30-19 Minami Ikebukuro, Toshima-ku, *Tokyo 171*

KOREA
CHULPANMUL, *Phenjan*

NORWAY
TANUM-CAMMERMEYER, Karl Johansgatan 41—43, *1000 Oslo*

POLAND
WĘGIERSKI INSTYTUT KULTURY, Marszalkowska 80, *Warszawa*
CKP I W ul. Towarowa 28 *00-958 Warsaw*

ROMANIA
D. E. P., *Bucureşti*
ROMLIBRI, Str. Biserica Amzei 7, *Bucureşti*

SOVIET UNION
SOJUZPETCHATI — IMPORT, *Moscow*
and the post offices in each town
MEZHDUNARODNAYA KNIGA, *Moscow G-200*

SPAIN
DIAZ DE SANTOS, Lagasca 95, *Madrid 6*

SWEDEN
ALMQVIST AND WIKSELL, Gamla Brogatan 26, *101 20 Stockholm*
GUMPERTS UNIVERSITETSBOKHANDEL AB, Box 346, *401 25 Göteborg 1*

SWITZERLAND
KARGER LIBRI AG, Petersgraben 31, *4011 Basel*

USA
EBSCO SUBSCRIPTION SERVICES, P.O. Box 1943, *Birmingham*, Alabama 35201
F. W. FAXON COMPANY, INC., 15 Southwest Park, *Westwood*, Mass. 02090
THE MOORE-COTTRELL SUBSCRIPTION AGENCIES, *North Cohocton, N. Y. 14868*
READ-MORE PUBLICATIONS, INC., 140 Cedar Street, *New York, N. Y. 10006*
STECHERT-MACMILLAN, INC., 7250 Westfield Avenue, *Pennsauken* N. J. 08110

VIETNAM
XUNHASABA, 32, Hai Ba Trung, *Hanoi*

YUGOSLAVIA
JUGOSLAVENSKA KNJIGA, Terazije 27, *Beograd*
FORUM, Vojvode Mišiča 1, *21000 Novi Sad*

Index: 26.025
Acta Phys. Hung. Tom. 43. No. 3—4. Budapest, 30. VI. 1978 HU-ISSN 0001-6705